A Standardized Database to Describe and Classify Offshore Benthic Marine Habitats and Its Use for Designating the Critical Habitat of Species at Risk

J.-D. Dutil, S. Proulx, P.-M. Chouinard, D. Borcard, C. Laurian, H. Tamdrari, and C. Nozères

Fisheries and Oceans Canada
Science Branch, Québec Region
Maurice Lamontagne Institute
PO Box 1000, 850 route de la Mer
Mont-Joli, Québec G5H 3Z4

2013

Canadian Manuscript Report of Fisheries and Aquatic Sciences 3014

Fisheries and Oceans Canada
Pêches et Océans Canada

Canada

Canadian Manuscript Report of
Fisheries and Aquatic Sciences

Manuscript reports contain scientific and technical information that contribute to existing knowledge but that deal with national or regional problems. Distribution is restricted to institutions or individuals located in particular regions of Canada. However, no restriction is placed on subject matter, and the series reflects the broad interests and policies of the Department of Fisheries and Oceans, namely, fisheries and aquatic sciences.

Manuscript reports may be cited as full publications. The correct citation appears above the abstract of each report. Each report is indexed in the data base Aquatic Sciences and Fisheries Abstracts.

Numbers 1-900 in this series were issued as Manuscript Reports (Biological Series) of the Biological Board of Canada, and subsequent to 1937 when the name of the Board was changed by Act of Parliament, as Manuscript Reports (Biological Series) of the Fisheries Research Board of Canada. Numbers 901-1425 were issued as Manuscript Reports of the Fisheries Research Board of Canada. Numbers 1426-1550 were issued as Department of Fisheries and Environment, Fisheries and Marine Service Manuscript Reports. The current series name was changed with report number 1551.

Manuscript reports are produced regionally but are numbered nationally. Requests for individual reports will be filled by the issuing establishment listed on the front cover and title page. Out-of-stock reports will be supplied for a fee by commercial agents.

Rapport manuscrit canadien des
sciences halieutiques et aquatiques

Les rapports manuscrits contiennent des renseignements scientifiques et techniques qui constituent une contribution aux connaissances actuelles, mais qui traitent de problèmes nationaux ou régionaux. La distribution en est limitée aux organismes et aux personnes de régions particulières du Canada. Il n’y a aucune restriction quant au sujet; de fait, la série reflète la vaste gamme des intérêts et des politiques du ministère des Pêches et des Océans, c’est-à-dire les sciences halieutiques et aquatiques.

Les rapports manuscrits peuvent être cités comme des publications intégrales. Le titre exact paraît au-dessus du résumé de chaque rapport. Les rapports manuscrits sont indexés dans la base de données Aquatic Sciences and Fisheries Abstracts.

Les numéros 1 à 900 de cette série ont été publiés à titre de manuscrits (série biologique) de l’Office de biologie du Canada, et après le changement de la désignation de cet organisme par décret du Parlement, en 1937, ont été classés comme manuscrits (série biologique) de l’Office des recherches sur les pêcheries du Canada. Les numéros 901 à 1425 ont été publiés à titre de rapports manuscrits de l’Office des recherches sur les pêcheries du Canada. Les numéros 1426 à 1550 sont parus à titre de rapports manuscrits du Service des pêches et de la mer, ministère des Pêches et de l’Environnement. Le nom actuel de la série a été établi lors de la parution du numéro 1551.

Les rapports manuscrits sont produits à l’échelon régional, mais numérotés à l’échelon national. Les demandes de rapports seront satisfaites par l'établissement d’origine dont le nom figure sur la couverture et la page du titre. Les rapports épuisés seront fournis contre rétribution par des agents commerciaux.

Canadian Manuscript Report of
Fisheries and Aquatic Sciences 3014

2013

A standardized database to describe and classify offshore benthic marine habitats and its use for designating the critical habitat of species at risk

by

J.-D. Dutil, S. Proulx, P.-M. Chouinard, D. Borcard, C. Laurian, H. Tamdrari, and C. Nozères

Fisheries and Oceans Canada
Science Branch, Québec Region
Maurice Lamontagne Institute
PO Box 1000, 850 route de la Mer
Mont-Joli, Québec
G5H 3Z4

Cat. No. Fs 97-4/3014E-PDF ISSN 1488-5387 (Online version)

Correct citation for this publication:

Dutil, J.-D., S. Proulx, P.-M. Chouinard, D. Borcard, C. Laurian, H. Tamdrari, and C. Nozères. 2013. A standardized database to describe and classify offshore benthic marine habitats and its use for designating the critical habitat of species at risk. Can. Manuscr. Rep. Fish. Aquat. Sci 3014: vi + 347 pp.

TABLE OF CONTENTS

ABSTRACT v
RÉSUMÉ vi
PREFACE vii
INTRODUCTION 1
1. DESCRIPTION OF BENTHIC HABITATS 2
 HABITATS AS OBTAINED BY CLUSTER ANALYSIS 3
 SPLIT INTO TWO CATEGORIES: SHALLOW WATER AND DEEP WATER HABITATS 5
 DEEP WATER HABITATS 9
 SHALLOW WATER HABITATS 16
2. SPATIAL CHARACTERISTICS OF BENTHIC HABITATS 42
 SPATIAL PATTERN ANALYSIS USING FRAGSTATS 42
 SPLIT INTO TWO CATEGORIES: SHALLOW WATER AND DEEP WATER HABITATS 44
 DEEP WATER HABITATS LANDSCAPE 45
 SHALLOW WATER HABITATS LANDSCAPE 46
 REGIONAL LANDSCAPE DIFFERENCES 49
3. LOCATING FISH HABITATS AND DEFINING KEY HABITAT FEATURES 51
 MATERIALS AND METHODS 51
4. STRIPED WOLFFISH 69
 AREA OF OCCUPANCY 69
 PATTERNS AND CLUSTERS OF DISTRIBUTION 70
 HABITAT RELATIONSHIPS 72
 ENVIRONMENTAL RELATIONSHIPS 81
5. SPOTTED WOLFFISH 88
 AREA OF OCCUPANCY 88
 PATTERNS AND CLUSTERS OF DISTRIBUTION 89
 HABITAT RELATIONSHIPS 90
 ENVIRONMENTAL RELATIONSHIPS 98
6. NORTHERN WOLFFISH 106
 AREA OF OCCUPANCY 106
 PATTERNS AND CLUSTERS OF DISTRIBUTION 107
 HABITAT RELATIONSHIPS 108
 ENVIRONMENTAL RELATIONSHIPS 115
7. COMPARING WOLFFISH HABITATS 122
 CLUSTER ANALYSIS 124
 REDUNDANCY ANALYSIS 126
 MULTIVARIATE REGRESSION TREE 130
8. AMERICAN PLAICE 134
 AREA OF OCCUPANCY 136
 PATTERNS AND CLUSTERS OF DISTRIBUTION 141
 HABITAT RELATIONSHIPS BY PERIOD AND SIZE CATEGORY 178
 ENVIRONMENTAL RELATIONSHIPS 230
 REDUNDANCY ANALYSIS 276
 MULTIVARIATE REGRESSION TREE 281

9. MULTIVARIATE TREE ANALYSIS OF FISH SPECIES ASSEMBLAGES 284
MATERIALS AND METHODS 284
CAPTURES AND SPECIES RICHNESS 288
MULTIVARIATE REGRESSION TREE 292
CONCLUSION 327
ACKNOWLEDGMENTS 328
REFERENCES 329
APPENDICES 331
APPENDIX 1. SUMMARY STATISTICS FOR DESCRIPTORS USED IN CLUSTER ANALYSIS OF SEAFLOOR HABITATS 332
APPENDIX 2. MEGAHABITAT FLOWCHARTS 334
APPENDIX 3. DESCRIPTION OF VARIABLES FROM GEOSPATIAL ANALYSIS 338
APPENDIX 4. ENVIRONMENTAL VARIABLES RETAINED FOR MULTIVARIATE REGRESSION TREE ANALYSIS 339
APPENDIX 5. TAXA CAUGHT DURING THE BOTTOM TRAWL SURVEYS 340
APPENDIX 6. TAXA CAUGHT OCCASIONALLY AND NOT CONSIDERED FOR ANALYSIS 343
APPENDIX 7. LIST OF TRAWL SURVEY VARIABLES 345
APPENDIX 8. SUMMARY OF INDICATOR SPECIES ASSOCIATED WITH TERMINAL GROUPS OF CELLS 346
APPENDIX 9. INTRAGROUP CONCORDANCE (KENDALL'S COEFFICIENT) 348

ABSTRACT

Dutil, J.-D., S. Proulx, P.-M. Chouinard, D. Borcard, C. Laurian, H. Tamdrari, and C. Nozères 2013. A standardized database to describe and classify offshore benthic marine habitats and its use for designating the critical habitat of species at risk. Can. Manuscr. Rep. Fish. Aquat. Sci. 3014: vi+347 pp.

This report includes the material presented at a workshop organized by the Species at Risk Program Management and held from 20 to 22 March 2012 in Ottawa (day 3 of the workshop). A standardized methodology was proposed to describe the critical habitat of species at risk when using data available from annual research surveys conducted to assess the relative abundance of groundfish. The method uses a single spatial reference system made of 100 km^2 cells to gather data on species and habitats. The classification of benthic habitats has been described previously; here, it was sought to fully describe the characteristics of each of these habitats and to analyze the spatial fragmentation. Wolffish habitats are described using presence/absence data (relative occurrence), while those of the American plaice are described from data on relative occurrence and abundance as well as for two size classes and three periods. Statistical analysis was used to examine the relationship of these species with their environment and to identify habitats that seem to be the most important for stages vulnerable to trawling. The data on other fish species are used as biological descriptors pointing to potential interspecific relationships within assemblages. Although there were differences in habitat classification when using physical descriptors only as compared to both physical and biological descriptors, there were still many points in common between the two classifications. Spatial analysis has, in turn, highlighted the hot spots of distribution and biodiversity, thus revealing the spatial context in which interspecific relationships are likely to take place. The proposed method can be useful for studying the risks associated with human activities as long as the spatial distribution of the considered factor (fishing effort, contaminant dispersion, location of drill sites) is known.

RÉSUMÉ

Dutil, J.-D., S. Proulx, P.-M. Chouinard, D. Borcard, C. Laurian, H. Tamdrari, and C. Nozères 2013. A standardized database to describe and classify offshore benthic marine habitats and its use for designating the critical habitat of species at risk. Can. Manuscr. Rep. Fish. Aquat. Sci. 3014: vi+347 pp.

Voici un compte-rendu de présentations faites au 3e jour d'un atelier organisé par les gestionnaires du programme des espèces en péril et tenu à Ottawa du 20 au 22 mars 2012. Nous avons proposé une approche standardisée pour décrire l'habitat essentiel des espèces en péril lorsque les données disponibles proviennent des relevés annuels de l'abondance du poisson de fond. La méthode consiste à utiliser un même système de référence spatiale unique (grille de cellules de 100 km^2) pour colliger les données sur les espèces et sur les habitats. La classification des habitats benthiques a été décrite précédemment, mais on a cherché à mieux décrire les caractéristiques de chacun de ces habitats et à en analyser la fragmentation spatiale. L'habitat du loup est décrit à partir des données de présence/absence (occurrence relative), alors que celui de la plie canadienne est décrit à partir des données d'occurrence relative et d'abondance, et ce pour deux classes de taille et trois périodes. L'analyse statistique a permis d'examiner les relations de ces espèces avec leur environnement et d'identifier les habitats qui semblent les plus importants pour les stades vulnérables au chalut. Les liens potentiels entre les espèces en péril et les autres espèces formant les communautés ont été évalués à partir des données d'abondance des autres espèces de poissons inventoriés lors des relevés. Bien qu'il existe des différences dans la classification des habitats selon que l'on tienne compte des seuls descripteurs physiques ou à la fois des descripteurs physiques et biologiques, on note tout de même de nombreux points en commun entre les deux classifications. L'analyse spatiale a quant à elle mis en évidence les hauts lieux de distribution et de biodiversité révélant ainsi le cadre spatial dans lequel les relations interspécifiques sont susceptibles de s'exercer. La méthode proposée peut s'avérer utile pour étudier les risques associés aux activités humaines pour peu que la distribution spatiale du facteur considéré (effort de pêche, dispersion des contaminants, localisation de sites de forage) soit connue.

PREFACE

In March 2012, the Species at Risk (SAR) Program Management held a Species at Risk Modelling Workshop in Ottawa. The purpose was to familiarize Species at Risk practitioners with different models that will help them identify critical habitat. One of the models was presented by Jean-Denis Dutil, Serge Proulx, and Pierre-Marc Chouinard, under the title:

SAR Critical Habit Methodology - A standardized database to describe and classify offshore benthic marine habitats and its use for designating the critical habitat of species at risk.

This presentation focussed on habitat classification and species–habitat relationships, looking specifically at occurrence/abundance data obtained from routine bottom trawl research surveys. This workshop presentation gave an overview of the approach along with practical examples with species at risk. A summary was prepared and materials were made available for workshop attendees. To enable public access to the materials, this work is compiled here as a manuscript report.

INTRODUCTION

By the Species at Risk Act (SARA), the Canadian government has pledged to halt the decline and prevent the extinction of species in Canada. To promote the recovery of species at risk, government agencies must protect their habitats. This requires that the habitats be identified and described, and that a link be established between the distribution of these species and habitats. For offshore marine areas, this poses a challenge since the observations are dispersed and generally indirect, and data on habitats and species are usually collected independently. Recent reports on coastal and epipelagic habitats (Dutil et al. 2012) and benthic habitats (Dutil et al. 2011) have proposed a classification scheme at the scale of the megahabitat. The 2011 report examined the topographic and oceanographic features of cells each representing a planimetric area of 100 km^2. We have used the same spatial reference system (grid) to report the catch data obtained from routine bottom trawl research surveys and to identify areas of occupancy and areas of concentration as well as the habitat characteristics of those areas for three species of the genus *Anarhichas* and the American plaice (*Hippoglossoides platessoides*). The striped wolffish (*A. lupus*), also known as the common or Atlantic wolffish, is a species listed as of *special concern* in Canada, whereas both the spotted (*A. minor*) and northern (*A. denticulatus)* wolffish are considered as being *threatened*. Wolffish occur locally in the study area, and the analyses were conducted on the basis of their relative occurrence (presence/absence). The American plaice is a more widely distributed benthic species. The catch in number statistics are reliable, allowing a comparison of the outcome of analyses based on relative occurrence and relative abundance. The American plaice is not currently listed under SARA.

The presentation at the workshop was prepared as blocks of information, each with a summary of the methods followed by results presented as a series of tables of statistical analyses. Multivariate statistical methods produced figures shown here as cluster dendrograms, ordination graphs, and partitioning trees. Map figures were also generated to display the results of the statistical groupings and modelling. This report is organized similarly. The different sections showcase the examples and analyses for different aspects of the species–habitat approach. It begins with an extensive description of benthic habitats (section 1), followed by a summary of their spatial characteristics (section 2). The methodology for an exercise at defining key habitat features is given in section 3. The results for this exercise are then presented for the selected species, with wolffish habitats examined by individual species (sections 4–6) and in comparisons for all three species (relative occurrence data; section 7). The exercise continues in section 8 with American plaice, including more detailed analyses and comparing the relative occurrence and relative abundance data. The final section (section 9) is a follow-up to work described by Chouinard and Dutil (2011), presenting an ecosystem classification that integrates both environmental and biological features in an effort to produce advice that includes species assemblages.

The purpose of the report is to propose a set of tools to improve our capacity to inform decision makers concerning such items as the diversity and characteristics of benthic habitats, the relative importance of different habitats for a given species, and the potential species interactions and species habitat relationships that might be worth exploring. It is hoped that by making available the material presented at the workshop, this approach can be applied to other species in the St. Lawrence and extended to similar matters in other areas.

1. DESCRIPTION OF BENTHIC HABITATS

The first portion of the presentation focussed on the benthic habitat classification proposed by Dutil et al. (2011). Of note, while several descriptors of the physical and oceanographic features were available on which to base the classification, the scale of measurement varied considerably. Although the size of a unit cell used to obtain a classification is large (100 km^2), there were over 2000 cells to describe, with many cells having few observations for many of the features. Whereas the purpose of the report by Dutil et al. (2011) was to create a database of environmental descriptors, it fell short of fully describing the habitats obtained through classification. This section presents a cluster analysis of cells based on the environmental descriptors. Starting with all cells, successive splits resulted in clusters that emphasize the similarities between cells within a group and dissimilarities among groups. The input variables for cluster analysis are listed in Appendix 1, with a summary of habitat area classification presented as flowcharts in Appendix 2. The areas mentioned in this report are shown in Figure 1.

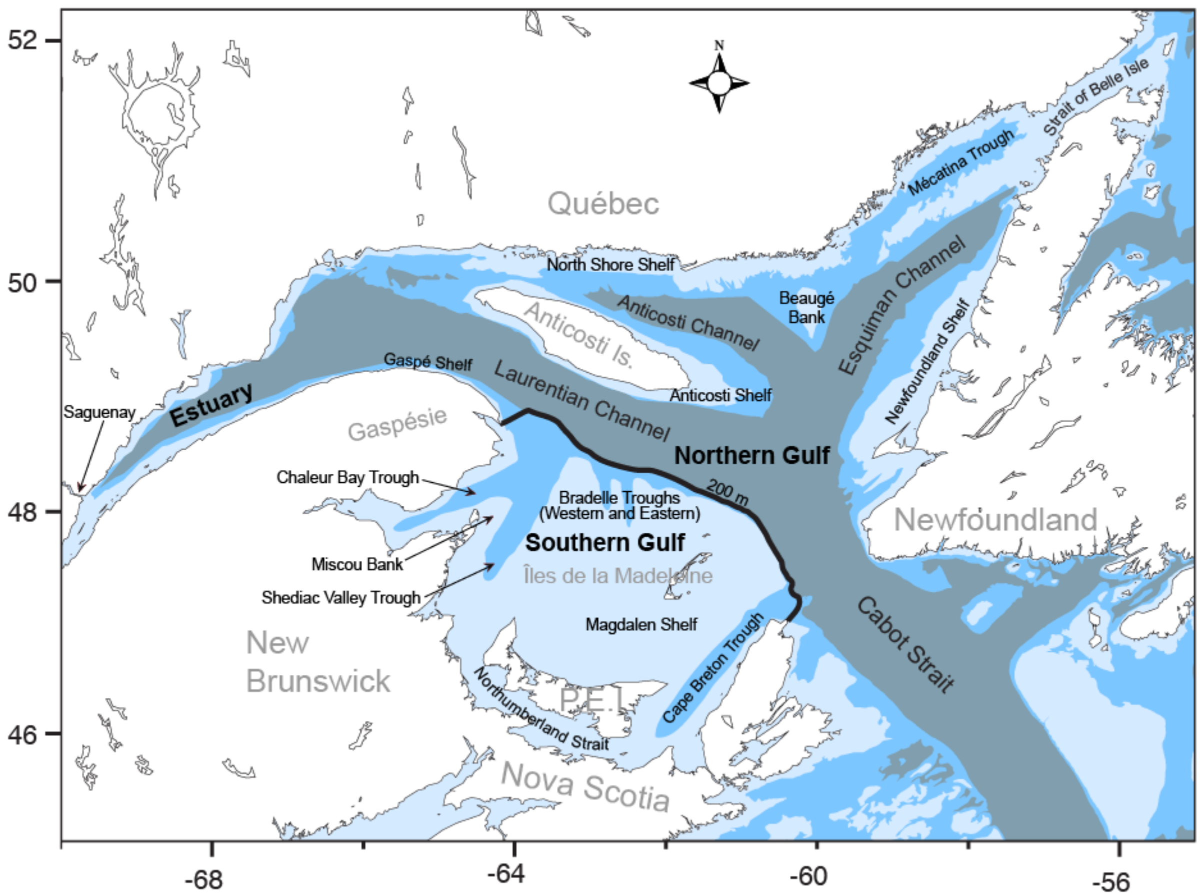

Figure 1. Undersea features of the Gulf of St. Lawrence. Depth >200 m: Laurentian Channel, Anticosti Channel, Esquiman Channel. Depth <200 m: Gaspe Shelf, North Shore Shelf, Anticosti Shelf, Beaugé Bank, Newfoundland Shelf, Magdalen Shelf, Miscou Bank, Mécatina Trough, Chaleur Bay Trough, Shediac Valley Trough, Cape Breton Trough, Bradelle Troughs. The northern region is separated from the southern Gulf by the 200 m isobath (black line). The southern features are drawn approximately.

Habitats as obtained by cluster analysis

The study area (St. Lawrence estuary and northern Gulf) was divided using a grid made of 2810 cells, each cell representing a square area of 100 km^2 (10 × 10 km). Classes of benthic megahabitats were obtained by a cluster analysis of cells based on nine descriptors. Four of those were obtained through four separate principal component analyses (PCA): depth (four variables), slope (four variables), salinity (nine variables), and temperature (nine variables). PCA scores for each cell were submitted to a cluster analysis. The resulting groups were used as four descriptors. Three descriptors were categorical (nominal) variables: proximity to the shoreline and two descriptors of landscape. Two others were categorical (ordinal) variables (dissolved oxygen and sediments). The methodology is described in Dutil et al. 2011.

Statistical analyses (SIMPROF test) classified the seafloor into significantly different clusters that were called *megahabitats* (Figure 2). Whereas 13 clusters were described and discussed in Dutil et al. 2011, significant clusters were also formed at higher similarity values. Megahabitat M, for instance, could have been split into three megahabitats (Figure 3).

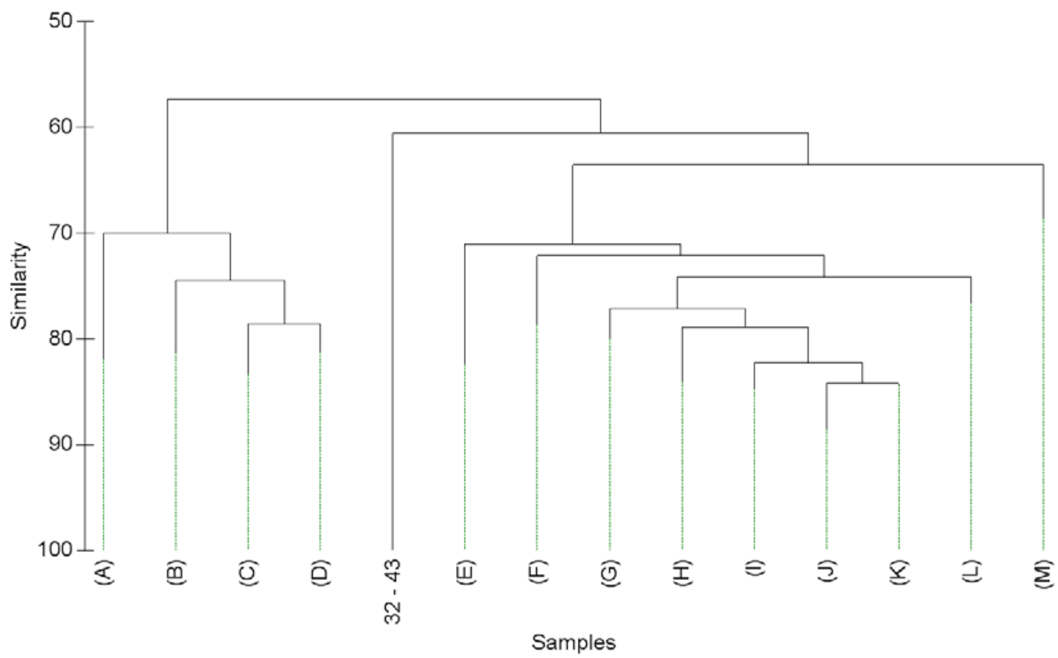

Figure 2. Group-average cluster analysis of a spatial grid based on nine habitat descriptors using the Gower similarity distance.

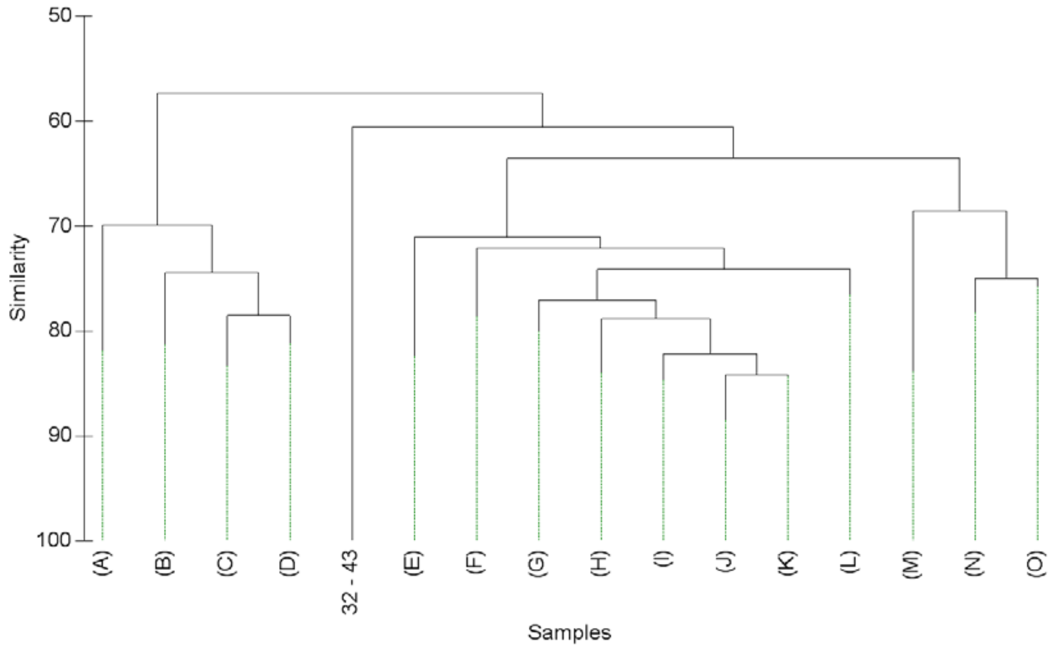

Figure 3. Cluster analysis performed at a higher similarity level with megahabitat M split into three clusters.

The earlier report (Dutil et al. 2011) fell short of explaining how the cells clustered at lower similarity values. The present document examines the coarse-level structure in the habitat data, starting with the two most dissimilar groups of cells, in an effort to better show dissimilarities between the megahabitats. Within-cluster similarity was high and ranged from 81 to 92% (Table 1). In addition to the detailed descriptions, each subsection below includes a closing summary statement.

Table 1. Within-cluster similarity for 15 megahabitats.

Habitat	Similarity (%)
A	91.61
B	85.95
C	87.60
D	86.36
E	92.22
F	83.09
G	87.35
H	88.59
I	88.14
J	90.70
K	89.05
L	82.63
M	81.82
N	83.38
O	81.82

Split into two categories: shallow water and deep water habitats

Two groups were formed at a similarity value of 57.35, with megahabitats A, B, C, and D forming one cluster (*a*) and the other megahabitats forming a second cluster (*b*). Cluster *a* included the Esquiman, Anticosti, and Laurentian channels as well as the Mecatina Trough (blue area; Figure 4).

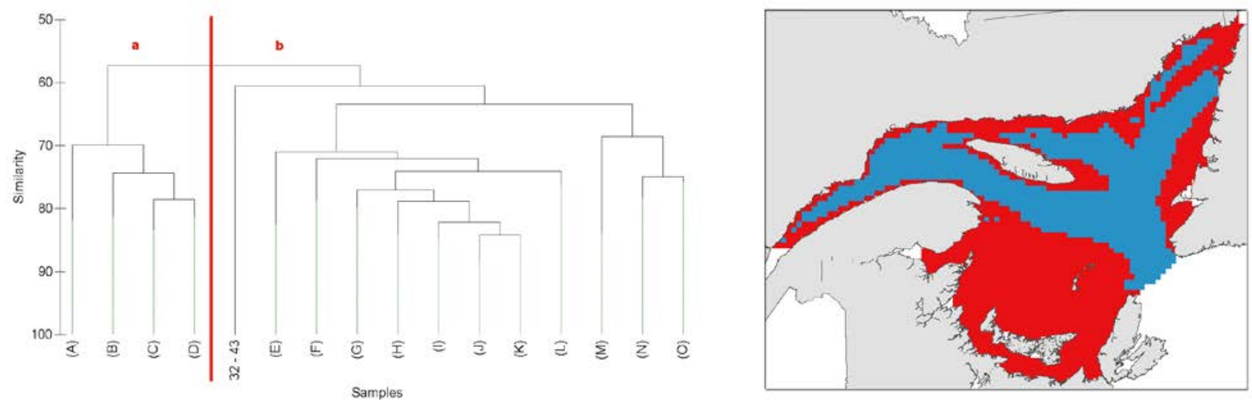

Figure 4. Cluster analysis with first level split at 57.35 similarity level (left) and map (right) of cells split into cluster *a* with blue area and cluster *b* with red area.

There were significant differences in depth distribution (i.e., frequency distribution of cells across groups defined by PCA, and based on mean, minimum, maximum, and standard deviation values calculated from 400 depth observations for each cell) between cells of the two clusters, with cells of cluster *a* falling into depth categories 3 to 5 and cells of cluster *b* falling into depth categories 1 to 3 (Table 2). Depth categories are described in Appendix 1.

Table 2. Statistical test and frequency distribution of cells for clusters *a* and *b* on the descriptor of depth.

Test statistic	Value	df	Prob
Pearson Chi-square	1777.101	4	<0.001

Gr_Bathy no.	Column no.					
Line no.	1	2	3	4	5	Gen. Total
Cluster *a*	0	4	303	196	457	960
Cluster *b*	534	631	307	0	0	1472
Gen. Total	534	635	610	196	457	2432

Thus, cluster *a* cells were in deep water (depth of 274 m on average) whereas cluster *b* cells were in shallow water (depth of 61 m on average). The two clusters overlapped the Cold Intermediate Layer (CIL, 80–270 m). There were also significant differences in salinity and temperature between cells of the two clusters, with cells of cluster *a* falling into salinity and temperature categories 2 and 3, and cells of cluster *b* falling into other categories (Table 3). Average salinity and temperature in cluster *a* cells were greater on average (salinity 34.3 and 4.31°C) than in cells of cluster *b* (salinity 31.5 and 1.99°C) at mean depth.

Table 3. Statistical tests and frequency distributions of cells for clusters *a* and *b* on the descriptors of salinity and temperature.

Salinity

Test statistic	Value	df	Prob
Pearson Chi-square	2265.739	6	<0.001

Gr_S	Column no.							
Line no.	1	2	3	4	5	6	7	Gen. Total
Cluster *a*	0	592	344	0	19	4	1	960
Cluster *b*	293	0	18	291	250	502	118	1472
Gen. Total	293	592	362	291	269	506	119	2432

Temperature

Test statistic	Value	df	Prob
Pearson Chi-square	2209.469	5	<0.001

Gr_T	Column no.						
Line no.	1	2	3	4	5	6	Gen. Total
Cluster *a*	0	592	352	14	2	0	960
Cluster *b*	271	0	42	573	181	405	1472
Gen. Total	271	592	294	587	183	405	2432

There were differences in the distribution of cells among the slope categories (groups defined by PCA based on mean, minimum, maximum, and standard deviation values derived from 400 depth observations in each cell), but only slight differences were observed in mean slope with cluster *b* cells having greater maximum slopes (Table 4).

Table 4. Statistical test and frequency distribution of cells for clusters *a* and *b* on the descriptor of slope.

Test statistic	Value	df	Prob
Pearson Chi-square	133.139	6	<0.001

Gr_Pente	Column no.							
Line no.	1	2	3	4	5	6	7	Gen. Total
Cluster (a)	296	142	211	150	77	76	8	960
Cluster (b)	375	474	174	147	137	148	17	1472
Gen. Total	671	616	385	297	214	224	25	2432

The majority of cluster *a* cells (68%) were classified as channels (< 0.1% for cluster *b* cells) and 19% as shelves (88% for cluster *b* cells); a similar proportion of cells were classified as slopes in both clusters (12%) (Table 5). Both groups were largely dominated by uniform terrain (Geomorph_2). Cells dominated by humps and pits (Geomorph_2) and classified as coastal cells (Geomorph_3), occurred primarily in cluster *b*.

Table 5. Statistical tests and frequency distributions for clusters *a* and *b* on the descriptors of terrain (Geomorph_1), terrain uniformity (Geomorph_2), and coastal forms (Geomorph_3).

Geomorph_1

Test statistic	Value	df	Prob
Pearson Chi-square	1459.382	2	<0.001

Gr_Geomorph_1	Column no.			
Line no.	1	2	3	Gen. Total
Cluster *a*	187	113	660	960
Cluster *b*	1301	170	1	1472
Gen. Total	1488	283	661	2432

Geomorph_2

Test statistic	Value	df	Prob
Pearson Chi-square	55.050	2	<0.001

Gr_Geomorph_2	Column no.			
Line no.	1	2	3	Gen. Total
Cluster *a*	958	2	0	960
Cluster *b*	1383	64	25	1472
Gen. Total	2341	66	25	2432

Geomorph_3

Test statistic	Value	df	Prob
Pearson Chi-square	369.433	1	<0.001

Gr_Geomorph_3	Column no.		
Line no.	0	1	Gen. Total
Cluster *a*	946	14	960
Cluster *b*	971	501	1472
Gen. Total	1917	515	2432

Cluster *a* cells were mainly hypoxic (46% dissolved oxygen saturation on average), whereas cluster *b* cells were not (83% dissolved oxygen saturation on average) (Table 6).

Table 6. Statistical test and frequency distribution of cells for clusters *a* and *b* on the descriptor of dissolved oxygen.

Test statistic	Value	df	Prob
Pearson Chi-square	1548.048	7	<0.001

Classe_oxygene	Column no.								
Line no.	1	2	3	4	5	6	7	8	Gen. Total
Cluster *a*	72	153	267	283	113	30	10	32	960
Cluster *b*	4	21	30	50	99	216	308	744	1472
Gen. Total	76	174	297	333	212	246	318	776	2432

They were also characterized by having very fine sediments (pelite series 110-120-130) in contrast to cluster *b* cells, which ranged mainly from sand to gravel (210-310-410). Where rock was present, it was associated with pelite for cluster *a* cells (512) and with sand and gravel for cluster *b* cells (530-540) (Table 7).

Table 7. Statistical test and frequency distribution of cells for clusters *a* and *b* on the descriptor of sediments.

Test statistic	Value	df	Prob
Pearson Chi-square	1363.314	8	<0.001

Classe_Sediment	Column no.									
Line no.	110	120	130	210	310	410	512	530	540	Gen. Total
Cluster *a*	386	232	142	23	33	0	131	11	2	960
Cluster *b*	6	88	112	210	414	104	108	252	178	1472
Gen. Total	392	320	254	233	447	104	239	263	180	2432

Overall, cluster *a* cells were located deeper, had higher salinities, experienced less extreme temperatures, and lower levels of dissolved oxygen saturation than cluster *b* cells. Cluster *a* cells occupied slopes and deep channels (rarely shelves) whereas cluster *b* cells occupied shelves and slopes (never channels). Cluster *b* cells occasionally had a rough seafloor always covered with coarser sediments than cluster *a* cells. The southern Gulf fits entirely in the shallow water category whereas in the northern Gulf both shallow and deep water areas are well represented. The cluster *a* cells are referred to as the *deep water habitats* and cluster *b* cells as the *shallow water habitats*.

Deep water habitats

<u>Subdivision of the deep water habitats: deep channels (megahabitat A) and shelves and slopes below the CIL (megahabitats B, C, D).</u>

Cluster *a* cells formed two groups at a similarity value of 69.96, megahabitat A forming one cluster *aa* and the other megahabitats forming a second cluster *ab* (Figure 5).

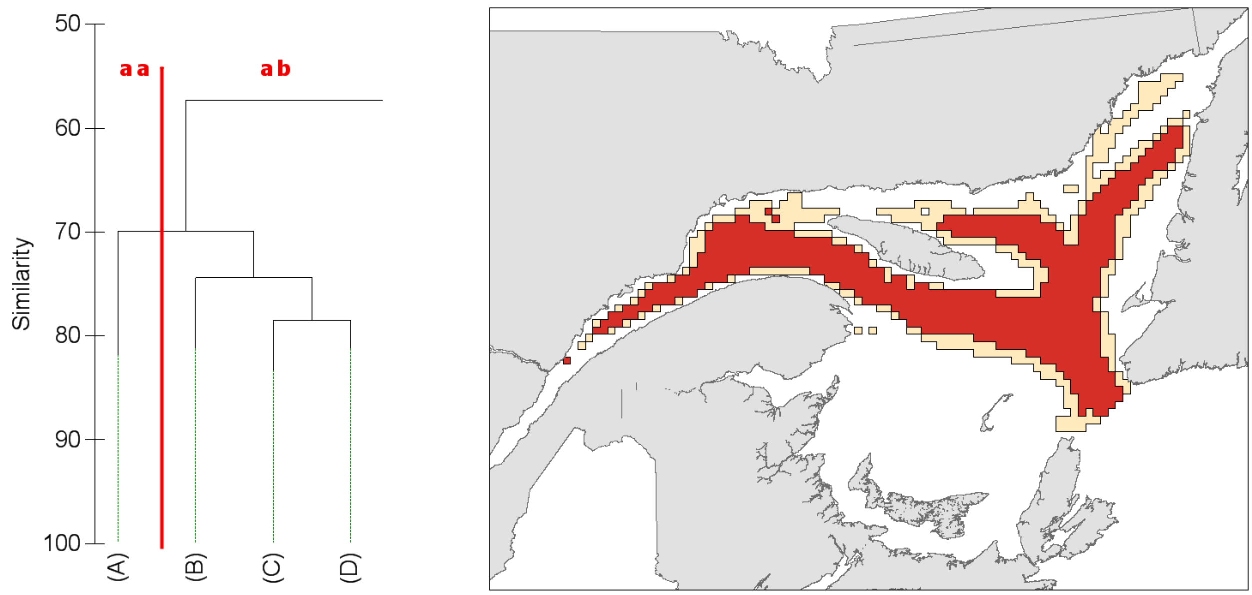

Figure 5. Splitting of cluster *a* into groups cluster *aa* and *ab*, shown as a dendrogram (left) and a map of grid cells (right) with cluster *aa* in red (megahabitat A) and *ab* in beige (megahabitats B-C-D).

There were significant differences in depth between cells of the two clusters, with cells of cluster *aa* falling into depth categories 4 and 5 and cells of cluster *ab* falling into depth category 3 (Table 8).

Table 8. Statistical tests for clusters *aa* and *ab* on the descriptor of depth (Gr_Bathy).

Test statistic	Value	df	Prob
Pearson Chi-square	811.964	2	<0.001

The Chi-square test was performed including Gr_Bathy 3, 4, 5 only to avoid too many fitted cells being sparse (calculated frequency < 5).

Gr_Bathy	Column no.				
Line no.	2	3	4	5	Gen. Total
Cluster *aa*	0	2	195	425	622
Cluster *ab*	4	301	1	32	338
Gen. Total	4	303	196	457	960

The depth of cluster *aa* cells was 324 m on average (mean minimum depth 288 m) compared to 182 m on average for cluster *ab* cells (mean maximum depth 243 m). There were also significant differences in salinity and temperature between cells of the two clusters, with cells of cluster *aa* falling into salinity and temperature category 2: highly saline waters (mean, minimum, and maximum salinity > 34 at mean, minimum, and maximum depths) and a very narrow range of mean, minimum, and maximum temperatures at mean, minimum, and maximum depths (4.2 to 5.4°C). Cells of cluster *ab* had lower salinities and lower temperatures, except at maximum depth: mean and minimum salinity (temperature in parentheses) at minimum depth averaged 32.5 (0.4°C) and 32.8 (1.2°C), respectively, and mean and minimum salinity (temperature) at mean depth averaged 33.5 (2.5°C) and 33.7 (3.2°C) (Table 9).

Table 9. Statistical tests and frequency distributions of cells for clusters *aa* and *ab* on the descriptors of salinity and temperature.

Salinity

Test statistic	Value	df	Prob
Pearson Chi-square	733.336	1	<0.001

Gr_S	Column no.					
Line no.	2	3	5	6	7	Gen. Tot.
Cluster *aa*	582	40	0	0	0	622
Cluster *ab*	10	304	19	4	1	338
Gen. Tot.	592	344	19	4	1	960

Temperature

Test statistic	Value	df	Prob
Pearson Chi-square	742.508	1	<0.001

Gr_T	Column no.				
Line no.	2	3	4	5	Gen. Tot.
Cluster *aa*	582	40	0	0	622
Cluster *ab*	10	312	14	2	338
Gen. Tot.	592	352	14	2	960

Cells of the two clusters also differed in slope, with cells of cluster *ab* having steeper slopes (mean and maximum 0.7 and 2.3°) than cells of cluster *aa* (0.3 and 0.9°) on average (Table 10).

Table 10. Statistical test and frequency distribution of cells for clusters *aa* and *ab* on the descriptor of slope.

Test statistic	Value	df	Prob
Pearson Chi-square	366.10	6	<0.001

Gr_Pente	Column no.							
Line no.	1	2	3	4	5	6	7	Gen. Tot.
Cluster *aa*	263	141	132	62	11	9	4	622
Cluster *ab*	33	1	79	88	66	67	4	338
Gen. Tot.	296	142	211	150	77	76	8	960

All cluster *aa* cells classified as channels whereas cluster *ab* cells classified in all three categories: shelf (55%), slope (33%), and channel (11%). In both *aa* and *ab* cells, terrain was rather uniform and cells were located away from the coastline; Chi-square tests were not performed due to many fitted cells being sparse (calculated frequency < 5) (Table 11).

Table 11. Statistical tests and frequency distributions of cells for clusters *aa* and *ab* on the descriptors of terrain (Geomorph_1), terrain uniformity (Geomorph_2), and coastal forms (Geomorph_3).

Geomorph_1

Test statistic	Value	df	Prob
Pearson Chi-square	803.02	2	<0.001

Geomorph_1	Column no.			
Line no.	1	2	3	Gen. Tot.
Cluster *aa*	0	0	622	622
Cluster *ab*	187	113	38	338
Gen. Tot.	187	113	660	960

Geomorph_2

Geomorph_2	Column no.		
Line no.	1	2	Gen. Tot.
Cluster *aa*	622	0	622
Cluster *ab*	336	2	338
Gen. Tot.	958	2	960

no observation in group 3

Geomorph_3

Geomorph_3	Column no.		
Line no.	0	1	Gen. Tot.
Cluster *aa*	621	1	622
Cluster *ab*	325	13	338
Gen. Tot.	946	14	960

Cluster *aa* cells were hypoxic and were covered with fine surface sediments (dominated by pelites and sandy pelites) whereas cluster *ab* cells were less hypoxic with a wider range of dissolved oxygen values and a greater diversity of sediment types (Table 12).

Table 12. Statistical tests and frequency distributions of cells for clusters *aa* and *ab* on the descriptors of dissolved oxygen and sediments.

Dissolved oxygen

Test statistic	Value	df	Prob
Pearson Chi-square	233.763	7	<0.001

Classe_oxygene	Column no.								
Line no.	1	2	3	4	5	6	7	8	Gen. Tot.
Cluster *aa*	69	125	209	173	46	0	0	0	622
Cluster *ab*	3	28	58	110	67	30	10	32	338
Gen. Tot.	72	153	267	283	113	30	10	32	960

Sediments

Test statistic	Value	df	Prob
Pearson Chi-square	336.505	7	<0.001

Classe_Sed2	Column no.								
Line no.	110	120	130	210	310	512	530	540	Gen. Tot.
Cluster *aa*	356	157	39	0	2	67	1	0	622
Cluster *ab*	30	75	103	23	31	64	10	2	338
Gen. Tot.	386	232	142	23	33	131	11	2	960

Thus the seafloor of deep channels of the St. Lawrence makes up a very homogeneous habitat (megahabitat A) characterized by having the highest salinity, lowest dissolved oxygen saturation, a narrow range of intermediate temperatures, very low slopes, and a uniform terrain covered with very fine sediments. There is more variability in the second cluster, which generally corresponds to the zone above deep channels and adjacent to the lower portion of the cold intermediate layer (megahabitats B, C, D). Megahabitat A is referred to as the *deep channel megahabitat*.

Deep water shelves (megahabitat C), slopes (megahabitat D), and steep-sloped (megahabitat B) megahabitats

Only 14 cells were classified as belonging to megahabitat B, with most being located at the entrance of Cabot Strait at the southwest tip of Newfoundland (Figure 6).

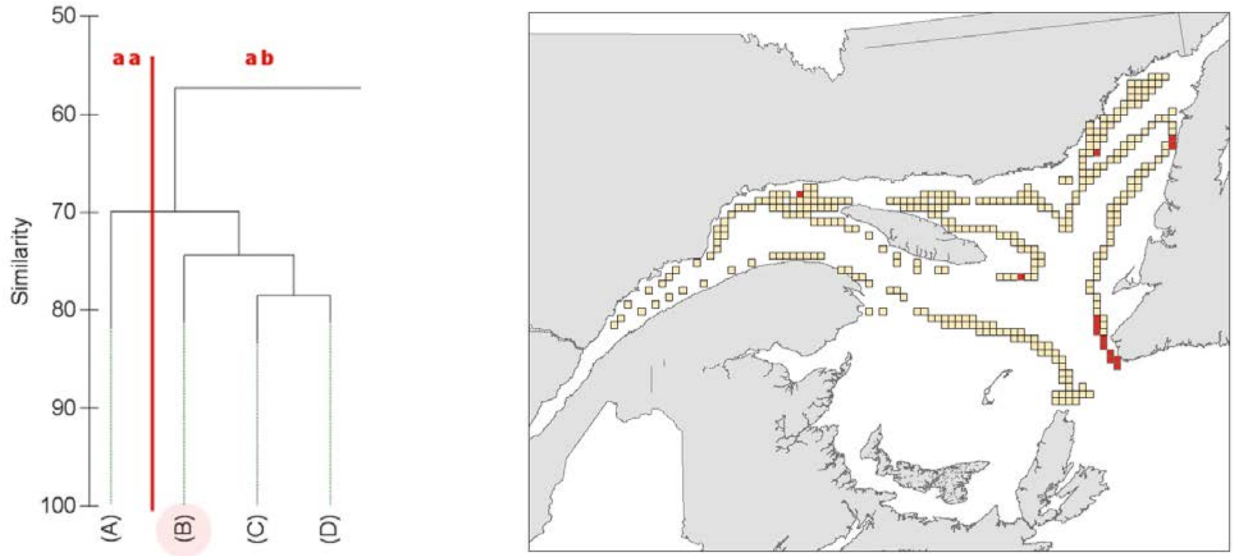

Figure 6. Dendogram (left) highlighting megahabitat B and a map of grid cells (right; red = B, beige = C, D).

These cells all classified as slopes. Minimum slope was steeper on average in megahabitat B (0.19° compared to 0.08° in megahabitats C and D), minimum dissolved oxygen saturation was above 55% (24% in megahabitats C and D), and surface sediments were always coarse (coarse sands to sandy gravel). This narrow combination of characteristics was unique within the *ab* cell clusters, but no single characteristic was unique to that megahabitat, which can referred to as the *deep water steep-sloped megahabitat*. Megahabitats C and D, in contrast, both included a large number of cells (Figure 7).

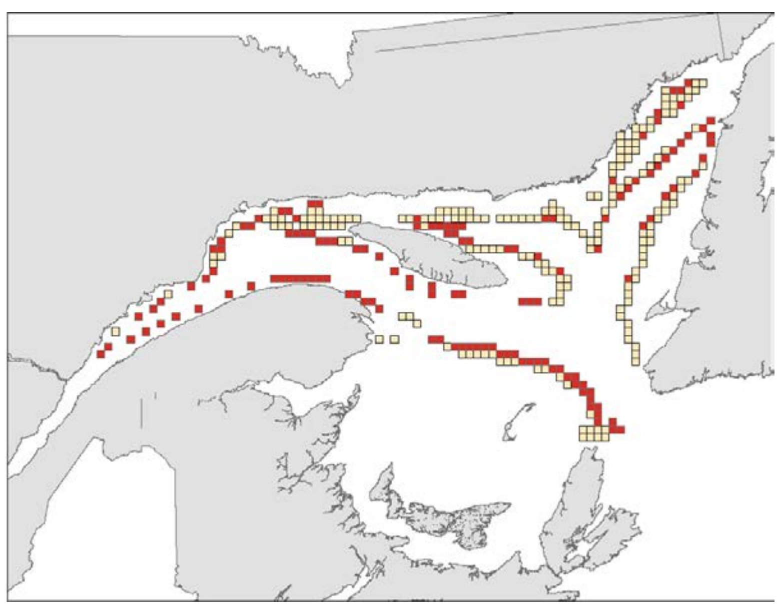

Figure 7. Map of grid cells for megahabitat groups C (beige) and D (red).

The variable *Geomorph_1* was the single most important criterion to separate megahabitats C and D, as all cells of megahabitat C classified as shelves (depths less than 200 m and slope less than 0.8), whereas cells of megahabitat D classified in the two other categories (Table 13).

Table 13. Frequency distributions of cells for megahabitat groups C and D on the descriptor of terrain (Geomorph_1).

Geomorph_1	Column no.			
Line no.	1	2	3	Gen. Tot.
Megahabitat C	187	0	0	187
Megahabitat D	0	98	38	136
Gen. Tot.	187	98	38	323

Megahabitat C is referred to as the *deep water shelf megahabitat* and megahabitat D as the *deep water slope megahabitat*. Megahabitats C and D cells appeared to be contiguous (Figure 8).

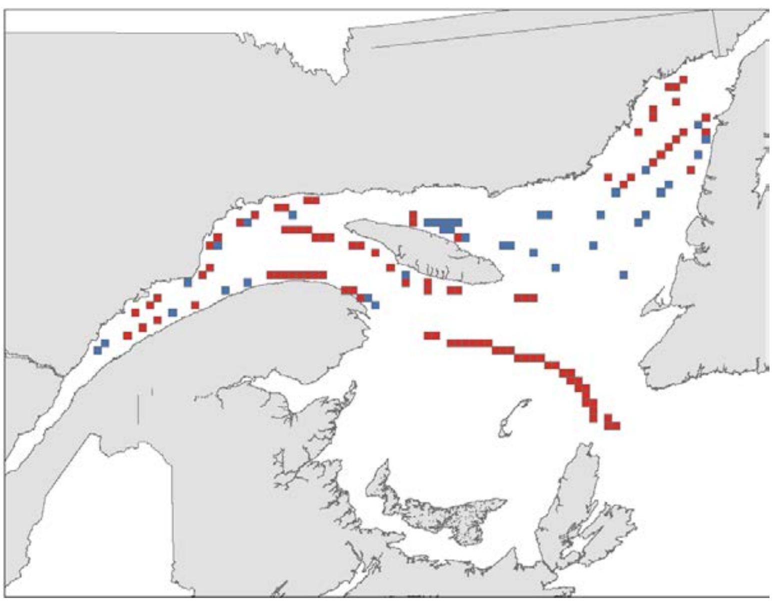

Figure 8. Map of grid cells for megahabitats C and D on Geomorph_1 classes (red = 2, blue = 3).

The deep water shelves of megahabitat C were shallower than the deep water slopes of megahabitat D (155 and 213 m on average, respectively), and thus exhibited a slightly lower salinity (33.5 and 34.0, respectively), lower temperature (2.6 and 4.0°C, respectively), and higher dissolved oxygen content (61 and 47%, respectively) at mean depth.

Within megahabitats C and D, dissolved oxygen varied with cells located in the Mecatina Trough, which had markedly higher dissolved oxygen saturation values (C: 91 vs. 55%; D: 93 vs. 45%; Figure 9). In Mecatina, mean bottom temperature in megahabitat D was also colder than elsewhere (2.4 vs. 4.0 on average at mean depth). The specific characteristics of megahabitats A to D are given in Dutil et al. (2011; Table 5).

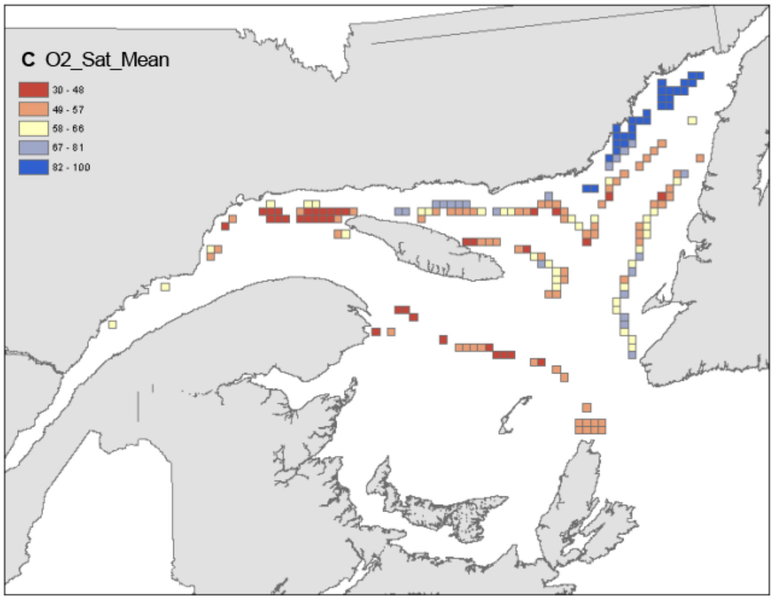

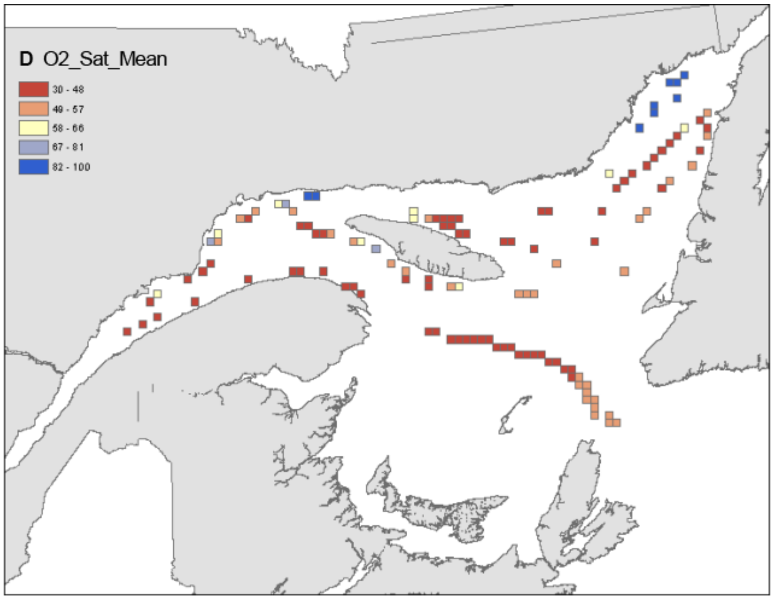

Figure 9. Map of oxygen saturation in grid cells of megahabitats C (above) and D (below).

Shallow water habitats

<u>Subdivision of the shallow water habitats: shallow water shelf habitats (megahabitats E–L) and shallow water slope habitats (megahabitats M–O)</u>

Within the shallow water cluster, two groups were formed at a similarity value of 63.54 (Figure 10). A single cell (cell 32–49) stemmed out at 60.59 but was ignored in further analyses as it represented a very small planimetric area in the nearshore zone. Cluster *bb* corresponds to megahabitat M in Dutil et al. (2011), but it will be dealt with as a cluster of 3 megahabitats (M, N, O) herein.

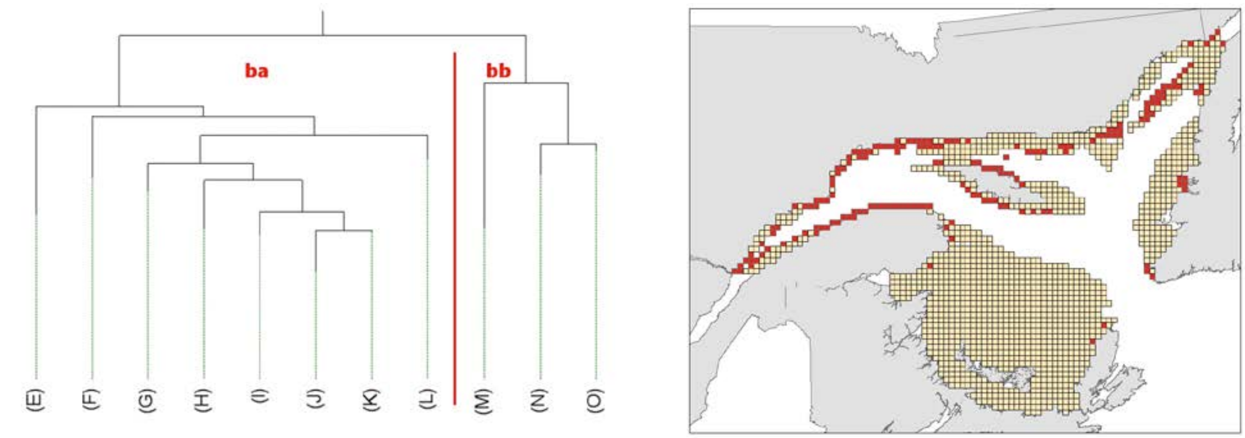

Figure 10. Splitting of cluster *b* into clusters *ba* (megahabitats E–L) and *bb* (megahabitats M–O) shown as a dendrogram (left) and a map (right) of grid cells (beige = *ba*, red = *bb*).

There were significant differences in depth between cells of the two clusters, with cells of cluster *ba* falling mainly into depth categories 1 and 2 and cells of cluster *bb* falling mainly into depth categories 2 and 3 (Table 14).

Table 14. Statistical test and frequency distribution of cells for clusters *ba* and *bb* on the descriptor of depth.

Test statistic	Value	df	Prob
Pearson Chi-square	178.325	2	<0.001

Gr_Bathy	Column no.			
Line no.	1	2	3	Gen. Tot.
Cluster *ba*	514	579	205	1298
Cluster *bb*	19	52	102	173
Gen. Tot.	533	631	307	1471

The depth of cluster *ba* cells was 56 m on average (mean minimum and maximum depths 37 and 78 m, respectively) compared to 94 m on average for cluster *bb* cells (mean minimum and maximum depth 17 and 178 m, respectively). There were also significant differences in salinity and temperature (Table 15).

Table 15. Statistical tests and frequency distribution of cells for clusters *ba* and *bb* on the descriptors of salinity and temperature.

Salinity

Test statistic	Value	df	Prob
Pearson Chi-square	417.168	5	<0.001

Gr_S	Column no.						
Line no.	1	3	4	5	6	7	Gen. Tot.
Cluster *ba*	292	6	291	197	464	48	1298
Cluster *bb*	0	12	0	53	38	70	173
Gen. Tot.	292	18	291	250	502	118	1471

Temperature

Test statistic	Value	df	Prob
Pearson Chi-square	232.464	4	<0.001

Gr_T	Column no.					
Line no.	1	3	4	5	6	Gen. Tot.
Cluster *ba*	271	18	551	158	300	1298
Cluster *bb*	0	24	22	22	105	173
Gen. Tot.	271	42	573	180	405	1471

Cluster *ba* and *bb* cells shared several salinity and temperature categories, but only cluster *ba* cells exhibited the lowest and relatively constant salinities (S_1 and S_4 categories) and the most variable temperatures (T_1 category), which are typical of surface waters (Table 16).

Table 16. Statistical test and frequency distribution of cells for clusters *ba* and *bb* on the descriptor of slope.

Test statistic	Value	df	Prob
Pearson Chi-square	732.053	6	<0.001

Gr_Pente	Column no.							
Line no.	1	2	3	4	5	6	7	Gen. Tot.
Cluster *ba*	375	474	173	139	82	52	3	1298
Cluster *bb*	0	0	0	8	55	96	14	173
Gen. Tot.	375	474	173	147	137	148	17	1471

Cluster *ba* cells had more gentle slopes than cluster *bb* cells and all classified as shelves (Geomorph_1 = 1), whereas nearly all cluster *d* cells classified as slopes (Geomorph_1 = 2). The frequency distribution of *ba* and *bb* cells across Geomorph_2 and Geomorph_3 classes varied significantly, with cluster *bb* having a much larger proportion of cells with humps and pits and located in the coastal zone (Table 17).

Table 17. Statistical tests and frequency distributions of cells for clusters *ba* and *bb* on the descriptors of terrain (Geomorph_1), terrain uniformity (Geomorph_2), and coastal forms (Geomorph_3).

Geomorph_1

Geomorph_1	Column no.			
Line no.	1	2	3	Gen. Tot.
Cluster *ba*	1298	0	0	1298
Cluster *bb*	3	169	1	173
Gen. Tot.	1301	169	1	1471

Chi-square tests were not performed due to many fitted cells being sparse (calculated frequency < 5).

Geomorph_2

Test statistic	Value	df	Prob
Pearson Chi-square	466.931	2	<0.001

Geomorph_2	Column no.			
Line no.	1	2	3	Gen. Tot.
Cluster *ba*	1283	15	0	1298
Cluster *bb*	100	48	25	173
Gen. Tot.	1383	63	25	1471

Geomorph_3

Test statistic	Value	df	Prob
Pearson Chi-square	57.030	1	<0.001

Geomorph_3	Column no.		
Line no.	1	2	Gen. Tot.
Cluster *ba*	901	397	1298
Cluster *bb*	70	103	173
Gen. Tot.	971	500	1471

A much larger proportion of cluster *ba* cells were classified as having high dissolved oxygen saturation values (Table 18).

Table 18. Statistical test and frequency distribution of cells for clusters *ba* and *bb* on the descriptor of dissolved oxygen.

Test statistic	Value	df	Prob
Pearson Chi-square	205.795	6	<0.001

The Chi-square test was performed excluding class 1 to avoid too many fitted cells being sparse (calculated frequency < 5).

Classe_oxygene	Column no.								
Line no.	1	2	3	4	5	6	7	8	Gen. Tot.
Cluster *ba*	0	5	17	27	77	198	274	700	1298
Cluster *bb*	4	16	13	22	22	18	34	44	173
Gen. Tot.	4	21	30	49	99	216	308	744	1471

There was no striking difference in sediment type between the two clusters. The Chi-square test was not performed due to many fitted cells being sparse (calculated frequency < 5) (Table 19).

Table 19. Frequency distribution of cells for clusters *ba* and *bb* on the descriptor of sediment.

Classe_Sed2	Column no.									
Line no.	110	120	130	210	310	410	512	530	540	Gen. Tot.
Cluster *ba*	5	71	76	210	341	103	97	229	166	1298
Cluster *bb*	1	17	36	0	72	1	11	23	12	173
Gen. Tot.	6	88	112	210	413	104	108	252	178	1471

Overall, the shallow water habitats were divided into shelves (characterized by gentle slopes, low salinity, highly variable temperatures, and high dissolved oxygen saturation values) or nearshore and offshore steep sloped areas (characterized by rough terrain). Deeper areas of the shelves and steep sloped areas overlapped in depth, salinity, and temperature characteristics and, in contrast to deep water habitats, included the CIL.

Shallow water slopes centered below the CIL (megahabitat M) and into the CIL (megahabitats N and O)

Within the shallow water slope cluster, two groups were formed at a similarity value of 68.57, one that included few cells (megahabitat M, nine cells) and the other that split at a similarity value of 75.02 (Figure 11).

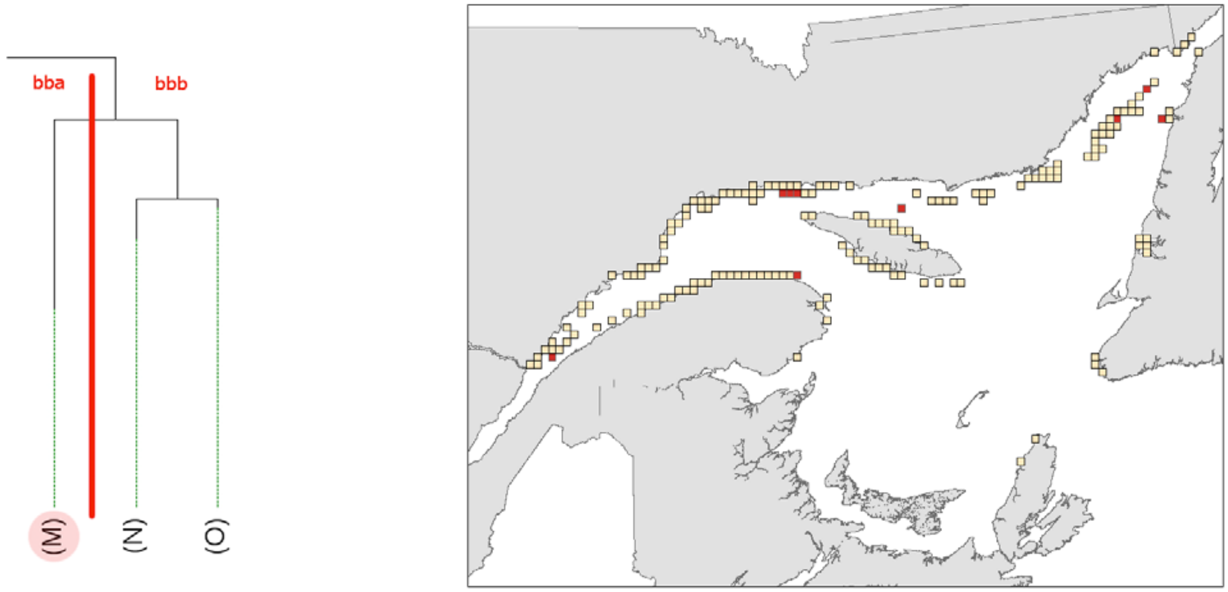

Figure 11. Splitting of cluster *bb* into clusters *bba* (megahabitat M) and *bbb* (megahabitats N, O), shown as a dendrogram highlighting M (left) and a map (right) of grid cells (red = *bba*, beige = *bbb*).

Megahabitat M (cluster *bba*) was made of shallow water slopes with pits and located deeper than other shallow water slopes. Depth was 149 m (mean value for nine cells); minimum and maximum depths were 54 and 237 m, respectively. Maximum temperature at minimum depth averaged 2.5°C (minimum temperature was -1.0°C on average). Maximum temperature at maximum depth averaged 5.0°C. However, mean temperature at mean depth averaged 2.3°C, indicating that megahabitat M was located immediately below the CIL and was not influenced by the surface layer.

Megahabitats N and O were quite similar and occupied the same portion of the study area (estuary and northern Gulf of St. Lawrence; Figure 12). However, they occupied different depths; cells of megahabitat N were distributed among three depth categories that were centered at 71 m, whereas megahabitat O occupied two depth categories and was centered at 100 m (Table 20).

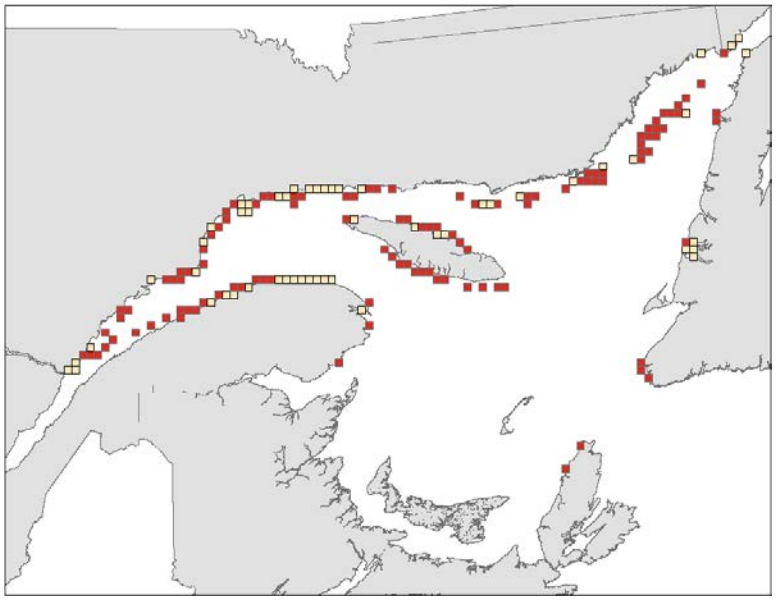

Figure 12. Map of grid cells for megahabitats N (beige) and O (red).

Table 20. Statistical test and frequency distribution of cells for megahabitats N and O on the descriptor of depth.

Test statistic	Value	df	Prob
Pearson Chi-square	23.556	2	<0.001

Gr_Bathy	Column no.			
Line no.	1	2	3	Gen. Totl
N	14	21	18	53
O	5	31	75	111
Gen. Tot.	19	52	93	164

Both megahabitats were under a strong influence of the CIL and some influence of the surface layer, as demonstrated by the high maximum temperature at minimum depth (N: 10.8°C; O: 8.2°C). However, megahabitat O was also partly influenced by the higher salinity and milder temperature of the upper portion of the bottom layer (salinity group S_5 and temperature group T_3) (Table 21).

Table 21. Statistical tests and frequency distribution of cells for megahabitats N and O on the descriptors of salinity and temperature.

Salinity

Test statistic	Value	df	Prob
Pearson Chi-square	15.599	2	<0.001

Chi-square test was performed excluding class 3 to avoid too many fitted cells being sparse (calculated frequency < 5).

Gr_S	Column no.				
Line no.	3	5	6	7	Gen. Tot.
N	1	7	20	25	53
O	6	44	18	43	111
Gen. Tot.	7	51	38	68	164

Temperature

Test statistic	Value	df	Prob
Pearson Chi-square	14.011	3	0.003

Gr_T	Column no.				
Line no.	3	4	5	6	Gen. Tot.
N	0	3	10	40	53
O	15	19	12	65	111
Gen. Tot.	15	22	22	105	164

A larger proportion of cells classified in group P-5 (steeper slopes) in megahabitat N (Table 22).

Table 22. Statistical test and frequency distribution of cells for megahabitats N and O on the descriptor of slope.

Test statistic	Value	df	Prob
Pearson Chi-square	7.605	2	0.022

Chi-square test was performed excluding class 4 to avoid too many fitted cells being sparse (calculated frequency < 5).

Gr_Pente	Column no.				
Line no.	4	5	6	7	Gen. Tot.
N	2	14	29	8	53
O	6	41	60	4	111
Gen. Tot.	8	55	89	12	164

Cells of megahabitats N and O all classified as slopes (Table 23), whereas cells of megahabitat O were characterized by uniform terrain, megahabitat N was made of non-uniform seabed, i.e., slopes with pits and humps (Table 24).

Table 23. Frequency distribution of cells for megahabitats N and O on the descriptor of Geomorph_1.

Geomorph_1	Column no.			
Line no.	1	2	3	Gen. Tot.
N	3	50		53
O		110	1	111
Gen. Tot.	3	160	1	164

Table 24. Statistical tests and frequency distributions of cells for megahabitats N and O on the descriptors of terrain uniformity (Geomorph_2) and coastal forms (Geomorph_3).

Geomorph_2

Test statistic	Value	df	Prob
Pearson Chi-square	125.235	2	<0.001

Geomorph_2	Column no.			
Line no.	1	2	3	Gen. Tot.
N		37	16	53
O	100	11		111
Gen. Tot.	100	48	16	164

Geomorph_3

Test statistic	Value	df	Prob
Pearson Chi-square	25.834	1	<0.001

Geomorph_3	Column no.		
Line no.	1	2	Gen. Tot.
N	5	48	53
O	56	55	111
Gen. Tot.	61	103	164

A larger proportion of cells with high oxygen saturation values and coarse sediments were classified as megahabitat N (Table 25). Megahabitat N was characterized by coarse sand and gravel, with or without rock outcrops. Megahabitat O included a large proportion of cells with pellitic sediments.

Table 25. Statistical tests and frequency distributions of cells for megahabitats N and O on the descriptors of dissolved oxygen and sediments.

Dissolved oxygen

Test statistic	Value	df	Prob
Pearson Chi-square	14.646	7	0.041

Classe_oxygene	Column no.								
Line no.	1	2	3	4	5	6	7	8	Gen. Tot.
N	1	7	5	5	5	1	9	20	53
O	3	9	5	16	17	17	22	22	111
Gen. Tot.	4	16	10	21	22	18	31	42	164

Sediments

Test statistic	Value	df	Prob
Pearson Chi-square	32.408	5	<0.001

Chi-square test was performed excluding class 110 or 410 to avoid too many fitted cells being sparse (calculated frequency < 5).

Classe_Sed2	Column no.								
Line no.	110	120	130	310	410	512	530	540	Gen. Tot.
N			2	34	1		11	5	53
O	1	16	29	37		9	12	7	111
Gen. Tot.	1	16	31	71	1	9	23	12	164

Within cluster *bb,* the few cells of megahabitat M are thus referred to as *shallow water slopes centered below the CIL*. They are not considered to be under the influence of the surface layer. In contrast to megahabitat M, megahabitats N and O were centered in the CIL and are considered to be under the influence of the surface layer. Megahabitats N and O differed slightly in average depth (N: 71 m; O: 100 m), with salinity, temperature, and dissolved oxygen differing accordingly and more markedly in terrain roughness and sediments. They are collectively referred to as *shallow water slopes centered in the CIL*; N overlays O and the two megahabitats are adjacent.

<u>Shallow water shelf habitats (megahabitats E–L)</u>

Megahabitat E: fringing shallow water shelf megahabitat of the southern Gulf

Within cluster *ba,* there was a clear separation among the shallow water shelves between fringing shelves located around the Magdalen Islands (les Îles de la Madeleine) and along the New Brunswick, Nova Scotia, and PEI coasts (megahabitat E), and those of the Magdalen Shelf, estuary and northern Gulf (Figure 13).

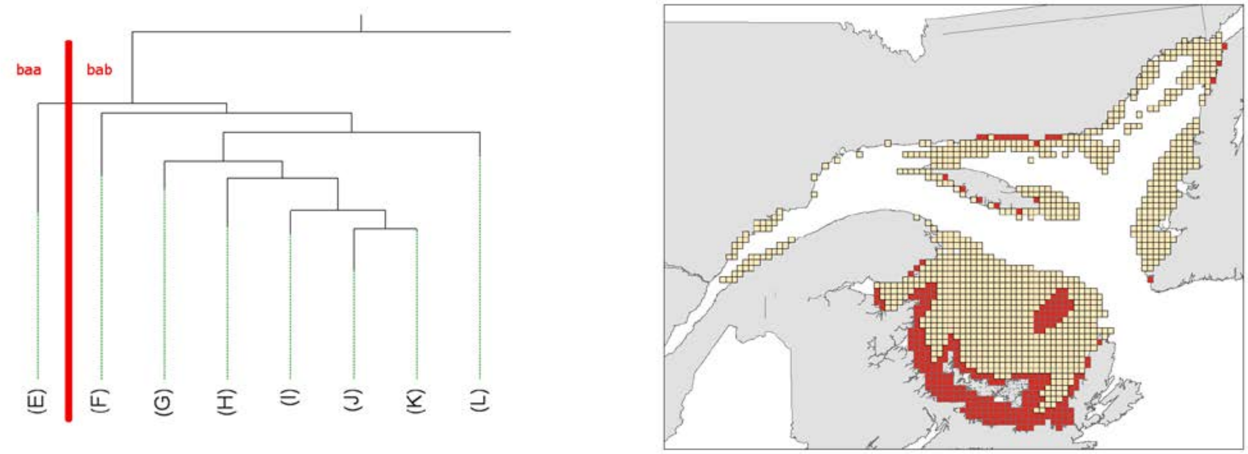

Figure 13. Splitting of cluster *ba* into cluster *baa* (megahabitat E) and *bab* (megahabitats F–L) shown as a dendrogram (left) and a map (right) of grid cells (*baa* = red, *bab* = beige).

Megahabitat E was comprised of shallower cells (average depth 15.8 m) than other shallow water shelf habitats (average depth 67.0 m) that also spanned a greater range in depth, 8.6 m and 31.2 m, respectively (Table 26).

Table 26. Statistical test and frequency distribution of cells for clusters *baa* and *bab* on the descriptor of depth.

Test statistic	Value	df	Prob
Pearson Chi-square	507.095	2	<0.001

Gr_Bathy	Column no.			
Line no.	1	2	3	Gen. Tot.
Cluster *baa*	269			269
Cluster *bab*	245	579	205	1029
Gen. Tot.	514	579	205	1298

Salinity was markedly lower in megahabitat E (Table 27).

Table 27. Statistical test and frequency distribution of cells for clusters *baa* and *bab* on the descriptor of salinity.

Test statistic	Value	df	Prob
Pearson Chi-square	733.190	5	<0.001

Gr_S	Column no.						
Line no.	1	3	4	5	6	7	Gen. Tot.
Cluster *baa*	224		43		2		269
Cluster *bab*	68	6	248	197	462	48	1029
Gen. Tot.	292	6	291	197	464	48	1298

Though all shallow water shelves exhibited minimum temperatures near 0°C (at mean, minimum, and maximum cell depth), mean and maximum temperatures at minimum cell depth were much higher in megahabitat E than in other shallow water shelves, reflecting large winter and summer differentials (Table 28).

Table 28. Statistical test and frequency distribution of cells for clusters *baa* and *bab* on the descriptor of temperature.

Test statistic	Value	df	Prob
Pearson Chi-square	1264.896	4	<0.001

Gr_T	Column no.					
Line no.	1	3	4	5	6	Gen. Tot.
Cluster *baa*	269					269
Cluster *bab*	2	18	551	158	300	1029
Gen. Tot.	271	18	551	158	300	1298

A larger proportion of cells had very gentle slopes (Gr_Pente 1 and 2) in megahabitat E (Table 29).

Table 29. Classification of clusters *baa* and *bab* on the descriptor of slope.

Test statistic	Value	df	Prob
Pearson Chi-square	110.475	6	<0.001

Gr_Pente	Column no.							
Line no.	1	2	3	4	5	6	7	Gen. Tot.
Cluster *baa*	123	118	27	1				269
Cluster *bab*	252	356	146	138	82	52	3	1029
Gen. Tot.	375	474	173	139	82	52	3	1298

Geomorph_1 and Geomorph_2 did not allow a separation of these two clusters (Table 30).

Table 30. Frequency distribution of clusters *baa* and *bab* on the descriptors of terrain (Geomorph_1) and terrain uniformity (Geomorph_2).

Geomorph_1	Column no.	
Line no.	1	Gen. Tot.
Cluster *baa*	269	269
Cluster *bab*	1029	1029
Gen. Tot.	1298	1298

Geomorph_2	Column no.		
Line no.	1	2	Gen. Tot.
Cluster *baa*	266	3	269
Cluster *bab*	1017	12	1029
Gen. Tot.	1283	15	1298

A majority of cells in megahabitat E (66%) and a minority of cells in other shallow water shelf areas (21%) are classified as *coastal*, i.e., are adjacent to the coastline (Table 31).

Table 31. Statistical test and frequency distribution of cells for clusters *baa* and *bab* on the descriptor of coastal forms (Geomorph_3).

Test statistic	Value	df	Prob
Pearson Chi-square	198.569	1	<0.001

Geomorph_3	Column no.		
Line no.	0	1	Gen. Tot.
Cluster *baa*	90	179	269
Cluster *bab*	811	218	1029
Gen. Tot.	901	397	1298

All of megahabitat E was classified as normoxic (see data limitations in Dutil et al. 2011).
A great proportion of shelf area was normoxic or slightly hypoxic (Table 32).

Table 32. Statistical test and frequency distribution of cells for clusters *baa* and *bab* on the descriptor of dissolved oxygen.

Test statistic	Value	df	Prob
Pearson Chi-square	215.932	4	<0.001

The Chi-square test was performed on data for class 4 and above to avoid too many fitted cells being sparse (calculated frequency < 5).

Classe_oxygene	Column no.							
Line no.	2	3	4	5	6	7	8	Gen. Tot.
Cluster *baa*			2		3	9	255	269
Cluster *bab*	5	17	25	77	195	265	445	1029
Gen. Tot.	5	17	27	77	198	274	700	1298

There was no striking difference in sediments between the two clusters, though proportions vary significantly (Table 33).

Table 33. Statistical test and frequency distribution of cells for clusters *baa* and *bab* on the descriptor of sediments.

Test statistic	Value	df	Prob
Pearson Chi-square	145.250	8	<0.001

Classe_Sed2 Line no.	Column no. 110	120	130	210	310	410	512	530	540	Gen. Tot.
Cluster *baa*		10	19	27	47	63	2	63	38	269
Cluster *bab*	5	61	57	183	294	40	95	166	128	1029
Gen. Tot.	5	71	76	210	341	103	97	229	166	1298

Megahabitat E is referred to as *fringing shallow water shelf of the southern Gulf* (Îles-de-la-Madeleine, and the New Brunswick, Nova Scotia, and PEI coasts).

Megahabitat F: fringing shallow water shelf with humps

Within cluster *bab*, two clusters are formed at a similarity value of 72.11, close to the similarity value at which megahabitat E separated from other shallow water shelves (71.03). Megahabitat F is comprised of only six cells , all of them on the coastline and with a surface area of marine habitat less than 100 km² (roughly 137 km^2 total) (Figure 14).

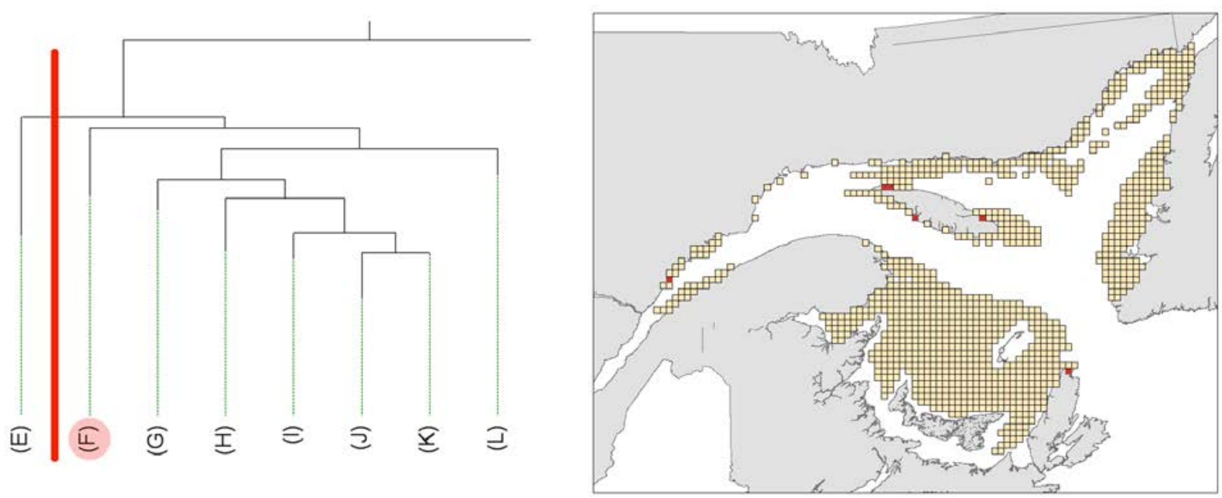

Figure 14. Dendrogram highlighting megahabitat F (left) and a map (right) of grid cells, with F in red and G–L in beige.

These cells are unique by virtue of their landscape, which is dominated by humps as opposed to a uniform seafloor in other clusters; variable Geomorph_2 had a value of *2* for all cells of megahabitat F. Other differences included shallower depths (14 m for megahabitat F, 67 m for other clusters), lower salinity in general, higher maximum temperature at minimum depth (reflecting depth and proximity to the coastline), and greater slopes on average (0.66° for megahabitat F, 0.30° for other clusters). Megahabitat F was termed *fringing shallow water shelf megahabitat with humps*.

Megahabitat L: sloping hypoxic shallow water shelf megahabitat

Cells of megahabitat L mainly fell into Bathy_3 category, but in fact ranged widely in depth (mean cell depth 80 m, mean minimum and maximum cell depths of 11 and 171 m, respectively; Figure 15, Table 34).

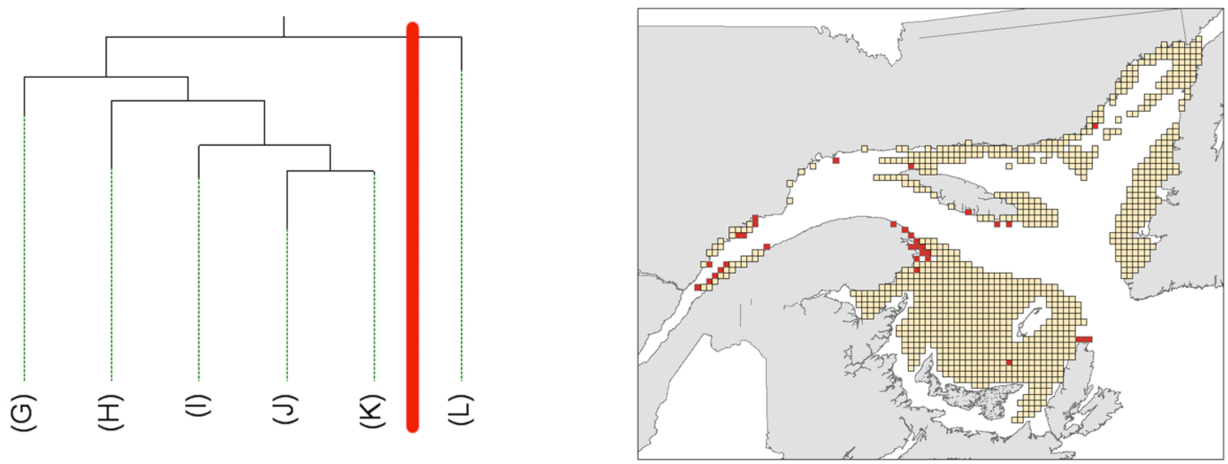

Figure 15. Dendrogram splitting megahabitat L (left) and a map of grid cells (right), with L in red.

Table 34. Statistical test and frequency distribution of cells for megahabitats G–K and L on the descriptor of depth.

Test statistic	Value	df	Prob
Pearson Chi-square	52.69	2	<0.001

Gr_Bathy Line no.	Column no. 1	2	3	Gen. Tot.
G–K	237	571	182	990
L	2	8	23	33
Gen. Tot.	239	579	205	1023

In contrast to megahabitats G–K, which mainly fell in Gr-S 4–6, megahabitat L mainly fell into Gr-S 7, i.e., large differences in mean salinity between mean, minimum, and maximum depth (Table 35).

Table 35. Frequency distribution of cells for megahabitats G–K and L on the descriptor of salinity.

Gr_S	Column no.						
Line no.	1	3	4	5	6	7	Gen. Tot.
G–K	68	5	242	194	458	23	990
L		1	2	3	3	24	33
Gen. Tot.	68	6	244	197	461	47	1023

Chi-square tests were not performed due to many fitted cells being sparse (calculated frequency < 5).

At minimum depth, cells of megahabitat L were under the influence of temperature from surface waters. In contrast, the seafloor was under of the influence of the CIL and the top of the bottom layer at other depths (Table 36).

Table 36. Statistical test and frequency distribution of cells for megahabitats G–K and L on the descriptor of temperature.

Test statistic	Value	df	Prob
Pearson Chi-square	43.366	3	<0.001

Gr_T	Column no.				
Line no.	3	4	5	6	Gen. Tot.
G–K	18	550	150	272	990
L		1	7	25	33
Gen. Tot.	18	551	157	297	1023

Whereas megahabitats G–K mainly fell in Gr-Pente 1–4, megahabitat L mainly fell into Gr-Pente 5 and 6, i.e., had steeper slopes than other shelf areas. Chi-square tests were not performed due to many fitted cells being sparse (calculated frequency < 5) (Table 37).

Table 37. Frequency distribution of cells of megahabitats G–K and L on the descriptor of slope.

Gr_Pente	Column no.							
Line no.	1	2	3	4	5	6	7	Gen. Tot.
G–K	252	356	144	132	71	35		990
L				3	10	17	3	33
Gen. Tot.	252	356	144	135	81	52	3	1023

In terms of the binary variables (Geomorph_1, Geomorph_2, and Geomorph_3), there was no variability in landscape (Geomorph_1, Geomorph_2) between the two clusters, but a larger proportion of the megahabitat L cells were located on the coast (Table 38).

Table 38. Statistical test for megahabitats G–K and L on the descriptor of landscape.

Test statistic	Value	df	Prob
Pearson Chi-square	28.189	1.000	<0.001

Cells of megahabitat L exhibited lower dissolved oxygen saturation (58% at mean depth) than cells in the other cluster, an unusual feature for coastal cells. Sediments were generally sand with gravel (Table 39). Chi-square tests could not be performed on the dissolved oxygen and sediments contingency tables due to many fitted cells being sparse (calculated frequency < 5).

Table 39. Frequency distribution of cells for megahabitats G–K and L on the descriptors of dissolved oxygen and sediments.

Oxygen

Classe_oxygene	Column no.							
Line no.	2	3	4	5	6	7	8	Gen. Tot.
G–K	5	6	21	68	187	261	442	990
L		11	4	7	5	3	3	33
Gen. Tot.	5	17	25	75	192	264	445	1023

Sediments

Classe_Sed2	Column no.									
Line no.	110	120	130	210	310	410	512	530	540	Gen. Tot.
G–K	5	61	49	183	272	40	90	165	125	990
L			8		18		4	1	2	33
Gen. Tot.	5	61	57	183	290	40	94	166	127	1023

Megahabitat L is thus made of coastal cells with slopes greater than other shelf habitats. These cells were not classified as slopes, though slope averaged greater than 0.8°, by virtue of their depth, which is less than 200 m on average. Thus cells of megahabitat L range widely in depth. They are characterized by a wide range of salinity and temperature conditions, depending on depth. The occurrence of low dissolved oxygen saturation at relatively shallow depths is a striking characteristic of cells in megahabitat L. Megahabitat L was *sloping hypoxic shallow water shelf megahabitat*.

Megahabitat G: flat hypoxic shallow water shelf megahabitat

Megahabitat G separated from other cells in that cluster at a similarity value of 77.11 (Figure 16). Low dissolved oxygen saturation was the most prominent feature of these shallow water shelf areas, which spanned dissolved oxygen classes 2 to 4 (<50% on average) compared to classes 5 to 8 (>75% on average) for the cells in the other cluster (Table 40).

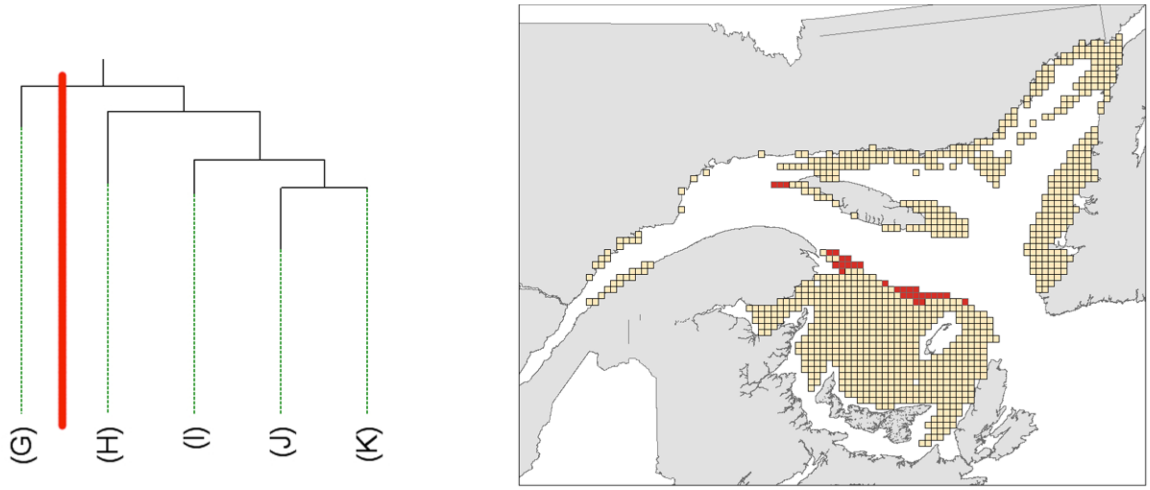

Figure 16. Dendrogram (left) splitting megahabitat G from megahabitats H–K and a map (right) of grid cells (red = G, beige = H–K).

Table 40. Frequency distribution of cells for megahabitats G–K and L on the descriptors of depth, salinity, temperature, slope, dissolved oxygen, and sediments.

Depth

Gr_Bathy	Column no.			
Line no.	1	2	3	Gen. Tot.
G		17	12	29
H–K	237	554	170	961
Gen. Tot.	237	571	182	990

Salinity

Gr_S	Column no.						
Line no.	1	3	4	5	6	7	Gen. Tot.
G		5		8	16		29
H–K	68		242	186	442	23	961
Gen. Tot.	68	5	242	194	458	23	990

Temperature

Gr_T	Column no.				
Line no.	3	4	5	6	Gen. Tot.
G	5	24			29
H–K	13	526	150	272	961
Gen. Tot.	18	550	150	272	990

Slope

Gr_Pente	Column no.						
Line no.	1	2	3	4	5	6	Gen. Tot.
G	16	7	2	1	2	1	29
H–K	236	349	142	131	69	34	961
Gen. Tot.	252	356	144	132	71	35	990

Dissolved oxygen

Classe_oxygene	Column no.							
Line no.	2	3	4	5	6	7	8	Gen. Tot.
G	2	6	21					29
H–K	3			68	187	261	442	961
Gen. Tot.	5	6	21	68	187	261	442	990

Sediments

Classe_Sed2	Column no.									
Line no.	110	120	130	210	310	410	512	530	540	Gen. Tot.
G				8	7			2	12	29
H–K	5	61	49	175	265	40	90	163	113	961
Gen. Tot.	5	61	49	183	272	40	90	165	125	990

In contrast to megahabitat L, gentle slopes characterized these hypoxic shelf areas, which we therefore termed *flat hypoxic shallow water shelf*. They correspond to the northeast limit for the troughs of Bradelle, Shediac Valley, and Chaleur Bay.

Megahabitat H: relatively warm intermediate shallow water shelf megahabitat

Megahabitat H was made of those cells adjacent to and slightly deeper than cells of megahabitat E. Most cells (88%) fitted in the same depth group as megahabitat E (Gr_Bathy = 1), but they averaged slightly deeper (35 m) than megahabitat E (16 m). Cells of megahabitat H were shallower than cells of the other cluster (megahabitats I, J, K) (Figure 17, Table 41).

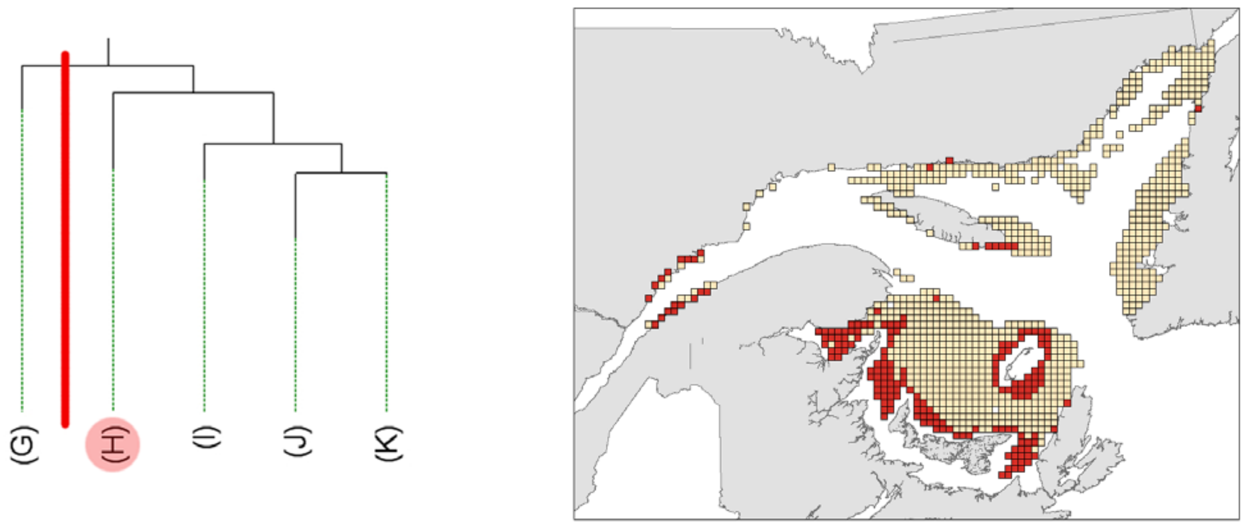

Figure 17. Dendrogram (left) highlighting megahabitat H and a map (right) of grid cells (red = H, beige = I–K).

Table 41. Statistical test and frequency distribution of cells for megahabitats H and I–K on the descriptor of depth.

Test statistic	Value	df	Prob
Pearson Chi-square	506.361	2	<0.001

Gr_Bathy	Column no.			
Line no.	1	2	3	Gen. Tot.
H	165	22		187
I–K	72	532	170	774
Gen. Tot.	237	554	170	961

Salinity was low at all depths, and temperature on the seafloor was under the influence of warm surface waters, in contrast to most cells of megahabitats I–K. Warm summer temperatures were experienced only at minimum cell depths in megahabitat H, whereas they occured at minimum and maximum depths in cells of megahabitat E (Table 42).

Table 42. Statistical tests and frequency distribution of cells for megahabitats H and I–K on the descriptors of salinity, temperature, slope, dissolved oxygen, and sediments.

Salinity

Test statistic	Value	df	Prob
Pearson Chi-square	532.941	4	<0.001

Gr_S	Column no.					
Line no.	1	4	5	6	7	Gen. Tot.
H	68	112	2	5		187
I–K		130	184	437	23	774
Gen. Tot.	68	242	186	442	23	961

Temperature

Test statistic	Value	df	Prob
Pearson Chi-square	382.296	3	<0.001

Gr_T	Column no.				
Line no.	3	4	5	6	Gen. Tot.
H		3	26	158	187
I–K	13	523	124	114	774
Gen. Tot.	13	526	150	272	961

Slope

Test statistic	Value	df	Prob
Pearson Chi-square	90.930	5	<0.001

Gr_Pente	Column no.						
Line no.	1	2	3	4	5	6	Gen. Tot.
H	47	117	16	4	3		187
I–K	189	232	126	127	66	34	774
Gen. Tot.	236	349	142	131	69	34	961

Dissolved oxygen

Test statistic	Value	df	Prob
Pearson Chi-square	107.681	4	<0.001

Classe_oxygene	Column no.					
Line no.	2	5	6	7	8	Gen. Tot.
H		2	12	24	149	187
I–K	3	66	175	237	293	774
Gen. Tot.	3	68	187	261	442	961

Sediments

Test statistic	Value	df	Prob
Pearson Chi-square	77.227	8	<0.001

Classe_Sed2	Column no.									
Line no.	110	120	130	210	310	410	512	530	540	Gen. Total
H	3	22	16	30	31	3		45	37	187
I–K	2	39	33	145	234	37	90	118	76	774
Gen. Tot.	5	61	49	175	265	40	90	163	113	961

Most of megahabitat H was located at the periphery of the Magdalen Shelf and into Chaleur Bay in the southern Gulf. Megahabitat H is referred to as the *intermediate shallow water shelf*, as it represents a transition between two megahabitats, one that reflects conditions prevailing at the surface (megahabitat E) and one that does not (megahabitat J).

Megahabitat I: fringing shallow water shelf areas of the northern Gulf

The frequency distribution of cells of megahabitat I differed from that of cells in the other cluster (megahabitats J and K; Figure 18, Table 43). There was no variability in landscape (Geomorph_1, Geomorph_2) between the two clusters, but a larger proportion of megahabitat I cells were located on the coast (Geomorph_3=1). All other variables showed significant differences, with cells of megahabitat I found in shallower water and characterized by a lower salinity and higher maximum temperature at minimum depth. Although cells are distributed over several slope groups (Gr_pente), cells of megahabitat I are characterized by steeper slopes than cells in the other cluster. Cells of megahabitat I are well oxygenated, with a high proportion having coarse sediments, rock outcrops with coarse sand, and gravel (Table 43).

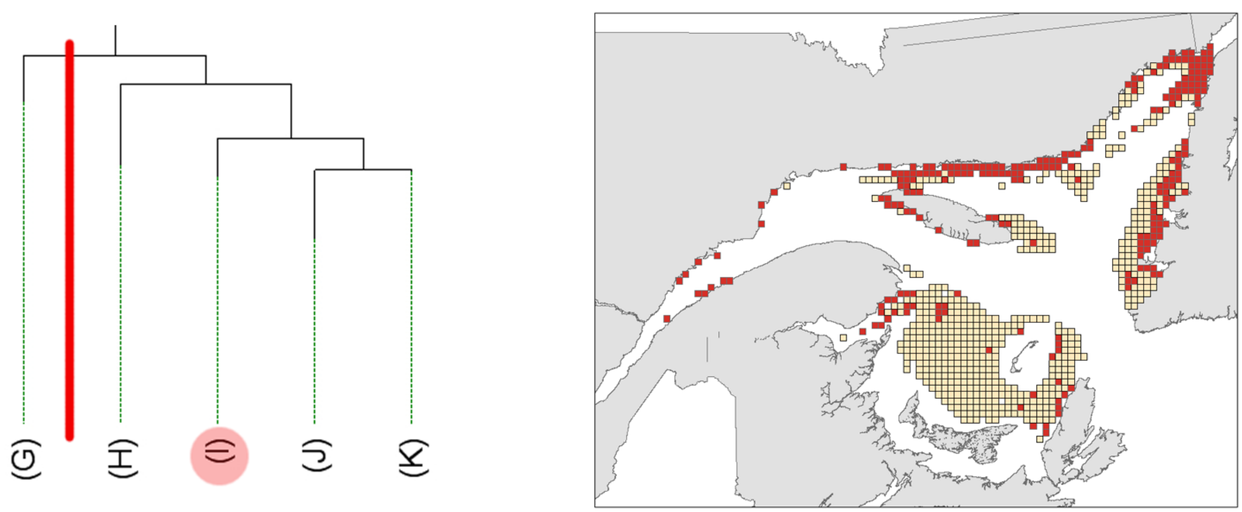

Figure 18. Dendrogram (left) highlighting megahabitat I and a map (right) of grid cells (red = I).

Table 43. Statistical tests and frequency distribution of cells for megahabitats I and J–K on the descriptors of depth, salinity, temperature, slope, landscape, dissolved oxygen, and sediments.

Depth

Test statistic	Value	df	Prob
Pearson Chi-square	232.513	2	<0.001

Gr_Bathy	Column no.			
Line no.	1	2	3	Gen. Tot.
I	72	163	2	237
J–K		369	168	537
Gen. Tot.	72	532	170	774

Salinity

Test statistic	Value	df	Prob
Pearson Chi-square	170.182	3	<0.001

Gr_S	Column no.				
Line no.	4	5	6	7	Gen. Tot.
I	3	20	191	23	237
J–K	127	164	246		537
Gen. Tot.	130	184	437	23	774

Temperature

Test statistic	Value	df	Prob
Pearson Chi-square	407.640	3	<0.001

Gr_T	Column no.				
Line no.	3	4	5	6	Gen. Tot.
I		51	74	112	237
J–K	13	472	50	2	537
Gen. Tot.	13	523	124	114	774

Slope

Test statistic	Value	df	Prob
Pearson Chi-square	293.507	5	<0.001

Gr_Pente	Column no.						
Line no.	1	2	3	4	5	6	Gen. Tot.
I	10	13	59	89	42	24	237
J–K	179	219	67	38	24	10	537
Gen. Tot.	189	232	126	127	66	34	774

Landscape

Test statistic	Value	df	Prob
Pearson Chi-square	169.914	1	<0.001

Geomorph_3	Column no.		
Line no.	0	1	Gen. Tot.
I	125	112	237
J–K	499	38	537
Gen. Tot.	624	150	774

Dissolved oxygen

Test statistic	Value	df	Prob
Pearson Chi-square	182.120	4	<0.001

Classe_oxygene	Column no.					
Line no.	2	5	6	7	8	Gen. Tot.
I		12	16	36	173	237
J–K	3	54	159	201	120	537
Gen. Tot.	3	66	175	237	293	774

Sediments

Test statistic	Value	df	Prob
Pearson Chi-square	130.355	8	<0.001

Classe_Sed2	Column no.									
Line no.	110	120	130	210	310	410	512	530	540	Gen. Total
I		11	4	11	103	28	5	47	28	237
J–K	2	28	29	134	131	9	85	71	48	537
Gen. Tot.	2	39	33	145	234	37	90	118	76	774

Megahabitat I is referred to as the *fringing shallow water shelf of the northern Gulf*. In contrast to fringing shallow water shelf areas of the southern Gulf, fringing shallow water shelf areas of the northern Gulf have a greater average depth, a higher salinity, and a colder temperature (at mean, minimum, and maximum cell depth). Temperature conditions in megahabitat I are more similar to those prevailing in megahabitat H (intermediate shallow water shelf) than in megahabitat E (fringing shallow water shelf areas of the southern Gulf). Slopes are also steeper in fringing shallow water shelf areas of the northeast Gulf (parts of the Anticosti, North Shore, and Newfoundland shelves).

Megahabitat J: cold shallow water shelf area; megahabitat K: relatively cold intermediate shallow water shelf habitat

Megahabitats J and K differed by depth and salinity (J shallower and K lower salinity). Both megahabitats were under the influence of the CIL, with inverse temperature gradients. Average temperature decreased with depth in megahabitat J, whereas it increased with depth in megahabitat K. Megahabitat J had very gentle slopes; more variability in slope was observed in megahabitat K. There was no variability in terrain (Geomorph_1, Geomorph_2) between the two clusters, but the coast (Geomorph_3=1) had a larger proportion of megahabitat I cells (Figure 19, Table 44).

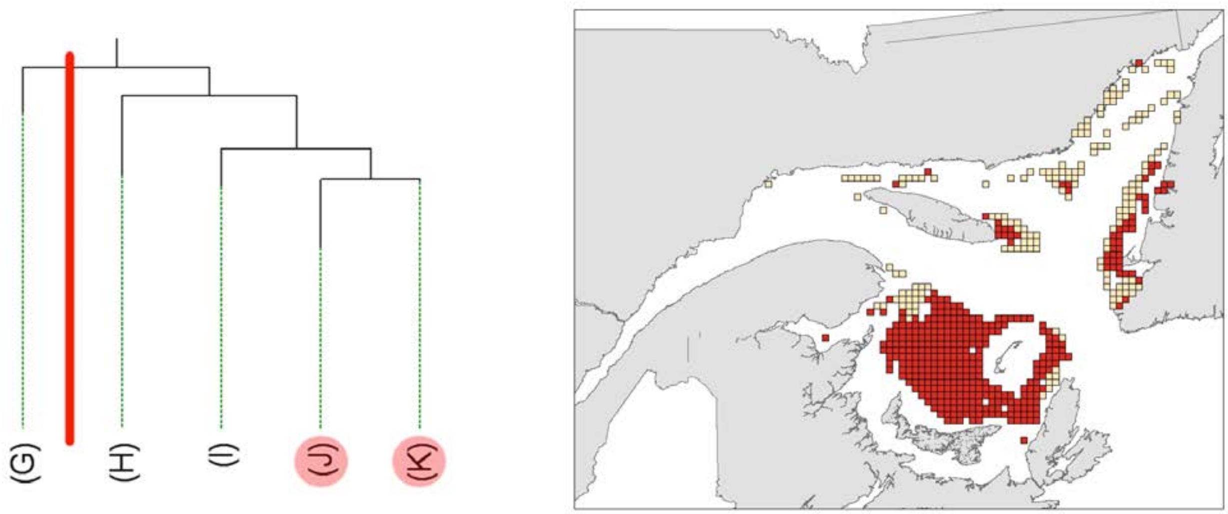

Figure 19. Dendrogram (left) highlighting megahabitats J and K, and a map (right) of grid cells (red = J, beige = K).

Table 44. Statistical test and frequency distribution of cells for megahabitats J and K on the descriptors of depth, salinity, temperature, slope, landscape, dissolved oxygen, and sediments.

Depth

Test statistic	Value	df	Prob
Pearson Chi-square	537.000	1	<0.001

Gr_Bathy	Column no.		
Line no.	2	3	Gen. Tot.
J	369		369
K		168	168
Gen. Tot.	369	168	537

Salinity

Test statistic	Value	df	Prob
Pearson Chi-square	440.155	2	<0.001

Gr_S	Column no.			
Line no.	4	5	6	Gen. Tot.
J	127	9	233	369
K		155	13	168
Gen. Tot.	127	164	246	537

Temperature

Test statistic	Value	df	Prob
Pearson Chi-square	41.267	2	<0.001

Chi-square test was performed excluding class 6 to avoid too many fitted cells being sparse (calculated frequency < 5).

Gr_T	Column no.				
Line no.	3	4	5	6	Gen. Tot.
J		322	46	1	369
K	13	150	4	1	168
Gen. Tot.	13	472	50	2	537

Slope

Test statistic	Value	df	Prob
Pearson Chi-square	294.943	5	<0.001

Gr_Pente	Column no.						
Line no.	1	2	3	4	5	6	Gen. Tot.
J	132	216	21				369
K	47	3	46	38	24	10	168
Gen. Tot.	179	219	67	38	24	10	537

Landscape

Test statistic	Value	df	Prob
Pearson Chi-square	16.265	1	<0.001

Geomorph_3	Column no.		
Line no.	0	1	Gen. Tot.
J	354	15	369
K	145	23	168
Gen. Tot.	499	38	537

Dissolved oxygen

Test statistic	Value	df	Prob
Pearson Chi-square	22.522	4	<0.001

Classe_oxygene	Column no.					
Line no.	2	5	6	7	8	Gen. Tot.
J		27	105	155	82	369
K	3	27	54	46	38	168
Gen. Tot.	3	54	159	201	120	537

Sediments

Test statistic	Value	df	Prob
Pearson Chi-square	139.656	8	<0.001

Classe_Sed2	Column no.									
Line no.	110	120	130	210	310	410	512	530	540	Gen. Tot.
J		13	4	129	86	9	39	44	45	369
K	2	15	25	5	45		46	27	3	168
Gen. Tot.	2	28	29	134	131	9	85	71	48	537

When considering mean, minimum, and maximum temperatures at mean, minimum, and maximum depths, Megahabitat J is overall the coldest environment in the study area and is referred to as *cold shallow water shelf*. It includes much of the Magdalen Shelf and part of the Shediac Valley Trough and the Cape Breton Trough, as well as very discrete areas on the Anticosti, North Shore (Beaugé Bank), and Newfoundland shelves. Megahabitat K is the next coldest environment, a characteristic shared with the more hypoxic megahabitat G. In contrast to megahabitat J, it is mainly located in the northeastern Gulf, Anticosti Shelf, much of Beaugé Bank, around the Mecatina Trough, and at the edge of the Newfoundland Shelf. In the southern Gulf, megahabitat K is located in two areas at the edge of the Laurentian Channel: the confluence of Chaleur Bay and Shediac Valley Trough, and the Cape Breton Trough. Megahabitat K is referred to as *relatively cold intermediate shallow water shelf*.

2. SPATIAL CHARACTERISTICS OF BENTHIC HABITATS

A prominent feature of the habitat classification described in the previous section (Ch. 1) is the fact that cells belonging to the same habitat tend to be clustered as opposed to being randomly distributed in the study area. This suggests that the descriptors selected, and the cluster analyses run on the basis of those descriptors, reflected spatially coherent processes and features. The degree of spatial organization varied, however, between habitat categories. This section looks for patterns in spatial organization using the FRAGSTATS software package. FRAGSTATS performs patch analysis and is principally used in the field of terrestrial ecology (McGarigal et al. 2002).

Spatial pattern analysis using FRAGSTATS

The grid of megahabitat cells (100 km^2) in vector format was converted to raster format (ERDAS IMAGINE) at a spatial resolution of 500 m and used for computing several landscape metrics with the FRAGSTATS software, version 3.3. FRAGSTATS analyzes categorical map patterns and produces a host of metrics describing the spatial distribution of patches within a landscape (Table 45; for a full description of methods, see McGarigal et al. 2002). Patches were defined as contiguous cells of the same category (class level in FRAGSTATS), i.e., cells of the same class level sharing a boundary point or a boundary line. Two sets of analyses were conducted. One set considered the whole study area as the landscape unit. The fragmentation pattern of shallow water patches (i.e., patches made of cells belonging to megahabitats E to M) was compared to that of deep water patches (i.e., patches made of cells belonging to megahabitats A to D). In a second analysis, fragmentation patterns of megahabitats were compared using megahabitat category as the class level. The second set considered subareas (estuary, northern and southern Gulf) as discrete landscapes. Habitat fragmentation was examined for each subarea (landscape level in FRAGSTATS) and for shared megahabitats (class level in FRAGSTATS) in the northern and southern Gulf of St. Lawrence.

Table 45. Landscape pattern metrics used to describe benthic megahabitats of the estuary and Gulf of St. Lawrence. A: FRAGSTATS code and measurement units; B: Description of each metric used.

A

Variable	FRAGSTATS code	Megahabitat features	Patch feature distribution	Units
Total area of megahabitat	CA	x		km^2
Proportion of total study area	PLAND	x		%
Number of patches	NP	x		-
Patch density	PD	x		no/10^4 km^2
Largest patch index 1	LPI (1)	x		%
Largest patch index 2	LPI (2)	x		%
Total edge 1	TE (1)	x		km
Total edge 2	TE (2)	x		km
Edge density 1	ED (1)	x		m/km^2
Edge density 2	ED (2)	x		m/km^2

Contrast weighted edge density	CWED	x		m/km^2
Total edge contrast index	TECI	x		%
Perimeter-area fractal dimension	PAFRAC	x		-
Clumpiness index	CLUMPY	x		-
Interspersion index	IJI	x		%
Patch area	AREA		x	km^2
Patch radius of gyration	GYRATE		x	km
Patch shape index	SHAPE		x	-
Patch similarity index	SIMI		x	-
Patch edge contrast index	ECON		x	-

B

Variable	Description
Total area of megahabitat	Surface area of the megahabitat
Proportion of total study area	Surface area of a megahabitat as a proportion of total study area
Number of patches	Number of patches of a megahabitat in the study area
Patch density	Number of patches of a megahabitat per unit total area
Largest patch index 1	Proportion of the study area occupied by the largest patch of the megahabitat
Largest patch index 2	Proportion of the megahabitat occupied by the largest patch of that megahabitat
Total edge 1	Total edge length of all patches of a megahabitat between megahabitats
Total edge 2	Total edge length of all patches of a megahabitat[2]
Edge density 1	Total edge (1) length per unit total area
Edge density 2	Total edge (2) length per unit total area[2]
Contrast weighted edge density	Total edge length per unit total area, weighted by the dissimilarity between megahabitats[3]
Total edge contrast index	Total contrast weighted edge length per unit total edge length of that megahabitat[3]
Perimeter-area fractal dimension	Shape complexity based on number of patches, and their area and perimeter
Clumpiness index	Measure of patch aggregation for a megahabitat[1]
Interspersion index	Measure of intermixing of patches of a megahabitat with those of other megahabitats
Patch area	Surface area of all patches of a megahabitat: AREA_MN, AREA_AM, AREA_RA[4]
Patch radius of gyration	Distance of each cell in a patch to the patch centroid: GYRATE_MN, GYRATE_AM, GYRATE_RA[4]
Patch shape index	Normalized ratio of patch perimeter to patch area: SHAPE_MN, SHAPE_AM, SHAPE_RA[4]
Patch similarity index	Similarity with neighbouring patches within 15 km: SIMI_MN, SIMI_AM, SIMI_RA[4,5]
Patch edge contrast index	Dissimilarity between adjacent patches: ECON_MN, ECON_AM, ECON_RA[3,4]

[1] Measure of distance from a random distribution (0), varies from -1, maximally disaggregated, to +1, maximally aggregated
[2] In contrast to TE (1) and ED (1), this metric includes the edge of the study area, which generally corresponds to the coastline
[3] This metric factors in the contrast with the edge of the study area, which generally corresponds to the coastline (dissimilarity value set arbitrarily to 1)
[4] MN-mean, AM-area-weighted mean, RA, range; metrics measured across all patches of a megahabitat
[5] Values calculated by FRAGSTATS were divided by 1000

Split into two categories: shallow water and deep water habitats

Shallow and deep waters each occupied a large proportion of the study area (58 and 43% for deep and shallow waters, respectively) (Table 46). Both split up into a small number of patches, with the largest patch in deep water occupying 99% of the surface area of deep waters and as much as 42% of the surface of the study area. The largest patch in shallow waters represented 60% of the surface area of shallow water megahabitats and 34% of the surface of the study area, suggesting a more evenly distributed surface area across patches in shallow waters. When the coastline was included in the calculations, the edge was much more important for shallow water megahabitats than for deep water megahabitats: shallow water megahabitats had a longer edge, a greater edge density, a greater highly contrasted edge density, and a greater dissimilarity between adjacent patches. Both megahabitats were strongly aggregated (clumpiness index > 0.95), but patches of shallow water megahabitats had a greater shape complexity, as the spreading of these megahabitats along the coastline would indicate. Overall, shallow waters represented a larger area divided into a few large patches, some being regular in shape (southern Gulf) while others were spread out and more indented (estuary and northern Gulf). Though also representing a large area, deep water megahabitats were strongly aggregated into a single elongated patch of low complexity.

Table 46. Landscape pattern metrics of the shallow and deep water habitats in the estuary and Gulf of St. Lawrence calculated using the FRAGSTATS software. The whole study area was considered as the landscape unit and cells were grouped into two classes: cells belonging to megahabitats E to M formed the shallow water patches, and cells belonging to megahabitats A to D formed the deep water patches.

Variable	Deep water megahabitats	Shallow water megahabitats	Units
Total area	95,871.5	129,789.8	km^2
Proportion of total study area	42.5	57.5	%
Number of patches	5	7	-
Patch density	0.52	0.54	number/10^4 km^2
Largest patch index 1	42.3	34.4	%
Largest patch index 2	99.5	59.8	%
Total edge 1	4,332.5	4,332.5	km
Total edge 2	4,582.0	12,645.0	km
Edge density 1	19.2	19.2	m/km^2
Edge density 2	20.3	56.0	m/km^2
Contrast weighted edge density	9.3	45.0	m/km^2
Total edge contrast index	45.8	80.4	%
Perimeter-area fractal dimension	N/A	N/A	-
Clumpiness index	0.99	0.97	-
Interspersion index	N/A	N/A	%
Patch area – MN	19,174.3	18,541.4	km^2
Patch area – AM	94,883.8	55,020.3	km^2
Patch area – RA	95,280.5	77,592.8	km^2

Patch radius of gyration - MN	42.1	61.0	km
Patch radius of gyration - AM	192.3	119.5	km
Patch radius of gyration - RA	189.6	181.7	km
Patch shape index - MN	1.5	3.2	-
Patch shape index - AM	3.5	4.6	-
Patch shape index - RA	2.6	7.0	-
Patch similarity index - MN	157,934	219,429	-
Patch similarity index - AM	296,782	219,265	-
Patch similarity index - RA	230,054	2,289	-
Patch edge contrast index - MN	44.7	72.3	-
Patch edge contrast index - AM	45.8	85.0	-
Patch edge contrast index - RA	7.2	49.0	-

Deep water habitats landscape

The deep water channels megahabitat (megahabitat A) represented a unique landscape pattern as it was made of only 3 patches, the largest patch representing 27% of the surface of the study area and 99% of the surface of megahabitat A (Table 47). The patch radius of gyration was therefore very high. In contrast, deep water shelves (megahabitat C) and slopes (megahabitat D) were broken down into a large number of patches, 29 and 50, respectively, resulting in long edges, high edge densities with neighbouring habitats, and large perimeter-area fractal dimensions. Deep water slopes were the most fragmented megahabitat in the study area, with the greatest number of patches and the highest perimeter-area fractal dimension. On the other hand, patches of megahabitat surrounding deep water shelves and slopes were not very dissimilar, as the high similarity index and low edge contrast index suggested. Compared to the shallow water habitats, deep water channels and bordering habitats formed a rather simple landscape, with fragmentation occurring mainly at the periphery.

Table 47. Landscape pattern metrics of the estuary and Gulf of St. Lawrence calculated using the FRAGSTATS software comparing four deep water megahabitats. The whole study area was considered as the landscape unit. Patches were formed by contiguous cells of the same megahabitat (class level in FRAGSTATS).

	Megahabitat				
Variable	A	B	C	D	Units
Total area of megahabitat	62,196.0	1,391.0	18,629.0	13,656.0	km^2
Proportion of total study area	27.6	0.6	8.3	6.1	%
Number of patches	3	5	29	50	-
Patch density	0.13	0.22	1.29	2.22	$no/10^4\ km^2$
Largest patch index 1	27.4	0.4	1.3	1.2	%
Largest patch index 2	99.5	64.1	16.1	19.0	%
Total edge 1	3,335.0	367.0	4,307.0	4,165.0	km
Total edge 2	3,400.0	423.0	4,379.0	4,220.0	km

Edge density 1	14.8	1.6	19.1	18.5	m/km^2
Edge density 2	15.1	1.9	19.4	18.7	m/km^2
Contrast weighted edge density	5.0	0.8	7.0	6.2	m/km^2
Total edge contrast index	33.2	41.2	35.9	33.2	%
Perimeter-area fractal dimension	N/A	N/A	1.58	1.69	-
Clumpiness index	0.99	0.98	0.97	0.96	-
Interspersion index	49.20	60.80	74.50	62.10	%
Patch area - MN	20,732.0	278.0	642.0	273.0	km^2
Patch area - AM	61,607.0	621.0	1,428.0	796.0	km^2
Patch area - RA	61,805.0	791.0	2,900.0	2,500.0	km^2
Patch radius of gyration - MN	65.0	8.0	13.0	8.0	km
Patch radius of gyration - AM	181.0	17.0	27.0	20.0	km
Patch radius of gyration - RA	178.0	19.0	63.0	58.0	km
Patch shape index - MN	1.9	1.2	1.4	1.2	-
Patch shape index - AM	3.3	1.7	2.0	1.7	-
Patch shape index - RA	2.3	1.0	2.4	2.0	-
Patch similarity index - MN	40,504.0	113,190.0	140,987.0	152,674.0	-
Patch similarity index - AM	107,060.0	158,507.0	141,198.0	174,617.0	-
Patch similarity index - RA	105,104.0	175,540.0	251,399.0	245,744.0	-
Patch edge contrast index - MN	37.6	39.0	36.0	33.7	-
Patch edge contrast index - AM	33.1	41.8	36.3	33.2	-
Patch edge contrast index - RA	19.8	23.0	18.4	30.9	-

Shallow water habitats landscape

Among the four megahabitats mainly found in the southern Gulf, the fringing shallow water shelf megahabitat (megahabitat E) had a unique set of landscape features, suggesting some form of isolation from other megahabitats (Table 48). It had a high edge density when including the landward edge, and got the highest scores of all megahabitats in terms of total edge contrast, area-weighted patch edge contrast, and contrast-weighted edge density. The interspersion index of the patches of that megahabitat was the lowest of all megahabitats. The cold shallow water Magdalen Shelf (megahabitat J; 16% of total study area), though split up into more than 20 patches, was made of one large-sized patch representing 85% of the surface area of the megahabitat. Shape complexity and contrast with neighbouring megahabitats were low: the perimeter-area fractal dimension, total edge contrast, and area-weighted patch edge contrast were the lowest of all megahabitats. The relatively warm intermediate shallow water shelf (megahabitat H), which also occupied a large surface area, exhibited average landscape characteristics compared to other megahabitats in the study area.

Similarly, among the remaining five megahabitats, the fringing shallow water shelf of the northern Gulf (megahabitat I), which represented 9% of the surface of the study area, got the highest scores of all megahabitats in terms of total edge and high scores for edge density and contrast-weighted edge density when including the landward edge, reflecting the large number of patches and wide spatial distribution on the coastline (Table 48). The similarity index was low and interspersion index very high. The shallow water slopes below the CIL (megahabitat M; 6% of total study area) represented a landscape similar to megahabitat I in that they were both split up into a large number of patches of a small size and spread out over a wide area, with high scores for edge density and contrast-weighted edge density. The similarity index was rather low and the interspersion index was very high.

The relatively cold intermediate shallow water shelf megahabitat K (7.1% of total surface area and split up into 30 small discrete patches) also had high total edge lengths, but the contrast-weighted edge density was less than for megahabitats I and M. The interspersion index was high and the patch similarity index greater than for megahabitats I and M. Overall, the two megahabitats that were classified as being “intermediate” in environmental characteristics performed similarly in terms of landscape features except that total edge contrast index, contrast-weighted edge density, and patch edge contrast index were greater, and patch similarity index was less for megahabitat I than for megahabitat K.

The sloping hypoxic shallow water shelf in the Gaspé area (megahabitat L), which represented only 1.2% of the total study area, had a low patch similarity index and high interspersion index, reflecting the diversity of habitats in the area.

Table 48. Landscape pattern metrics of the estuary and Gulf St. Lawrence calculated using the FRAGSTATS software comparing nine shallow water megahabitats. The whole study area was considered as the landscape unit. Patches were formed by contiguous cells of the same megahabitat (class level in FRAGSTATS).

	Megahabitat				
Variable	E	G	H	J	Units
Total area of megahabitat	20,202.3	2,900.0	16,662.3	36,202.0	km^2
Proportion of total study area	9.0	1.3	7.4	16.0	%
Number of patches	24	5	25	21	-
Patch density	1.06	0.22	1.11	0.93	$no/10^4\ km^2$
Largest patch index 1	7.1	0.6	2.8	13.7	%
Largest patch index 2	79.6	48.3	38.4	85.4	%
Total edge 1	1,524.5	620.0	2,785.0	2,947.0	km
Total edge 2	4,989.0	620.0	3,487.0	3,144.0	km
Edge density 1	6.8	2.8	12.3	13.1	m/km^2
Edge density 2	22.1	2.8	15.5	13.9	m/km^2
Contrast weighted edge density	17.3	0.9	6.2	3.6	m/km^2
Total edge contrast index	78.4	33.5	40.1	25.7	%
Perimeter-area fractal dimension	1.34	N/A	1.24	1.12	-
Clumpiness index	0.97	0.98	0.98	0.99	-
Interspersion index	30.83	64.28	54.11	63.38	%
Patch area - MN	841.8	580.0	666.5	1,723.9	km^2
Patch area - AM	13,296.1	1,058.6	4,177.8	26,518.6	km^2

Patch area - RA	16,083.8	1,300.0	6,397.3	30,898.8	km^2
Patch radius of gyration - MN	7.9	10.4	8.8	9.5	km
Patch radius of gyration - AM	80.8	16.4	38.4	69.3	km
Patch radius of gyration - RA	96.0	16.7	53.5	78.0	km
Patch shape index - MN	1.9	1.3	1.7	1.3	-
Patch shape index - AM	6.0	1.6	2.6	2.3	-
Patch shape index - RA	5.9	0.7	2.0	1.5	-
Patch similarity index - MN	14,050.6	110,453.2	31,258.7	20,380.9	-
Patch similarity index - AM	106,885.3	118,227.1	115,333.6	110,746.4	-
Patch similarity index - RA	121,084.2	75,596.2	150,007.6	126,376.1	-
Patch edge contrast index - MN	72.5	34.1	58.4	36.2	-
Patch edge contrast index - AM	78.7	33.2	32.2	22.8	-
Patch edge contrast index - RA	36.3	8.2	68.0	77.2	-
Total area of megahabitat	124.0	21,145.5	16,068.0	2,817.0	13,641.0
Proportion of total study area	0.1	9.4	7.1	1.2	6.0
Number of patches	6	44	30	19	38
Patch density	0.27	1.95	1.33	0.84	1.68
Largest patch index 1	0.0	2.5	1.0	0.3	0.9
Largest patch index 2	31.3	26.8	13.7	24.5	15.4
Total edge 1	78.5	3,746.0	3,541.0	883.5	3,187.0
Total edge 2	168.0	5,467.0	3,877.0	1,107.0	4,717.0
Edge density 1	0.4	16.6	15.7	3.9	14.1
Edge density 2	0.7	24.2	17.2	4.9	20.9
Contrast weighted edge density	0.5	11.9	6.3	2.3	12.4
Total edge contrast index	67.8	49.0	36.4	47.2	59.2
Perimeter-area fractal dimension	N/A	1.38	1.48	1.34	1.54
Clumpiness index	0.87	0.97	0.97	0.96	0.96
Interspersion index	52.36	74.99	70.42	83.75	77.84
Patch area - MN	20.7	480.6	535.6	148.3	359.0
Patch area - AM	27.8	2,764.9	1,267.7	313.4	1,003.8
Patch area - RA	29.5	5,662.8	2,125.0	670.3	2,083.3
Patch radius of gyration - MN	2.3	9.2	10.1	4.9	10.3
Patch radius of gyration - AM	2.6	34.9	18.3	8.1	24.9
Patch radius of gyration - RA	1.5	77.6	29.8	12.7	57.0
Patch shape index - MN	1.6	1.4	1.4	1.2	1.6
Patch shape index - AM	1.5	2.5	1.8	1.5	2.3
Patch shape index - RA	0.4	3.0	1.4	1.1	2.8
Patch similarity index - MN	5,071.6	48,387.0	55,086.8	54,341.7	58,835.5
Patch similarity index - AM	4,452.4	37,947.3	93,187.3	57,363.3	71,425.6
Patch similarity index - RA	15,547.8	172,922.5	194,539.9	144,617.0	147,735.8
Patch edge contrast index - MN	68.2	45.1	38.0	48.1	59.0
Patch edge contrast index - RA	10.6	70.7	59.4	45.5	50.4

Regional landscape differences

Habitats appeared to be much more fragmented in the estuary than in the northern and southern Gulf (Table 49). Patch density, edge density, and contrast-weighted edge density were much higher while the largest patch index, patch area, patch shape index, patch radius of gyration, and patch similarity index were much lower for the estuary compared with either the northern or southern Gulf. In contrast, the northern and southern Gulf landscapes exhibited marginal differences. This can be interpreted as a more diversified or a less predictable environment in the estuary compared to the northern and southern Gulf. Only two megahabitats occupied a large area in both the northern and southern Gulf (I and K). Habitat fragmentation was greater in the northern Gulf in both cases as evidenced by greater values in the northern Gulf for edge density, contrast-weighted edge density, total edge contrast index, and patch edge contrast index (Table 50).

Table 49. Habitat fragmentation in three landscapes, the estuary and northern and southern Gulf of St. Lawrence, as calculated using FRAGSTATS software. Statistics are also shown for the whole study area.

Variable	Estuary	Northern Gulf	Southern Gulf	Study Area	Units
Total area	8,446.8	136,456.8	80,730.0	225,633.5	km^2
Number of patches	46	195	70	299	-
Patch density	54.46	14.29	8.67	13.25	$no/10^4\ km^2$
Largest patch index	29.6	43.5	38.3	27.4	%
Total edge 1	1,092.5	9,821.5	4,375.5	15,742.5	km
Total edge 2	1,866.5	14,578.5	8,454.5	24,255.5	km
Edge density 1	129.3	72.0	54.2	69.8	m/km^2
Edge density 2	220.97	106.84	104.73	107.5	m/km^2
Contrast weighted edge density	137.4	58.0	64.4	59.0	m/km^2
Total edge contrast index	62.2	54.3	61.5	54.9	%
Perimeter-area fractal dimension	1.24	1.28	1.37	1.31	-
Interspersion index	77.5	67.3	62.2	74.8	%
Patch area - MN	183.6	699.8	1,153.3	754.6	km^2
Patch area - AM	917.0	26,756.4	16,148.5	23,333.1	km^2
Patch area - RA	2,497.3	59,399.3	30,894.0	61,899.3	km^2
Patch radius of gyration - MN	5.4	9.9	10.5	9.7	km
Patch radius of gyration - AM	14.7	88.5	60.4	81.1	km
Patch radius of gyration - RA	30.8	169.8	95.1	181.9	km
Patch shape index - MN	1.3	1.5	1.4	1.5	-
Patch shape index - AM	1.6	2.5	3.2	2.8	-
Patch shape index - RA	1.2	3.0	5.9	5.9	-
Patch similarity index - MN	4,705	66,569	57,514	72,204	-
Patch similarity index - AM	7,151	83,273	109,979	105,319	-
Patch similarity index - RA	9,467	187,629	154,567	255,379	-
Patch edge contrast index - MN	54.3	48.4	44.9	46.3	-

Patch edge contrast index - AM	48.5	41.0	40.5	39.0	-
Patch edge contrast index - RA	54.9	83.1	65.9	79.1	-

Table 50. Habitat fragmentation in two landscapes, the northern and southern Gulf of St. Lawrence, and for two shallow water megahabitats (I and K) calculated using FRAGSTATS software.

Variable	Megahabitat I		Megahabitat K		Units
	Northern Gulf	Southern Gulf	Northern Gulf	Southern Gulf	
Total area of megahabitat	16531.5	3738.3	12968.0	3100.0	km^2
Proportion of total study area	12.1	4.6	9.5	3.8	%
Number of patches	24	14	26	5	-
Patch density	1.76	1.73	1.91	0.62	$no/10^4\ km^2$
Largest patch index 1	4.2	1.3	1.6	2.2	%
Largest patch index 2	34.3	28.1	17.0	58.1	%
Total edge 1	2369.5	1101.5	2921.0	560.0	km
Total edge 2	3904.0	1193.0	3277.0	600.0	km
Edge density 1	17.4	13.6	21.4	6.9	m/km^2
Edge density 2	28.6	14.8	24.0	7.4	m/km^2
Contrast weighted edge density	15.9	4.0	9.5	1.9	m/km^2
Total edge contrast index	55.7	27.0	39.5	25.6	%
Perimeter-area fractal dimension	1.3039	1.7155	1.5223	N/A	-
Clumpiness index	0.97	0.97	0.97	0.98	-
Interspersion index	68.50	65.42	64.26	70.68	%
Patch area - MN	688.8	267.0	498.8	620.0	km^2
Patch area - AM	3408.8	524.8	1270.8	1241.9	km^2
Patch area - RA	5662.8	950.8	2125.0	1600.0	km^2
Patch radius of gyration - MN	11.2	7.3	9.8	10.0	km
Patch radius of gyration - AM	41.4	12.8	19.1	14.5	km
Patch radius of gyration - RA	77.6	19.9	29.8	11.8	km
Patch shape index - MN	1.6	1.2	1.4	1.3	-
Patch shape index - AM	2.8	1.7	1.9	1.4	-
Patch shape index - RA	3.0	1.7	1.4	0.5	-
Patch similarity index - MN	13429	102220	45795	69956	-
Patch similarity index - AM	22369	99590	76806	104866	-
Patch similarity index - RA	73821	126536	146144	120135	-
Patch edge contrast index - MN	56.9	23.4	42.0	28.4	-
Patch edge contrast index - AM	55.2	26.5	37.0	23.0	-
Patch edge contrast index - RA	70.7	26.8	53.5	38.6	-

3. LOCATING FISH HABITATS AND DEFINING KEY HABITAT FEATURES

This section describes how the fish data were prepared for analysis in the sections that follow. The methodology required that data for individual trawl sets be reported at the cell level. Two avenues were explored, one to be applied to rare species or data-poor situations (wolffish, occurrence data; sections 4 to 7) and one applied to data-rich situations (American plaice, reliable abundance data; section 8). The two datasets were analyzed using the same methodology. The relationships between fish data and environmental descriptors, and between fish data and habitat categories, were then examined using a suite of spatial and multivariate statistical analyses.

Materials and Methods

The distribution and habitat associations of three species of wolffish (*Anarhichas denticulatus*, *A. minor*, and *A. lupus*) as well as American plaice (*Hippoglossoides platessoides*) were studied based on catches made during the bottom trawl surveys conducted by the Department of Fisheries and Oceans to assess groundfish abundance in the St. Lawrence lower estuary and Gulf. The surveys have been conducted annually from 1978 in the northern Gulf (Québec Region of DFO) and from 1971 in the southern Gulf (Gulf Region of DFO). In the present report, however, the terms “northern Gulf” and “southern Gulf” refer to the location of an observation relative to the 200 m isobath south of the Laurentian Channel.

Survey methodology

The groundfish surveys focus on commercial species. Depth strata are predetermined, and the number of sets per depth stratum is adjusted according to the planimetric area (area herein) of the stratum. The areal coverage of these surveys in the St. Lawrence estuary and Gulf is extensive, but pelagic and nearshore habitats as well as rough bottoms are not sampled. Juvenile stages may be misrepresented due to their small size or their settling on the seafloor later in the fall, but the surveys are considered adequate to estimate the biomass of pre-recruit and fully recruited groundfish. Whereas the sampling strategy has remained relatively unchanged over time, other factors have changed and methods have differed between the two DFO regions concerned (Gulf and Québec). Surveys were generally conducted in summer, but also occurred in winter. They were not conducted concurrently in the two regions. Spatial coverage changed over time and was less in winter as a result of ice conditions. Finally, gears and vessels have changed over time and differed between regions.

Habitat characterization

Habitat characteristics were obtained from Dutil et al. (2011). In that report, the St. Lawrence estuary and Gulf was divided using a grid made up of 100 km^2 cells (10 km × 10 km), and a hierarchical classification of the seabed at the scale of the megahabitat was proposed based on physiographic and oceanographic features of the study area. The dataset includes each cell’s features, and each cell is assigned to one of 13 different megahabitats. The data are available as a DVD attached to the report (http:/ / www.dfo-mpo.gc.ca/ Library/ 342703.zip). Catch and effort data were matched with habitat categories and corresponding characteristics based on set position in the grid, as described below. Only sets located within cells for which a habitat classification was available were included.

<u>Catch data by set and by cell</u>

Wolffish species

During research surveys, wolffish were identified to species by science staff. These identifications are considered reliable, but whether all catches were recorded in all years in the northern Gulf is unclear (Dutil et al. 2006). Catches are reported by weight, and numbers of wolffish in the catch are available only for some sets in some years. Furthermore, the catch of any species of wolffish is very small and does not allow making corrections for catchability issues. Thus our analyses were conducted using presence/absence data, as opposed to catch in number or in weight.

Catch and effort data were aggregated using a grid made of 100 km^2 square cells (Dutil et al. 2011). The number of sets in which a species was recorded and the number of sets made were determined for each cell. The probability of catching wolffish of a given species in a set and within a cell was calculated as the ratio of the number of sets in which a species was recorded and the total number of sets made. The number of sets in which a species was recorded is considered as its frequency of occurrence and is termed “occurrence,” the number of sets made is considered as the level of effort and is termed “fishing effort.” The term relative occurrence designates the ratio of these two frequencies. The data from both regions until 2008 were considered in our analyses (Figure 20, Table 51).

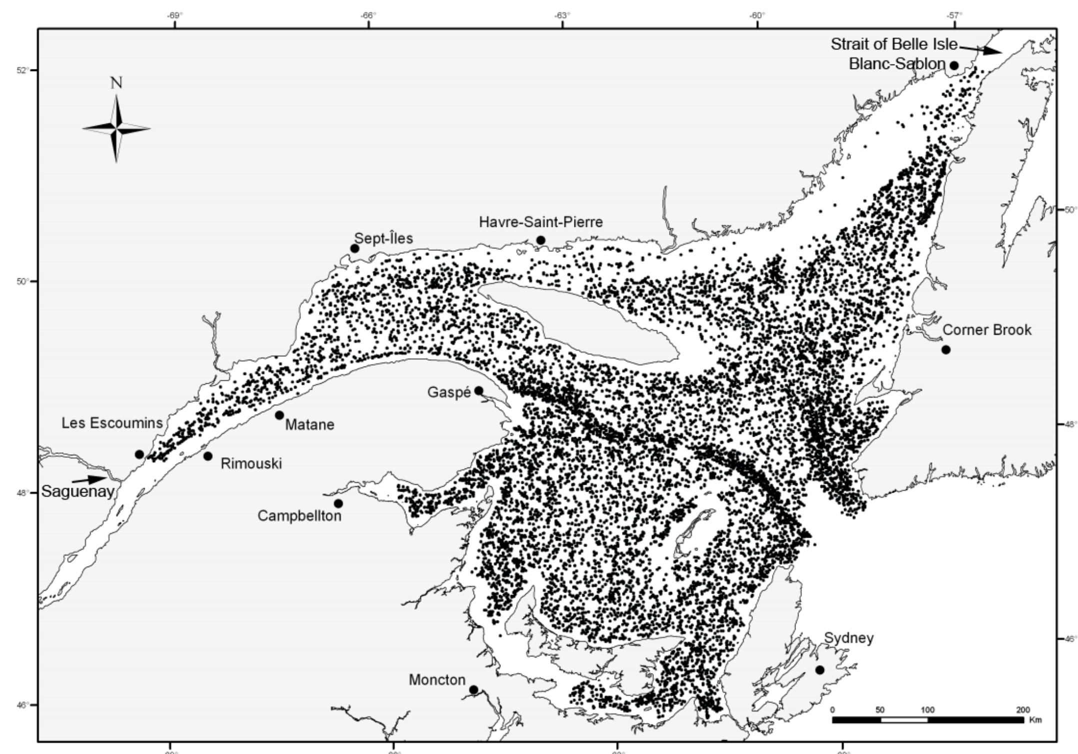

Figure 20. Location of trawl sets (black dots) done between 1971 and 2008 during the annual surveys conducted by the Department of Fisheries and Oceans to assess groundfish abundance in the study area (Gulf and Québec regions). Sets corresponding to cells without a megahabitat classification (near the Saguenay Fjord and into the Strait of Belle Isle) were excluded from the analysis and are not shown.

Table 51. List of variables describing catch and effort data for wolffish species in the DFO annual groundfish surveys conducted in the St. Lawrence estuary and Gulf during the period from 1971 to 2008. Each line in the dataset represents a different cell in a grid, with each cell having a 100 km^2 planimetric area (Dutil et al. 2011). The location of the cell in the grid and the corresponding megahabitat class are given.

Variable	Legend	Description
COL_ROW	Cell ID	Location of cell in a grid. Cell designation uses column number from left to right (1 to 115) and row number from top to bottom (1 to 85). Each cell represents 100 km^2 (10 km × 10 km).
MEGAHABITA	Megahabitat	Class of megahabitat to which the cell belongs; classes described in Dutil et al. 2011.
RR_EFF	Sets 71–08	Number of sets done in the cell during the period from 1971 to 2008.
RR_LAT	Sets with striped wolffish	Number of sets with striped wolffish present in the catch during the period from 1971 to 2008.
RR_LTA	Sets with spotted wolffish	Number of sets with spotted wolffish present in the catch during the period from 1971 to 2008.
RR_LTL	Sets with northern wolffish	Number of sets with northern wolffish present in the catch during the period from 1971 to 2008.
RR_RO_LAT	Relative occurrence of striped wolffish	Proportion of sets with striped wolffish present in the catch during the period from 1984 to 2008 (RR_LAT/RR_EFF).
RR_RO_LTA	Relative occurrence of spotted wolffish	Proportion of sets with spotted wolffish present in the catch during the period from 1984 to 2008 (RR_LTA/RR_EFF).
RR_RO_LTL	Relative occurrence of northern wolffish	Proportion of sets with northern wolffish present in the catch during the period from 1984 to 2008 (RR_LTL/RR_EFF).
OBJECTID		Sequential number attributed automatically by the program (ESRI ArcGIS software).
SHAPE		Vector data type in the geodatabase (information generated by ESRI ArcGIS).

American plaice

Given the reliability of the data for this commercially important species, catch in number and catch in weight were also considered in the analyses. Numbers and weights caught needed to be adjusted to account for catchability issues resulting from differences in gear and vessel over time and between regions. Catchability issues are addressed through comparative fishing operations using the two gears/vessels and parallel tows, but comparative fishing operations were not conducted for all vessel and gear combinations. Differences in catchability were assessed by also considering the potential effects of fish size, fishing depth, and time of day (Benoit and Swain 2003a, 2003b; Bourdages et al. 2007).

The research survey data for the Gulf region (1971–2010) and the Québec region (1978–1981 and 1983–2010) were combined (Figure 21) and used differently depending on whether catch data could be corrected for differences in catchability. When no correction factor was available, catches in number and weight were used for presence/absence analyses only. A species was considered present in a set when catch in either number or weight was > 0. When a correction factor was available, catches in number and weight were expressed as CCGS *Alfred Needler* (vessel) and Western IIa (trawl) equivalent per km^2 of seafloor swept by the trawl. Catch in number was broken down into two size categories, fish smaller and fish larger than 20.5 cm in total length. Correction factors were available for all surveys conducted in the Gulf region and part of the surveys conducted in the Québec region, where catch data for the RV *Gadus atlantica* (all years, both species) and the RV *Lady Hammond* (1984–1986, plaice only) could not be corrected for differences in catchability.

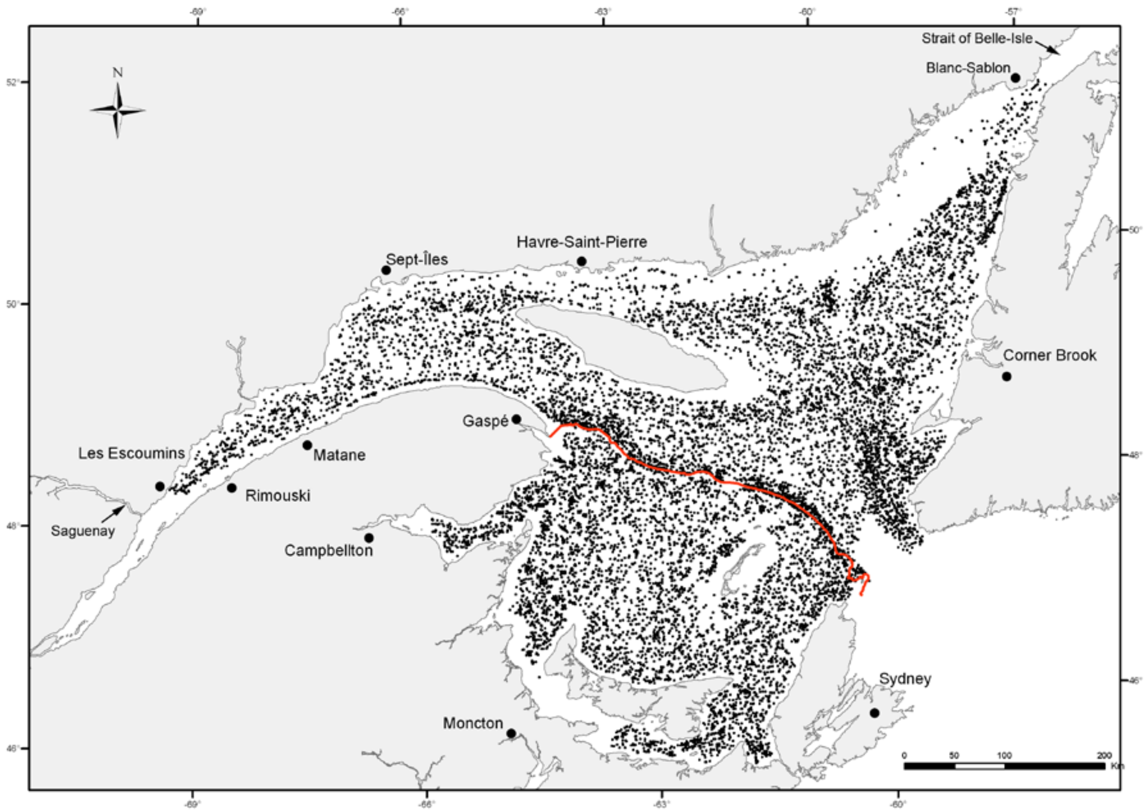

Figure 21. Location of trawl sets (black dots) done between 1971 and 2010 during the annual surveys conducted by the Department of Fisheries and Oceans to assess groundfish abundance in the study area (Gulf and Québec regions). The red line arbitrarily divides the data for the northern and southern Gulf of St. Lawrence and corresponds to the 200 m isobath south of the Laurentian Channel. Sets corresponding to cells without a megahabitat classification (near the Saguenay Fjord and into the Strait of Belle Isle) were excluded from the analysis and are not shown.

For presence/absence analyses, the number of sets done in a cell was considered as a measure of fishing effort in that cell. Frequency occurrence was defined as the number of sets in a cell in which a species was present (number or weight > 0). Relative occurrence was calculated as the ratio of frequency occurrence and fishing effort. For the calculation of the relative occurrence of small and large fish, fishing effort excluded the RV *Gadus atlantica* and the RV *Lady Hammond* (1984–1986) sets for the Québec region, and frequency occurrence in a cell was defined as the number of sets in which small or large fish were present. The relative occurrence in summer and winter was compared; summer observations were those made in August and September, winter observations were those made in January. The mean catch was calculated on sets with species present. Numbers and weights caught (data corrected for changes in catchability) were log transformed ($\log_{10}$), averaged for each cell, and are reported as back-transformed values. For the study area as a whole, the proportion of cells with species present represents the prevalence. Table 52 shows a list and description of the relative occurrence and catch in number and in weight data used in the present study.

Table 53 describes the source data by set (Gulf and Québec, data corrected for differences in catchability). The number of sets selected and corresponding number of cells available for the analyses are shown in Table 54 (wolffish species) and Table 55 (American plaice). The species–environment variables are listed in Table 56.

Table 52. List of variables describing catch and effort data for American plaice in the DFO annual groundfish surveys conducted in the St. Lawrence estuary and Gulf during the period from 1971 to 2010. Each line in the dataset represents a different cell in a grid with each cell having a 100 km^2 planimetric area (Dutil et al. 2011). The location of cells in the grid and corresponding megahabitat class are given.

Variable	Legend	Description
COL_ROW	Cell ID	Location of cell in a grid. Cell designation uses column number from left to right (1 to 115) and row number from top to bottom (1 to 85). Each cell represents 100 km^2 (10 km × 10 km).
MEGAHABITA	Megahabitat	Class of megahabitat to which the cell belongs; classes described in Dutil et al. 2011.
EFF_7110	Number of sets 71–10	Number of sets done in the cell during the period from 1971 to 2010.
P_OC_7110	Number of sets with plaice 71–10	Number of sets with plaice present in the catch during the period from 1971 to 2010.
P_RO_7110	Relative occurrence of plaice 71–10	Proportion of sets with plaice present in the catch during the period from 1971 to 2010 (P_OC_7110/EFF_7110).
EFF_8410	Number of sets 84–10	Number of sets done in the cell during the period from 1984 to 2010.
P_OC_8410	Number of sets with plaice 84–10	Number of sets with plaice present in the catch during the period from 1984 to 2010.
P_RO_8410	Relative occurrence of plaice 84–10	Proportion of sets with plaice present in the catch during the period from 1984 to 2010 (P_OC_8410/EFF_8410).
EFF_8410SL	Number of sets 84–10 (breakdown by size available)	Number of sets done in the cell during the period from 1984 to 2010, excluding surveys and sets for which the catch in number cannot be broken down into size categories.
P_OC_8410S	Number of sets with small plaice 84–10	Number of sets with small plaice (fish < 20.5 cm total length) present in the catch during the period from 1984 to 2010.
P_RO_8410S	Relative occurrence of small plaice 84–10	Proportion of sets with small plaice (fish < 20.5 cm total length) present in the catch during the period 1984 to 2010 (P_OC_8410S/EFF_8410SL).
P_OC_8410L	Number of sets with large plaice 84–10	Number of sets with large plaice (fish > 20.5 cm total length) present in the catch during the period from 1984 to 2010.
P_RO_8410L	Relative occurrence of large plaice 84–10	Proportion of sets with large plaice (fish > 20.5 cm total length) present in the catch during the period from 1984 to 2010 (P_OC_8410L/EFF_8410SL).
EFF_7183	Number of sets 71–83	Number of sets done in the cell during the period from 1971 to 1983.
P_OC_7183	Number of sets with plaice 71–83	Number of sets with plaice present in the catch during the period from 1971 to 1983.
P_RO_7183	Relative occurrence of plaice 71–83	Proportion of sets with plaice present in the catch during the period from 1971 to 1983 (P_OC_7183/EFF_7183).
EFF_8492	Number of sets 84–92	Number of sets done in the cell during the period from 1984 to 1992.
P_OC_8492	Number of sets with	Number of sets with plaice present in the catch during the period from 1984 to 1992.

Variable	Legend	Description
	plaice 84–92	
P_RO_8492	Relative occurrence of plaice 84–92	Proportion of sets with plaice present in the catch during the period from 1984 to 1992 (P_OC_8492/EFF_8492).
EFF_8492SL	Number of sets 84–92 (breakdown by size available)	Number of sets done in the cell during the period from 1984 to 1992, excluding surveys and sets for which the catch in number cannot be broken down into size categories.
P_OC_8492S	Number of sets with small plaice 84–92	Number of sets with small plaice (fish < 20.5 cm total length) present in the catch during the period from 1984 to 1992.
P_RO_8492S	Relative occurrence of small plaice 84–92	Proportion of sets with small plaice (fish < 20.5 cm total length) present in the catch during the period from 1984 to 1992 (P_OC_8492S/EFF_8492SL).
P_OC_8492L	Number of sets with large plaice 84–92	Number of sets with large plaice (fish > 20.5 cm total length) present in the catch during the period from 1984 to 1992.
P_RO_8492L	Relative occurrence of large plaice 84–92	Proportion of sets with large plaice (fish > 20.5 cm total length) present in the catch during the period from 1984 to 1992 (P_OC_8492L/EFF_8492SL).
EFF_9301	Number of sets 93–01	Number of sets done in the cell during the period from 1993 to 2001.
P_OC_9301	Number of sets with plaice 93–01	Number of sets with plaice present in the catch during the period from 1993 to 2001.
P_RO_9301	Relative occurrence of plaice 93–01	Proportion of sets with plaice present in the catch during the period from 1993 to 2001 (P_OC_9301/EFF_9301).
EFF_9301SL	Number of sets 93–01 (breakdown by size available	Number of sets done in the cell during the period from 1993 to 2001, excluding surveys and sets for which the catch in number cannot be broken down into size categories.
P_OC_9301S	Number of sets with small plaice 93–01	Number of sets with small plaice (fish < 20.5 cm total length) present in the catch during the period from 1993 to 2001.
P_RO_9301S	Relative occurrence of small plaice 93–01	Proportion of sets with small plaice (fish < 20.5 cm total length) present in the catch during the period from 1993 to 2001 (P_OC_9301S/EFF_9301SL).
P_OC_9301L	Number of sets with large plaice 93–01	Number of sets with large plaice (fish > 20.5 cm total length) present in the catch during the period from 1993 to 2001.
P_RO_9301L	Relative occurrence of large plaice 93–01	Proportion of sets with large plaice (fish > 20.5 cm total length) present in the catch during the period from 1993 to 2001 (P_OC_9301L/EFF_9301SL).
EFF_0210	Number of sets 02–10	Number of sets done in the cell during the period from 2002 to 2010.
P_OC_0210	Number of sets with plaice 02–10	Number of sets with plaice present in the catch during the period from 2002 to 2010.
P_RO_0210	Relative occurrence of plaice 02–10	Proportion of sets with plaice present in the catch during the period from 2002 to 2010 (P_OC_0210/EFF_0210).
EFF_0210SL	Number of sets 02–10 (breakdown by size	Number of sets done in the cell during the period from 2002 to 2010, excluding surveys and sets for which the catch in number cannot be broken down into size categories.

Variable	Legend	Description
	available)	
P_OC_0210S	Number of sets with small plaice 02–10	Number of sets with small plaice (fish < 20.5 cm total length) present in the catch during the period from 2002 to 2010.
P_RO_0210S	Relative occurrence of small plaice 02–10	Proportion of sets with small plaice (fish < 20.5 cm total length) present in the catch during the period from 2002 to 2010 (P_OC_0210S/EFF_0210SL).
P_OC_0210L	Number of sets with large plaice 02–10	Number of sets with large plaice (fish > 20.5 cm total length) present in the catch during the period from 2002 to 2010.
P_RO_0210L	Relative occurrence of large plaice 02–10	Proportion of sets with large plaice (fish > 20.5 cm total length) present in the catch during the period from 2002 to 2010 (P_OC_0210L/EFF_0210SL).
EFF_S8492	Number of sets, summer 84–92	Number of sets done in the cell in summer during the period from 1984 to 1992.
P_OC_S8492	Number of sets with plaice, summer 84–92	Number of sets with plaice present in the catch in summer during the period from 1984 to 1992.
P_RO_S8492	Relative occurrence of plaice, summer 84–92	Proportion of sets with plaice present in the catch in summer during the period from 1984 to 1992 (P_OC_S8492/EFF_S8492).
EFF_W8492	Number of sets, winter 84–92	Number of sets done in the cell in winter during the period from 1984 to 1992.
P_OC_W8492	Number of sets with plaice, winter 84–92	Number of sets with plaice present in the catch in winter during the period from 1984 to 1992.
P_RO_W8492	Relative occurrence of plaice, winter 84–92	Proportion of sets with plaice present in the catch in winter during the period from 1984 to 1992 (P_OC_W8492/EFF_S8492).
P_CW_8410	Catch in weight of plaice 84–10	Mean catch in weight of plaice per cell during the period from 1984 to 2010, as CCGS *Alfred Needler* (vessel) and Western IIa (trawl) equivalent weight per km^2 of seafloor swept by the trawl. The mean was calculated on sets with species present.
P_CW_8492	Catch in weight of plaice 84–92	Mean catch in weight of plaice per cell during the period from 1984 to 1992, as CCGS *Alfred Needler* (vessel) and Western IIa (trawl) equivalent weight per km^2 of seafloor swept by the trawl.
P_CW_9301	Catch in weight of plaice 93–01	Mean catch in weight of plaice per cell during the period from 1993 to 2001, as CCGS *Alfred Needler* (vessel) and Western IIa (trawl) equivalent weight per km^2 of seafloor swept by the trawl. The mean was calculated on sets with species present.
P_CW_0210	Catch in weight of plaice 02–10	Mean catch in weight of plaice per cell during the period from 2002 to 2010, as CCGS *Alfred Needler* (vessel) and Western IIa (trawl) equivalent weight per km^2 of seafloor swept by the trawl. The mean was calculated on sets with species present.
P_CN_8410	Catch in number of plaice 84–10	Mean catch in number of plaice per cell during the period from 1984 to 2010, as CCGS *Alfred Needler* (vessel) and Western IIa (trawl) equivalent number per km^2 of seafloor swept by the trawl. The mean was calculated on sets with species present.
P_CN_8410S	Catch in number of small plaice 84–10	Mean catch in number of small plaice (fish < 20.5 cm total length) per cell during the period from 1984 to 2010, as CCGS *Alfred Needler* (vessel) and Western IIa (trawl) equivalent number per km^2 of seafloor swept by the trawl. The mean was calculated on sets with small fish present.

Variable	Legend	Description
P_CN_8410L	Catch in number of large plaice 84–10	Mean catch in number of large plaice (fish > 20.5 cm total length) per cell during the period from 1984 to 2010, as CCGS *Alfred Needler* (vessel) and Western IIa (trawl) equivalent number per km^2 of seafloor swept by the trawl. The mean was calculated on sets with large fish present.
P_CN_8492	Catch in number of plaice 84–92	Mean catch in number of plaice per cell during the period from 1984 to 1992, as CCGS *Alfred Needler* (vessel) and Western IIa (trawl) equivalent number per km^2 of seafloor swept by the trawl. The mean was calculated on sets with species present.
P_CN_8492S	Catch in number of small plaice 84–92	Mean catch in number of small plaice (fish < 20.5 cm total length) per cell during the period from 1984 to 1992, as CCGS *Alfred Needler* (vessel) and Western IIa (trawl) equivalent number per km^2 of seafloor swept by the trawl. The mean was calculated on sets with small fish present.
P_CN_8492L	Catch in number of large plaice 84–92	Mean catch in number of large plaice (fish > 20.5 cm total length) per cell during the period from 1984 to 1992, as CCGS *Alfred Needler* (vessel) and Western IIa (trawl) equivalent number per km^2 of seafloor swept by the trawl. The mean was calculated on sets with large fish present.
P_CN_9301	Catch in number of plaice 93–01	Mean catch in number of plaice per cell during the period from 1993 to 2001, as CCGS *Alfred Needler* (vessel) and Western IIa (trawl) equivalent number per km^2 of seafloor swept by the trawl. The mean was calculated on sets with species present.
P_CN_9301S	Catch in number of small plaice 93–01	Mean catch in number of small plaice (fish < 20.5 cm total length) per cell during the period from 1993 to 2001, as CCGS *Alfred Needler* (vessel) and Western IIa (trawl) equivalent number per km^2 of seafloor swept by the trawl. The mean was calculated on sets with small fish present.
P_CN_9301L	Catch in number of large plaice 93–01	Mean catch in number of large plaice (fish > 20.5 cm total length) per cell during the period from 1993 to 2001, as CCGS *Alfred Needler* (vessel) and Western IIa (trawl) equivalent number per km^2 of seafloor swept by the trawl. The mean was calculated on sets with large fish present.
P_CN_0210	Catch in number of plaice 02–10	Mean catch in number of plaice per cell during the period from 2002 to 2010, as CCGS *Alfred Needler* (vessel) and Western IIa (trawl) equivalent number per km^2 of seafloor swept by the trawl. The mean was calculated on sets with species present.
P_CN_0210S	Catch in number of small plaice 02–10	Mean catch in number of small plaice (fish < 20.5 cm total length) per cell during the period from 2002 to 2010, as CCGS *Alfred Needler* (vessel) and Western IIa (trawl) equivalent number per km^2 of seafloor swept by the trawl. The mean was calculated on sets with small fish present.
P_CN_0210L	Catch in number of large plaice 02–10	Mean catch in number of large plaice (fish > 20.5 cm total length) per cell during the period from 2002 to 2010, as CCGS *Alfred Needler* (vessel) and Western IIa (trawl) equivalent number per km^2 of seafloor swept by the trawl. The mean was calculated on sets with large fish present.
OBJECTID		Sequential number attributed automatically by the program (ESRI ArcGIS software).
SHAPE		Vector data type in the geodatabase (information generated by ESRI ArcGIS).

Table 53. List of variables describing bottom trawl sets and associated catches of American plaice in the DFO annual groundfish surveys conducted in the St. Lawrence estuary and Gulf during the period from 1971 to 2010.

Variable	Legend	Description
REGION	DFO region	DFO region responsible for the data and the surveys. NR: Québec Region; SR:Gulf Region.
SET_ID	Trawl set ID	Trawl set identification. The code contains the information required to trace set data in the corporate databases. The first two digits designate the DFO region (variable REGION). For the DFO Québec region surveys, the code indicates the source project, survey number, vessel code, and set number. For the DFO Gulf region surveys, the code indicates the cruise number, vessel code, and set number.
SET_LAT	Latitude of set	Position of the trawl set in decimal degrees – WGS84 (World Geodetic System, 1984 revision).
SET_LON	Longitude of set	Position of the trawl set in decimal degrees – WGS84 (World Geodetic System, 1984 revision).
DATE	Date	Trawl set date as DD-MMM-YYYY.
YEAR	Year	Year of the survey.
MONTH	Month	Month when the trawl set took place.
DAY	Day	Day when the trawl set took place.
TIME	Hour	Time of day (24-hour clock) when the trawl set took place.
NAFO	NAFO division	NAFO division where the trawl set occurred.
NAFO_SUB	NAFO subdivision	NAFO subdivision where the trawl set occurred.
P_OC	Plaice occurrence	Presence of plaice in the catch *Yes*= plaice present; *No*= plaice absent.
P_CW	Catch in weight	Catch in weight of American plaice as CCGS *Alfred Needler* (vessel) and Western IIa (trawl) equivalent per km^2 of seafloor swept by the trawl.
P_CN	Catch in number	Catch in number of American plaice as CCGS *Alfred Needler* (vessel) and Western IIa (trawl) equivalent per km^2 of seafloor swept by the trawl.
P_CN_S	Number < 20.5 cm	Catch in number of small American plaice, fish < 20.5 cm total length.
P_CN_L	Number > 20.5 cm	Catch in number of large American plaice, fish > 20.5 cm total length.
COL_ROW	Cell ID	Location of set in a grid. Cell designation uses column number from left to right (1 to 115) and row number from top to bottom (1 to 85). Each cell represents 100 km^2 (10 km × 10 km).
MEGAHABITA	Megahabitat	Class of megahabitat to which the cell belongs; classes described in Dutil et al. 2011.

Table 54. Number of trawl sets and number of cells selected (LAT: striped wolffish, LTA: spotted wolffish, LTL: northern wolffish). Only cells for which both a catch and a megahabitat classification are available were considered (1971–2008). Variable names refer to Tables 51–53 above.

Variable	Number of sets selected	Number of cells
RR_EFF	13117	1906
RR_LAT	1306	493
RR_LTA	248	187
RR_LTL	102	90
RR_RO_LAT	1306	493
RR_RO_LTA	248	187
RR_RO_LTL	102	90

Table 55. Number of trawl sets and number of cells selected for American plaice. Only cells for which both a fishing effort and a megahabitat classification are available were considered (1971–2010). Variable names refer to Tables 51–53 above.

Variable	Number of sets selected	Number of cells
EFF_7110	12742	1899
P_OC_7110	9888	1804
P_RO_7110		1899
EFF_8410	11275	1873
P_OC_8410	8655	1764
P_RO_8410		1873
EFF_8410SL	9676	1824
P_OC_8410S	6413	1476
P_RO_8410S		1824
P_OC_8410L	7793	1608
P_RO_8410L		1824
EFF_7183	1467	850
P_OC_7183	1233	766
P_RO_7183		850
EFF_8492	4359	1473
P_OC_8492	3222	1281
P_RO_8492		1473
EFF_8492SL	2940	1254
P_OC_8492S	1612	759
P_RO_8492S		1254
P_OC_8492L	2090	951

P_RO_8492L		1254
EFF_9301	3655	1465
P_OC_9301	2668	1226
P_RO_9301		1465
EFF_9301SL	3478	1442
P_OC_9301S	1938	960
P_RO_9301S		1442
P_OC_9301L	2382	1107
P_RO_9301L		1442
EFF_0210	3261	1421
P_OC_0210	2765	1283
P_RO_0210		1421
EFF_0210SL	3258	1420
P_OC_0210S	2278	1154
P_RO_0210S		1420
P_OC_0210L	2577	1216
P_RO_0210L		1420
EFF_S8492	3257	1350
P_OC_S8492	2367	1079
P_RO_S8492		1350
EFF_W8492	952	467
P_OC_W8492	771	422
P_RO_W8492		467
P_CW_8410	7661	1684
P_CW_8492	2385	1072
P_CW_9301	2511	1165
P_CW_0210	2765	1288
P_CN_8410	7704	1681
P_CN_8410S	5828	1772
P_CN_8410L	7049	1598
P_CN_8492	2438	1094
P_CN_8492S	1612	759
P_CN_8492L	2090	951
P_CN_9301	2504	1163
P_CN_9301S	1938	960
P_CN_9301L	2382	1107
P_CN_0210	2762	1282
P_CN_0210S	2278	1154
P_CN_0210L	2577	1216

Table 56. List of variables used to examine species–environment relationships. Variable name and legend are in French in the database; a description is provided for each variable or group of variables.

Variable	Legend	Description
MHVar_3x3	Diversité des habitats	Number of megahabitats in a 15 km radius around the cell.
MHVar_3x3_2		Squared value of MHVar_3x3.
Relief_var	Variabilité du relief	Number of reliefs (maximum of 9) represented in the cell.
Relief_var_2		Squared value of Relief_var.
Pro_Protege		Planimetric area of sheltered marine environment, expressed as a proportion of the area of the cell marine environment (calculated from Sup_Protege, Sup_SemiExp, Sup_Exp).
Pro_Protege_2		Squared value of Sup_Protege.
Pro_SemiExp		Planimetric area of semi-exposed marine environment, expressed as a proportion of the area of the cell marine environment (calculated from Sup_Protege, Sup_SemiExp, Sup_Exp).
Pro_SemiExp_2		Squared value of Sup_SemiExp.
Cote_Dist	Distance à la côte	Distance between the cell centroid and the nearest shore (m) at low tide on the mainland and on islands longer than 1.5 km on their longer axis (based on the CanVec data product -NRCan, spatial resolution of 1:50,000).
Cote_Dist_2		Squared value of Cote_Dist.
Bathy_Mean	Profondeur moyenne	Mean depth for the cell.
Bathy_Mean_2		Squared value of Bathy_Mean.
Bathy_STD	Profondeur moyenne (e.t.)	Standard deviation of depths for the cell.
Bathy_STD_2		Squared value of Bathy_STD.
Bathy_Max	Profondeur maximale	Maximum depth.
Bathy_Max_2		Squared value of Bathy_Max.
Bathy_Min	Profondeur minimale	Minimum depth.
Bathy_Min_2		Squared value of Bathy_Min.
Pente_Mean	Pente moyenne	Mean slope for the cell.
Pente_Mean_2		Squared value of Pente_Mean.
Pente_STD	Pente (e.t.)	Standard deviation of slopes for the cell.
Pente_STD_2		Squared value of Pente_STD.
Pente_Max	Pente maximale	Maximum slope.
Pente_Max_2		Squared value of Pente_Max.
Pente_Min	Pente minimale	Minimum slope.
Pente_Min_2		Squared value of Pente_Min.
Geo2_Bosse	Proportion - Bosse	Proportion of the cell surface area classified as being humps, based on Geomorph_2.
Geo2_Bosse_2		Squared value of Geo2_Bosse.
Geo2_Creux	Proportion - Creux	Proportion of the cell surface area classified as being pits, based on Geomorph_2.

Geo2_Creux_2	Salinité	Squared value of Geo2_Creux.
SalMoyMoy	MoPrMo	Bottom mean annual salinity according to BathyMoy_ajustée.
SalMoyMoy_2		Squared value of SalMoyMoy.
SalMinMoy	Salinité MiPrMo	Bottom monthly minimal salinity according to BathyMoy_ajustée.
SalMinMoy_2		Squared value of SalMinMoy.
SalMaxMoy	Salinité MaPrMo	Bottom monthly maximal salinity according to BathyMoy_ajustée.
SalMaxMoy_2		Squared value of SalMaxMoy.
SalMoyMin	Salinité MoPrMi	Bottom mean annual salinity according to BathyMin_ajustée.
SalMoyMin_2		Squared value of SalMoyMin.
SalMinMin	Salinité MiPrMi	Bottom monthly minimal salinity according to BathyMin_ajustée.
SalMinMin_2		Squared value of SalMinMin.
SalMaxMin	Salinité MaPrMi	Bottom monthly maximal salinity according to BathyMin_ajustée.
SalMaxMin_2		Squared value of SalMaxMin.
SalMoyMax	Salinité MoPrMa	Bottom mean annual salinity according to BathyMax_ajustée.
SalMoyMax_2		Squared value of SalMoyMax.
SalMinMax	Salinité MiPrMa	Bottom monthly minimal salinity according to BathyMax_ajustée.
SalMinMax_2		Squared value of SalMinMax.
SalMaxMax	Salinité MaPrMa	Bottom monthly maximal salinity according to BathyMax_ajustée.
SalMaxMax_2		Squared value of SalMaxMax.
TempMoyMoy	Température MoPrMo	Bottom mean annual temperature (°C) according to BathyMoy_ajustée.
TempMoyMoy_2		Squared value of TempMoyMoy.
TempMinMoy	Température MiPrMo	Bottom monthly minimal temperature (°C) according to BathyMoy_ajustée.
TempMinMoy_2		Squared value of TempMinMoy.
TempMaxMoy	Température MaPrMo	Bottom monthly maximal temperature (°C) according to BathyMoy_ajustée.
TempMaxMoy_2		Squared value of TempMaxMoy.
TempMoyMin	Température MoPrMi	Bottom mean annual temperature (°C) according to BathyMin_ajustée.
TempMoyMin_2		Squared value of TempMoyMin.
TempMinMin	Température MiPrMi	Bottom monthly minimal temperature (°C) according to BathyMin_ajustée.
TempMinMin_2		Squared value of TempMinMin.
TempMaxMin	Température MaPrMi	Bottom monthly maximal temperature (°C) according to BathyMin_ajustée.
TempMaxMin_2		Squared value of TempMaxMin.
TempMoyMax	Température MoPrMa	Bottom mean annual temperature (°C) according to BathyMax_ajustée.
TempMoyMax_2		Squared value of TempMoyMax.
TempMinMax	Température MiPrMa	Bottom monthly minimal temperature (°C) according to BathyMax_ajustée.
TempMinMax_2	Température	Squared value of TempMinMax.
TempMaxMax	MaPrMa	Bottom monthly maximal temperature (°C) according to BathyMax_ajustée.

TempMaxMax_2	Squared value of TempMaxMax.
Geo_Plateau	Class with greatest area within the cell: plateau (depth < 200 m and slope < 0.8° (binary).
Geo_Talus	Class with greatest area within the cell: slope (slope≥ 0.8° (binary).
Geo_Chenal	Class with greatest area within the cell: channel (depth > 200 m and slope < 0.8° (binary).
Oxy_12	Class 1 and 2 of mean dissolved oxygen saturation: 0 to 35% (binary).
Oxy_34	Class 3 and 4 of mean dissolved oxygen saturation: 35 to 55% (binary).
Oxy_56	Class 5 and 6 of mean dissolved oxygen saturation: 55 to 75% (binary).
Oxy_78	Class 7 and 8 of mean dissolved oxygen saturation: 75 to 100% (binary).
Sed1_100	Sediments code: mainly pelites (binary).
Sed1_200	Sediments code: mainly sand (binary).
Sed1_300	Sediments code: gravely sand (binary).
Sed1_400	Sediments code: various coarse sediments (binary).
Sed2	Outcrop present or absent (binary).

Spatial analysis

In the present report, “northern Gulf” and “southern Gulf” refer to the location of an observation relative to the 200 m isobath, south of the Laurentian Channel (Figure 21). Similar methods were used to assess the distribution, habitat associations, and environmental relationships of all species. For wolffish species, only relative occurrence data were considered for a single period. In contrast, catch in number and in weight as well as relative occurrence data were compared for two size categories and several periods for American plaice.

Area of occupancy

The area of occupancy was determined by overlapping species occurrence (presence/absence data, by cell) with the 100 km^2 grid used to study habitat classification in the study area (Dutil et al. 2011). A species was considered present in a cell when reported in at least one set done in that cell during the bottom trawl research surveys conducted annually by DFO. Conversely, a species was considered absent when not reported in any of the sets done in that cell. Cells with no observation (no fishing done) were excluded from the analyses. The Hernández and Navarro (2007) cartographic and conglomerate method was applied to centroids of cells in which the species was present. The method identifies clusters of observations (referred to as conglomerates) and isolated observations (referred to as satellite observations). The maximum distance between observations (cell centroids in the present study) within a conglomerate determines the scale of the grid used to determine the area corresponding to each observation within that conglomerate. Thus the scale of the grid varies with the size of the conglomerate. The area of occupancy is shown as a multiple grid map based on presence and its size is determined by summing the planimetric area of cells across conglomerates and satellites (land excluded). When two grids overlapped, the overlapping surface was reported to the smallest conglomerate. Satellite observations were considered to occupy a minimum planimetric area of 1 km^2, since the side of square cells in the finest grid (smallest conglomerate) measured 1 km, i.e., 10% of the shortest distance between centroids in the input grid (10 km) (Hernández and Navarro 2007).

Patterns and clusters of distribution

Density maps of relative occurrence were generated with ESRI ArcGIS 10.0 software and the Spatial Analyst extension using the kernel density estimate method (quartic kernel function). A 20 km search radius was used. Results are shown as a map of volume density (kernel density broken down by geometrical interval). Planimetric areas corresponding to the 50%, 90%, and 95% volume density contours were calculated to be compared with the Hernández and Navarro (2007) area of occupancy estimates.

The spatial pattern of distribution of relative occurrence of a species in the study area was determined as follows. The Moran’s *I* global spatial autocorrelation parameter was calculated. The Global Moran's *I* tool in ArcGIS calculates a Z-score and associated p value based on the randomization null hypothesis. Moran’s *I* value is expected to be near zero under the null hypothesis of no spatial pattern. A positive value indicates clustering, a negative value indicates dispersion. The spatial pattern observed was considered clustered when the Global Moran's *I* index was significant at $\alpha = 0.10$.

When a positive and significant Global Moran's *I* index was obtained, indicating clustering, the Getis and Ord (1992) G_i* local spatial autocorrelation statistic (actually a Z-score) was calculated for each cell in the grid (cells with fishing effort > 0 for wolffish, all cells for American plaice). Concentrations of low relative occurrence (cold spots) have negative G_i* scores whereas concentrations of high relative occurrence (hot spots) have positive G_i* scores. G_i* scores were considered significant at $\alpha = 0.10$. For both the Moran’s *I* and the Getis and Ord G_i* statistics, the Euclidean distance was used as the distance method and spatial relationships were examined within a 20 km distance band (zone of indifference model in the application). G_i* values for significant hot spots and cold spots are shown as a map (broken down by geometrical interval) and were used in subsequent species–environment statistical analyses.

These analyses with occurrence data were repeated using the catch in number and catch in weight data for American plaice.

<u>Habitat relationships</u>

The degree of association between species and megahabitats was determined by cluster analysis (Primer, version 6.1.13). The following characteristics were obtained for each megahabitat: number of cells in which the species occurred, expressed as a proportion of the total number of cells in that megahabitat; mean relative occurrence of species; mean Getis and Ord G_i* statistic, based on relative occurrence, for all cells of the megahabitat as well as only for cells where the species occurred; and degree of overlap of megahabitat with distribution features (area of occupancy, kernel density contour limits, and cold- and hot-spot classification, based on relative occurrence). For American plaice, additional characteristics were used: mean relative occurrence of species and mean Getis and Ord G_i* statistic, based on catch in number, for all cells of the megahabitat as well as only for cells where the species occurred, and degree of overlap of megahabitat with distribution features (area of occupancy, kernel density contour limits, and cold- and hot-spot classification, based on catch in number).

A cell was considered to be located within the area of occupancy when more than 50% of its planimetric area (marine environment only) overlapped any of the conglomerates and satellites described above (coded 0 or 1). Similarly, a surface area criterion was used to classify cells into three categories based on the kernel density estimates: cells with more than 50% of their planimetric area located within the 90% contour line were split into high density (within the 50% volume contour) and low density (50–90% volume contour) cells (coded 50 and 90, respectively). Cells with more than 50% of their planimetric area located outside of the 90% volume contour were coded 100. Cells were also classified into cold spots (coded 1) and hot spots (coded 2) based on the value of the G_i* index as described above. The frequency occurrence of cells coded 1 based on the area of occupancy, 50 or 90 based on the kernel density estimates, and 1 or 2 based on the G_i* index value was reported as a proportion of the total number of cells in that megahabitat (e.g., number of cells of megahabitat A classified as hot spots/number of cells classified as megahabitat A), and as a proportion of the number of cells where the species occurred in each megahabitat (e.g., number of cells of megahabitat A having a relative occurrence value > 0 and classified as hot spots / number of cells classified as megahabitat A and having a relative occurrence value > 0). The procedure was repeated for catch in number with American plaice.

The cluster analysis used a distance matrix (Euclidean distance) based on the data standardized to 0 mean and unit standard deviation (14 variables for the wolffish species and 27 for American plaice; see tables in Results). The group average option was selected for wolffish species, whereas the complete linkage option was selected for American plaice. The significance was tested with similarity profile permutation tests (SIMPROF, using 1000 permutations; $\alpha = 0.05$). The relative distance between megahabitats is shown as 2-D MDS graphs based on the distance matrix (Euclidean distance) and the Kruskal stress value is shown. Considering that the size of the megahabitats varies and to account for a potentially significant overall contribution of a large megahabitat with a low average relative occurrence (wolffish species) or low average catch in number, two additional variables were created. For each wolffish species, the number of cells where the presence of the species had been confirmed was multiplied by the mean relative occurrence. For American plaice, the number of cells where the presence of the species had been confirmed was multiplied by the mean catch in number (based on sets with catches > 0). These variables are referred to as the *relative occurrence weighted area* and *catch in number weighted area* herein. They are used in the MDS graphs as an index of overall contribution of the megahabitat to the status of the species in the study area.

<u>Environmental relationships</u>

Two sets of analyses were conducted on each wolffish species and American plaice. One analysis sought to determine which environmental variables could explain the variability in relative occurrence, catch in number, or catch in weight. The other sought to identify the environmental variables that contributed most to explaining the degree of spatial correlation (G_i* as the dependent variable), i.e., the degree of clustering and hot-spot formation in relative occurrence, catch in number, or catch in weight. For wolffish species, only cells with relative occurrence values > 0 were used in the first analysis and only cells with G_i* values > 0 were used in the second analysis. Relative occurrence (all species), catch in number or catch in weight (American plaice only) data were transformed to a normal distribution (square root of fourth root transform). Latitude and longitude of cells were transformed into coordinates (distance in km from a reference cell in the lower left corner of the grid), and their effects on relative occurrence, catch in number, or catch in weight as well as their effects on G_i* values based on relative occurrence, catch in number, or catch in weight were tested with a multiple linear regression model. When the model was significant, the residuals were used as the dependent variable in subsequent analyses.

The potential explanatory variables were obtained from the megahabitat database. The quantitative variables and their quadratic form (n=33) were centered. Categorical variables in the source database (Geomorph_1, O2_Sat_Classe, Classe_oxygene) were split into binary variables (n=12) (Table 58). A multiple linear regression was fitted by permutation under a reduced model and the resulting model R^2 value used, in combination with the 0.05 critical value, as a stopping criterion in a forward selection multiple linear regression analysis (Blanchet et al. 2008). Variance inflation factors above 20 were considered collinear and the number of significant variables in the model was adjusted accordingly. Multiple linear regression model results (R^2 value adjusted) are presented and partial R^2 values are reported.

For quantitative variables describing environmental conditions, the mean, median, 5th, 25th, 75th, and 95th percentiles are reported for cells where the species was found to occur (relative occurrence > 0) and cells where the species was found to cluster (local spatial autocorrelation G_i* statistic value > 1.645). The number of cells and proportion of cells meeting the classification criteria were also calculated for 12 binary variables describing environmental conditions for cells where the species was found to occur (relative occurrence > 0) and cells where the species was found to cluster (local spatial autocorrelation G_i* statistic value > 1.645).

The environmental relationships of the three species of wolffish were compared through redundancy analysis (scaling 2 method, with weighted averages). Two sets of analyses were done, one that considered all cells in which at least one of the three species was present (578 cells with relative occurrence > 0) and one that considered all cells with a G_i* value > 0 for any of the three species (902 cells). Relative occurrence data were square-root transformed and G_i* data were fourth-root transformed. Latitude and longitude effects were assessed through linear regression and the residuals from those regressions were used as the three response variables. The quantitative environmental variables and their quadratic form were centered and the categorical environmental variables were considered as factors in the multivariate regressions. A stepwise regression model was used (Vegan package RDA and *ordistep* procedures in R). Variance inflation factors above 20 were considered collinear and the number of significant variables in the model was adjusted accordingly. The global and partial R^2 values were calculated for the remaining variables in the final model. The significance of the model and canonical axes were tested by permutation (999 permutations; Vegan package RDA and *anova* procedures in R). The biplots presented used the weighted average scores.

<u>Relationships with other species</u>

For striped and spotted wolffishes (section 7) and plaice (section 8), cells were grouped using a multivariate regression tree based on both catch composition and environmental conditions. Groupings important to these species are presented in their respective sections. Details of tree methods and additional group results are presented in the final chapter (section 9).

4. STRIPED WOLFFISH

Using the relative occurrence data and analyses as described in the Methods (section 3), a set of standardized output maps and tables were produced for striped wolffish. They include a description of the area of occupancy, density maps of occurrence, and global and local spatial autocorrelation statistics and maps. Tables are shown that summarize a set of species scores for each megahabitat category. The scores were then used in cluster analyses and MDS plots to identify the most important and the least important megahabitats for this species. Summary statistics and multiple forward linear regression statistics are provided describing environmental conditions and relationships in areas where striped wolffish occurs and where clusters of higher relative occurrence are found.

Area of occupancy

Striped wolffish were present principally in a single large conglomerate (no. 21) in the northern Gulf (Figure 22), along with several smaller ones (Table 57).

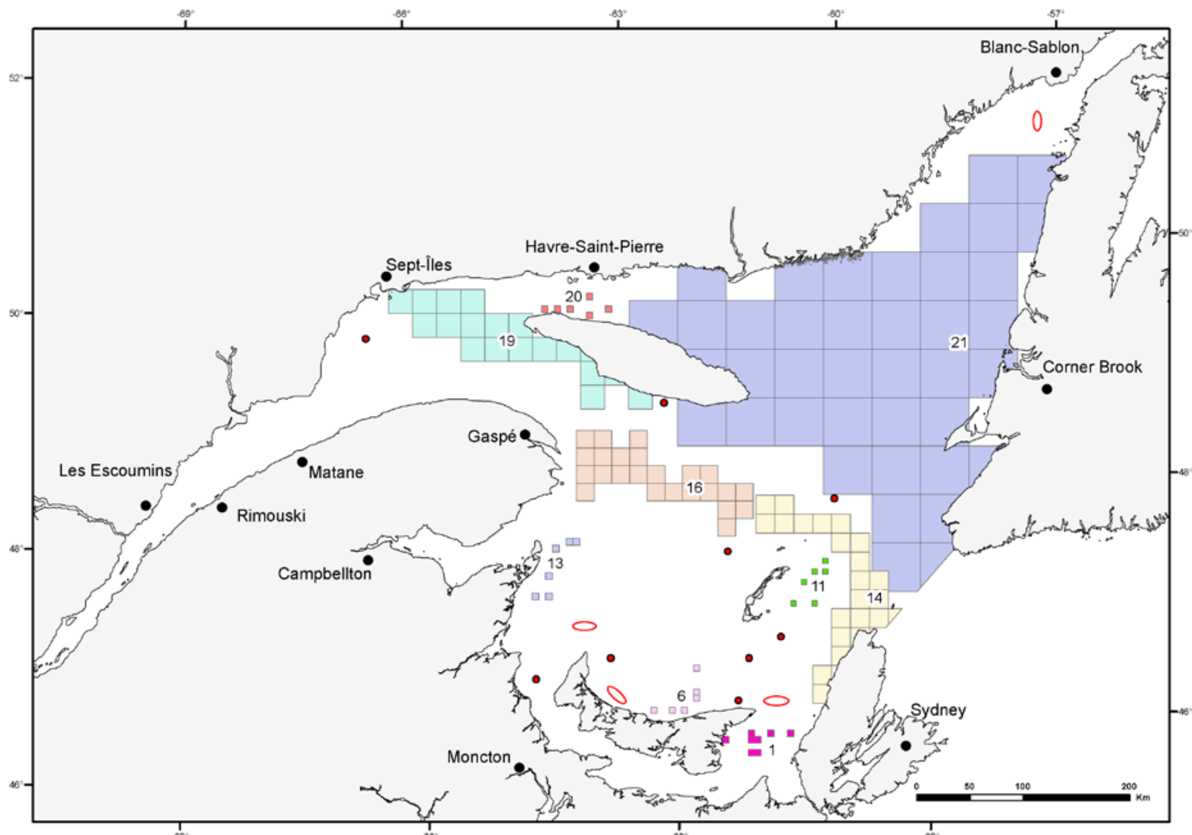

Figure 22. Area of occupancy of striped wolffish in the St. Lawrence estuary and Gulf based on annual bottom trawl surveys conducted by DFO (1971–2008). The numbered grids were produced based on presence data using the Hernández and Navarro (2007) cartographic and conglomerate method. Conglomerates less than 100 km^2 are shown as ovals (not to scale), and satellites (isolated observations) are shown as red dots.

Table 57. Size of the area of occupancy of striped wolffish broken down by conglomerate and satellite groups of observations, based on presence data obtained from annual bottom trawl surveys conducted by DFO (1971–2008). Conglomerate numbers refer to Figure 21.

Conglomerate	Satellite	Planimetric area (km^2)
21		72,625*
19		8,352
14		6,698
16		6,613
01		298
13		287
20		216
06		195
11		150
Others (less than 100 km^2 individually)		10
	n = 9	9
Total area of occupancy		**95,453**

* A 300 km^2 overlap between conglomerates 21 and 14 was subtracted from the planimetric area of conglomerate 21.

Patterns and clusters of distribution

The kernel density estimate method applied to relative occurrence data yielded planimetric areas of 88,465 km^2, 68,678 km^2, and 20,042 km^2 for the 95%, 90% (low density), and 50% (high density) volume density contours, respectively (Figure 23).

The Moran's *I* global spatial autocorrelation parameter yielded a positive (index value=0.486), highly significant ($P<0.0001$) Z-score of 49.4, which clearly indicates a high degree of clustering of striped wolffish relative occurrence in the study area (Figure 24). The local spatial autocorrelation statistic applied to relative occurrence data yielded planimetric areas of 27,700 km^2 for cold spots at $p=0.10$, and 31,669 km^2 for hot spots at $p=0.10$ (including 28,678 km^2 at $p=0.05$ and 23,871 km^2 at $p=0.01$).

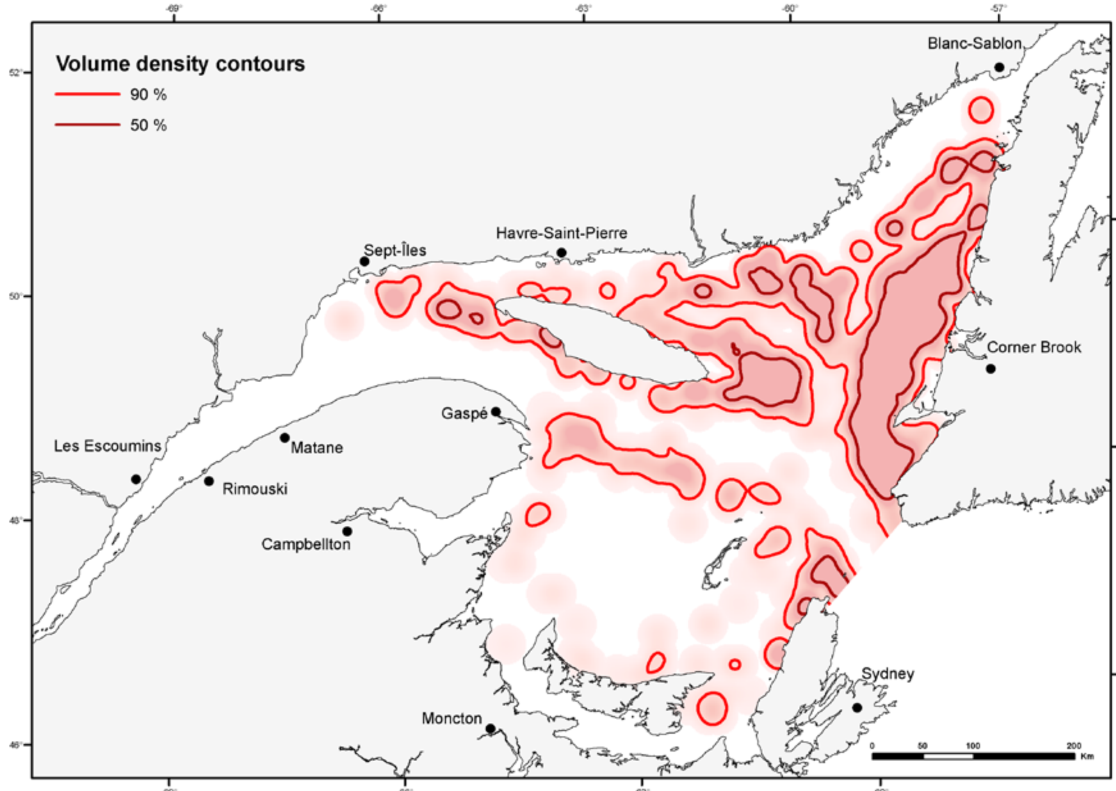

Figure 23. Density map of relative occurrence for striped wolffish in the St. Lawrence estuary and Gulf based on annual bottom trawl surveys conducted by DFO (1971–2008). The 50% and 90% volume density contours are shown.

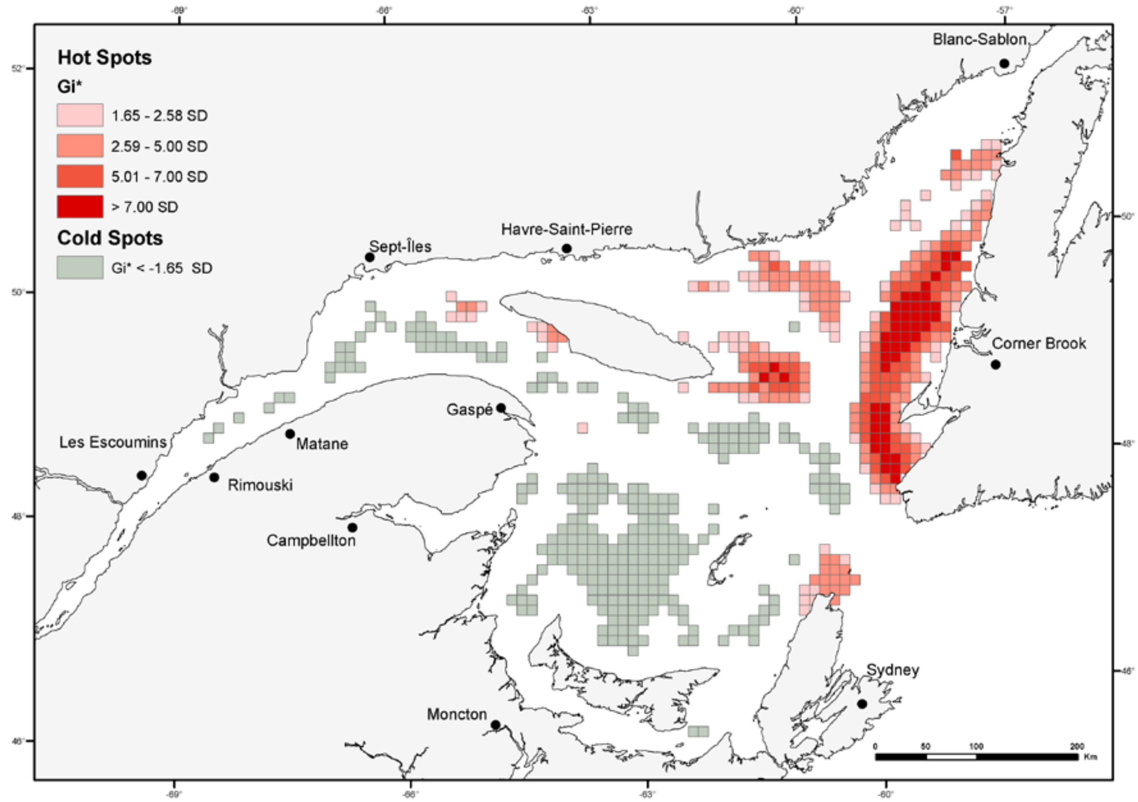

Figure 24. Location of statistically significant clusters of low relative occurrence (cold spots) and high relative occurrence (hot spots) (G_i* Z-scores significant at α=0.10) for striped wolffish in the St. Lawrence estuary and Gulf based on annual bottom trawl surveys conducted by DFO (1971–2008). Significant hot spots are broken down by intervals of Z-score standard deviations (SD). A 20 km bandwith (zone of indifference model) was used.

Habitat relationships

Even though they occurred in 12 different megahabitats, striped wolffish used three contiguous megahabitats most intensively. Deep water megahabitats B (deep water, steep-sloped habitats) and C (deep water shelf habitats), and megahabitat K (relatively cold shallow to mid-depth shelf habitats) occur mainly in the northern Gulf and represented a distinct group of megahabitats on the basis of striped wolffish spatial distribution and relative occurrence (Tables 58 and 59). The cluster analysis formed 5 significant clusters with megahabitats B and C forming a significant group (SIMPROF, p<0.05) with megahabitat K, and being most distant to other groups (Figure 25). That group was characterized by a unique combination of a large proportion of cells overlapping the area of occupancy and within the 50 and 90% volume contours, a low proportion of cells classified as cold spots and a large proportion of cells classified as hot spots. The mean relative occurrence of each of the three megahabitats was high (<0.2) and the local spatial autocorrelation G_i* value was positive and significant (P<0.01) indicating that high relative occurrence values tended to cluster in these megahabitats. The MDS graph (stress value = 0.03; Figure 26) confirmed that megahabitats B, C, and K were similar to each other, i.e., were close to each other in the MDS graph, and dissimilar from other megahabitats. These differences are exemplified by the large size of the bubbles for these megahabitats in three MDS graphs (proportion of cells classified as hot spots, and mean relative occurrence, and G_i* value of cells; Figures 27–29) and small size of the bubbles in the other (proportion of cells classified as cold spots, Figure 26). Striped wolffish megahabitats were most dissimilar to shallow water shelf megahabitats E, H, and J found in the southern Gulf of St. Lawrence. The megahabitat A (deep channels) was singled out when the relative occurrence weighted area was plotted in the MDS graph (Figure 30).

Table 58. Number of cells overlapping the distribution features for striped wolffish, reported as a proportion of the number of cells in each megahabitat. The area of occupancy was determined by the Hernández and Navarro (2007) method using presence/absence data. The other features are based on the species relative occurrence. Cold spots and hot spots were determined based on the Getis and Ord local spatial autocorrelation Gi* statistic (Z-score). Mean relative occurrence and Gi* value are given for each megahabitat. Prime habitats for the species are highlighted.

Megahabitat	Number of cells	Area of occupancy	KDE 90% volume	KDE 50% volume	Cold spot	Hot spot	Relative occurrence	Z-score
A	609	0.622	0.273	0.034	0.161	0.089	0.040	-0.46
B	14	0.929	0.500	0.357	0.000	0.571	0.275	2.34
C	161	0.851	0.385	0.342	0.000	0.460	0.284	2.26
D	129	0.651	0.388	0.109	0.000	0.147	0.113	0.14
E	111	0.009	0.027	0.000	0.009	0.000	0.010	-1.16
G	29	0.759	0.759	0.034	0.000	0.138	0.118	0.41
H	149	0.027	0.074	0.000	0.094	0.000	0.018	-1.23
I	125	0.368	0.272	0.112	0.064	0.264	0.126	0.47
J	351	0.148	0.071	0.074	0.422	0.091	0.038	-0.76
K	134	0.769	0.321	0.418	0.052	0.590	0.305	3.04
L	18	0.444	0.278	0.000	0.056	0.167	0.053	-0.05
M	76	0.395	0.250	0.066	0.000	0.158	0.113	-0.13

Table 59. Number of cells where the species presence was confirmed and overlap between these cells and the distribution features, reported as a proportion of the number of cells in each megahabitat. The area of occupancy was determined by the Hernández and Navarro (2007) method using presence/absence data. The other features are based on the species relative occurrence. Cold spots and hot spots were determined based on the Getis and Ord local spatial autocorrelation Gi* statistic (Z-score). Mean relative occurrence and Gi* value are given for each megahabitat. Prime habitats for the species are highlighted.

Megahabitat	Number of cells	Area of occupancy	KDE 90% volume	KDE 50% volume	Cold spot	Hot spot	Relative occurrence	Z-score
A	109	1.000	0.642	0.183	0.000	0.367	0.225	1.43
B	11	1.000	0.545	0.455	0.000	0.636	0.350	2.93
C	98	0.990	0.439	0.520	0.000	0.663	0.467	3.59
D	54	1.000	0.667	0.259	0.000	0.296	0.270	1.33
E	7	0.143	0.429	0.000	0.000	0.000	0.159	-0.73
G	12	1.000	0.917	0.083	0.000	0.250	0.285	0.95
H	20	0.150	0.300	0.000	0.000	0.000	0.136	-0.91
I	34	0.824	0.559	0.412	0.000	0.588	0.464	2.67
J	40	0.800	0.250	0.525	0.000	0.600	0.333	2.86
K	86	0.977	0.314	0.640	0.000	0.837	0.475	4.86
L	3	0.667	0.667	0.000	0.000	0.333	0.317	0.96
M	19	1.000	0.684	0.263	0.000	0.474	0.450	1.89

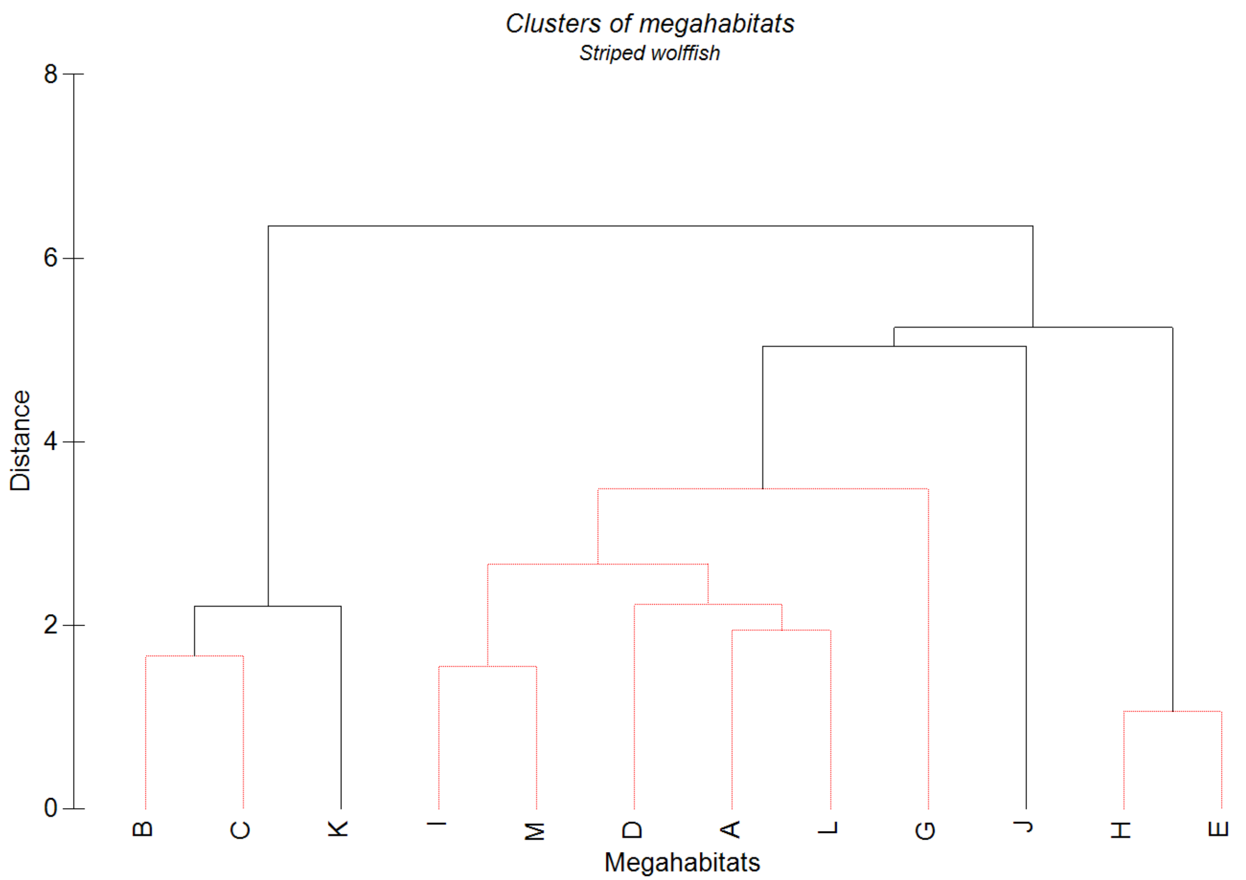

Figure 25. Tree diagram showing significant (black line) clusters of megahabitats based on striped wolffish spatial distribution and relative occurrence descriptors: proportion of cells overlapping the area of occupancy and within the 50 and 90% volume contours, proportion of cells classified as hot spots or cold spots, mean relative occurrence, and local spatial autocorrelation G_i* statistic.

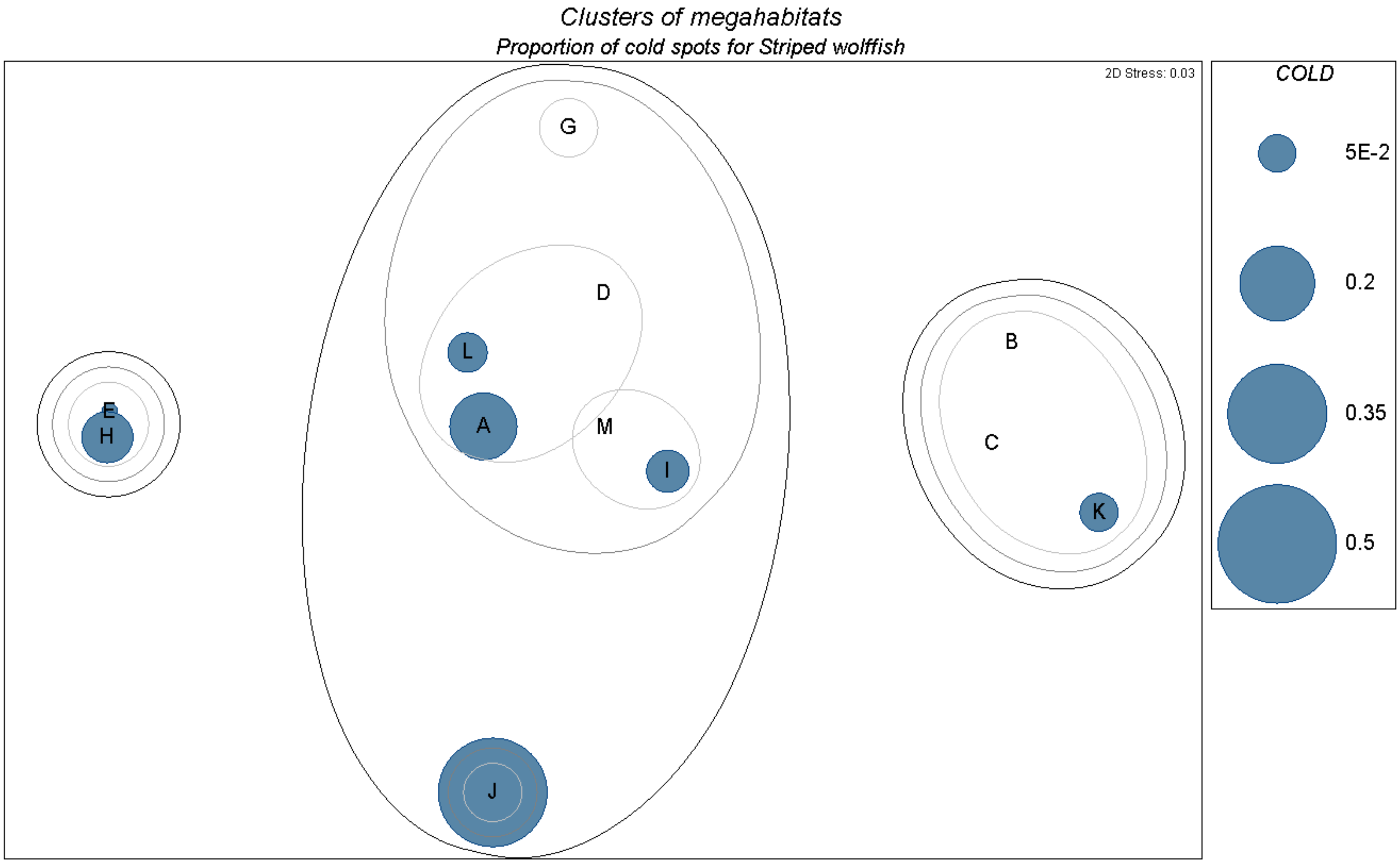

Figure 26. Multidimensional scaling plot of megahabitats based on striped wolffish spatial distribution and relative occurrence descriptors: proportion of cells overlapping the area of occupancy and within the 50 and 90% volume contours, proportion of cells classified as hot spots or cold spots, mean relative occurrence, and local spatial autocorrelation G_i* statistic. Bubble size is proportional to the proportion of cells classified as cold spots in the megahabitat.

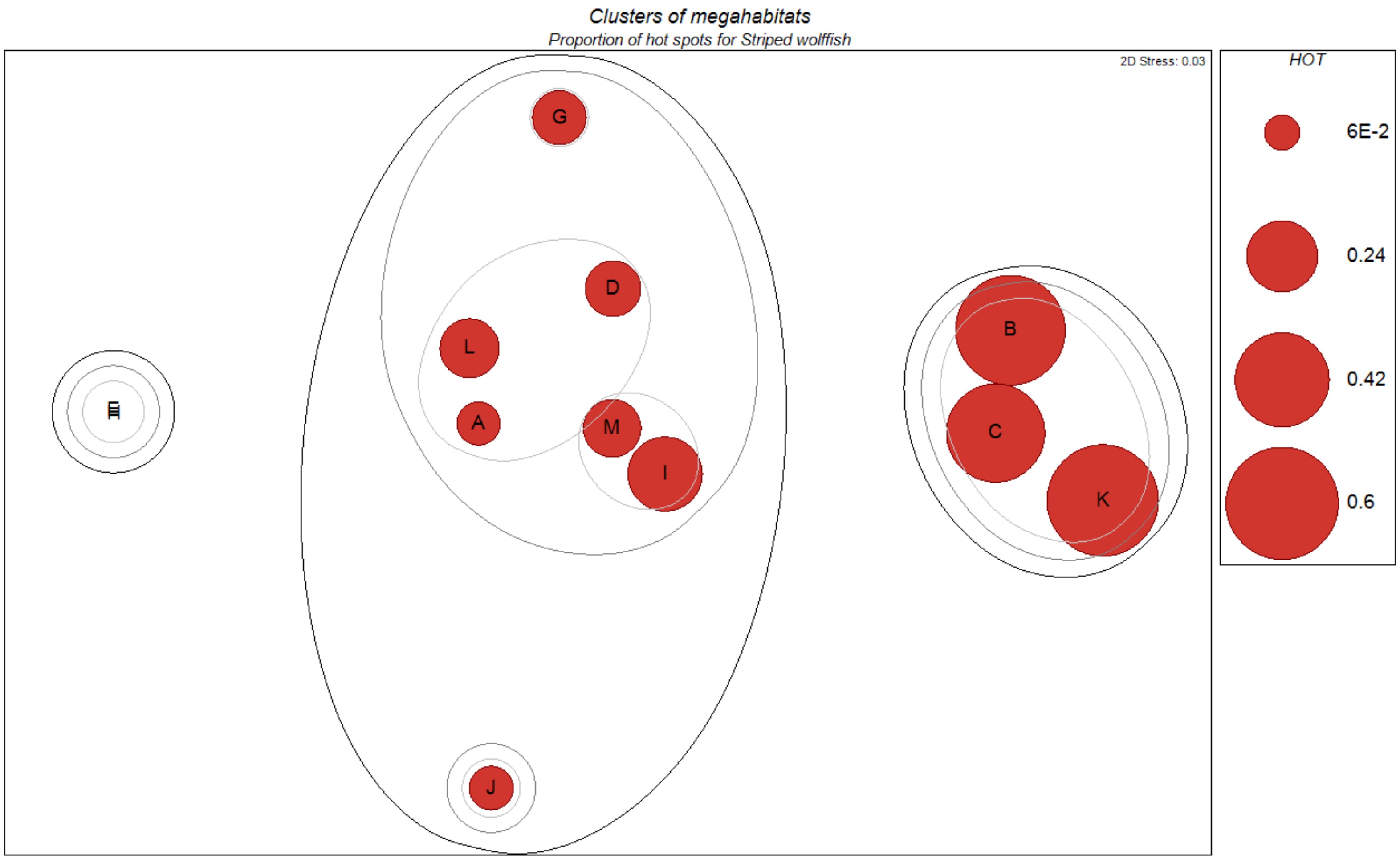

Figure 27. Multidimensional scaling plot of megahabitats based on striped wolffish spatial distribution and relative occurrence descriptors: proportion of cells overlapping the area of occupancy and within the 50 and 90% volume contours, proportion of cells classified as hot spots or cold spots, mean relative occurrence, and local spatial autocorrelation G_i* statistic. Bubble size is proportional to the proportion of cells classified as hot spots in the megahabitat.

Figure 28. Multidimensional scaling plot of megahabitats based on striped wolffish spatial distribution and relative occurrence descriptors: proportion of cells overlapping the area of occupancy and within the 50 and 90% volume contours, proportion of cells classified as hot spots or cold spots, mean relative occurrence, and local spatial autocorrelation G_i* statistic. Bubble size is proportional to the mean relative occurrence value of cells in the megahabitat.

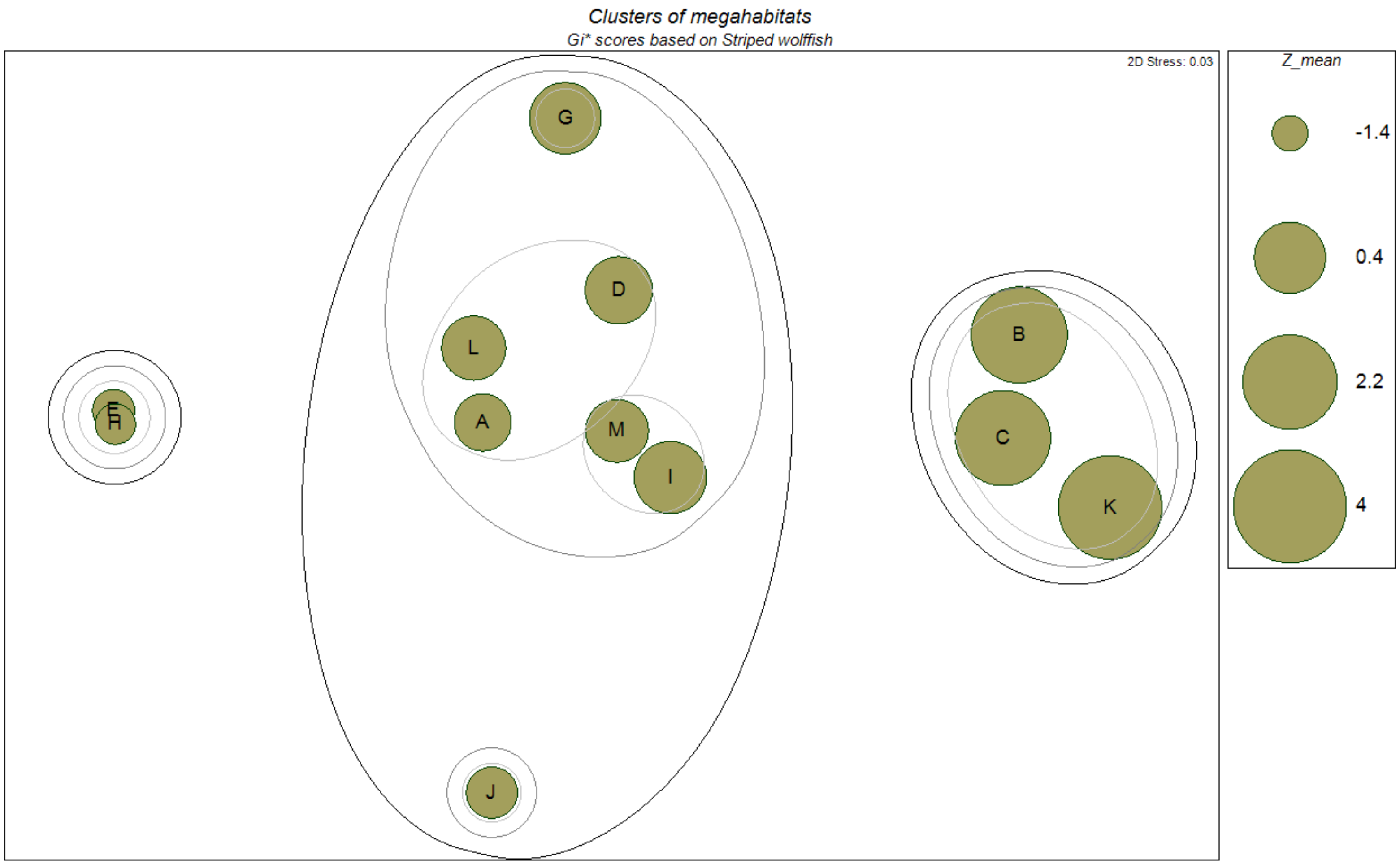

Figure 29. Multidimensional scaling plot of megahabitats based on striped wolffish spatial distribution and relative occurrence descriptors: proportion of cells overlapping the area of occupancy and within the 50 and 90% volume contours, proportion of cells classified as hot spots or cold spots, mean relative occurrence, and local spatial autocorrelation G_i* statistic. Bubble size is proportional to the mean local spatial autocorrelation G_i* value of cells in the megahabitat.

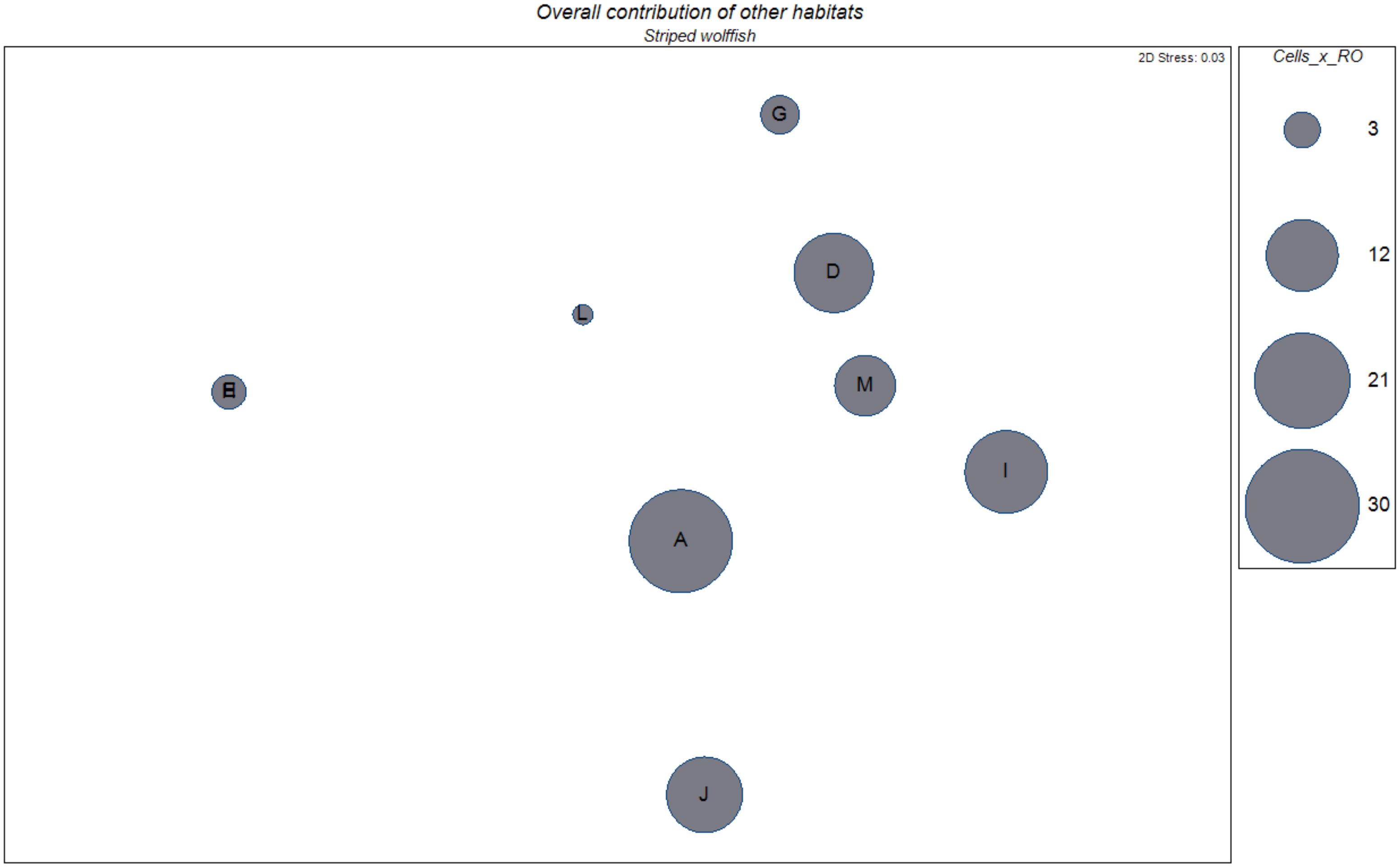

Figure 30. Multidimensional scaling plot of megahabitats based on striped wolffish spatial distribution and relative occurrence descriptors: proportion of cells overlapping the area of occupancy and within the 50 and 90% volume contours, proportion of cells classified as hot spots or cold spots, mean relative occurrence, and local spatial autocorrelation G_i* statistic. Bubble size is proportional to the product of mean relative occurrence and number of cells where the species was found to occur (relative occurrence weighted area).

Environmental relationships

Tables 60–63 summarize the environmental conditions that prevail where striped wolffish was found to occur and to cluster; mean values and confidence intervals are reported for quantitative variables, and number and proportion of cells meeting the classification criteria are reported for qualitative variables.

Table 60. Mean, 5th, 25th, median, 75th, and 95th percentiles for quantitative variables describing environmental conditions for cells where striped wolffish was found to occur (relative occurrence > 0).

Variable	Mean	5%	25%	Median	75%	95%
MHVar_3x3	3.28	1.00	3.00	3.00	4.00	5.00
Relief_var	4.16	1.00	2.00	4.00	6.00	8.00
Pro_Protege	0.00	0.00	0.00	0.00	0.00	0.00
Pro_SemiExp	0.00	0.00	0.00	0.00	0.00	0.00
Cote_Dist	36227	5362	17269	32712	51317	80848
Bathy_Mean	-156.8	-291.2	-210.4	-140.7	-95.0	-38.9
Bathy_STD	20.7	3.0	9.0	15.5	27.0	56.9
Bathy_Max	-200.2	-356.2	-261.0	-198.0	-136.5	-48.3
Bathy_Min	-114.1	-254.5	-163.6	-94.2	-58.1	-9.3
Pente_Mean	0.47	0.10	0.22	0.36	0.64	1.15
Pente_STD	0.26	0.05	0.11	0.18	0.33	0.68
Pente_Max	0.05	0.00	0.01	0.02	0.05	0.23
Pente_Min	1.39	0.30	0.65	1.04	1.80	3.47
Geo2_Bosse	0.06	0.00	0.00	0.01	0.08	0.23
Geo2_Creux	0.04	0.00	0.00	0.01	0.06	0.21
SalMoyMoy	33.25	31.27	32.65	33.38	34.08	34.57
SalMinMoy	32.95	30.20	32.32	33.02	33.82	34.46
SalMaxMoy	33.52	31.61	32.82	33.62	34.32	34.72
SalMoyMin	32.69	30.49	32.03	32.65	33.38	34.41
SalMinMin	32.33	29.51	31.84	32.35	33.15	34.29
SalMaxMin	33.01	31.48	32.31	32.83	33.66	34.57
SalMoyMax	33.70	31.29	33.31	34.04	34.46	34.78
SalMinMax	33.44	30.91	32.94	33.82	34.32	34.64
SalMaxMax	33.94	32.14	33.56	34.22	34.58	34.86
TempMoyMoy	2.70	0.18	0.82	2.41	4.40	5.13
TempMinMoy	1.82	-1.45	-0.22	1.74	3.97	4.90
TempMaxMoy	3.60	0.99	1.65	3.00	5.32	6.21
TempMoyMin	2.23	0.17	0.56	1.84	4.22	5.13
TempMinMin	0.77	-1.54	-0.75	0.15	1.96	4.61
TempMaxMin	3.88	0.99	1.25	2.87	5.10	12.54
TempMoyMax	3.48	0.39	1.96	4.29	5.04	5.32
TempMinMax	2.79	-1.21	1.43	3.81	4.44	4.97
TempMaxMax	4.22	1.11	2.97	4.76	5.37	5.90

Table 61. Number and proportion of cells where striped wolffish was found to occur (relative occurrence > 0) and meeting the dichotomous classification criterion for 12 binary variables describing environmental conditions.

Variable	Count	Proportion
Geo_Plateau	300	0.61
Geo_Talus	67	0.14
Geo_Chenal	126	0.26
Oxy_12	20	0.04
Oxy_34	199	0.40
Oxy_56	138	0.28
Oxy_78	136	0.28
Sed1_100	291	0.59
Sed1_200	34	0.07
Sed1_300	132	0.27
Sed1_400	36	0.07
Sed2	153	0.31

Table 62. Mean, 5th, 25th, median, 75th, and 95th percentiles for quantitative variables describing environmental conditions where striped wolffish was found to cluster (local spatial autocorrelation G_i* statistic value > 1.645).

Variable	Mean	5%	25%	Median	75%	95%
MHVar_3x3	3.37	2.00	3.00	3.00	4.00	5.00
Relief_var	4.23	1.00	2.00	4.00	6.00	8.00
Pro_Protege	0.00	0.00	0.00	0.00	0.00	0.00
Pro_SemiExp	0.00	0.00	0.00	0.00	0.00	0.00
Cote_Dist	34672	4824	16248	31688	48678	75938
Bathy_Mean	-145.2	-253.0	-196.2	-132.2	-94.7	-51.4
Bathy_STD	18.6	5.0	9.8	14.8	24.5	44.1
Bathy_Max	-185.1	-299.8	-233.0	-180.7	-132.8	-79.6
Bathy_Min	-106.3	-215.2	-145.9	-93.7	-61.2	-19.7
Pente_Mean	0.44	0.14	0.25	0.36	0.55	0.96
Pente_STD	0.24	0.07	0.12	0.18	0.30	0.58
Pente_Max	0.04	0.00	0.01	0.02	0.04	0.17
Pente_Min	1.33	0.44	0.71	1.01	1.59	3.10
Geo2_Bosse	0.05	0.00	0.00	0.01	0.07	0.22
Geo2_Creux	0.04	0.00	0.00	0.01	0.05	0.20
SalMoyMoy	33.25	32.03	32.65	33.31	34.04	34.47
SalMinMoy	33.00	31.84	32.35	33.02	33.75	34.32
SalMaxMoy	33.48	32.20	32.81	33.56	34.22	34.58
SalMoyMin	32.75	31.60	32.32	32.65	33.38	34.08
SalMinMin	32.45	31.11	31.98	32.35	33.02	33.90
SalMaxMin	33.02	32.09	32.55	32.81	33.62	34.32
SalMoyMax	33.70	32.43	33.31	34.00	34.41	34.63
SalMinMax	33.46	32.15	32.98	33.63	34.25	34.53
SalMaxMax	33.91	32.64	33.50	34.17	34.57	34.72
TempMoyMoy	2.28	0.17	0.56	1.96	4.40	5.13
TempMinMoy	1.62	-0.79	-0.24	1.43	3.82	4.90

TempMaxMoy	2.99	0.99	1.25	2.87	4.76	5.56
TempMoyMin	1.90	0.17	0.56	1.15	2.81	5.13
TempMinMin	0.67	-1.13	-0.72	0.15	1.90	4.00
TempMaxMin	3.36	0.99	1.16	2.60	4.76	9.18
TempMoyMax	3.22	0.17	1.96	4.11	4.92	5.30
TempMinMax	2.69	-0.62	1.19	3.67	4.35	4.90
TempMaxMax	3.77	0.99	2.82	4.46	5.33	5.70

Table 63. Number and proportion of cells meeting the classification criteria for 12 binary variables describing environmental conditions where striped wolffish was found to cluster (local spatial auto-correlation G_i* statistic value > 1.645).

Variable	Count	Proportion
Geo_Plateau	225	0.71
Geo_Talus	28	0.09
Geo_Chenal	65	0.20
Oxy_12	2	0.01
Oxy_34	98	0.31
Oxy_56	113	0.36
Oxy_78	105	0.33
Sed1_100	197	0.62
Sed1_200	4	0.01
Sed1_300	107	0.34
Sed1_400	10	0.03
Sed2	108	0.34

Striped wolffish tend to occur in areas where a great diversity of habitats are found, closer to shore and more rarely in channels than the two other species of wolffish. They mainly occur less than 200 m deep and cluster at depths of less than 150 m, 20–30 m above hot-spot areas for spotted wolffish. They are associated with outcrops and gravelly sand more often than the two other species at salinities below 34 and temperatures below 4°C. They cluster in areas slightly cooler than the spotted wolffish hot-spot areas, but also avoid cells with minimum temperature below 0.5–1.0°C.

Latitude and longitude explained 13% of the variance in the relative occurrence data (p<0.001, F-statistic: 39.0 on 2 and 490 DF) and 19% of the variance in the G_i* data (p<0.001, F-statistic: 68.1 on 2 and 564 DF). The relative occurrence data were square-root-transformed, and the G_i* data were fourth-root-transformed.

<u>Relative occurrence</u>

Eleven different variables, including 6 quadratic terms, correlated significantly with relative occurrence of striped wolffish (p< 0.001, F-statistic: 20.92 on 11 and 481 DF, R^2=0.31). The minimum temperature at minimum cell depth (quadratic term) was the single most important parameter in terms of the proportion of the variance explained (14% of 31%). The negative coefficient suggested a dome-shaped relationship in contrast to maximum temperature at minimum cell depth, which had a positive effect on the relative occurrence of striped wolffish

(Table 64). Similarly, plateaus, coarse sediments, and outcrops had a positive effect. The residuals of the linear regression of relative occurrence with latitude and longitude were used for the regression, which included only cells where the species is known to occur.

Table 64. Results of a multiple forward linear regression between relative occurrence of striped wolffish and potential explanatory variables obtained from the megahabitat database (adapted from Dutil et al. 2011). *: p<0.10; **: p<0.05; ***: p<0.001; +: positive effect; -: negative effect.

Variable RO

	Estimate	Standard error	t value	p	Partial R^2	+/-
(Intercept)	-0.045	0.018	-2.467	*		
TempMinMin2	-0.0065	0.0020	-3.20	**	0.14	-
Geo_Plateau	0.080	0.019	4.32	***	0.04	+
TempMaxMin2	0.00104	0.00029	3.61	***	0.03	+
Sed2	0.063	0.016	3.87	***	0.03	+
SalMaxMax2	-0.031	0.007	-4.71	***	0.02	-
Sed1_300	0.105	0.018	5.77	***	0.02	+
Bathy_Max2	$1.635 \cdot 10^{-6}$	$0.66 \cdot 10^{-6}$	-2.48	*	0.01	+
Pro_Protege2	-6527	2184	-2.99	**	0.01	-
Pro_Protege	59.17	25.87	2.29	*	0.01	+
Cote_Dist	0.00	0.00	2.13	*	0.01	+
Sed1_400	0.077	0.033	2.35	*	0.01	+

Striped wolffish avoided areas where minimum temperature at minimum cell depth approached the freezing point (Figure 31) and were over-represented (relative to stratum availability) in cells where maximum temperature at minimum cell depth was in the range 0–3°C (Figure 32). They generally occurred over plateaus (60.8% of cells where they occurred whereas plateaus represent 56.6% of all cells) and in cells with outcrops (31.0% of cells where they occurred whereas outcrops represent 24.3% of all cells).

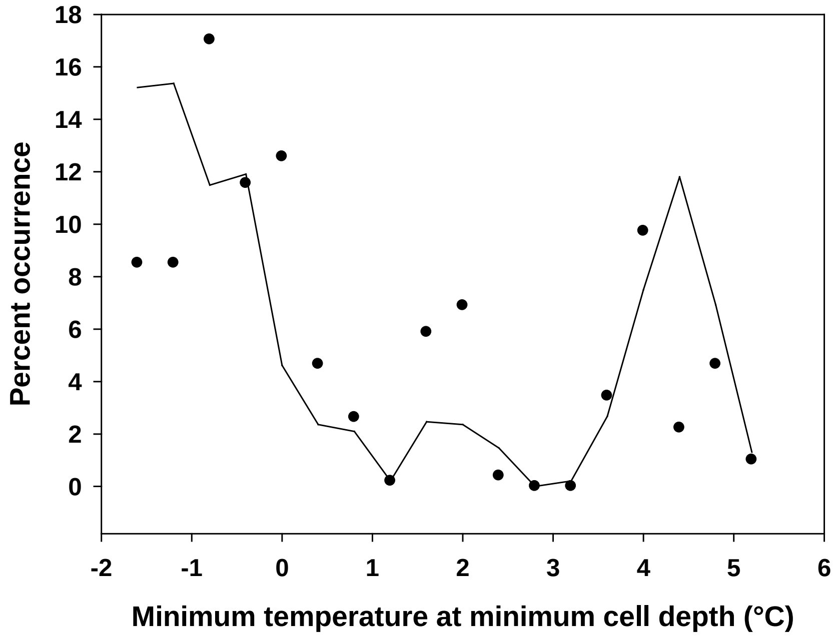

Figure 31. Percent frequency occurrence of cells in which striped wolffish occurred (•; relative occurrence > 0) and percent frequency of cells in the study area (−) as a function of minimum temperature at minimum cell depth.

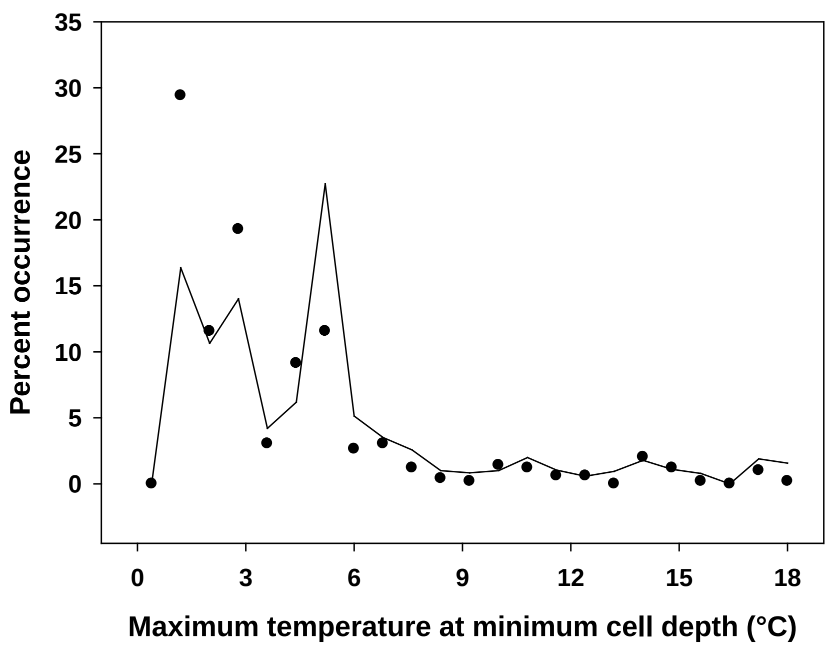

Figure 32. Percent frequency occurrence of cells in which striped wolffish occurred (•; relative occurrence > 0) and percent frequency of cells in the study area (−) as a function of maximum temperature at minimum cell depth.

Clustering of high relative occurrences

When the latitude and longitude effects are taken into account, 18 different variables (including 6 quadratic terms) appear to have a significant effect on G_i* values (Table 65) for the striped wolffish in cells where positive values of the local spatial autocorrelation G_i* statistic were observed, with as much as 44% of the variance explained (p< 0.001, F-statistic: 25.58 on 18 and 548 DF, R^2=0.44). The minimum cell depth (quadratic term) was the single most important parameter in terms of the proportion of the variance explained (15% of 44%). The negative coefficient suggested a dome-shaped relationship in contrast to maximum temperature at maximum cell depth, which had a positive effect on the relative occurrence of striped wolffish. Two other factors, coarse sediments and outcrops, explained 12% of the variance, with a higher degree of clustering (hot spots) being observed in cells with these characteristics. The residuals of the linear regression of G_i* with latitude and longitude were used, and only cells where positive values of the local spatial autocorrelation G_i* statistic were observed were included in the regression.

Table 65. Results of a multiple forward linear regression for striped wolffish using G_i* (clusters of high relative occurrence for the species) and the potential explanatory variables obtained from the megahabitat database (adapted from Dutil et al. 2011). *: p<0.10; **: p<0.05; ***: p<0.001; +: positive effect; -: negative effect.

Variable: G_i*

	Estimate	Standard error	t value	p	Partial R^2	+/-
(Intercept)	0.323	0.044	7.30	***		+
Bathy_Min2	$-1.13 \cdot 10^{-5}$	$0.22 \cdot 10^{-5}$	-5.21	***	0.150	-
Sed1_300	0.142	0.027	5.31	***	0.066	+
Sed2	0.092	0.024	3.84	***	0.055	+
Pente_Min	-0.29	0.14	-2.16	*	0.029	-
Oxy_34	-0.194	0.043	-4.53	***	0.021	-
Sed1_200	-0.225	0.053	-4.28	***	0.020	-
SalMoyMax2	-0.129	0.023	-5.66	***	0.018	-
Oxy_12	-0.372	0.058	-6.40	***	0.018	-
Geo2_Creux	-1.00	0.23	-4.39	***	0.018	-
MHVar_3x32	-0.0187	0.0059	-3.14	**	0.014	-
Pro_Protege2	-106.7	52.8	-2.02	*	0.009	-
Pente_STD	0.254	0.083	3.08	**	0.007	+
Cote_Dist2	$-6.12 \cdot 10^{-11}$	$1.76 \cdot 10^{-11}$	-3.47	***	0.007	-
Oxy_56	-0.088	0.036	-2.45	*	0.006	-
Cote_Dist	$2.55 \cdot 10^{-6}$	$0.61 \cdot 10^{-6}$	4.21	***	0.005	+
SalMaxMax	-0.074	0.033	-2.26	*	0.005	-
TempMoyMoy2	-0.0153	0.0048	-3.15	**	0.004	-
TempMoyMin	0.0197	0.0084	2.35	*	0.003	+

Striped wolffish clusters did not occur in cells with minimum depth greater than 300 m. They clustered preferentially in cells with a minimum depth ranging from 60 to 200 m (Figure 33), and cells with coarse sediments and outcrops represented a greater proportion of significant clusters than expected considering the availability of these habitats in the study area, i.e., 21.6 vs. 27.5% for coarse sediments and 24.3 vs. 26.8% for outcrops.

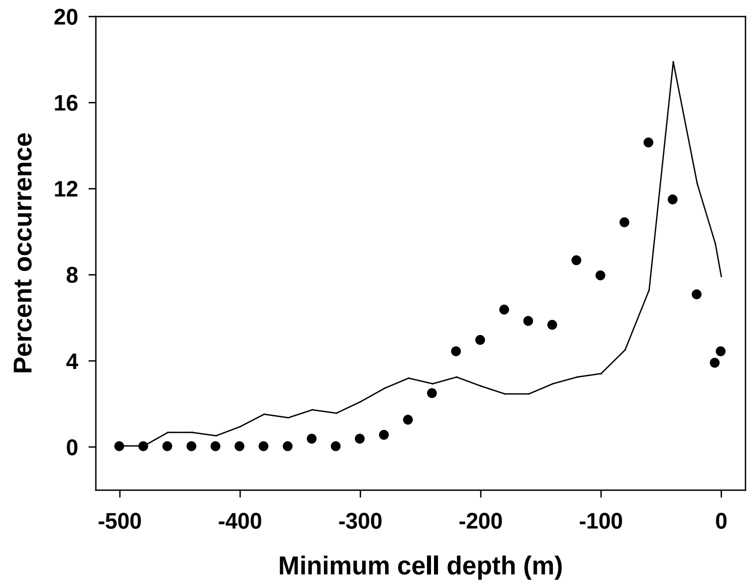

Figure 33. Percent frequency occurrence of cells in which striped wolffish clustered (•; relative occurrence > 0) and percent frequency of cells in the study area (−) as a function of minimum (absolute value) cell depth.

5. SPOTTED WOLFFISH

In the same manner as the preceding section 4 on striped wolffish, a set of standardized output maps and tables are presented here for spotted wolffish, produced from the analyses described in the Methods (section 3) using relative occurrence data. They include a description of the area of occupancy, density maps of occurrence, and global and local spatial autocorrelation statistics and maps. Tables are shown that summarize a set of species scores for each megahabitat category. The scores were then used in cluster analyses and MDS plots to identify the most important and the least important megahabitats for spotted wolffish. Summary statistics and multiple forward linear regression statistics are provided describing environmental conditions and relationships in areas where the species occurs and where clusters of higher relative occurrence are found.

Area of occupancy

Spotted wolffish were present primarily in conglomerate 1, located in the northeastern sector of the Gulf (west coast of Newfoundland; Figure 34). Two much smaller conglomerates and satellites were also located primarily in the Gulf north of the 200 m isobath (Table 66).

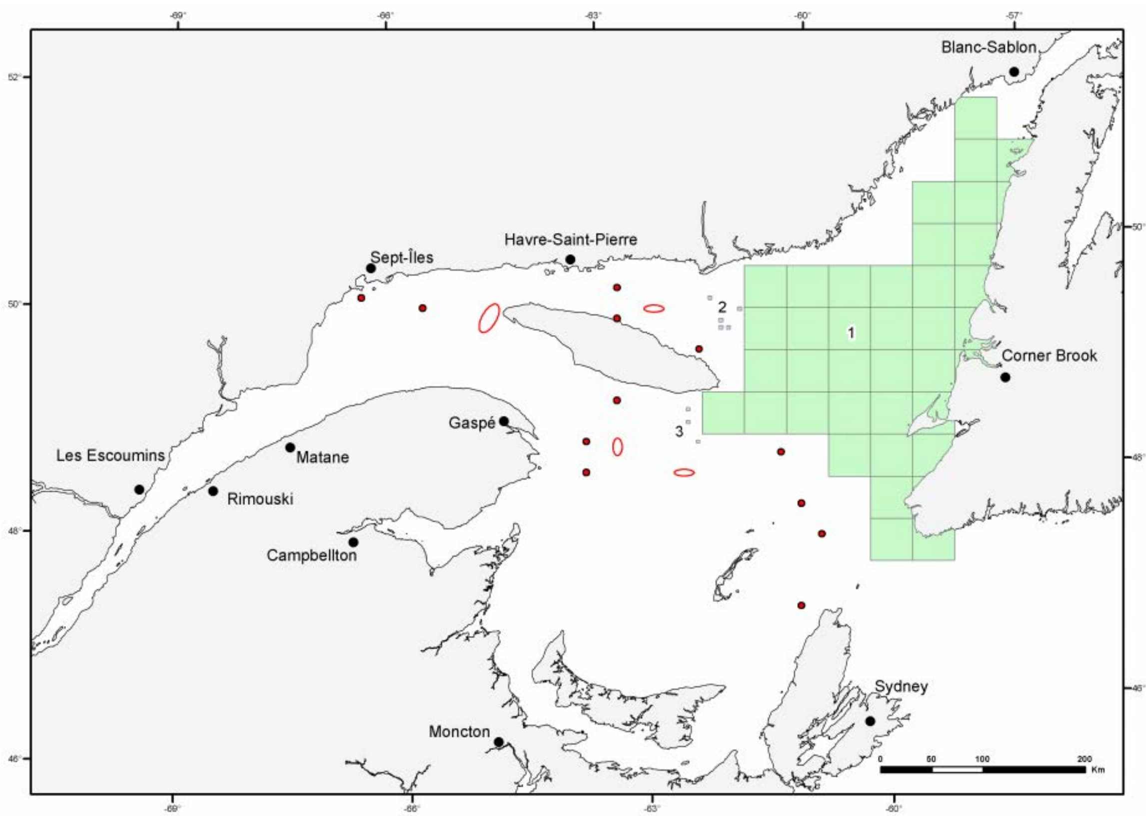

Figure 34. Area of occupancy of spotted wolffish in the St. Lawrence estuary and Gulf based on annual bottom trawl surveys conducted by DFO (1971–2008). The grids were produced based on presence data using the Hernández and Navarro (2007) cartographic and conglomerate method. Conglomerates less than 100 km^2 are shown as ovals (not to scale), and satellites (isolated observations) are shown as red dots.

Table 66. Size of the area of occupancy of spotted wolffish by conglomerate and satellite groups of observations, as determined by the Hernández and Navarro (2007) cartographic and conglomerate method and based on presence data obtained from annual bottom trawl surveys conducted by DFO (1971–2008). Numbers refer to Figure 33.

Conglomerate	Satellite	Planimetric area (km^2)
1		56,375
2		66
3		30
Others (less than 20 km^2 individually)		16
	n = 12	12
Total area of occupancy		**56,499**

Patterns and clusters of distribution

The kernel density estimate method applied to relative occurrence data yielded planimetric areas of 52,496 km^2, 45,289 km^2, and 14,362 km^2 for the 95%, 90% (low density), and 50% (high density) volume density contours, respectively (Figure 35).

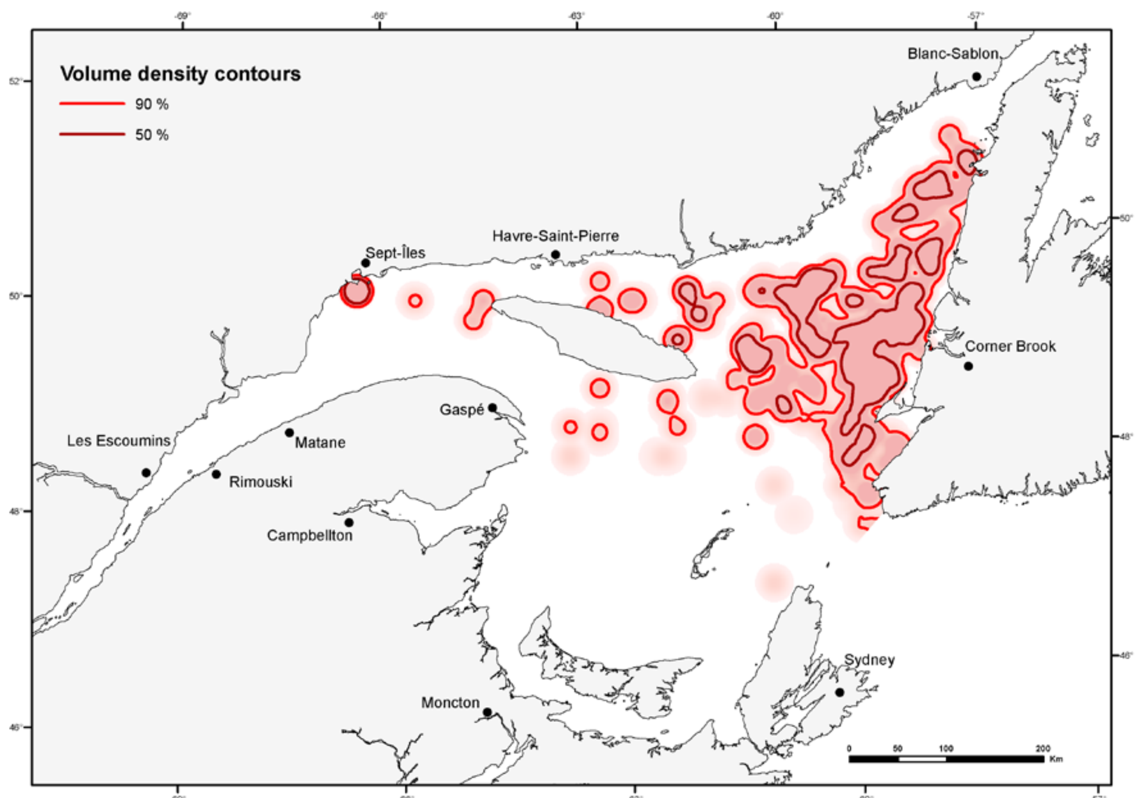

Figure 35. Density map of relative occurrence for spotted wolffish in the St. Lawrence estuary and Gulf based on annual bottom trawl surveys conducted by DFO (1971–2008). The 50% and 90% volume density contours are shown. A 20 km search radius was used.

The Moran's *I* global spatial autocorrelation parameter yielded a positive (index value=0.141), highly significant (P<0.0001) Z-score of 14.6, which clearly indicates a high degree of clustering of spotted wolffish relative occurrence in the study area (Figure 36). The local spatial autocorrelation statistic applied to relative occurrence data yielded planimetric areas of 26,182 km^2 for hot spots at p=0.10 (including 23,392 km^2 at p=0.05 and 16,961 km^2 at p=0.01).

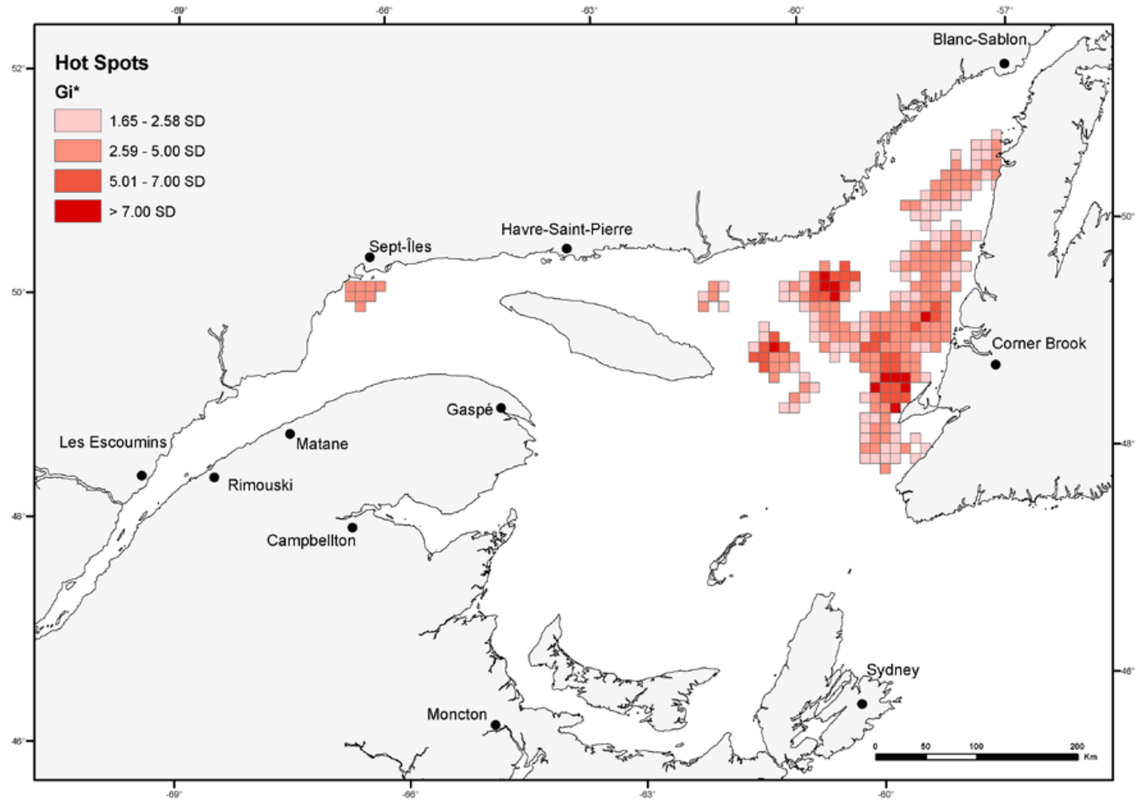

Figure 36. Location of statistically significant clusters of high relative occurrence (hot spots) (G_i* Z-scores significant at α=0.10) for spotted wolffish in the St. Lawrence estuary and Gulf based on annual bottom trawl surveys conducted by DFO (1971–2008). No significant clusters of low relative occurrence (cold spots) were identified. Significant hot spots are shown by intervals of Z-score standard deviations (SD). A 20 km bandwith (zone of indifference model) was used.

Habitat relationships

The cluster analysis identified six different clusters including two very dissimilar groups of megahabitats on the basis of spatial distribution and relative occurrence of spotted wolffish (SIMPROF, p<0.05; Figure 37). One group included megahabitats E, G, H, and L, where the species does not occur. The other group was divided into three categories, megahabitats B, C, and K, where spotted wolffish appear to concentrate, and other more marginal megahabitats, including cold, shallow water shelf megahabitat J, where spotted wolffish are less likely to occur. Spotted wolffish used two contiguous megahabitats most intensively: megahabitats C (deep water shelf habitats) and K (relatively cold shallow to mid-depth shelf habitats) in the northern

Gulf. Megahabitats C and K were characterized by the highest relative occurrence of spotted wolffish, and a large proportion of the cells were classified as hot spots, as shown in Table 67 and by the size of the bubbles (proportion of cells classified as hot spots, and mean relative occurrence and G_i* value of cells) in the three MDS graphs (stress value = 0.03; Figures 38–40). Though deep water megahabitat B (deep water, steep-sloped habitats) was also used by spotted wolffish (large bubbles in two of the MDS graphs), it represented a distinct group. Megahabitat B, which is contiguous to megahabitat C and very limited in terms of planimetric area, was also characterized by greater relative occurrence, volume density was lower, and frequency occurrence of clusters of high relative occurrence (hot spots at $p<0.01$) was low. Spotted wolffish appeared to be associated to none of the megahabitats found mainly in the southern Gulf of St. Lawrence. However, deep channels (megahabitat A) appeared to be of some importance when the surface area was considered and weighted by relative occurrence (relative occurrence weighted area) in the MDS graph (Figure 41).

Table 67. Number of cells overlapping the distribution features for spotted wolffish, reported as a proportion of the number of cells in each megahabitat. The area of occupancy was determined by the Hernández and Navarro (2007) method using presence/absence data. The other features are based on the species relative occurrence. Cold spots and hot spots were determined based on the Getis and Ord local spatial autocorrelation Gi* statistic (Z-score). Mean relative occurrence and Gi* value are given for each megahabitat. Prime habitats for the species are highlighted.

Megahabitat	Number of cells	Area of occupancy	KDE 90% volume	KDE 50% volume	Cold spot	Hot spot	Relative occurrence	Z-score
A	609	0.392	0.243	0.057	0.000	0.136	0.018	0.094
B	14	0.857	0.571	0.071	0.000	0.071	0.039	0.732
C	161	0.447	0.280	0.155	0.000	0.304	0.040	0.965
D	129	0.233	0.171	0.070	0.000	0.147	0.018	0.026
E	111	0.000	0.000	0.000	0.000	0.000	0.000	-0.735
G	29	0.034	0.069	0.000	0.000	0.000	0.004	-0.686
H	149	0.000	0.000	0.000	0.000	0.000	0.000	-0.846
I	125	0.320	0.160	0.064	0.000	0.168	0.018	0.143
J	351	0.097	0.028	0.060	0.000	0.080	0.013	-0.395
K	134	0.619	0.276	0.254	0.000	0.410	0.054	1.460
L	18	0.000	0.000	0.000	0.000	0.000	0.000	-0.662
M	76	0.197	0.118	0.039	0.000	0.092	0.026	-0.163

Table 68. Number of cells where the presence of spotted wolffish was confirmed and overlap between these cells and the distribution features, reported as a proportion of the number of cells in each megahabitat. The area of occupancy was determined by the Hernández and Navarro (2007) method using presence/absence data. The other features are based on the species relative occurrence. Cold spots and hot spots were determined based on the Getis and Ord local spatial autocorrelation Gi* statistic (Z-score). Mean relative occurrence and Gi* value are given for each megahabitat. Prime habitats for the species are highlighted.

Megahabitat	Number of cells	Area of occupancy	KDE 90% volume	KDE 50% volume	Cold spot	Hot spot	Relative occurrence	Z-score
A	70	0.857	0.571	0.357	0.000	0.486	0.161	1.629
B	4	1.000	0.750	0.250	0.000	0.250	0.136	1.324
C	29	0.931	0.379	0.621	0.000	0.655	0.221	2.925
D	17	0.706	0.471	0.294	0.000	0.412	0.139	1.197
E	0	0.000	0.000	0.000	0.000	0.000	0.000	0.000
G	1	1.000	1.000	0.000	0.000	0.000	0.125	-0.447
H	0	0.000	0.000	0.000	0.000	0.000	0.000	0.000
I	9	1.000	0.444	0.556	0.000	0.778	0.244	2.852
J	15	1.000	0.133	0.867	0.000	0.933	0.303	4.867
K	37	1.000	0.324	0.622	0.000	0.811	0.194	3.054
L	0	0.000	0.000	0.000	0.000	0.000	0.000	0.000
M	5	1.000	0.600	0.400	0.000	0.600	0.394	2.392

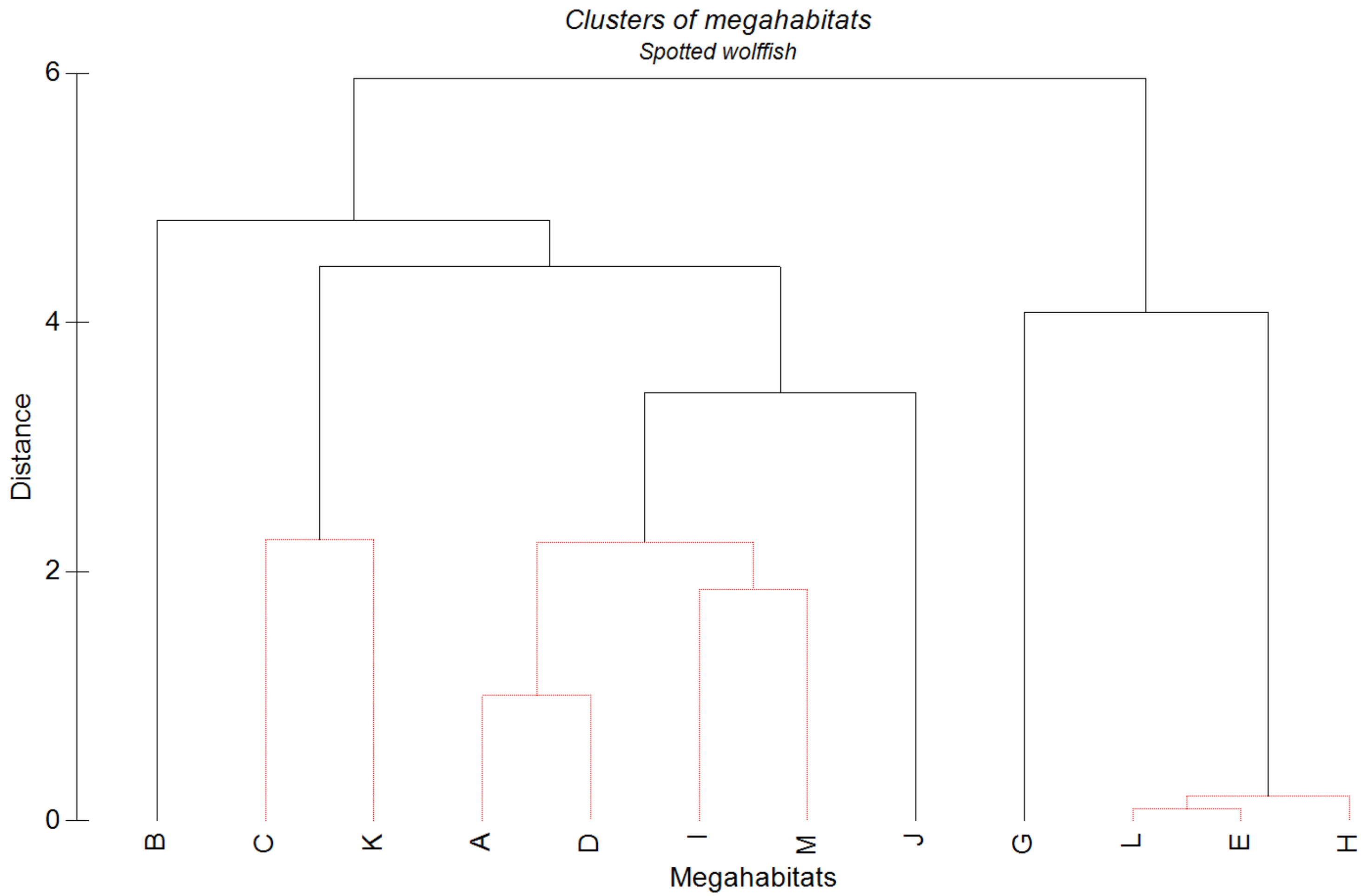

Figure 37. Tree diagram showing significant (black line) clusters of megahabitats based on spotted wolffish spatial distribution and relative occurrence descriptors: proportion of cells overlapping the area of occupancy and within the 50 and 90% volume contours, proportion of cells classified as hot spots or cold spots, mean relative occurrence, and local spatial autocorrelation G_i* statistic.

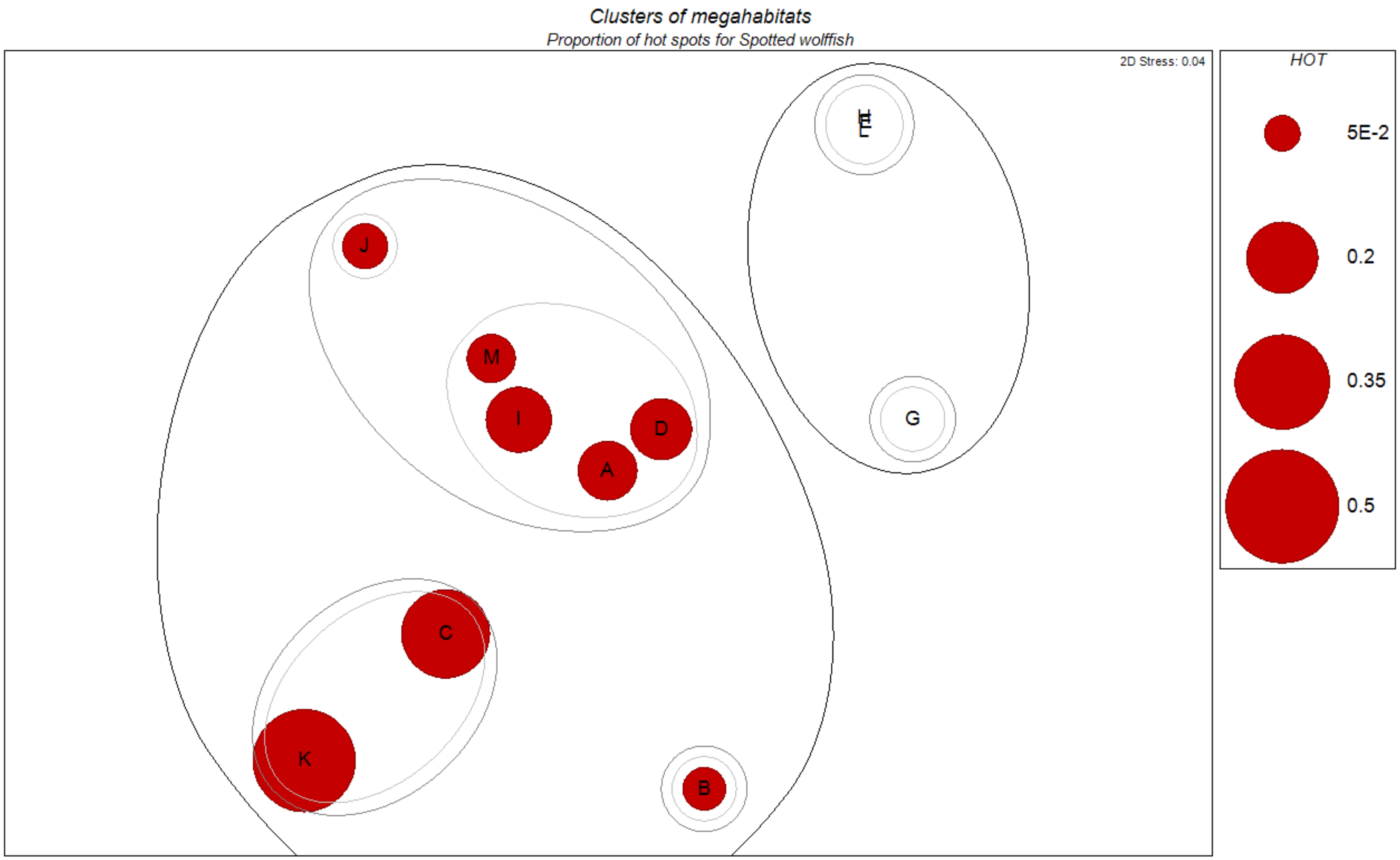

Figure 38. Multidimensional scaling plot of megahabitats based on spotted wolffish spatial distribution and relative occurrence descriptors: proportion of cells overlapping the area of occupancy and within the 50 and 90% volume contours, proportion of cells classified as hot spots or cold spots, mean relative occurrence, and local spatial autocorrelation G_i* statistic. Bubble size is proportional to the proportion of cells classified as hot spots in the megahabitat.

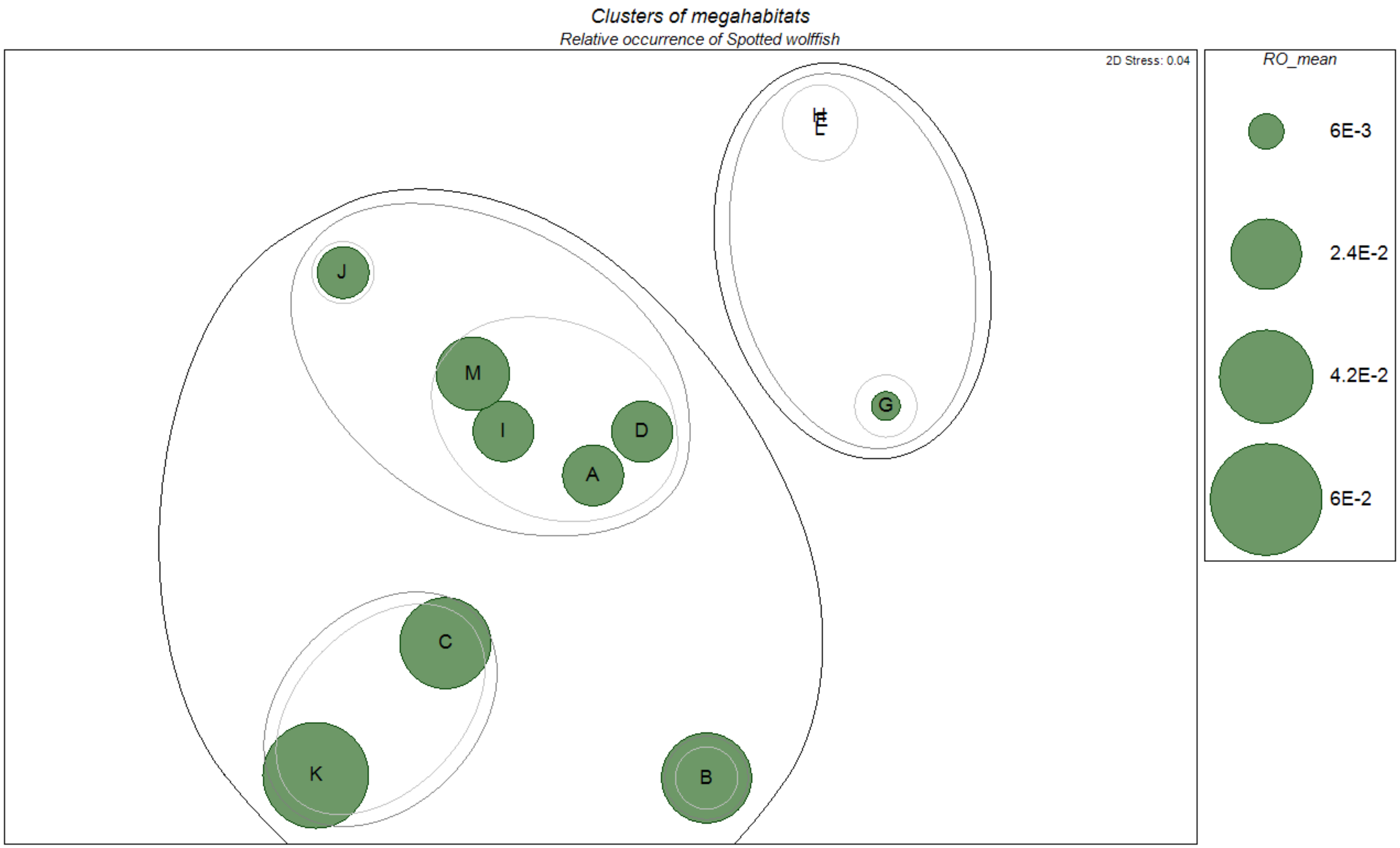

Figure 39. Multidimensional scaling plot of megahabitats based on spotted wolffish spatial distribution and relative occurrence descriptors: proportion of cells overlapping the area of occupancy and within the 50 and 90% volume contours, proportion of cells classified as hot spots or cold spots, mean relative occurrence, and local spatial autocorrelation G_i* statistic. Bubble size is proportional to the mean relative occurrence value of cells in the megahabitat.

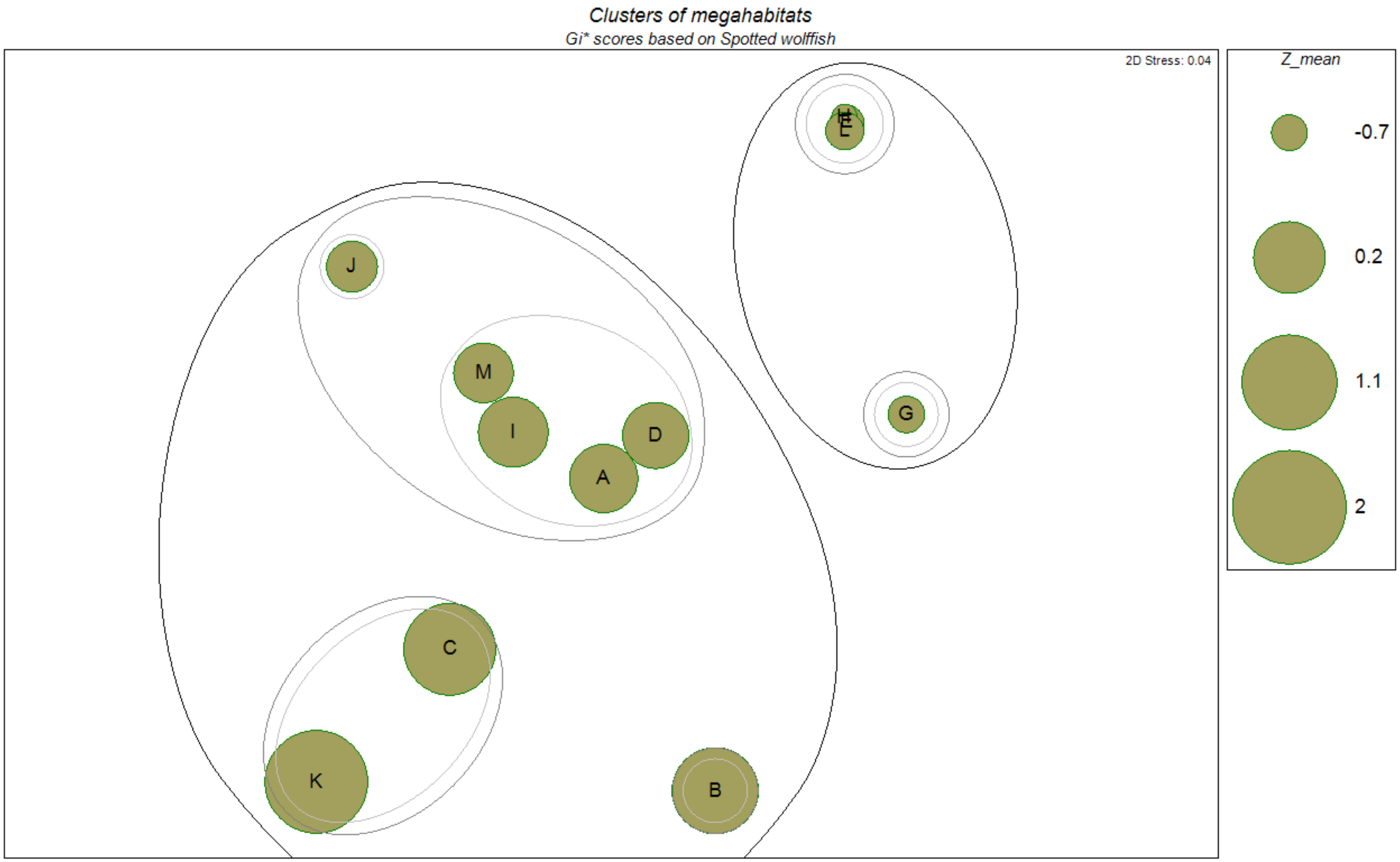

Figure 40. Multidimensional scaling plot of megahabitats based on spotted wolffish spatial distribution and relative occurrence descriptors: proportion of cells overlapping the area of occupancy and within the 50 and 90% volume contours, proportion of cells classified as hot spots or cold spots, mean relative occurrence, and local spatial autocorrelation G_i* statistic. Bubble size is proportional to the mean local spatial autocorrelation G_i* value of cells in the megahabitat.

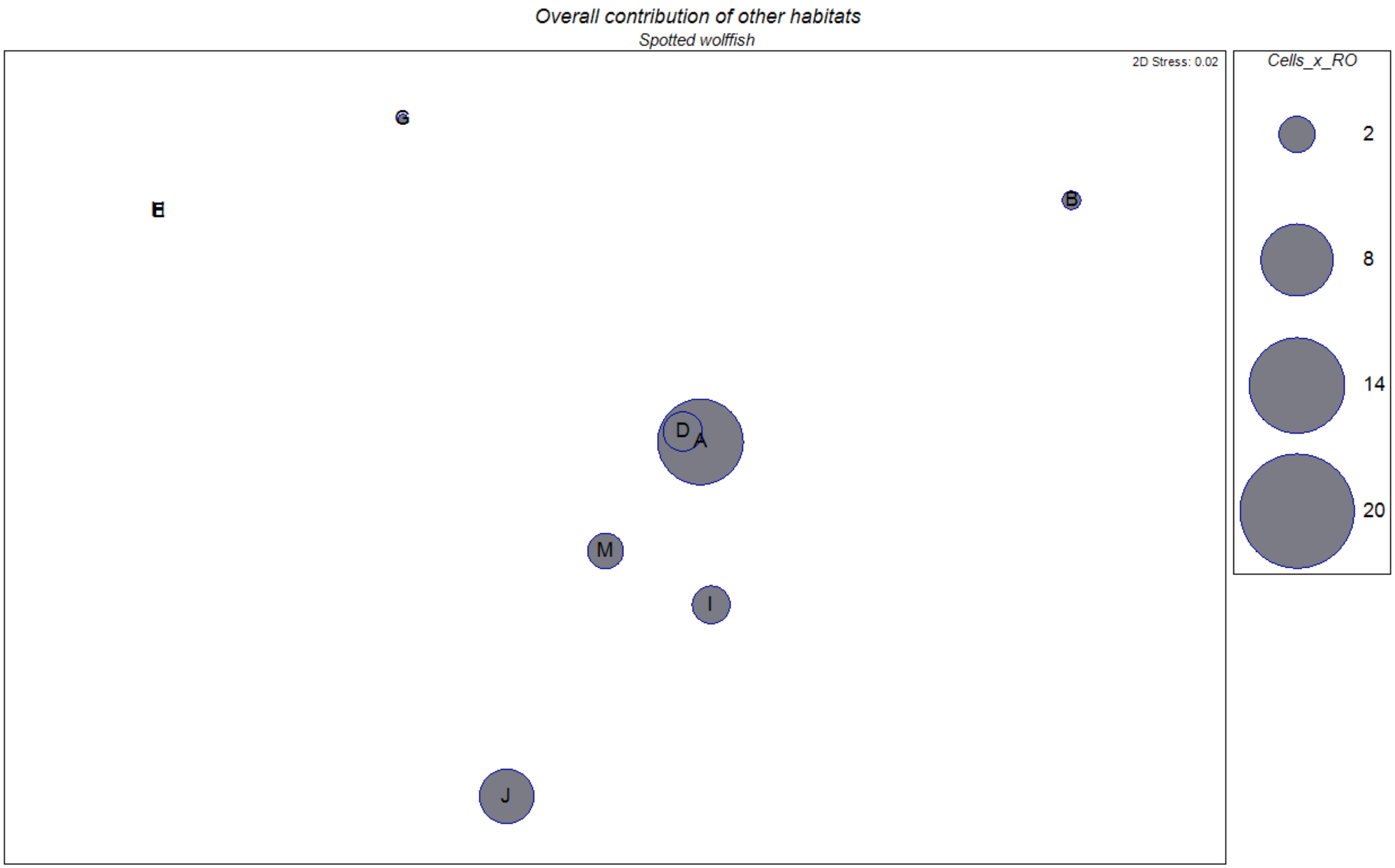

Figure 41. Multidimensional scaling plot of megahabitats based on spotted wolffish spatial distribution and relative occurrence descriptors: proportion of cells overlapping the area of occupancy and within the 50 and 90% volume contours, proportion of cells classified as hot spots or cold spots, mean relative occurrence, and local spatial autocorrelation G_i* statistic. Bubble size is proportional to the product of mean relative occurrence and number of cells where the species was found to occur (relative occurrence weighted area).

Environmental relationships

Tables 69–73 summarize the environmental conditions that prevail where spotted wolffish was found to occur and to cluster; mean values and confidence intervals are reported for quantitative variables, and number of cells and proportion of cells meeting the classification criteria are reported for qualitative variables.

Table 69. Mean, 5th, 25th, median, 75th, and 95th percentiles for quantitative variables describing environmental conditions for cells where spotted wolffish was found to occur (relative occurrence > 0).

Variable	Mean	5%	25%	Median	75%	95%
MHVar_3x3	3.00	1.00	2.00	3.00	4.00	5.00
Relief_var	3.88	1.00	1.50	4.00	6.00	8.00
Pro_Protege	0.00	0.00	0.00	0.00	0.00	0.00
Pro_SemiExp	0.00	0.00	0.00	0.00	0.00	0.00
Cote_Dist	42303	5671	23420	41304	56574	85289
Bathy_Mean	-189.3	-340.9	-248.8	-190.6	-107.9	-79.7
Bathy_STD	18.6	4.3	8.9	13.6	25.8	43.4
Bathy_Max	-228.0	-387.9	-282.9	-231.5	-147.9	-98.0
Bathy_Min	-148.0	-295.0	-210.0	-134.2	-79.7	-34.8
Pente_Mean	0.43	0.14	0.21	0.33	0.57	1.11
Pente_STD	0.22	0.07	0.11	0.17	0.26	0.52
Pente_Max	0.05	0.00	0.01	0.02	0.05	0.22
Pente_Min	1.25	0.37	0.61	0.91	1.52	2.94
Geo2_Bosse	0.04	0.00	0.00	0.01	0.04	0.23
Geo2_Creux	0.04	0.00	0.00	0.00	0.04	0.19
SalMoyMoy	33.67	32.40	32.78	34.04	34.46	34.65
SalMinMoy	33.45	32.13	32.53	33.73	34.29	34.55
SalMaxMoy	33.87	32.59	33.10	34.22	34.58	34.76
SalMoyMin	33.20	31.69	32.43	33.21	34.08	34.54
SalMinMin	32.94	31.30	32.15	32.92	33.82	34.42
SalMaxMin	33.43	32.09	32.64	33.56	34.26	34.72
SalMoyMax	33.99	32.62	33.38	34.41	34.54	34.80
SalMinMax	33.80	32.35	33.02	34.25	34.42	34.71
SalMaxMax	34.17	32.73	33.62	34.57	34.69	34.86
TempMoyMoy	3.15	0.21	0.90	4.11	5.12	5.34
TempMinMoy	2.60	-0.62	0.19	3.67	4.61	5.04
TempMaxMoy	3.71	0.99	1.65	4.46	5.37	5.83
TempMoyMin	2.53	0.17	0.56	2.41	4.40	5.13
TempMinMin	1.61	-0.79	-0.59	0.59	3.97	4.90
TempMaxMin	3.57	0.99	1.16	2.99	5.28	6.88
TempMoyMax	3.83	0.39	2.41	4.80	5.13	5.34
TempMinMax	3.33	-0.27	1.96	4.18	4.70	5.04
TempMaxMax	4.34	1.03	2.99	5.23	5.50	5.90

Table 70. Number of cells and proportion of cells meeting the classification criteria for 12 binary variables describing environmental conditions for cells where spotted wolffish was found to occur (relative occurrence > 0).

Variable	Count	Proportion
Geo_Plateau	91	0.49
Geo_Talus	19	0.10
Geo_Chenal	77	0.41
Oxy_12	12	0.06
Oxy_34	78	0.42
Oxy_56	53	0.28
Oxy_78	44	0.24
Sed1_100	130	0.70
Sed1_200	0	0.00
Sed1_300	55	0.29
Sed1_400	2	0.01
Sed2	55	0.29

Table 71. Mean, 5th, 25th, median, 75th, and 95th percentiles for quantitative variables describing environmental conditions where spotted wolffish was found to cluster (local spatial autocorrelation G_i* statistic value > 1.645).

Variable	Mean	5%	25%	Median	75%	95%
MHVar_3x3	3.08	1.00	2.00	3.00	4.00	5.00
Relief_var	3.81	1.00	2.00	4.00	6.00	8.00
Pro_Protege	0.00	0.00	0.00	0.00	0.00	0.00
Pro_SemiExp	0.00	0.00	0.00	0.00	0.00	0.00
Cote_Dist	42566	6647	23292	40586	58833	87992
Bathy_Mean	-163.5	-273.3	-223.7	-154.4	-102.2	-57.3
Bathy_STD	16.2	4.3	8.2	13.1	22.6	37.0
Bathy_Max	-198.7	-301.5	-263.2	-205.0	-135.7	-80.0
Bathy_Min	-128.2	-248.9	-187.1	-112.3	-73.6	-31.3
Pente_Mean	0.40	0.14	0.22	0.31	0.50	0.88
Pente_STD	0.22	0.07	0.11	0.15	0.24	0.61
Pente_Max	0.03	0.00	0.01	0.02	0.04	0.13
Pente_Min	1.24	0.37	0.62	0.91	1.24	3.37
Geo2_Bosse	0.04	0.00	0.00	0.01	0.04	0.20
Geo2_Creux	0.04	0.00	0.00	0.00	0.03	0.22
SalMoyMoy	33.46	32.07	32.78	33.38	34.16	34.49
SalMinMoy	33.24	31.86	32.53	33.02	34.00	34.42
SalMaxMoy	33.68	32.24	33.10	33.62	34.44	34.58
SalMoyMin	33.03	31.69	32.39	32.78	34.04	34.41
SalMinMin	32.76	31.30	32.13	32.53	33.73	34.29
SalMaxMin	33.27	32.09	32.57	33.10	34.22	34.57
SalMoyMax	33.81	32.43	33.31	34.04	34.47	34.60
SalMinMax	33.61	32.15	33.02	33.82	34.33	34.55
SalMaxMax	34.01	32.64	33.62	34.22	34.58	34.72
TempMoyMoy	2.76	0.17	0.56	2.41	4.47	5.13
TempMinMoy	2.16	-0.75	0.19	1.96	4.19	4.90

TempMaxMoy	3.38	0.99	1.16	3.00	5.21	5.69
TempMoyMin	2.24	0.17	0.56	1.86	4.40	5.13
TempMinMin	1.23	-0.79	-0.62	0.19	3.74	4.90
TempMaxMin	3.36	0.99	1.16	2.99	5.10	6.88
TempMoyMax	3.51	0.19	1.96	4.40	5.12	5.34
TempMinMax	2.99	-0.62	1.43	3.97	4.61	5.04
TempMaxMax	4.04	0.99	2.99	4.76	5.50	5.90

Table 72. Number of cells and proportion of cells meeting the classification criteria for 12 binary variables describing environmental conditions where spotted wolffish was found to cluster (local spatial autocorrelation G_i* statistic value > 1.645).

Variable	Count	Proportion
Geo_Plateau	153	0.58
Geo_Talus	17	0.06
Geo_Chenal	93	0.35
Oxy_12	16	0.06
Oxy_34	97	0.37
Oxy_56	71	0.27
Oxy_78	79	0.30
Sed1_100	177	0.67
Sed1_200	0	0.00
Sed1_300	82	0.31
Sed1_400	4	0.02
Sed2	68	0.26

Spotted wolffish tend to occur in areas where a great diversity of habitats are found; they are associated in a greater proportion with plateaus than channels and within a narrow range of temperatures (2–4°C) and at intermediate depths and dissolved oxygen saturations. They tend to cluster in the upper portion of that range, i.e., right below the CIL and 100–150 m above hot spot areas for northern wolffish. The relative occurrence data were log transformed, and the G_i* data were square-root transformed.

Latitude and longitude explained 9% of the variance in the relative occurrence data ($p<0.001$, F-statistic: 9.4 on 2 and 184 DF) and 6% of the variance in the G_i* data ($p<0.001$, F-statistic: 15.8 on 2 and 505 DF).

Relative occurrence

There was a significant relationship between the relative occurrence of spotted wolffish and the environmental variables ($p<0.001$, F-statistic: 9.69 on 6 and 180 DF, $R^2=0.22$). Six environmental variables (including three quadratic terms) showed significant relationships, including three that explained a greater percentage of the variance in the relative occurrence data: maximum depth (10%), minimum slope (4%), and mean temperature at minimum depth (3%) (Table 73). The residuals of the linear regression of relative occurrence with latitude and longitude were used for the regression, which included only cells where the species is known to occur.

Table 73. Results of a multiple forward linear regression between relative occurrence of spotted wolffish and potential explanatory variables obtained from the megahabitat database (adapted from Dutil et al. 2011). *: p<0.10; **: p<0.05; ***: p<0.001; +: positive effect; -: negative effect.

Variable RO	Estimate	Standard error	t value	p	Partial R^2	+/-
Bathy_Max	0.00141	0.00046	3.06	**	0.10	+
Pente_Min2	-5.18	1.45	-3.57	***	0.04	-
TempMoyMin2	-0.062	0.019	-3.30	**	0.03	-
Geo2_Bosse	2.48	1.00	2.48	*	0.03	+
SalMinMin2	0.115	0.034	3.39	***	0.02	+
Geo2_Creux	-4.09	1.22	-3.36	***	0.02	-

The relative occurrence of spotted wolffish increased with decreasing depth (Bathy_Max is a negative variable). Spotted wolffish selected cells less than 250 m deep and avoided near-surface waters (Figure 42). Cells with a maximum depth of 40 m, for instance, represent 11% of all cells in the study area but do not account for more than 1% of the spotted wolffish occurrences, whereas cells with a maximum depth of 260 m represent less than 6% of all cells in the study area but account for 12% of spotted wolffish occurrences.

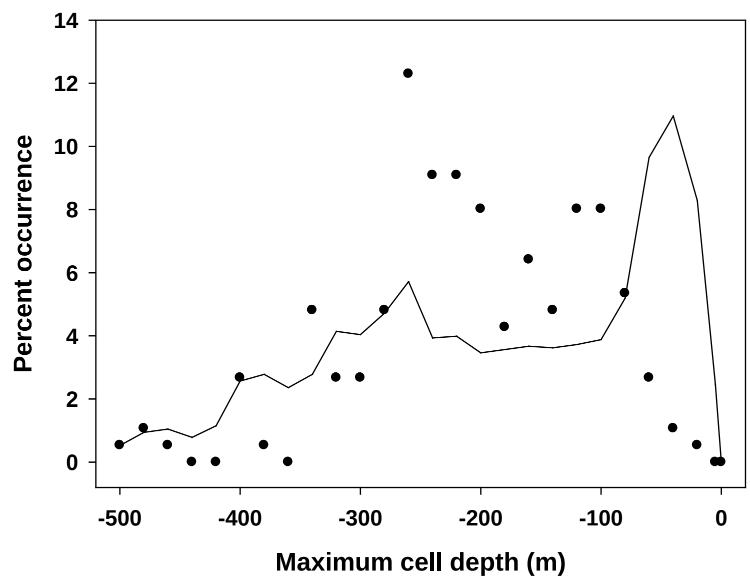

Figure 42. Percent frequency occurrence of cells in which spotted wolffish occurred (•; relative occurrence > 0) and percent frequency of cells in the study area (−) as a function of maximum (absolute value) cell depth.

The pattern was not as clear for the two other variables, which contributed most to explained variance (quadratic terms of minimum slope and mean temperature at minimum cell depth): spotted wolffish were present in cells with minimum slope values of 0 and greater than 0.15 (Figure 43), and in two groups of cells based on mean temperature at minimum depth (in absolute value)—mean temperatures below 3°C and between 4.0 and 5.5°C (Figure 44). Cells with a mean temperature at minimum depth of about 2.5°C and 5.0°C were selected.

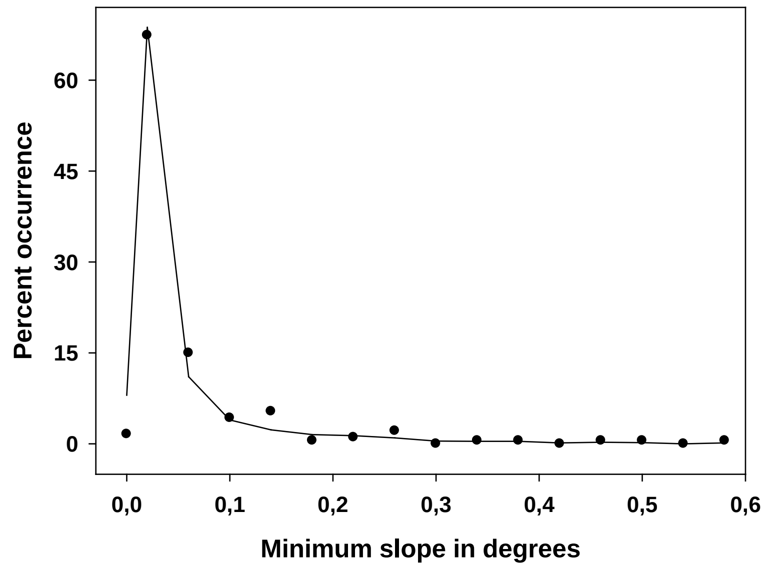

Figure 43. Percent frequency occurrence of cells in which spotted wolffish occurred (•; relative occurrence > 0) and percent frequency of cells in the study area (−), as a function of minimum slope.

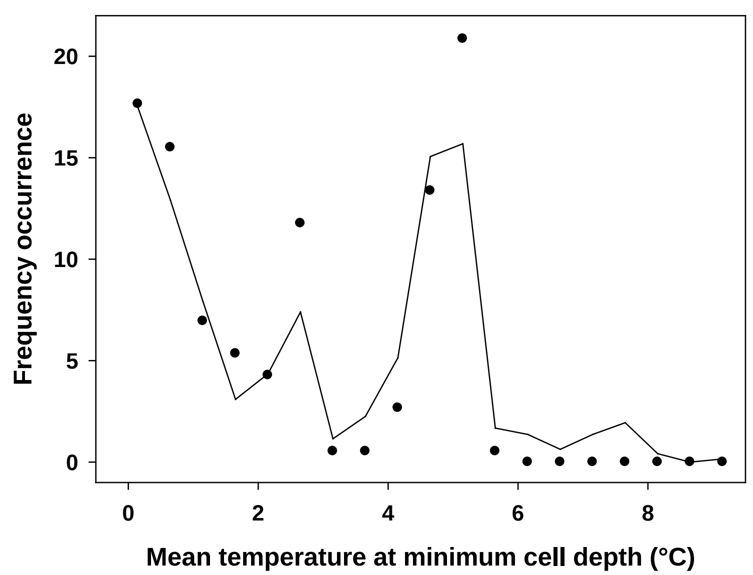

Figure 44. Percent frequency occurrence of cells in which spotted wolffish occurred (•; relative occurrence > 0) and percent frequency of cells in the study area (−), as a function of mean temperature at minimum depth.

Clustering of high relative occurrences

When the latitude and longitude effects are taken into account, 10 variables appear to have a significant effect on the degree of clustering of spotted wolffish in cells where positive values of the local spatial autocorrelation G_i* statistic were observed (p< 0.001, F-statistic: 23.17 on 11 and 497 DF, R^2=0.30). Four of those contributed most to explained variance: minimum cell depth (Bathy_min2, quadratic term) rugosity of the terrain (Geo2_Bosse), minimum salinity at minimum cell depth (SalMinMin), and distance to the shoreline (Cote_Dist) (Table 74). Other significant variables included slope, sediment type, and variability of neighbouring habitats. The residuals of the linear regression of G_i* with latitude and longitude were used, and only cells where positive values of the local spatial autocorrelation G_i* statistic were observed were included in the regression.

Table 74. Results of a multiple forward linear regression between G_i* (clusters of high relative occurrence for the species) and potential explanatory variables obtained from the megahabitat database (adapted from Dutil et al. 2011). *: p<0.10; **: p<0.05; ***: p<0.001; +: positive effect; -: negative effect.

Variable: G_i*	Estimate	Standard error	t value	p	Partial R^2	+/-
Bathy_Min2	$-1.03 \cdot 10^{-5}$	$0.23 \cdot 10^{-5}$	-4.45	***	0.10	-
Geo2_Bosse	-2.51	0.38	-6.65	***	0.06	-
SalMinMin	-0.199	0.035	-5.67	***	0.05	-
Cote_Dist	$7.17 \cdot 10^{-6}$	$1.28 \cdot 10^{-6}$	5.59	***	0.03	+
Sed2	0.237	0.055	4.30	***	0.02	+
Sed1_300	0.303	0.068	4.46	***	0.02	+
Pente_Mean2	0.43	0.13	3.45	***	0.02	+
Pente_Min2	-4.71	1.25	-3.79	***	0.01	-
MHVar_3x3	0.077	0.026	2.99	**	0.01	+
MHVar_3x32	-0.031	0.013	-2.29	*	0.01	-

Clusters of spotted wolffish occurrence (positive values of the G_i*) occured in cells with a minimum depth less than 300 m (Figure 45) and rugosity near 0 (Figure 46). Cells with a minimum depth of 100–250 m appear to be selected (Figure 45). This is consistent with the results for minimum salinity at minimum depth: clusters that occurred at salinities above 32 were over-represented (Figure 47), i.e., hot spots occurred in those cells at a greater frequency than expected considering the frequency occurrence of such cells in the study area. The species also clustered at any distance from the coast but predominantly in cells with a centroid located more than 40 km from the coast (Figure 48).

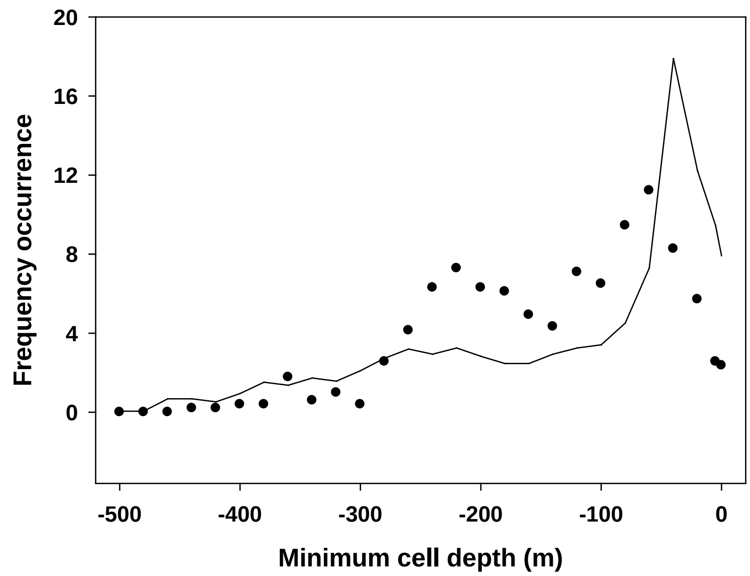

Figure 45. Percent frequency occurrence of cells in which spotted wolffish clustered (•; Gi* > 0) and percent frequency of cells in the study area (−), as a function of minimum (absolute value) cell depth.

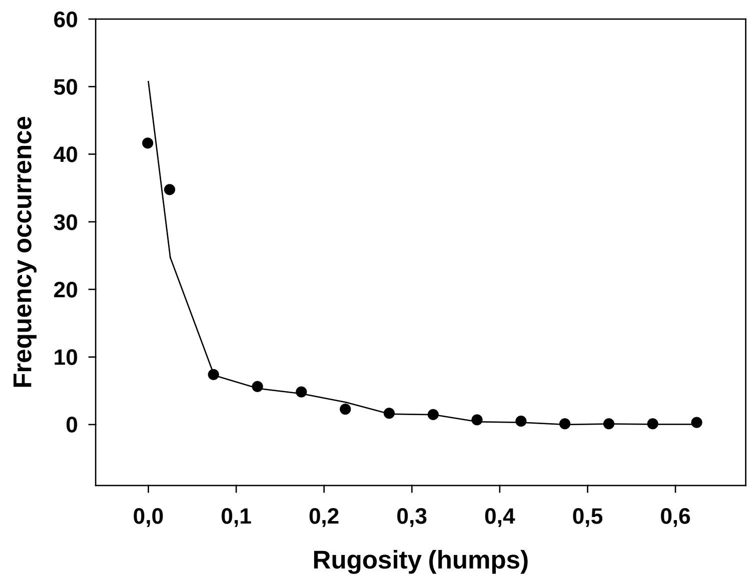

Figure 46. Percent frequency occurrence of cells in which spotted wolffish clustered (•; G_i* > 0) and percent frequency of cells in the study area (−) as a function of rugosity, i.e., the proportion of the seafloor classified as humps.

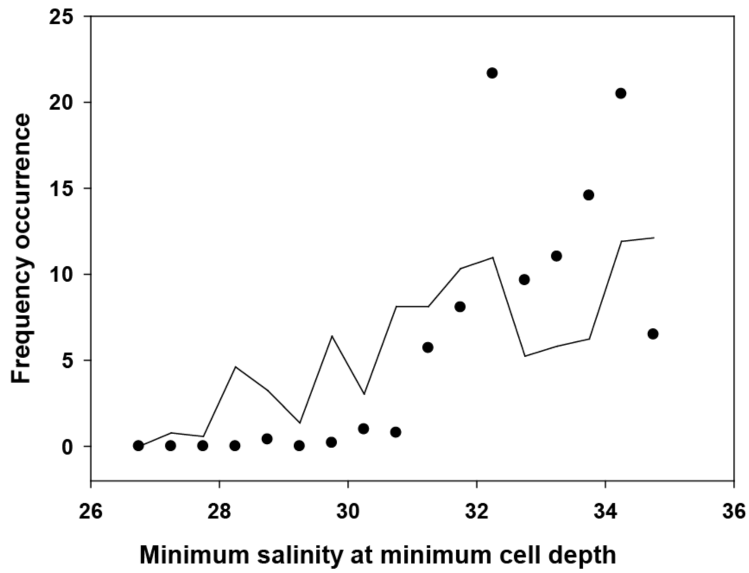

Figure 47. Percent frequency occurrence of cells in which spotted wolffish clustered (•; $G_i^* > 0$) and percent frequency of cells in the study area (−) as a function of minimum salinity at minimum cell depth.

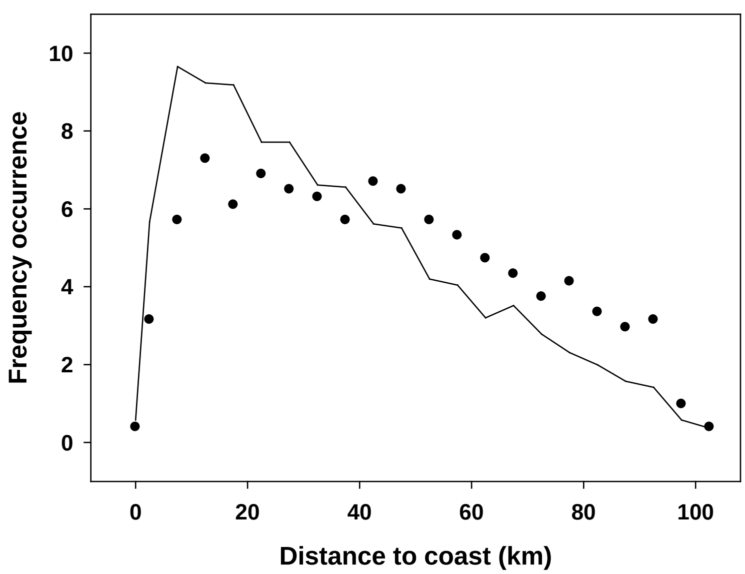

Figure 48. Percent frequency occurrence of cells in which spotted wolffish clustered (•; $G_i^* > 0$) and percent frequency of cells in the study area (−) as a function of distance between cell centroid and the nearest coast.

6. NORTHERN WOLFFISH

As was done for the other wolffish species (sections 4 and 5), a set of standardized output maps and tables are presented here for northern wolffish, produced with the analyses described in the Methods (section 3) using relative occurrence data. They include a description of the area of occupancy, density maps of occurrence, and global and local spatial autocorrelation statistics and maps. Tables are shown that summarize a set of species scores for each megahabitat category. The scores were then used in cluster analyses and MDS plots to identify the most important and the least important megahabitats for northern wolffish. Summary statistics and multiple forward linear regression statistics are provided describing environmental conditions and relationships in areas where the species occurs and where clusters of higher relative occurrence are found.

Area of occupancy

Northern wolffish were located primarily in conglomerate 1 (Table 75), located at the the south-western tip of Newfoundland at Cabot Strait, with smaller groups scattered in the area (Figure 49).

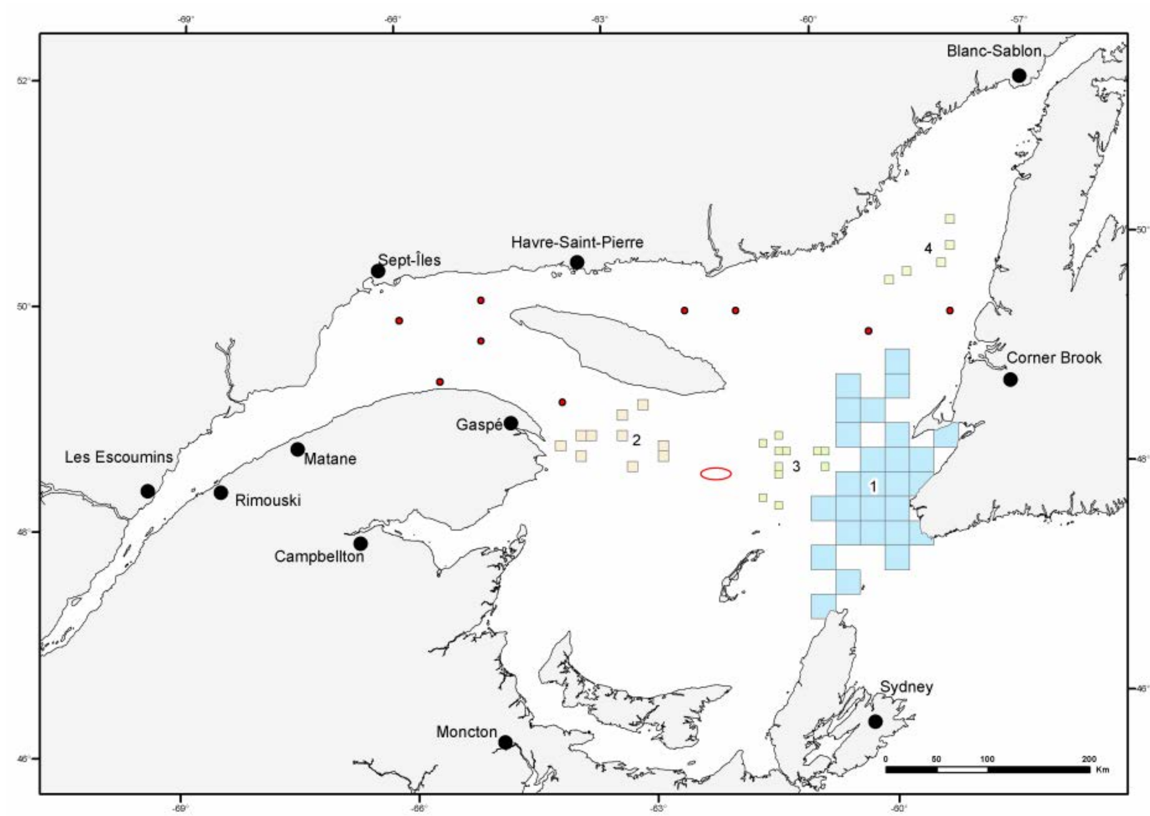

Figure 49. Area of occupancy of northern wolffish in the St. Lawrence estuary and Gulf based on annual bottom trawl surveys conducted by DFO (1971–2008). The grids were produced based on presence data using the Hernández and Navarro (2007) cartographic and conglomerate method. Conglomerates less than 100 km^2 are shown as ovals (not to scale), and satellites (isolated observations) are shown as red dots.

Table 75. Size of the area of occupancy of northern wolffish broken down by conglomerate and satellite groups of observations as determined by the Hernández and Navarro (2007) cartographic and conglomerate method and based on presence data obtained from annual bottom trawl surveys conducted by DFO (1971–2008). Conglomerates are mapped in Figure 48.

Conglomerate	Satellite	Planimetric area (km^2)
1		15,070
2		1,017
3		638
4		360
Others (less than 100 km^2 individually)		8
	n = 9	36
Total area of occupancy		**17,129**

Patterns and clusters of distribution

The kernel density estimate method applied to relative occurrence data yielded planimetric areas of 35,240 km^2, 29450 km^2, and 9,578 km^2 for the 95%, 90% (low density), and 50% (high density) volume density contours, respectively (Figure 50).

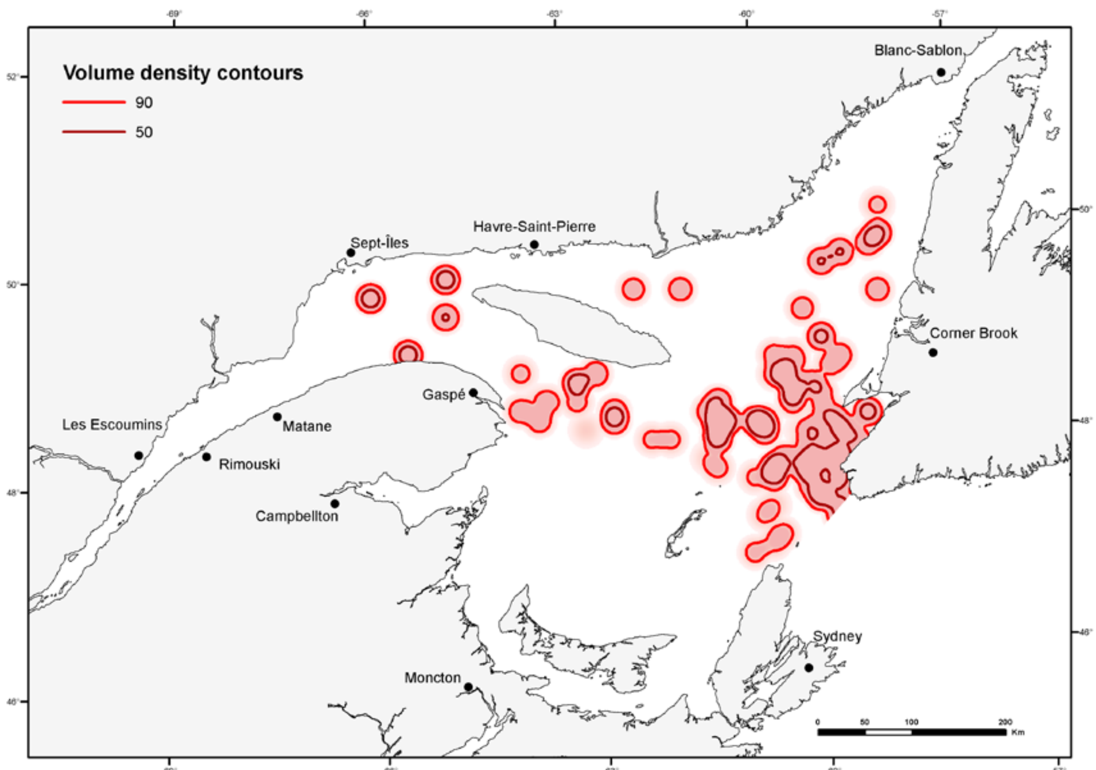

Figure 50. Density map of relative occurrence for northern wolffish in the St. Lawrence estuary and Gulf based on annual bottom trawl surveys conducted by DFO (1971–2008). The 50% and 90% volume density contours are shown. A 20 km search radius was used.

The Moran's *I* global spatial autocorrelation parameter yielded a positive (index value=0.119), highly significant (P<0.0001) Z-score of 12.3, which clearly indicates a high degree of clustering of northern wolffish relative occurrence in the study area (Figure 51). The local spatial autocorrelation statistic applied to relative occurrence data yielded planimetric areas of 19,960 km^2 for hot spots at p=0.10 (including 17,860 km^2 at p=0.05 and 12,186 km^2 at p=0.01).

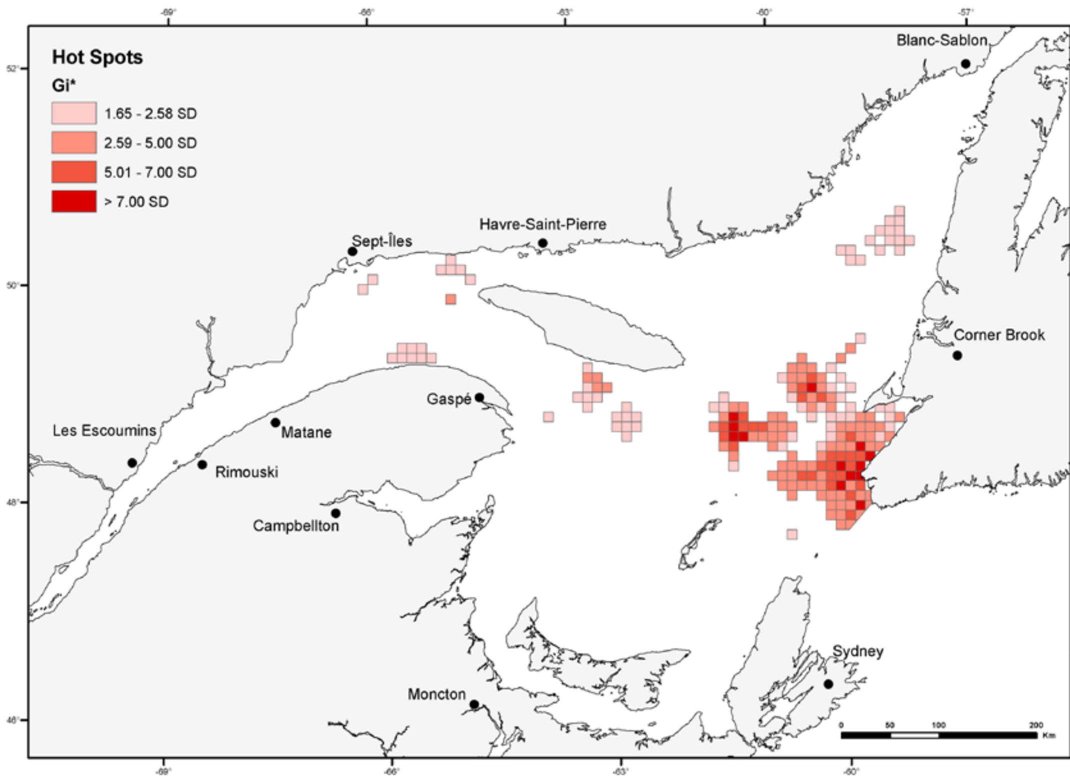

Figure 51. Location of statistically significant clusters of high relative occurrence (hot spots) (G_i* Z-scores significant at α=0.10) for northern wolffish in the St. Lawrence estuary and Gulf based on annual bottom trawl surveys conducted by DFO (1971–2008). No significant clusters of low relative occurrence (cold spots) were identified. Significant hot spots are broken down by intervals of Z-score standard deviations (SD). A 20 km bandwith (zone of indifference model) was used.

Habitat relationships

Not only do northern wolffish occupy a small portion of the study area, but they appear to be associated with a single megahabitat, namely the deep water, steep-sloped megahabitat B (Tables 76 and 77). This is shown clearly in the cluster analysis, with megahabitat B being significantly different from all other megahabitats (SIMPROF, p<0.05; Figure 52), and in the MDS graphs (stress value = 0.03; Figures 53–55), with megahabitat B being very dissimilar from all other megahabitats. Megahabitat B was also characterized by very high values of the G_i* statistic. This is shown by the large size of the bubbles only for megahabitat B in the MDS graphs (proportion of cells classified as hot spots, and mean relative occurrence and G_i* value of cells). Deep channels (megahabitat A) turned out to be the only other significant habitat when the size of the megahabitat was factored in the MDS graph (relative occurrence weighted area; Figure 56).

Table 76. Number of cells overlapping the distribution features, reported as a proportion of the number of cells in each megahabitat. The area of occupancy was determined by the Hernández and Navarro (2007) method using presence/absence data. The other features are based on the species relative occurrence. Cold spots and hot spots were determined based on the Getis and Ord local spatial autocorrelation Gi* statistic (Z-score). Mean relative occurrence and Gi* value are given for each megahabitat. The prime habitat for the species is highlighted.

Megahabitat	Number of cells	Area of occupancy	KDE 90% volume	KDE 50% volume	Cold spot	Hot spot	Relative occurrence	Z-score
A	609	0.172	0.184	0.108	0.000	0.218	0.012	0.68
B	14	0.643	0.143	0.500	0.000	0.643	0.021	3.21
C	161	0.112	0.180	0.019	0.000	0.106	0.004	0.12
D	129	0.054	0.109	0.016	0.000	0.078	0.005	-0.09
E	111	0.000	0.000	0.000	0.000	0.000	0.000	-0.57
G	29	0.034	0.276	0.000	0.000	0.069	0.004	0.10
H	149	0.000	0.000	0.000	0.000	0.000	0.000	-0.65
I	125	0.048	0.048	0.016	0.000	0.056	0.001	-0.32
J	351	0.031	0.026	0.003	0.000	0.011	0.001	-0.55
K	134	0.157	0.142	0.060	0.000	0.134	0.010	0.13
L	18	0.056	0.111	0.000	0.000	0.000	0.000	-0.23
M	76	0.053	0.026	0.026	0.000	0.053	0.003	-0.21

Table 77. Number of cells where the species presence was confirmed and overlap between these cells and the distribution features, reported as a proportion of the number of cells in each megahabitat. The area of occupancy was determined by the Hernández and Navarro (2007) method using presence/absence data. The other features are based on the species relative occurrence. Cold spots and hot spots were determined based on the Getis and Ord local spatial autocorrelation Gi* statistic (Z-score). Mean relative occurrence and Gi* value are given for each megahabitat. The prime habitat for the species is highlighted.

Megahabitat	Number of cells	Area of occupancy	KDE 90% volume	KDE 50% volume	Cold spot	Hot spot	Relative occurrence	Z-score
A	53	0.849	0.283	0.717	0.000	0.736	0.141	3.34
B	4	1.000	0.250	0.750	0.000	1.000	0.073	5.64
C	7	1.000	0.714	0.286	0.000	0.286	0.100	2.00
D	7	0.571	0.714	0.143	0.000	0.143	0.089	0.82
E	0	0.000	0.000	0.000	0.000	0.000	0.000	0.00
G	1	1.000	1.000	0.000	0.000	0.000	0.111	0.65
H	0	0.000	0.000	0.000	0.000	0.000	0.000	0.00
I	2	1.000	0.000	1.000	0.000	1.000	0.088	3.70
J	3	1.000	0.667	0.333	0.000	0.333	0.133	1.15
K	12	1.000	0.500	0.500	0.000	0.667	0.109	3.12
L	0	0.000	0.000	0.000	0.000	0.000	0.000	0.00
M	1	1.000	0.000	1.000	0.000	1.000	0.222	6.71

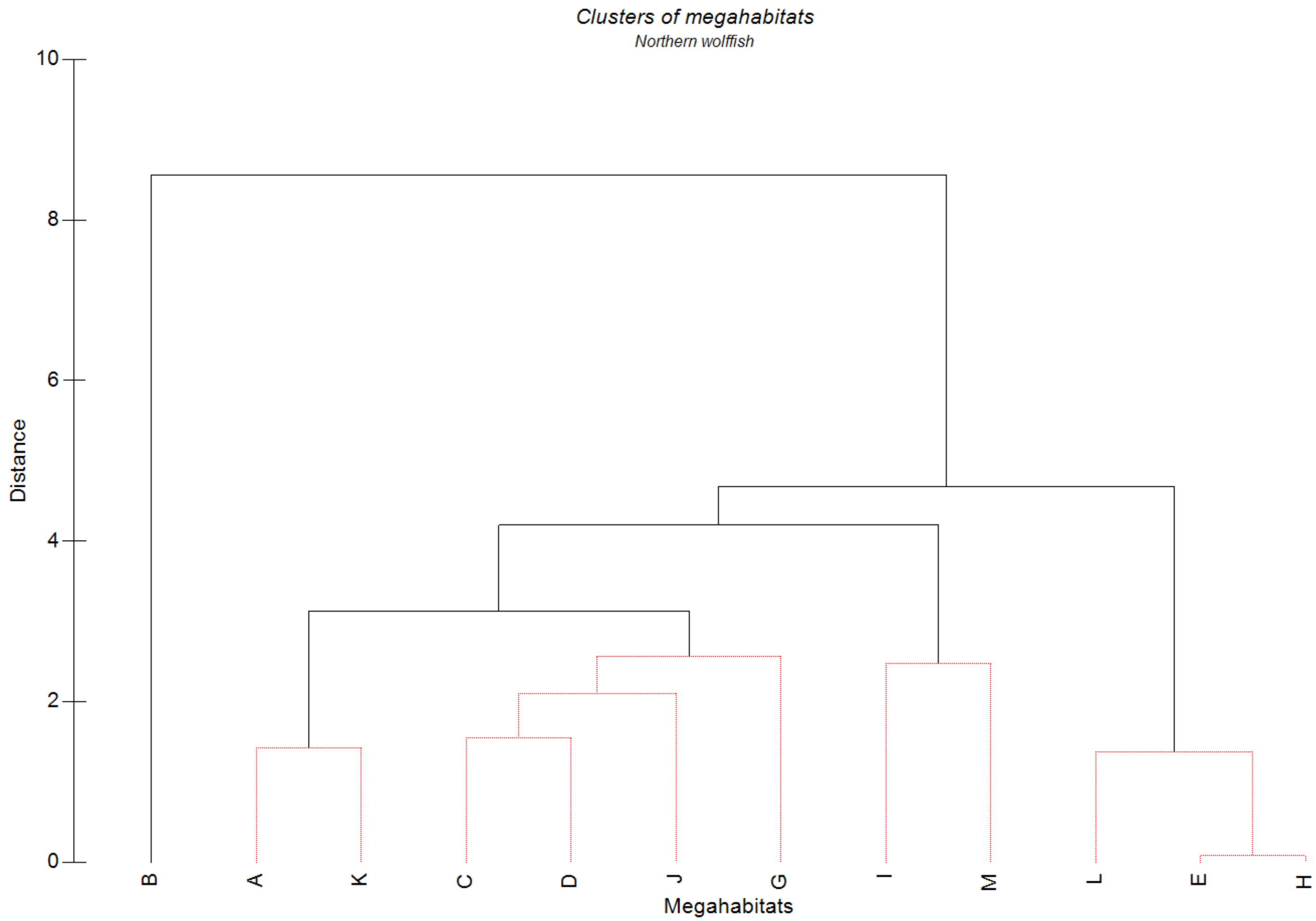

Figure 52. Tree diagram showing significant (black line) clusters of megahabitats based on northern wolffish spatial distribution and relative occurrence descriptors: proportion of cells overlapping the area of occupancy and within the 50 and 90% volume contours, proportion of cells classified as hot spots or cold spots, mean relative occurrence, and local spatial autocorrelation G_i* statistic.

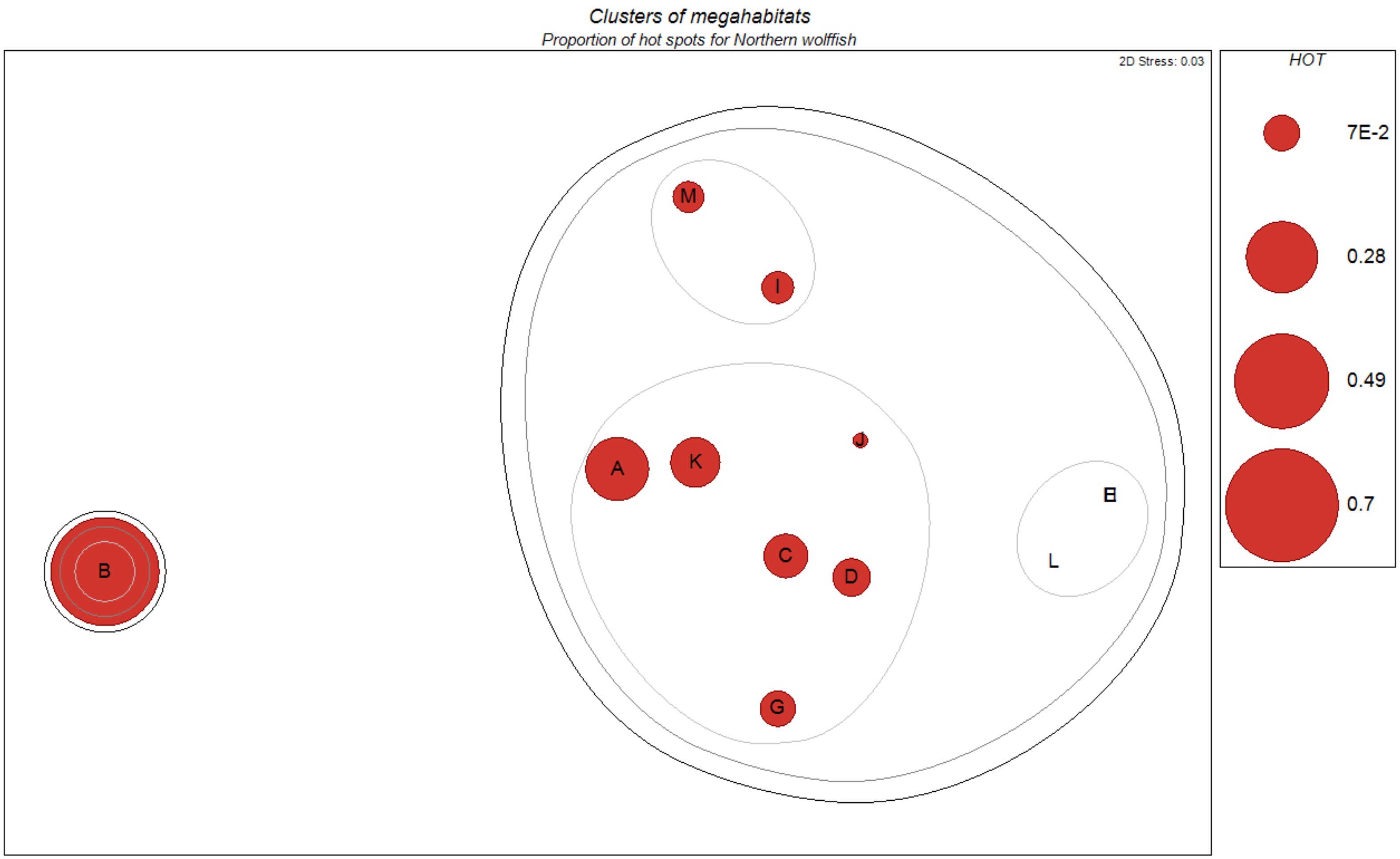

Figure 53. Multidimensional scaling plot of megahabitats based on northern wolffish spatial distribution and relative occurrence descriptors: proportion of cells overlapping the area of occupancy and within the 50 and 90% volume contours, proportion of cells classified as hot spots or cold spots, mean relative occurrence, and local spatial autocorrelation G_i* statistic. Bubble size is proportional to the proportion of cells classified as hot spots in the megahabitat.

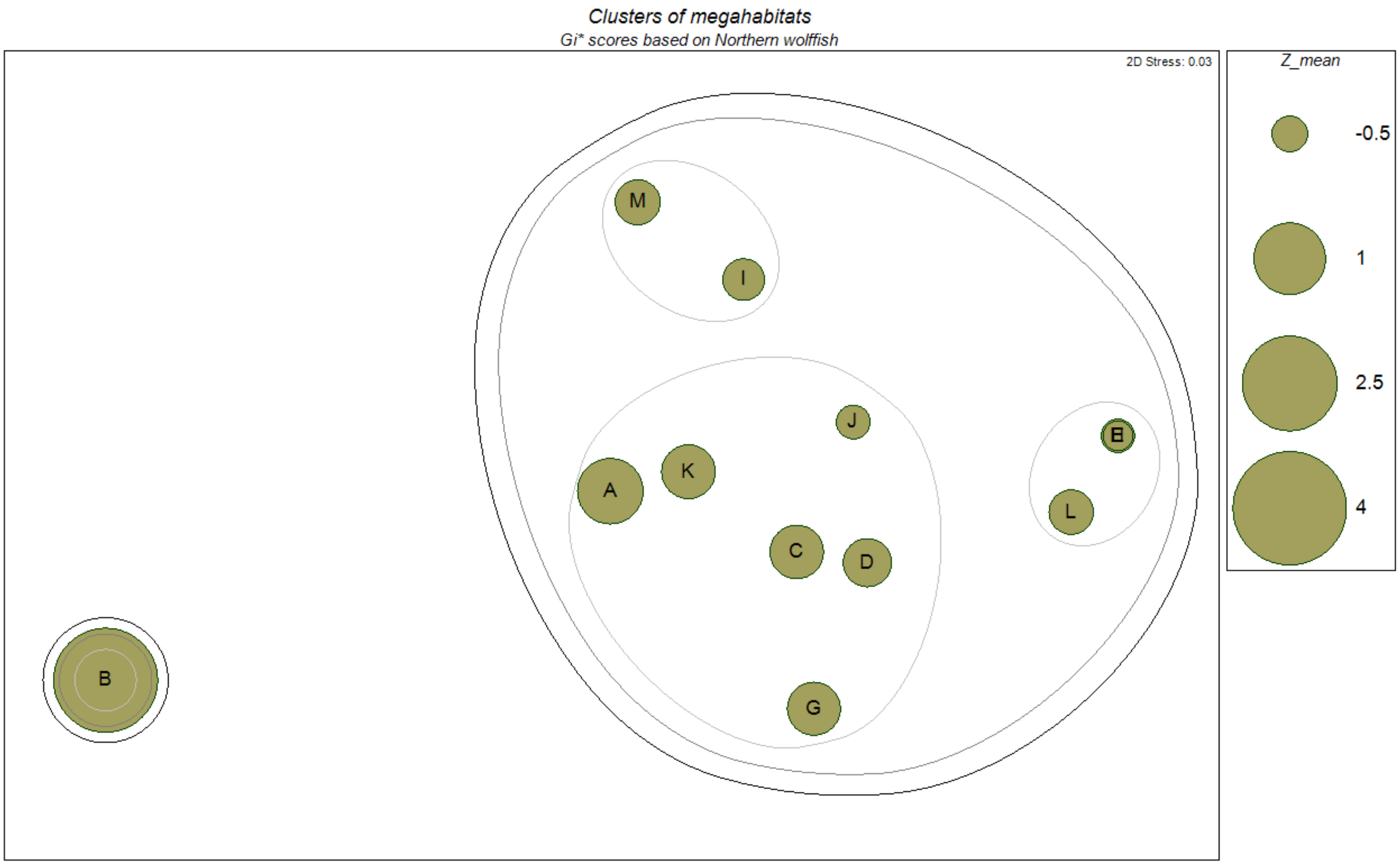

Figure 54. Multidimensional scaling plot of megahabitats based on northern wolffish spatial distribution and relative occurrence descriptors: proportion of cells overlapping the area of occupancy and within the 50 and 90% volume contours, proportion of cells classified as hot spots or cold spots, mean relative occurrence, and local spatial autocorrelation G_i* statistic. Bubble size is proportional to the mean relative occurrence value of cells in the megahabitat.

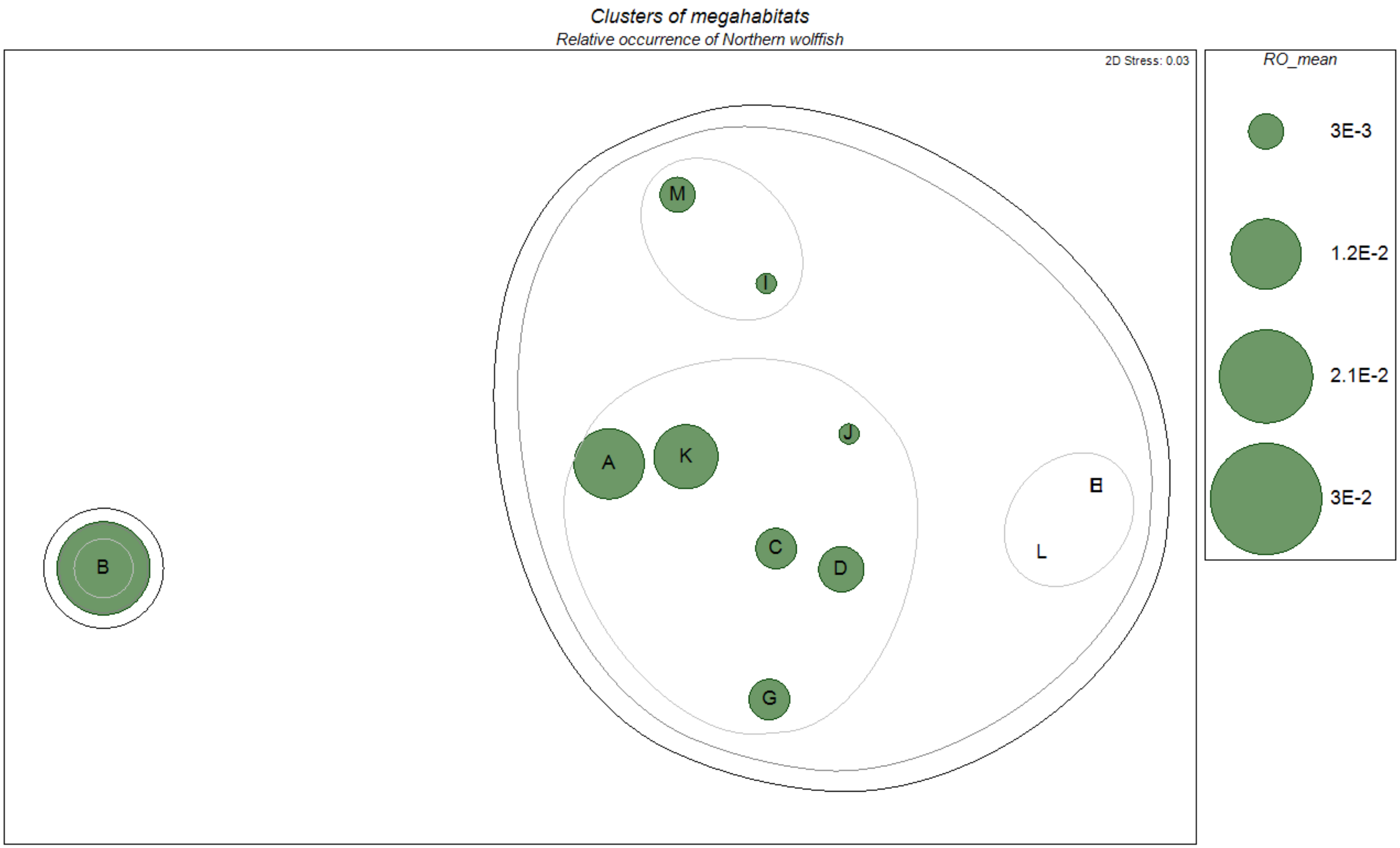

Figure 55. Multidimensional scaling plot of megahabitats based on northern wolffish spatial distribution and relative occurrence descriptors: proportion of cells overlapping the area of occupancy and within the 50 and 90% volume contours, proportion of cells classified as hot spots or cold spots, mean relative occurrence, and local spatial autocorrelation G_i* statistic. Bubble size is proportional to the mean local spatial autocorrelation G_i* value of cells in the megahabitat.

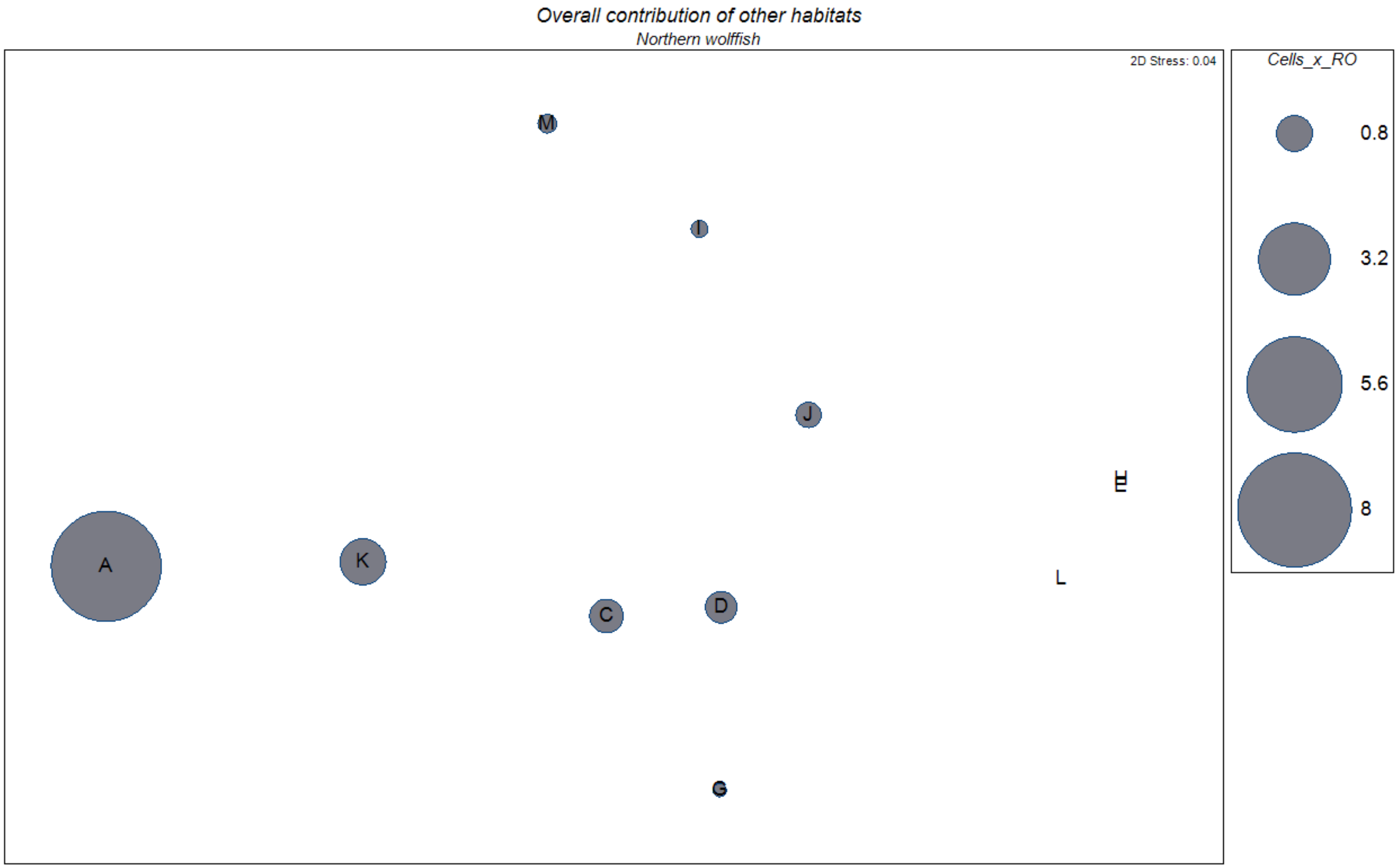

Figure 56. Multidimensional scaling plot of megahabitats based on northern wolffish spatial distribution and relative occurrence descriptors: proportion of cells overlapping the area of occupancy and within the 50 and 90% volume contours, proportion of cells classified as hot spots or cold spots, mean relative occurrence, and local spatial autocorrelation G_i* statistic. Bubble size is proportional to the product of mean relative occurrence and number of cells where the species was found to occur (relative occurrence weighted area).

Environmental relationships

Tables 78–81 summarize the environmental conditions that prevail where northern wolffish was found to occur and to cluster; mean values and confidence interval are reported for quantitative variables, and number of cells and proportion of cells meeting the classification criteria are reported for qualitative variables.

Table 78. Mean, 5th, 25th, median, 75th, and 95th percentiles for quantitative variables describing environmental conditions for cells where northern wolffish was found to occur (relative occurrence > 0).

Variable	Mean	5%	25%	Median	75%	95%
MHVar_3x3	2.32	1.00	1.00	2.00	3.00	4.00
Relief_var	3.53	1.00	1.00	3.00	6.00	7.00
Pro_Protege	0.00	0.00	0.00	0.00	0.00	0.00
Pro_SemiExp	0.00	0.00	0.00	0.00	0.00	0.00
Cote_Dist	41955	11547	23450	37235	59416	82871
Bathy_Mean	-280.2	-478.5	-399.6	-274.9	-159.5	-94.6
Bathy_STD	21.1	3.9	8.1	15.7	26.6	62.4
Bathy_Max	-320.5	-494.1	-423.7	-319.4	-242.4	-128.8
Bathy_Min	-232.3	-461.2	-356.7	-213.1	-96.6	-58.3
Pente_Mean	0.46	0.13	0.193	0.403	0.6	1.202
Pente_STD	0.22	0.06	0.10	0.17	0.30	0.52
Pente_Max	0.07	0.00	0.01	0.02	0.07	0.30
Pente_Min	1.19	0.31	0.57	0.89	1.59	2.71
Geo2_Bosse	0.04	0.00	0.00	0.00	0.06	0.17
Geo2_Creux	0.03	0.00	0.00	0.01	0.05	0.14
SalMoyMoy	34.16	32.65	33.60	34.52	34.80	34.80
SalMinMoy	33.99	32.35	33.31	34.39	34.70	34.76
SalMaxMoy	34.32	32.81	33.85	34.68	34.84	35.00
SalMoyMin	33.76	32.11	32.65	34.12	34.77	34.80
SalMinMin	33.55	31.85	32.27	33.90	34.65	34.76
SalMaxMin	33.93	32.25	32.81	34.41	34.83	34.91
SalMoyMax	34.36	33.33	34.38	34.60	34.80	34.80
SalMinMax	34.20	32.94	34.17	34.52	34.71	34.76
SalMaxMax	34.50	33.48	34.57	34.72	34.85	35.04
TempMoyMoy	4.01	0.81	2.87	4.80	5.02	5.34
TempMinMoy	3.57	0.19	2.27	4.33	4.70	5.04
TempMaxMoy	4.49	1.16	3.32	5.28	5.42	5.90
TempMoyMin	3.46	0.49	1.12	4.58	4.94	5.34
TempMinMin	2.82	-0.57	0.59	4.04	4.60	5.04
TempMaxMin	4.21	1.12	2.60	5.03	5.42	5.90
TempMoyMax	4.35	2.35	4.53	4.89	5.11	5.34
TempMinMax	3.94	1.74	4.10	4.45	4.70	5.04
TempMaxMax	4.85	2.87	4.91	5.37	5.51	5.90

Table 79. Number of cells and proportion of cells meeting the classification criteria for 12 binary variables describing environmental conditions for cells where northern wolffish was found to occur (relative occurrence > 0).

Variable	Count	Proportion
Geo_Plateau	25	0.28
Geo_Talus	12	0.13
Geo_Chenal	53	0.59
Oxy_12	8	0.09
Oxy_34	45	0.50
Oxy_56	23	0.26
Oxy_78	14	0.16
Sed1_100	66	0.73
Sed1_200	5	0.06
Sed1_300	19	0.21
Sed1_400	0	0.00
Sed2	20	0.22

Table 80. Mean, 5th, 25th, median, 75th, and 95th percentiles for quantitative variables describing environmental conditions where northern wolffish was found to cluster (local spatial autocorrelation G_i* statistic value > 1.645).

Variable	Mean	5%	25%	Median	75%	95%
MHVar_3x3	2.13	1.00	1.00	2.00	3.00	4.00
Relief_var	3.28	1.00	1.00	2.50	5.25	7.00
Pro_Protege	0.00	0.00	0.00	0.00	0.00	0.00
Pro_SemiExp	0.00	0.00	0.00	0.00	0.00	0.00
Cote_Dist	42475	6158	19594	41267	62896	83497
Bathy_Mean	-300.0	-486.3	-406.6	-320.6	-187.7	-88.4
Bathy_STD	17.6	3.8	7.1	12.3	23.0	49.8
Bathy_Max	-333.7	-503.0	-429.1	-345.8	-244.1	-113.0
Bathy_Min	-258.9	-472.2	-382.4	-279.1	-114.5	-55.1
Pente_Mean	0.40	0.11	0.17	0.28	0.51	1.13
Pente_STD	0.19	0.04	0.08	0.15	0.28	0.48
Pente_Max	0.06	0.00	0.01	0.02	0.06	0.26
Pente_Min	1.07	0.26	0.44	0.83	1.49	2.68
Geo2_Bosse	0.03	0.00	0.00	0.00	0.04	0.19
Geo2_Creux	0.03	0.00	0.00	0.00	0.04	0.14
SalMoyMoy	34.22	32.65	34.04	34.54	34.80	34.80
SalMinMoy	34.07	32.35	33.82	34.39	34.71	34.76
SalMaxMoy	34.37	32.81	34.22	34.72	34.85	35.04
SalMoyMin	33.91	32.11	32.77	34.54	34.79	34.80
SalMinMin	33.73	31.96	32.51	34.39	34.71	34.76
SalMaxMin	34.07	32.25	32.98	34.63	34.85	35.04
SalMoyMax	34.39	32.67	34.41	34.62	34.80	34.80
SalMinMax	34.26	32.38	34.17	34.54	34.74	34.76
SalMaxMax	34.52	32.85	34.57	34.72	34.85	35.04
TempMoyMoy	4.15	1.04	4.05	4.81	5.04	5.34
TempMinMoy	3.72	0.25	3.67	4.40	4.70	5.04

TempMaxMoy	4.67	1.65	4.42	5.32	5.42	5.90
TempMoyMin	3.77	0.56	2.16	4.77	4.94	5.34
TempMinMin	3.10	-0.62	0.59	4.31	4.61	5.04
TempMaxMin	4.63	1.29	2.99	5.23	5.42	5.90
TempMoyMax	4.41	1.12	4.64	4.91	5.10	5.34
TempMinMax	4.01	0.59	4.14	4.46	4.70	5.04
TempMaxMax	4.90	1.65	4.93	5.37	5.48	5.90

Table 81. Number of cells and proportion of cells meeting the classification criteria for 12 binarybinary variables describing environmental conditions where northern wolffish was found to cluster (local spatial autocorrelation G_i* statistic value > 1.645).

Variable	Count	Proportion
Geo_Plateau	48	0.2353
Geo_Talus	21	0.1029
Geo_Chenal	135	0.6617
Oxy_12	14	0.0686
Oxy_34	101	0.4951
Oxy_56	62	0.3039
Oxy_78	27	0.1323
Sed1_100	162	0.7941
Sed1_200	1	0.0049
Sed1_300	39	0.1911
Sed1_400	2	0.0098
Sed2	47	0.2303

Northern wolffish tend to occur in poorly diversified habitats. They are associated with very fine sediments and channels offshore, i.e., in a greater proportion than the two other species of wolffish (sections 4 and 5). They mainly occur at depths greater than 200 m and cluster at depths between 250 and 300 m, in a high salinity (34) constant temperature (3–5°C) environment with relatively low levels of oxygen saturation.

Latitude and longitude explained only 6% of the variance in the relative occurrence data (p=0.03, F-statistic: 3.7 on 2 and 87 DF) and 5% of the variance in the G_i* data (p<0.001, F-statistic: 15.5 on 2 and 509 DF). The relative occurrence data were log transformed, and the G_i* data were fourth-root transformed.

Relative occurrence

Only three environmental variables (quadratic term) showed significant relationships with northern wolffish relative occurrence: minimum depth, distance to the coast, and mean temperature at minimum depth (p<0.001, F-statistic: 14.99 on 3 and 86 DF, R^2=0.32). Minimum depth and mean temperature at minimum depth had the greatest correlation coefficients and explained 15 and 13% of the variance, respectively (Table 82). The residuals of the linear regression of relative occurrence with latitude and longitude were used for the regression, which included only cells where the species is known to occur.

Table 82. Results of a multiple forward linear regression between relative occurrence of northern wolffish and potential explanatory variables obtained from the megahabitat database (adapted from Dutil et al. 2011). *: p<0.10; **: p<0.05; ***: p<0.001; +: positive effect; -: negative effect.

Variable RO	Estimate	Standard error	t value	p	Partial R^2	+/-
Bathy_Min_2	0.0000132	0.0000029	4.57	***	0.15	+
TempMoyMin_2	-0.0688	0.0167	-4.13	***	0.13	-
Cote_Dist_2	$2.32 \cdot 10^{-10}$	$0.80 \cdot 10^{-10}$	2.91	**	0.06	+

Northern wolffish avoided cells with minimum depths between 0 and 50 m and appeared to be over-represented (relative to stratum availability) in cells where minimum depth was great, i.e., below 300 m (Figure 57). Cells with a minimum depth of 20 m, for instance, represent 12.2% of all cells in the study area but do not account for any northern wolffish occurrences, whereas cells with a minimum depth of 360 m represent 1.4% of all cells in the study area but account for 7.8% of northern wolffish occurrences.

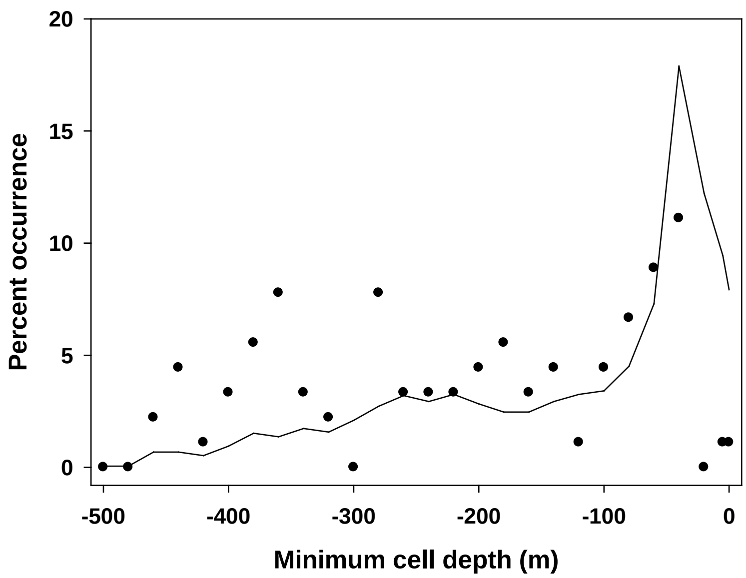

Figure 57. Percent frequency occurrence of cells in which northern wolffish occurred (•; relative occurrence > 0) and percent frequency of cells in the study area (−), as a function of minimum (absolute value) cell depth.

Northern wolffish were absent from the few cells with mean temperature at minimum depth above 6°C, avoided cells where mean temperature at minimum depth was cold (0.5°C), and favoured cells where mean temperature at minimum depth was between 5 and 6°C (Figure 58). The latter are representative of deep channels in the study area.

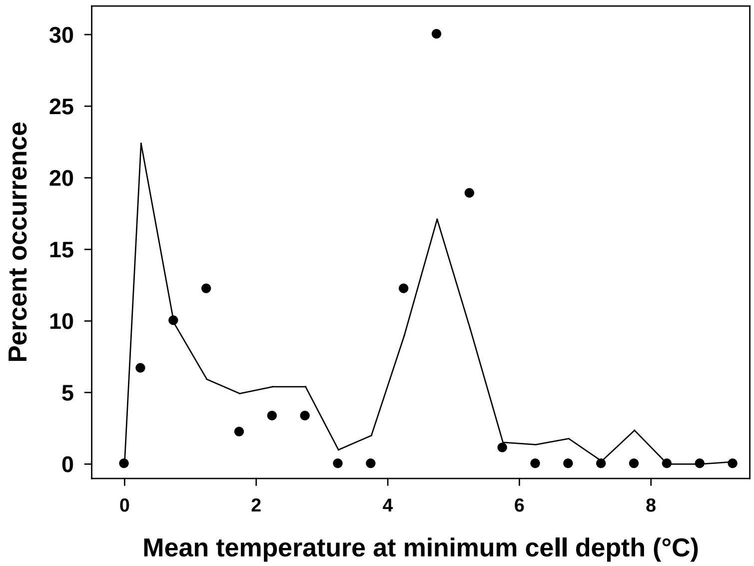

Figure 58. Percent frequency occurrence of cells in which northern wolffish occurred (•; relative occurrence > 0) and percent frequency of cells in the study area (−), as a function of mean temperature at minimum depth.

Whereas a large number of cells are located at short distances from the coast (cell centroid to coast distance less than 30 km), northern wolffish appeared to occur more frequently relative to stratum availability at greater distances from the coast (Figure 59).

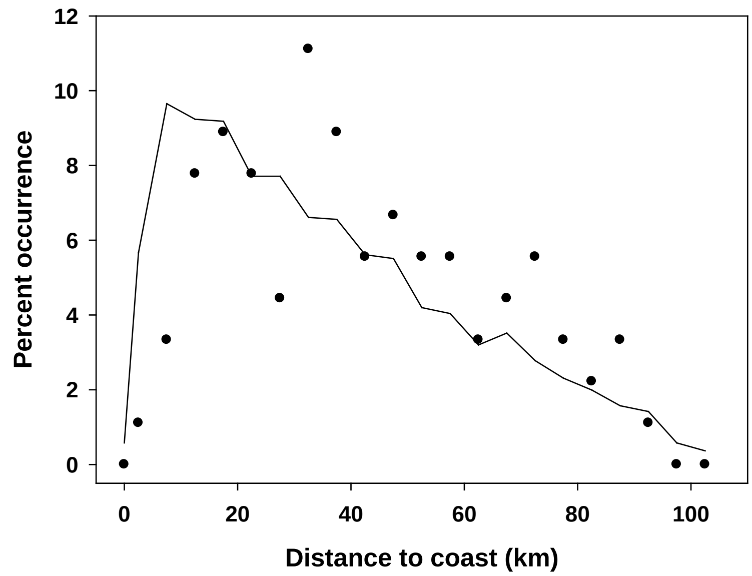

Figure 59. Percent frequency occurrence of cells in which northern wolffish occurred (•; relative occurrence > 0) and percent frequency of cells in the study area (−) as a function of distance to coast.

Clustering of high relative occurrences

When the latitude and longitude effects are taken into account, nine variables appear to have a significant effect on the degree of clustering of northern wolffish in cells where positive values of the local spatial autocorrelation G_i* statistic were observed ($p<0.001$, F-statistic: 13.09 on 9 and 502 DF, $R^2=0.18$; Table 83). Two binary variables appeared to explain a greater proportion of the variance, with a higher degree of clustering (hot spots) being observed over coarse sediments. Relationships with other variables were more complex, as indicated by the significant quadratic terms. The residuals of the linear regression of G_i* with latitude and longitude were used for the regression, which included only cells where positive values of the local spatial autocorrelation G_i* statistic were observed.

Table 83. Results of a multiple forward linear regression between G_i* (clusters of high relative occurrence for the species) and potential explanatory variables obtained from the megahabitat database (adapted from Dutil et al. 2011). *: p<0.10; **: p<0.05; ***: p<0.001; +: positive effect; -: negative effect.

Variable: G_i*	Estimate	Standard error	t value	p	Partial R^2	+/-
(Intercept)	-0.056	0.024	-2.29	*		-
Sed1_200	-0.207	0.069	-2.99	**	0.06	-
Bathy_Min2	$4.04 \cdot 10^{-6}$	$0.87 \cdot 10^{-6}$	4.66	***	0.03	+
Sed1_300	0.214	0.045	4.79	***	0.03	+
TempMinMoy2	-0.026	0.007	-3.46	***	0.02	-
Pente_STD2	-0.68	0.17	-4.01	***	0.02	-
SalMaxMoy2	0.101	0.045	2.58	*	0.01	+
Pro_SemiExp2	-126.4	58.6	-2.16	*	0.01	-
TempMaxMax	0.050	0.019	2.62	**	0.01	+
Geo2_Creux2	4.37	1.92	2.28	*	0.01	+

Although clusters occurred most frequently over fine sediments (79% of the cells classified as hot spots), the degree of clustering was most influenced by other types of sediments, with no clustering occurring over sandy bottoms (Sed1_200) and some clustering occurring over gravely sands (Sed1_300). Northern wolffish clustered preferentially in cells with minimum depth (absolute value) greater than 180 m, i.e., below the CIL (Figure 60).

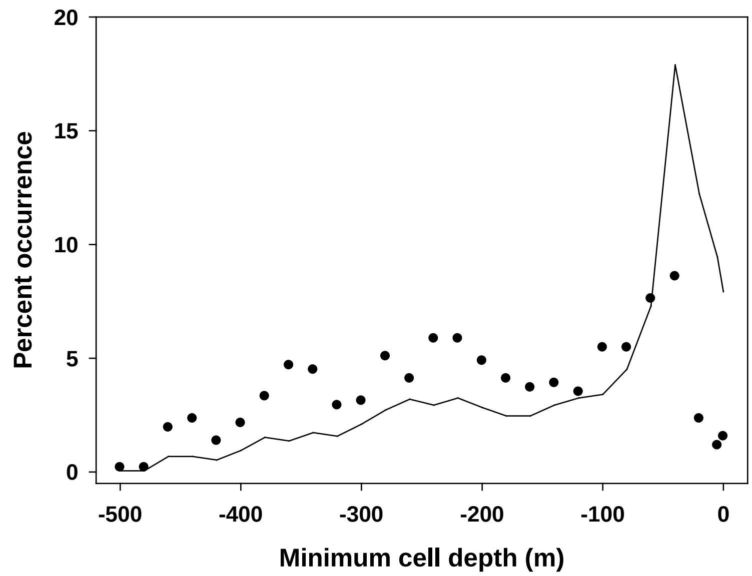

Figure 60. Percent frequency occurrence of cells in which northern wolffish clustered (•; $G_i^* > 0$) and percent frequency of cells in the study area (−) as a function of minimum (absolute value) cell depth.

7. COMPARING WOLFFISH HABITATS

The results presented in sections 4 to 6 suggest commonalities in habitat features among the wolffish species. The cells and megahabitat categories that were important for more than one species might deserve more attention from a protection and management perspective. To this end, the degree of overlap between species was examined with a redundancy analysis conducted on the data to explore how the species differed in their relationship to environmental conditions. A final series of analyses examined the composition of species caught in association with the wolffishes and their groupings when using recursive tree partitioning based on environmental and biological data. Further details on the tree partitioning method of analysis are described and presented in the final chapter (section 9) on fish assemblages.

Size of the habitat by species

The two species listed as threatened (northern and spotted wolffish) occurred in a small proportion of all trawl sets (8.4% and 14.3%, respectively) and cells (4.7% and 9.8%, respectively), compared to striped wolffish (36.0% of sets and 26.0% of cells, respectively) (Table 84). These differences are significant for both sets (Chi-square =2615.6, 2 degrees of freedom; $p<0.001$) and cells (Chi-square =348.0, 2 degrees of freedom; $p<0.001$).

Table 84. Size (km^2) of the area of occupancy, area within the 50% volume density contour (KDE), area of hot spots based on the local G_i* statistic, number of cells where the species was caught, and prime habitats for northern, spotted, and striped wolffish.

Species	Area of occupancy	50% volume density	Hot spots	Number of cells	Prime habitats
Northern wolffish	17,129	9,578	12,186	90	A, B
Spotted wolffish	56,499	14,362	16,961	187	C, K
Striped wolffish	95,453	20,042	23,871	493	B, C, K

Degree of overlap between species

As expected from its abundance, the striped wolffish overlapped the most with the other species both in zones of 50% volume density and in hot spots (Tables 85 and 86). Of particular interest was the the difference in degree of overlap between the two approaches. A larger proportion of hot spot cells was shared by the three species than in two-way overlaps: 326 vs. 192 and 57 for striped wolffish with the others in shared hot spots, compared with 193 vs. 172 and 48 in overlapping 50% volume density zones. Cells with all wolffish species are of special interest to examine for their environmental features (Figure 61).

Table 85. Overlap of zones within the 50% volume density contour (km^2, based on KDE) between northern, spotted, and striped wolffish.

50% volume density	Northern wolffish	Spotted wolffish	Striped wolffish	Two other species
Northern wolffish (no. of cells)	-	556.9 (22)	1825.8 (48)	39.5 (49)
Spotted wolffish (no. of cells)	-	-	9080.4 (172)	9189.0 (173)
Striped wolffish (no. of cells)	-	-	-	10457.9 (193)

Table 86. Overlap of hot spots (km^2, G_i*>1.645) between northern, spotted, and striped wolffish.

Hot spots	Northern wolffish	Spotted wolffish	Striped wolffish	Two other species
Northern wolffish (no. of cells)	-	3979.3 (40)	5638.9 (57)	6138.9 (62)
Spotted wolffish (no. of cells)	-	-	19131.6 (192)	19631.6 (198)
Striped wolffish (no. of cells)	-	-	-	31828.4 (326)

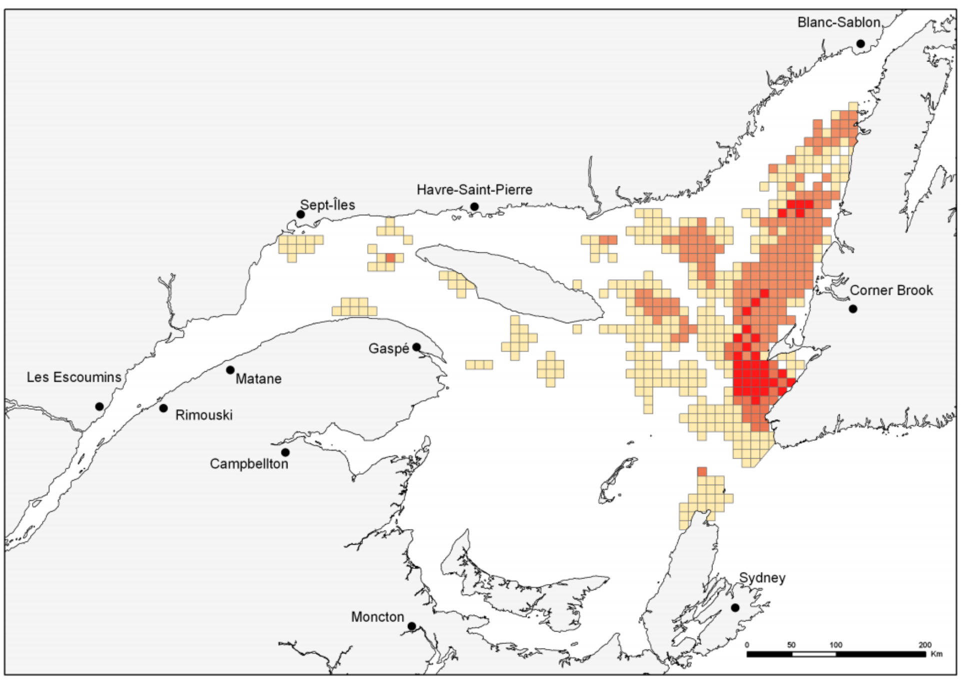

Figure 61. Overlap of hot spots (G_i*>1.645) between northern, spotted, and striped wolffish. Red: cells where hot spots of the three species overlap; light red: cells where hot spots of two species overlap; beige: no overlap.

Cluster analysis

Northern wolffish appear to have significantly different habitat requirements than the two other species (Figures 62–63). Megahabitat B is considered, with megahabitats C and K, as most favourable to wolffish in the study area (Figure 64). Megahabitats A and D have a secondary importance, depending on species and variable considered. Megahabitats G, L, E, and H have no importance.

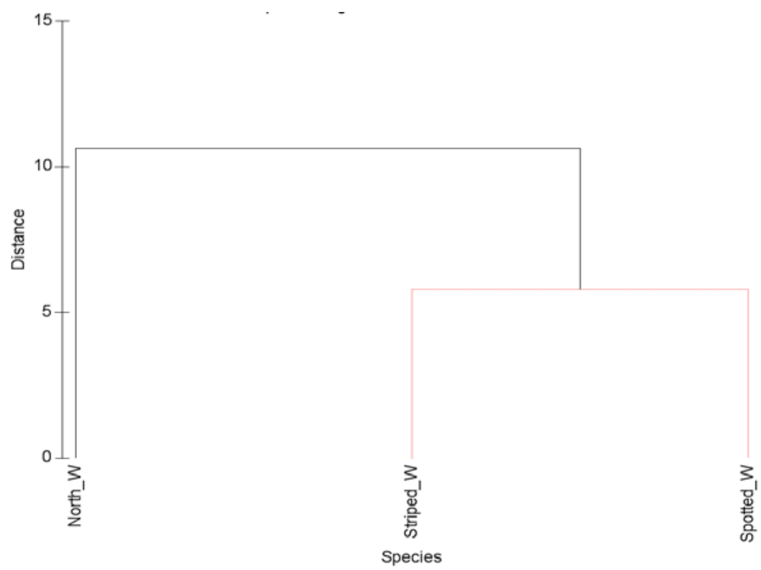

Figure 62. Species clusters based on enviromental data. The mean values for each of the environmental descriptors in the megahabitat database were used as species descriptors in the analysis.

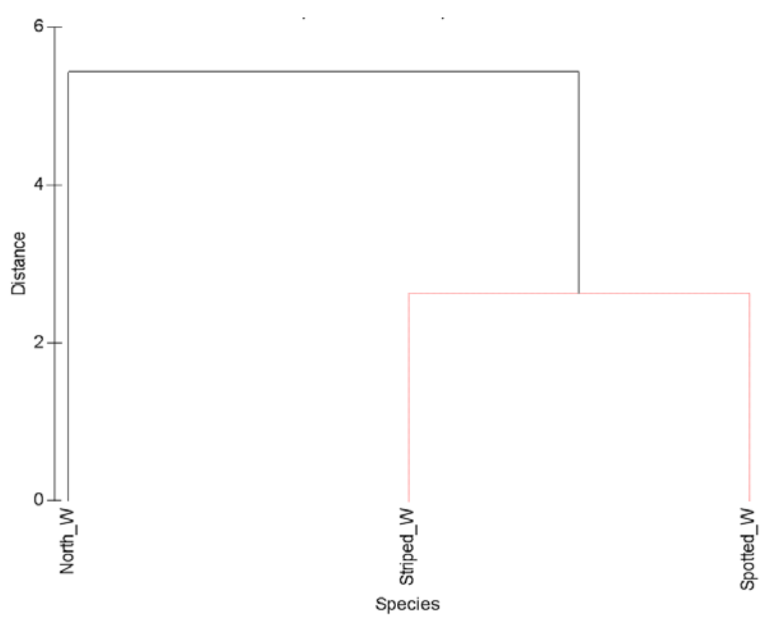

Figure 63. Species clusters based on Euclidean distance between megahabitat B and other megahabitats. Species are considered as samples and megahabitats as variables in the analysis.

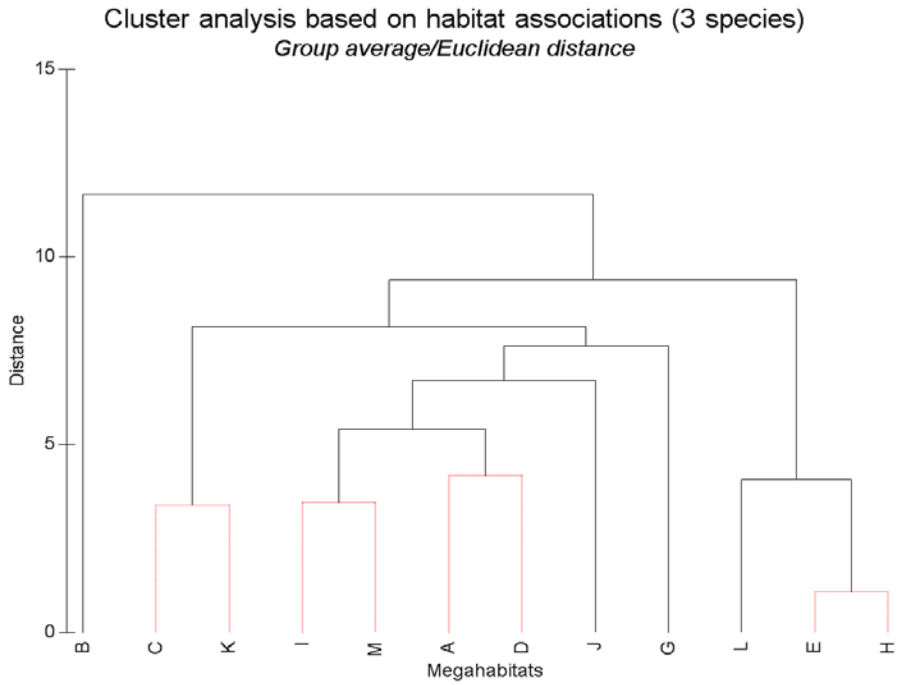

Figure 64. Clusters of megahabitats based on the outcome of geospatial analyses for the three wolffish species. Megahabitats B, C, and K are the most favourable to the three species overall.

An MDS plot confirms the cluster results, with favourable cells in megahabitat B as well as K and C (Figure 65). These were all projected on the same side along one axis, suggesting shared features, although B was distinguished from K and C on the secondary axis.

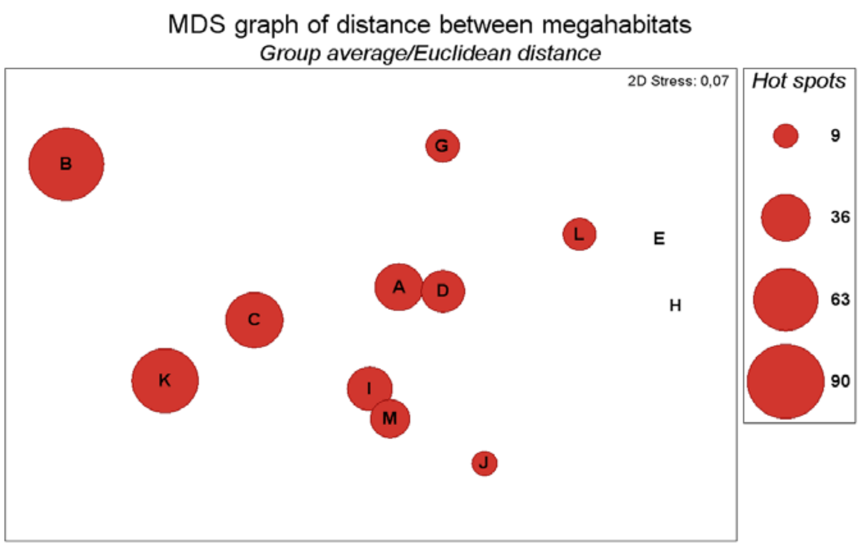

Figure 65. MDS graph of distance between megahabitats based on descriptors of distribution and relative occurrence for the three wolffish species in the study area. Bubble size reflects the proportion of cells classified as hot spots for any species of wolffish.

Redundancy analysis

Relative occurrence

There were significant effects of latitude and longitude for all three species (Table 87). The relationship between the three species responses and the 22 significant explanatory variables selected by the stepwise regression was significant (P<0.001). The three canonical axes were significant (P<0.001), but they explained together only 30% (27% adjusted) of the variance in the relative occurrence of the three wolffish species, with the first axis accounting for 89% of that value. The first principal component explained 35% of the unconstrained variance (Table 88).

Table 87. Linear regression model statistics for the effects of latitude and longitude on the relative occurrence of northern, spotted, and striped wolffish.

Species	F-statistic*	P value	P value for latitude	P value for longitude	Adjusted R^2
Striped	17.23	< 0.001	< 0.001	< 0.05	0.05
Spotted	39.64	< 0.001	< 0.001	< 0.001	0.12
Northern	8.81	< 0.001	> 0.05	< 0.001	0.03

* 2 and 575 degrees of freedom

Table 88. Redundancy analysis statistics for the effects of 22 environmental variables on the relative occurrence of northern, spotted, and striped wolffish.

	Degrees of freedom	Variance	F	N. perm	Pr (>F)	
Model	29	0.0382	8.26	999	0.001	
Residual	548	0.0874				
RDA1	1	0.0339	222.40	999	0.001	
RDA2	1	0.0023	15.28	999	0.001	
RDA3	1	0.0020	13.15	999	0.001	
Residual	574	0.0874				
Eigenvalue and contribution						
	RDA1	RDA2	RDA3	PC1	PC2	PC3
Eigenvalue	0.0339	0.0023	0.0020	0.0439	0.0321	0.0114
Proportion explained	0.27	0.02	0.02	0.35	0.26	0.09
Cumulative proportion	0.27	0.29	0.30	0.65	0.91	1.00
Species scores						
Striped	-1.462	0.042	-0.088	1.280	-0.963	0.133
Spotted	-0.078	-0.386	-0.083	-1.152	-1.087	0.091
Northern	0.390	0.081	-0.348	-0.076	0.261	0.865

Hot spots based on relative occurrence

There were significant effects of latitude and longitude for all three species (Table 89). The relationship between the three species responses and the 23 significant explanatory variables selected by the stepwise regression was significant (P<0.001). The three canonical axes were significant (P<0.001), but they explained together 54% (52% adjusted) of the variance in the relative occurrence of the three wolffish species, with the first axis accounting for 90% of that value. The first principal component explained 79% of the unconstrained variance (Table 90).

Table 89. Linear regression model statistics for the effects of latitude and longitude on the Getis and Ord local spatial autocorrelation Gi* statistic (Z-score) as determined from the relative occurrence of northern, spotted, and striped wolffish.

Species	F-statistic*	P value	P value for latitude	P value for longitude	Adjusted R^2
Striped	102.5	< 0.001	< 0.001	< 0.05	0.18
Spotted	332.3	< 0.001	< 0.001	< 0.001	0.42
Northern	121.6	< 0.001	> 0.05	< 0.001	0.21

* 2 and 899 degrees of freedom

Table 90. Redundancy analysis statistics for the effects of 23 environmental variables on the Getis and Ord local spatial autocorrelation Gi* statistic (Z-score) as determined from the relative occurrence of northern, spotted, and striped wolffish.

	Degrees of freedom	Variance	F	N. perm	Pr (>F)	
Model	28	0.1038	36.12	999	0.001	
Residual	873	0.0896				
RDA1	1	0.0934	936.18	999	0.001	
RDA2	1	0.0069	69.62	999	0.001	
RDA3	1	0.0034	34.41	999	0.001	
Residual	898	0.0896				
Eigenvalue and contribution						
	RDA1	RDA2	RDA3	PC1	PC2	PC3
Eigenvalue	0.0933	0.0069	0.0034	0.0485	0.0232	0.0179
Proportion explained	0.48	0.04	0.02	0.25	0.12	0.09
Cumulative proportion	0.48	0.52	0.54	0.79	0.91	1.00
Species scores						
Striped	2.3955	-0.045	-0.150	1.751	-0.079	0.293
Spotted	0.6107	-0.331	0.408	0.450	-0.253	-1.049
Northern	-0.5133	-0.602	-0.213	-0.205	-1.229	0.198

The results of the RDA in terms of environmental variables, wolffish species, and cells are projected on a triplot in Figure 66; a scaled-up view is presented in Figure 67 to reveal the categorical factors (orange circles). The northern wolffish was projected with an opposing vector to the other two wolffish species, in the same direction as some of the temperature variables and away from others such as maximum depth variables.

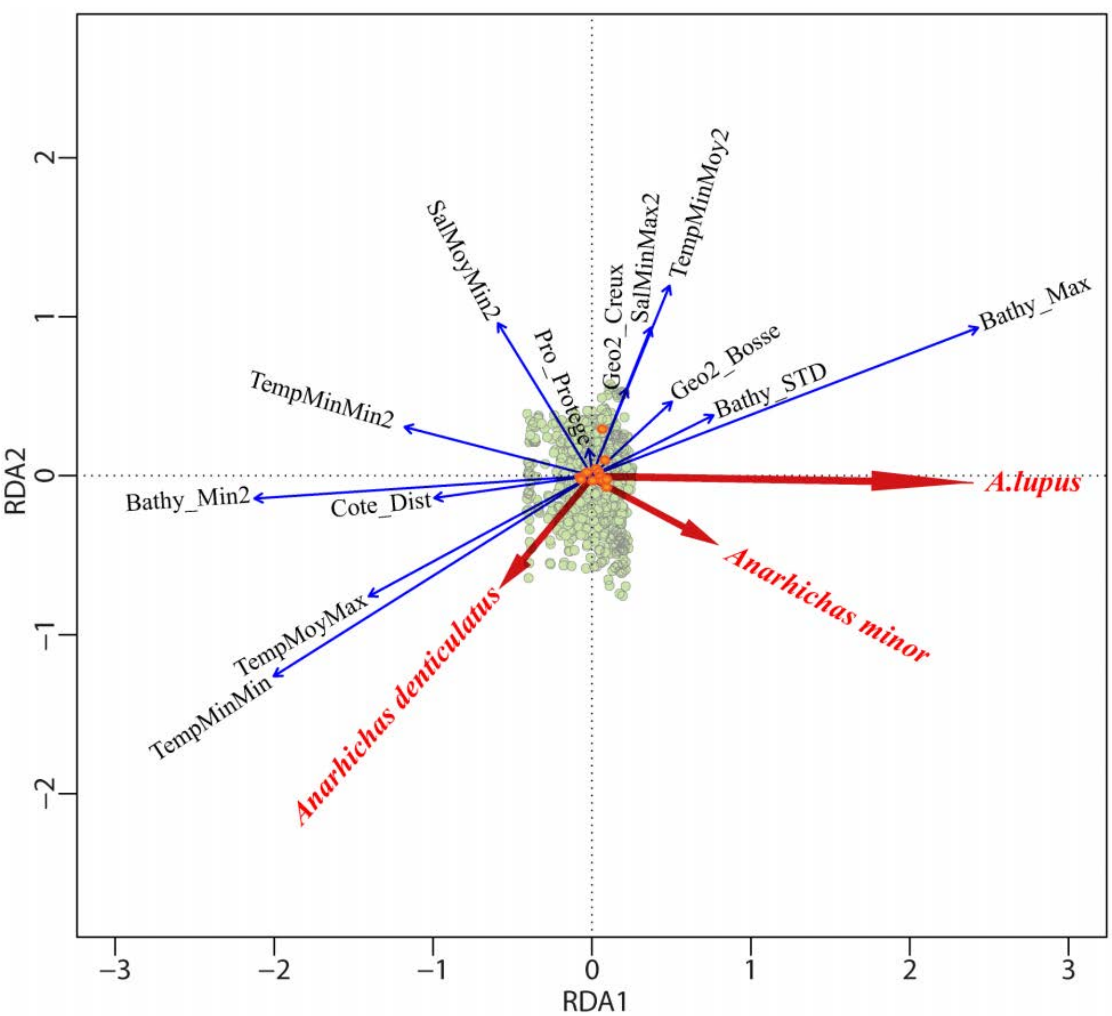

Figure 66. Triplot of species (red arrows), environmental variables (blue arrows and orange circles), and cells classified as clusters of high relative occurrence (green circles) for three wolffish species (northern = *A. denticulatus*, spotted = *A. minor*, striped = *A. lupus*) in the St. Lawrence estuary and Gulf, based on a redundancy analysis using the scaling 2 method and weighted averages scores, and showing the first two RDA axes.

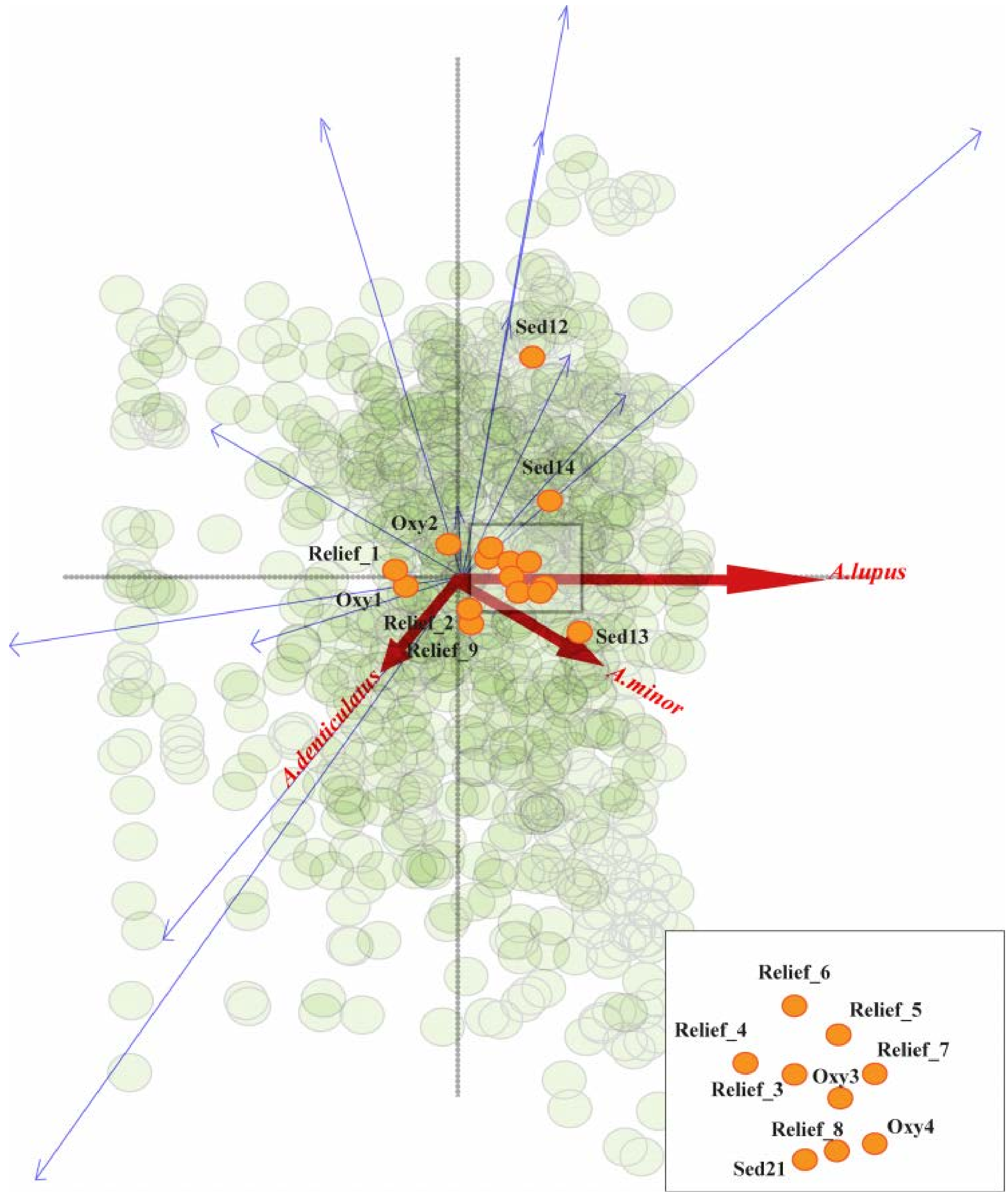

Figure 67. Magnified version of the triplot in Figure 65, with inset box to identify categorical factors.

Multivariate regression tree

Based on their catch in number data, striped and spotted wolffish occurred predominantly in group 3 and less frequently in group 10 of a regression tree partitioning cells into 10 different groups using environmental and fish assemblage data. The environmental variables and their split levels are shown in Figure 68. The partitioning of the catch into groups is highlighted in Figure 69 for striped wolffish and Figure 70 for spotted wolffish. Group 3 includes 120 cells representing roughly 10% of the study area and 7% of the catch (based on average cell values). The details on methods and full results of the tree analysis are presented in section 9.

Species compositions

Figures and tables on the other species forming groups 3 and 10 are presented in section 9 on fish assemblages; the results specific to wolffish are summarized here.

Fifty-six fish species occurred in group 3 cells, with a maximum species richness of 29 species per cell. The most abundant species, and thus the species that striped and spotted wolffish are likely to interact with most frequently, included Atlantic cod, American plaice, redfish species, moustache sculpin, and daubed shanny. Eleven species had a significant indicator value (IndVal, see methods in section 9), and were thus representative of that group based on distribution, fidelity, and abundance criteria. Values for IndVal were low in general, though greater than 0.2 for striped wolffish and five non-commercial species. Other species with a significant IndVal value included spotted wolffish, Atlantic cod (a commercial species), and several non-commercial species.

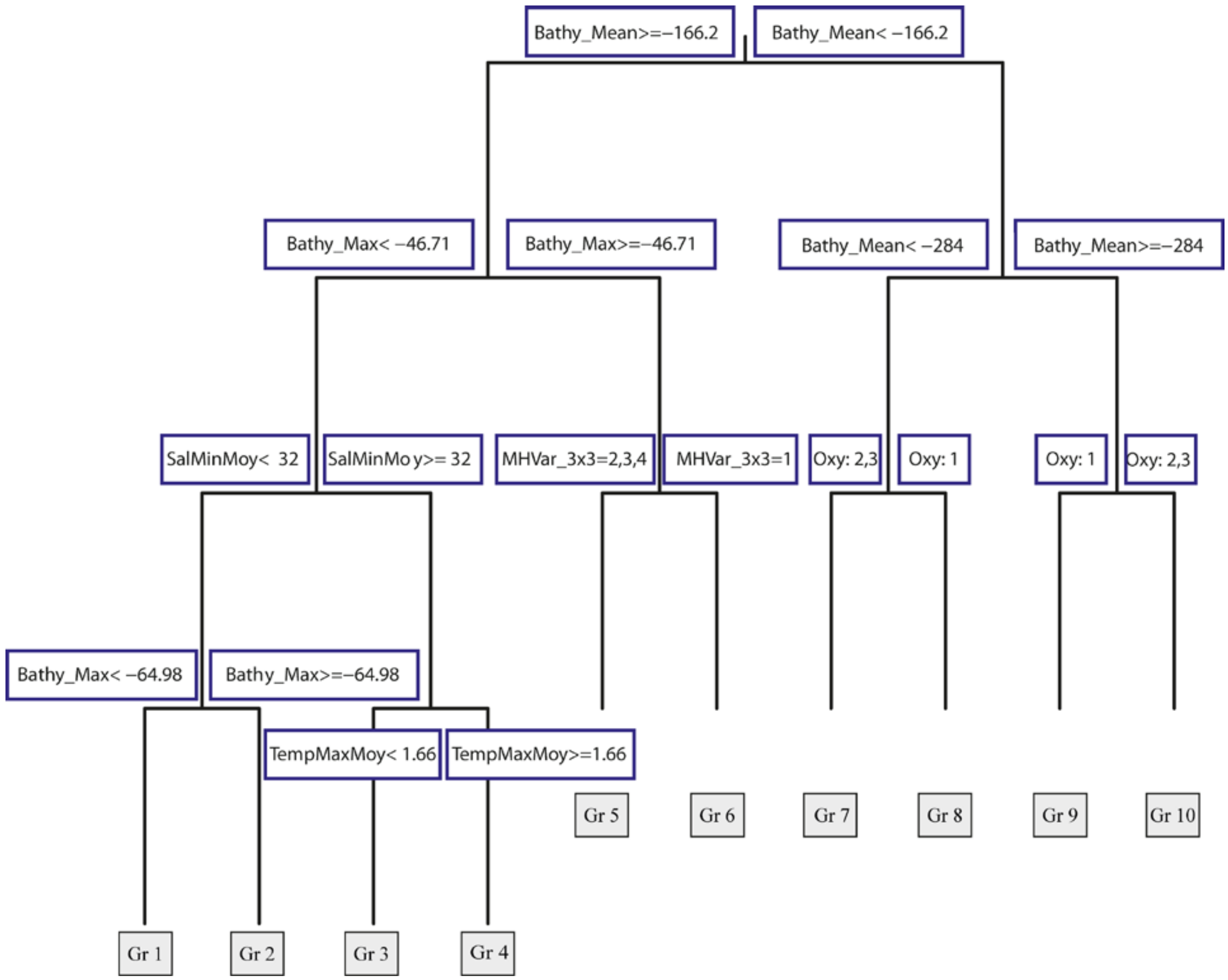

Figure 68. Regression tree partitioning cells into 10 groups (gray boxes) based on environmental and fish assemblage data. The decision criteria are shown at each node (blue-outlined boxes).

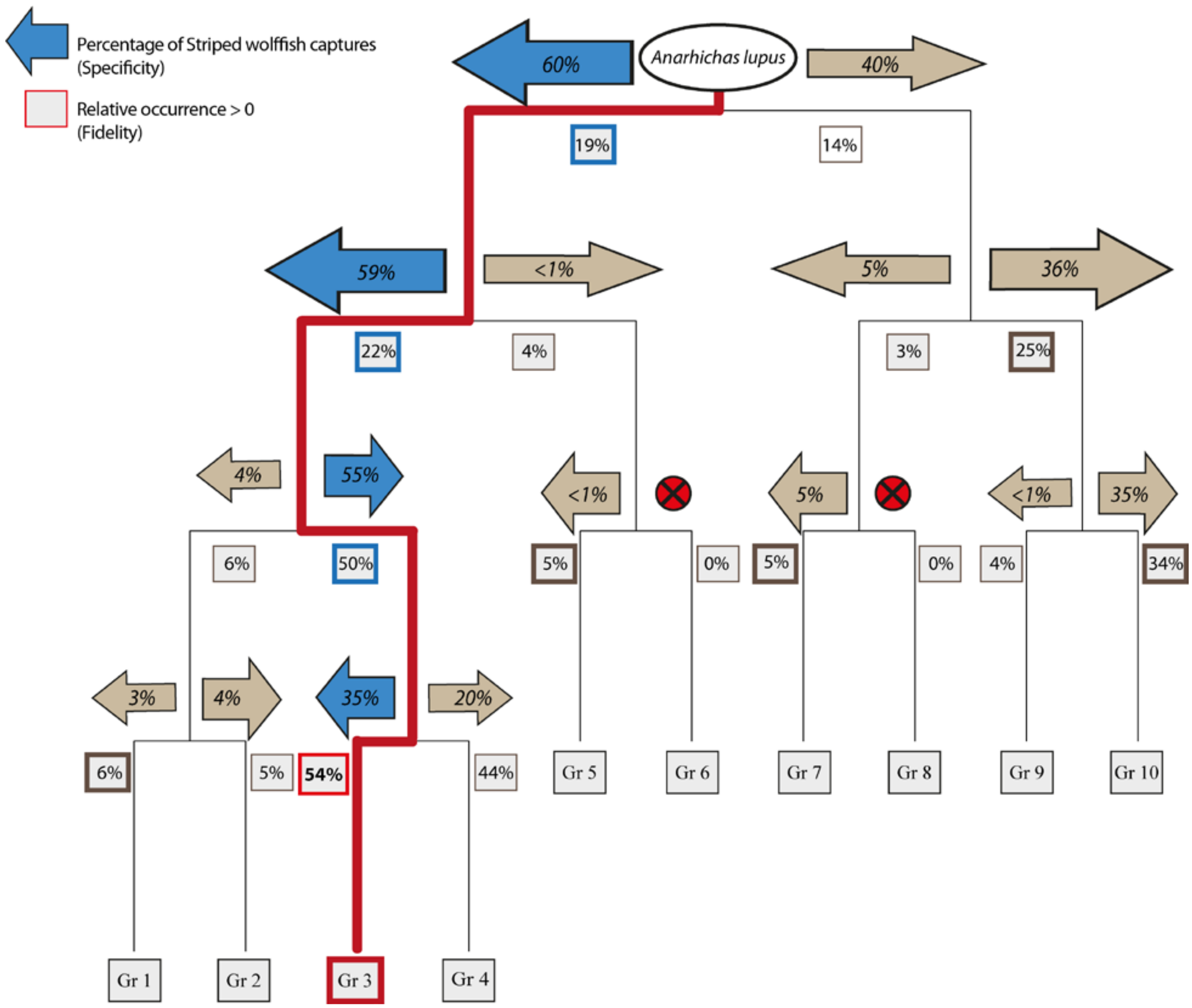

Figure 69. Recursive partitioning of striped wolffish abundance data highlighting the pathway of catches to group 3 cells and secondarily to group 10 cells.

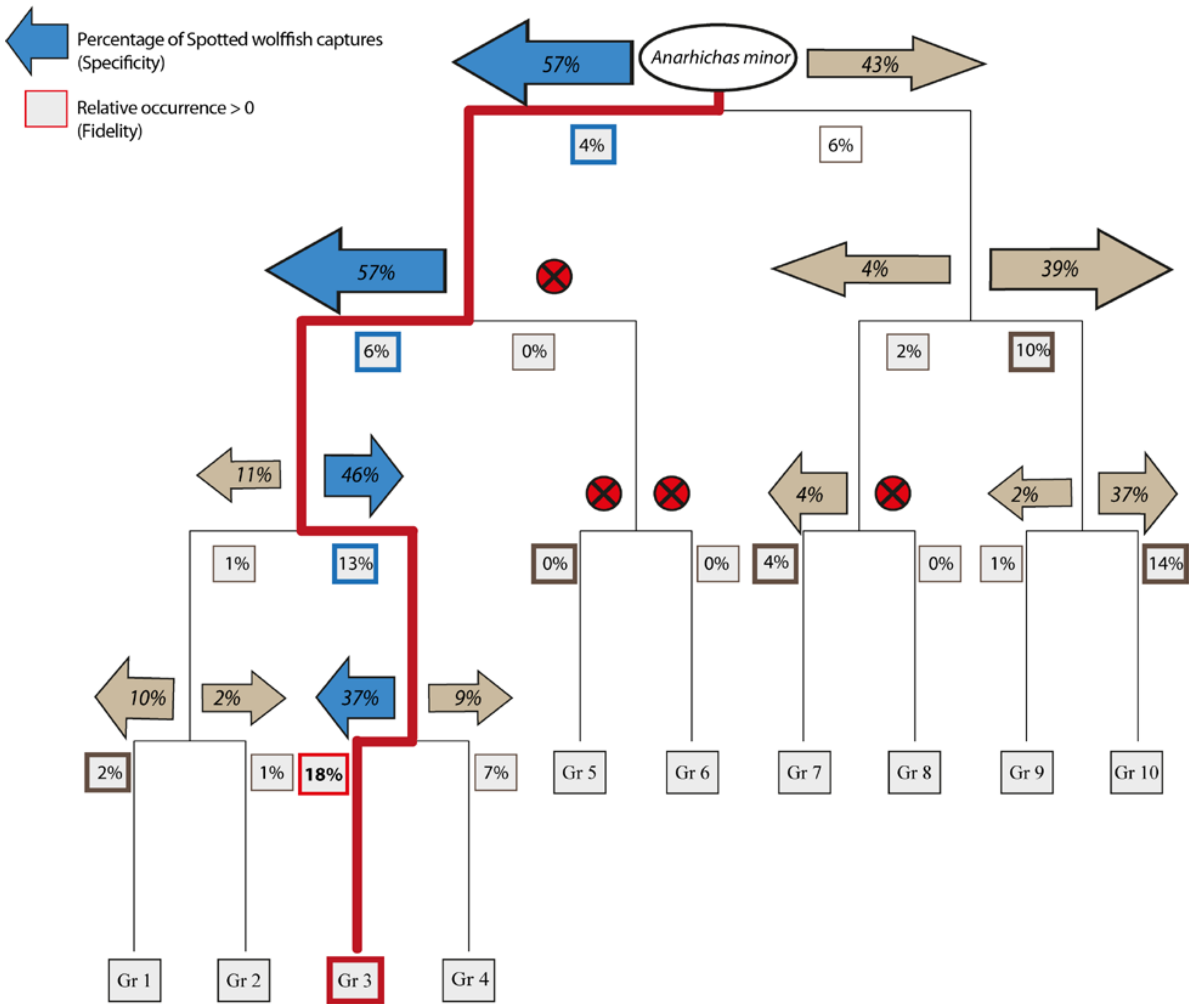

Figure 70. Recursive partitioning of spotted wolffish abundance data highlighting the pathway of catches to group 3 cells and secondarily to group 10 cells.

8. AMERICAN PLAICE

The same analyses as performed earlier for the wolffish species (sections 4–6) were conducted on American plaice data. Since the catch in number and catch in weight data were available and considered reliable, three series of maps and tables were produced, one based on the relative occurrence (presence/absence), one based on catch in number, and one based on catch in weight. Furthermore, two size categories and three time periods were considered (see Methods, section 3). A final series presents descriptive statistics of the environmental conditions as well as multivariate statistics to investigate the relationships of plaice with other species using redundancy analysis and recursive tree partitioning. The tree partitioning analysis of species assemblages is described and presented in further detail in the final chapter (section 9). For a full list of the comparative map figures that follow, refer to Tables 91 and 92.

Table 91. Summary of figures for American plaice presented in this section. Three parameters are considered (relative occurrence, catch in number, and catch in weight) for different time periods (years) and fish size categories. Cells: number of cells sampled; P/A: area of occupancy based on presence/absence and using the Hernández and Navarro’s (2007) cartographic and conglomerate method; KDE: kernel density estimate based on the quartic kernel function and a 20 km search radius; Hot/cold spot: concentrations of low (cold spots) and high relative occurrences (hot spots) within a 20 km distance band based on the Getis and Ord G_i* local spatial autocorrelation statistic. A check mark indicates that a corresponding map is available below.

Period	Parameter	Fish size	Cells	Figures		
				P/A	KDE	Hot/cold spot
71–10	Relative occurrence	Small and large	1899	✓	✓	✓
71–83	Relative occurrence	Small and large	850		✓	✓
84–10	Relative occurrence	Small and large	1873	✓	✓	✓
84–10	Relative occurrence	Small	1824		✓	✓
84–10	Relative occurrence	Large	1824		✓	✓
84–10	Catch in number	Small and large	1824		✓	✓
84–10	Catch in number	Small	1824		✓	✓
84–10	Catch in number	Large	1824		✓	✓
84–10	Catch in weight	Small and large	1824		✓	✓
84–92	Relative occurrence	Small and large	1473	✓	✓	✓
84–92	Relative occurrence	Small	1254	✓	✓	✓
84–92	Relative occurrence	Large	1254	✓	✓	✓
84–92	Catch in number	Small and large	1254		✓	✓
84–92	Catch in number	Small	1254		✓	✓
84–92	Catch in number	Large	1254		✓	✓
84–92	Catch in weight	Small and large	1254		✓	✓
93–01	Relative occurrence	Small and large	1465		✓	✓
93–01	Relative occurrence	Small	1442		✓	✓
93–01	Relative occurrence	Large	1442		✓	✓
93–01	Catch in number	Small and large	1442		✓	✓

93–01	Catch in number	Small	1442		✓	✓
93–01	Catch in number	Large	1442		✓	✓
93–01	Catch in weight	Small and large	1442		✓	✓
02–10	Relative occurrence	Small and large	1421	✓	✓	✓
02–10	Relative occurrence	Small	1420	✓	✓	✓
02–10	Relative occurrence	Large	1420	✓	✓	✓
02–10	Catch in number	Small and large	1420		✓	✓
02–10	Catch in number	Small	1420		✓	✓
02–10	Catch in number	Large	1420		✓	✓
02–10	Catch in weight	Small and large	1420		✓	✓
84–92	Relative occurrence–summer	Small and large	1350		✓	✓
84–92	Relative occurrence–winter	Small and large	467		✓	✓

Table 92. List of statistical analyses conducted for American plaice on species–environment relationships and presented in this section. Two sets of analyses were conducted for different time periods (years) and fish size categories; one determined which environmental variables could explain the variability in relative occurrence and catch in number or in weight, and the other determined which environmental variables contributed most to explaining the degree of spatial correlation, i.e., the degree of clustering and hot-spot formation (Getis and Ord G_i* local spatial autocorrelation statistic based on the relative occurrence, catch in number, or catch in weight). Cells = number of cells sampled. A check mark indicates that a corresponding map is available below.

Period	Parameter	Fish size	Cells	Analysis		
				Multiple regression	Forward regression	Statistics
71–10	Relative occurrence	Small and large	1899	✓	✓	✓
71–83	Relative occurrence	Small and large	850		✓	✓
84–10	Relative occurrence	Small and large	1873	✓	✓	✓
84–10	Relative occurrence	Small	1824		✓	✓
84–10	Relative occurrence	Large	1824		✓	✓
84–10	Catch in number	Small and large	1824		✓	✓
84–10	Catch in number	Small	1824		✓	✓
84–10	Catch in number	Large	1824		✓	✓
84–10	Catch in weight	Small and large	1824		✓	✓
84–92	Relative occurrence	Small and large	1473	✓	✓	✓
84–92	Relative occurrence	Small	1254	✓	✓	✓
84–92	Relative occurrence	Large	1254	✓	✓	✓
84–92	Catch in number	Small and large	1254		✓	✓
84–92	Catch in number	Small	1254		✓	✓
84–92	Catch in number	Large	1254		✓	✓
84–92	Catch in weight	Small and large	1254		✓	✓
93–01	Relative occurrence	Small and large	1465		✓	✓
93–01	Relative occurrence	Small	1442		✓	✓

93–01	Relative occurrence	Large	1442		✓	✓
93–01	Catch in number	Small and large	1442		✓	✓
93–01	Catch in number	Small	1442		✓	✓
93–01	Catch in number	Large	1442		✓	✓
93–01	Catch in weight	Small and large	1442		✓	✓
02–10	Relative occurrence	Small and large	1421	✓	✓	✓
02–10	Relative occurrence	Small	1420	✓	✓	✓
02–10	Relative occurrence	Large	1420	✓	✓	✓
02–10	Catch in number	Small and large	1420		✓	✓
02–10	Catch in number	Small	1420		✓	✓
02–10	Catch in number	Large	1420		✓	✓
02–10	Catch in weight	Small and large	1420		✓	✓
84–92	Relative occurrence–summer	Small and large	1350		✓	✓
84–92	Relative occurrence–winter	Small and large	467		✓	✓

Area of occupancy

The dataset includes presence/absence data for 12834 sets. Plaice was present in 5019 sets in the Gulf region surveys and 4912 sets in the Québec region surveys. Corrected catch data were available for 5019 sets for plaice in the Gulf region (1971–2010) and 3498 sets for plaice in the Québec region (1984–2010). These values exclude sets that failed for any reason, such as a damaged trawl. In most cases, catch in both number and weight were recorded. Only 68 sets with a catch in number recorded had no associated catch in weight recorded (both regions). Similarly, only 27 sets with a catch in weight recorded had no associated catch in number recorded. Sets corresponding to cells with no matching megahabitat category, as a result of lacking environmental data, were left out (92 of 12834 sets). The areas are summarized in Table 93 and the resulting maps shown in Figures 71–78.

Table 93. Size of the area of occupancy of American plaice broken down by conglomerate and satellite groups of observations as determined by the Hernández and Navarro (2007) cartographic and conglomerate method and based on presence data obtained from annual bottom trawl surveys conducted by DFO (1971–2008). Conglomerates are mapped by number in the corresponding figures.

Period	Fish size	Conglomerate							Satellites	Total
		1	2	3	4	5	6	Others		
71–10	Small and large	225,248	2						2	225,252
84–10	Small and large	224,128								224,128
84–92	Small and large	213,704	2,238	1,117	4				6	217,069
84–92	Small	82,428	34,878	13,233	7,139	1,260	252	205	16	139,411
84–92	Large	91,695	75,980	20,264	2,000	586	4		24	190,553
02–10	Small and large	223,729	2						1	223,732
02–10	Small	219,060	261	40					20	219,381

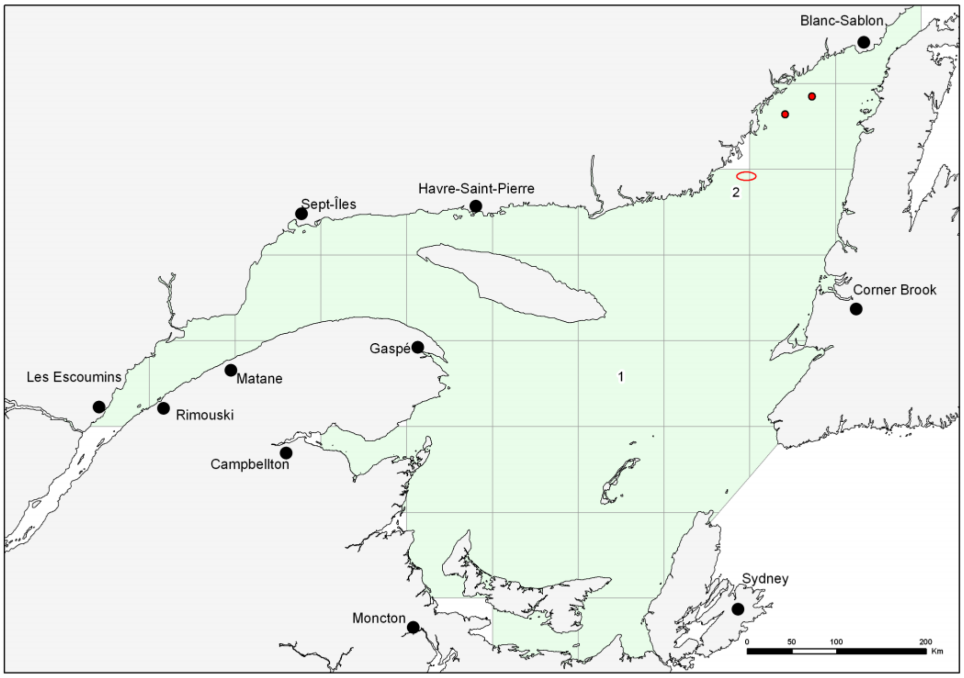

Figure 71. Area of occupancy of American plaice in the St. Lawrence estuary and Gulf based on presence data from annual bottom trawl surveys conducted by DFO (1971–2010). Conglomerates are numbered (1: green area; 2: red oval , not to scale), with satellites (isolated observations) shown as red dots.

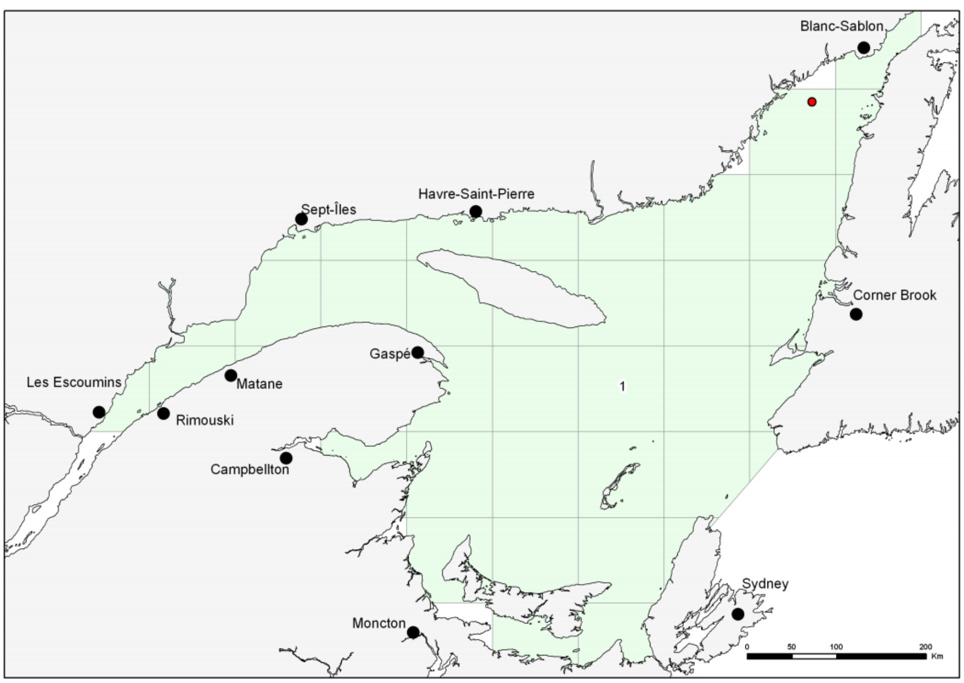

Figure 72. Area of occupancy of American plaice in the St. Lawrence estuary and Gulf based on presence data from annual bottom trawl surveys conducted by DFO (1984–2010). Conglomerate 1 is labeled (green area), with a satellite observation shown as a red dot.

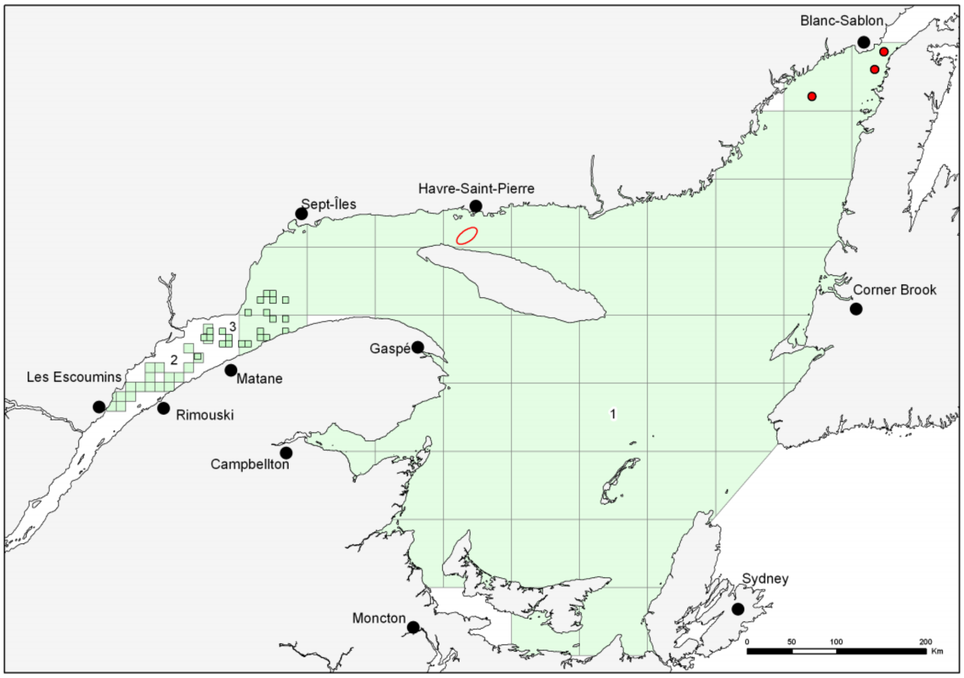

Figure 73. Area of occupancy of American plaice in the St. Lawrence estuary and Gulf based on presence data from annual bottom trawl surveys conducted by DFO (1984–1992). Conglomerates are numbered, with those less than 100 km^2 shown as ovals (not to scale), and satellites shown as red dots.

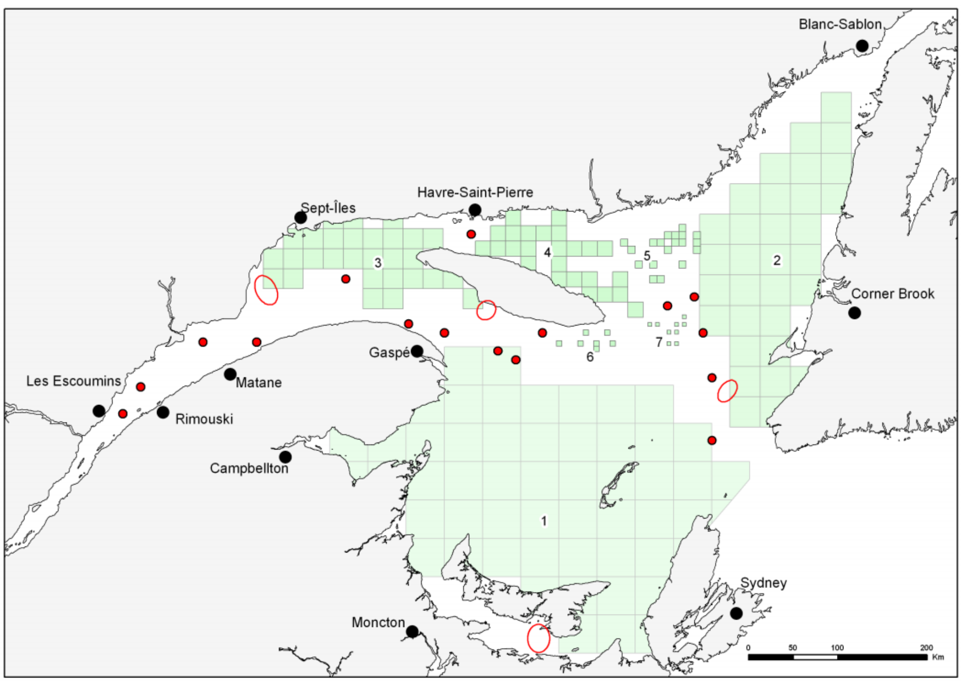

Figure 74. Area of occupancy of American plaice in the St. Lawrence estuary and Gulf based on presence data from annual bottom trawl surveys conducted by DFO (1984–1992, fish < 20.5 cm total length). Conglomerates are numbered, with those less than 100 km^2 shown as ovals (not to scale), and satellites shown as red dots.

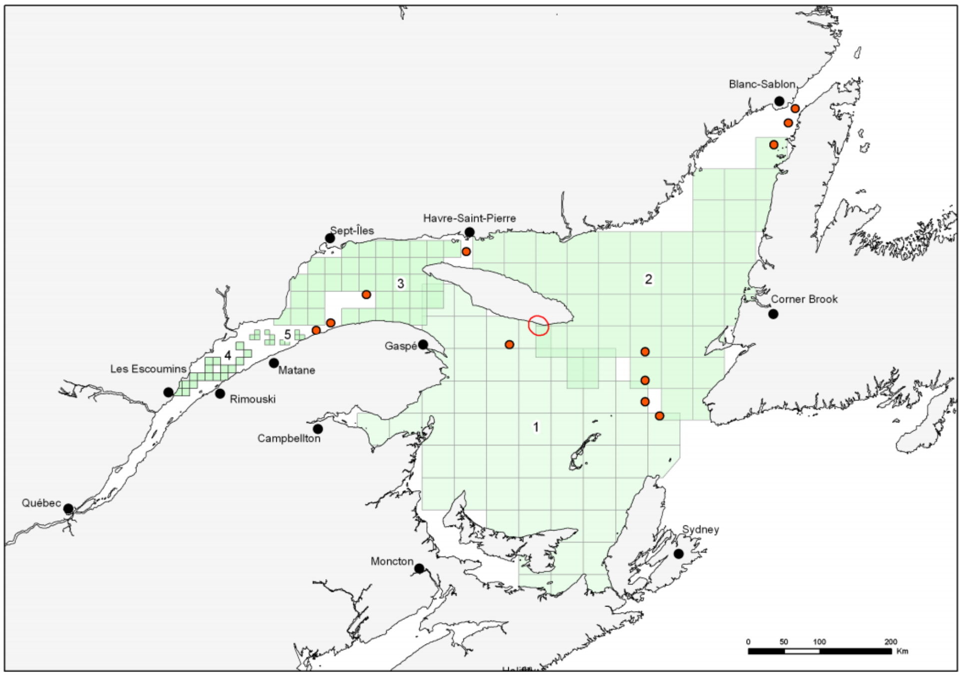

Figure 75. Area of occupancy of American plaice in the St. Lawrence estuary and Gulf based on presence data from annual bottom trawl surveys conducted by DFO (1984–1992, fish > 20.5 cm total length). Conglomerates are numbered, with those less than 100 km^2 shown as ovals (not to scale), and satellites shown as red dots.

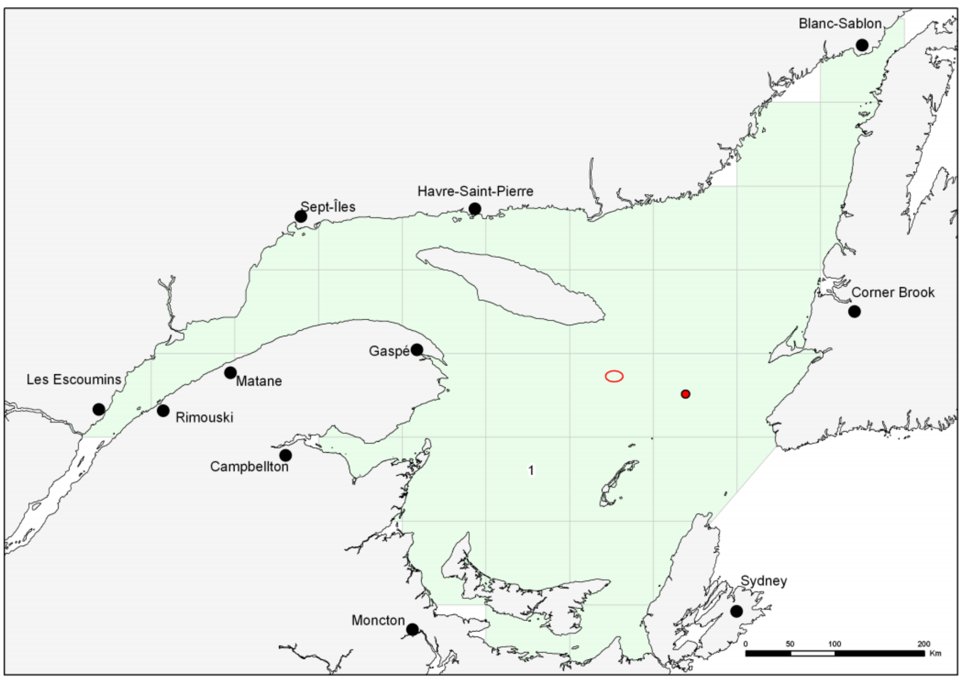

Figure 76. Area of occupancy of American plaice in the St. Lawrence estuary and Gulf based on presence data from annual bottom trawl surveys conducted by DFO (2002–2010). Conglomerates are numbered, with those less than 100 km^2 shown as ovals (not to scale), and satellites shown as red dots.

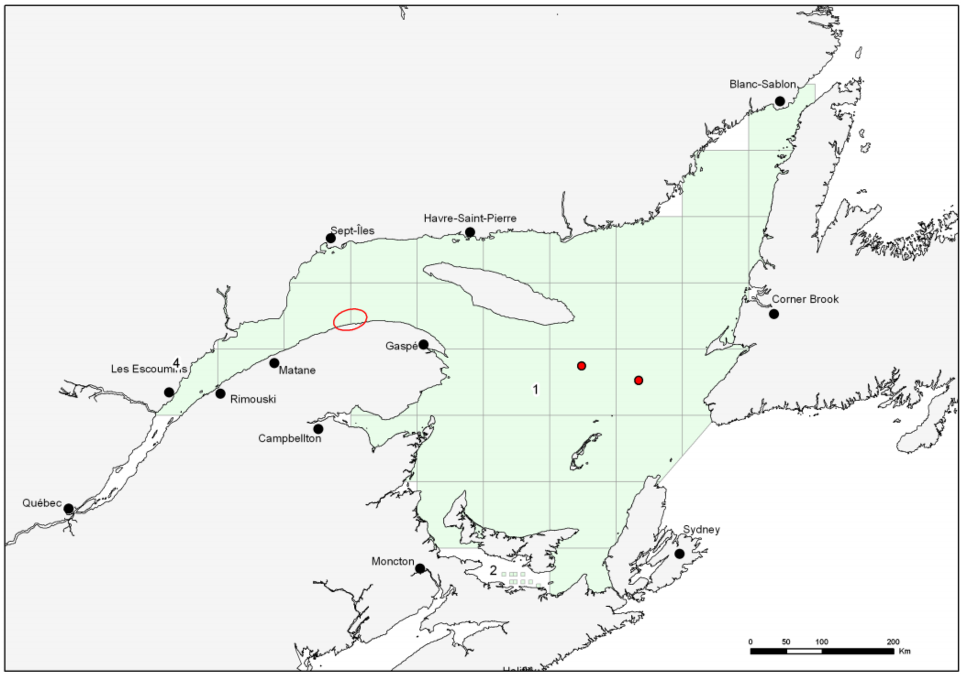

Figure 77. Area of occupancy of American plaice in the St. Lawrence estuary and Gulf based on presence data from annual bottom trawl surveys conducted by DFO (2002–2010, fish < 20.5 cm total length). Conglomerates are numbered, with those less than 100 km^2 shown as ovals (not to scale), and satellites shown as red dots.

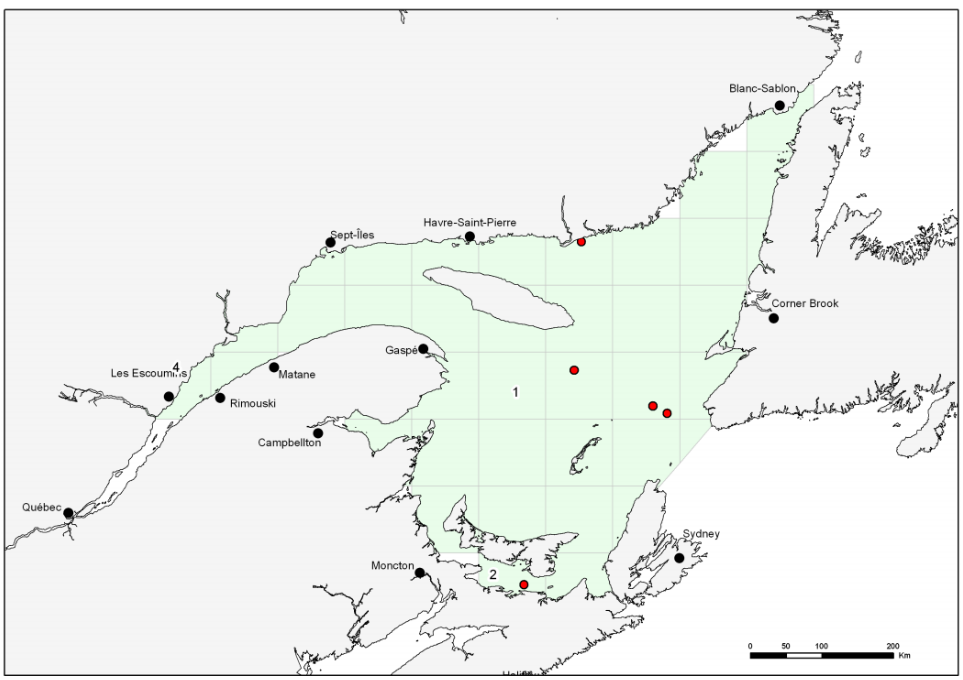

Figure 78. Area of occupancy of American plaice in the St. Lawrence estuary and Gulf based on presence data from annual bottom trawl surveys conducted by DFO (2002–2010, fish > 20.5 cm total length). Conglomerates are numbered and satellites shown as red dots.

Patterns and clusters of distribution

Results for American plaice are presented for kernel density estimates (KDE) of volume density and spatial autocorrelation statistics (Moran's *I*) for significant clusters. See section 3 for further details on methods.

Kernel density estimates

American plaice density distribution on the three sets of parameters is summarized in area and numbers of cells in Table 94. The results are presented as a series of volume density contour maps (Figures 79–110). The maps were generated with ESRI ArcGIS 10.0 software and the Spatial Analyst extension using the kernel density estimate method (quartic kernel function and a 20 km search radius).

Table 94. Total planimetric area (km^2) of American plaice density distribution in the study area. Three contour lines were drawn (95%, 90% [low density], and 50% [high density]) for each of three parameters (relative occurrence, catch in number, and catch in weight) and different time periods (years) and fish size categories (fish less than or greater than 20.5 cm). The probability density function is based on the quartic kernel function and a 20 km search radius. N. of cells: number of cells overlapping the polygons defined by the contour lines.

Period	Parameter	Fish size	KDE 95%		KDE 90%		KDE 50%	
			Area	N. of cells	Area	N. of cells	Area	N. of cells
71–10	Relative occurrence	Small and large	181,426	1,875	175,074	1,847	78,265	1,090
71–83	Relative occurrence	Small and large	82,152	841	80,375	831	44,031	629
84–10	Relative occurrence	Small and large	179,347	1,852	159,770	1,749	76,558	1,077
84–10	Relative occurrence	Small	147,690	1,644	126,632	1,463	47,442	669
84–10	Relative occurrence	Large	159,799	1,689	149,767	1,624	68,325	977
84–10	Catch in number	Small and large	115,732	1,333	90,604	1,120	26,318	393
84–10	Catch in number	Small	118,233	1,377	94,730	1,174	28,170	422
84–10	Catch in number	Large	116,385	1,346	89,457	1,104	24,812	363
84–10	Catch in weight	Small and large	115,732	1,333	90,604	1,120	26,318	393
84–92	Relative occurrence	Small and large	140,294	1,448	130,903	1,408	67,847	948
84–92	Relative occurrence	Small	87,997	986	80,264	926	39,914	571
84–92	Relative occurrence	Large	106,430	1,141	99,930	1,090	50,489	692
84–92	Catch in number	Small and large	55,254	657	42,800	533	12,466	187
84–92	Catch in number	Small	57,678	698	45,748	587	11,473	184

84–92	Catch in number	Large	55,107	661	42,282	518	12,042	178
84–92	Catch in weight	Small and large	62,529	747	49,416	616	14,379	199
93–01	Relative occurrence	Small and large	134,191	1,429	123,615	1,368	59,033	804
93–01	Relative occurrence	Small	110,457	1,242	99,490	1,159	44,321	607
93–01	Relative occurrence	Large	122,447	1,343	111,953	1,262	53,418	724
93–01	Catch in number	Small and large	86,440	1,017	66,947	844	18,553	302
93–01	Catch in number	Small	83,280	1,008	65,092	816	15,816	265
93–01	Catch in number	Large	87,478	1,015	67,943	850	18,758	304
93–01	Catch in weight	Small and large	84,943	964	68,483	833	19,860	312
02–10	Relative occurrence	Small and large	136,975	1,411	124,683	1343	65,838	966
02–10	Relative occurrence	Small	125,392	1,355	117,083	1298	57,246	833
02–10	Relative occurrence	Large	126,603	1,334	119,391	1294	61,852	892
02–10	Catch in number	Small and large	95,983	1,120	77,686	974	24,474	364
02–10	Catch in number	Small	92,152	1,080	75,643	936	25,147	386
02–10	Catch in number	Large	96,284	1,123	77,293	976	22,228	321
02–10	Catch in weight	Small and large	98,425	1,139	79,903	996	24,329	354
84–92	Relative occurrence–summer	Small and large	121,949	1,287	111,336	1,228	57,030	780
84–92	Relative occurrence–winter	Small and large	45,276	462	43,198	452	23,442	344

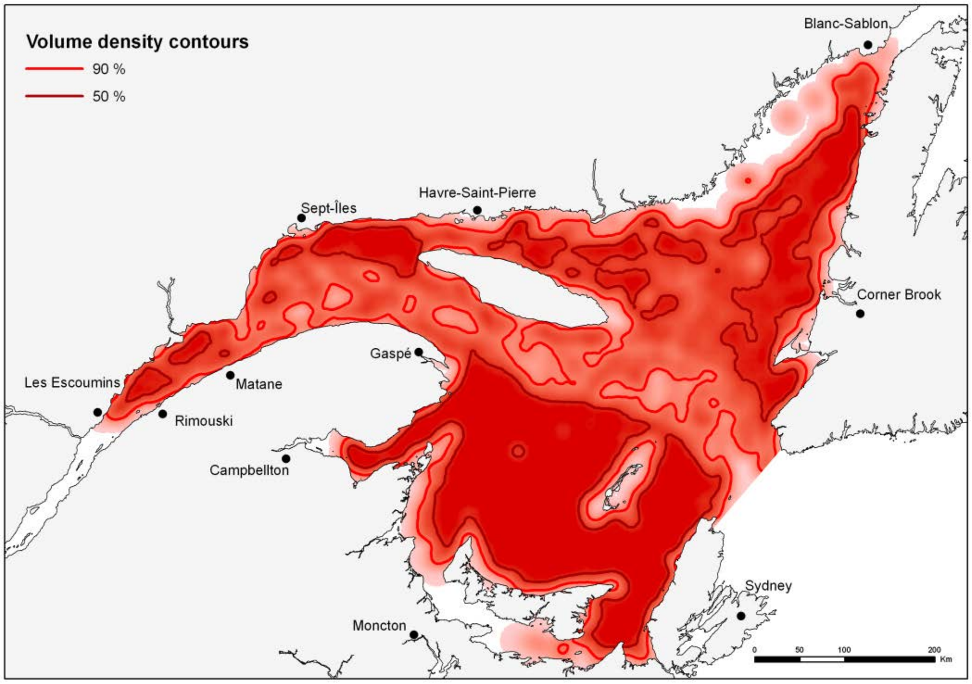

Figure 79. Map of relative occurrence (50% and 90% volume density contours) for American plaice in the St. Lawrence estuary and Gulf based on annual bottom trawl surveys conducted by DFO (1971–2010).

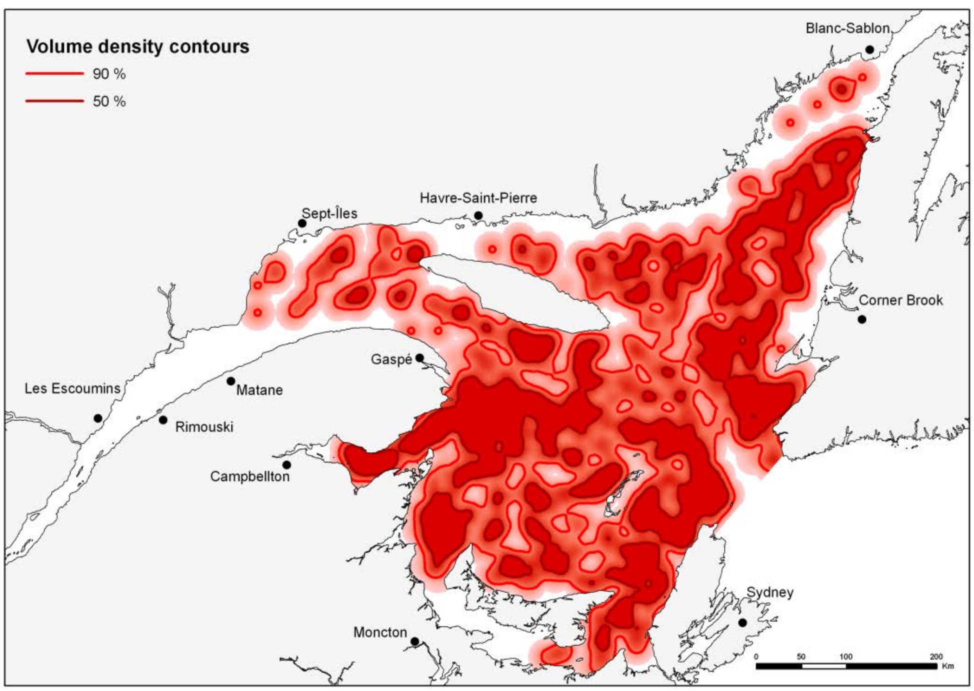

Figure 80. Map of relative occurrence (50% and 90% volume density contours) for American plaice in the St. Lawrence estuary and Gulf based on annual bottom trawl surveys conducted by DFO (1971–1983).

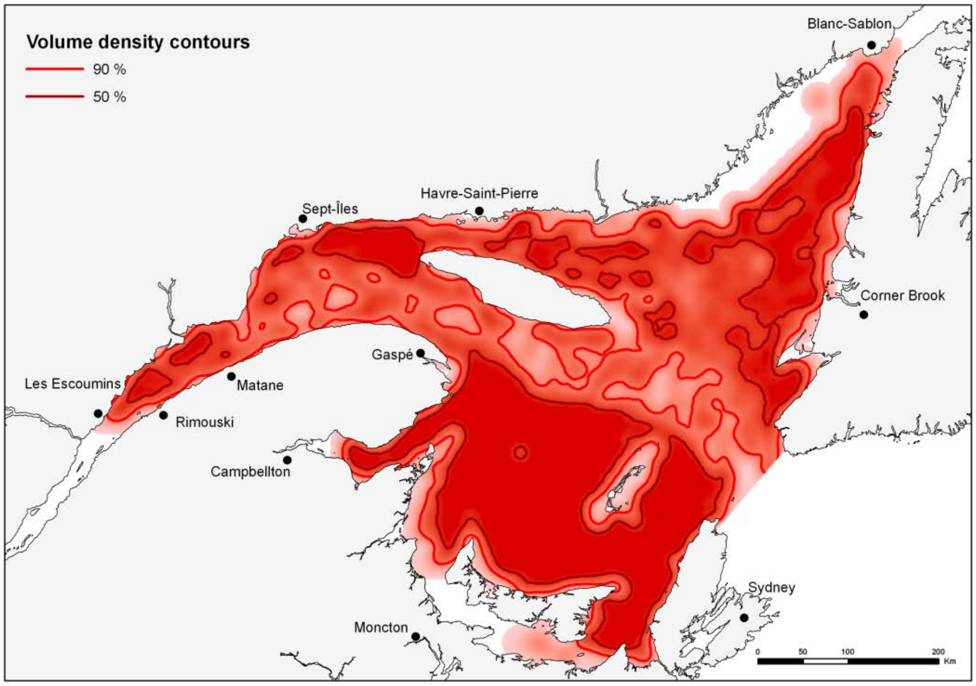

Figure 81. Map of relative occurrence (50% and 90% volume density contours) for American plaice in the St. Lawrence estuary and Gulf based on annual bottom trawl surveys conducted by DFO (1984–2010).

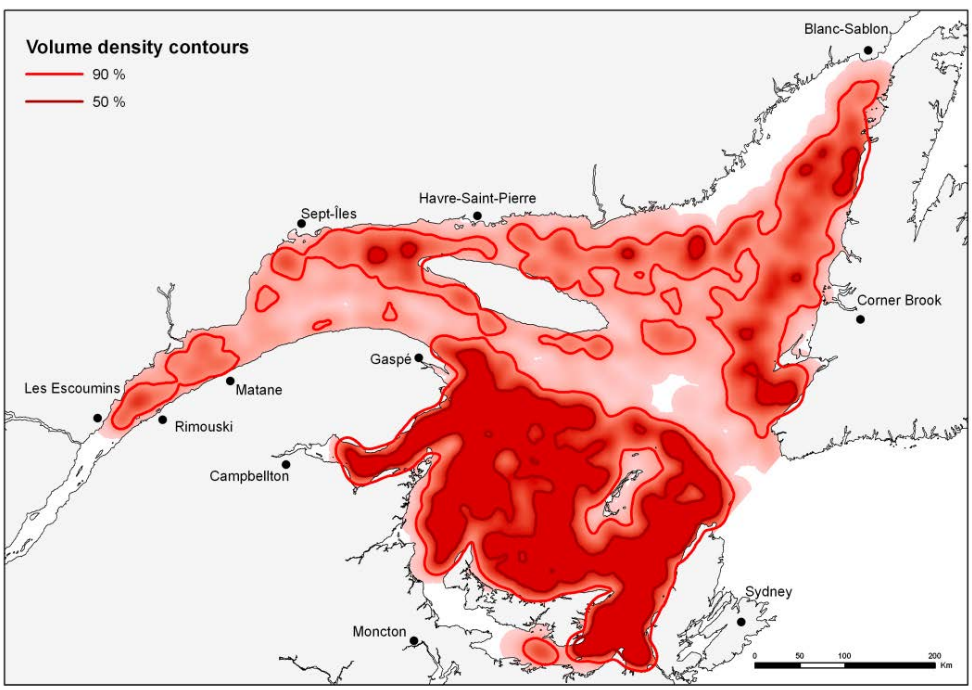

Figure 82. Map of relative occurrence (50% and 90% volume density contours) for American plaice in the St. Lawrence estuary and Gulf, based on annual bottom trawl surveys conducted by DFO (1984–2010, fish < 20.5 cm total length).

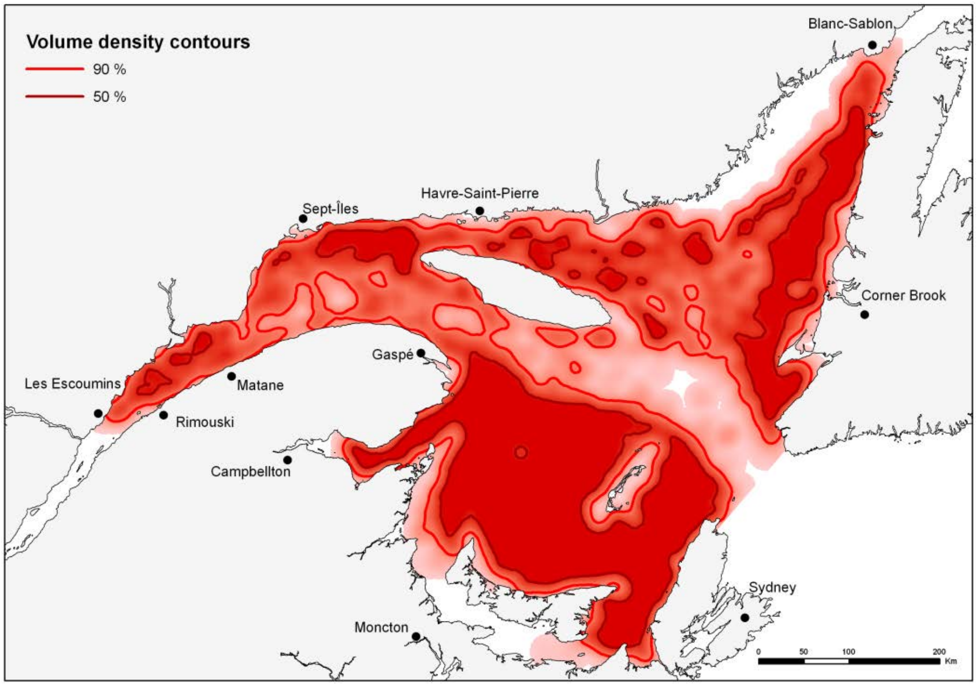

Figure 83. Map of relative occurrence (50 and 90% volume density contours) for American plaice in the St. Lawrence estuary and Gulf based on annual bottom trawl surveys conducted by DFO (1984–2010, fish > 20.5 cm total length).

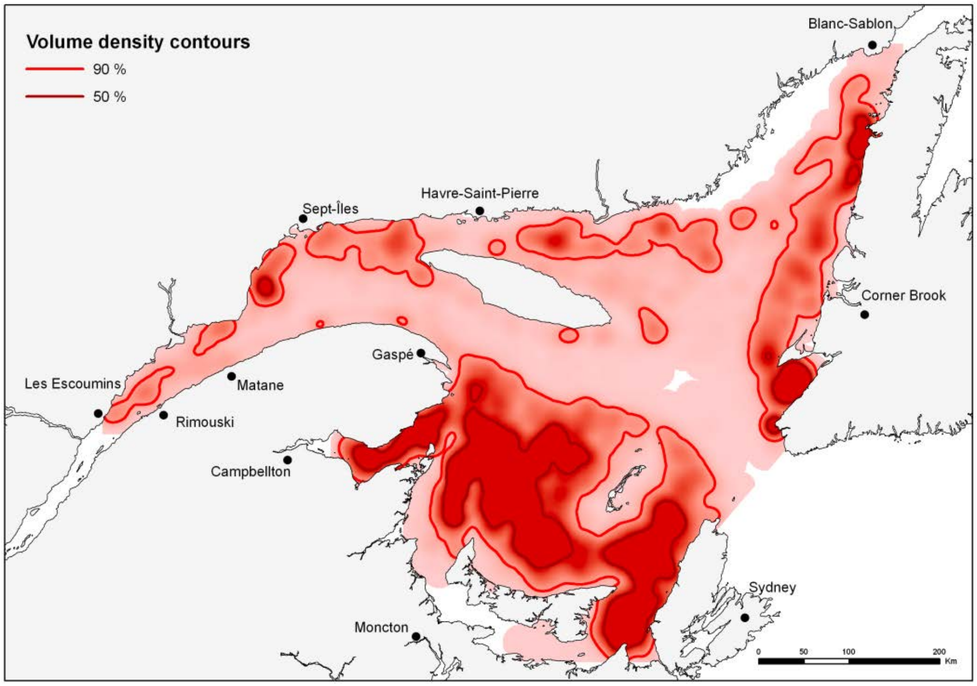

Figure 84. Map of catch in number (50% and 90% volume density contours) for American plaice in the St. Lawrence estuary and Gulf based on annual bottom trawl surveys conducted by DFO (1984–2010).

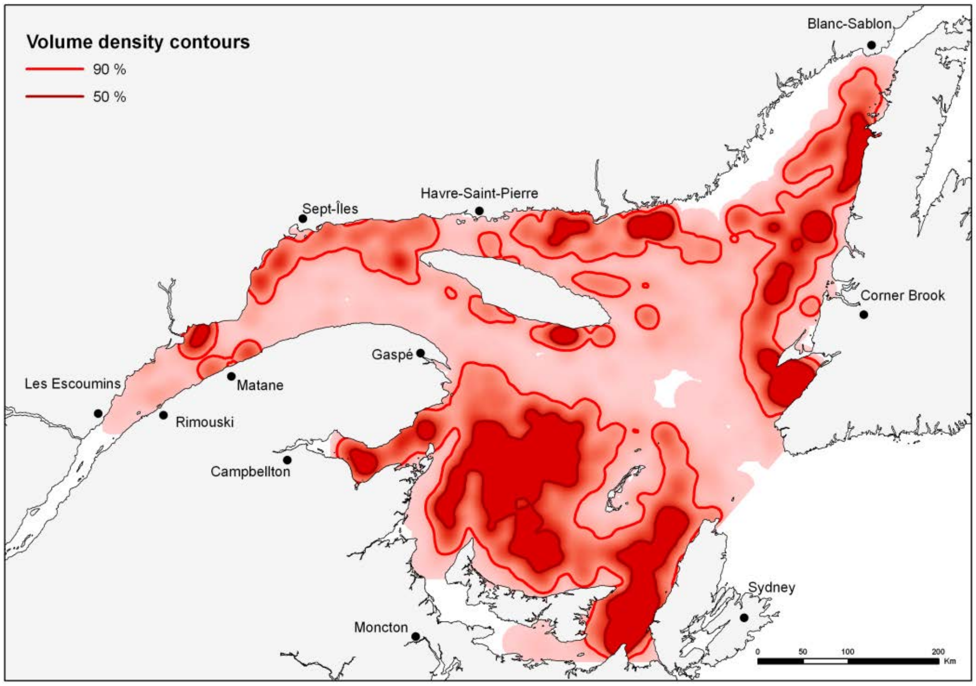

Figure 85. Map of catch in number (50% and 90% volume density contours) for American plaice in the St. Lawrence estuary and Gulf based on annual bottom trawl surveys conducted by DFO (1984–2010, fish < 20.5 cm total length).

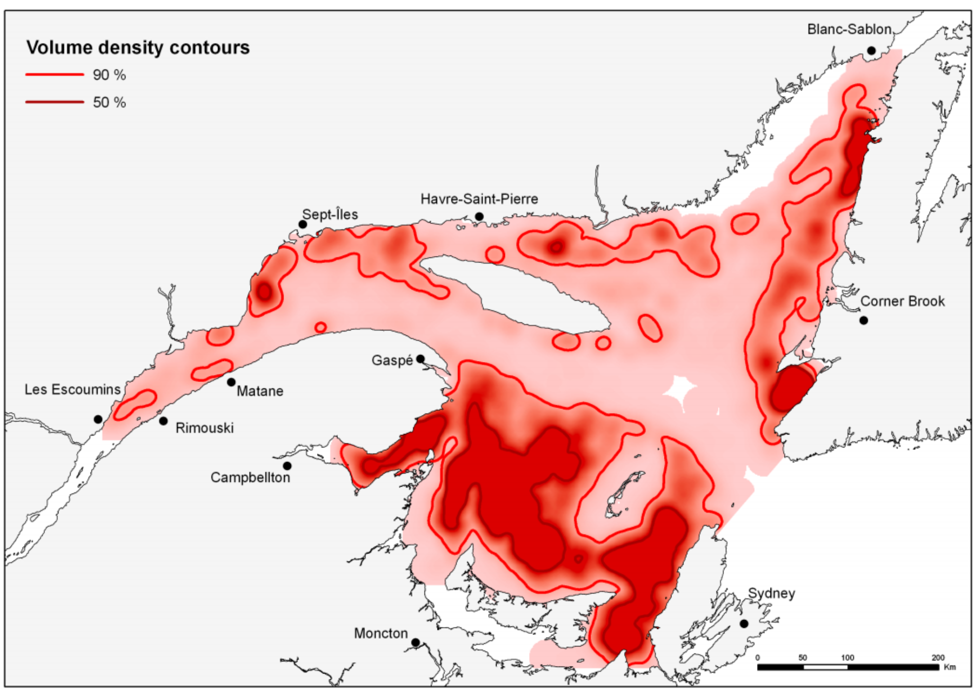

Figure 86. Map of catch in number (50% and 90% volume density contours) for American plaice in the St. Lawrence estuary and Gulf based on annual bottom trawl surveys conducted by DFO (1984–2010, fish > 20.5 cm total length).

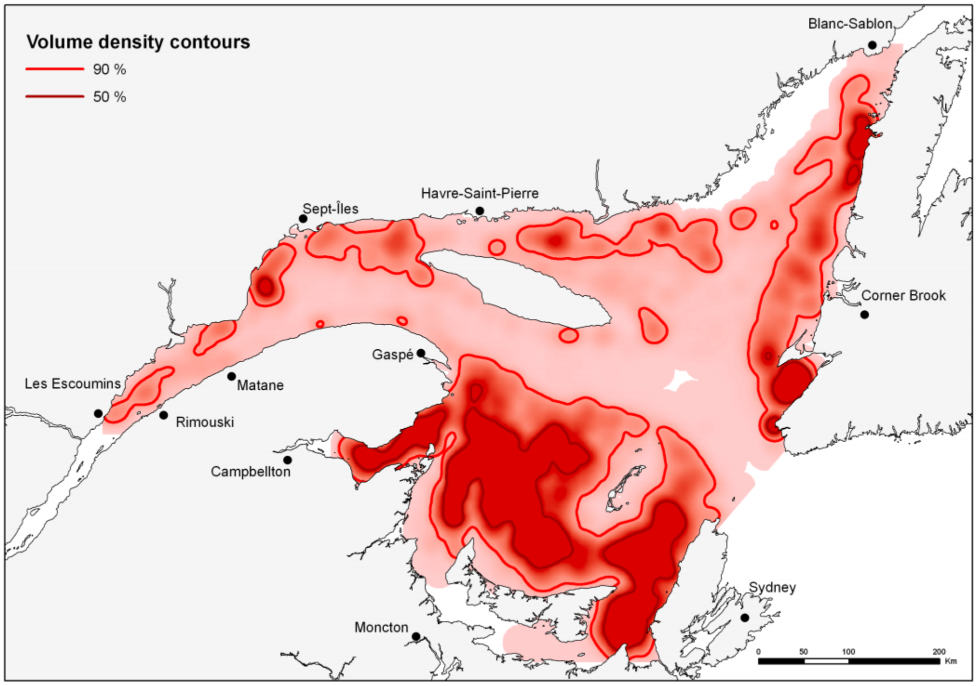

Figure 87. Map of catch in weight (50% and 90% volume density contours) for American plaice in the St. Lawrence estuary and Gulf based on annual bottom trawl surveys conducted by DFO (1984–2010).

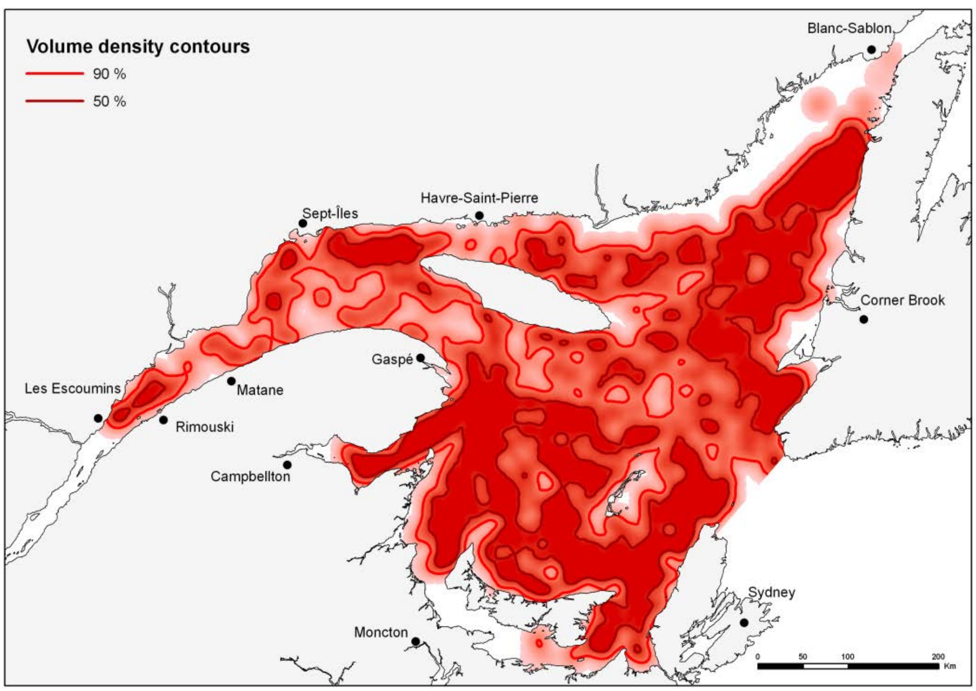

Figure 88. Map of relative occurrence (50% and 90% volume density contours) for American plaice in the St. Lawrence estuary and Gulf based on annual bottom trawl surveys conducted by DFO (1984–1992).

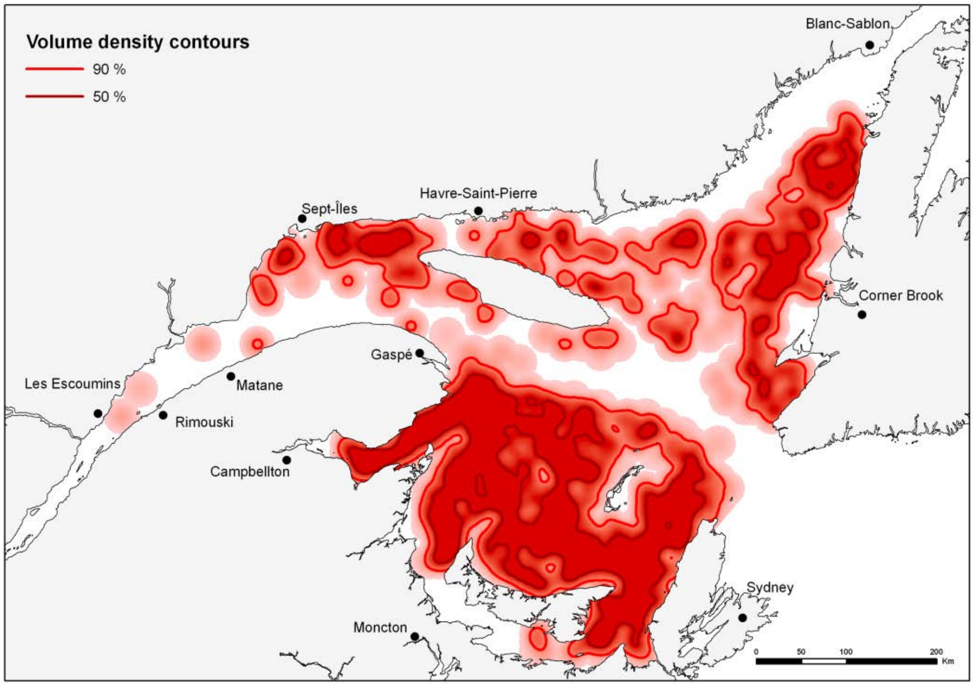

Figure 89. Map of relative occurrence (50% and 90% volume density contours) for American plaice in the St. Lawrence estuary and Gulf based on annual bottom trawl surveys conducted by DFO (1984–1992, fish < 20.5 cm total length).

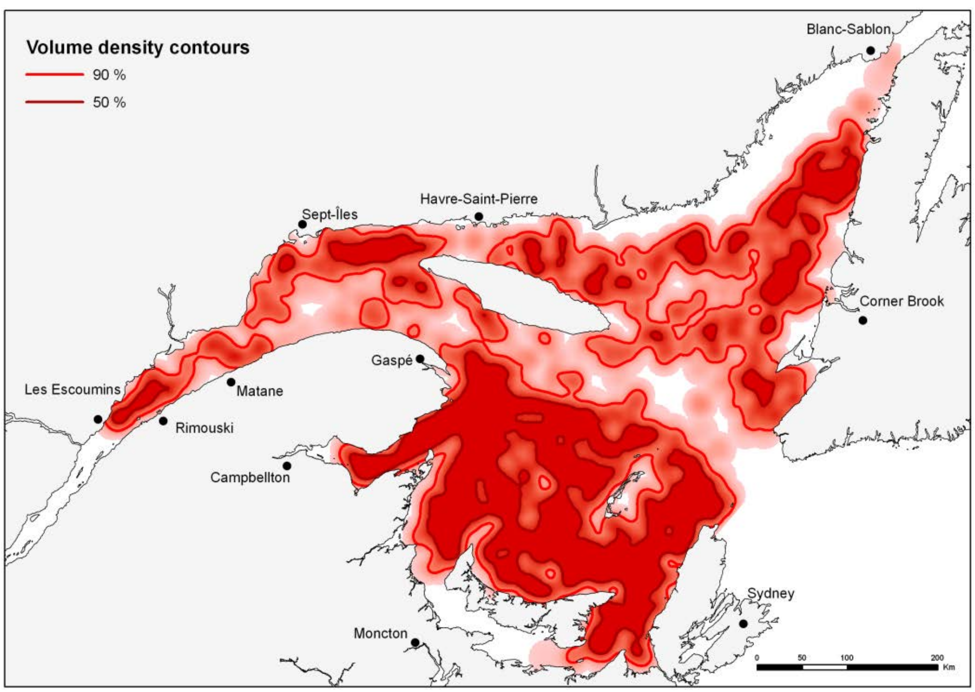

Figure 90. Map of relative occurrence (50% and 90% volume density contours) for American plaice in the St. Lawrence estuary and Gulf based on annual bottom trawl surveys conducted by DFO (1984–1992, fish > 20.5 cm total length).

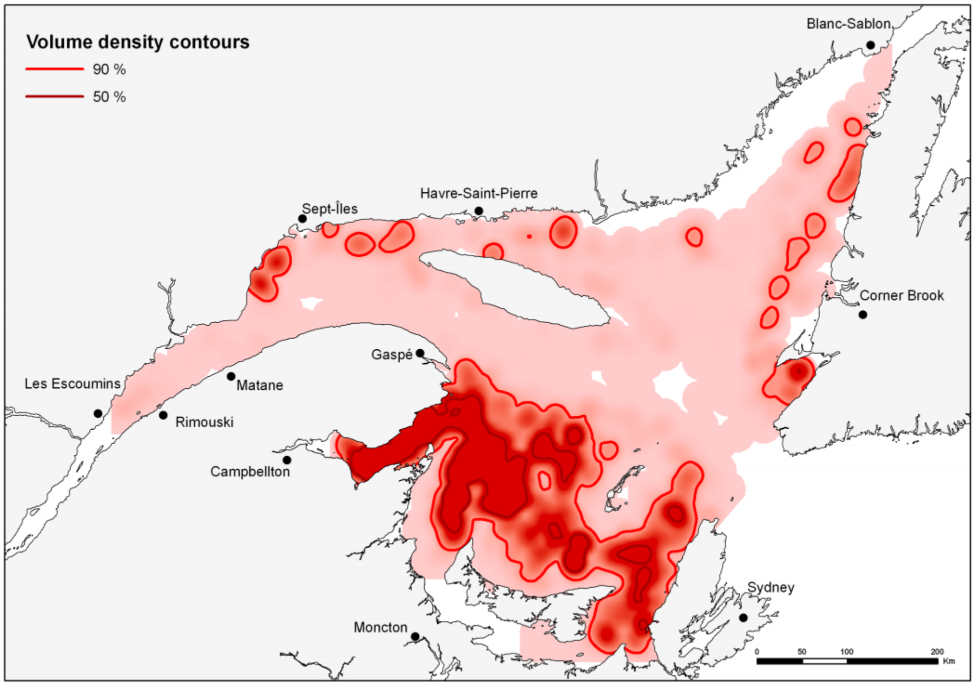

Figure 91. Map of catch in number (50% and 90% volume density contours) for American plaice in the St. Lawrence estuary and Gulf based on annual bottom trawl surveys conducted by DFO (1984–1992).

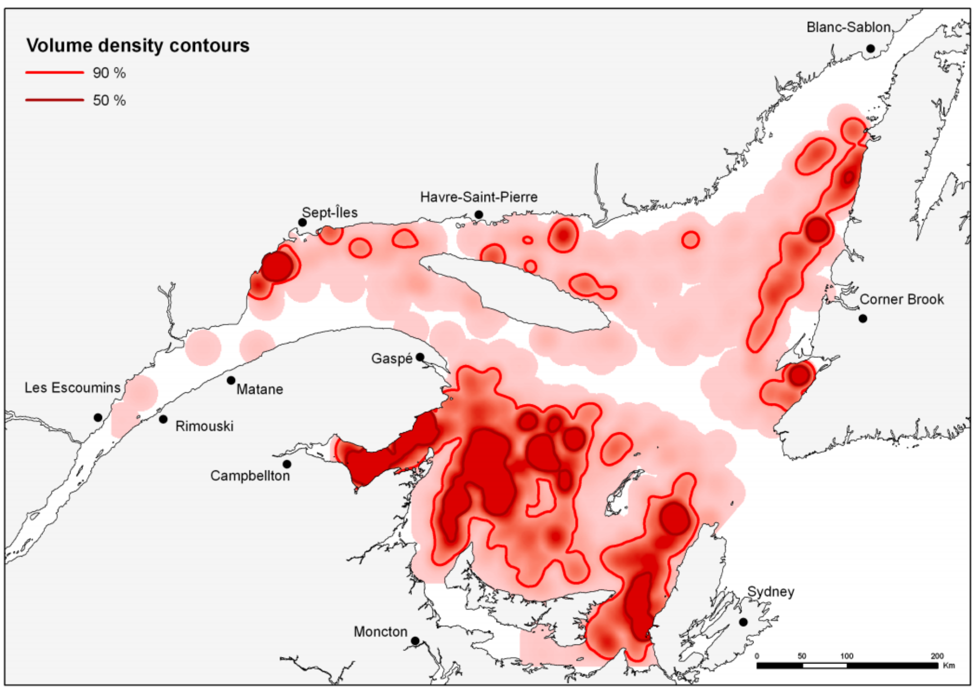

Figure 92. Map of catch in number (50% and 90% volume density contours) for American plaice in the St. Lawrence estuary and Gulf based on annual bottom trawl surveys conducted by DFO (1984–1992, fish < 20.5 cm total length).

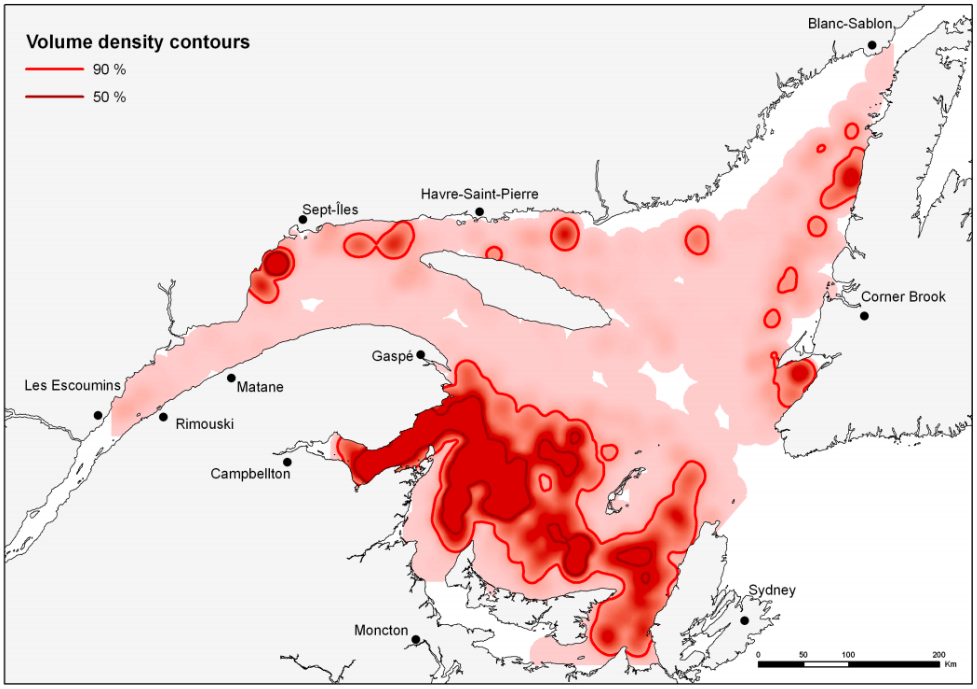

Figure 93. Map of catch in number (50% and 90% volume density contours) for American plaice in the St. Lawrence estuary and Gulf based on annual bottom trawl surveys conducted by DFO (1984–1992, fish > 20.5 cm total length).

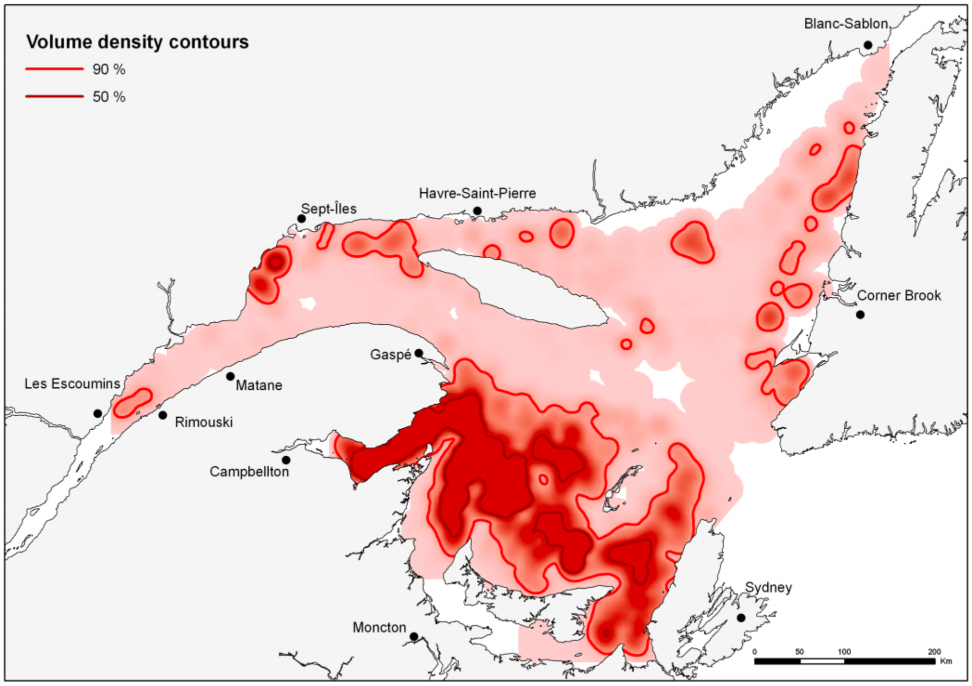

Figure 94. Map of catch in weight (50% and 90% volume density contours) for American plaice in the St. Lawrence estuary and Gulf based on annual bottom trawl surveys conducted by DFO (1984–1992).

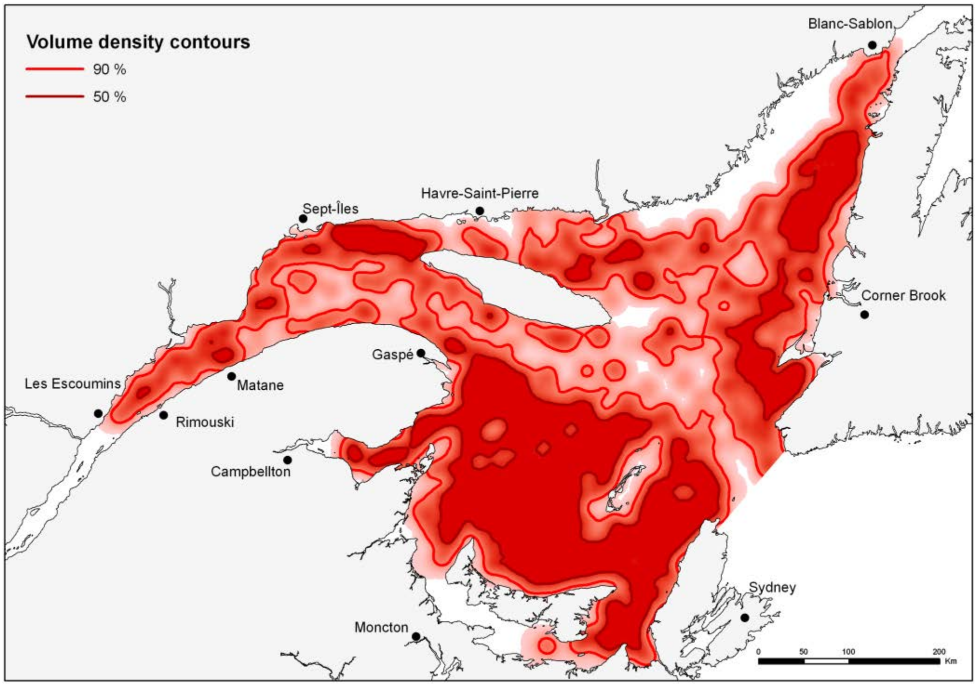

Figure 95. Map of relative occurrence (50% and 90% volume density contours) for American plaice in the St. Lawrence estuary and Gulf based on annual bottom trawl surveys conducted by DFO (1993–2001).

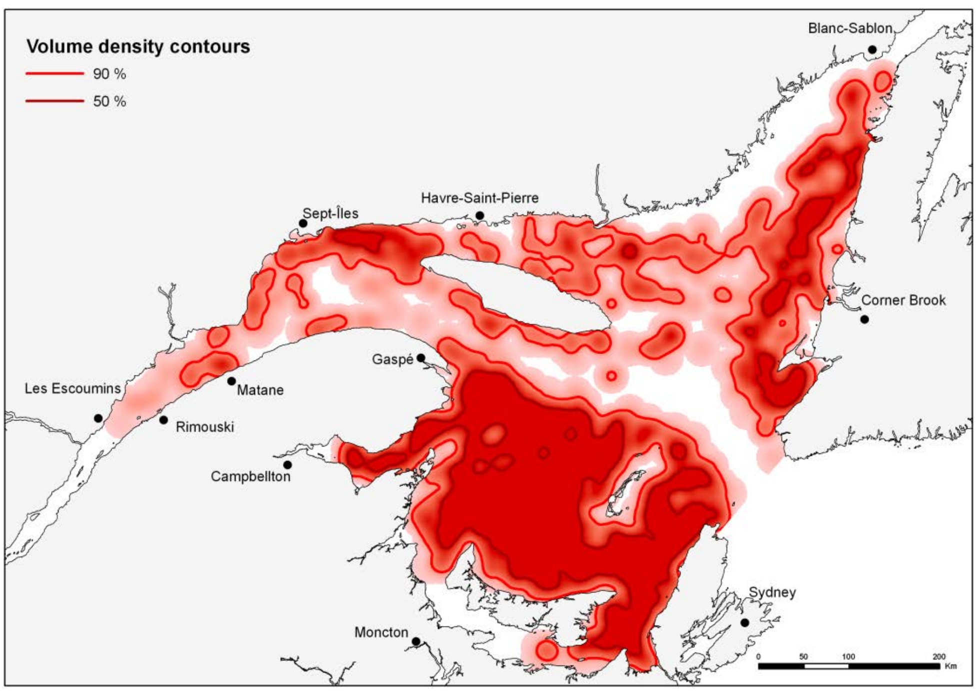

Figure 96. Map of relative occurrence (50% and 90% volume density contours) for American plaice in the St. Lawrence estuary and Gulf based on annual bottom trawl surveys conducted by DFO (1993–2001, fish < 20.5 cm total length).

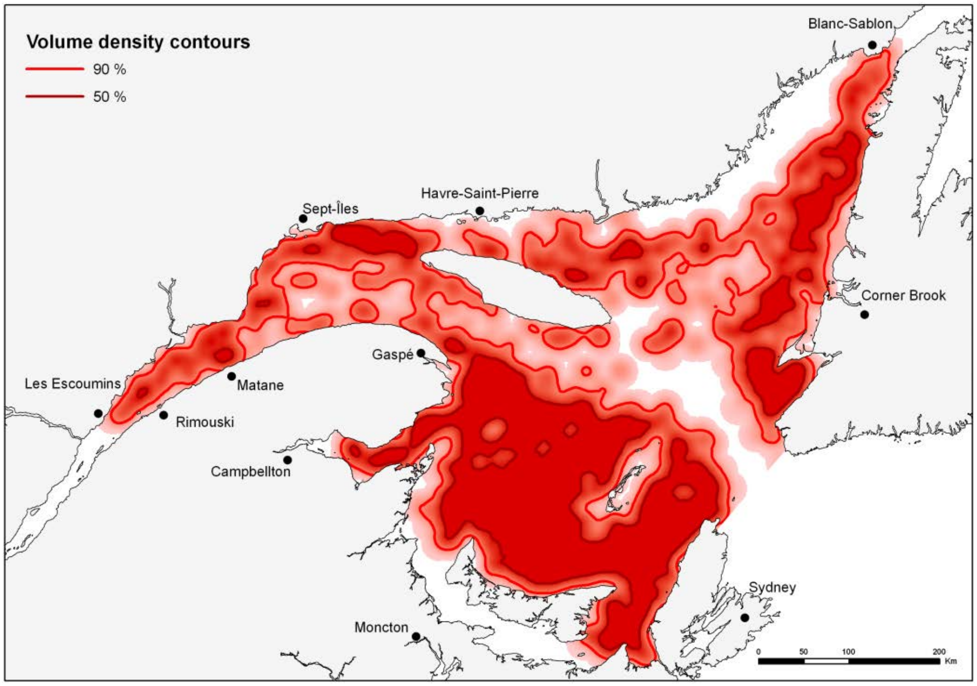

Figure 97. Map of relative occurrence (50% and 90% volume density contours) for American plaice in the St. Lawrence estuary and Gulf based on annual bottom trawl surveys conducted by DFO (1993–2001, fish > 20.5 cm total length).

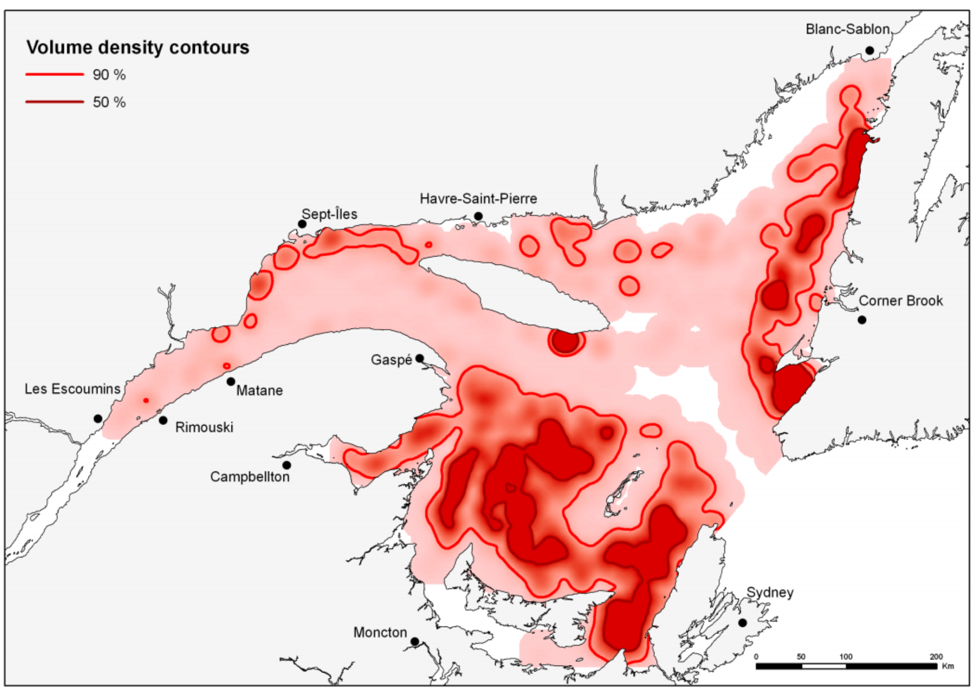

Figure 98. Map of catch in number (50% and 90% volume density contours) for American plaice in the St. Lawrence estuary and Gulf based on annual bottom trawl surveys conducted by DFO (1993–2001).

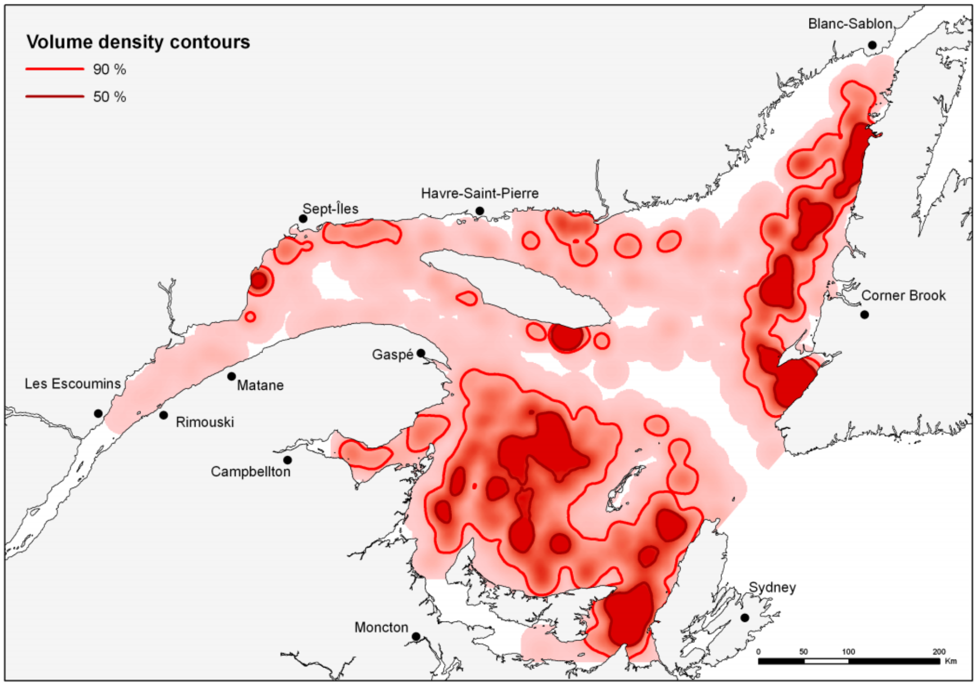

Figure 99. Map of catch in number (50% and 90% volume density contours) for American plaice in the St. Lawrence estuary and Gulf based on annual bottom trawl surveys conducted by DFO (1993–2001, fish < 20.5 cm total length).

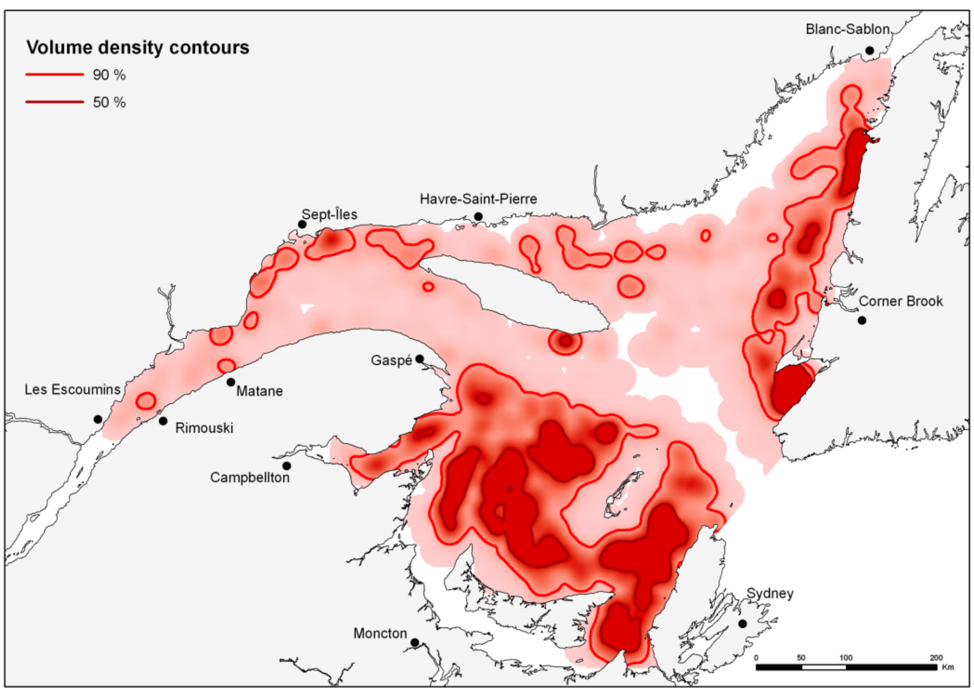

Figure 100. Map of catch in number (50% and 90% volume density contours) for American plaice in the St. Lawrence estuary and Gulf based on annual bottom trawl surveys conducted by DFO (1993–2001, fish > 20.5 cm total length).

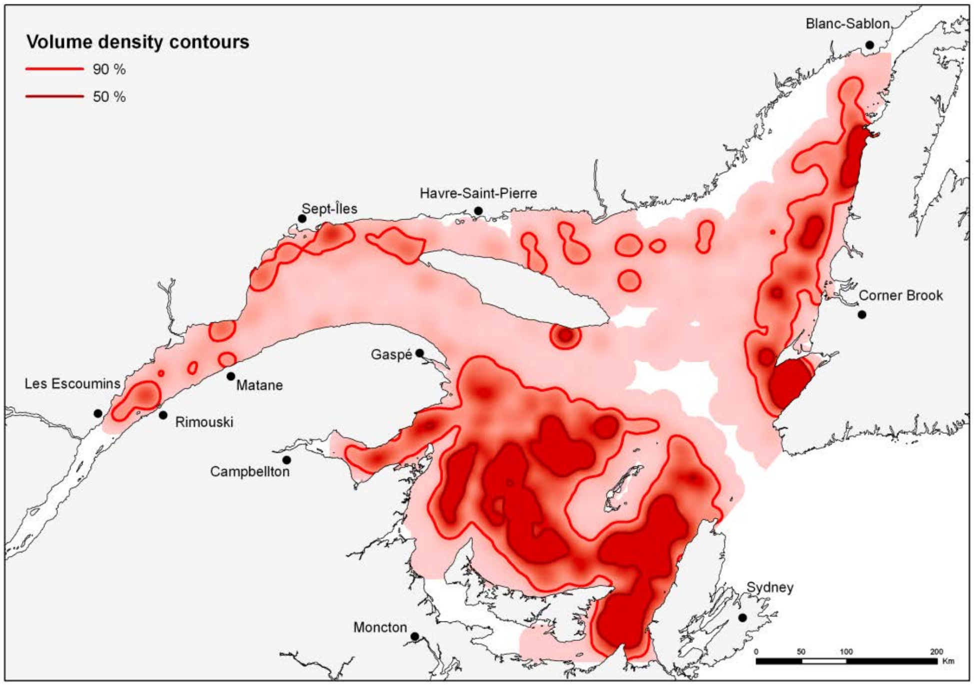

Figure 101. Map of catch in weight (50% and 90% volume density contours) for American plaice in the St. Lawrence estuary and Gulf based on annual bottom trawl surveys conducted by DFO (1993–2001).

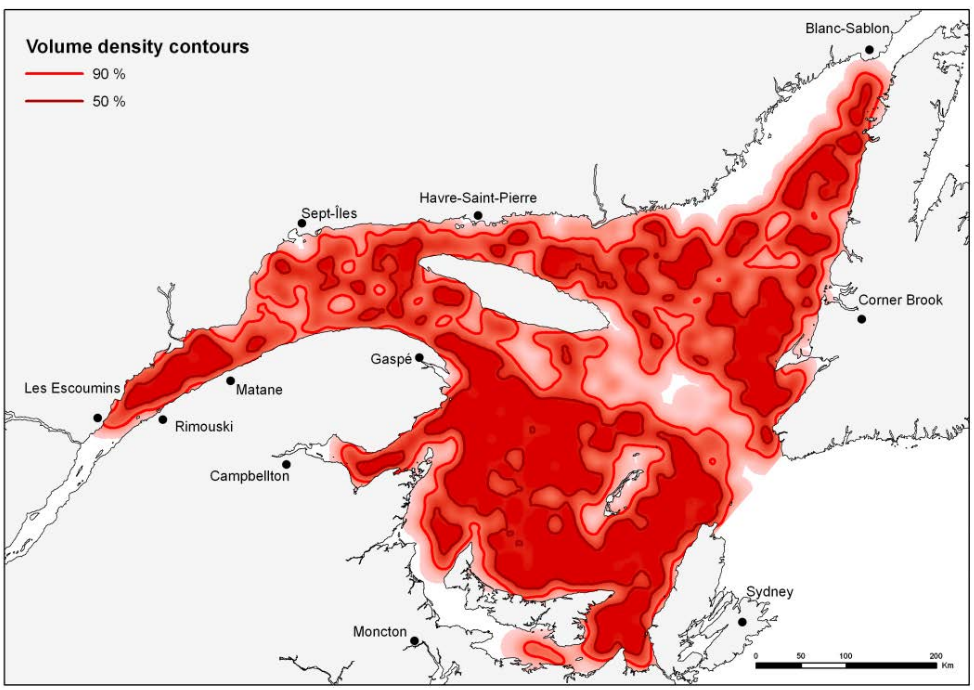

Figure 102. Map of relative occurrence (50% and 90% volume density contours) for American plaice in the St. Lawrence estuary and Gulf based on annual bottom trawl surveys conducted by DFO (2002–2010).

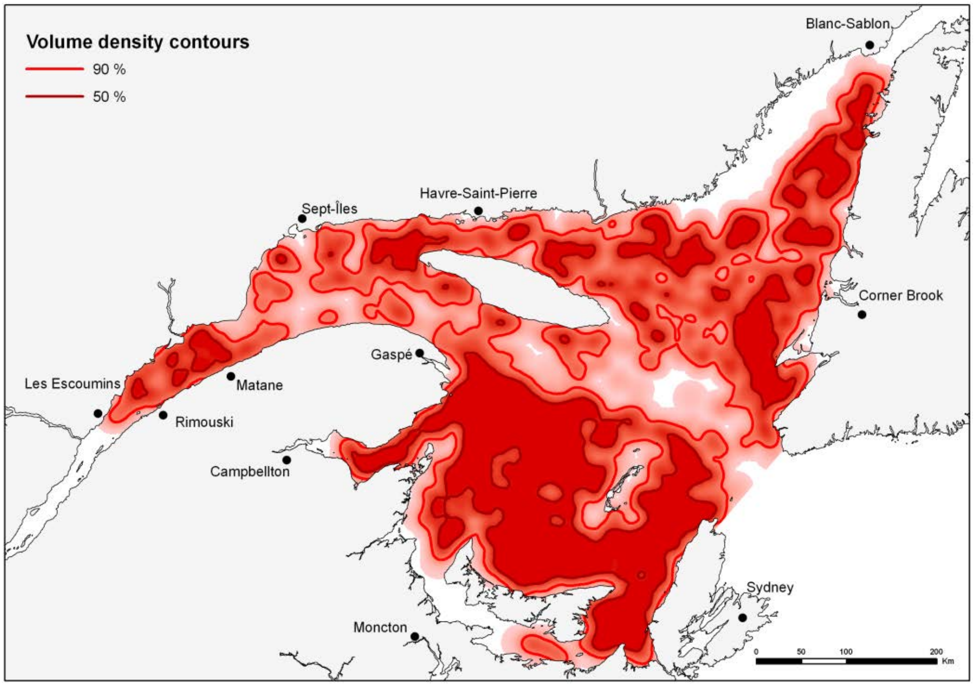

Figure 103. Map of relative occurrence (50% and 90% volume density contours) for American plaice in the St. Lawrence estuary and Gulf based on annual bottom trawl surveys conducted by DFO (2002–2010, fish < 20.5 cm total length).

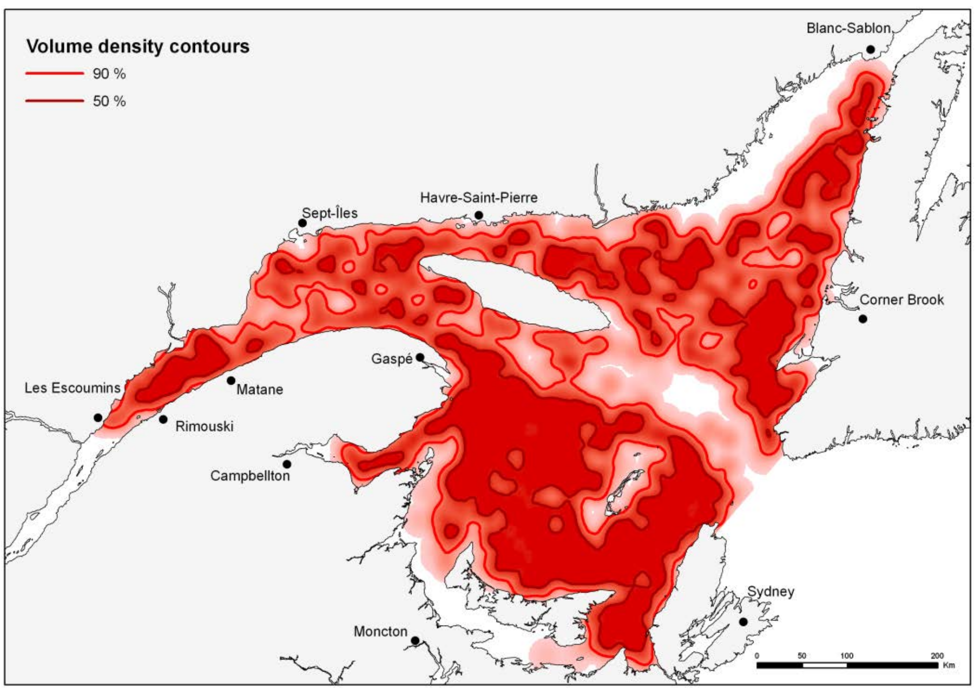

Figure 104. Map of relative occurrence (50% and 90% volume density contours) for American plaice in the St. Lawrence estuary and Gulf based on annual bottom trawl surveys conducted by DFO (2002–2010, fish > 20.5 cm total length).

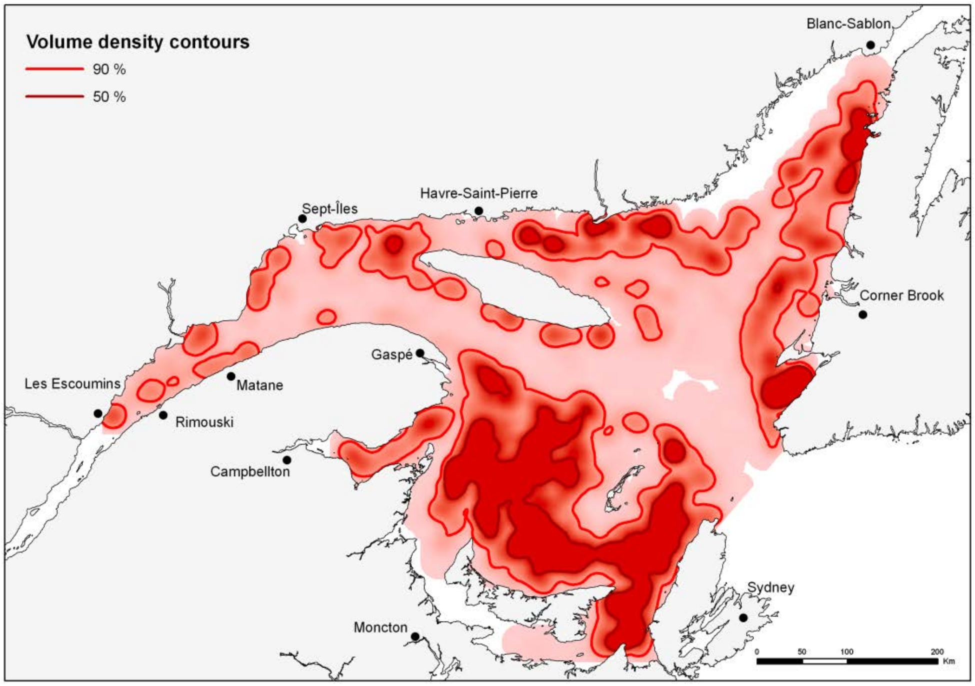

Figure 105. Map of catch in number (50% and 90% volume density contours) for American plaice in the St. Lawrence estuary and Gulf based on annual bottom trawl surveys conducted by DFO (2002–2010).

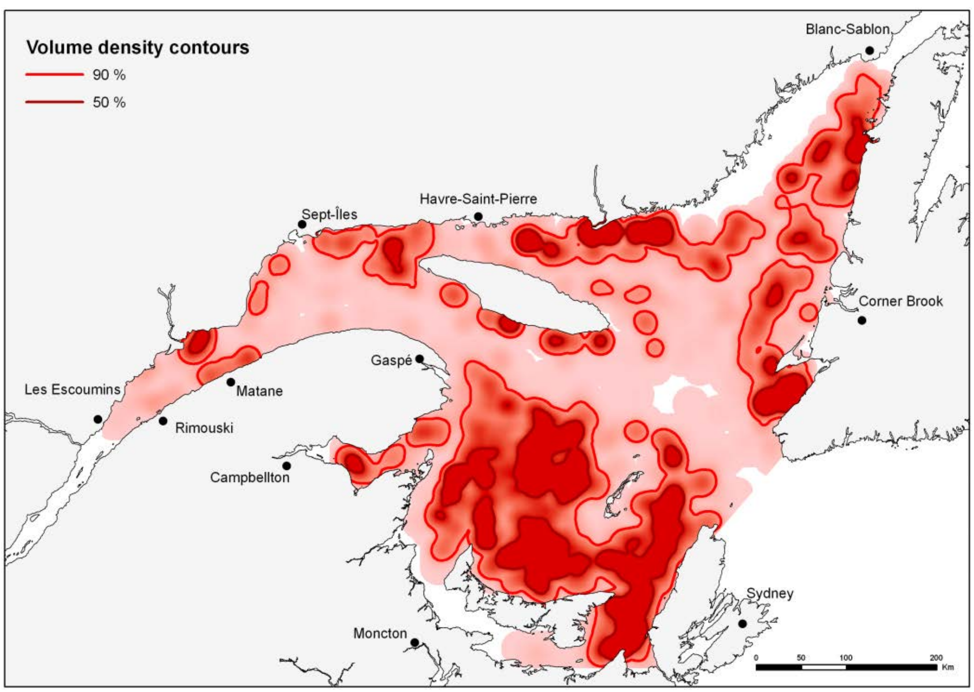

Figure 106. Map of catch in number (50% and 90% volume density contours) for American plaice in the St. Lawrence estuary and Gulf based on annual bottom trawl surveys conducted by DFO (2002–2010, fish < 20.5 cm total length).

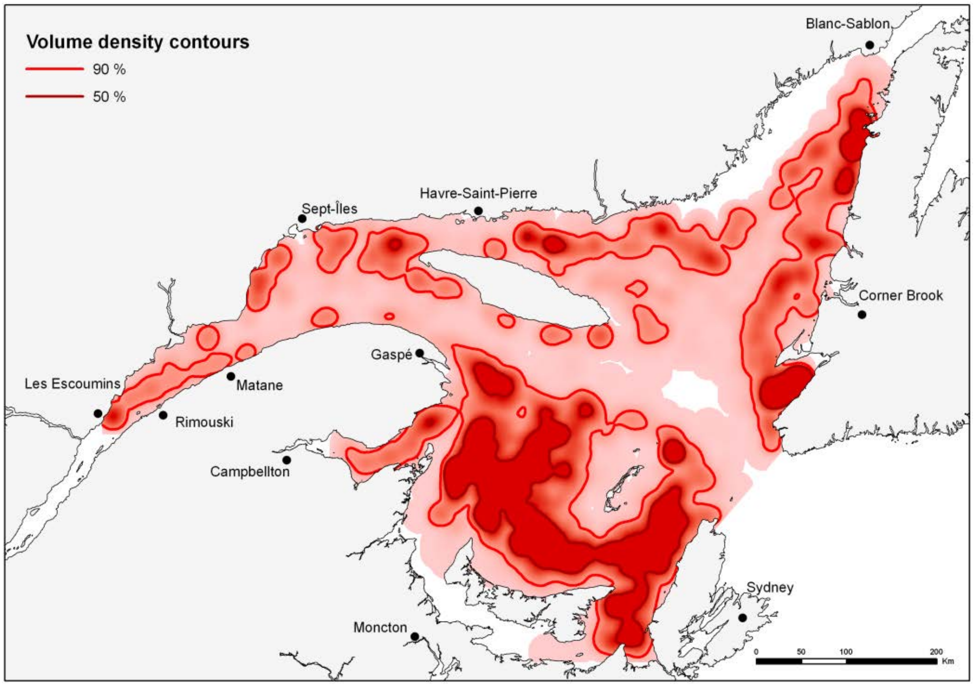

Figure 107. Map of catch in number (50% and 90% volume density contours) for American plaice in the St. Lawrence estuary and Gulf based on annual bottom trawl surveys conducted by DFO (2002–2010, fish > 20.5 cm total length).

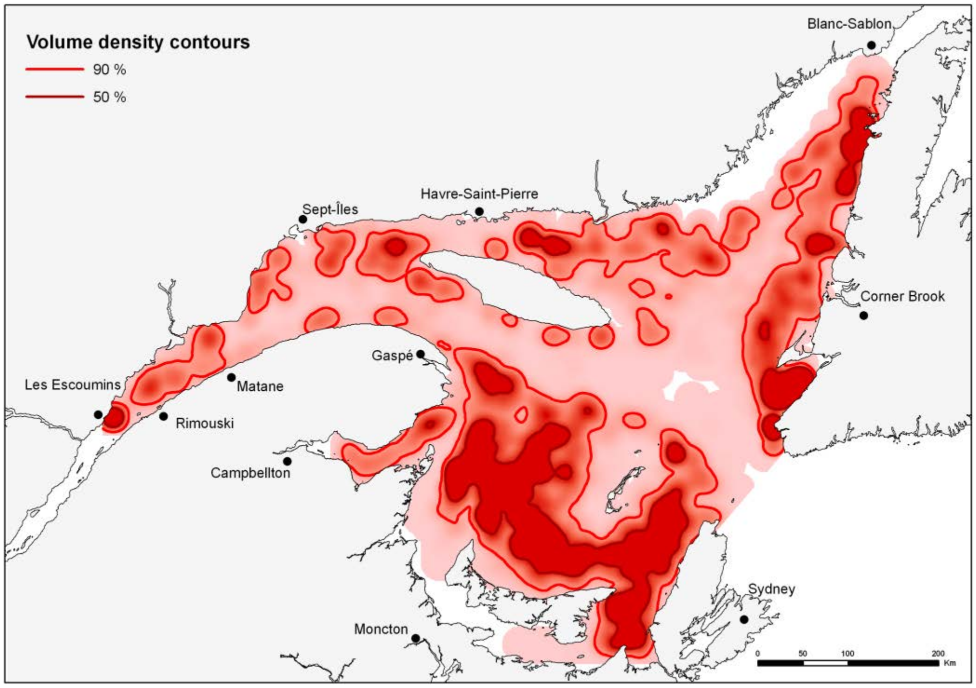

Figure 108. Map of catch in weight (50% and 90% volume density contours) for American plaice in the St. Lawrence estuary and Gulf based on annual bottom trawl surveys conducted by DFO (2002–2010).

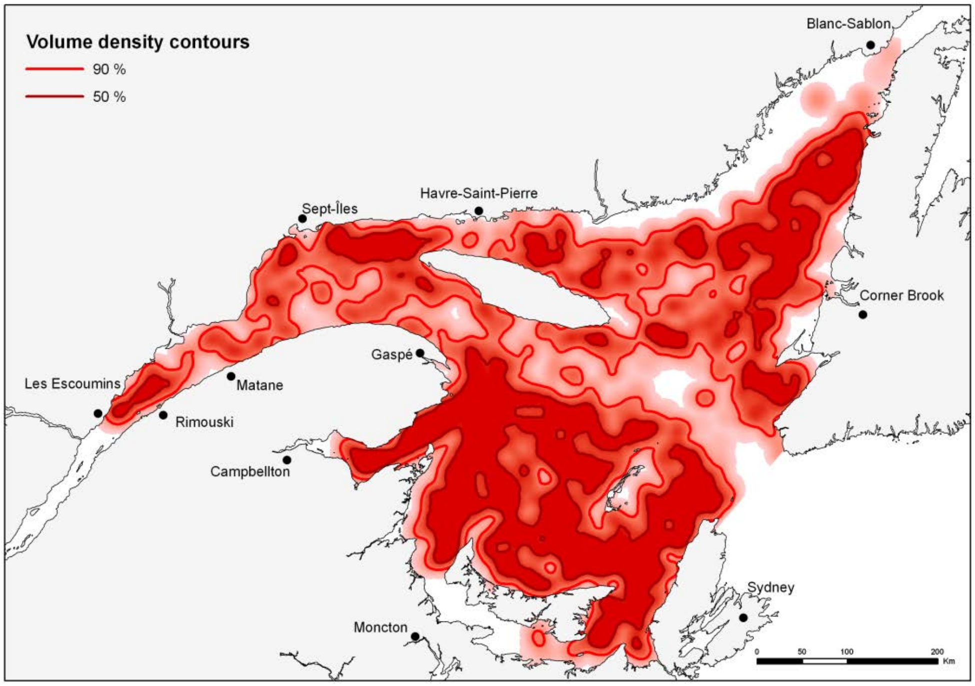

Figure 109. Map of relative occurrence (50% and 90% volume density contours) for American plaice in the St. Lawrence estuary and Gulf based on annual bottom trawl surveys conducted by DFO (1984–1992, summer).

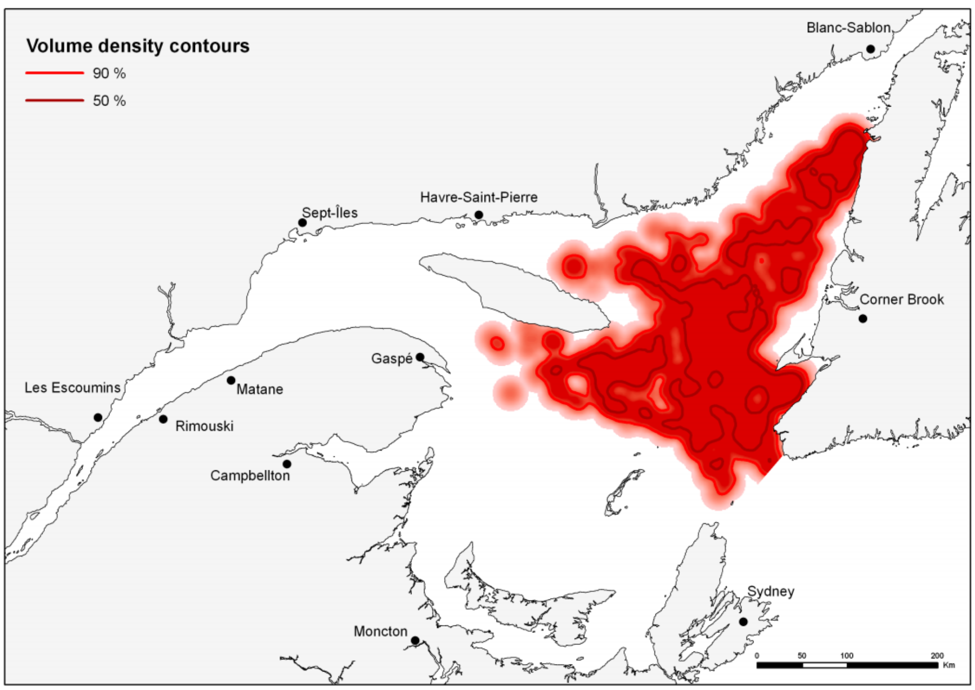

Figure 110. Map of relative occurrence (50% and 90% volume density contours) for American plaice in the St. Lawrence estuary and Gulf based on annual bottom trawl surveys conducted by DFO (1984–1992, winter).

Global and local spatial autocorrelation statistic

The statistics for the different periods, categories, and parameters are summarized in Table 95. The resulting maps (Figures 111–142) present the locations of significant clusters for low and high data values of plaice (hot spots and cold spots, respectively). Scores for G_i* Z are significant at α=0.10. Significant hot spots and cold spots are broken down by intervals of Z-score standard deviations (SD). A 20 km bandwith (zone of indifference model) was used. Whereas the number of cells classified as hot spots and cold spots varies considerably, due in part to the number of observations and power of the statistical tests, the location of hot spots and cold spots is largely consistent whether relative occurrences or catches in number or in weight are considered.

Table 95. Moran's *I* global spatial autocorrelation index value, Z-score, and associated probability based on the randomization null hypothesis for American plaice in the St. Lawrence estuary and Gulf. The index was calculated for each of three parameters (relative occurrence, catch in number, and catch in weight during the annual bottom trawl surveys) and different time periods (years) and fish size categories (fish less than or greater than 20.5 cm). Moran's *I* value is expected to be near zero under the null hypothesis of no spatial pattern. A positive value indicates clustering and a negative value indicates dispersion. The spatial pattern observed was considered clustered when the Global Moran's *I* index was significant at $\alpha = 0.10$.

Period	Parameter	Size of fish	Index value (*I*)	Z-score	p value
71–10	Relative occurrence	Small and large	0.412	41.52	<0.001
71–83	Relative occurrence	Small and large	0.161	8.23	<0.001
84–10	Relative occurrence	Small and large	0.450	44.92	<0.001
84–10	Relative occurrence	Small	0.601	58.59	<0.001
84–10	Relative occurrence	Large	0.571	55.71	<0.001
84–10	Catch in number	Small and large	0.511	50.40	<0.001
84–10	Catch in number	Small	0.303	30.43	<0.001
84–10	Catch in number	Large	0.474	47.29	<0.001
84–10	Catch in weight	Small and large	0.548	53.66	<0.001
84–92	Relative occurrence	Small and large	0.332	27.20	<0.001
84–92	Relative occurrence	Small	0.597	41.62	<0.001
84–92	Relative occurrence	Large	0.499	34.82	<0.001
84–92	Catch in number	Small and large	0.368	26.88	<0.001
84–92	Catch in number	Small	0.186	13.82	<0.001
84–92	Catch in number	Large	0.345	25.04	<0.001
84–92	Catch in weight	Small and large	0.409	29.42	<0.001
93–01	Relative occurrence	Small and large	0.381	30.70	<0.001
93–01	Relative occurrence	Small	0.546	43.38	<0.001
93–01	Relative occurrence	Large	0.459	36.52	<0.001
93–01	Catch in number	Small and large	0.298	25.56	<0.001
93–01	Catch in number	Small	0.203	17.60	<0.001
93–01	Catch in number	Large	0.325	27.57	<0.001
93–01	Catch in weight	Small and large	0.315	26.44	<0.001
02–10	Relative occurrence	Small and large	0.388	30.05	<0.001
02–10	Relative occurrence	Small	0.394	30.52	<0.001
02–10	Relative occurrence	Large	0.449	34.75	<0.001
02–10	Catch in number	Small and large	0.354	27.91	<0.001
02–10	Catch in number	Small	0.249	19.54	<0.001
02–10	Catch in number	Large	0.328	26.32	<0.001
02–10	Catch in weight	Small and large	0.325	25.63	<0.001
84–92	Rel. occurrence - summer	Small and large	0.472	35.10	<0.001
84–92	Rel. occurrence - winter	Small and large	0.109	4.92	<0.001

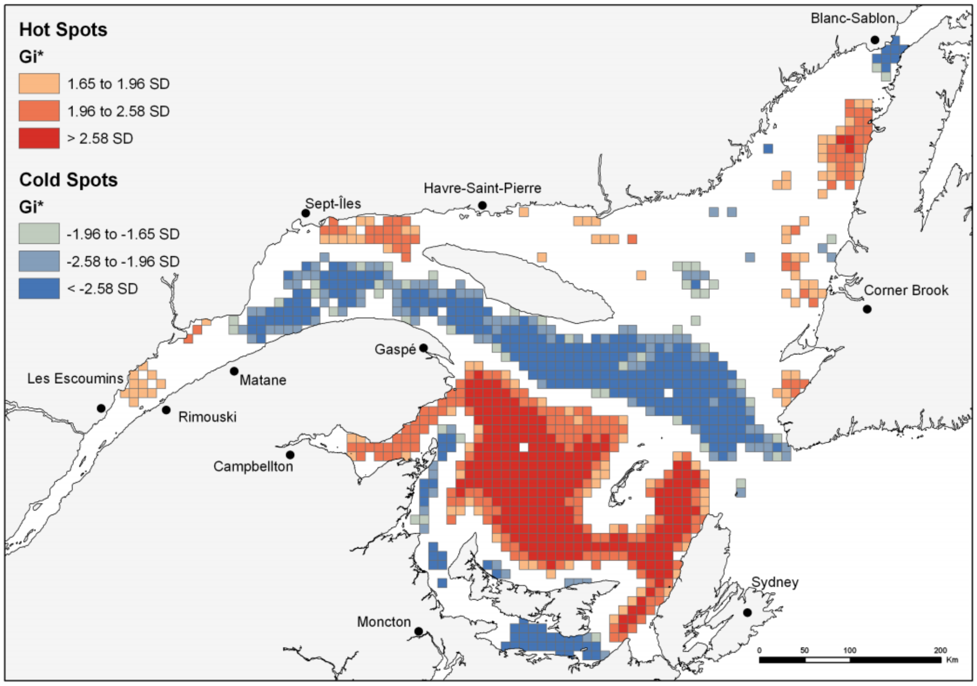

Figure 111. Location of statistically significant clusters of low relative occurrence (cold spots) and high relative occurrence (hot spots) for American plaice in the St. Lawrence estuary and Gulf based on annual bottom trawl surveys conducted by DFO (1971–2010).

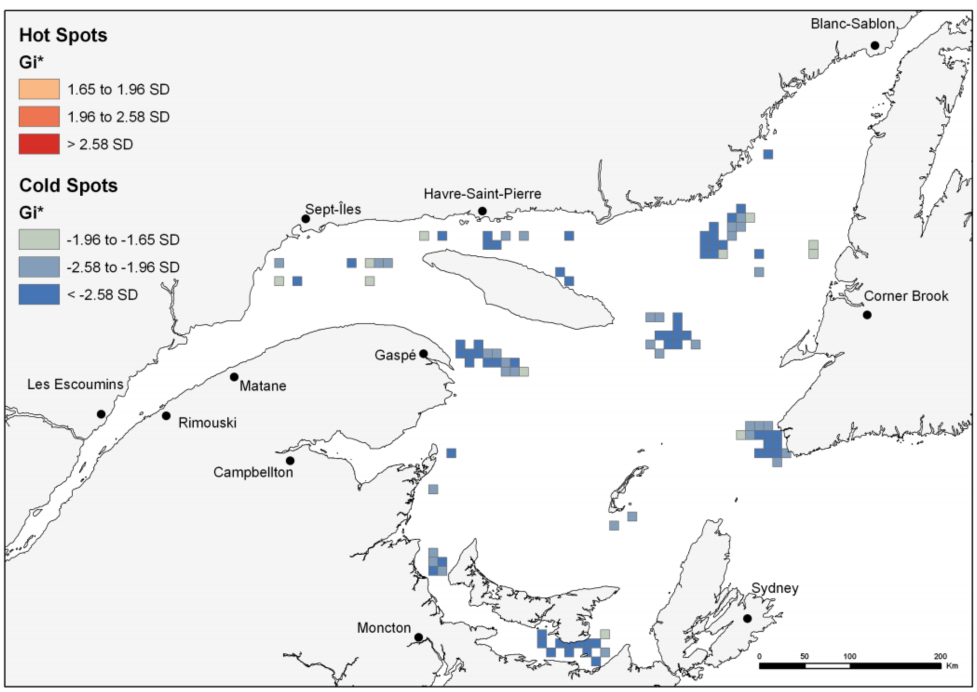

Figure 112. Location of statistically significant clusters of low relative occurrence (cold spots) and high relative occurrence (hot spots) for American plaice in the St. Lawrence estuary and Gulf based on annual bottom trawl surveys conducted by DFO (1971–1983).

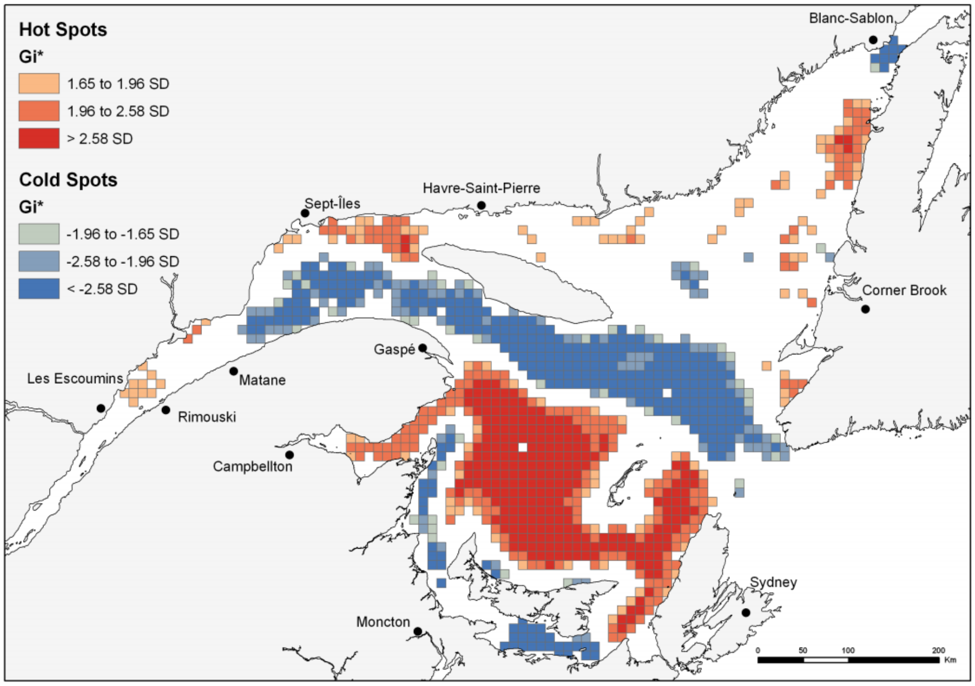

Figure 113. Location of statistically significant clusters of low relative occurrence (cold spots) and high relative occurrence (hot spots) for American plaice in the St. Lawrence estuary and Gulf based on annual bottom trawl surveys conducted by DFO (1984–2010).

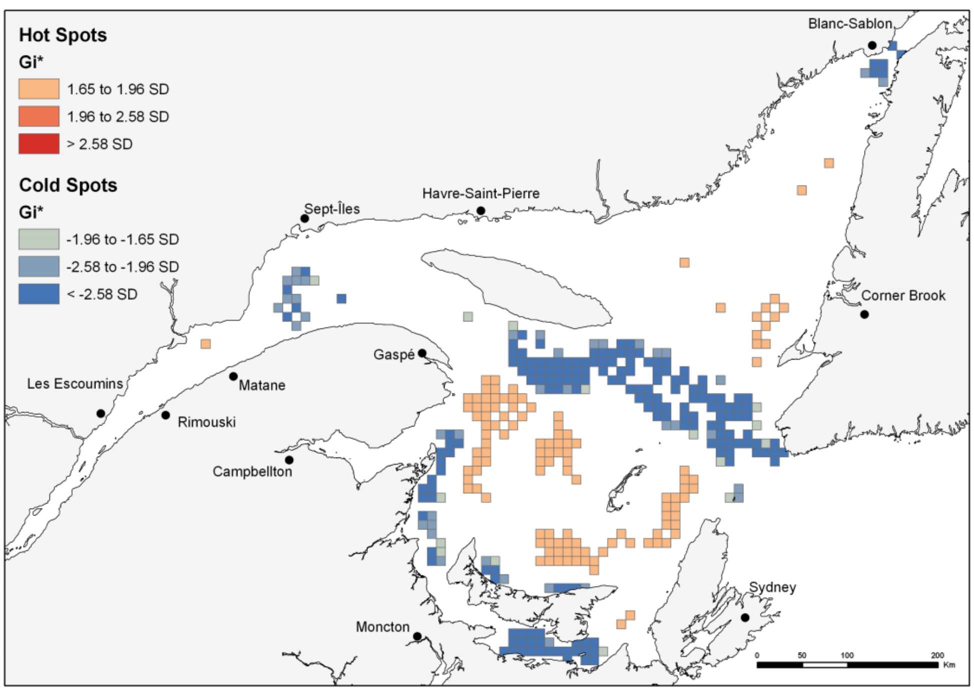

Figure 114. Location of statistically significant clusters of low relative occurrence (cold spots) and high relative occurrence (hot spots) for American plaice in the St. Lawrence estuary and Gulf based on annual bottom trawl surveys conducted by DFO (1984–2010, fish < 20.5 cm total length).

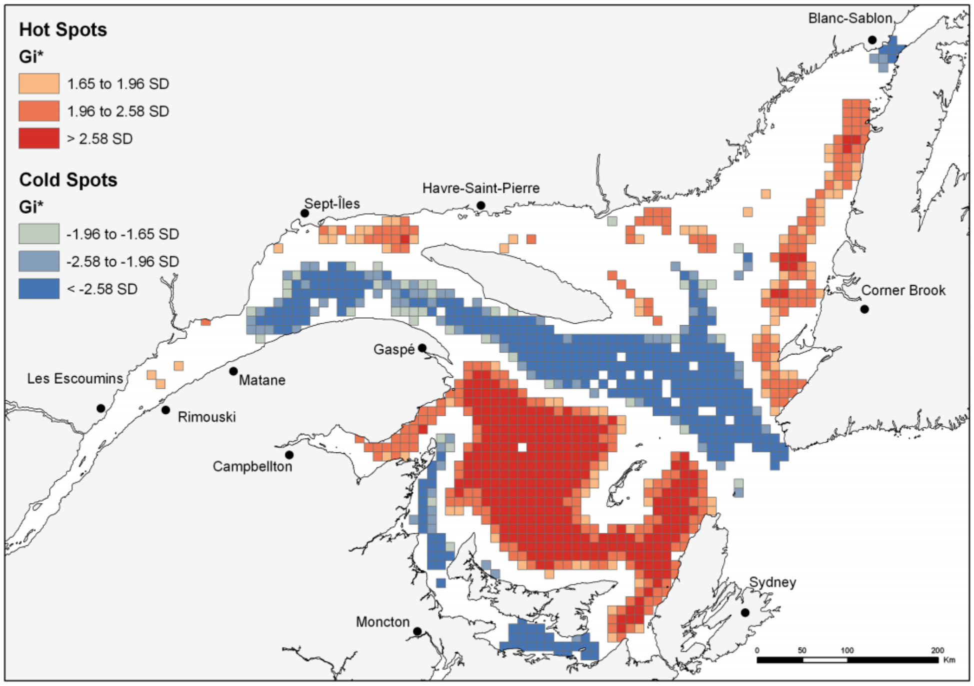

Figure 115. Location of statistically significant clusters of low relative occurrence (cold spots) and high relative occurrence (hot spots) for American plaice in the St. Lawrence estuary and Gulf based on annual bottom trawl surveys conducted by DFO (1984–2010, fish > 20.5 cm total length).

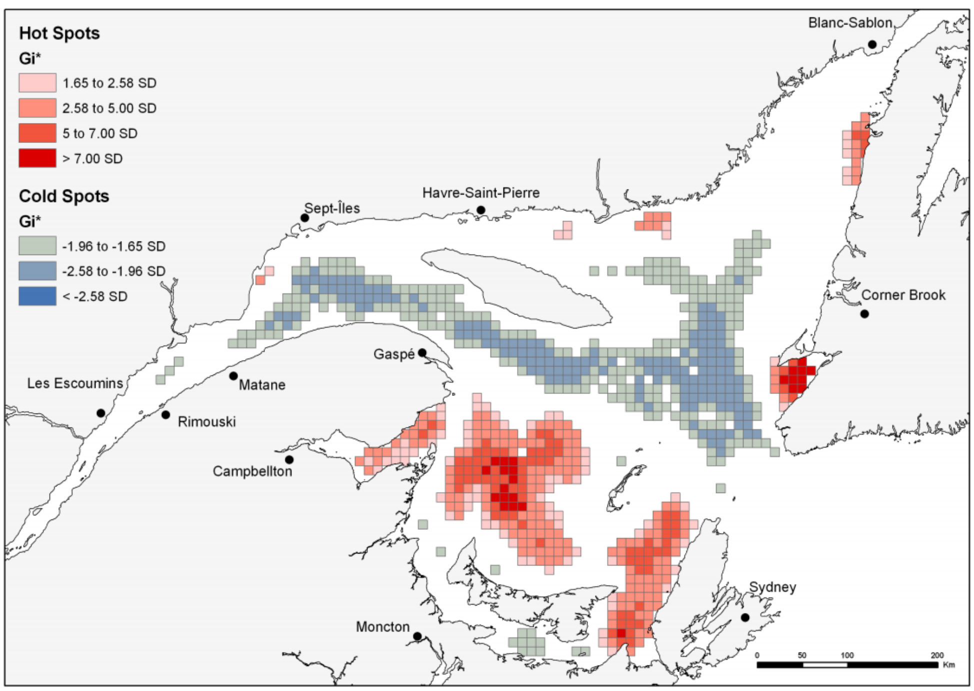

Figure 116. Location of statistically significant clusters of low catch in number (cold spots) and high catch in number (hot spots) for American plaice in the St. Lawrence estuary and Gulf based on annual bottom trawl surveys conducted by DFO (1984–2010).

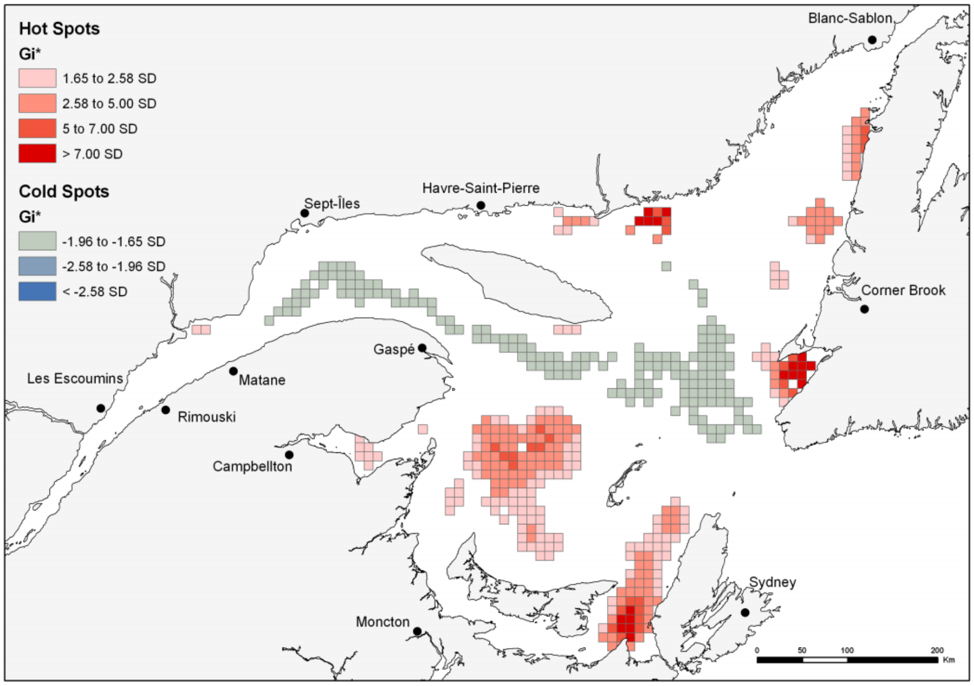

Figure 117. Location of statistically significant clusters of low catch in number (cold spots) and high catch in number (hot spots) for American plaice in the St. Lawrence estuary and Gulf based on annual bottom trawl surveys conducted by DFO (1984–2010, fish < 20.5 cm total length).

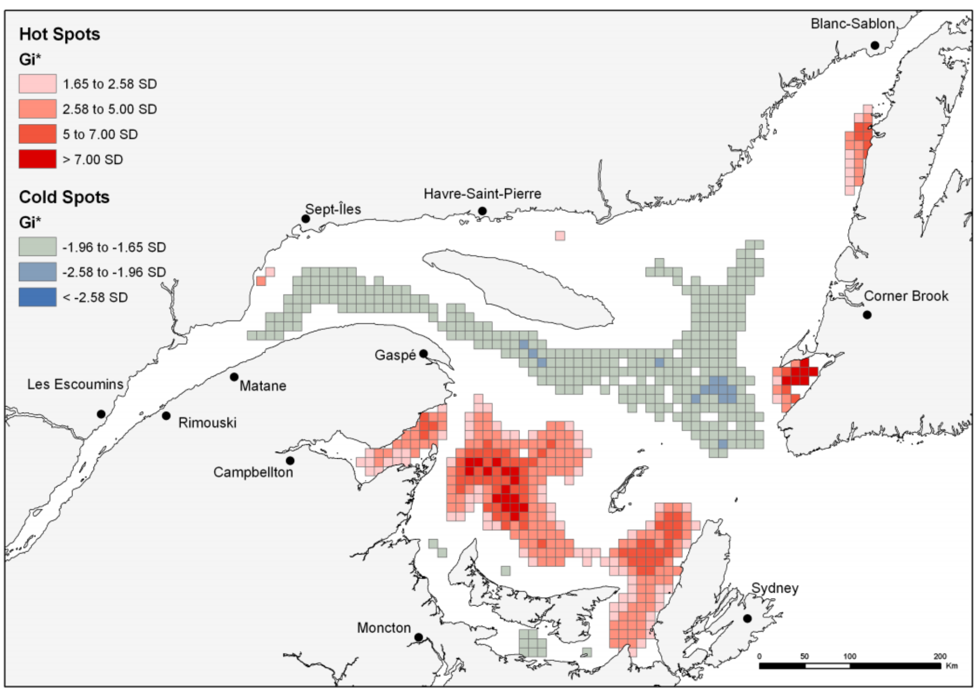

Figure 118. Location of statistically significant clusters of low catch in number (cold spots) and high catch in number (hot spots) for American plaice in the St. Lawrence estuary and Gulf based on annual bottom trawl surveys conducted by DFO (1984–2010, fish > 20.5 cm total length).

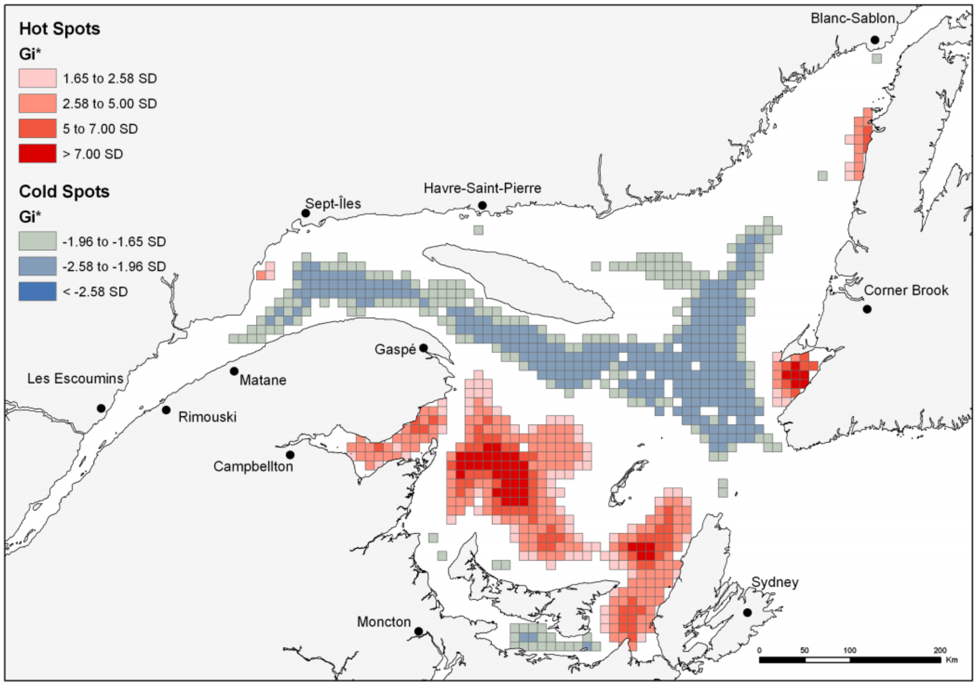

Figure 119. Location of statistically significant clusters of low catch in weight (cold spots) and high catch in weight (hot spots) for American plaice in the St. Lawrence estuary and Gulf based on annual bottom trawl surveys conducted by DFO (1984–2010).

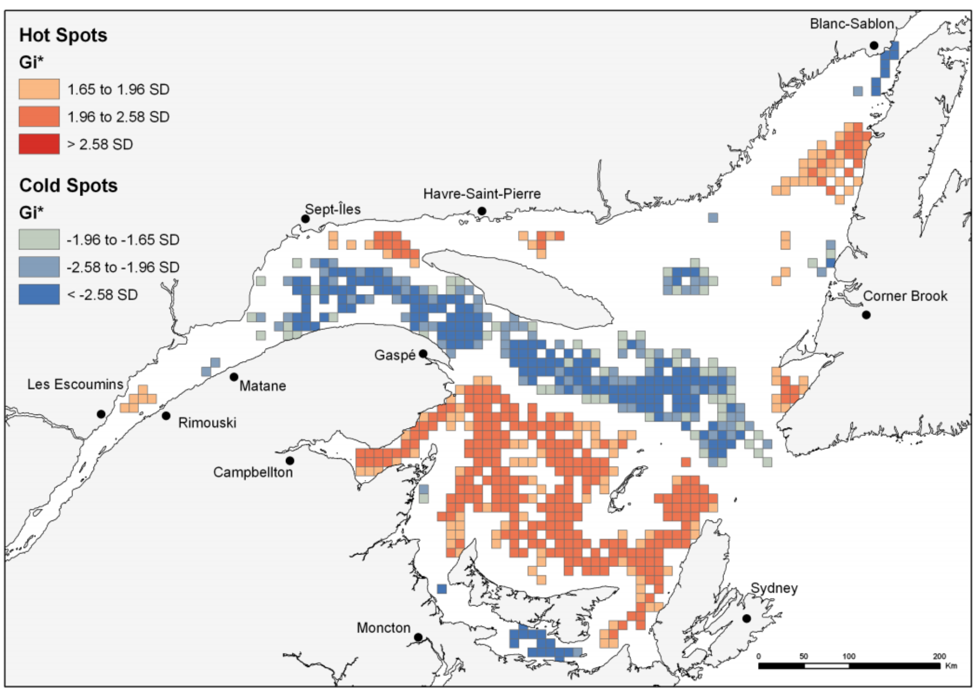

Figure 120. Location of statistically significant clusters of low relative occurrence (cold spots) and high relative occurrence (hot spots) for American plaice in the St. Lawrence estuary and Gulf based on annual bottom trawl surveys conducted by DFO (1984–1992).

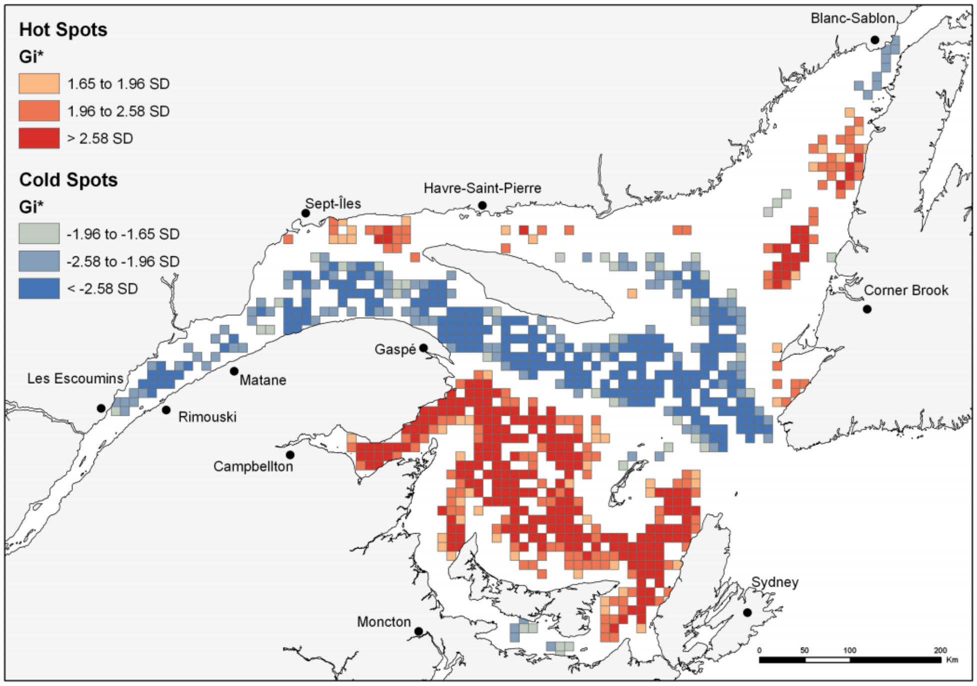

Figure 121. Location of statistically significant clusters of low relative occurrence (cold spots) and high relative occurrence (hot spots) for American plaice in the St. Lawrence estuary and Gulf based on annual bottom trawl surveys conducted by DFO (1984–1992, fish < 20.5 cm total length).

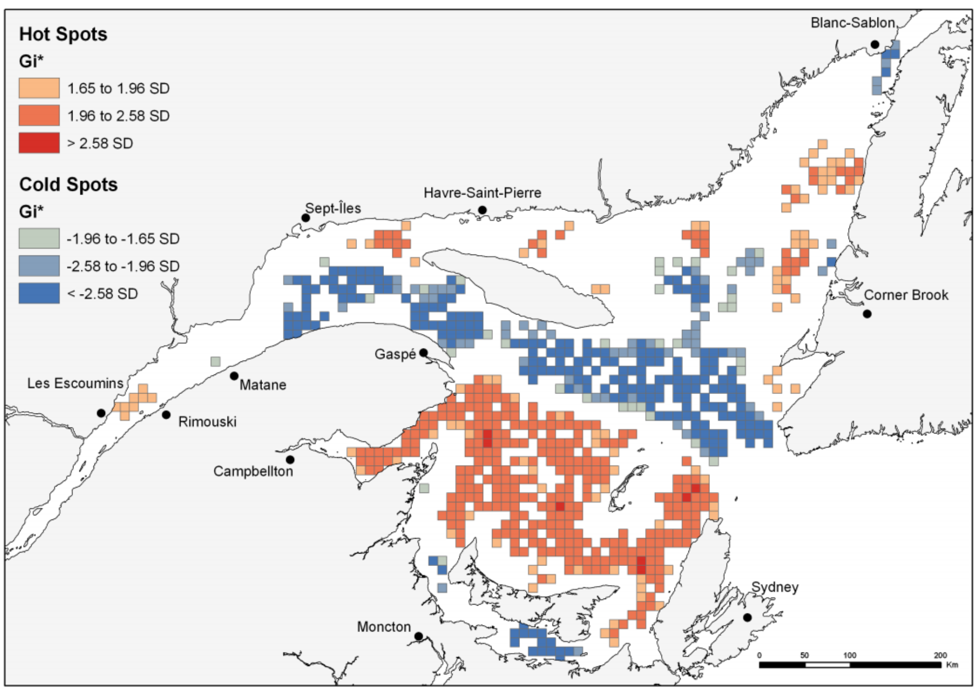

Figure 122. Location of statistically significant clusters of low relative occurrence (cold spots) and high relative occurrence (hot spots) for American plaice in the St. Lawrence estuary and Gulf based on annual bottom trawl surveys conducted by DFO (1984–1992, fish > 20.5 cm total length).

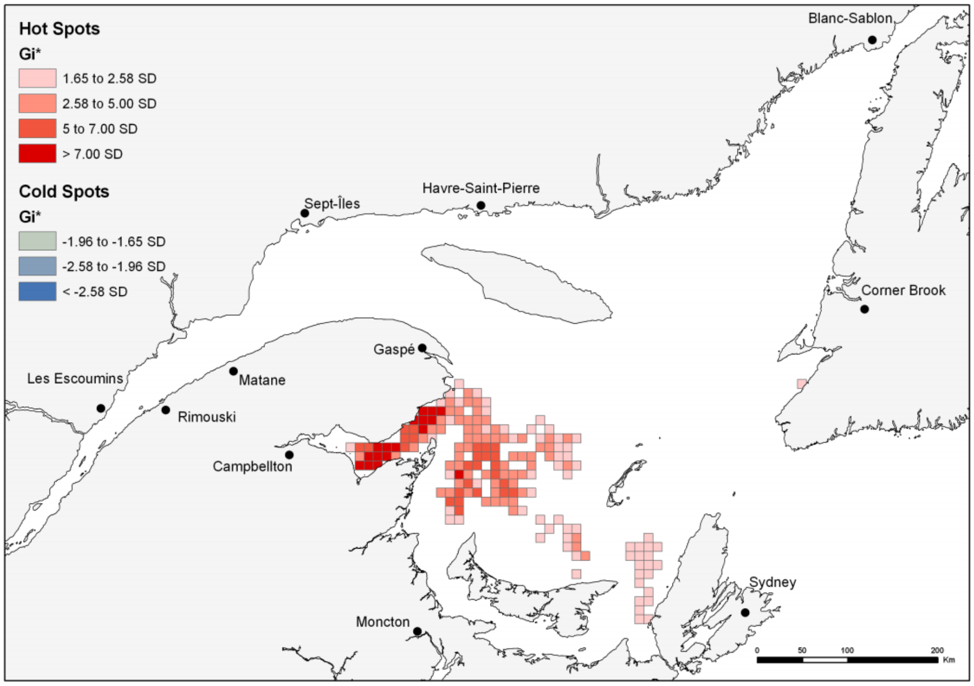

Figure 123. Location of statistically significant clusters of low catch in number (cold spots) and high catch in number (hot spots) for American plaice in the St. Lawrence estuary and Gulf based on annual bottom trawl surveys conducted by DFO (1984–1992).

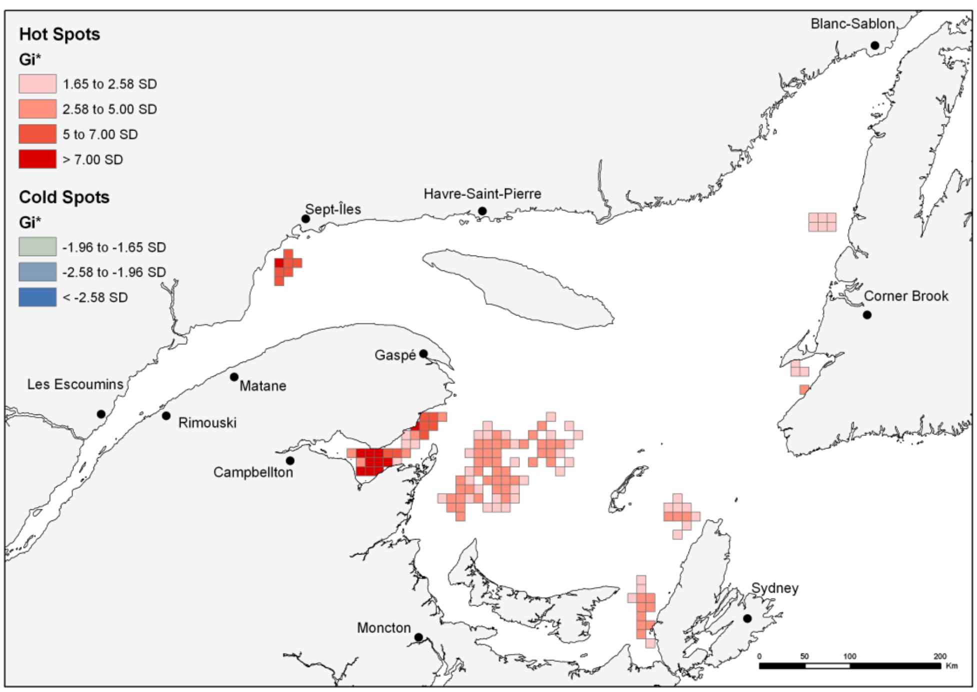

Figure 124. Location of statistically significant clusters of low catch in number (cold spots) and high catch in number (hot spots) for American plaice in the St. Lawrence estuary and Gulf based on annual bottom trawl surveys conducted by DFO (1984–1992, fish < 20.5 cm total length).

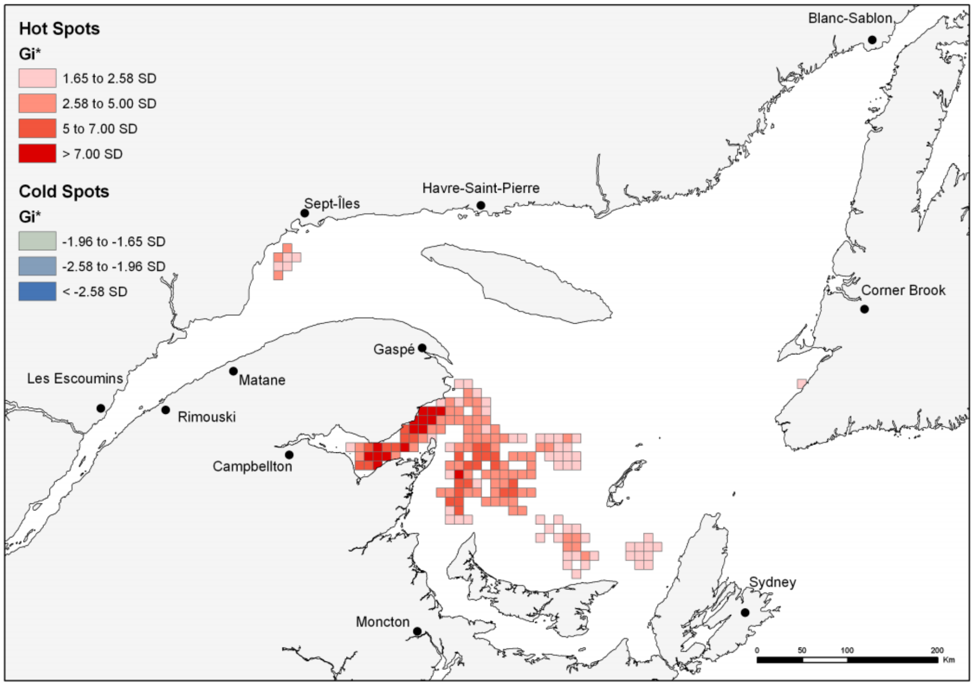

Figure 125. Location of statistically significant clusters of low catch in number (cold spots) and high catch in number (hot spots) (G_i* Z-scores significant at α=0.10) for American plaice in the St. Lawrence estuary and Gulf based on annual bottom trawl surveys conducted by DFO (1984–1992, fish > 20.5 cm total length).

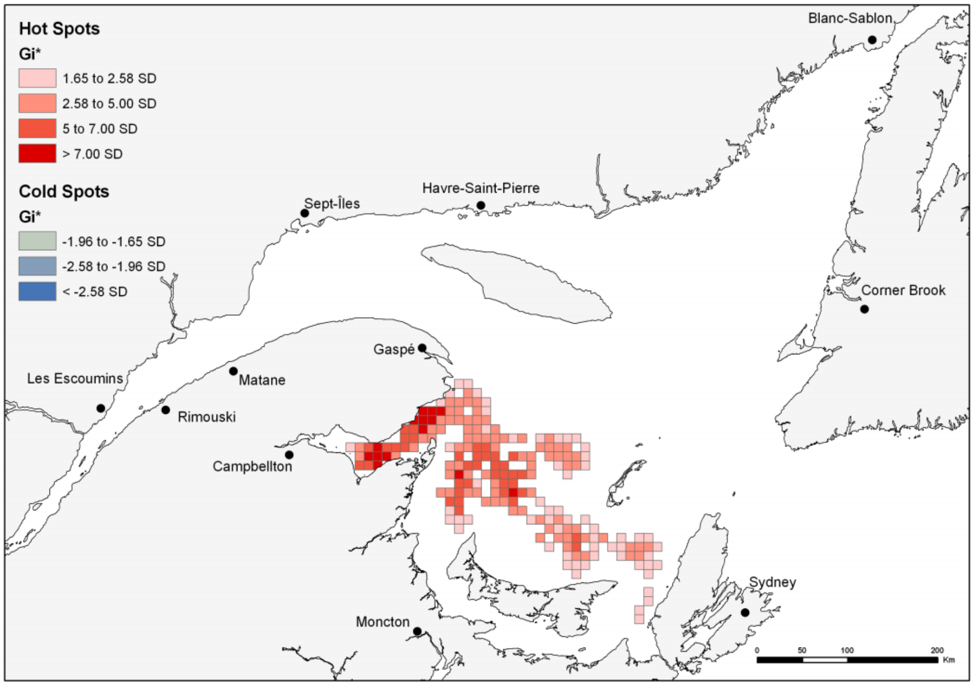

Figure 126. Location of statistically significant clusters of low catch in weight (cold spots) and high catch in weight (hot spots) for American plaice in the St. Lawrence estuary and Gulf based on annual bottom trawl surveys conducted by DFO (1984–1992).

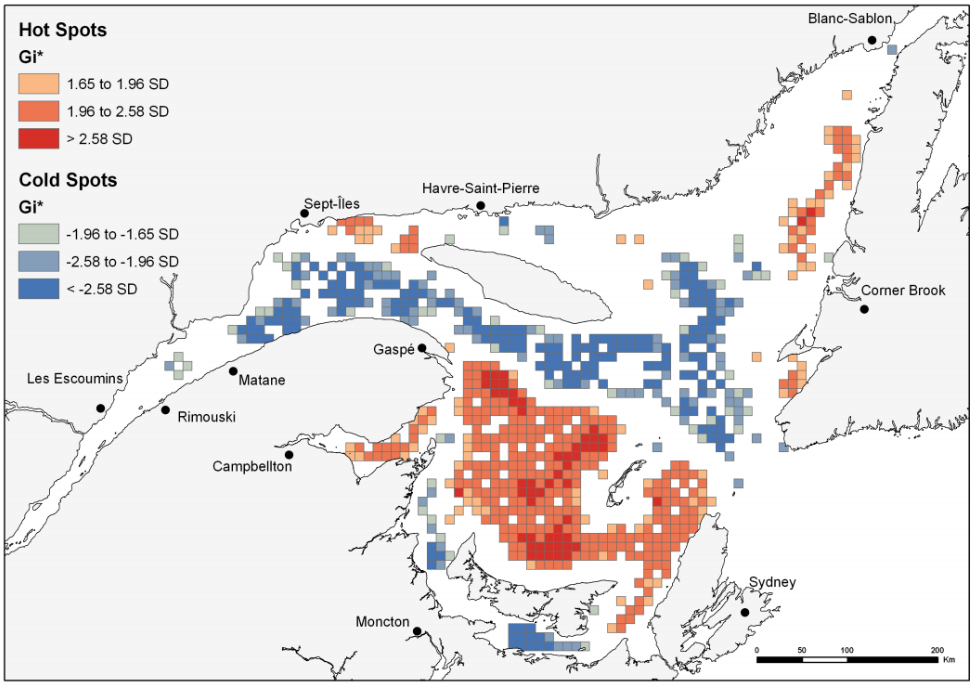

Figure 127. Location of statistically significant clusters of low relative occurrence (cold spots) and high relative occurrence (hot spots) for American plaice in the St. Lawrence estuary and Gulf based on annual bottom trawl surveys conducted by DFO (1993–2001).

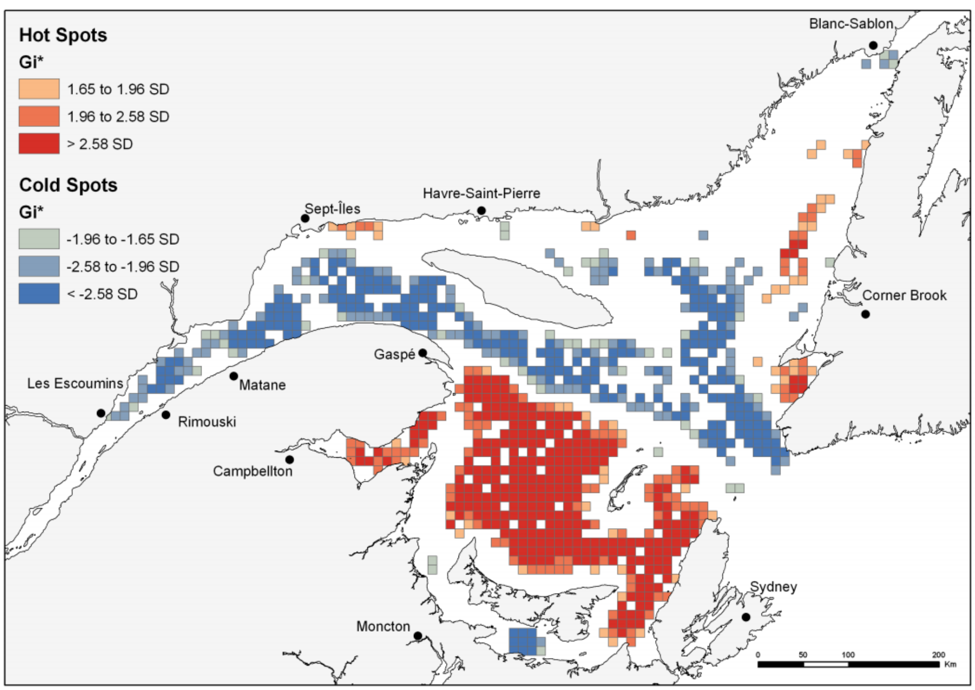

Figure 128. Location of statistically significant clusters of low relative occurrence (cold spots) and high relative occurrence (hot spots) for American plaice in the St. Lawrence estuary and Gulf based on annual bottom trawl surveys conducted by DFO (1993–2001, fish < 20.5 cm total length).

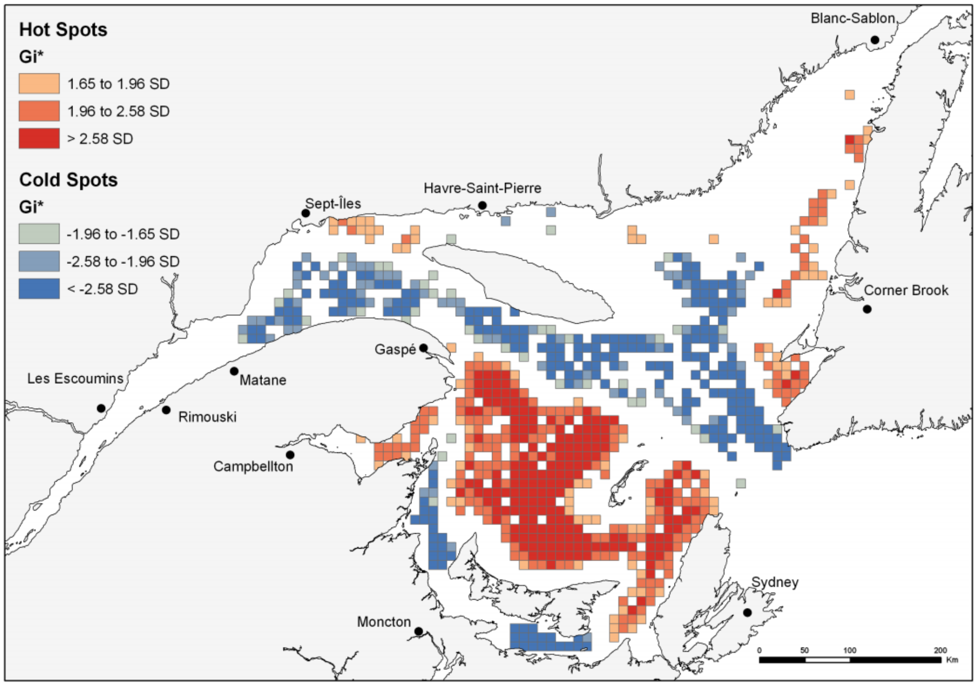

Figure 129. Location of statistically significant clusters of low relative occurrence (cold spots) and high relative occurrence (hot spots) for American plaice in the St. Lawrence estuary and Gulf based on annual bottom trawl surveys conducted by DFO (1993–2001, fish > 20.5 cm total length).

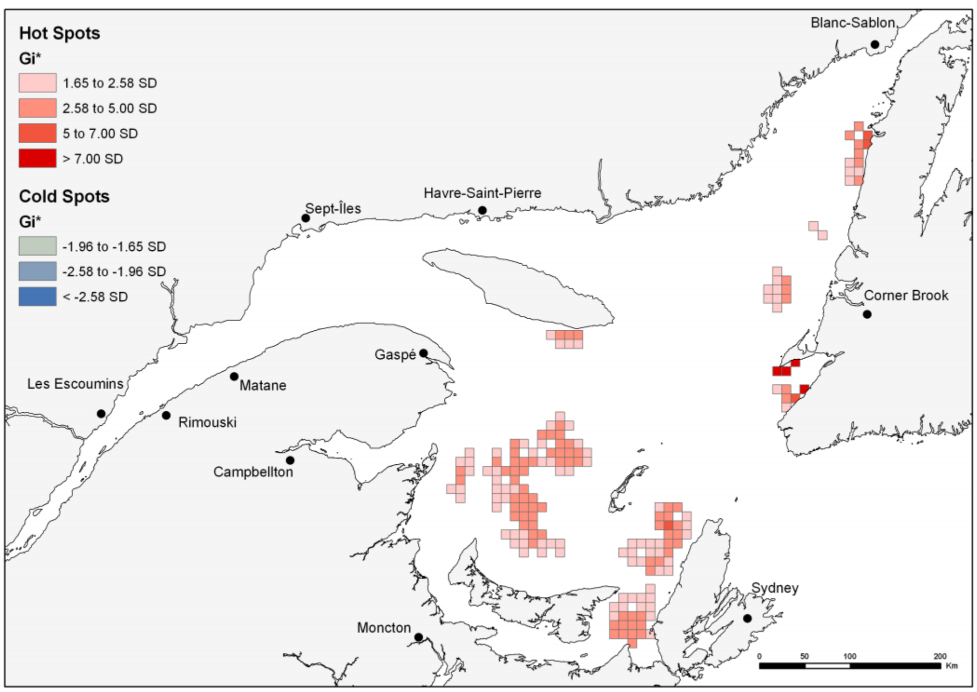

Figure 130. Location of statistically significant clusters of low catch in number (cold spots) and high catch in number (hot spots) for American plaice in the St. Lawrence estuary and Gulf based on annual bottom trawl surveys conducted by DFO (1993–2001).

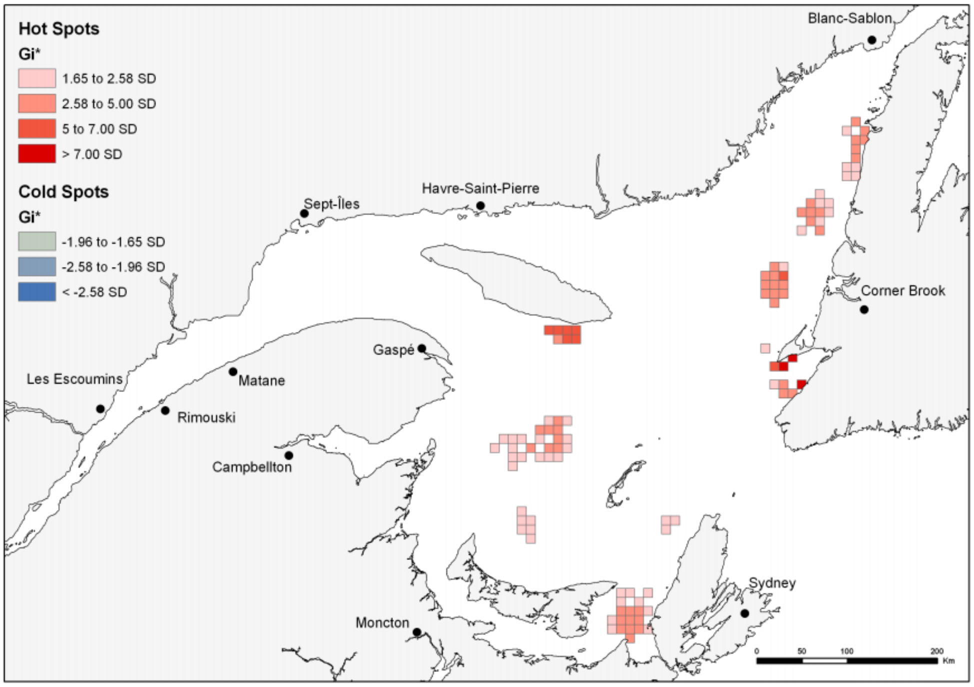

Figure 131. Location of statistically significant clusters of low catch in number (cold spots) and high catch in number (hot spots) for American plaice in the St. Lawrence estuary and Gulf based on annual bottom trawl surveys conducted by DFO (1993–2001, fish < 20.5 cm total length).

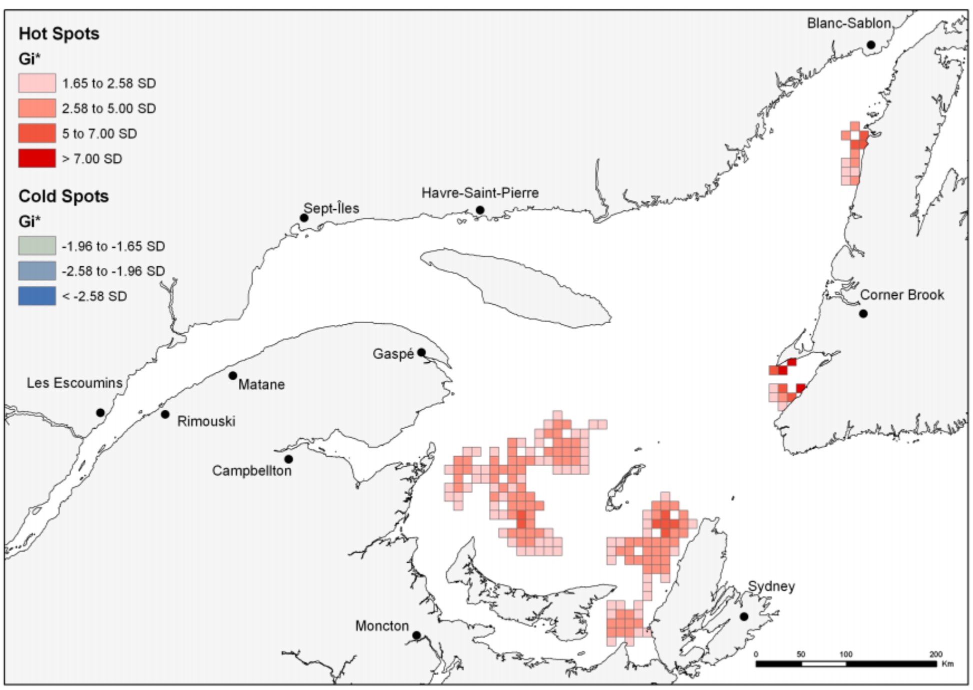

Figure 132. Location of statistically significant clusters of low catch in number (cold spots) and high catch in number (hot spots) for American plaice in the St. Lawrence estuary and Gulf based on annual bottom trawl surveys conducted by DFO (1993–2001, fish > 20.5 cm total length).

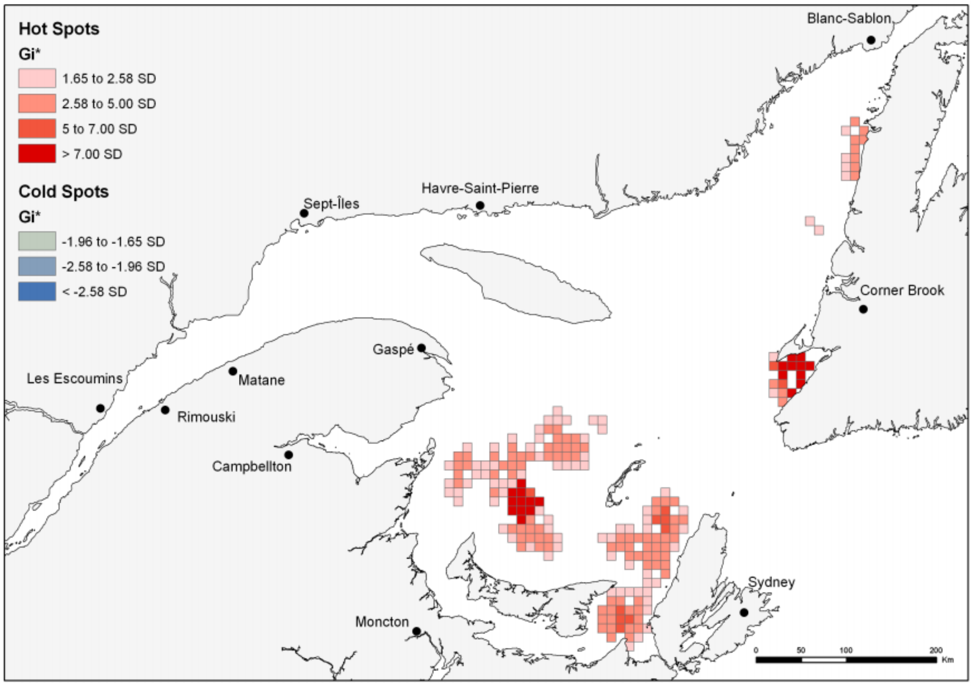

Figure 133. Location of statistically significant clusters of low catch in weight (cold spots) and high catch in weight (hot spots) for American plaice in the St. Lawrence estuary and Gulf based on annual bottom trawl surveys conducted by DFO (1993–2001).

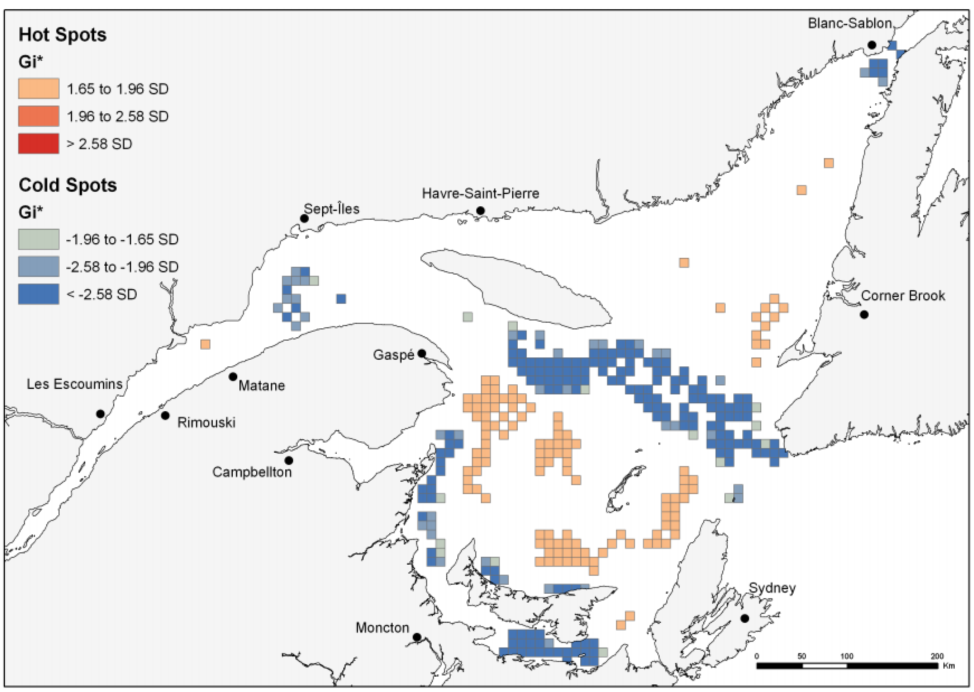

Figure 134. Location of statistically significant clusters of low relative occurrence (cold spots) and high relative occurrence (hot spots) for American plaice in the St. Lawrence estuary and Gulf based on annual bottom trawl surveys conducted by DFO (2002–2010).

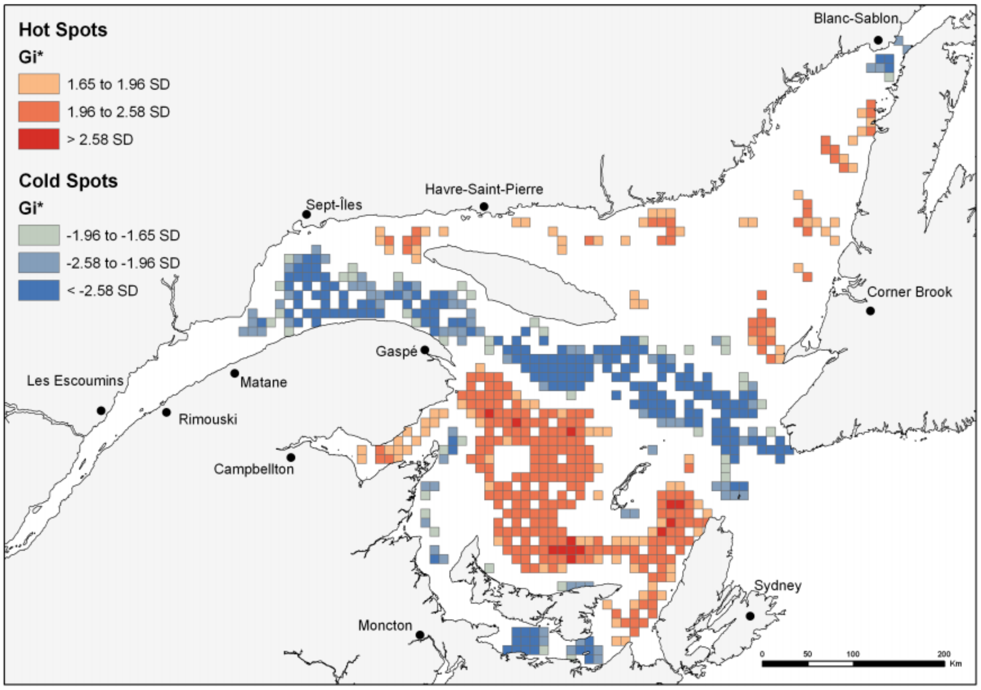

Figure 135. Location of statistically significant clusters of low relative occurrence (cold spots) and high relative occurrence (hot spots) for American plaice in the St. Lawrence estuary and Gulf based on annual bottom trawl surveys conducted by DFO (2002–2010, fish < 20.5 cm total length).

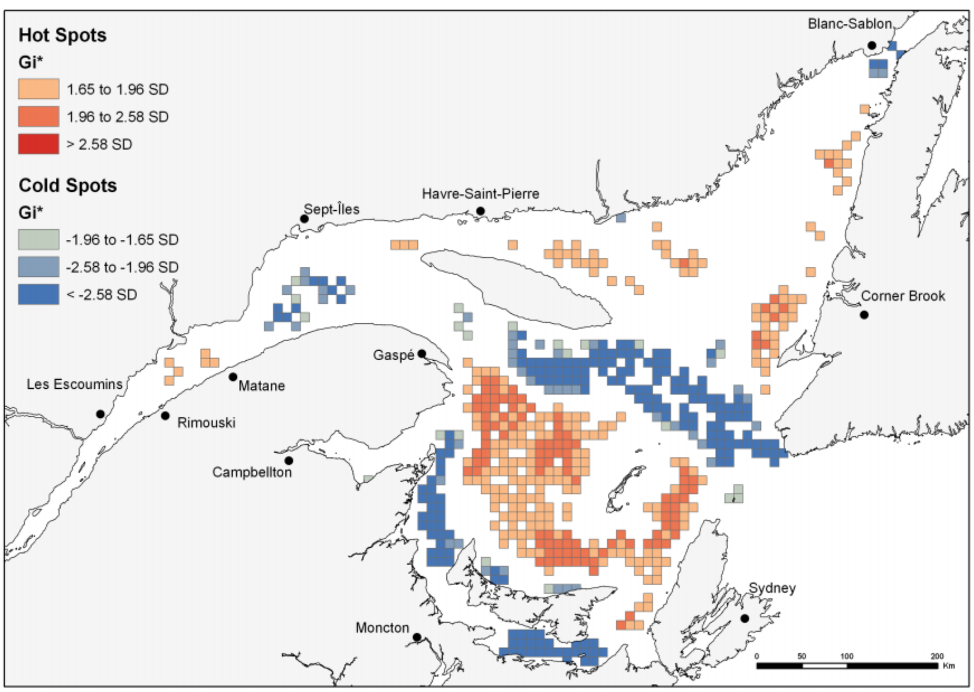

Figure 136. Location of statistically significant clusters of low relative occurrence (cold spots) and high relative occurrence (hot spots) for American plaice in the St. Lawrence estuary and Gulf based on annual bottom trawl surveys conducted by DFO (2002–2010, fish > 20.5 cm total length).

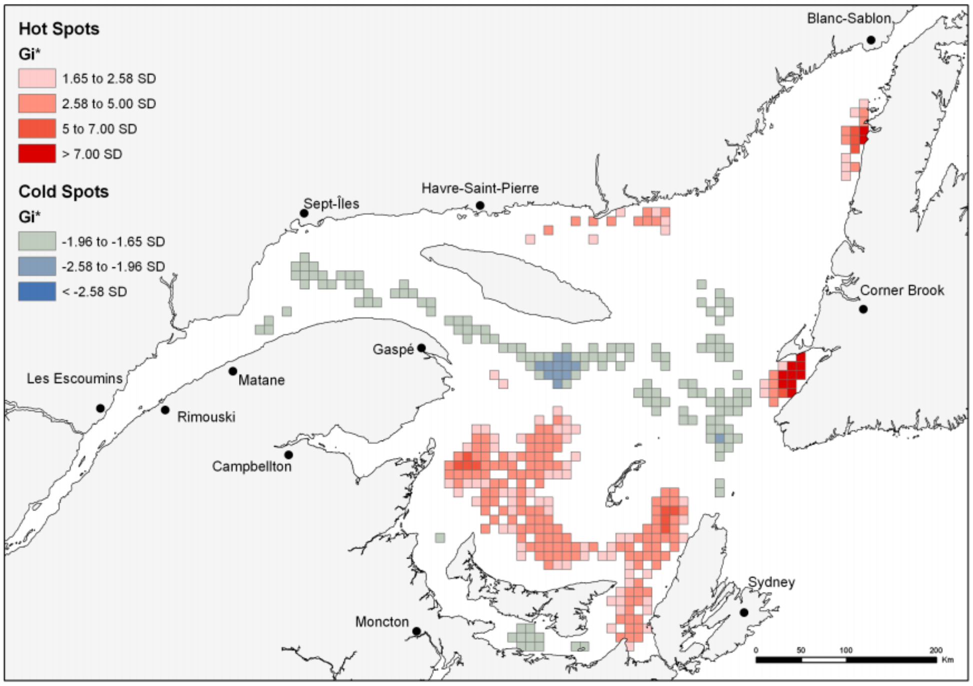

Figure 137. Location of statistically significant clusters of low catch in number (cold spots) and high catch in number (hot spots) for American plaice in the St. Lawrence estuary and Gulf based on annual bottom trawl surveys conducted by DFO (2002–2010).

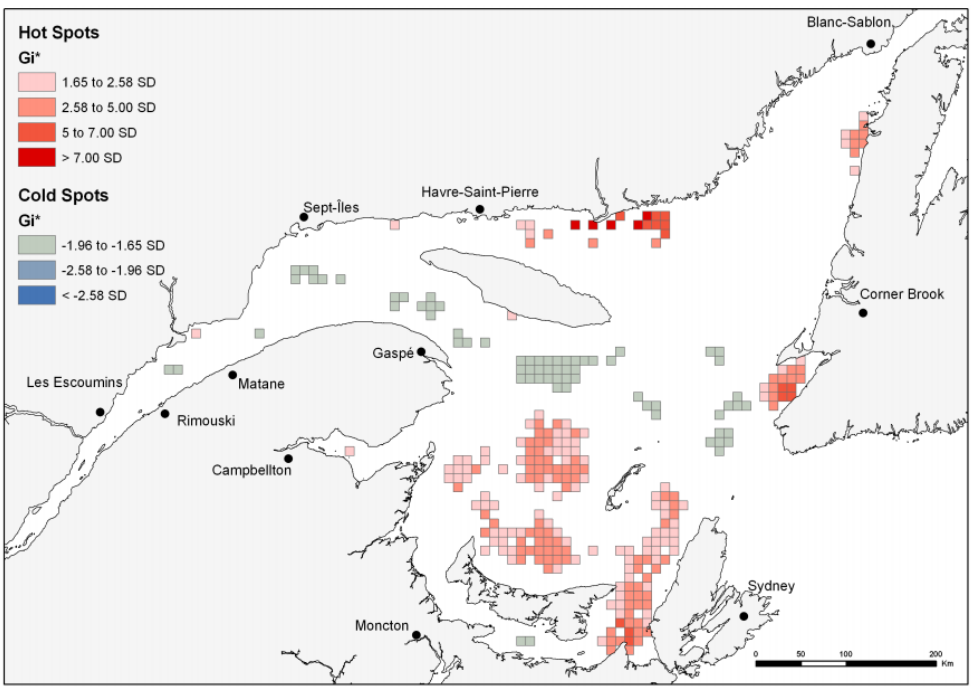

Figure 138. Location of statistically significant clusters of low catch in number (cold spots) and high catch in number (hot spots) for American plaice in the St. Lawrence estuary and Gulf based on annual bottom trawl surveys conducted by DFO (2002–2010, fish < 20.5 cm total length).

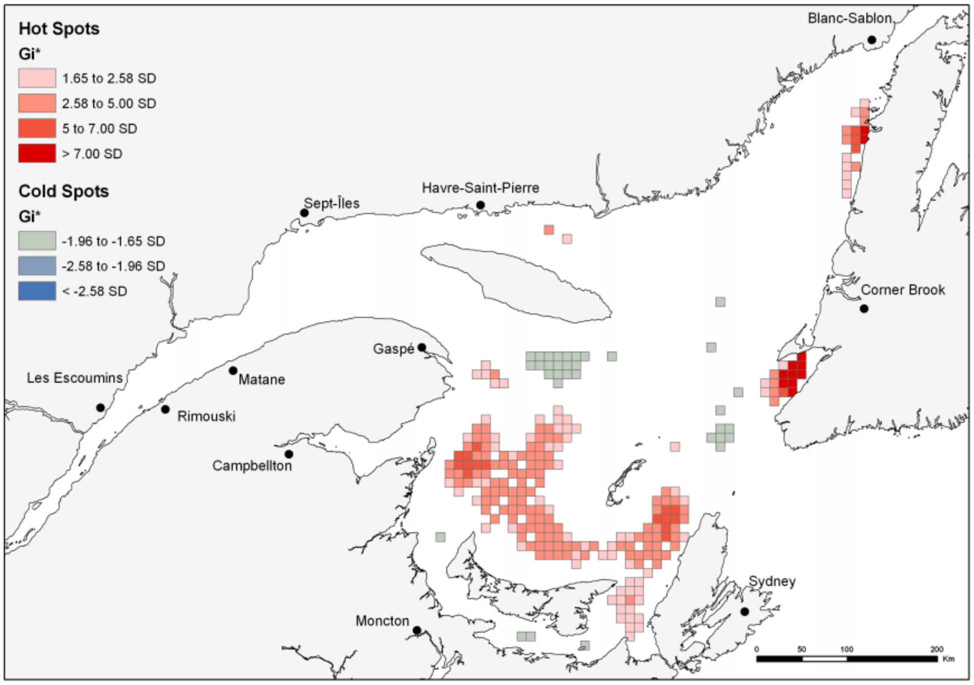

Figure 139. Location of statistically significant clusters of low catch in number (cold spots) and high catch in number (hot spots) for American plaice in the St. Lawrence estuary and Gulf based on annual bottom trawl surveys conducted by DFO (2002–2010, fish > 20.5 cm total length).

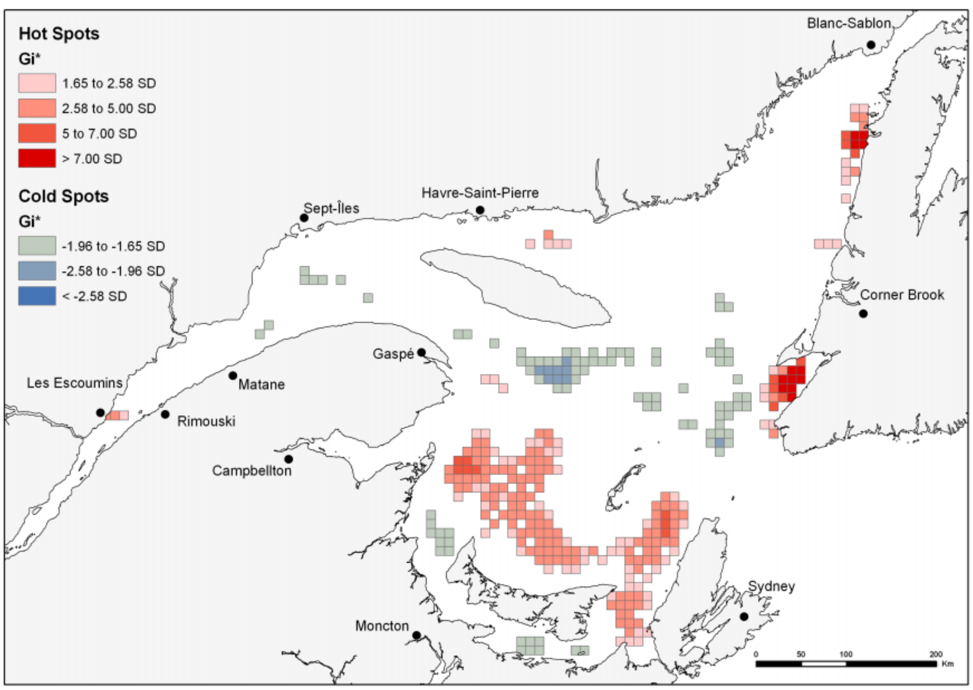

Figure 140. Location of statistically significant clusters of low catch in weight (cold spots) and high catch in weight (hot spots) for American plaice in the St. Lawrence estuary and Gulf based on annual bottom trawl surveys conducted by DFO (2002–2010).

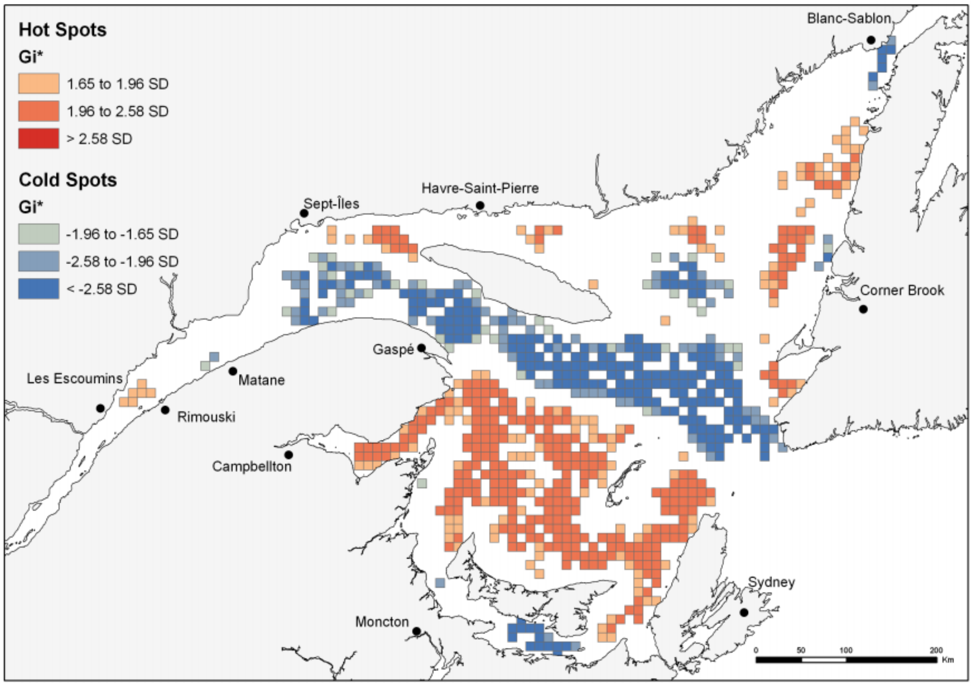

Figure 141. Location of statistically significant clusters of low relative occurrence (cold spots) and high relative occurrence (hot spots) for American plaice in the St. Lawrence estuary and Gulf based on annual bottom trawl surveys conducted by DFO (1984–1992, summer).

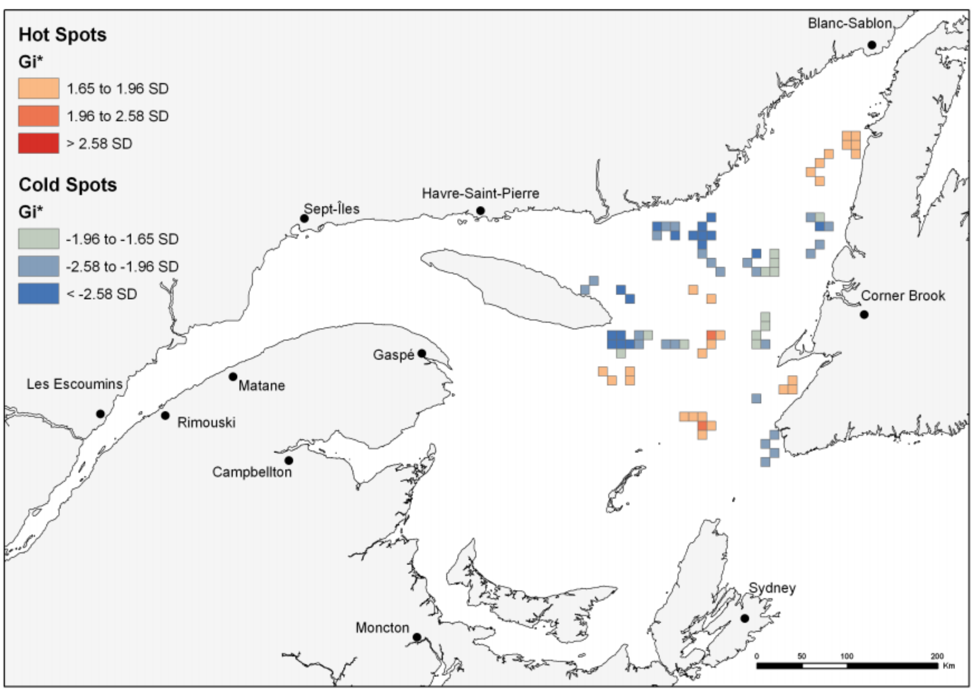

Figure 142. Location of statistically significant clusters of low relative occurrence (cold spots) and high relative occurrence (hot spots) for American plaice in the St. Lawrence estuary and Gulf based on annual bottom trawl surveys conducted by DFO (1984–1992, winter).

Habitat relationships by period and size category

American plaice occur over a large portion of the study area but appear to be strongly associated with a single megahabitat, namely the cold water shelf areas, megahabitat J. Adjacent megahabitats H, I, and K are also important, when all periods and fish sizes are considered. Habitat use by plaice is summarized for the different categories in Tables 96–123. To reveal habitat relationships, cluster analyses and MDS plots by sampling period and category of fish size are presented in Figures 143–165. The cold shallow water shelf areas (megahabitat J) stems out as a key habitat for American plaice. Megahabitats I and K have a secondary importance and there appears to be overall only slight differences in plaice-habitat associations between size categories and between time periods.

1984–2010

Table 96. Habitat use by American plaice in the St. Lawrence estuary and Gulf (1984–2010) based on relative occurrence data. The number of cells overlapping the distribution features is reported as a proportion of the number of cells in each megahabitat. The area of occupancy was determined by the Hernández and Navarro (2007) method using presence/absence data. Other features are based on the species relative occurrence. The kernel density estimates (KDE) were generated with ESRI ArcGIS 10.0 software and the Spatial Analyst extension (quartic kernel function). Clusters of high (hot spot) and low (cold spot) relative occurrences were determined using the Getis and Ord local spatial autocorrelation Gi* statistic (Z-score). Mean relative occurrence and Gi* value are given for each megahabitat. Prime habitats for the species are highlighted.

Megahabitat	Number of cells	Area of occupancy	KDE 90% volume	KDE 50% volume	Cold spot	Hot spot	Relative occurrence	Z-score
A	601	0.998	0.656	0.130	0.566	0.025	0.575	-1.927
B	13	0.923	0.769	0.077	0.385	0.231	0.665	-0.732
C	147	1.000	0.435	0.551	0.000	0.265	0.905	0.969
D	128	1.000	0.633	0.297	0.211	0.125	0.786	-0.254
E	108	1.000	0.444	0.074	0.454	0.093	0.502	-1.447
G	29	1.000	0.069	0.931	0.000	0.690	0.975	1.906
H	149	1.000	0.423	0.530	0.094	0.403	0.834	0.753
I	128	1.000	0.477	0.320	0.078	0.320	0.818	0.703
J	351	1.000	0.088	0.912	0.000	0.803	0.976	2.261
K	126	1.000	0.421	0.571	0.016	0.452	0.896	1.369
L	17	1.000	0.529	0.353	0.000	0.529	0.958	1.461
M	76	1.000	0.763	0.066	0.158	0.250	0.840	0.328

Table 97. Habitat use by American plaice in the St. Lawrence estuary and Gulf (1984–2010) based on relative occurrence data and cells where the species presence was confirmed. The number of cells overlapping the distribution features is reported as a proportion of the number of cells in each megahabitat. The area of occupancy was determined by the Hernández and Navarro (2007) method using presence/absence data. Other features are based on the species relative occurrence. The kernel density estimates (KDE) were generated with ESRI ArcGIS 10.0 software and the Spatial Analyst extension (quartic kernel function). Clusters of high (hot spot) and low (cold spot) relative occurrences were determined using the Getis and Ord local spatial autocorrelation Gi* statistic (Z-score). Mean relative occurrence and Gi* value are given for each megahabitat. Prime habitats for the species are highlighted.

Megahabitat	Number of cells	Area of occupancy	KDE 90% volume	KDE 50% volume	Cold spot	Hot spot	Relative occurrence	Z-score
A	550	0.998	0.695	0.142	0.535	0.027	0.629	-1.742
B	13	0.923	0.769	0.077	0.385	0.231	0.665	-0.732
C	145	1.000	0.434	0.559	0.000	0.269	0.917	0.990
D	124	1.000	0.653	0.306	0.185	0.129	0.811	-0.137
E	77	1.000	0.610	0.104	0.299	0.130	0.704	-0.684
G	29	1.000	0.069	0.931	0.000	0.690	0.975	1.906
H	145	1.000	0.421	0.545	0.090	0.414	0.857	0.804
I	117	1.000	0.513	0.350	0.043	0.350	0.895	0.953
J	351	1.000	0.088	0.912	0.000	0.803	0.976	2.261
K	125	1.000	0.424	0.576	0.008	0.456	0.903	1.402
L	17	1.000	0.529	0.353	0.000	0.529	0.958	1.461
M	71	1.000	0.775	0.070	0.155	0.268	0.899	0.422

Table 98. Habitat use by American plaice in the St. Lawrence estuary and Gulf (1984–2010) based on catch in number. The number of cells overlapping the distribution features is reported as a proportion of the number of cells in each megahabitat. The kernel density estimates (KDE) were generated with ESRI ArcGIS 10.0 software and the Spatial Analyst extension (quartic kernel function). Clusters of high (hot spot) and low (cold spot) catch in number were determined using the Getis and Ord local spatial autocorrelation Gi* statistic (Z-score). Mean catch in number and Gi* value are given for each megahabitat. Prime habitats for the species are highlighted.

Megahabitat	Number of cells	KDE 90% volume	KDE 50% volume	Cold spot	Hot spot	CN_mean	Z-score
A	581	0.084	0.000	0.682	0.005	213.6	-1.670
B	13	0.308	0.077	0.308	0.154	1685.3	-0.661
C	134	0.746	0.015	0.022	0.037	1725.2	-0.485
D	127	0.291	0.031	0.118	0.055	1002.7	-0.928
E	108	0.278	0.083	0.111	0.176	1185.1	-0.181
G	28	1.000	0.000	0.000	0.000	2329.0	-0.087
H	149	0.450	0.275	0.020	0.362	2297.2	0.912
I	126	0.476	0.119	0.000	0.254	1948.5	0.599
J	350	0.477	0.477	0.000	0.609	4357.7	2.734
K	118	0.712	0.144	0.000	0.237	3348.0	0.984
L	17	0.529	0.000	0.000	0.059	1998.9	-0.268
M	73	0.342	0.068	0.000	0.082	1692.2	-0.391

Table 99. Habitat use by American plaice in the St. Lawrence estuary and Gulf (1984–2010) based on cells where the species presence was confirmed. The number of cells overlapping the distribution features is reported as a proportion of the number of cells in each megahabitat. The kernel density estimates (KDE) were generated with ESRI ArcGIS 10.0 software and the Spatial Analyst extension (quartic kernel function). Clusters of high (hot spot) and low (cold spot) catch in number were determined using the Getis and Ord local spatial autocorrelation Gi* statistic (Z-score). Mean catch in number and Gi* value are given for each megahabitat. Prime habitats for the species are highlighted.

Megahabitat	Number of cells	KDE 90% volume	KDE 50% volume	Cold spot	Hot spot	CN_mean	Z-score
A	476	0.101	0.000	0.628	0.006	260.7	-1.618
B	13	0.308	0.077	0.308	0.154	1685.3	-0.661
C	134	0.746	0.015	0.022	0.037	1725.2	-0.485
D	123	0.301	0.033	0.106	0.057	1035.4	-0.905
E	77	0.351	0.117	0.104	0.247	1662.3	0.231
G	28	1.000	0.000	0.000	0.000	2329.0	-0.087
H	145	0.448	0.283	0.021	0.372	2360.5	0.938
I	116	0.500	0.129	0.000	0.276	2116.5	0.747
J	350	0.477	0.477	0.000	0.609	4357.7	2.734
K	118	0.712	0.144	0.000	0.237	3348.0	0.984
L	17	0.529	0.000	0.000	0.059	1998.9	-0.268
M	68	0.353	0.074	0.000	0.088	1816.6	-0.332

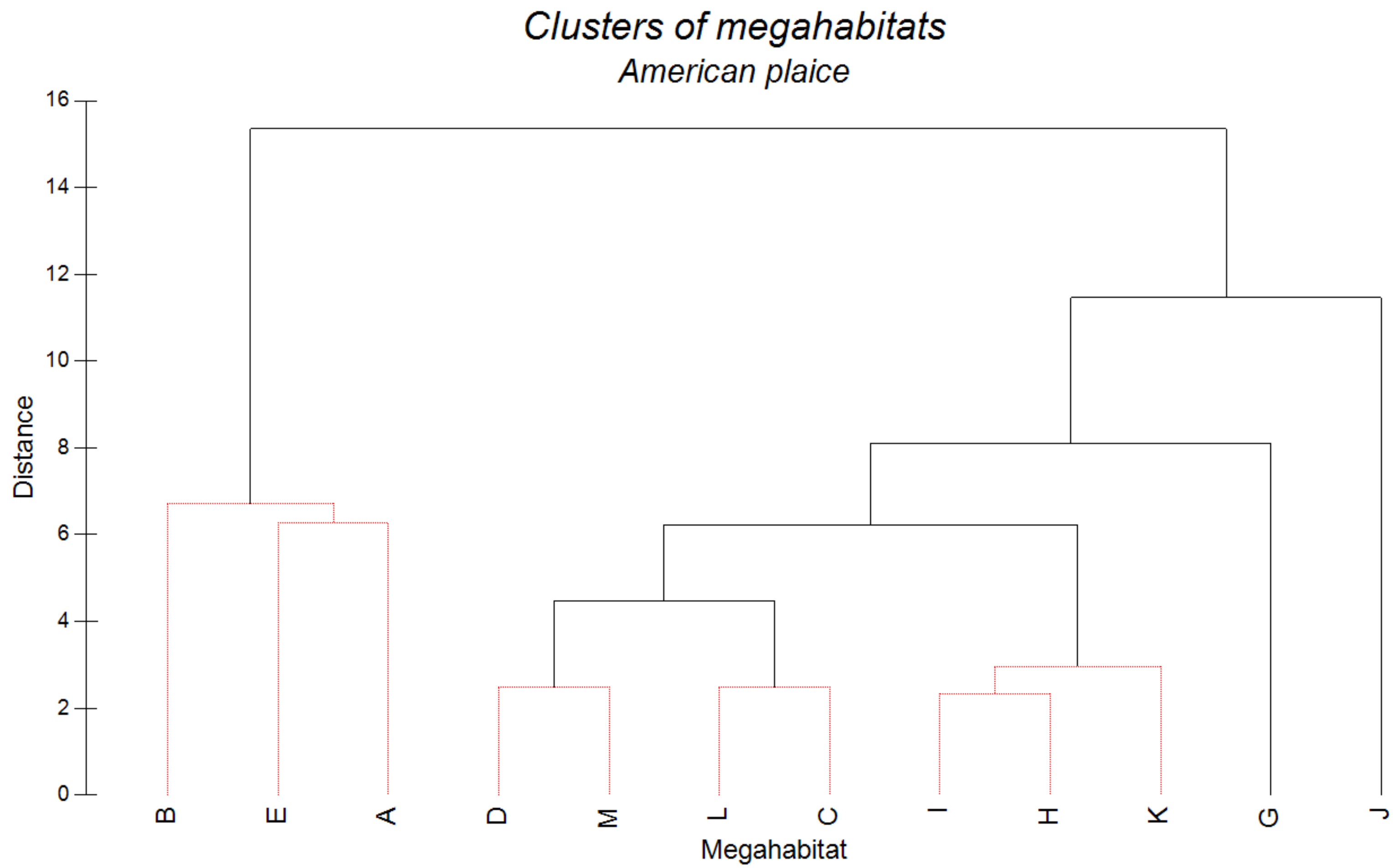

Figure 143. Clusters of megahabitats determined using 27 different descriptors of spatial distribution and abundance of American plaice, based on relative occurrence, catch in number and catch in weight in the annual bottom trawl research surveys (1984-2010). Habitats are ordered from left to right by decreasing distance from megahabitat J which is considered most important to American plaice.

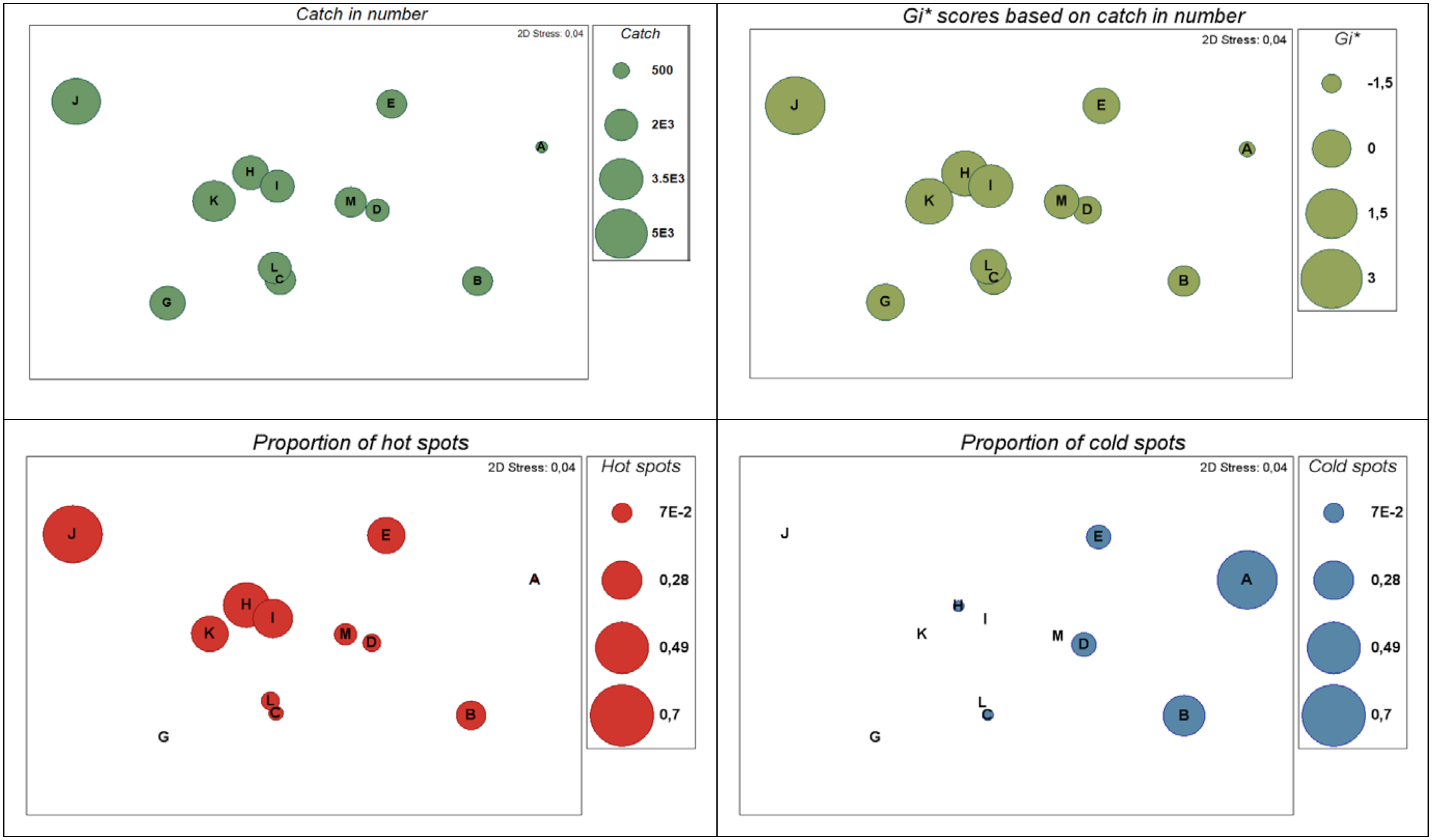

Figure 144. Multidimensional scaling plot of megahabitats based on American plaice spatial distribution and relative occurrence and abundance descriptors (27 descriptors, 1984–2010). Bubble size reflects mean catch in number in sets where the species is present (upper left panel), local spatial autocorrelation G_i* statistic (upper right panel), and proportion of cells classified as hot spots or cold spots (lower left and lower right panels, respectively).

Table 100. Habitat use by American plaice in the St. Lawrence estuary and Gulf (1984–1992) based on relative occurrence data. The number of cells overlapping the distribution features is reported as a proportion of the number of cells in each megahabitat. The area of occupancy was determined by the Hernández and Navarro (2007) method using presence/absence data. Other features are based on the species relative occurrence. The kernel density estimates (KDE) were generated with ESRI ArcGIS 10.0 software and the Spatial Analyst extension (quartic kernel function). Clusters of high (hot spot) and low (cold spot) relative occurrences were determined using the Getis and Ord local spatial autocorrelation Gi* statistic (Z-score). Mean relative occurrence and Gi* value are given for each megahabitat. Prime habitats for the species are highlighted.

Megahabitat	Number of cells	Area of occupancy	KDE 90% volume	KDE 50% volume	Cold spot	Hot spot	Relative occurrence	Z-score
A	541	0.989	0.564	0.299	0.490	0.035	0.562	-1.479
B	13	0.923	0.692	0.308	0.000	0.077	0.696	-0.110
C	125	1.000	0.320	0.656	0.016	0.232	0.902	0.764
D	106	0.991	0.585	0.321	0.236	0.132	0.712	-0.387
E	71	0.972	0.577	0.127	0.239	0.113	0.564	-0.547
G	21	1.000	0.143	0.857	0.000	0.381	0.929	1.257
H	114	1.000	0.404	0.561	0.009	0.412	0.869	1.011
I	57	1.000	0.298	0.404	0.211	0.404	0.723	0.372
J	257	1.000	0.121	0.860	0.008	0.805	0.972	1.879
K	115	1.000	0.313	0.600	0.026	0.374	0.874	0.990
L	8	1.000	0.625	0.375	0.000	0.500	0.875	1.501
M	45	0.956	0.822	0.089	0.222	0.133	0.859	-0.093

Table 101. Habitat use by American plaice in the St. Lawrence estuary and Gulf (1984–1992) based on relative occurrence data and cells where the species presence was confirmed. The number of cells overlapping the distribution features is reported as a proportion of the number of cells in each megahabitat. The area of occupancy was determined by the Hernández and Navarro (2007) method using presence/absence data. Other features are based on the species relative occurrence. The kernel density estimates (KDE) were generated with ESRI ArcGIS 10.0 software and the Spatial Analyst extension (quartic kernel function). Clusters of high (hot spot) and low (cold spot) relative occurrences were determined using the Getis and Ord local spatial autocorrelation Gi* statistic (Z-score). Mean relative occurrence and Gi* value are given for each megahabitat. Prime habitats for the species are highlighted.

Megahabitat	Number of cells	Area of occupancy	KDE 90% volume	KDE 50% volume	Cold spot	Hot spot	Relative occurrence	Z-score
A	425	0.991	0.569	0.369	0.402	0.045	0.715	-1.117
B	13	0.923	0.692	0.308	0.000	0.077	0.696	-0.110
C	120	1.000	0.308	0.683	0.008	0.242	0.940	0.825
D	96	1.000	0.583	0.354	0.219	0.146	0.786	-0.287
E	47	1.000	0.681	0.191	0.128	0.170	0.852	0.097
G	21	1.000	0.143	0.857	0.000	0.381	0.929	1.257
H	104	1.000	0.375	0.615	0.000	0.452	0.952	1.169
I	44	1.000	0.341	0.523	0.068	0.523	0.937	1.041
J	252	1.000	0.119	0.877	0.004	0.821	0.991	1.940
K	111	1.000	0.306	0.622	0.018	0.387	0.905	1.030
L	7	1.000	0.571	0.429	0.000	0.571	1.000	1.629
M	41	1.000	0.878	0.098	0.195	0.146	0.943	0.064

Table 102. Habitat use by American plaice in the St. Lawrence estuary and Gulf (1984–1992) based on catch in number. The number of cells overlapping the distribution features, based on the species catch in number, is reported as a proportion of the number of cells in each megahabitat. The kernel density estimates (KDE) were generated with ESRI ArcGIS 10.0 software and the Spatial Analyst extension (quartic kernel function). Clusters of high (hot spot) and low (cold spot) catch in number were determined using the Getis and Ord local spatial autocorrelation Gi* statistic (Z-score). Mean catch in number and Gi* value are given for each megahabitat. Prime habitats for the species are highlighted.

Megahabitat	Number of cells	KDE 90% volume	KDE 50% volume	Cold spot	Hot spot	CN_mean	Z-score
A	422	0.014	0.000	0.000	0.000	105.1	-1.075
B	10	0.300	0.000	0.000	0.000	1549.3	-0.688
C	91	0.220	0.000	0.000	0.011	1565.2	-0.611
D	93	0.097	0.000	0.000	0.000	820.4	-0.865
E	71	0.324	0.042	0.000	0.070	2346.1	-0.051
G	20	0.350	0.000	0.000	0.000	1427.2	-0.374
H	114	0.272	0.228	0.000	0.272	6489.9	1.316
I	53	0.358	0.208	0.000	0.264	7011.0	1.042
J	252	0.560	0.306	0.000	0.433	8186.4	1.715
K	88	0.432	0.102	0.000	0.125	3347.1	0.094
L	7	0.286	0.143	0.000	0.143	2522.1	0.389
M	33	0.091	0.030	0.000	0.030	1915.3	-0.231

Table 103. Habitat use by American plaice in the St. Lawrence estuary and Gulf (1984–1992) based on catch in number and cells where the species presence was confirmed. The number of cells overlapping the distribution features, based on the species catch in number, is reported as a proportion of the number of cells in each megahabitat. The kernel density estimates (KDE) were generated with ESRI ArcGIS 10.0 software and the Spatial Analyst extension (quartic kernel function). Clusters of high (hot spot) and low (cold spot) catch in number were determined using the Getis and Ord local spatial autocorrelation Gi* statistic (Z-score). Mean catch in number and Gi* value are given for each megahabitat. Prime habitats for the species are highlighted.

Megahabitat	Number of cells	KDE 90% volume	KDE 50% volume	Cold spot	Hot spot	CN_mean	Z-score
A	253	0.020	0.000	0.000	0.000	175.3	-1.053
B	8	0.375	0.000	0.000	0.000	1936.7	-0.696
C	90	0.222	0.000	0.000	0.011	1582.6	-0.625
D	79	0.101	0.000	0.000	0.000	965.8	-0.854
E	47	0.447	0.064	0.000	0.106	3544.1	0.226
G	20	0.350	0.000	0.000	0.000	1427.2	-0.374
H	104	0.298	0.250	0.000	0.298	7114.0	1.522
I	41	0.439	0.268	0.000	0.341	9063.0	1.491
J	247	0.571	0.312	0.000	0.441	8352.1	1.759
K	87	0.437	0.103	0.000	0.126	3385.6	0.102
L	6	0.333	0.167	0.000	0.167	2942.4	0.579
M	29	0.103	0.034	0.000	0.034	2179.5	-0.166

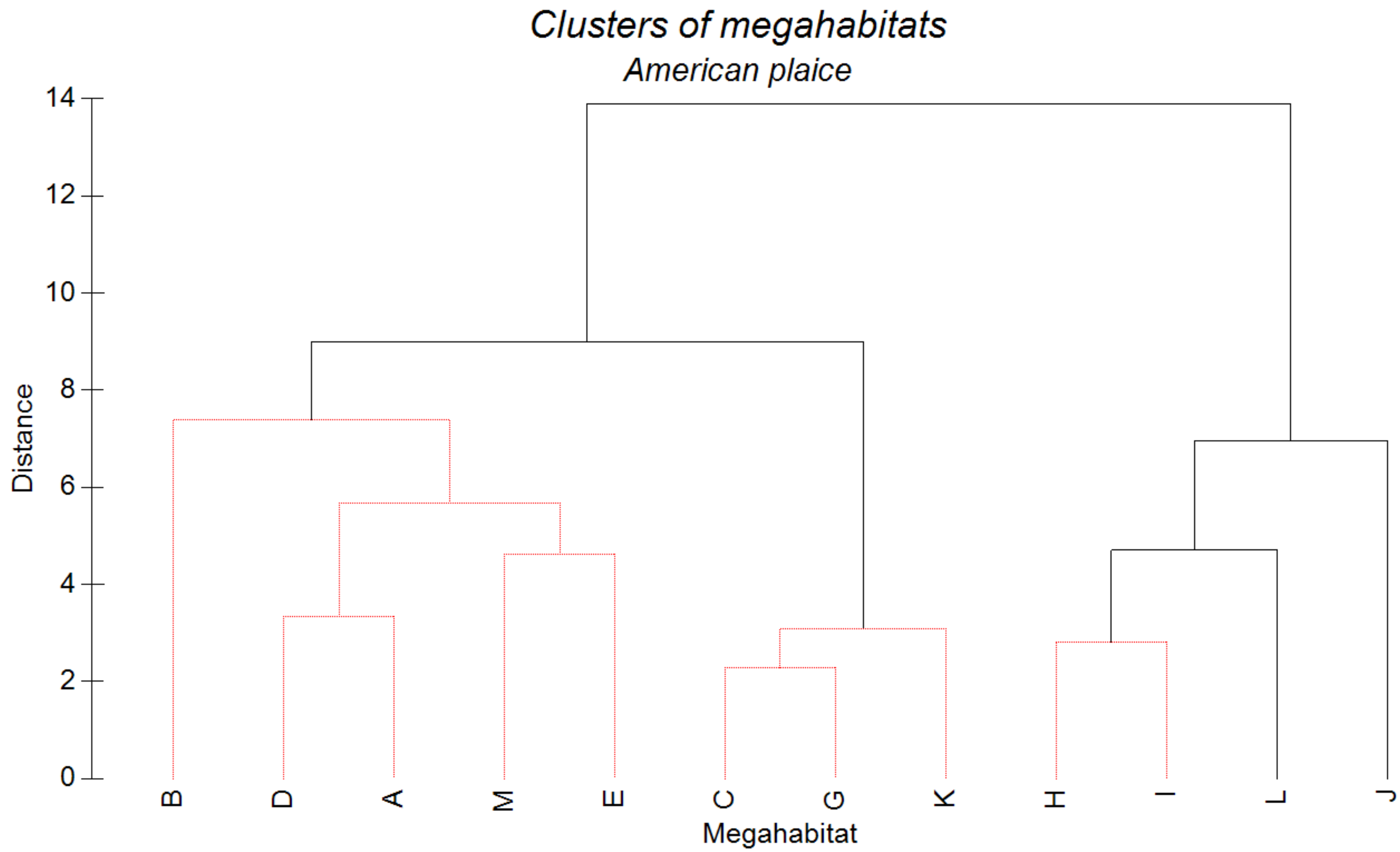

Figure 145. Clusters of megahabitats determined using 27 different descriptors of spatial distribution and abundance of American plaice based on relative occurrence, catch in number, and catch in weight in the annual bottom trawl research surveys (1984–1992). Habitats are ordered from left to right by decreasing distance from megahabitat J, which is considered most important to American plaice.

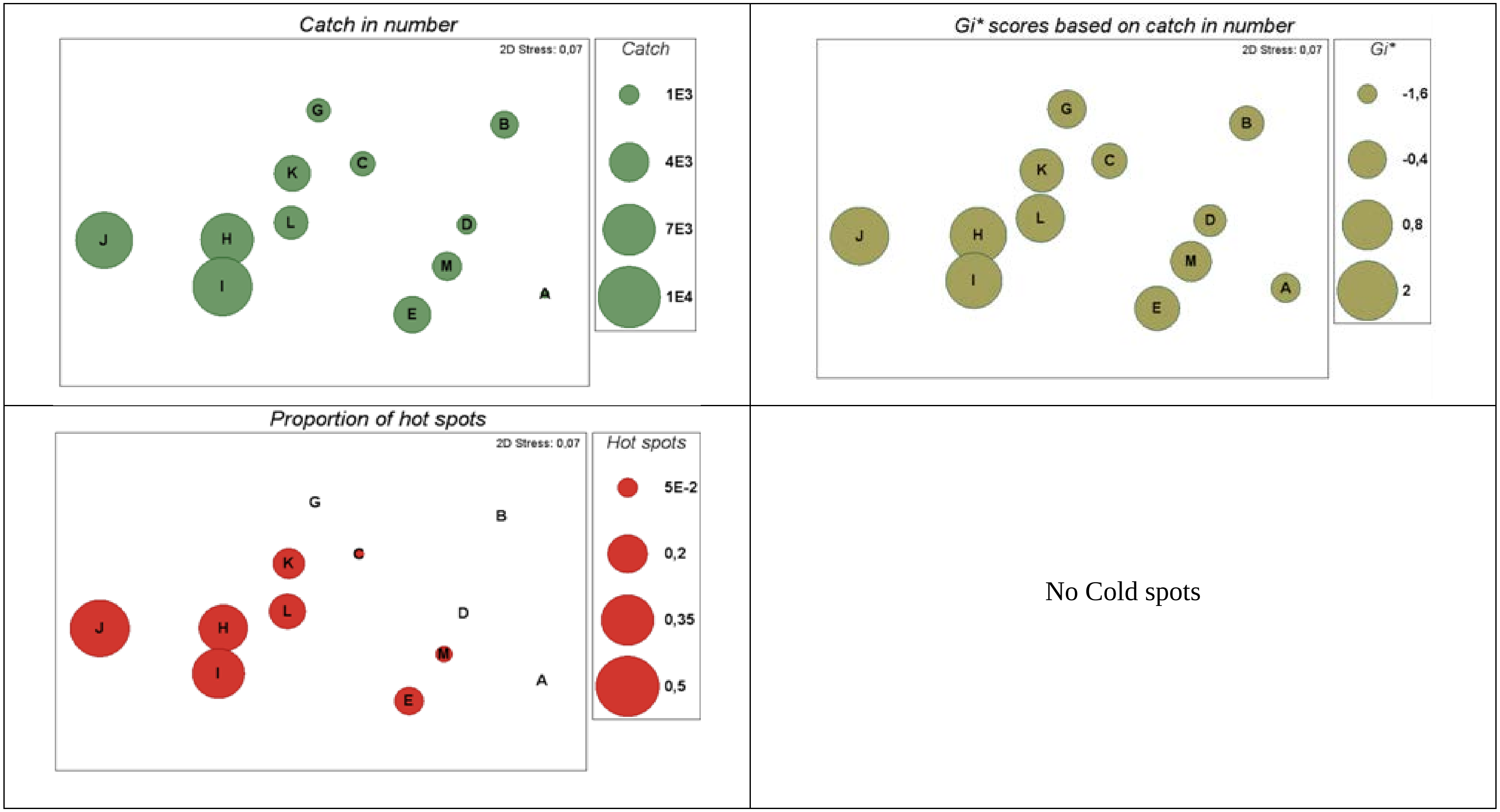

Figure 146. Multidimensional scaling plot of megahabitats based on American plaice spatial distribution and relative occurrence and abundance descriptors (27 descriptors, 1984–1992). Bubble size reflects mean catch in number in sets where the species is present (upper left panel), local spatial autocorrelation G_i* statistic (upper right panel), and proportion of cells classified as hot spots or cold spots (lower left and lower right panel, respectively).

1984–1992, fish <20.5 cm total length

Table 104. Habitat use by American plaice in the St. Lawrence estuary and Gulf (1984–1992, fish <20.5 cm total length) based on relative occurrence data. The number of cells overlapping the distribution features is reported as a proportion of the number of cells in each megahabitat. The area of occupancy was determined by the Hernández and Navarro (2007) method using presence/absence data. Other features are based on the species relative occurrence. The kernel density estimates (KDE) were generated with ESRI ArcGIS 10.0 software and the Spatial Analyst extension (quartic kernel function). Clusters of high (hot spot) and low (cold spot) relative occurrences were determined using the Getis and Ord local spatial autocorrelation G_i* statistic (Z-score). Mean relative occurrence and G_i* value are given for each megahabitat. Prime habitats for the species are highlighted.

Megahabitat	Number of cells	Area of occupancy	KDE 90% volume	KDE 50% volume	Cold spot	Hot spot	Relative occurrence	Z-score
A	422	0.441	0.216	0.031	0.727	0.036	0.165	-2.138
B	10	0.700	0.300	0.200	0.400	0.300	0.383	-0.640
C	91	0.923	0.516	0.407	0.033	0.319	0.801	0.933
D	93	0.677	0.473	0.065	0.398	0.097	0.347	-1.092
E	71	0.789	0.521	0.197	0.155	0.239	0.440	0.252
G	20	1.000	0.500	0.500	0.000	0.300	0.688	0.859
H	114	1.000	0.456	0.526	0.018	0.456	0.728	1.310
I	53	0.755	0.340	0.358	0.189	0.509	0.606	1.020
J	252	1.000	0.175	0.798	0.000	0.817	0.887	2.415
K	88	0.886	0.466	0.477	0.023	0.557	0.867	1.666
L	7	0.714	0.286	0.429	0.143	0.429	0.714	0.862
M	33	0.485	0.424	0.061	0.424	0.182	0.460	-0.653

Table 105. Habitat use by American plaice in the St. Lawrence estuary and Gulf (1984–1992, fish <20.5 cm total length) based on relative occurrence data and cells where the species presence was confirmed. The number of cells overlapping the distribution features is reported as a proportion of the number of cells in each megahabitat. The area of occupancy was determined by the Hernández and Navarro (2007) method using presence/absence data. Other features are based on the species relative occurrence. The kernel density estimates (KDE) were generated with ESRI ArcGIS 10.0 software and the Spatial Analyst extension (quartic kernel function). Clusters of high (hot spot) and low (cold spot) relative occurrences were determined using the Getis and Ord local spatial autocorrelation Gi* statistic (Z-score). Mean relative occurrence and Gi* value are given for each megahabitat. Prime habitats for the species are highlighted.

Megahabitat	Number of cells	Area of occupancy	KDE 90% volume	KDE 50% volume	Cold spot	Hot spot	Relative occurrence	Z-score
A	102	0.765	0.578	0.127	0.333	0.127	0.684	-0.769
B	5	1.000	0.600	0.400	0.000	0.600	0.767	1.023
C	83	0.952	0.530	0.446	0.012	0.349	0.878	1.108
D	45	0.911	0.822	0.133	0.111	0.200	0.717	0.032
E	38	0.895	0.579	0.368	0.026	0.447	0.822	1.239
G	17	1.000	0.412	0.588	0.000	0.353	0.809	1.147
H	97	1.000	0.381	0.619	0.010	0.536	0.855	1.617
I	35	0.971	0.429	0.543	0.000	0.771	0.918	2.097
J	235	1.000	0.149	0.851	0.000	0.864	0.951	2.549
K	80	0.925	0.463	0.525	0.000	0.613	0.954	1.908
L	5	0.800	0.400	0.600	0.000	0.600	1.000	2.018
M	17	0.765	0.706	0.118	0.118	0.353	0.892	0.547

Table 106. Habitat use by American plaice in the St. Lawrence estuary and Gulf (1984–1992, fish < 20.5 cm total length) based on catch in number. The number of cells overlapping the distribution features, based on the species catch in number, is reported as a proportion of the number of cells in each megahabitat. The kernel density estimates (KDE) were generated with ESRI ArcGIS 10.0 software and the Spatial Analyst extension (quartic kernel function). Clusters of high (hot spot) and low (cold spot) catch in number were determined using the Getis and Ord local spatial autocorrelation Gi* statistic (Z-score). Mean catch in number and Gi* value are given for each megahabitat. Prime habitats for the species are highlighted.

Megahabitat	Number of cells	KDE 90% volume	KDE 50% volume	Cold spot	Hot spot	CN_mean	Z-score
A	422	0.017	0.007	0.000	0.012	51.8	-0.773
B	10	0.200	0.000	0.000	0.000	523.2	-0.389
C	91	0.363	0.033	0.000	0.044	960.5	-0.168
D	93	0.140	0.000	0.000	0.000	316.1	-0.623
E	71	0.366	0.042	0.000	0.070	681.5	0.051
G	20	0.550	0.050	0.000	0.000	456.4	-0.112
H	114	0.298	0.237	0.000	0.246	1592.7	1.034
I	53	0.358	0.132	0.000	0.132	1356.2	0.540
J	252	0.548	0.254	0.000	0.302	1563.2	0.963
K	88	0.568	0.068	0.000	0.102	1024.6	0.207
L	7	0.286	0.000	0.000	0.000	370.8	-0.270
M	33	0.152	0.030	0.000	0.030	404.1	-0.248

Table 107. Habitat use by American plaice in the St. Lawrence estuary and Gulf (1984–1992, fish < 20.5 cm total length) based on catch in number and cells where the species presence was confirmed. The number of cells overlapping the distribution features, based on the species catch in number, is reported as a proportion of the number of cells in each megahabitat. The kernel density estimates (KDE) were generated with ESRI ArcGIS 10.0 software and the Spatial Analyst extension (quartic kernel function). Clusters of high (hot spot) and low (cold spot) catch in number were determined using the Getis and Ord local spatial autocorrelation Gi* statistic (Z-score). Mean catch in number and Gi* value are given for each megahabitat. Prime habitats for the species are highlighted.

Megahabitat	Number of cells	KDE 90% volume	KDE 50% volume	Cold spot	Hot spot	CN_mean	Z-score
A	102	0.049	0.020	0.000	0.029	214.4	-0.528
B	5	0.400	0.000	0.000	0.000	1046.4	0.014
C	83	0.398	0.036	0.000	0.048	1053.1	-0.122
D	45	0.267	0.000	0.000	0.000	653.4	-0.460
E	38	0.605	0.079	0.000	0.105	1273.4	0.502
G	17	0.647	0.059	0.000	0.000	537.0	-0.020
H	97	0.340	0.278	0.000	0.289	1871.9	1.302
I	35	0.486	0.200	0.000	0.171	2053.7	0.975
J	235	0.566	0.264	0.000	0.311	1676.3	1.022
K	80	0.625	0.075	0.000	0.113	1127.0	0.293
L	5	0.400	0.000	0.000	0.000	519.1	-0.125
M	17	0.294	0.059	0.000	0.059	784.4	0.147

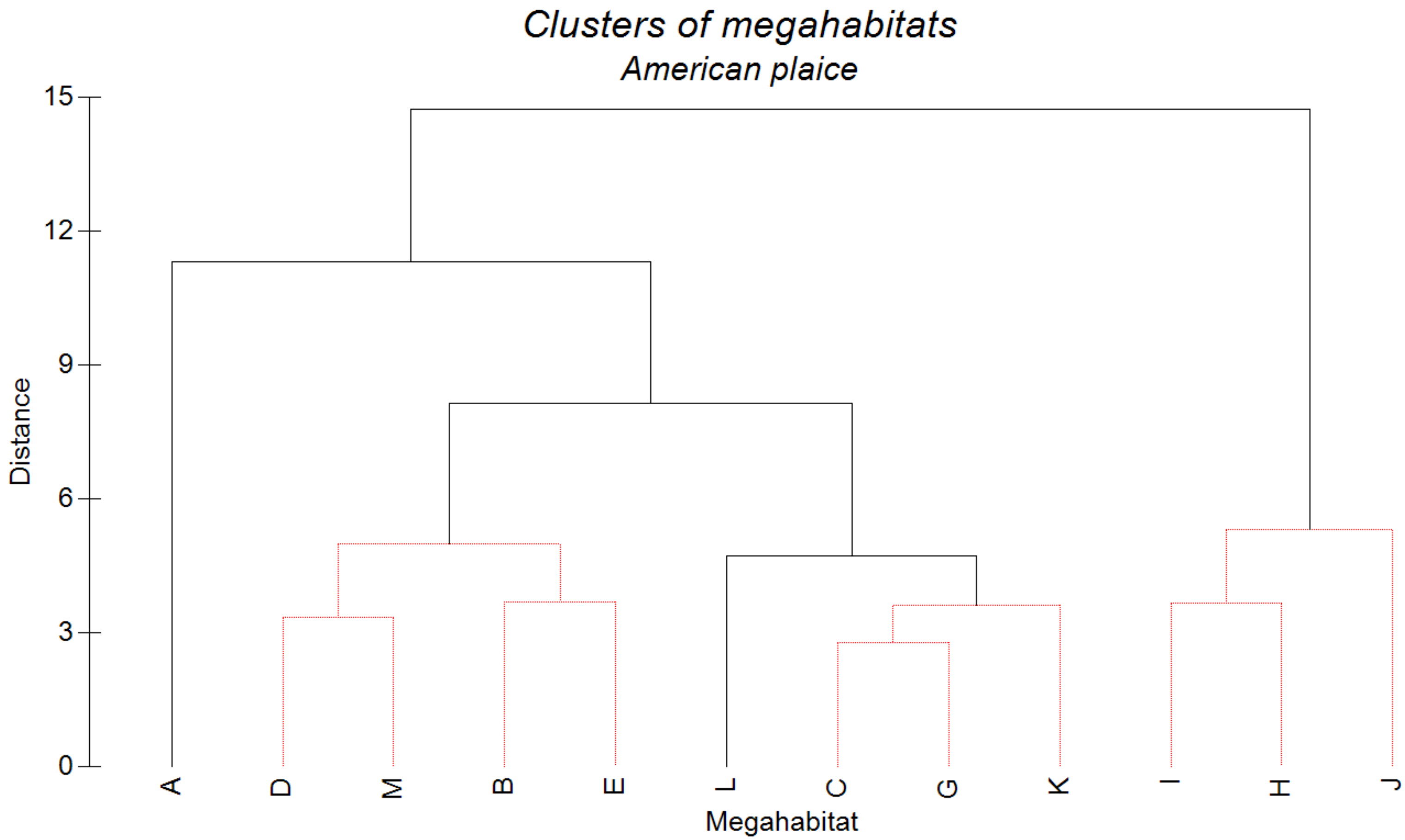

Figure 147. Clusters of megahabitats determined using 27 different descriptors of spatial distribution and abundance of American plaice based on relative occurrence, catch in number, and catch in weight in the annual bottom trawl research surveys (1984–1992, fish less than 20.5 cm). Habitats are ordered from left to right by decreasing distance from megahabitat J, which is considered most important to American plaice.

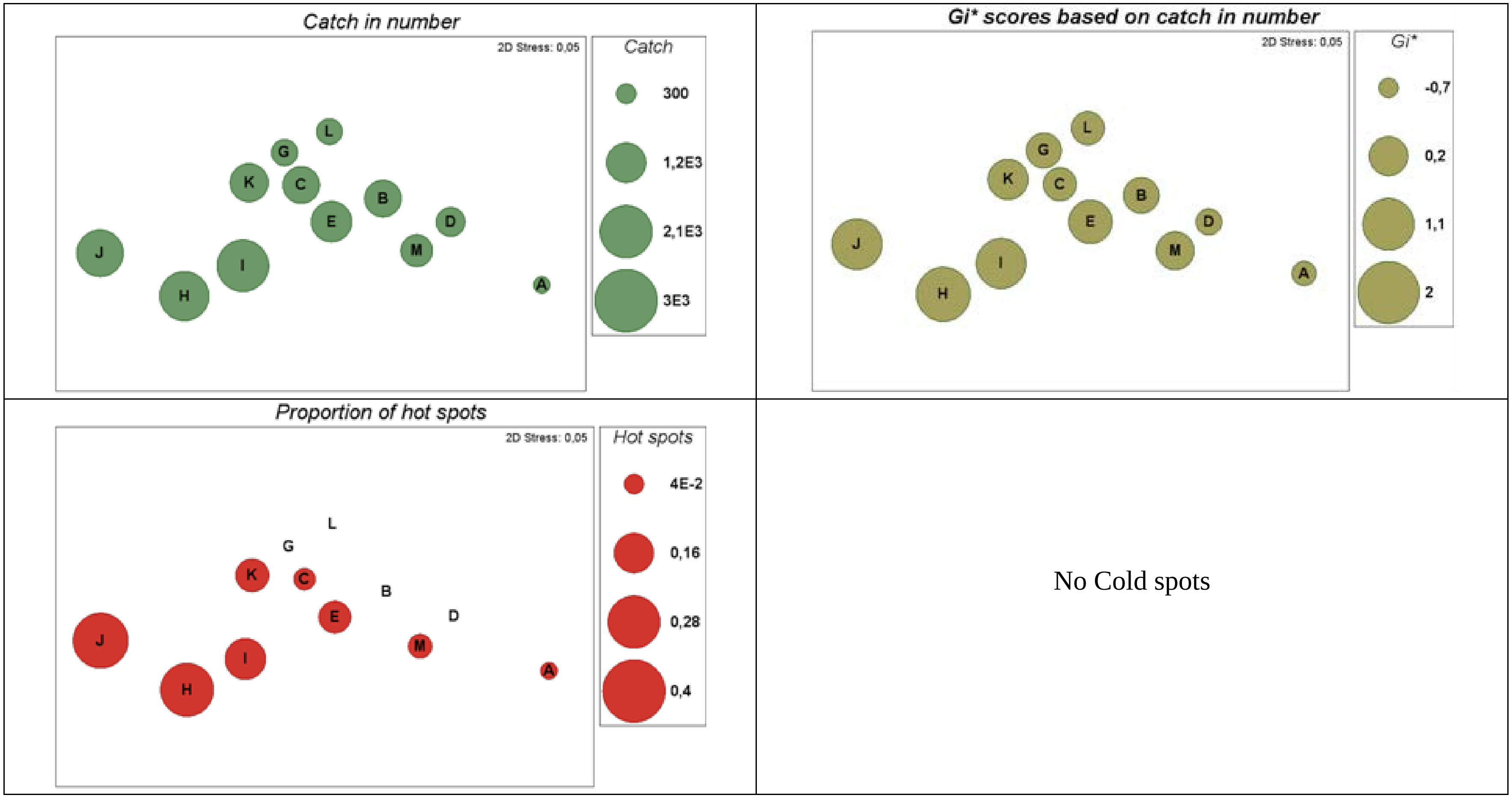

Figure 148. Multidimensional scaling plot of megahabitats based on American plaice spatial distribution and relative occurrence and abundance descriptors (27 descriptors, 1984–1992, fish < 20.5 cm). Bubble size reflects mean catch in number in sets where the species is present (upper left panel), local spatial autocorrelation G_i* statistic (upper right panel), and proportion of cells classified as hot spots or cold spots (lower left and lower right panel, respectively).

1984–1992, fish >20.5 cm total length

Table 108. Habitat use by American plaice in the St. Lawrence estuary and Gulf (1984–1992, fish >20.5 cm total length) based on relative occurrence data. The number of cells overlapping the distribution features is reported as a proportion of the number of cells in each megahabitat. The area of occupancy was determined by the Hernández and Navarro (2007) method using presence/absence data. Other features are based on the species relative occurrence. The kernel density estimates (KDE) were generated with ESRI ArcGIS 10.0 software and the Spatial Analyst extension (quartic kernel function). Clusters of high (hot spot) and low (cold spot) relative occurrences were determined using the Getis and Ord local spatial autocorrelation Gi* statistic (Z-score). Mean relative occurrence and Gi* value are given for each megahabitat. Prime habitats for the species are highlighted.

Megahabitat	Number of cells	Area of occupancy	KDE 90% volume	KDE 50% volume	Cold spot	Hot spot	Relative occurrence	Z-score
A	422	0.931	0.500	0.083	0.592	0.040	0.366	-1.959
B	10	0.900	0.400	0.300	0.400	0.200	0.577	-0.766
C	91	1.000	0.418	0.582	0.011	0.308	0.910	0.969
D	93	0.968	0.742	0.140	0.247	0.075	0.646	-0.535
E	71	0.831	0.535	0.183	0.268	0.127	0.512	-0.441
G	20	1.000	0.100	0.900	0.000	0.500	0.925	1.578
H	114	0.991	0.360	0.632	0.009	0.421	0.856	1.183
I	53	0.849	0.283	0.415	0.189	0.491	0.703	0.578
J	252	1.000	0.099	0.881	0.004	0.861	0.980	2.068
K	88	0.989	0.432	0.534	0.011	0.545	0.968	1.522
L	7	1.000	0.571	0.429	0.000	0.714	0.857	1.464
M	33	0.848	0.727	0.121	0.182	0.212	0.808	0.108

Table 109. Habitat use by American plaice in the St. Lawrence estuary and Gulf (1984–1992, fish >20.5 cm total length) based on relative occurrence data and cells where the species presence was confirmed. The number of cells overlapping the distribution features is reported as a proportion of the number of cells in each megahabitat. The area of occupancy was determined by the Hernández and Navarro (2007) method using presence/absence data. Other features are based on the species relative occurrence. The kernel density estimates (KDE) were generated with ESRI ArcGIS 10.0 software and the Spatial Analyst extension (quartic kernel function). Clusters of high (hot spot) and low (cold spot) relative occurrences were determined using the Getis and Ord local spatial autocorrelation Gi* statistic (Z-score). Mean relative occurrence and Gi* value are given for each megahabitat. Prime habitats for the species are highlighted.

Megahabitat	Number of cells	Area of occupancy	KDE 90% volume	KDE 50% volume	Cold spot	Hot spot	Relative occurrence	Z-score
A	207	0.961	0.705	0.164	0.348	0.082	0.746	-0.975
B	7	1.000	0.429	0.429	0.286	0.286	0.824	-0.094
C	86	1.000	0.384	0.616	0.000	0.326	0.963	1.065
D	78	0.974	0.795	0.167	0.192	0.090	0.770	-0.348
E	43	1.000	0.628	0.302	0.093	0.209	0.845	0.480
G	20	1.000	0.100	0.900	0.000	0.500	0.925	1.578
H	103	1.000	0.301	0.699	0.010	0.466	0.947	1.334
I	40	0.950	0.325	0.550	0.075	0.650	0.931	1.307
J	247	1.000	0.097	0.899	0.000	0.879	0.999	2.119
K	86	0.988	0.430	0.547	0.000	0.558	0.990	1.577
L	6	1.000	0.500	0.500	0.000	0.833	1.000	1.606
M	28	0.929	0.786	0.143	0.143	0.250	0.952	0.403

Table 110. Habitat use by American plaice in the St. Lawrence estuary and Gulf (1984–1992, fish > 20.5 cm total length) based on catch in number. The number of cells overlapping the distribution features, based on the species catch in number, is reported as a proportion of the number of cells in each megahabitat. The kernel density estimates (KDE) were generated with ESRI ArcGIS 10.0 software and the Spatial Analyst extension (quartic kernel function). Clusters of high (hot spot) and low (cold spot) catch in number were determined using the Getis and Ord local spatial autocorrelation Gi* statistic (Z-score). Mean catch in number and Gi* value are given for each megahabitat. Prime habitats for the species are highlighted.

Megahabitat	Number of cells	KDE 90% volume	KDE 50% volume	Cold spot	Hot spot	CN_mean	Z-score
A	422	0.014	0.005	0.000	0.012	101.3	-1.019
B	10	0.300	0.000	0.000	0.000	1149.6	-0.485
C	91	0.209	0.011	0.000	0.033	1923.6	-0.510
D	93	0.075	0.000	0.000	0.000	783.3	-0.839
E	71	0.338	0.028	0.000	0.070	1652.8	-0.138
G	20	0.350	0.000	0.000	0.000	1025.6	-0.465
H	114	0.289	0.211	0.000	0.246	4885.3	1.150
I	53	0.340	0.189	0.000	0.226	5687.9	1.028
J	252	0.575	0.294	0.000	0.429	6587.2	1.678
K	88	0.398	0.091	0.000	0.125	2541.9	0.081
L	7	0.286	0.143	0.000	0.286	2145.7	0.461
M	33	0.061	0.030	0.000	0.030	1553.3	-0.235

Table 111. Habitat use by American plaice in the St. Lawrence estuary and Gulf (1984–1992, fish > 20.5 cm total length) based on catch in number and cells where the species presence was confirmed. The number of cells overlapping the distribution features, based on the species catch in number, is reported as a proportion of the number of cells in each megahabitat. The kernel density estimates (KDE) were generated with ESRI ArcGIS 10.0 software and the Spatial Analyst extension (quartic kernel function). Clusters of high (hot spot) and low (cold spot) catch in number were determined using the Getis and Ord local spatial autocorrelation Gi* statistic (Z-score). Mean catch in number and Gi* value are given for each megahabitat. Prime habitats for the species are highlighted.

Megahabitat	Number of cells	KDE 90% volume	KDE 50% volume	Cold spot	Hot spot	CN_mean	Z-score
A	207	0.019	0.010	0.000	0.014	206.6	-0.963
B	7	0.429	0.000	0.000	0.000	1642.3	-0.342
C	86	0.221	0.012	0.000	0.035	2035.4	-0.500
D	78	0.077	0.000	0.000	0.000	933.9	-0.826
E	43	0.512	0.047	0.000	0.116	2729.0	0.208
G	20	0.350	0.000	0.000	0.000	1025.6	-0.465
H	103	0.320	0.233	0.000	0.272	5407.1	1.365
I	40	0.425	0.250	0.000	0.300	7536.5	1.518
J	247	0.587	0.300	0.000	0.437	6720.5	1.721
K	86	0.407	0.093	0.000	0.128	2601.0	0.102
L	6	0.333	0.167	0.000	0.333	2503.3	0.659
M	28	0.071	0.036	0.000	0.036	1830.7	-0.154

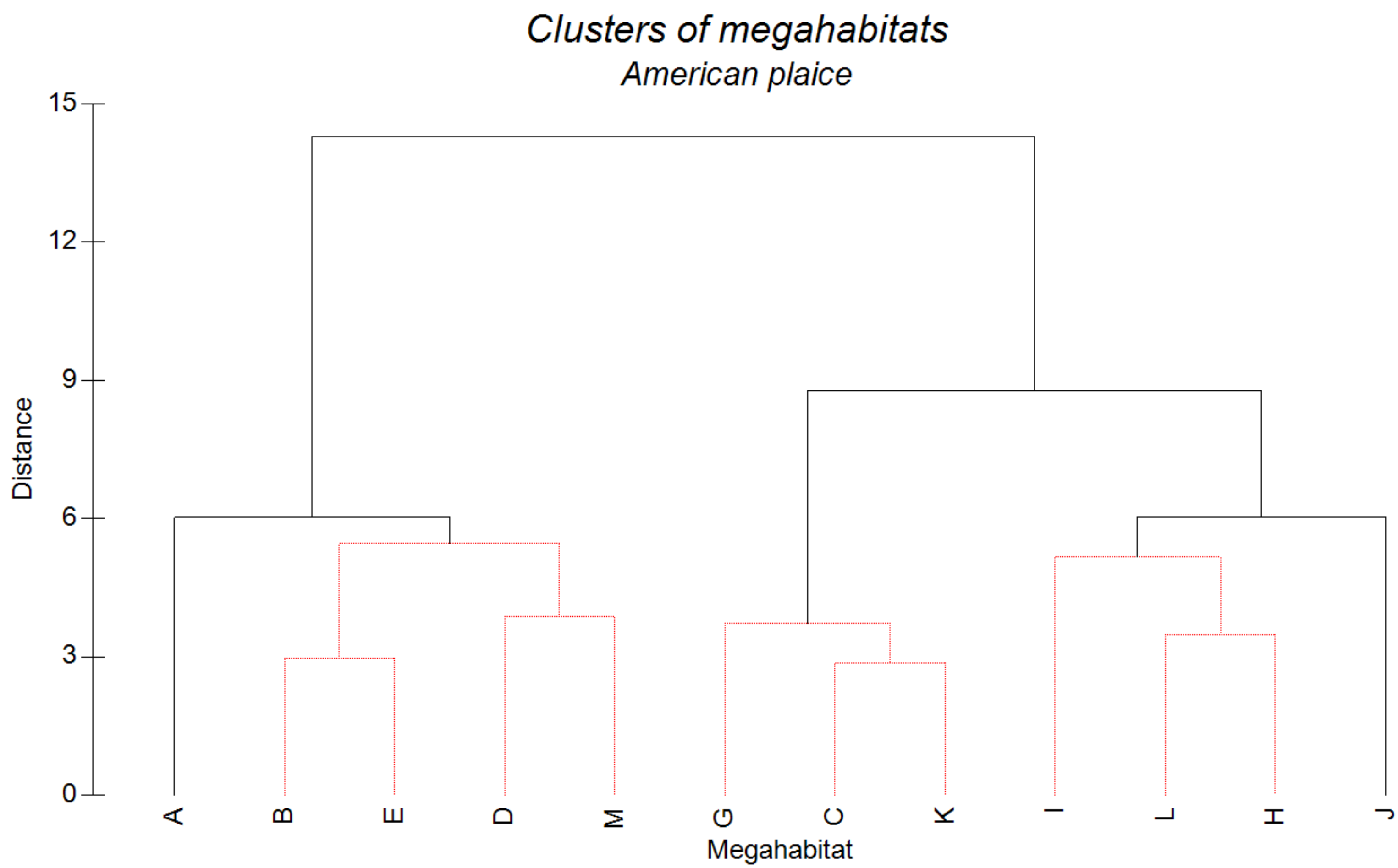

Figure 149. Clusters of megahabitats determined using 27 different descriptors of spatial distribution and abundance of American plaice based on relative occurrence, catch in number, and catch in weight in the annual bottom trawl research surveys (1984–1992, fish > 20.5 cm). Habitats are ordered from left to right by decreasing distance from megahabitat J, which is considered most important to American plaice.

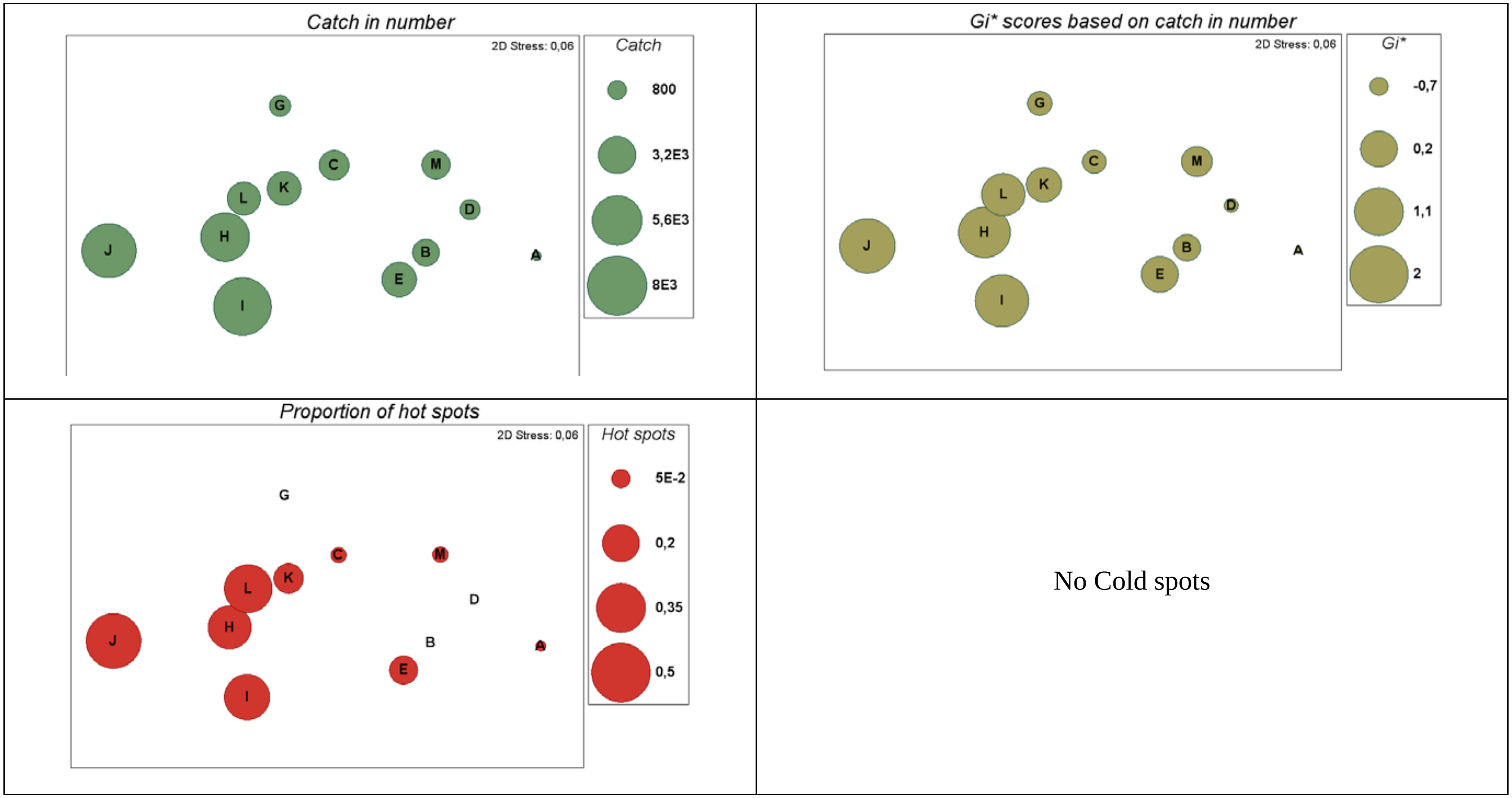

Figure 150. Multidimensional scaling plot of megahabitats based on American plaice spatial distribution and relative occurrence and abundance descriptors (27 descriptors, 1984–1992, fish > 20.5 cm). Bubble size reflects mean catch in number in sets where the species is present (upper left panel), local spatial autocorrelation G_i* statistic (upper right panel), and proportion of cells classified as hot spots or cold spots (lower left and lower right panel, respectively).

2002–2010

Table 112. Habitat use by American plaice in the St. Lawrence estuary and Gulf (2002–2010) based on relative occurrence data. The number of cells overlapping the distribution features is reported as a proportion of the number of cells in each megahabitat. The area of occupancy was determined by the Hernández and Navarro (2007) method using presence/absence data. Other features are based on the species relative occurrence. The kernel density estimates (KDE) were generated with ESRI ArcGIS 10.0 software and the Spatial Analyst extension (quartic kernel function). Clusters of high (hot spot) and low (cold spot) relative occurrences were determined using the Getis and Ord local spatial autocorrelation Gi* statistic (Z-score). Mean relative occurrence and Gi* value are given for each megahabitat. Prime habitats for the species are highlighted.

Megahabitat	Number of cells	Area of occupancy	KDE 90% volume	KDE 50% volume	Cold spot	Hot spot	Relative occurrence	Z-score
A	432	1.000	0.509	0.294	0.324	0.012	0.706	-1.051
B	9	1.000	0.667	0.111	0.444	0.000	0.730	-1.271
C	104	1.000	0.404	0.577	0.010	0.038	0.974	0.981
D	96	1.000	0.469	0.469	0.094	0.010	0.890	0.179
E	86	1.000	0.558	0.093	0.477	0.000	0.518	-1.884
G	26	1.000	0.115	0.885	0.000	0.115	1.000	1.370
H	126	1.000	0.460	0.460	0.175	0.032	0.836	-0.054
I	94	1.000	0.479	0.372	0.074	0.064	0.870	0.531
J	296	1.000	0.142	0.858	0.000	0.264	0.987	1.360
K	92	1.000	0.435	0.565	0.000	0.185	0.995	1.178
L	16	1.000	0.625	0.375	0.000	0.000	1.000	1.052
M	44	1.000	0.773	0.114	0.023	0.000	0.908	0.427

Table 113. Habitat use by American plaice in the St. Lawrence estuary and Gulf (2002–2010) based on relative occurrence data and cells where the species presence was confirmed. The number of cells overlapping the distribution features is reported as a proportion of the number of cells in each megahabitat. The area of occupancy was determined by the Hernández and Navarro (2007) method using presence/absence data. Other features are based on the species relative occurrence. The kernel density estimates (KDE) were generated with ESRI ArcGIS 10.0 software and the Spatial Analyst extension (quartic kernel function). Clusters of high (hot spot) and low (cold spot) relative occurrences were determined using the Getis and Ord local spatial autocorrelation Gi* statistic (Z-score). Mean relative occurrence and Gi* value are given for each megahabitat. Prime habitats for the species are highlighted.

Megahabitat	Number of cells	Area of occupancy	KDE 90% volume	KDE 50% volume	Cold spot	Hot spot	Relative occurrence	Z-score
A	350	1.000	0.566	0.363	0.214	0.014	0.872	-0.370
B	8	1.000	0.750	0.125	0.375	0.000	0.821	-1.026
C	104	1.000	0.404	0.577	0.010	0.038	0.974	0.981
D	93	1.000	0.484	0.484	0.065	0.011	0.919	0.296
E	58	1.000	0.741	0.138	0.276	0.000	0.768	-0.991
G	26	1.000	0.115	0.885	0.000	0.115	1.000	1.370
H	115	1.000	0.461	0.504	0.130	0.035	0.916	0.165
I	85	1.000	0.506	0.412	0.035	0.071	0.962	0.791
J	294	1.000	0.136	0.864	0.000	0.265	0.993	1.377
K	92	1.000	0.435	0.565	0.000	0.185	0.995	1.178
L	16	1.000	0.625	0.375	0.000	0.000	1.000	1.052
M	42	1.000	0.786	0.119	0.000	0.000	0.952	0.561

Table 114. Habitat use by American plaice in the St. Lawrence estuary and Gulf (2002–2010) based on catch in number. The number of cells overlapping the distribution features, based on the species catch in number, is reported as a proportion of the number of cells in each megahabitat. The kernel density estimates (KDE) were generated with ESRI ArcGIS 10.0 software and the Spatial Analyst extension (quartic kernel function). Clusters of high (hot spot) and low (cold spot) catch in number were determined using the Getis and Ord local spatial autocorrelation Gi* statistic (Z-score). Mean catch in number and Gi* value are given for each megahabitat. Prime habitats for the species are highlighted.

Megahabitat	Number of cells	KDE 90% volume	KDE 50% volume	Cold spot	Hot spot	CN_mean	Z-score
A	431	0.160	0.002	0.313	0.005	317.4	-1.317
B	9	0.333	0.111	0.000	0.111	1615.5	-0.548
C	104	0.769	0.077	0.010	0.058	2481.2	-0.010
D	96	0.500	0.031	0.021	0.042	1551.8	-0.566
E	86	0.198	0.081	0.128	0.105	955.2	-0.554
G	26	0.654	0.231	0.000	0.038	3197.5	0.220
H	126	0.492	0.143	0.008	0.159	1702.2	0.074
I	94	0.511	0.117	0.000	0.191	1874.3	0.411
J	296	0.355	0.561	0.000	0.561	3961.0	1.981
K	92	0.652	0.228	0.000	0.207	3894.6	0.983
L	16	0.563	0.063	0.000	0.063	1949.6	-0.349
M	44	0.477	0.091	0.000	0.114	2372.2	0.094

Table 115. Habitat use by American plaice in the St. Lawrence estuary and Gulf (2002–2010) based on catch in number and cells where the species presence was confirmed. The number of cells overlapping the distribution features, based on the species catch in number, is reported as a proportion of the number of cells in each megahabitat. The kernel density estimates (KDE) were generated with ESRI ArcGIS 10.0 software and the Spatial Analyst extension (quartic kernel function). Clusters of high (hot spot) and low (cold spot) catch in number were determined using the Getis and Ord local spatial autocorrelation Gi* statistic (Z-score). Mean catch in number and Gi* value are given for each megahabitat. Prime habitats for the species are highlighted.

Megahabitat	Number of cells	KDE 90% volume	KDE 50% volume	Cold spot	Hot spot	CN_mean	Z-score
A	348	0.193	0.003	0.250	0.006	393.1	-1.251
B	8	0.375	0.125	0.000	0.125	1817.4	-0.501
C	104	0.769	0.077	0.010	0.058	2481.2	-0.010
D	93	0.516	0.032	0.022	0.043	1601.8	-0.539
E	58	0.276	0.121	0.103	0.155	1416.4	-0.217
G	26	0.654	0.231	0.000	0.038	3197.5	0.220
H	115	0.513	0.157	0.009	0.174	1865.1	0.148
I	85	0.553	0.118	0.000	0.200	2072.7	0.436
J	294	0.354	0.561	0.000	0.561	3988.0	1.961
K	92	0.652	0.228	0.000	0.207	3894.6	0.983
L	16	0.563	0.063	0.000	0.063	1949.6	-0.349
M	42	0.500	0.095	0.000	0.119	2485.1	0.145

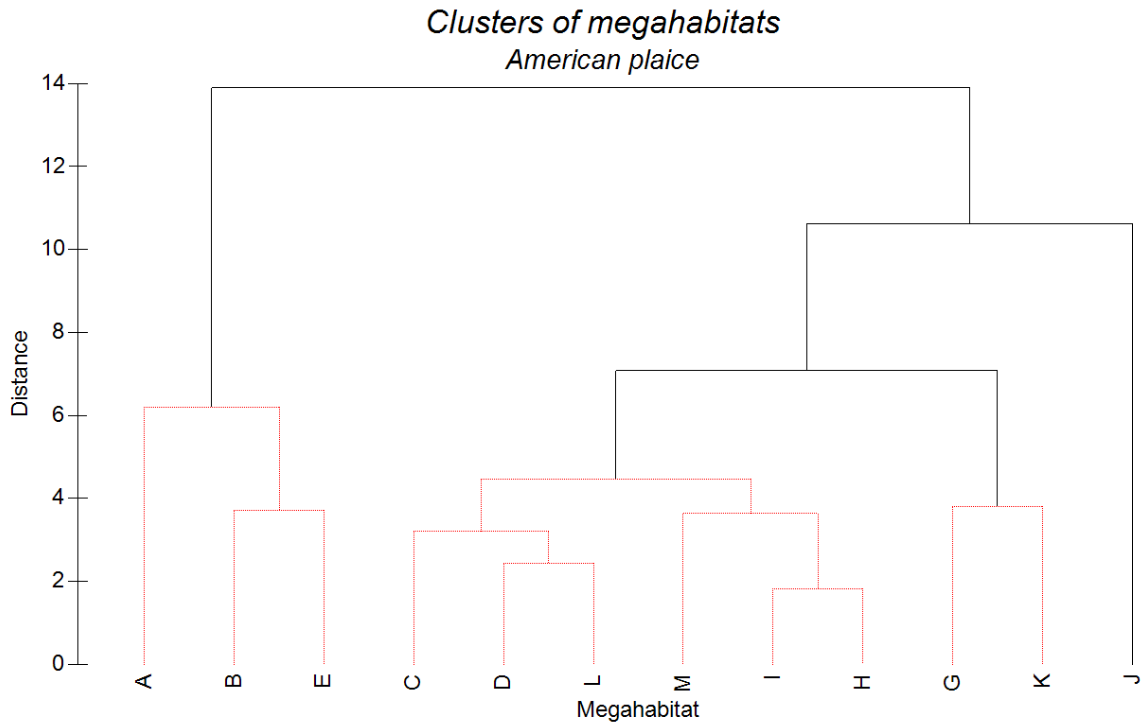

Figure 151. Clusters of megahabitats determined using 27 different descriptors of spatial distribution and abundance of American plaice based on relative occurrence, catch in number, and catch in weight in the annual bottom trawl research surveys (2002–2010). Habitats are ordered from left to right by decreasing distance from megahabitat J, which is considered most important to American plaice.

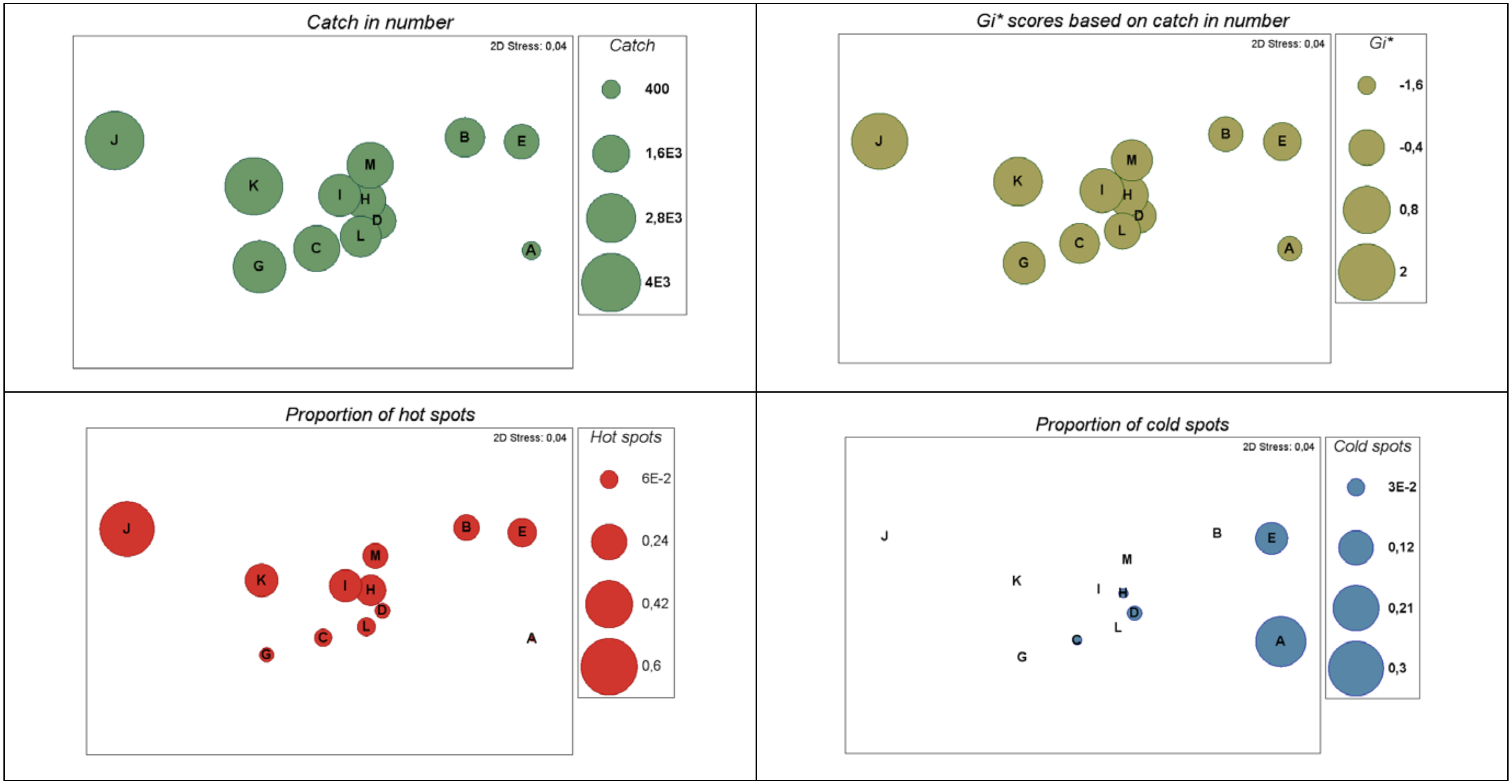

Figure 152. Multidimensional scaling plot of megahabitats based on American plaice spatial distribution and relative occurrence and abundance descriptors (27 descriptors, 2002–2010). Bubble size reflects mean catch in number in sets where the species is present (upper left panel), local spatial autocorrelation G_i* statistic (upper right panel), and proportion of cells classified as hot spots or cold spots (lower left and lower right panel, respectively).

2002–2010, fish <20.5 cm total length

Table 116. Habitat use by American plaice in the St. Lawrence estuary and Gulf (2002–2010, fish <20.5 cm total length) based on relative occurrence data. The number of cells overlapping the distribution features is reported as a proportion of the number of cells in each megahabitat. The area of occupancy was determined by the Hernández and Navarro (2007) method using presence/absence data. Other features are based on the species relative occurrence. The kernel density estimates (KDE) were generated with ESRI ArcGIS 10.0 software and the Spatial Analyst extension (quartic kernel function). Clusters of high (hot spot) and low (cold spot) relative occurrences were determined using the Getis and Ord local spatial autocorrelation Gi* statistic (Z-score). Mean relative occurrence and Gi* value are given for each megahabitat. Prime habitats for the species are highlighted.

Megahabitat	Number of cells	Area of occupancy	KDE 90% volume	KDE 50% volume	Cold spot	Hot spot	Relative occurrence	Z-score
A	431	1.000	0.515	0.116	0.513	0.037	0.437	-1.666
B	9	1.000	0.778	0.000	0.556	0.000	0.563	-1.405
C	104	1.000	0.481	0.500	0.029	0.240	0.928	0.792
D	96	1.000	0.625	0.208	0.260	0.073	0.669	-0.516
E	86	0.767	0.535	0.140	0.395	0.047	0.490	-0.812
G	26	1.000	0.231	0.769	0.000	0.385	0.942	1.247
W	126	1.000	0.452	0.484	0.087	0.278	0.743	0.443
I	94	1.000	0.447	0.372	0.074	0.277	0.806	0.794
J	296	1.000	0.169	0.831	0.003	0.662	0.934	1.780
K	92	1.000	0.337	0.663	0.000	0.435	0.932	1.410
L	16	1.000	0.688	0.313	0.000	0.250	0.969	1.007
M	44	1.000	0.750	0.091	0.114	0.136	0.744	0.065

Table 117. Habitat use by American plaice in the St. Lawrence estuary and Gulf (2002–2010, fish <20.5 cm total length) based on relative occurrence data and cells where the species presence was confirmed. The number of cells overlapping the distribution features is reported as a proportion of the number of cells in each megahabitat. The area of occupancy was determined by the Hernández and Navarro (2007) method using presence/absence data. Other features are based on the species relative occurrence. The kernel density estimates (KDE) were generated with ESRI ArcGIS 10.0 software and the Spatial Analyst extension (quartic kernel function). Clusters of high (hot spot) and low (cold spot) relative occurrences were determined using the Getis and Ord local spatial autocorrelation Gi* statistic (Z-score). Mean relative occurrence and Gi* value are given for each megahabitat. Prime habitats for the species are highlighted.

Megahabitat	Number of cells	Area of occupancy	KDE 90% volume	KDE 50% volume	Cold spot	Hot spot	Relative occurrence	Z-score
A	257	1.000	0.642	0.195	0.354	0.062	0.733	-0.918
B	7	1.000	0.857	0.000	0.571	0.000	0.724	-1.334
C	103	1.000	0.485	0.505	0.029	0.243	0.937	0.792
D	83	1.000	0.675	0.241	0.205	0.084	0.774	-0.278
E	56	0.839	0.750	0.214	0.179	0.071	0.752	0.023
G	25	1.000	0.200	0.800	0.000	0.400	0.980	1.292
W	109	1.000	0.404	0.560	0.037	0.321	0.859	0.683
I	81	1.000	0.494	0.420	0.025	0.321	0.936	1.078
J	289	1.000	0.152	0.848	0.000	0.678	0.957	1.821
K	90	1.000	0.322	0.678	0.000	0.444	0.953	1.436
L	16	1.000	0.688	0.313	0.000	0.250	0.969	1.007
M	38	1.000	0.789	0.105	0.105	0.158	0.861	0.134

Table 118. Habitat use by American plaice in the St. Lawrence estuary and Gulf (2002–2010, fish < 20.5 cm total length) based on catch in number. The number of cells overlapping the distribution features, based on the species catch in number, is reported as a proportion of the number of cells in each megahabitat. The kernel density estimates (KDE) were generated with ESRI ArcGIS 10.0 software and the Spatial Analyst extension (quartic kernel function). Clusters of high (hot spot) and low (cold spot) catch in number were determined using the Getis and Ord local spatial autocorrelation Gi* statistic (Z-score). Mean catch in number and Gi* value are given for each megahabitat. Prime habitats for the species are highlighted.

Megahabitat	Number of cells	KDE 90% volume	KDE 50% volume	Cold spot	Hot spot	CN_mean	Z-score
A	431	0.132	0.000	0.153	0.002	92.901	-1.208
B	9	0.333	0.111	0.000	0.111	721.469	-0.540
C	104	0.644	0.144	0.000	0.058	974.081	0.081
D	96	0.365	0.063	0.010	0.042	461.846	-0.589
E	86	0.279	0.116	0.023	0.140	451.115	-0.158
G	26	0.654	0.115	0.000	0.000	963.502	-0.286
H	126	0.556	0.214	0.000	0.198	873.669	0.491
I	94	0.489	0.128	0.000	0.191	943.369	0.652
J	296	0.382	0.524	0.000	0.446	1237.950	1.410
K	92	0.620	0.185	0.000	0.152	1143.024	0.551
L	16	0.438	0.063	0.000	0.125	746.418	-0.307
M	44	0.341	0.182	0.000	0.159	1084.798	0.204

Table 119. Habitat use by American plaice in the St. Lawrence estuary and Gulf (2002–2010, fish < 20.5 cm total length) based on catch in number and cells where the species presence was confirmed. The number of cells overlapping the distribution features, based on the species catch in number, is reported as a proportion of the number of cells in each megahabitat. The kernel density estimates (KDE) were generated with ESRI ArcGIS 10.0 software and the Spatial Analyst extension (quartic kernel function). Clusters of high (hot spot) and low (cold spot) catch in number were determined using the Getis and Ord local spatial autocorrelation Gi* statistic (Z-score). Mean catch in number and Gi* value are given for each megahabitat. Prime habitats for the species are highlighted.

Megahabitat	Number of cells	KDE 90% volume	KDE 50% volume	Cold spot	Hot spot	CN_mean	Z-score
A	257	0.206	0.000	0.113	0.004	155.798	-1.082
B	7	0.286	0.143	0.000	0.143	927.603	-0.649
C	103	0.650	0.136	0.000	0.049	983.538	0.054
D	83	0.422	0.072	0.000	0.048	534.183	-0.478
E	56	0.357	0.179	0.036	0.196	692.784	0.261
G	25	0.640	0.120	0.000	0.000	1002.042	-0.258
H	109	0.569	0.248	0.000	0.229	1009.929	0.646
I	81	0.531	0.136	0.000	0.210	1094.774	0.802
J	289	0.374	0.533	0.000	0.453	1267.935	1.431
K	90	0.622	0.189	0.000	0.156	1168.424	0.567
L	16	0.438	0.063	0.000	0.125	746.418	-0.307
M	38	0.368	0.211	0.000	0.158	1256.082	0.299

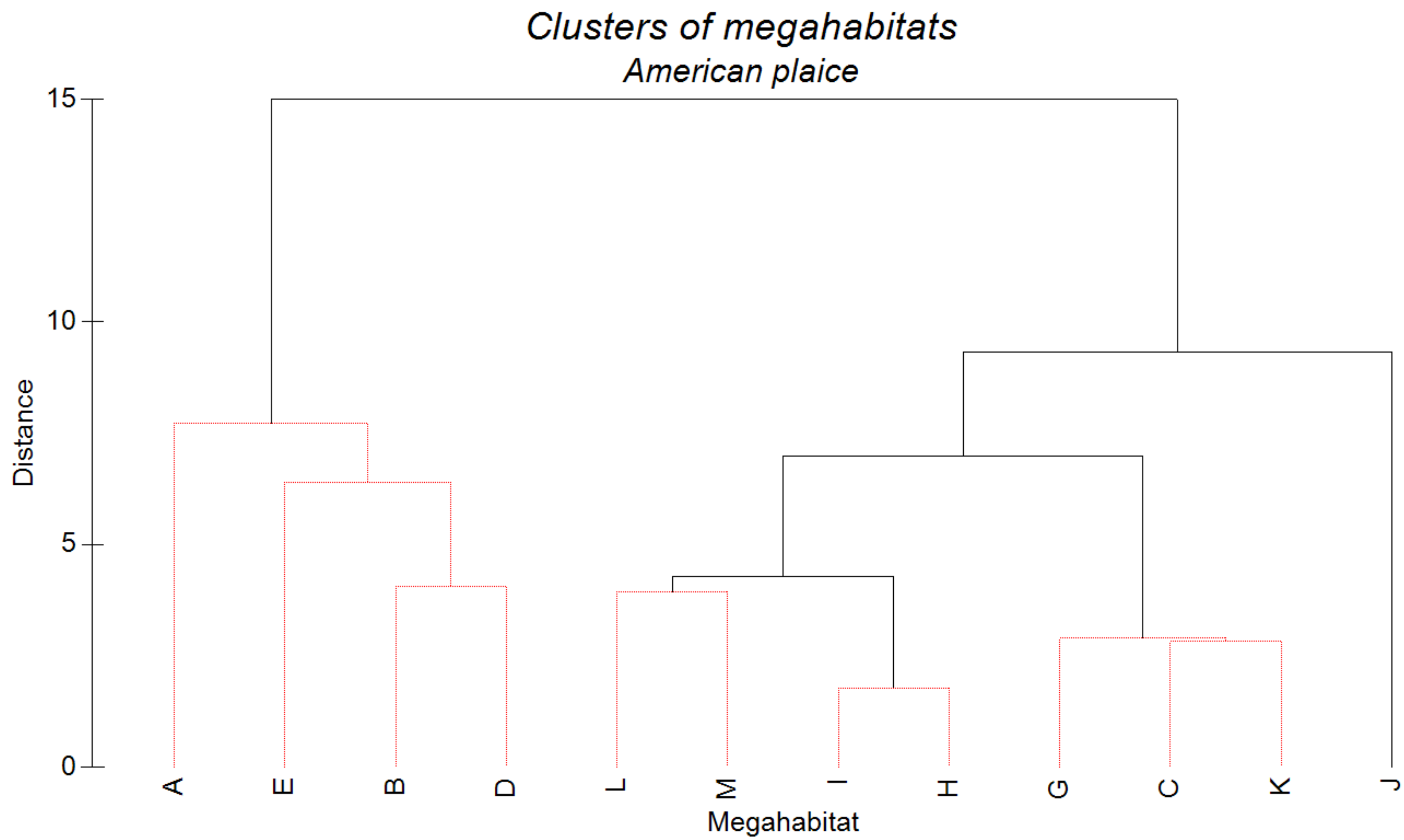

Figure 153. Clusters of megahabitats determined using 27 different descriptors of spatial distribution and abundance of American plaice based on relative occurrence, catch in number, and catch in weight in the annual bottom trawl research surveys (2002–2010, fish < 20.5 cm). Habitats are ordered from left to right by decreasing distance from megahabitat J, which is considered most important to American plaice.

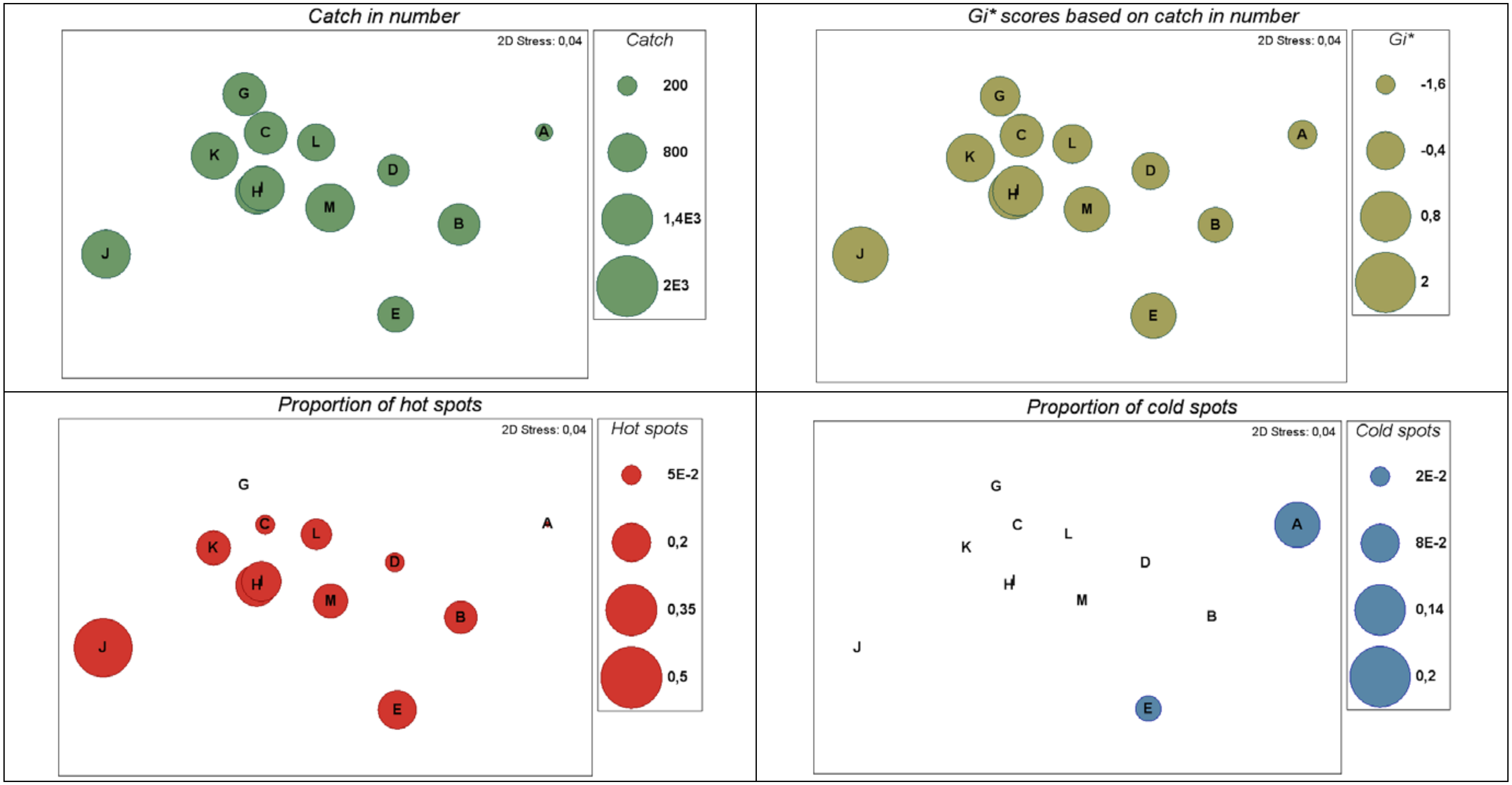

Figure 154. Multidimensional scaling plot of megahabitats based on American plaice spatial distribution and relative occurrence and abundance descriptors (27 descriptors, 2002–2010, fish < 20.5 cm). Bubble size reflects mean catch in number in sets where the species is present (upper left panel), local spatial autocorrelation G_i* statistic (upper right panel), and proportion of cells classified as hot spots or cold spots (lower left and lower right panel, respectively).

2002–2010, fish >20.5 cm total length

Table 120. Habitat use by American plaice in the St. Lawrence estuary and Gulf (2002–2010, fish >20.5 cm total length) based on relative occurrence data. The number of cells overlapping the distribution features is reported as a proportion of the number of cells in each megahabitat. The area of occupancy was determined by the Hernández and Navarro (2007) method using presence/absence data. Other features are based on the species relative occurrence. The kernel density estimates (KDE) were generated with ESRI ArcGIS 10.0 software and the Spatial Analyst extension (quartic kernel function). Clusters of high (hot spot) and (cold spot) low relative occurrences were determined using the Getis and Ord local spatial autocorrelation Gi* statistic (Z-score). Mean relative occurrence and Gi* value are given for each megahabitat. Prime habitats for the species are highlighted.

Megahabitat	Number of cells	Area of occupancy	KDE 90% volume	KDE 50% volume	Cold spot	Hot spot	Relative occurrence	Z-score
A	431	1.000	0.508	0.232	0.355	0.084	0.623	-1.091
B	9	1.000	0.667	0.111	0.333	0.000	0.630	-1.315
C	104	1.000	0.423	0.558	0.010	0.288	0.956	1.082
D	96	1.000	0.542	0.396	0.115	0.167	0.876	0.263
E	86	1.000	0.407	0.093	0.488	0.000	0.382	-2.322
G	26	1.000	0.115	0.885	0.000	0.615	1.000	1.489
H	126	1.000	0.476	0.365	0.254	0.103	0.729	-0.392
I	94	1.000	0.457	0.372	0.064	0.149	0.805	0.638
J	296	1.000	0.145	0.855	0.000	0.703	0.978	1.591
K	92	1.000	0.424	0.576	0.000	0.413	0.973	1.324
L	16	1.000	0.625	0.375	0.000	0.188	0.969	0.839
M	44	1.000	0.773	0.091	0.023	0.045	0.879	0.331

Table 121. Habitat use by American plaice in the St. Lawrence estuary and Gulf (2002–2010, fish >20.5 cm total length) based on relative occurrence data and cells where the species presence was confirmed. The number of cells overlapping the distribution features is reported as a proportion of the number of cells in each megahabitat. The area of occupancy was determined by the Hernández and Navarro (2007) method using presence/absence data. Other features are based on the species relative occurrence. The kernel density estimates (KDE) were generated with ESRI ArcGIS 10.0 software and the Spatial Analyst extension (quartic kernel function). Clusters of high (hot spot) and low (cold spot) relative occurrences were determined using the Getis and Ord local spatial autocorrelation Gi* statistic (Z-score). Mean relative occurrence and Gi* value are given for each megahabitat. Prime habitats for the species are highlighted.

Megahabitat	Number of cells	Area of occupancy	KDE 90% volume	KDE 50% volume	Cold spot	Hot spot	Relative occurrence	Z-score
A	317	1.000	0.606	0.315	0.205	0.114	0.846	-1.082
B	7	1.000	0.857	0.143	0.143	0.000	0.810	-0.649
C	103	1.000	0.417	0.563	0.010	0.291	0.966	0.054
D	92	1.000	0.554	0.413	0.076	0.174	0.914	-0.478
E	44	1.000	0.682	0.159	0.159	0.000	0.746	0.261
G	26	1.000	0.115	0.885	0.000	0.615	1.000	-0.258
H	105	1.000	0.486	0.438	0.152	0.124	0.874	0.646
I	80	1.000	0.500	0.438	0.025	0.175	0.946	0.802
J	293	1.000	0.137	0.863	0.000	0.710	0.988	1.431
K	91	1.000	0.418	0.582	0.000	0.418	0.984	0.567
L	16	1.000	0.625	0.375	0.000	0.188	0.969	-0.307
M	42	1.000	0.786	0.095	0.000	0.048	0.921	0.299

Table 122. Habitat use by American plaice in the St. Lawrence estuary and Gulf (2002–2010, fish > 20.5 cm total length) based on catch in number. The number of cells overlapping the distribution features, based on the species catch in number, is reported as a proportion of the number of cells in each megahabitat. The kernel density estimates (KDE) were generated with ESRI ArcGIS 10.0 software and the Spatial Analyst extension (quartic kernel function). Clusters of high (hot spot) and low (cold spot) catch in number were determined using the Getis and Ord local spatial autocorrelation Gi* statistic (Z-score). Mean catch in number and Gi* value are given for each megahabitat. Prime habitats for the species are highlighted.

Megahabitat	Number of cells	KDE 90% volume	KDE 50% volume	Cold spot	Hot spot	CN_mean	Z-score
A	431	0.174	0.002	0.067	0.005	244.208	-1.142
B	9	0.556	0.000	0.000	0.111	1005.627	-0.271
C	104	0.788	0.058	0.000	0.038	1540.874	-0.027
D	96	0.552	0.042	0.000	0.042	1108.072	-0.452
E	86	0.198	0.070	0.035	0.058	510.227	-0.675
G	26	0.731	0.192	0.000	0.154	2192.195	0.425
H	126	0.413	0.127	0.008	0.135	839.205	-0.164
I	94	0.447	0.085	0.000	0.117	926.725	0.226
J	296	0.419	0.500	0.000	0.530	2663.780	1.907
K	92	0.663	0.239	0.000	0.217	2736.769	1.107
L	16	0.563	0.063	0.000	0.063	1146.756	-0.296
M	44	0.500	0.068	0.000	0.068	1299.587	0.027

Table 123. Habitat use by American plaice in the St. Lawrence estuary and Gulf (2002–2010, fish > 20.5 cm total length) based on catch in number and cells where the species presence was confirmed. The number of cells overlapping the distribution features, based on the species catch in number, is reported as a proportion of the number of cells in each megahabitat. The kernel density estimates (KDE) were generated with ESRI ArcGIS 10.0 software and the Spatial Analyst extension (quartic kernel function). Clusters of high (hot spot) and low (cold spot) catch in number were determined using the Getis and Ord local spatial autocorrelation Gi* statistic (Z-score). Mean catch in number and Gi* value are given for each megahabitat. Prime habitats for the species are highlighted.

Megahabitat	Number of cells	KDE 90% volume	KDE 50% volume	Cold spot	Hot spot	CN_mean	Z-score
A	317	0.230	0.003	0.044	0.006	332.030	-1.048
B	7	0.714	0.000	0.000	0.143	1292.949	-0.093
C	103	0.796	0.058	0.000	0.039	1555.834	-0.018
D	92	0.576	0.043	0.000	0.043	1156.249	-0.418
E	44	0.341	0.136	0.000	0.114	997.262	-0.185
G	26	0.731	0.192	0.000	0.154	2192.195	0.425
H	105	0.476	0.152	0.010	0.162	1007.047	-0.051
I	80	0.525	0.088	0.000	0.113	1088.902	0.158
J	293	0.420	0.502	0.000	0.532	2691.054	1.896
K	91	0.659	0.242	0.000	0.220	2766.843	1.115
L	16	0.563	0.063	0.000	0.063	1146.756	-0.296
M	42	0.524	0.071	0.000	0.071	1361.472	0.071

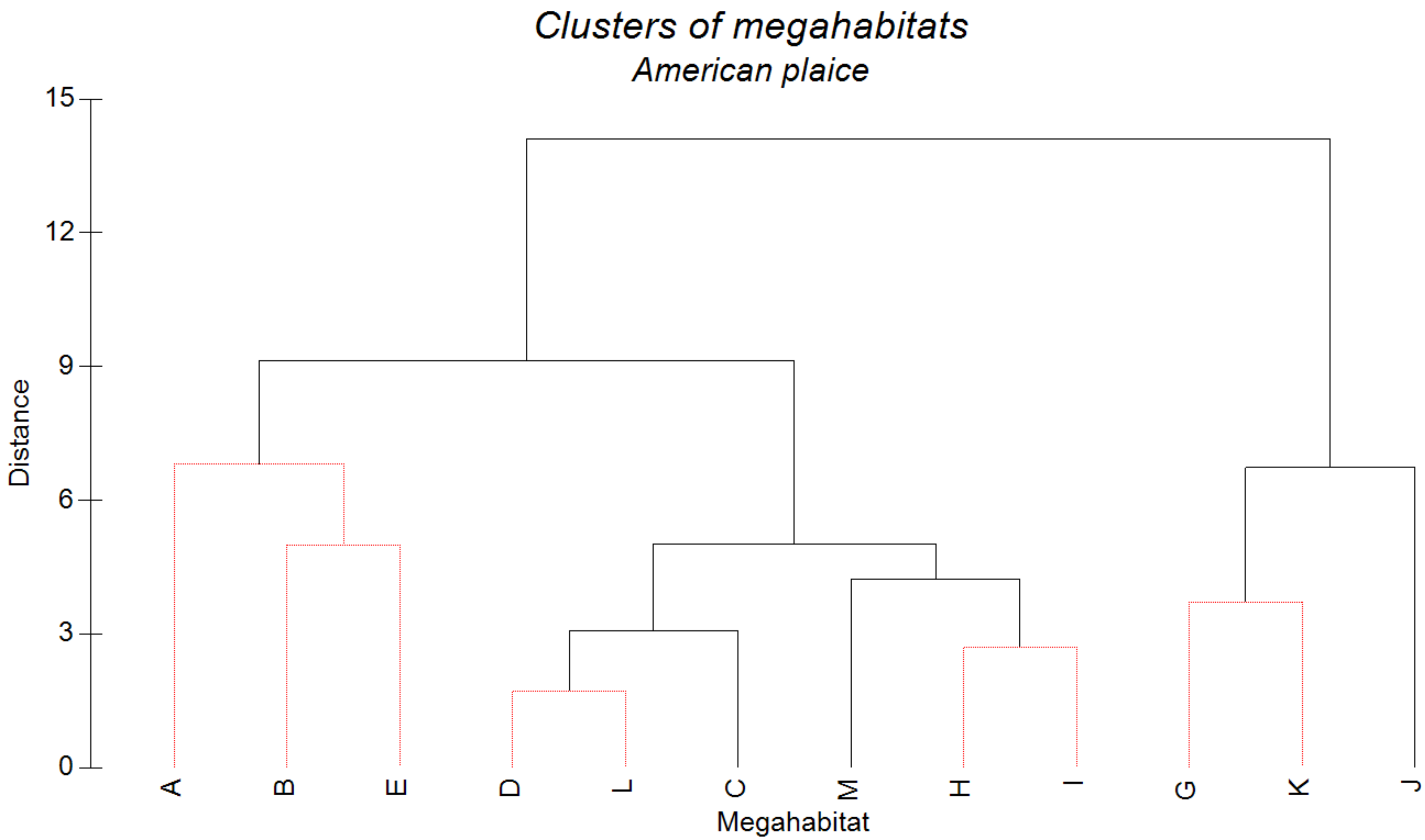

Figure 155. Clusters of megahabitats determined using 27 different descriptors of spatial distribution and abundance of American plaice, based on relative occurrence, catch in number, and catch in weight in the annual bottom trawl research surveys (2002–2010, fish > 20.5 cm). Habitats are ordered from left to right by decreasing distance from megahabitat J, which is considered most important to American plaice.

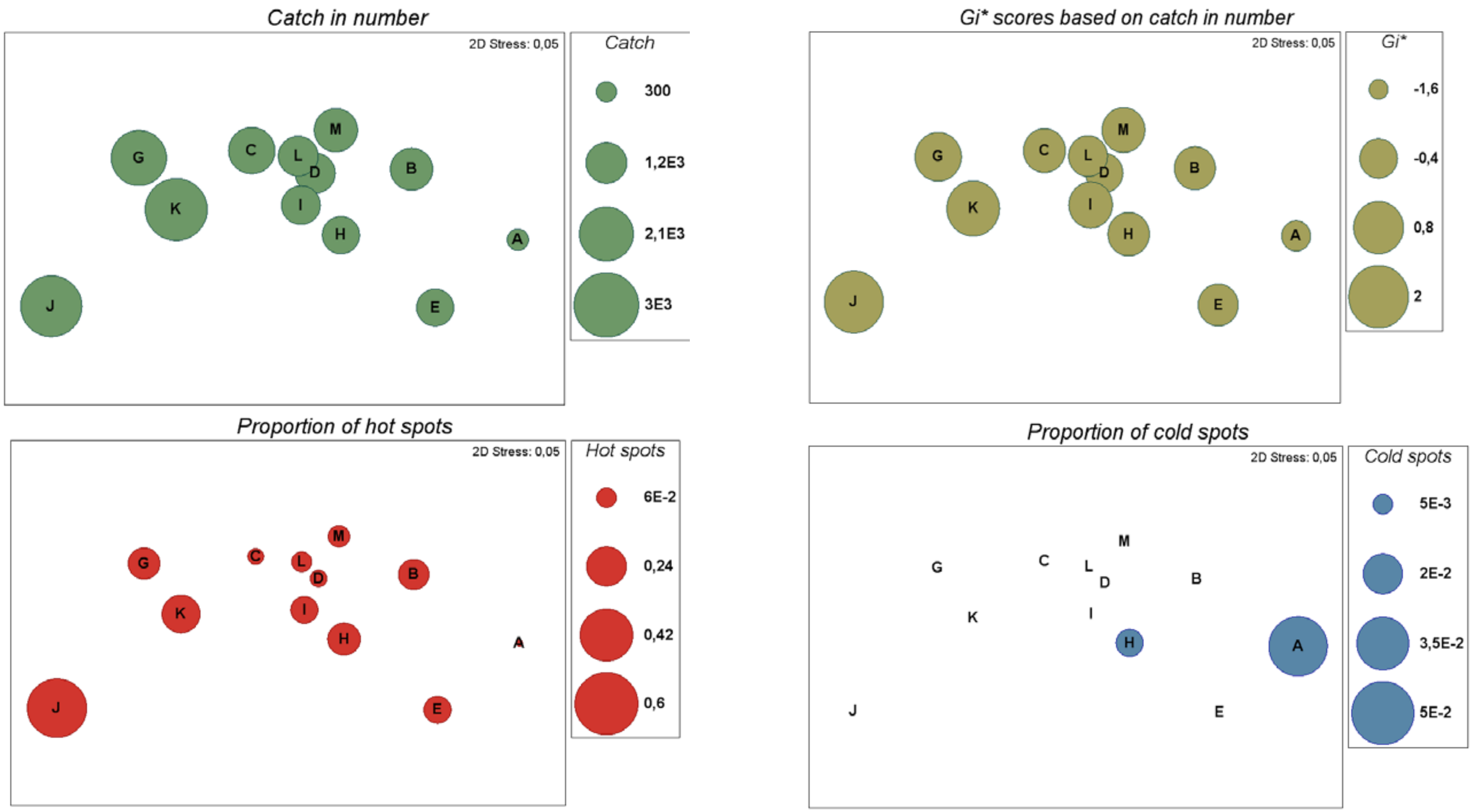

Figure 156. Multidimensional scaling plot of megahabitats based on American plaice spatial distribution and relative occurrence and abundance descriptors (27 descriptors, 2002–2010, fish > 20.5 cm). Bubble size reflects mean catch in number in sets where the species is present (upper left panel), local spatial autocorrelation G_i* statistic (upper right panel), and proportion of cells classified as hot spots or cold spots (lower left and lower right panel, respectively).

Combined periods and size categories

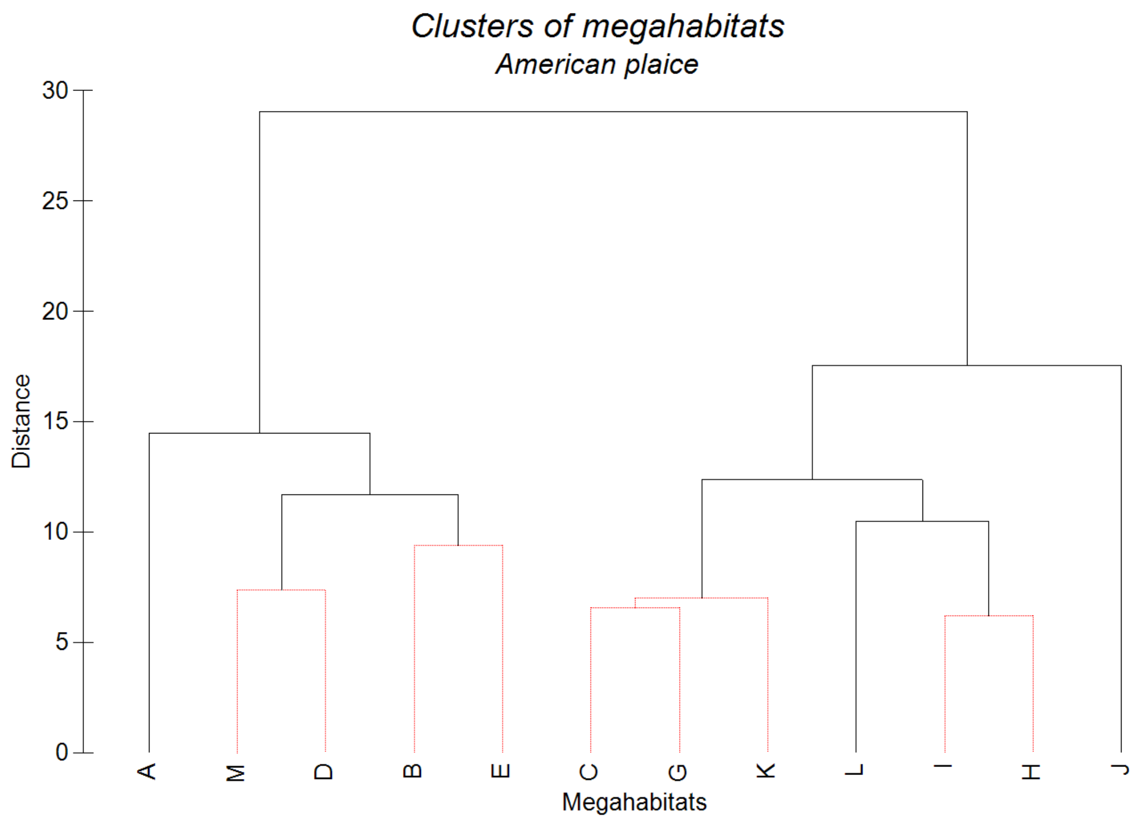

Figure 157. Clusters of megahabitats determined using 27 different descriptors of spatial distribution and abundance of American plaice based on relative occurrence, catch in number, and catch in weight in the annual bottom trawl research surveys. Two different time periods (1984–1992 and 2002–2010) and two different fish size categories (fish smaller and fish larger than 20.5 cm) were considered. Habitats are ordered from left to right by decreasing distance from megahabitat J, which is considered most important to American plaice.

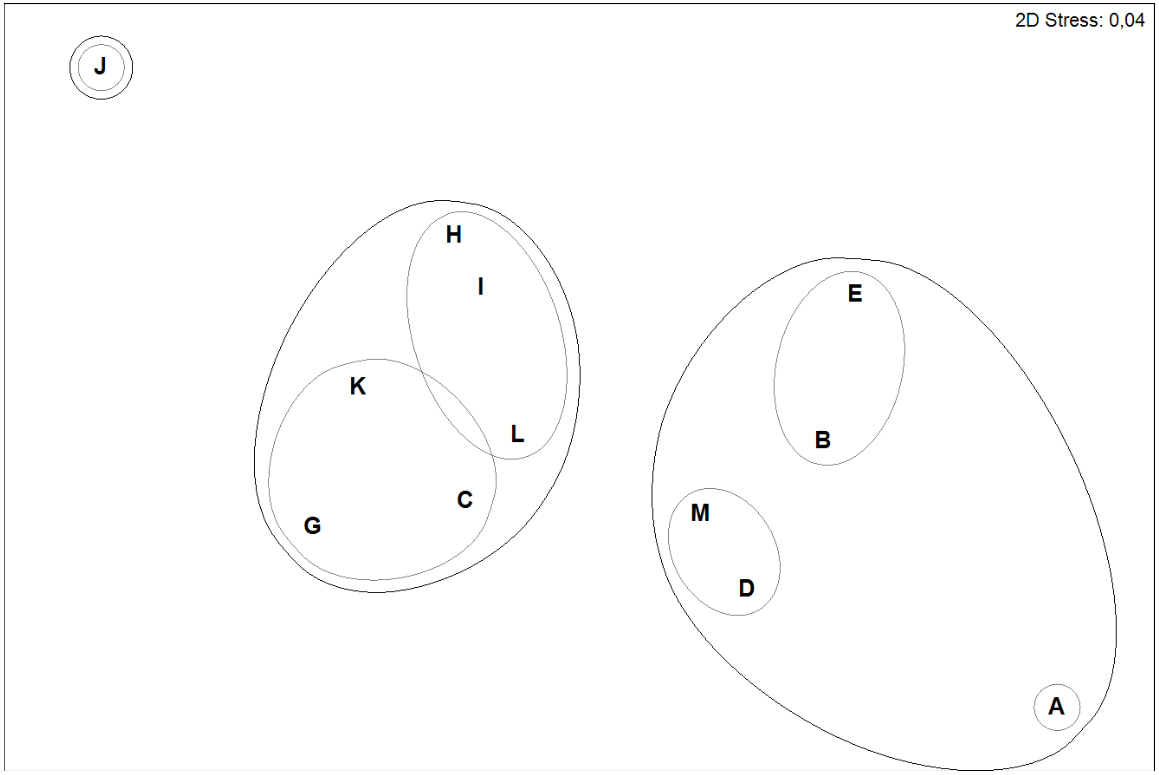

Figure 158. Multidimensional scaling plot of megahabitats based on American plaice spatial distribution and relative occurrence and abundance descriptors (27 descriptors) Two different time periods (1984–1992 and 2002–2010) and two different fish size categories (fish smaller and fish larger than 20.5 cm) were considered. Megahabitat J is considered most important to American plaice; megahabitats I and K have a secondary importance overall.

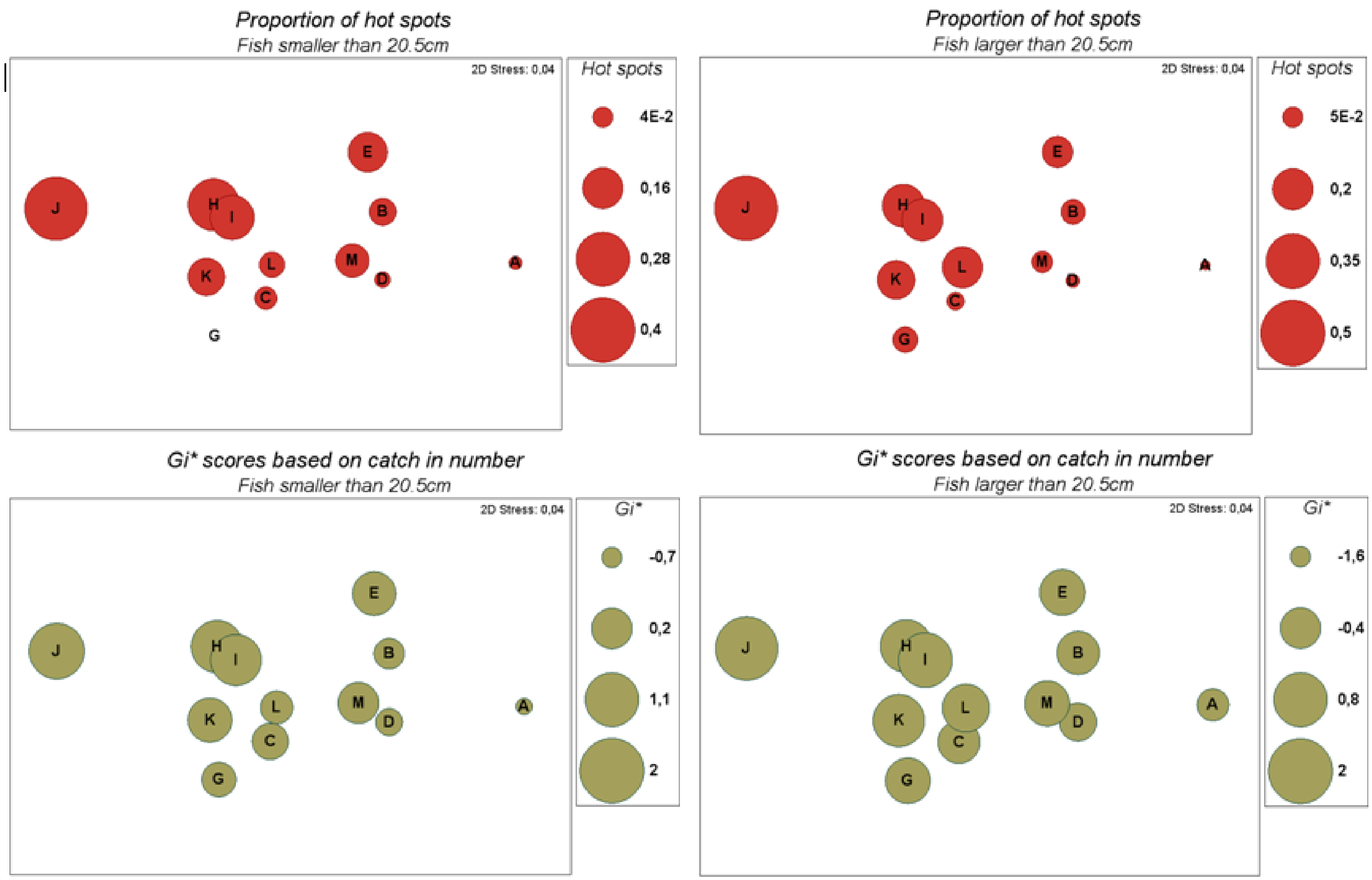

Figure 159. Multidimensional scaling plot of megahabitats based on American plaice spatial distribution and relative occurrence and abundance descriptors (27 descriptors). Fish smaller and fish larger than 20.5 cm are compared. Bubble size reflects the proportion of cells classified as hot spots (upper panels) and the local spatial autocorrelation G_i* statistic (lower panels) in cells where the species was present.

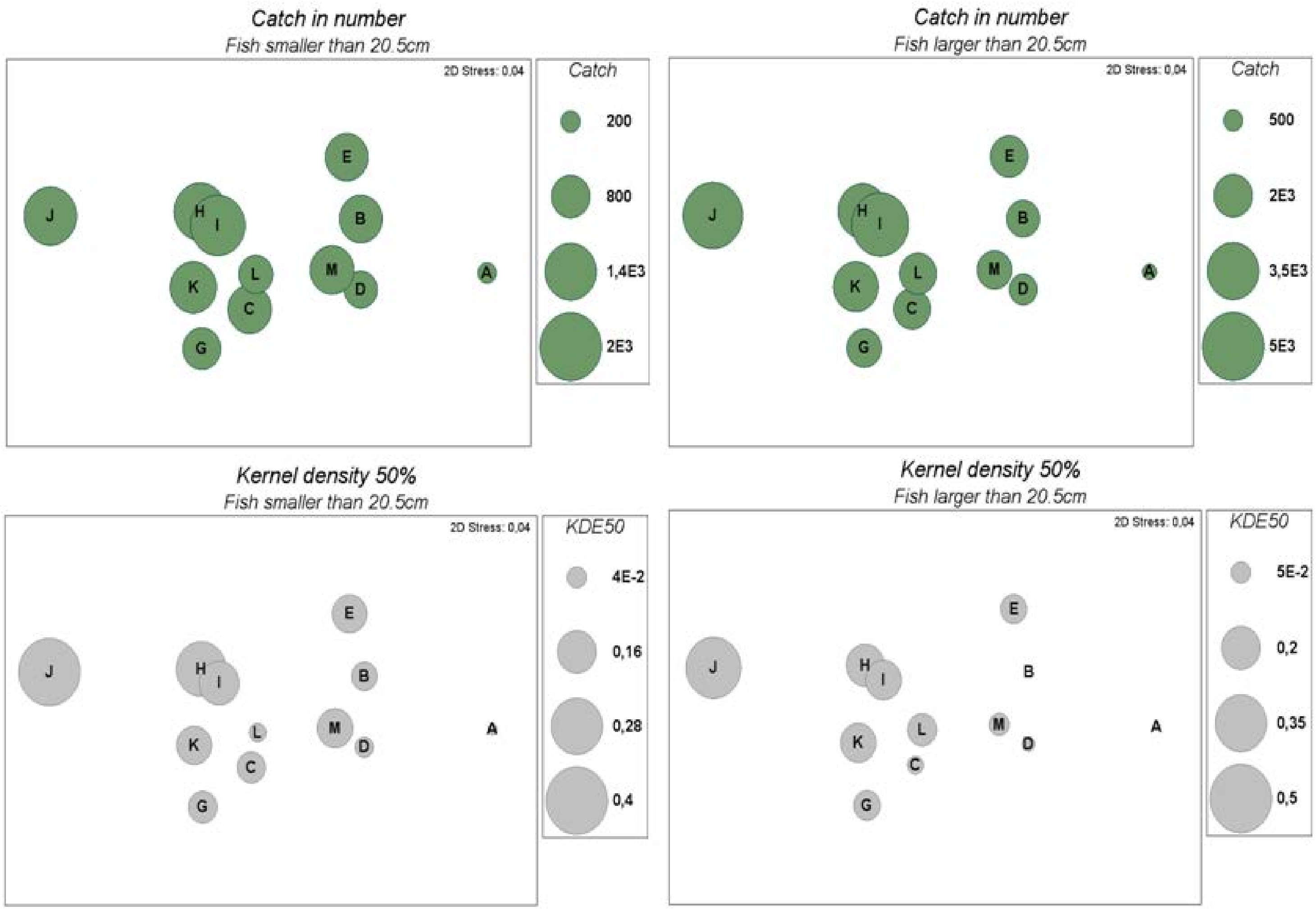

Figure 160. Multidimensional scaling plot of megahabitats based on American plaice spatial distribution and relative occurrence and abundance descriptors (27 descriptors). Fish smaller and fish larger than 20.5 cm are compared. Bubble size reflects mean catch in number in cells where the species is present (upper panels) and the proportion of cells within the 50% kernel density volume (lower panels) in cells where the species was present.

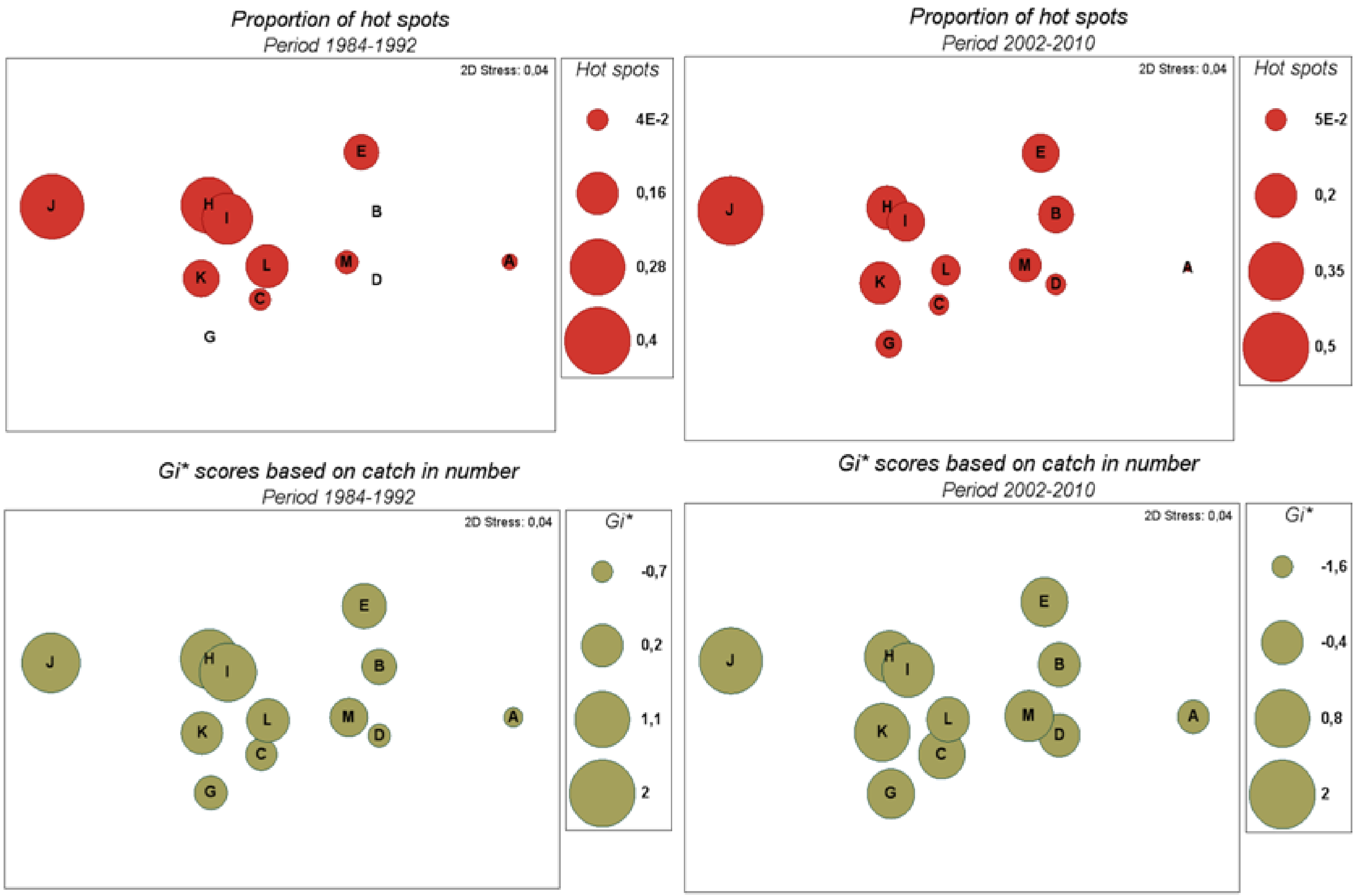

Figure 161. Multidimensional scaling plot of megahabitats based on American plaice spatial distribution and relative occurrence and abundance descriptors (27 descriptors). Two periods are compared (1984–1992 and 2002–2010). Bubble size reflects the proportion of cells classified as hot spots (upper panels) and local spatial autocorrelation G_i* statistic (lower panels) in cells where the species was present.

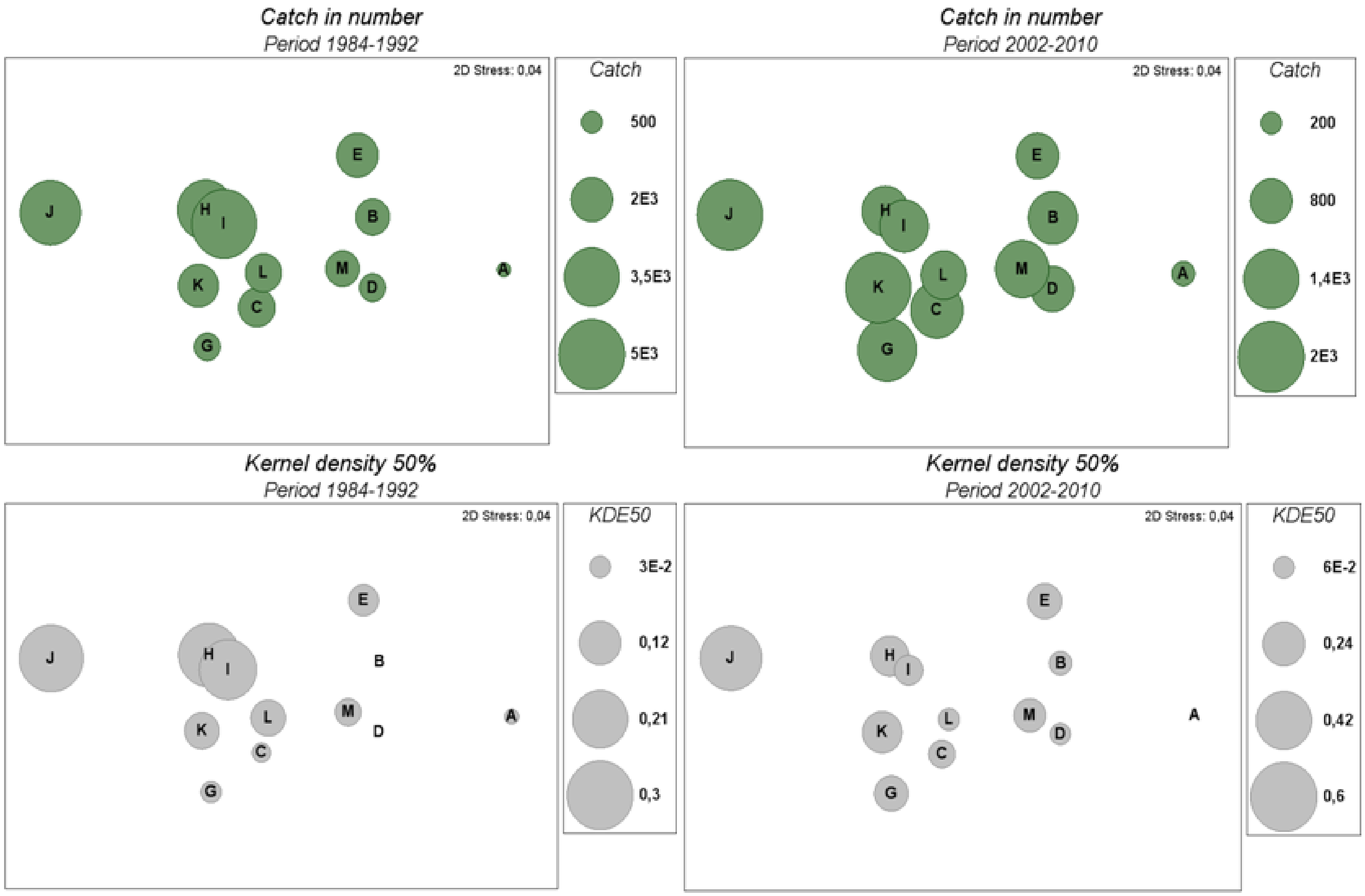

Figure 162. Multidimensional scaling plot of megahabitats based on American plaice spatial distribution and relative occurrence and abundance descriptors (27 descriptors). Two periods are compared (1984–1992 and 2002–2010). Bubble size reflects mean catch in number in cells where the species is present (upper panels) and the proportion of cells within the 50% kernel density volume (lower panels) in cells where the species was present.

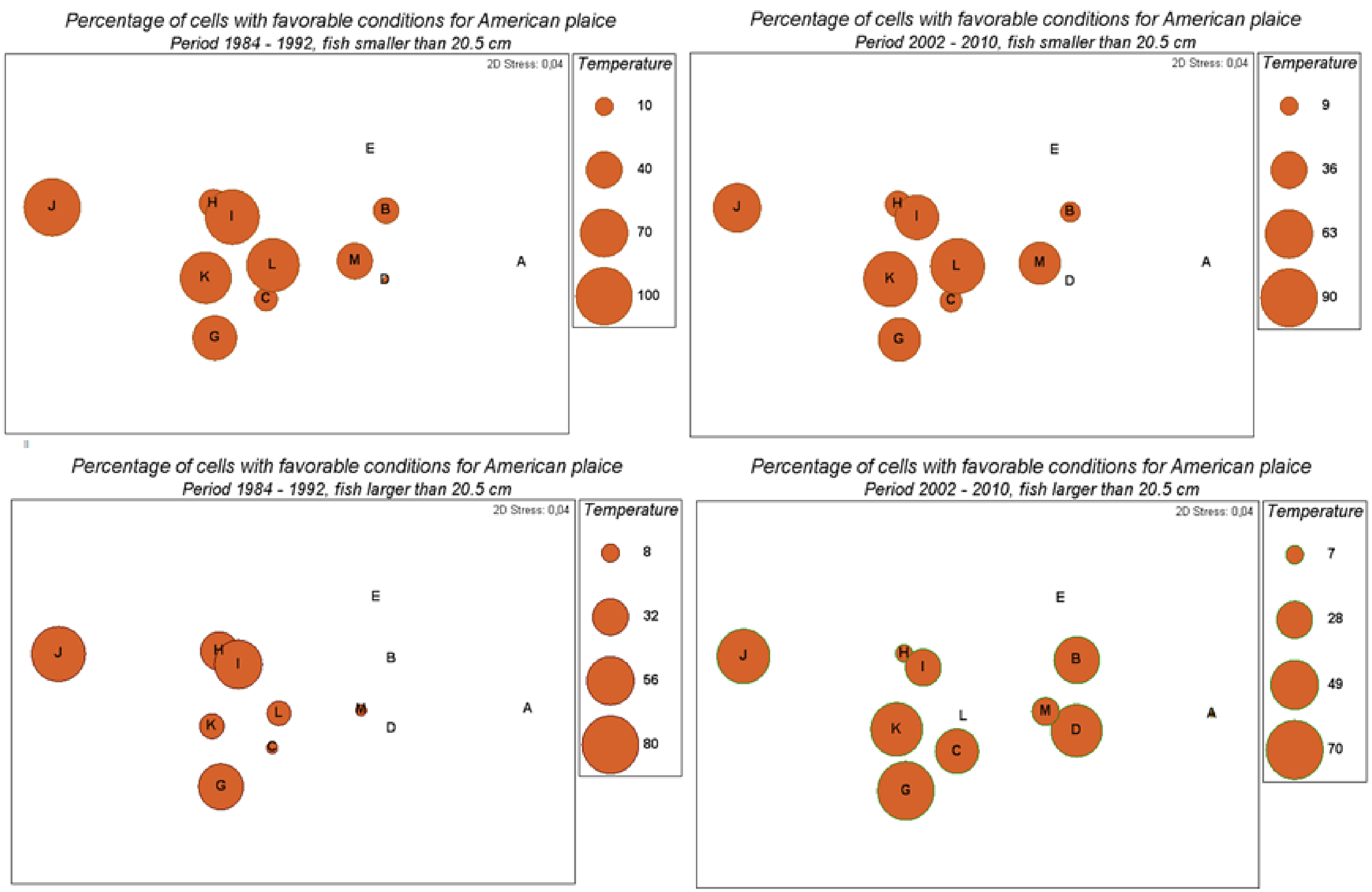

Figure 163. Multidimensional scaling plot of megahabitats based on American plaice spatial distribution and relative occurrence and abundance descriptors (27 descriptors) for two different time periods (1984–1992 and 2002–2010) and two different fish size categories (fish smaller and fish larger than 20.5 cm). Bubble size indicates the proportion of cells with temperature characteristics favourable to American plaice in each megahabitat, i.e., within the 25% and 75% percentiles. The parameter used in each panel varies and was selected from the forward selection regression as explaining the greatest proportion of the variance: upper panels: mean temperature at mean depth; lower left panel: mean temperature at maximum depth; lower right panel: mean temperature at minimum depth.

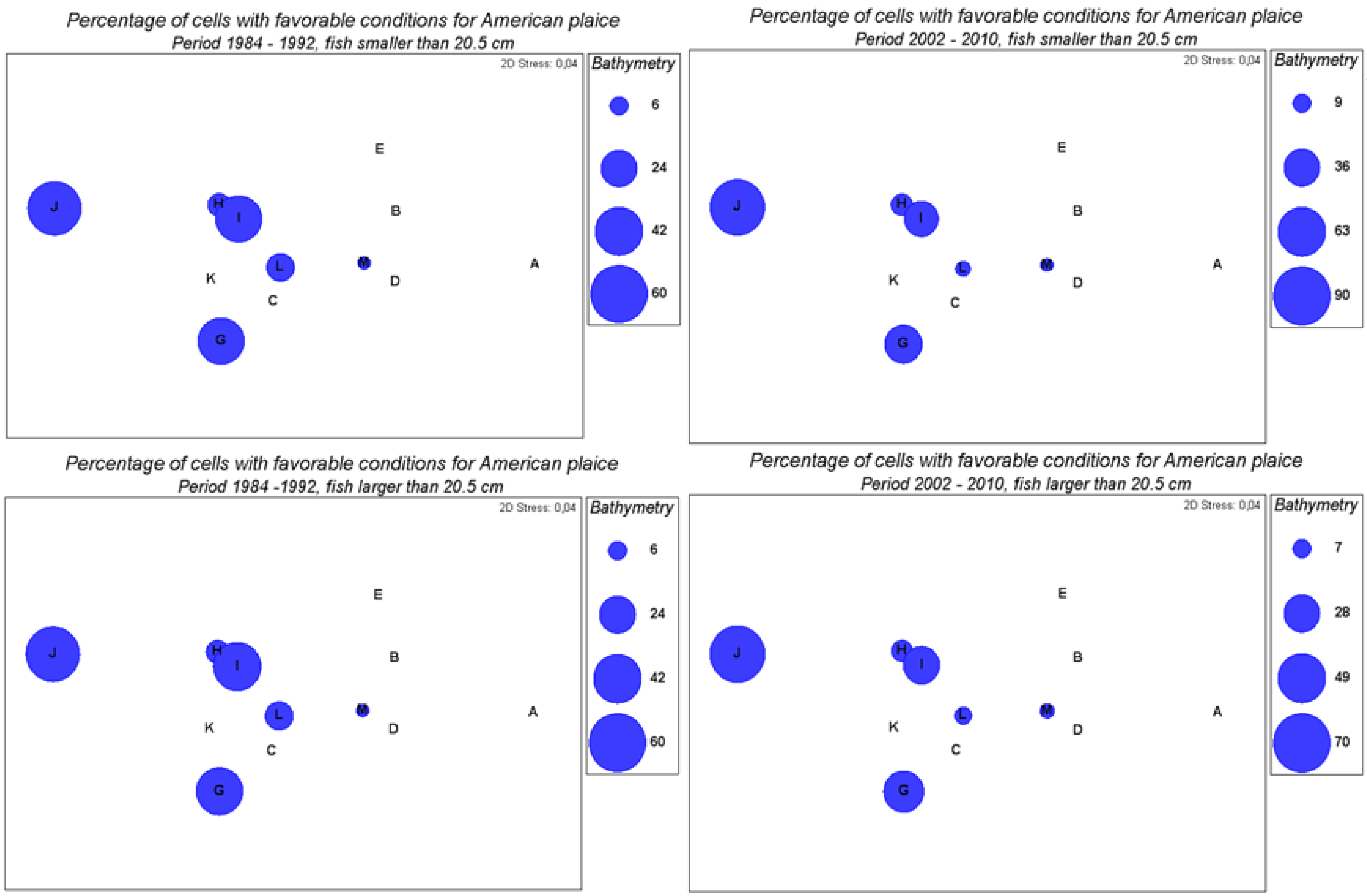

Figure 164. Multidimensional scaling plot of megahabitats based on American plaice spatial distribution and relative occurrence and abundance descriptors (27 descriptors) for two different time periods (1984–1992 and 2002–2010) and two different fish size categories (fish smaller and fish larger than 20.5 cm). Bubble size indicates the proportion of cells with depth characteristics (maximum cell depth) favourable to American plaice in each megahabitat, i.e., within the 25% and 75% percentiles.

.

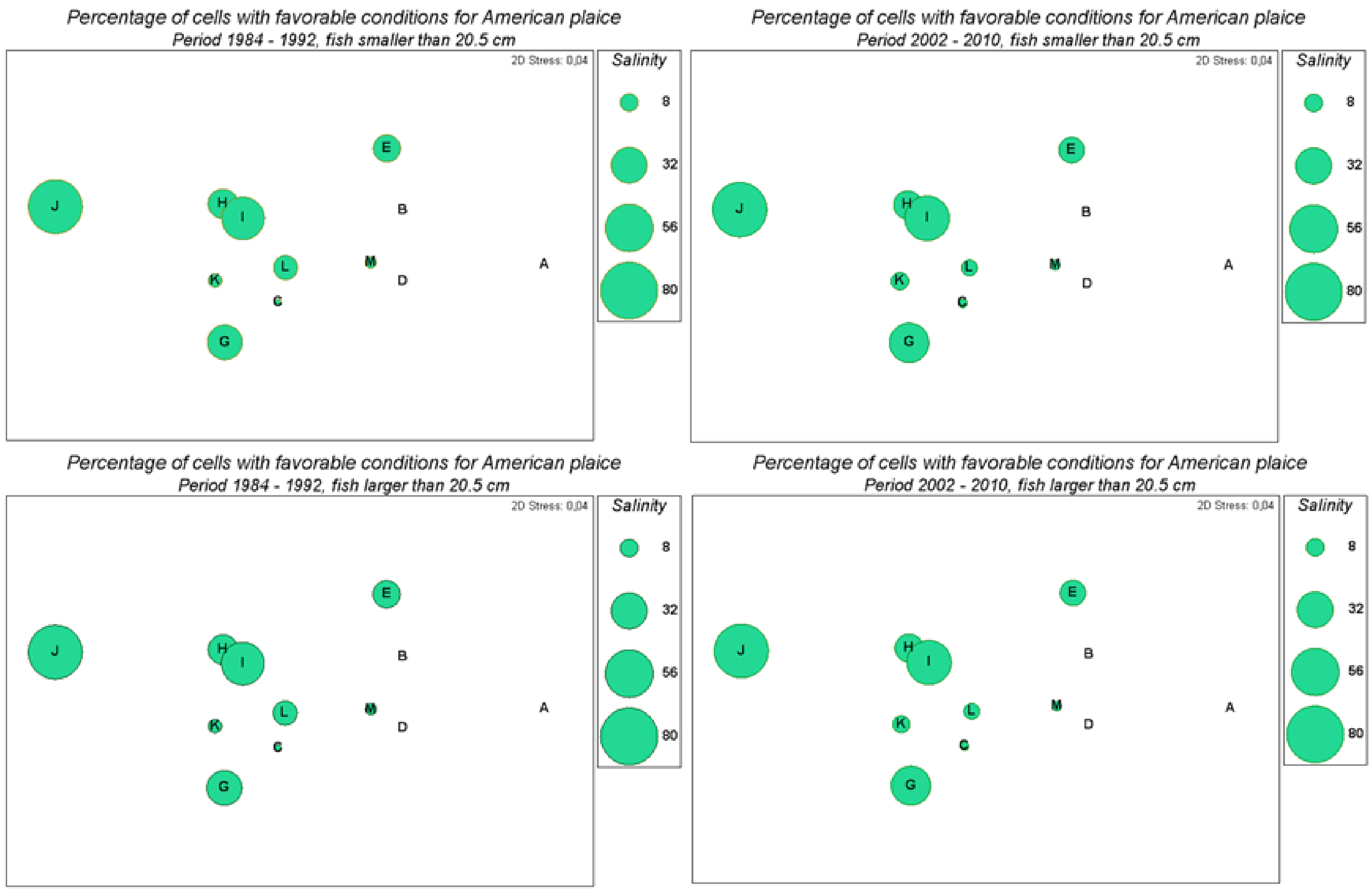

Figure 165. Multidimensional scaling plot of megahabitats based on American plaice spatial distribution and relative occurrence and abundance descriptors (27 descriptors) for two different time periods (1984–1992 and 2002–2010) and two different fish size categories (fish smaller and fish larger than 20.5 cm). Bubble size indicates the proportion of cells with salinity characteristics (maximum salinity at maximum cell depth) favourable to American plaice in each megahabitat, i.e., within the 25% and 75% percentiles.

Environmental relationships

Descriptive statistics

Environmental conditions associated with American plaice are summarized in Tables 124–153.

Table 124. Environmental conditions prevailing in hot spots and cold spots of American plaice distribution based on relative occurrence (1971–2010). Mean, median, and 5th, 25th, 75th, and 95th percentiles are shown for quantitative variables and cells where the local spatial autocorrelation G_i* statistic value was significant (>1.645 and <-1.645 for hot spots and cold spots, respectively).

	Hot spot						Cold spot					
Variable	Mean	5%	25%	Median	75%	95%	Mean	5%	25%	Median	75%	95%
MHVar_3x3	2.50	1.00	1.00	2.00	3.00	5.00	1.79	1.00	1.00	1.00	2.00	4.00
Sup_Protege	0.01	0.00	0.00	0.00	0.00	0.00	0.04	0.00	0.00	0.00	0.00	0.00
Sup_SemiExp	0.26	0.00	0.00	0.00	0.00	0.00	0.09	0.00	0.00	0.00	0.00	0.00
Cote_Dist	37525	4325	17960	34438	53121	84958	38811	3962	16782	36262	58107	83504
Bathy_Mean	-85.8	-204.5	-95.9	-67.9	-57.9	-40.0	-291.4	-468.0	-384.3	-327.9	-242.5	-18.9
Bathy_STD	10.4	1.6	3.0	4.9	11.2	36.9	16.3	2.6	5.7	10.7	20.7	49.0
Bathy_Max	-106.9	-250.9	-130.2	-79.7	-65.4	-49.2	-320.5	-487.1	-410.8	-358.3	-294.2	-27.4
Bathy_Min	-62.3	-143.0	-68.1	-57.0	-45.7	-7.5	-252.4	-445.9	-359.1	-287.0	-151.9	-2.5
Pente_Mean	0.28	0.06	0.10	0.14	0.30	1.00	0.36	0.07	0.14	0.27	0.48	0.98
Pente_STD	0.20	0.04	0.05	0.09	0.21	0.77	0.19	0.04	0.07	0.12	0.22	0.56
Pente_Min	0.01	0.00	0.00	0.01	0.01	0.06	0.06	0.00	0.01	0.02	0.06	0.26
Pente_Max	1.08	0.19	0.30	0.51	1.22	4.05	1.01	0.21	0.39	0.66	1.23	2.77
Geo2_Bosse	0.04	0.00	0.00	0.00	0.02	0.24	0.02	0.00	0.00	0.00	0.02	0.15
Geo2_Creux	0.04	0.00	0.00	0.00	0.03	0.23	0.03	0.00	0.00	0.00	0.03	0.15
Relief_var	2.75	1.00	1.00	1.00	5.00	7.00	2.80	1.00	1.00	2.00	4.50	6.00
SalMoyMoy	32.09	30.70	31.38	31.99	32.66	34.03	33.86	29.46	34.43	34.60	34.79	34.80
SalMinMoy	31.61	29.65	30.91	31.53	32.35	33.82	33.64	28.67	34.25	34.53	34.65	34.75
SalMaxMoy	32.50	31.13	32.01	32.31	33.02	34.22	34.10	30.04	34.58	34.67	34.85	35.04
SalMoyMin	31.57	29.21	31.25	31.54	32.03	33.38	33.58	29.21	33.43	34.55	34.77	34.80
SalMinMin	31.00	28.41	30.40	31.39	31.64	33.02	33.29	28.36	33.15	34.38	34.64	34.75
SalMaxMin	32.03	30.38	31.56	31.73	32.48	33.62	33.91	30.59	33.64	34.63	34.85	35.04
SalMoyMax	32.44	31.29	31.54	32.13	33.33	34.39	34.00	29.78	34.55	34.65	34.80	34.80
SalMinMax	31.97	30.40	30.91	31.64	32.94	34.25	33.82	29.11	34.38	34.60	34.71	34.75
SalMaxMax	32.86	31.57	32.16	32.51	33.48	34.48	34.20	30.73	34.63	34.72	34.85	35.04
TempMoyMoy	1.25	0.18	0.36	0.63	1.52	4.40	4.72	2.43	4.73	4.91	5.04	5.64
TempMinMoy	-0.05	-1.65	-0.95	-0.51	0.08	3.73	3.37	-1.54	4.14	4.36	4.54	4.90
TempMaxMoy	2.84	1.08	1.34	2.48	3.22	5.73	6.13	3.00	5.32	5.42	5.61	13.94
TempMoyMin	1.45	0.18	0.36	0.67	1.68	5.13	4.69	1.03	4.69	4.91	5.09	7.10
TempMinMin	-0.67	-1.65	-1.35	-0.92	-0.51	1.96	2.98	-1.54	1.58	4.31	4.54	4.74
TempMaxMin	3.87	1.16	1.94	2.64	4.69	12.30	6.58	2.34	5.29	5.42	5.61	17.25
TempMoyMax	1.50	0.18	0.53	0.63	2.41	4.47	4.63	2.35	4.73	4.91	4.92	5.13
TempMinMax	0.47	-1.65	-0.51	-0.28	1.93	3.97	3.53	-1.55	4.14	4.36	4.54	4.93
TempMaxMax	2.80	1.08	1.34	2.69	3.73	5.59	5.79	4.82	5.32	5.42	5.59	10.54

Table 125. Environmental conditions prevailing in hot spots and cold spots of American plaice distribution based on relative occurrence (1971–2010). Number of cells and proportion of cells meeting the classification criteria are shown for 10 binarybinary variables and cells where the local spatial autocorrelation G_i* statistic value was significant (>1.645 and <-1.645 for hot spots and cold spots, respectively).

	Hot spot		Cold spot	
Variable	Count	Proportion	Count	Proportion
Geo_Plateau	510	0.90	84	0.18
Geo_Talus	26	0.05	40	0.09
Geo_Chenal	28	0.05	339	0.73
O2_12	20	0.04	100	0.22
O2_34	60	0.11	239	0.52
O2_56	178	0.32	46	0.10
O2_78	306	0.54	78	0.17
Sed1_S<300	347	0.62	392	0.85
Sed1_S >300	217	0.38	71	0.15
Sed2_R	138	0.24	80	0.17

Table 126. Environmental conditions prevailing in hot spots and cold spots of American plaice distribution, based on relative occurrence (1984–2010). Mean, median, and 5th, 25th, 75th, and 95th percentiles are shown for quantitative variables and cells where the local spatial autocorrelation G_i* statistic value was significant (>1.645 and <-1.645 for hot spots and cold spots, respectively).

	Hot spot						Cold spot					
Variable	Mean	5%	25%	Median	75%	95%	Mean	5%	25%	Median	75%	95%
MHVar_3x3	2.54	1.00	1.00	2.00	4.00	5.00	1.76	1.00	1.00	1.00	2.00	4.00
Sup_Protege	0.01	0.00	0.00	0.00	0.00	0.00	0.04	0.00	0.00	0.00	0.00	0.00
Sup_SemiExp	0.26	0.00	0.00	0.00	0.00	0.00	0.09	0.00	0.00	0.00	0.00	0.00
Cote_Dist	37328	4511	18175	34142	52212	84958	39038	4471	17495	36420	58605	83184
Bathy_Mean	-85.9	-189.5	-99.3	-68.6	-58.4	-40.0	-293.9	-468.0	-384.4	-329.1	-250.8	-19.0
Bathy_STD	10.7	1.7	3.0	5.0	12.1	36.9	16.1	2.5	5.5	10.3	20.5	47.7
Bathy_Max	-108.0	-239.2	-137.0	-80.8	-65.5	-49.2	-322.8	-487.4	-410.8	-358.6	-297.3	-27.4
Bathy_Min	-61.8	-140.1	-68.1	-57.0	-45.9	-7.5	-255.5	-446.3	-360.0	-295.3	-163.3	-3.7
Pente_Mean	0.29	0.06	0.10	0.15	0.31	1.00	0.36	0.07	0.14	0.26	0.46	0.96
Pente_STD	0.21	0.04	0.05	0.10	0.23	0.77	0.18	0.037	0.065	0.117	0.217	0.517
Pente_Min	0.01	0.00	0.00	0.01	0.01	0.06	0.06	0.001	0.006	0.015	0.063	0.254
Pente_Max	1.13	0.19	0.30	0.52	1.32	4.05	0.97	0.21	0.36	0.64	1.21	2.66
Geo2_Bosse	0.04	0.00	0.00	0.00	0.03	0.24	0.02	0.00	0.00	0.00	0.01	0.14
Geo2_Creux	0.04	0.00	0.00	0.00	0.03	0.23	0.02	0.00	0.00	0.00	0.03	0.14
Relief_var	2.85	1.00	1.00	1.00	5.00	7.00	2.74	1.00	1.00	2.00	4.00	6.00
SalMoyMoy	32.10	30.69	31.38	31.99	32.71	34.03	33.87	29.46	34.45	34.60	34.79	34.80
SalMinMoy	31.62	29.65	30.91	31.53	32.35	33.82	33.66	28.67	34.32	34.53	34.65	34.75
SalMaxMoy	32.51	31.07	32.11	32.31	33.10	34.22	34.11	30.47	34.58	34.68	34.85	35.04
SalMoyMin	31.57	29.35	31.25	31.54	32.03	33.38	33.61	29.21	33.43	34.55	34.77	34.80
SalMinMin	31.01	28.41	30.40	31.39	31.64	33.02	33.32	28.36	33.22	34.39	34.64	34.75
SalMaxMin	32.03	30.38	31.56	31.73	32.51	33.62	33.93	30.59	33.75	34.66	34.85	35.04
SalMoyMax	32.46	31.29	31.54	32.13	33.38	34.39	34.01	29.78	34.55	34.65	34.80	34.80
SalMinMax	31.99	30.40	30.91	31.64	32.94	34.25	33.83	29.11	34.38	34.60	34.71	34.75
SalMaxMax	32.89	31.60	32.16	32.68	33.62	34.48	34.21	30.49	34.63	34.73	34.85	35.04
TempMoyMoy	1.23	0.18	0.36	0.63	1.52	4.40	4.74	2.52	4.81	4.91	5.04	5.64
TempMinMoy	-0.06	-1.65	-0.95	-0.51	0.19	3.73	3.43	-1.54	4.14	4.36	4.54	4.93
TempMaxMoy	2.81	1.08	1.34	2.48	3.00	5.73	6.11	4.32	5.32	5.42	5.61	13.94
TempMoyMin	1.41	0.18	0.36	0.57	1.64	5.13	4.74	1.83	4.69	4.91	5.11	6.98
TempMinMin	-0.70	-1.65	-1.36	-0.92	-0.51	1.96	3.05	-1.54	1.72	4.31	4.54	4.89
TempMaxMin	3.80	1.14	1.75	2.64	3.80	12.30	6.58	2.82	5.32	5.48	5.61	17.02
TempMoyMax	1.53	0.18	0.53	0.63	2.52	4.47	4.67	2.35	4.73	4.91	4.94	5.30
TempMinMax	0.51	-1.65	-0.51	-0.28	1.96	3.97	3.58	-1.55	4.14	4.36	4.54	4.93
TempMaxMax	2.83	1.08	1.34	2.77	4.38	5.59	5.81	5.10	5.32	5.42	5.61	10.54

Table 127. Environmental conditions prevailing in hot spots and cold spots of American plaice distribution based on relative occurrence (1984–2010). Number of cells and proportion of cells meeting the classification criteria are shown for 10 binarybinary variables and cells where the local spatial autocorrelation G_i* statistic value was significant (>1.645 and <-1.645 for hot spots and cold spots, respectively).

	Hot spot		Cold spot	
Variable	Count	Proportion	Count	Proportion
Geo_Plateau	519	0.91	76	0.17
Geo_Talus	30	0.05	41	0.09
Geo_Chenal	23	0.04	343	0.75
O2_12	16	0.03	97	0.21
O2_34	65	0.11	244	0.53
O2_56	188	0.33	44	0.10
O2_78	303	0.53	75	0.16
Sed1_S<300	356	0.62	391	0.85
Sed1_S >300	216	0.38	69	0.15
Sed2_R	147	0.26	83	0.18

Table 128. Environmental conditions prevailing in hot spots and cold spots of American plaice distribution based on catch in number (1984–2010). Mean, median, and 5th, 25th, 75th, and 95th percentiles are shown for quantitative variables and cells where the local spatial autocorrelation G_i* statistic value was significant (>1.645 and <-1.645 for hot spots and cold spots, respectively).

	Hot spot						Cold spot					
Variable	Mean	5%	25%	Median	75%	95%	Mean	5%	25%	Median	75%	95%
MHVar_3x3	2.18	1.00	1.00	2.00	3.00	4.00	1.55	1.00	1.00	1.00	2.00	3.00
Sup_Protege	0.04	0.00	0.00	0.00	0.00	0.00	0.003	0.00	0.00	0.00	0.00	0.00
Sup_SemiExp	0.32	0.00	0.00	0.00	0.00	0.00	0.004	0.00	0.00	0.00	0.00	0.00
Cote_Dist	37849	3640	14498	34217	56123	88985	49994	14472	30534	47748	69009	90572
Bathy_Mean	-71.0	-126.2	-78.2	-65.4	-55.2	-34.8	-326.6	-458.7	-380.7	-328.7	-278.9	-203.1
Bathy_STD	7.8	1.6	2.9	4.6	8.9	23.5	13.2	2.7	5.7	9.9	16.9	36.5
Bathy_Max	-87.6	-179.8	-94.3	-75.4	-64.0	-46.1	-350.6	-479.1	-407.9	-354.8	-301.7	-251.2
Bathy_Min	-53.3	-89.0	-63.7	-55.7	-41.9	-6.3	-294.5	-429.7	-353.8	-297.9	-249.8	-134.4
Pente_Mean	0.22	0.06	0.10	0.14	0.23	0.74	0.29	0.08	0.14	0.24	0.36	0.76
Pente_STD	0.15	0.037	0.052	0.085	0.166	0.447	0.15	0.039	0.070	0.112	0.185	0.365
Pente_Min	0.01	0.000	0.000	0.004	0.011	0.042	0.04	0.001	0.006	0.014	0.048	0.191
Pente_Max	0.82	0.19	0.30	0.46	0.92	2.51	0.79	0.23	0.39	0.62	0.98	1.89
Geo2_Bosse	0.025	0.000	0.000	0.000	0.010	0.167	0.011	0.000	0.000	0.000	0.005	0.061
Geo2_Creux	0.025	0.000	0.000	0.000	0.010	0.161	0.014	0.000	0.000	0.000	0.010	0.078
Relief_var	2.40	1.00	1.00	1.00	4.00	6.00	2.49	1.00	1.00	2.00	4.00	6.00
SalMoyMoy	31.73	29.78	31.29	31.99	32.13	33.31	34.45	34.05	34.54	34.60	34.77	34.80
SalMinMoy	31.19	29.11	30.70	31.48	31.64	33.10	34.32	33.77	34.38	34.53	34.65	34.75
SalMaxMoy	32.21	30.73	31.65	32.31	32.54	33.56	34.58	34.21	34.63	34.72	34.85	35.04
SalMoyMin	31.29	29.20	31.23	31.29	31.99	32.65	34.32	33.06	34.41	34.55	34.77	34.80
SalMinMin	30.68	28.36	29.72	30.91	31.53	32.10	34.16	32.72	34.25	34.42	34.64	34.75
SalMaxMin	31.81	30.30	31.56	31.73	32.31	32.82	34.49	33.31	34.58	34.66	34.85	35.04
SalMoyMax	32.13	31.24	31.38	32.03	32.66	34.00	34.50	34.39	34.55	34.65	34.79	34.80
SalMinMax	31.60	30.40	30.73	31.53	32.35	33.63	34.39	34.25	34.42	34.58	34.71	34.75
SalMaxMax	32.64	31.56	32.31	32.47	33.02	34.21	34.62	34.54	34.66	34.72	34.85	35.04
TempMoyMoy	1.18	0.18	0.30	0.59	1.32	4.56	4.95	4.68	4.81	4.92	5.12	5.34
TempMinMoy	-0.49	-1.66	-1.16	-0.51	-0.22	1.43	4.26	3.67	4.31	4.36	4.61	5.04
TempMaxMoy	3.23	1.09	1.34	2.35	3.59	10.54	5.69	5.10	5.32	5.42	5.61	5.90
TempMoyMin	1.64	0.18	0.36	0.82	1.65	6.46	4.81	3.93	4.81	4.91	5.12	5.34
TempMinMin	-0.92	-1.66	-1.55	-1.13	-0.51	0.15	4.07	0.64	4.14	4.36	4.61	4.93
TempMaxMin	4.56	1.34	2.16	2.64	5.59	15.16	5.61	4.38	5.32	5.42	5.58	5.90
TempMoyMax	1.14	0.18	0.53	0.59	1.52	4.40	4.95	4.69	4.87	4.92	5.09	5.34
TempMinMax	-0.09	-1.66	-0.51	-0.28	-0.15	3.67	4.29	4.02	4.31	4.44	4.61	5.04
TempMaxMax	2.71	1.08	1.34	2.30	2.97	5.59	5.64	5.14	5.32	5.42	5.61	5.90

Table 129. Environmental conditions prevailing in hot spots and cold spots of American plaice distribution based on catch in number (1984–2010). Number of cells and proportion of cells meeting the classification criteria are shown for 10 binarybinary variables and cells where the local spatial autocorrelation G_i* statistic value was significant (>1.645 and <-1.645 for hot spots and cold spots, respectively).

	Hot spot		Cold spot	
Variable	Count	Proportion	Count	Proportion
Geo_Plateau	352	0.95	18	0.04
Geo_Talus	12	0.03	17	0.04
Geo_Chenal	6	0.02	399	0.92
O2_12	3	0.01	115	0.26
O2_34	9	0.02	272	0.63
O2_56	111	0.30	32	0.07
O2_78	247	0.67	15	0.03
Sed1_S<300	251	0.68	425	0.98
Sed1_S >300	119	0.32	9	0.02
Sed2_R	74	0.20	46	0.11

Table 130. Environmental conditions prevailing in hot spots and cold spots of American plaice distribution based on relative occurrence (1984–1992). Mean, median, and 5th, 25th, 75th, and 95th percentiles are shown for quantitative variables and cells where the local spatial autocorrelation G_i* statistic value was significant (>1.645 and <-1.645 for hot spots and cold spots, respectively).

	Hot spot						Cold spot					
Variable	Mean	5%	25%	Median	75%	95%	Mean	5%	25%	Median	75%	95%
MHVar_3x3	2.45	1.00	1.00	2.00	3.00	5.00	1.82	1.00	1.00	1.00	2.00	4.00
Sup_Protege	0.01	0.00	0.00	0.00	0.00	0.00	0.01	0.00	0.00	0.00	0.00	0.00
Sup_SemiExp	0.16	0.00	0.00	0.00	0.00	0.00	0.09	0.00	0.00	0.00	0.00	0.00
Cote_Dist	37229	5556	18629	34933	51218	82412	42370	6858	22315	40821	61432	83240
Bathy_Mean	-90.4	-216.9	-99.3	-68.8	-58.2	-38.8	-310.5	-467.9	-393.1	-332.5	-272.0	-28.9
Bathy_STD	9.9	1.6	3.0	5.1	11.0	35.1	17.8	2.9	6.3	11.7	22.4	56.4
Bathy_Max	-110.6	-280.2	-132.0	-80.6	-65.5	-48.4	-342.6	-486.2	-411.1	-363.5	-305.4	-42.3
Bathy_Min	-66.8	-162.1	-70.9	-57.8	-47.1	-14.9	-268.3	-438.5	-363.7	-301.0	-205.9	-11.4
Pente_Mean	0.26	0.06	0.10	0.15	0.30	0.84	0.40	0.09	0.16	0.29	0.51	1.14
Pente_STD	0.19	0.04	0.05	0.10	0.21	0.57	0.21	0.04	0.08	0.14	0.25	0.59
Pente_Min	0.01	0.00	0.00	0.01	0.01	0.05	0.06	0.00	0.01	0.02	0.07	0.26
Pente_Max	1.02	0.19	0.30	0.50	1.27	3.22	1.10	0.24	0.42	0.77	1.32	3.02
Geo2_Bosse	0.03	0.00	0.00	0.00	0.02	0.19	0.03	0.00	0.00	0.000	0.02	0.17
Geo2_Creux	0.03	0.00	0.00	0.00	0.04	0.20	0.03	0.00	0.00	0.003	0.04	0.15
Relief_var	2.81	1.00	1.00	1.00	5.00	6.60	3.07	1.00	1.00	2.00	5.00	6.00
SalMoyMoy	32.11	30.69	31.38	31.99	32.66	34.16	34.21	30.08	34.46	34.63	34.80	34.80
SalMinMoy	31.64	29.58	30.73	31.53	32.35	34.00	34.04	29.11	34.33	34.53	34.65	34.75
SalMaxMoy	32.52	30.98	31.97	32.31	33.02	34.44	34.37	31.48	34.63	34.72	34.86	35.04
SalMoyMin	31.60	29.23	31.25	31.54	32.13	33.40	33.90	29.49	34.08	34.55	34.77	34.80
SalMinMin	31.05	28.41	30.40	31.39	31.64	33.15	33.66	28.42	33.81	34.42	34.65	34.75
SalMaxMin	32.05	30.38	31.56	31.73	32.51	33.70	34.13	30.88	34.36	34.66	34.85	35.04
SalMoyMax	32.45	31.24	31.54	32.13	33.33	34.40	34.33	31.12	34.60	34.67	34.80	34.80
SalMinMax	32.00	30.40	30.91	31.64	32.94	34.29	34.19	30.30	34.53	34.63	34.65	34.75
SalMaxMax	32.88	31.56	32.16	32.51	33.48	34.57	34.49	32.41	34.65	34.73	34.86	35.04
TempMoyMoy	1.42	0.18	0.36	0.75	1.96	4.56	4.61	0.82	4.81	4.91	5.01	5.34
TempMinMoy	0.09	-1.65	-0.92	-0.28	0.19	3.97	3.74	-1.27	4.14	4.35	4.54	4.90
TempMaxMoy	3.03	1.11	1.34	2.64	3.59	6.77	5.55	2.35	5.32	5.40	5.58	10.29
TempMoyMin	1.50	0.18	0.36	0.80	1.64	5.34	4.47	0.77	4.68	4.87	4.94	5.40
TempMinMin	-0.55	-1.65	-1.35	-0.92	-0.27	1.96	3.27	-1.39	3.67	4.31	4.54	4.74
TempMaxMin	3.79	1.16	2.00	2.64	4.69	11.43	5.82	1.98	5.23	5.40	5.61	13.64
TempMoyMax	1.60	0.18	0.53	0.75	2.41	5.13	4.70	3.83	4.81	4.91	4.94	5.13
TempMinMax	0.58	-1.46	-0.51	-0.28	1.93	4.90	3.92	-0.73	4.18	4.36	4.54	4.93
TempMaxMax	2.91	1.08	1.34	2.77	4.42	5.59	5.53	4.68	5.32	5.40	5.58	6.16

Table 131. Environmental conditions prevailing in hot spots and cold spots of American plaice distribution based on relative occurrence (1984–1992). Number of cells and proportion of cells meeting the classification criteria are shown for 10 binarybinary variables and cells where the local spatial autocorrelation G_i* statistic value was significant (>1.645 and <-1.645 for hot spots and cold spots, respectively).

	Hot spot		Cold spot	
Variable	Count	Proportion	Count	Proportion
Geo_Plateau	369	0.90	37	0.11
Geo_Talus	13	0.03	32	0.09
Geo_Chenal	27	0.07	268	0.80
O2_12	17	0.04	82	0.24
O2_34	49	0.12	195	0.58
O2_56	125	0.31	25	0.07
O2_78	218	0.53	35	0.10
Sed1_S<300	272	0.67	306	0.91
Sed1_S >300	137	0.33	31	0.09
Sed2_R	95	0.23	43	0.13

Table 132. Environmental conditions prevailing in hot spots of American plaice distribution based on catch in number (1984–1992). Mean, median, and 5th, 25th, 75th, and 95th percentiles are shown for quantitative variables and cells where the local spatial autocorrelation G_i* statistic value was significant (>1.645). No cold spots (G_i* statistic value <-1.645) were identified for this period.

	Hot spot						Cold spot					
Variable	Mean	5%	25%	Median	75%	95%	Mean	5%	25%	Median	75%	95%
MHVar_3x3	2.12	1.00	1.00	2.00	3.00	4.00	-	-	-	-	-	-
Sup_Protege	0.04	0.00	0.00	0.00	0.00	0.00	-	-	-	-	-	-
Sup_SemiExp	0.26	0.00	0.00	0.00	0.00	0.00	-	-	-	-	-	-
Cote_Dist	40463	4158	17590	38373	58298	88795	-	-	-	-	-	-
Bathy_Mean	-65.9	-97.2	-75.9	-66.3	-55.9	-33.9	-	-	-	-	-	-
Bathy_STD	6.8	1.7	2.9	4.5	8.6	18.1	-	-	-	-	-	-
Bathy_Max	-81.4	-127.8	-89.5	-78.0	-66.5	-52.7	-	-	-	-	-	-
Bathy_Min	-50.1	-76.4	-63.7	-57.1	-39.2	-6.9	-	-	-	-	-	-
Pente_Mean	0.19	0.06	0.10	0.14	0.23	0.45	-	-	-	-	-	-
Pente_STD	0.14	0.042	0.057	0.095	0.160	0.369	-	-	-	-	-	-
Pente_Min	0.01	0.000	0.000	0.003	0.010	0.025	-	-	-	-	-	-
Pente_Max	0.76	0.22	0.33	0.48	0.96	2.36	-	-	-	-	-	-
Geo2_Bosse	0.016	0.000	0.000	0.000	0.007	0.099	-	-	-	-	-	-
Geo2_Creux	0.017	0.000	0.000	0.000	0.010	0.108	-	-	-	-	-	-
Relief_var	2.33	1.00	1.00	1.00	4.00	6.00	-	-	-	-	-	-
SalMoyMoy	31.62	29.76	31.29	31.99	32.03	32.66	-	-	-	-	-	-
SalMinMoy	31.10	29.42	30.70	31.39	31.53	32.35	-	-	-	-	-	-
SalMaxMoy	32.09	30.38	31.73	32.31	32.47	33.02	-	-	-	-	-	-
SalMoyMin	31.07	28.61	30.69	31.29	31.99	32.07	-	-	-	-	-	-
SalMinMin	30.42	27.18	29.91	30.91	31.53	31.60	-	-	-	-	-	-
SalMaxMin	31.67	30.30	31.45	31.65	32.31	32.54	-	-	-	-	-	-
SalMoyMax	32.02	30.70	31.56	32.03	32.65	33.10	-	-	-	-	-	-
SalMinMax	31.49	30.38	30.73	31.53	32.10	32.94	-	-	-	-	-	-
SalMaxMax	32.47	31.03	32.16	32.36	33.02	33.39	-	-	-	-	-	-
TempMoyMoy	0.89	0.18	0.18	0.59	1.02	2.83	-	-	-	-	-	-
TempMinMoy	-0.68	-1.66	-1.16	-0.51	-0.28	0.18	-	-	-	-	-	-
TempMaxMoy	2.88	1.08	1.34	2.29	4.54	6.77	-	-	-	-	-	-
TempMoyMin	1.63	0.18	0.30	0.76	2.08	6.31	-	-	-	-	-	-
TempMinMin	-1.00	-1.66	-1.55	-1.16	-0.51	-0.22	-	-	-	-	-	-
TempMaxMin	4.58	1.34	2.00	2.64	5.59	13.00	-	-	-	-	-	-
TempMoyMax	0.78	0.18	0.30	0.59	0.93	2.52	-	-	-	-	-	-
TempMinMax	-0.36	-1.32	-0.51	-0.37	-0.17	1.03	-	-	-	-	-	-
TempMaxMax	2.21	1.07	1.34	2.00	2.77	5.09	-	-	-	-	-	-

Table 133. Environmental conditions prevailing in hot spots of American plaice distribution based on catch in number (1984–1992). Number of cells and proportion of cells meeting the classification criteria are shown for 10 binarybinary variables and cells where the local spatial autocorrelation G_i* statistic value was significant (>1.645). No cold spots (G_i* statistic value <-1.645) were identified for this period.

	Hot spot		Cold spot	
Variable	Count	Proportion	Count	Proportion
Geo_Plateau	172	0.99	-	-
Geo_Talus	1	0.01	-	-
Geo_Chenal	0	0.00	-	-
O2_12	0	0.00	-	-
O2_34	1	0.01	-	-
O2_56	50	0.29	-	-
O2_78	122	0.71	-	-
Sed1_S<300	123	0.71	-	-
Sed1_S >300	50	0.29	-	-
Sed2_R	24	0.14	-	-

Table 134. Environmental conditions prevailing in hot spots and cold spots of American plaice distribution based on relative occurrence (1984–1992, fish < 20.5 cm total length). Mean, median, and 5th, 25th, 75th, and 95th percentiles are shown for quantitative variables and cells where the local spatial autocorrelation G_i* statistic value was significant (>1.645 and <-1.645 for hot spots and cold spots, respectively).

	Hot spot						Cold spot					
Variable	Mean	5%	25%	Median	75%	95%	Mean	5%	25%	Median	75%	95%
MHVar_3x3	2.39	1.00	1.00	2.00	3.00	5.00	2.01	1.00	1.00	2.00	3.00	4.50
Sup_Protege	0.01	0.00	0.00	0.00	0.00	0.00	0.004	0.00	0.00	0.00	0.00	0.00
Sup_SemiExp	0.17	0.00	0.00	0.00	0.00	0.00	0.03	0.00	0.00	0.00	0.00	0.00
Cote_Dist	36519	5204	17694	34520	50282	81417	42202	7890	20452	40586	60768	85094
Bathy_Mean	-85.1	-196.0	-98.1	-67.5	-56.2	-34.2	-302.9	-438.0	-370.1	-314.1	-264.6	-77.1
Bathy_STD	8.9	1.6	3.0	5.2	10.2	29.6	20.6	3.3	6.9	12.9	24.5	69.6
Bathy_Max	-103.8	-231.4	-130.3	-79.0	-64.4	-44.0	-338.1	-471.6	-398.0	-345.6	-298.9	-115.5
Bathy_Min	-64.6	-161.5	-69.3	-57.0	-44.4	-9.6	-253.4	-421.4	-333.4	-273.3	-190.8	-19.0
Pente_Mean	0.24	0.06	0.10	0.15	0.28	0.77	0.44	0.09	0.18	0.30	0.55	1.36
Pente_STD	0.17	0.04	0.05	0.10	0.19	0.53	0.26	0.04	0.08	0.14	0.27	1.00
Pente_Min	0.01	0.00	0.00	0.01	0.01	0.04	0.06	0.00	0.01	0.02	0.07	0.27
Pente_Max	0.91	0.19	0.31	0.51	1.09	2.83	1.37	0.25	0.46	0.79	1.40	4.74
Geo2_Bosse	0.03	0.00	0.00	0.00	0.02	0.17	0.03	0.00	0.00	0.00	0.03	0.18
Geo2_Creux	0.03	0.00	0.00	0.00	0.03	0.17	0.04	0.00	0.00	0.002	0.04	0.23
Relief_var	2.69	1.00	1.00	1.00	5.00	6.00	3.20	1.00	1.00	2.00	5.00	7.00
SalMoyMoy	31.98	29.78	31.29	31.99	32.65	34.04	34.32	32.43	34.41	34.60	34.77	34.80
SalMinMoy	31.49	29.42	30.73	31.53	32.35	33.82	34.17	32.15	34.25	34.53	34.64	34.75
SalMaxMoy	32.42	30.73	31.69	32.31	33.00	34.22	34.47	32.64	34.58	34.66	34.85	35.04
SalMoyMin	31.51	29.20	31.25	31.54	32.12	33.38	33.89	30.44	34.06	34.49	34.65	34.80
SalMinMin	30.94	28.37	29.78	31.27	31.64	33.02	33.64	28.98	33.73	34.38	34.53	34.75
SalMaxMin	31.99	30.30	31.56	31.73	32.51	33.62	34.12	31.46	34.26	34.58	34.73	35.04
SalMoyMax	32.35	30.70	31.38	32.13	33.31	34.41	34.44	32.70	34.55	34.63	34.77	34.80
SalMinMax	31.87	30.34	30.73	31.64	32.94	34.29	34.32	32.48	34.38	34.55	34.65	34.75
SalMaxMax	32.81	31.07	32.16	32.51	33.48	34.57	34.57	32.92	34.63	34.72	34.85	35.04
TempMoyMoy	1.43	0.18	0.36	0.93	2.01	4.56	4.65	2.41	4.71	4.91	5.04	5.34
TempMinMoy	-0.04	-1.66	-1.15	-0.46	0.12	3.97	3.97	-0.62	4.14	4.36	4.61	4.99
TempMaxMoy	3.20	1.11	1.34	2.64	4.40	7.76	5.40	2.97	5.23	5.42	5.58	5.90
TempMoyMin	1.72	0.18	0.36	0.82	2.41	6.31	4.29	0.79	4.36	4.87	5.04	5.34
TempMinMin	-0.57	-1.65	-1.51	-0.92	-0.28	1.96	3.34	-1.30	3.60	4.32	4.54	4.90
TempMaxMin	4.25	1.11	2.00	2.64	4.76	13.93	5.37	1.67	5.10	5.37	5.58	6.88
TempMoyMax	1.60	0.18	0.53	0.93	2.41	5.13	4.75	4.47	4.81	4.91	5.03	5.34
TempMinMax	0.48	-1.66	-0.51	-0.28	1.43	4.90	4.09	-0.04	4.14	4.36	4.54	4.99
TempMaxMax	3.02	1.08	1.37	2.77	4.42	5.87	5.46	5.10	5.25	5.42	5.58	5.90

Table 135. Environmental conditions prevailing in hot spots and cold spots of American plaice distribution based on relative occurrence (1984–1992, fish < 20.5 cm total length). Number of cells and proportion of cells meeting the classification criteria are shown for 10 binarybinary variables and cells where the local spatial autocorrelation G_i* statistic value was significant (>1.645 and <-1.645 for hot spots and cold spots, respectively).

	Hot spot		Cold spot	
Variable	Count	Proportion	Count	Proportion
Geo_Plateau	389	0.92	29	0.07
Geo_Talus	14	0.03	46	0.12
Geo_Chenal	20	0.05	316	0.81
O2_12	10	0.02	127	0.32
O2_34	34	0.08	215	0.55
O2_56	132	0.31	26	0.07
O2_78	247	0.58	23	0.06
Sed1_S<300	280	0.66	366	0.94
Sed1_S >300	143	0.34	25	0.06
Sed2_R	109	0.26	59	0.15

Table 136. Environmental conditions prevailing in hot spots of American plaice distribution based on catch in number (1984–1992, fish < 20.5 cm total length). Mean, median, and 5th, 25th, 75th, and 95th percentiles are shown for quantitative variables and cells where the local spatial autocorrelation G_i* statistic value was significant (>1.645). No cold spots (G_i* statistic value <-1.645) were identified for this period.

	Hot spot						Cold spot					
Variable	Mean	5%	25%	Median	75%	95%	Mean	5%	25%	Median	75%	95%
MHVar_3x3	2.30	1.00	1.00	2.00	3.00	5.00	-	-	-	-	-	-
Sup_Protege	0.03	0.00	0.00	0.00	0.00	0.00	-	-	-	-	-	-
Sup_SemiExp	0.06	0.00	0.00	0.00	0.00	0.00	-	-	-	-	-	-
Cote_Dist	39462	3981	14220	36745	61868	90305	-	-	-	-	-	-
Bathy_Mean	-77.2	-156.2	-80.7	-68.9	-55.2	-34.0	-	-	-	-	-	-
Bathy_STD	7.9	2.2	3.6	5.7	10.0	21.2	-	-	-	-	-	-
Bathy_Max	-93.5	-208.9	-96.9	-82.0	-68.8	-48.6	-	-	-	-	-	-
Bathy_Min	-59.1	-116.2	-68.3	-59.0	-41.9	-6.2	-	-	-	-	-	-
Pente_Mean	0.20	0.07	0.11	0.16	0.24	0.48	-	-	-	-	-	-
Pente_STD	0.15	0.042	0.062	0.099	0.172	0.458	-	-	-	-	-	-
Pente_Min	0.009	0.000	0.000	0.003	0.010	0.044	-	-	-	-	-	-
Pente_Max	0.77	0.22	0.35	0.51	0.93	2.39	-	-	-	-	-	-
Geo2_Bosse	0.019	0.000	0.000	0.000	0.007	0.142	-	-	-	-	-	-
Geo2_Creux	0.019	0.000	0.000	0.000	0.015	0.100	-	-	-	-	-	-
Relief_var	2.39	1.00	1.00	1.00	3.50	6.00	-	-	-	-	-	-
SalMoyMoy	31.82	29.76	31.29	31.99	32.03	33.62	-	-	-	-	-	-
SalMinMoy	31.29	29.42	30.57	31.53	31.53	33.22	-	-	-	-	-	-
SalMaxMoy	32.27	30.38	31.97	32.31	32.57	33.97	-	-	-	-	-	-
SalMoyMin	31.30	28.61	30.70	31.54	31.99	32.94	-	-	-	-	-	-
SalMinMin	30.70	27.18	29.91	31.39	31.53	32.78	-	-	-	-	-	-
SalMaxMin	31.87	30.30	31.45	31.97	32.31	33.45	-	-	-	-	-	-
SalMoyMax	32.24	30.70	31.99	32.03	32.66	34.16	-	-	-	-	-	-
SalMinMax	31.75	30.34	31.27	31.53	32.35	33.97	-	-	-	-	-	-
SalMaxMax	32.68	30.98	32.31	32.51	33.02	34.33	-	-	-	-	-	-
TempMoyMoy	1.19	0.18	0.18	0.63	1.58	4.56	-	-	-	-	-	-
TempMinMoy	-0.41	-1.80	-1.16	-0.51	-0.28	2.29	-	-	-	-	-	-
TempMaxMoy	3.09	1.08	1.34	2.29	4.62	6.77	-	-	-	-	-	-
TempMoyMin	1.76	0.18	0.18	1.02	2.83	6.31	-	-	-	-	-	-
TempMinMin	-0.71	-1.66	-1.35	-0.79	-0.51	0.89	-	-	-	-	-	-
TempMaxMin	4.54	1.34	1.34	2.60	5.59	13.28	-	-	-	-	-	-
TempMoyMax	1.13	0.18	0.30	0.59	1.52	4.61	-	-	-	-	-	-
TempMinMax	-0.08	-1.66	-0.59	-0.37	-0.10	4.08	-	-	-	-	-	-
TempMaxMax	2.52	1.07	1.34	1.65	3.70	5.60	-	-	-	-	-	-

Table 137. Environmental conditions prevailing in hot spots of American plaice distribution based on catch in number (1984–1992, fish < 20.5 cm total length). Number of cells and proportion of cells meeting the classification criteria are shown for 10 binarybinary variables and cells where the local spatial autocorrelation G_i* statistic value was significant (>1.645). No cold spots (G_i* statistic value <-1.645) were identified for this period.

	Hot spot		Cold spot	
Variable	Count	Proportion	Count	Proportion
Geo_Plateau	129	0.96	-	-
Geo_Talus	1	0.01	-	-
Geo_Chenal	5	0.04	-	-
O2_12	5	0.04	-	-
O2_34	3	0.02	-	-
O2_56	40	0.30	-	-
O2_78	87	0.64	-	-
Sed1_S<300	115	0.85	-	-
Sed1_S >300	20	0.15	-	-
Sed2_R	8	0.06	-	-

Table 138. Environmental conditions prevailing in hot spots and cold spots of American plaice distribution based on relative occurrence (1984–1992, fish > 20.5 cm total length). Mean, median, and 5th, 25th, 75th, and 95th percentiles are shown for quantitative variables and cells where the local spatial autocorrelation G_i* statistic value was significant (>1.645 and <-1.645 for hot spots and cold spots, respectively).

	Hot spot						Cold spot					
Variable	Mean	5%	25%	Median	75%	95%	Mean	5%	25%	Median	75%	95%
MHVar_3x3	2.43	1.00	1.00	2.00	3.00	5.00	1.77	1.00	1.00	1.00	2.00	4.00
Sup_Protege	0.001	0.00	0.00	0.00	0.00	0.00	0.01	0.00	0.00	0.00	0.00	0.00
Sup_SemiExp	0.12	0.00	0.00	0.00	0.00	0.00	0.10	0.00	0.00	0.00	0.00	0.00
Cote_Dist	38290	7250	20792	36080	52335	82600	45195	6898	24966	45570	65537	86080
Bathy_Mean	-88.6	-213.2	-97.0	-68.4	-57.7	-39.1	-304.2	-452.1	-380.8	-326.6	-266.2	-24.3
Bathy_STD	9.4	1.6	3.0	5.2	10.6	29.6	17.3	2.8	6.1	11.9	20.9	58.8
Bathy_Max	-107.7	-251.8	-130.6	-80.8	-65.4	-49.0	-335.3	-474.1	-409.1	-356.3	-293.1	-34.5
Bathy_Min	-66.6	-163.7	-69.9	-57.3	-46.2	-11.0	-262.9	-425.1	-352.3	-282.5	-208.4	-10.7
Pente_Mean	0.24	0.06	0.10	0.15	0.28	0.77	0.38	0.09	0.16	0.28	0.49	1.14
Pente_STD	0.18	0.04	0.05	0.10	0.19	0.53	0.19	0.04	0.08	0.13	0.23	0.55
Pente_Min	0.01	0.00	0.00	0.01	0.01	0.05	0.06	0.00	0.01	0.02	0.06	0.23
Pente_Max	0.95	0.20	0.31	0.52	1.09	2.86	1.01	0.23	0.42	0.74	1.24	2.67
Geo2_Bosse	0.02	0.00	0.00	0.00	0.02	0.15	0.02	0.00	0.00	0.00	0.02	0.14
Geo2_Creux	0.03	0.00	0.00	0.00	0.03	0.16	0.03	0.00	0.00	0.00	0.03	0.15
Relief_var	2.66	1.00	1.00	1.00	5.00	6.00	2.98	1.00	1.00	2.00	5.00	6.00
SalMoyMoy	32.08	30.69	31.38	31.99	32.65	34.16	34.18	29.70	34.49	34.60	34.77	34.80
SalMinMoy	31.61	29.65	30.73	31.53	32.35	34.00	34.02	28.92	34.37	34.53	34.65	34.75
SalMaxMoy	32.49	30.98	31.97	32.31	32.99	34.44	34.35	30.85	34.58	34.69	34.85	35.04
SalMoyMin	31.59	29.20	31.25	31.54	32.13	33.41	33.89	29.25	34.08	34.55	34.77	34.80
SalMinMin	31.02	28.41	30.39	31.39	31.64	33.15	33.66	28.42	33.81	34.41	34.64	34.75
SalMaxMin	32.04	30.38	31.56	31.73	32.51	33.71	34.13	30.74	34.32	34.63	34.85	35.04
SalMoyMax	32.43	31.25	31.54	32.13	33.21	34.40	34.30	29.90	34.55	34.65	34.80	34.80
SalMinMax	31.96	30.40	30.91	31.64	32.94	34.25	34.16	29.54	34.42	34.60	34.71	34.75
SalMaxMax	32.85	31.56	32.16	32.51	33.58	34.56	34.45	30.73	34.65	34.73	34.85	35.04
TempMoyMoy	1.30	0.18	0.36	0.67	1.65	4.56	4.75	2.52	4.81	4.92	5.12	5.42
TempMinMoy	-0.02	-1.65	-0.95	-0.37	0.03	3.86	3.84	-1.30	4.18	4.36	4.61	4.93
TempMaxMoy	2.92	1.08	1.34	2.64	3.59	6.41	5.72	2.97	5.32	5.42	5.61	10.81
TempMoyMin	1.50	0.18	0.36	0.71	1.96	5.59	4.61	0.98	4.69	4.91	5.12	6.19
TempMinMin	-0.56	-1.65	-1.35	-0.92	-0.28	1.96	3.39	-1.39	3.67	4.32	4.60	4.90
TempMaxMin	3.80	1.16	2.00	2.64	4.69	13.00	5.96	2.35	5.23	5.42	5.61	13.94
TempMoyMax	1.50	0.18	0.53	0.65	2.36	4.69	4.77	4.54	4.81	4.91	5.03	5.34
TempMinMax	0.47	-1.65	-0.51	-0.28	1.03	4.15	3.96	-0.75	4.31	4.36	4.54	4.93
TempMaxMax	2.81	1.07	1.34	2.77	4.38	5.59	5.64	5.10	5.32	5.42	5.61	7.76

Table 139. Environmental conditions prevailing in hot spots and cold spots of American plaice distribution based on relative occurrence (1984–1992, fish > 20.5 cm total length). Number of cells and proportion of cells meeting the classification criteria are shown for 10 binary variables and cells where the local spatial autocorrelation G_i* statistic value was significant (>1.645 and <-1.645 for hot spots and cold spots, respectively).

	Hot spot		Cold spot	
Variable	Count	Proportion	Count	Proportion
Geo_Plateau	391	0.92	33	0.10
Geo_Talus	10	0.02	30	0.09
Geo_Chenal	23	0.05	253	0.80
O2_12	18	0.04	68	0.22
O2_34	36	0.08	193	0.61
O2_56	138	0.33	24	0.08
O2_78	232	0.55	31	0.10
Sed1_S<300	278	0.66	290	0.92
Sed1_S >300	146	0.34	26	0.08
Sed2_R	115	0.27	42	0.13

Table 140. Environmental conditions prevailing in hot spots of American plaice distribution based on catch in number (1984–1992, fish > 20.5 cm total length). Mean, median, and 5th, 25th, 75th, and 95th percentiles are shown for quantitative variables and cells where the local spatial autocorrelation G_i* statistic value was significant (>1.645). No cold spots (G_i* statistic value <-1.645) were identified for this period.

	Hot spot						Cold spot					
Variable	Mean	5%	25%	Median	75%	95%	Mean	5%	25%	Median	75%	95%
MHVar_3x3	2.17	1.00	1.00	2.00	3.00	5.00	-	-	-	-	-	-
Sup_Protege	0.02	0.00	0.00	0.00	0.00	0.00	-	-	-	-	-	-
Sup_SemiExp	0.25	0.00	0.00	0.00	0.00	0.00	-	-	-	-	-	-
Cote_Dist	39119	4878	17614	37499	55837	84523	-	-	-	-	-	-
Bathy_Mean	-72.6	-110.0	-77.0	-66.7	-56.9	-33.2	-	-	-	-	-	-
Bathy_STD	7.5	1.7	3.1	4.9	9.6	21.6	-	-	-	-	-	-
Bathy_Max	-89.8	-159.3	-92.9	-78.7	-68.6	-51.6	-	-	-	-	-	-
Bathy_Min	-55.1	-86.2	-64.0	-57.2	-38.9	-7.3	-	-	-	-	-	-
Pente_Mean	0.21	0.07	0.11	0.15	0.25	0.51	-	-	-	-	-	-
Pente_STD	0.149	0.043	0.059	0.100	0.178	0.486	-	-	-	-	-	-
Pente_Min	0.008	0.000	0.001	0.005	0.011	0.030	-	-	-	-	-	-
Pente_Max	0.83	0.23	0.35	0.51	1.03	2.45	-	-	-	-	-	-
Geo2_Bosse	0.020	0.000	0.000	0.000	0.007	0.135	-	-	-	-	-	-
Geo2_Creux	0.022	0.000	0.000	0.000	0.021	0.124	-	-	-	-	-	-
Relief_var	2.49	1.00	1.00	1.00	4.00	6.00	-	-	-	-	-	-
SalMoyMoy	31.70	29.76	31.29	31.99	32.03	32.77	-	-	-	-	-	-
SalMinMoy	31.20	29.42	30.70	31.39	31.53	32.51	-	-	-	-	-	-
SalMaxMoy	32.14	30.38	31.60	32.31	32.47	33.39	-	-	-	-	-	-
SalMoyMin	31.15	28.61	30.64	31.29	31.99	32.41	-	-	-	-	-	-
SalMinMin	30.54	27.18	29.91	30.91	31.53	32.15	-	-	-	-	-	-
SalMaxMin	31.71	30.30	31.45	31.63	32.31	32.61	-	-	-	-	-	-
SalMoyMax	32.09	30.70	31.56	32.03	32.65	33.46	-	-	-	-	-	-
SalMinMax	31.57	30.39	30.73	31.53	32.10	32.94	-	-	-	-	-	-
SalMaxMax	32.53	31.05	32.16	32.36	33.02	33.64	-	-	-	-	-	-
TempMoyMoy	1.01	0.18	0.18	0.56	1.02	4.29	-	-	-	-	-	-
TempMinMoy	-0.48	-1.65	-1.16	-0.51	-0.28	0.64	-	-	-	-	-	-
TempMaxMoy	2.91	1.24	1.34	2.30	4.54	6.77	-	-	-	-	-	-
TempMoyMin	1.69	0.18	0.36	0.76	2.83	6.31	-	-	-	-	-	-
TempMinMin	-0.87	-1.65	-1.55	-1.16	-0.51	0.58	-	-	-	-	-	-
TempMaxMin	4.52	1.34	2.00	2.64	5.75	13.00	-	-	-	-	-	-
TempMoyMax	0.90	0.18	0.30	0.59	0.93	2.83	-	-	-	-	-	-
TempMinMax	-0.15	-1.16	-0.51	-0.37	-0.15	1.99	-	-	-	-	-	-
TempMaxMax	2.29	1.07	1.34	2.00	2.77	5.15	-	-	-	-	-	-

Table 141. Environmental conditions prevailing in hot spots of American plaice distribution based on catch in number (1984–1992, fish > 20.5 cm total length). Number of cells and proportion of cells meeting the classification criteria are shown for 10 binary variables and cells where the local spatial autocorrelation G_i* statistic value was significant (>1.645). No cold spots (G_i* statistic value <-1.645) were identified for this period.

	Hot spot		Cold spot	
Variable	Count	Proportion	Count	Proportion
Geo_Plateau	170	0.97	-	-
Geo_Talus	1	0.01	-	-
Geo_Chenal	5	0.03	-	-
O2_12	5	0.03	-	-
O2_34	4	0.02	-	-
O2_56	48	0.27	-	-
O2_78	119	0.68	-	-
Sed1_S<300	119	0.68	-	-
Sed1_S >300	57	0.32	-	-
Sed2_R	32	0.18	-	-

Table 142. Environmental conditions prevailing in hot spots and cold spots of American plaice distribution based on relative occurrence (2002–2010). Mean, median, and 5th, 25th, 75th, and 95th percentiles are shown for quantitative variables and cells where the local spatial autocorrelation G_i* statistic value was significant (>1.645 and <-1.645 for hot spots and cold spots, respectively).

	Hot spot						Cold spot					
Variable	Mean	5%	25%	Median	75%	95%	Mean	5%	25%	Median	75%	95%
MHVar_3x3	2.10	1.00	1.00	2.00	3.00	4.00	1.70	1.00	1.00	1.00	2.00	3.00
Sup_Protege	0.00	0.00	0.00	0.00	0.00	0.00	0.07	0.00	0.00	0.00	0.00	0.00
Sup_SemiExp	0.00	0.00	0.00	0.00	0.00	0.00	0.15	0.00	0.00	0.00	0.00	0.00
Cote_Dist	49476	20114	34843	44760	64849	89048	36470	3553	13177	36263	56614	76098
Bathy_Mean	-91.2	-243.8	-95.5	-69.3	-60.9	-50.4	-266.3	-481.1	-405.6	-334.2	-32.6	-17.2
Bathy_STD	7.1	1.6	2.7	4.7	8.7	21.1	13.5	2.3	4.5	8.0	16.8	41.5
Bathy_Max	-107.2	-272.1	-119.0	-80.7	-68.1	-59.2	-291.1	-497.5	-426.6	-376.2	-45.1	-24.9
Bathy_Min	-75.8	-194.0	-76.1	-59.9	-55.0	-41.7	-233.6	-461.8	-379.0	-280.4	-24.7	-2.2
Pente_Mean	0.19	0.07	0.09	0.15	0.24	0.45	0.30	0.06	0.12	0.20	0.37	0.84
Pente_STD	0.12	0.04	0.05	0.09	0.15	0.27	0.14	0.03	0.06	0.09	0.19	0.37
Pente_Min	0.01	0.00	0.00	0.00	0.01	0.05	0.05	0.00	0.01	0.01	0.06	0.24
Pente_Max	0.68	0.19	0.29	0.48	0.80	1.55	0.79	0.18	0.31	0.53	0.95	2.22
Geo2_Bosse	0.01	0.00	0.00	0.00	0.005	0.05	0.02	0.00	0.00	0.00	0.01	0.10
Geo2_Creux	0.01	0.00	0.00	0.00	0.008	0.07	0.02	0.00	0.00	0.00	0.01	0.11
Relief_var	2.21	1.00	1.00	1.00	3.00	6.00	2.36	1.00	1.00	1.00	3.75	6.00
SalMoyMoy	32.21	31.25	31.38	31.99	32.66	34.40	33.27	29.46	30.47	34.65	34.80	34.80
SalMinMoy	31.71	29.65	30.91	31.53	32.35	34.29	32.96	28.67	29.91	34.53	34.71	34.76
SalMaxMoy	32.61	31.56	32.16	32.31	33.02	34.57	33.61	30.04	31.48	34.78	34.87	35.04
SalMoyMin	31.94	31.25	31.29	31.84	32.13	34.02	33.05	29.21	30.08	34.55	34.79	34.80
SalMinMin	31.44	29.65	30.91	31.39	31.84	33.69	32.66	28.21	29.54	34.38	34.65	34.76
SalMaxMin	32.28	31.56	31.65	32.20	32.54	34.20	33.49	30.04	31.48	34.66	34.86	35.04
SalMoyMax	32.46	31.32	31.99	32.13	32.71	34.41	33.41	29.78	31.29	34.77	34.80	34.80
SalMinMax	31.98	30.73	31.53	31.64	32.35	34.29	33.16	29.03	30.70	34.65	34.71	34.75
SalMaxMax	32.90	32.16	32.31	32.51	33.45	34.57	33.72	30.49	31.60	34.83	34.88	35.04
TempMoyMoy	1.07	0.18	0.18	0.56	0.98	5.12	4.69	2.35	4.69	4.91	5.00	5.64
TempMinMoy	0.05	-1.65	-0.51	-0.37	-0.15	4.51	2.67	-1.64	-1.06	4.31	4.54	4.74
TempMaxMoy	2.43	1.07	1.34	2.30	2.77	5.48	6.81	5.01	5.32	5.42	7.04	13.94
TempMoyMin	1.00	0.18	0.36	0.42	1.32	4.40	4.90	2.39	4.69	4.92	5.17	7.08
TempMinMin	-0.46	-1.65	-1.17	-0.92	-0.51	3.75	2.41	-1.64	-1.30	4.31	4.54	4.74
TempMaxMin	2.70	1.07	1.34	2.30	2.99	5.59	7.62	3.16	5.32	5.42	9.66	17.25
TempMoyMax	1.31	0.18	0.53	0.59	1.64	5.13	4.36	0.56	4.63	4.84	4.92	5.30
TempMinMax	0.43	-1.16	-0.51	-0.28	0.08	4.90	2.71	-1.65	-0.27	4.31	4.46	4.69
TempMaxMax	2.49	1.07	1.34	2.30	2.97	5.59	6.10	2.64	5.32	5.37	5.61	10.54

Table 143. Environmental conditions prevailing in hot spots and cold spots of American plaice distribution based on relative occurrence (2002–2010). Number of cells and proportion of cells meeting the classification criteria are shown for 10 binary variables and cells where the local spatial autocorrelation G_i* statistic value was significant (>1.645 and <-1.645 for hot spots and cold spots, respectively).

	Hot spot		Cold spot	
Variable	Count	Proportion	Count	Proportion
Geo_Plateau	193	0.92	72	0.32
Geo_Talus	1	0.00	13	0.06
Geo_Chenal	15	0.07	141	0.62
O2_12	7	0.03	16	0.07
O2_34	16	0.08	112	0.50
O2_56	69	0.33	27	0.12
O2_78	117	0.56	71	0.31
Sed1_S<300	126	0.60	168	0.74
Sed1_S >300	83	0.40	58	0.26
Sed2_R	59	0.28	66	0.29

Table 144. Environmental conditions prevailing in hot spots and cold spots of American plaice distribution based on catch in number (2002–2010). Mean, median, and 5th, 25th, 75th, and 95th percentiles are shown for quantitative variables and cells where the local spatial autocorrelation G_i* statistic value was significant (>1.645 and <-1.645 for hot spots and cold spots, respectively).

	Hot spot						Cold spot					
Variable	Mean	5%	25%	Median	75%	95%	Mean	5%	25%	Median	75%	95%
MHVar_3x3	2.10	1.00	1.00	2.00	3.00	4.00	1.30	1.00	1.00	1.00	1.00	2.00
Sup_Protege	0.02	0.00	0.00	0.00	0.00	0.00	0.01	0.00	0.00	0.00	0.00	0.00
Sup_SemiExp	0.24	0.00	0.00	0.00	0.00	0.00	0.01	0.00	0.00	0.00	0.00	0.00
Cote_Dist	39697	5574	18354	36487	56101	88668	46219	11873	33035	45550	60185	83043
Bathy_Mean	-73.9	-135.1	-79.1	-66.6	-58.0	-40.4	-338.4	-479.3	-401.8	-357.1	-310.7	-19.2
Bathy_STD	7.6	1.6	2.6	4.3	8.0	26.8	11.2	3.0	5.9	8.7	15.3	24.6
Bathy_Max	-90.4	-193.6	-96.5	-75.0	-64.0	-47.8	-359.1	-496.2	-421.2	-376.8	-333.5	-27.8
Bathy_Min	-56.7	-91.6	-63.9	-57.0	-46.5	-15.7	-311.5	-461.8	-377.0	-322.9	-278.8	-12.9
Pente_Mean	0.22	0.06	0.09	0.13	0.21	0.75	0.25	0.08	0.15	0.21	0.33	0.56
Pente_STD	0.15	0.034	0.050	0.078	0.151	0.458	0.127	0.035	0.065	0.101	0.161	0.282
Pente_Min	0.01	0.000	0.000	0.003	0.011	0.042	0.036	0.001	0.006	0.014	0.036	0.153
Pente_Max	0.82	0.18	0.28	0.42	0.82	2.73	0.69	0.22	0.38	0.57	0.83	1.51
Geo2_Bosse	0.027	0.000	0.000	0.000	0.007	0.198	0.008	0.000	0.000	0.000	0.004	0.043
Geo2_Creux	0.029	0.000	0.000	0.000	0.011	0.222	0.009	0.000	0.000	0.000	0.005	0.057
Relief_var	2.34	1.00	1.00	1.00	3.00	6.00	2.23	1.00	1.00	1.00	3.00	6.00
SalMoyMoy	31.89	31.23	31.29	31.99	32.13	33.33	34.26	29.46	34.55	34.67	34.80	34.80
SalMinMoy	31.36	29.65	30.73	31.53	31.64	33.13	34.10	28.67	34.40	34.63	34.65	34.75
SalMaxMoy	32.35	31.56	32.16	32.31	32.68	33.56	34.41	30.04	34.66	34.73	34.88	35.04
SalMoyMin	31.52	29.78	31.29	31.54	31.99	32.65	34.19	29.21	34.54	34.61	34.80	34.80
SalMinMin	30.95	29.11	30.40	30.99	31.53	32.35	34.02	28.42	34.38	34.53	34.65	34.75
SalMaxMin	31.96	30.73	31.56	31.73	32.31	32.83	34.39	30.59	34.63	34.72	34.86	35.04
SalMoyMax	32.20	31.29	31.38	31.99	32.66	34.04	34.30	29.78	34.60	34.77	34.80	34.80
SalMinMax	31.68	30.40	30.73	31.53	32.35	33.82	34.15	29.11	34.53	34.64	34.71	34.75
SalMaxMax	32.72	31.74	32.31	32.47	33.02	34.22	34.46	30.73	34.66	34.83	34.88	35.04
TempMoyMoy	1.02	0.18	0.29	0.53	1.31	4.45	4.99	4.69	4.81	4.91	5.10	5.64
TempMinMoy	-0.42	-1.66	-1.15	-0.51	-0.22	1.93	4.00	-1.54	4.31	4.36	4.61	5.04
TempMaxMoy	2.86	1.10	1.34	2.30	2.80	5.62	6.10	5.10	5.32	5.42	5.61	13.94
TempMoyMin	1.30	0.18	0.36	0.53	1.32	4.72	5.05	4.68	4.81	4.91	5.13	6.98
TempMinMin	-0.91	-1.65	-1.61	-1.13	-0.51	0.19	3.95	-1.30	4.15	4.36	4.63	5.04
TempMaxMin	3.92	1.34	2.29	2.64	3.68	12.74	6.31	5.10	5.32	5.48	5.61	17.25
TempMoyMax	1.17	0.18	0.36	0.59	1.65	4.40	4.94	4.69	4.81	4.91	5.03	5.34
TempMinMax	0.03	-1.66	-0.51	-0.28	-0.15	3.76	4.05	-1.15	4.31	4.36	4.54	5.04
TempMaxMax	2.70	1.08	1.34	2.30	2.87	5.59	5.93	5.10	5.32	5.37	5.61	10.54

Table 145. Environmental conditions prevailing in hot spots and cold spots of American plaice distribution, based on catch in number (2002–2010). Number of cells and proportion of cells meeting the classification criteria are shown for 10 binary variables and cells where the local spatial autocorrelation G_i* statistic value was significant (>1.645 and <-1.645 for hot spots and cold spots, respectively).

	Hot spot		Cold spot	
Variable	Count	Proportion	Count	Proportion
Geo_Plateau	262	0.95	13	0.09
Geo_Talus	8	0.03	2	0.01
Geo_Chenal	5	0.02	135	0.90
O2_12	2	0.01	35	0.23
O2_34	9	0.03	90	0.60
O2_56	90	0.33	13	0.09
O2_78	174	0.63	12	0.08
Sed1_S<300	180	0.65	145	0.97
Sed1_S >300	95	0.35	5	0.03
Sed2_R	76	0.28	20	0.13

Table 146. Environmental conditions prevailing in hot spots and cold spots of American plaice distribution based on relative occurrence (2002–2010, fish < 20.5 cm total length). Mean, median, and 5th, 25th, 75th, and 95th percentiles are shown for quantitative variables and cells where the local spatial autocorrelation G_i* statistic value was significant (>1.645 and <-1.645 for hot spots and cold spots, respectively).

	Hot spot						Cold spot					
Variable	Mean	5%	25%	Median	75%	95%	Mean	5%	25%	Median	75%	95%
MHVar_3x3	2.38	1.00	1.00	2.00	3.00	5.00	1.81	1.00	1.00	1.00	2.00	4.00
Sup_Protege	0.01	0.00	0.00	0.00	0.00	0.00	0.04	0.00	0.00	0.00	0.00	0.00
Sup_SemiExp	0.11	0.00	0.00	0.00	0.00	0.00	0.11	0.00	0.00	0.00	0.00	0.00
Cote_Dist	41046	7366	23424	38088	56043	86112	34926	4688	15327	32800	49637	75394
Bathy_Mean	-87.8	-205.0	-96.3	-69.3	-60.0	-44.7	-288.1	-469.8	-380.4	-325.4	-234.3	-19.0
Bathy_STD	8.8	1.6	2.9	5.0	10.7	28.1	17.7	2.4	5.9	11.0	20.9	65.9
Bathy_Max	-106.7	-245.0	-128.6	-81.5	-67.4	-51.0	-320.0	-492.1	-407.8	-357.2	-298.3	-27.0
Bathy_Min	-67.9	-168.2	-70.0	-59.0	-49.3	-17.9	-246.8	-449.2	-353.0	-288.0	-138.5	-4.0
Pente_Mean	0.25	0.06	0.09	0.16	0.28	0.76	0.39	0.08	0.15	0.28	0.47	1.27
Pente_STD	0.16	0.04	0.05	0.10	0.19	0.49	0.20	0.04	0.07	0.13	0.23	0.59
Pente_Min	0.01	0.00	0.00	0.005	0.01	0.05	0.06	0.00	0.01	0.02	0.06	0.28
Pente_Max	0.90	0.19	0.31	0.51	1.06	2.76	1.09	0.21	0.40	0.71	1.28	3.51
Geo2_Bosse	0.03	0.00	0.00	0.00	0.02	0.20	0.03	0.00	0.00	0.00	0.02	0.17
Geo2_Creux	0.03	0.00	0.00	0.00	0.03	0.20	0.03	0.00	0.00	0.00	0.03	0.18
Relief_var	2.65	1.00	1.00	1.00	5.00	6.00	2.91	1.00	1.00	2.00	5.00	7.00
SalMoyMoy	32.14	30.92	31.38	31.99	32.66	34.04	33.84	29.46	34.38	34.60	34.79	34.80
SalMinMoy	31.66	29.65	30.91	31.53	32.35	33.82	33.60	28.67	34.17	34.53	34.65	34.75
SalMaxMoy	32.55	31.56	32.16	32.31	33.02	34.22	34.08	30.04	34.58	34.66	34.85	35.04
SalMoyMin	31.73	29.78	31.29	31.54	32.13	33.38	33.53	29.21	33.19	34.55	34.77	34.80
SalMinMin	31.20	29.11	30.91	31.39	31.64	33.15	33.24	28.36	32.75	34.38	34.64	34.75
SalMaxMin	32.13	30.73	31.56	32.09	32.54	33.66	33.86	30.59	33.36	34.63	34.85	35.04
SalMoyMax	32.47	31.29	31.56	32.13	33.10	34.41	33.98	29.78	34.55	34.67	34.80	34.80
SalMinMax	32.00	30.40	30.91	31.64	32.94	34.29	33.79	29.11	34.38	34.63	34.68	34.75
SalMaxMax	32.90	31.65	32.31	32.71	33.45	34.57	34.18	30.49	34.63	34.72	34.85	35.04
TempMoyMoy	1.21	0.18	0.30	0.56	1.32	4.56	4.70	2.52	4.71	4.87	5.03	5.64
TempMinMoy	-0.01	-1.65	-0.92	-0.51	-0.10	3.97	3.37	-1.54	4.10	4.32	4.54	4.93
TempMaxMoy	2.71	1.07	1.34	2.30	2.97	5.59	6.13	3.83	5.32	5.42	5.61	13.94
TempMoyMin	1.32	0.18	0.36	0.45	1.52	5.13	4.58	0.77	4.68	4.87	5.04	6.98
TempMinMin	-0.60	-1.65	-1.33	-0.92	-0.51	1.96	2.87	-1.54	1.14	4.31	4.46	4.74
TempMaxMin	3.51	1.11	1.75	2.64	3.59	10.54	6.46	2.34	5.23	5.42	5.61	17.25
TempMoyMax	1.46	0.18	0.53	0.59	1.96	5.12	4.63	2.35	4.73	4.87	4.92	5.29
TempMinMax	0.49	-1.65	-0.51	-0.28	1.03	4.61	3.52	-1.55	4.14	4.36	4.54	4.93
TempMaxMax	2.72	1.07	1.34	2.64	3.22	5.59	5.83	5.10	5.25	5.42	5.61	10.54

Table 147. Environmental conditions prevailing in hot spots and cold spots of American plaice distribution based on relative occurrence (2002–2010, fish < 20.5 cm total length). Number of cells and proportion of cells meeting the classification criteria are shown for 10 binary variables and cells where the local spatial autocorrelation G_i* statistic value was significant (>1.645 and <-1.645 for hot spots and cold spots, respectively).

	Hot spot		Cold spot	
Variable	Count	Proportion	Count	Proportion
Geo_Plateau	340	0.92	57	0.18
Geo_Talus	7	0.02	34	0.11
Geo_Chenal	22	0.06	221	0.71
O2_12	7	0.02	89	0.29
O2_34	45	0.12	140	0.45
O2_56	119	0.32	30	0.10
O2_78	198	0.54	53	0.17
Sed1_S<300	221	0.60	268	0.86
Sed1_S >300	148	0.40	44	0.14
Sed2_R	105	0.28	62	0.20

Table 148. Environmental conditions prevailing in hot spots and cold spots of American plaice distribution based on catch in number (2002–2010, fish < 20.5 cm total length). Mean, median, and 5th, 25th, 75th, and 95th percentiles are shown for quantitative variables and cells where the local spatial autocorrelation G_i* statistic value was significant (>1.645 and <-1.645 for hot spots and cold spots, respectively).

	Hot spot						Cold spot					
Variable	Mean	5%	25%	Median	75%	95%	Mean	5%	25%	Median	75%	95%
MHVar_3x3	2.16	1.00	1.00	2.00	3.00	4.00	1.41	1.00	1.00	1.00	2.00	3.00
Sup_Protege	0.03	0.00	0.00	0.00	0.00	0.00	0.00	0.00	0.00	0.00	0.00	0.00
Sup_SemiExp	0.30	0.00	0.00	0.00	0.00	0.00	0.00	0.00	0.00	0.00	0.00	0.00
Cote_Dist	37015	4377	17249	31245	52666	90839	44003	18164	33300	45406	55215	65977
Bathy_Mean	-71.9	-139.3	-76.2	-64.6	-56.0	-36.7	-360.6	-478.4	-392.2	-368.6	-333.6	-288.5
Bathy_STD	8.2	1.6	2.5	4.0	8.8	28.4	13.0	4.0	7.1	10.1	17.0	29.9
Bathy_Max	-89.2	-199.5	-94.7	-74.4	-63.4	-43.5	-385.4	-498.1	-419.2	-393.1	-356.9	-312.2
Bathy_Min	-54.0	-90.1	-61.9	-55.5	-43.8	-9.6	-328.4	-451.7	-367.9	-335.1	-302.0	-203.8
Pente_Mean	0.24	0.05	0.08	0.12	0.22	0.79	0.29	0.10	0.18	0.26	0.35	0.61
Pente_STD	0.16	0.029	0.047	0.073	0.160	0.499	0.14	0.037	0.075	0.128	0.184	0.279
Pente_Min	0.01	0.000	0.000	0.003	0.013	0.047	0.05	0.001	0.007	0.016	0.054	0.206
Pente_Max	0.88	0.15	0.25	0.41	0.85	2.97	0.77	0.26	0.43	0.69	0.96	1.75
Geo2_Bosse	0.033	0.000	0.000	0.000	0.015	0.211	0.005	0.000	0.000	0.000	0.005	0.027
Geo2_Creux	0.032	0.000	0.000	0.000	0.010	0.224	0.012	0.000	0.000	0.001	0.012	0.051
Relief_var	2.39	1.00	1.00	1.00	3.00	6.00	2.57	1.00	1.00	2.00	4.00	6.00
SalMoyMoy	31.84	29.78	31.29	31.99	32.13	33.33	34.55	34.44	34.60	34.67	34.80	34.80
SalMinMoy	31.33	29.11	30.73	31.53	31.64	33.15	34.43	34.25	34.52	34.63	34.65	34.75
SalMaxMoy	32.29	30.73	31.73	32.31	32.64	33.56	34.70	34.58	34.66	34.83	35.04	35.04
SalMoyMin	31.45	29.72	31.25	31.45	31.99	32.65	34.47	33.88	34.55	34.64	34.80	34.80
SalMinMin	30.88	28.67	30.40	30.93	31.53	32.32	34.31	33.47	34.38	34.53	34.65	34.75
SalMaxMin	31.91	30.73	31.56	31.73	32.31	32.83	34.63	34.14	34.64	34.72	34.87	35.04
SalMoyMax	32.15	31.29	31.38	31.99	32.65	34.04	34.58	34.49	34.63	34.80	34.80	34.80
SalMinMax	31.64	30.40	30.73	31.53	32.32	33.82	34.46	34.34	34.60	34.65	34.65	34.75
SalMaxMax	32.65	31.56	32.31	32.47	33.02	34.22	34.73	34.58	34.68	34.85	35.04	35.04
TempMoyMoy	1.14	0.18	0.29	0.53	1.32	4.56	4.95	4.69	4.87	4.91	5.03	5.34
TempMinMoy	-0.47	-1.66	-1.17	-0.51	-0.22	1.93	4.31	4.02	4.31	4.36	4.70	4.93
TempMaxMoy	3.12	1.11	1.34	2.30	2.87	10.54	5.65	5.14	5.32	5.32	5.60	5.90
TempMoyMin	1.46	0.18	0.36	0.82	1.65	5.59	4.89	4.47	4.81	4.91	5.02	5.34
TempMinMin	-0.94	-1.66	-1.56	-1.15	-0.51	0.15	4.18	2.48	4.31	4.35	4.54	4.97
TempMaxMin	4.30	1.34	2.29	2.64	4.69	13.91	5.69	5.10	5.32	5.42	5.61	5.90
TempMoyMax	1.25	0.18	0.30	0.59	1.65	4.54	4.92	4.69	4.87	4.91	5.03	5.23
TempMinMax	-0.03	-1.66	-0.56	-0.37	-0.22	3.81	4.34	4.04	4.31	4.34	4.73	4.93
TempMaxMax	2.90	1.08	1.34	2.64	3.37	5.59	5.54	5.14	5.25	5.32	5.41	5.90

Table 149. Environmental conditions prevailing in hot spots and cold spots of American plaice distribution based on catch in number (2002–2010, fish < 20.5 cm total length). Number of cells and proportion of cells meeting the classification criteria are shown for 10 binary variables and cells where the local spatial autocorrelation G_i* statistic value was significant (>1.645 and <-1.645 for hot spots and cold spots, respectively).

	Hot spot		Cold spot	
Variable	Count	Proportion	Count	Proportion
Geo_Plateau	210	0.94	2	0.03
Geo_Talus	9	0.04	1	0.01
Geo_Chenal	4	0.02	71	0.96
O2_12	1	0.00	22	0.30
O2_34	9	0.04	43	0.58
O2_56	61	0.27	7	0.09
O2_78	152	0.68	2	0.03
Sed1_S<300	136	0.61	74	1.00
Sed1_S >300	87	0.39	0	0.00
Sed2_R	65	0.29	14	0.19

Table 150. Environmental conditions prevailing in hot spots and cold spots of American plaice distribution based on relative occurrence (2002–2010, fish > 20.5 cm total length). Mean, median, and 5th, 25th, 75th, and 95th percentiles are shown for quantitative variables and cells where the local spatial autocorrelation G_i* statistic value was significant (>1.645 and <-1.645 for hot spots and cold spots, respectively).

	Hot spot						Cold spot					
Variable	Mean	5%	25%	Median	75%	95%	Mean	5%	25%	Median	75%	95%
MHVar_3x3	2.32	1.00	1.00	2.00	3.00	4.25	1.68	1.00	1.00	1.00	2.00	3.00
Sup_Protege	0.001	0.000	0.000	0.000	0.000	0.000	0.06	0.00	0.00	0.00	0.00	0.00
Sup_SemiExp	0.04	0.00	0.00	0.00	0.00	0.00	0.13	0.00	0.00	0.00	0.00	0.00
Cote_Dist	44991	14344	27506	40674	60198	86667	36252	4037	15075	34933	54496	75470
Bathy_Mean	-103.8	-253.6	-124.0	-73.1	-62.0	-51.4	-260.9	-479.4	-396.2	-330.6	-33.0	-17.7
Bathy_STD	9.4	1.6	3.0	5.2	11.4	30.0	13.0	2.1	4.3	7.6	16.7	41.9
Bathy_Max	-123.7	-280.7	-163.1	-86.4	-70.9	-59.9	-284.8	-496.2	-421.9	-361.5	-45.0	-25.6
Bathy_Min	-83.0	-216.3	-87.7	-61.1	-55.0	-39.0	-229.4	-457.0	-370.5	-281.5	-25.7	-2.2
Pente_Mean	0.24	0.06	0.10	0.17	0.29	0.67	0.29	0.06	0.11	0.18	0.35	0.84
Pente_STD	0.15	0.04	0.06	0.10	0.17	0.45	0.14	0.03	0.06	0.09	0.17	0.35
Pente_Min	0.02	0.00	0.00	0.005	0.01	0.08	0.05	0.00	0.01	0.01	0.05	0.23
Pente_Max	0.85	0.19	0.33	0.56	0.99	2.51	0.75	0.18	0.31	0.49	0.89	2.13
Geo2_Bosse	0.02	0.00	0.00	0.00	0.01	0.13	0.014	0.000	0.000	0.000	0.005	0.081
Geo2_Creux	0.02	0.00	0.00	0.00	0.02	0.15	0.015	0.000	0.000	0.000	0.007	0.097
Relief_var	2.61	1.00	1.00	1.00	4.00	7.00	2.25	1.00	1.00	1.00	3.00	6.00
SalMoyMoy	32.44	31.29	31.84	32.03	33.13	34.41	33.20	29.46	30.46	34.63	34.80	34.80
SalMinMoy	32.00	30.40	31.39	31.64	32.92	34.25	32.90	28.64	29.91	34.53	34.65	34.75
SalMaxMoy	32.80	31.56	32.20	32.47	33.48	34.57	33.55	30.04	31.45	34.73	34.86	35.04
SalMoyMin	32.10	31.25	31.29	31.99	32.65	34.08	32.99	29.21	30.08	34.55	34.79	34.80
SalMinMin	31.65	29.65	30.91	31.53	32.15	33.82	32.60	28.21	29.54	34.38	34.65	34.75
SalMaxMin	32.42	31.56	31.73	32.31	32.83	34.32	33.43	30.04	31.48	34.66	34.85	35.04
SalMoyMax	32.71	31.38	31.99	32.65	33.46	34.49	33.35	29.78	31.23	34.77	34.80	34.80
SalMinMax	32.28	30.73	31.53	32.10	33.15	34.39	33.10	29.11	30.40	34.64	34.71	34.75
SalMaxMax	33.10	32.16	32.31	33.02	33.64	34.58	33.65	30.49	31.56	34.83	34.87	35.04
TempMoyMoy	1.38	0.18	0.18	0.59	1.96	4.92	4.68	2.35	4.69	4.91	5.04	5.64
TempMinMoy	0.41	-1.65	-0.51	-0.28	0.70	4.35	2.65	-1.64	-0.79	4.31	4.54	4.89
TempMaxMoy	2.63	1.07	1.34	2.30	2.99	5.40	6.80	5.09	5.32	5.42	7.22	13.94
TempMoyMin	1.15	0.18	0.36	0.47	1.32	4.49	4.94	2.41	4.69	4.91	5.17	7.45
TempMinMin	-0.26	-1.65	-1.17	-0.71	-0.22	3.97	2.41	-1.64	-1.30	4.31	4.54	4.83
TempMaxMin	2.79	1.07	1.34	2.35	3.04	5.61	7.61	3.16	5.32	5.51	7.76	17.25
TempMoyMax	1.73	0.18	0.53	0.59	2.99	5.12	4.33	1.02	4.63	4.81	4.92	5.34
TempMinMax	0.90	-0.92	-0.50	-0.28	1.99	4.61	2.68	-1.65	-0.17	4.31	4.54	4.73
TempMaxMax	2.80	1.07	1.34	2.77	4.40	5.56	6.09	4.69	5.32	5.42	5.61	10.54

Table 151. Environmental conditions prevailing in hot spots and cold spots of American plaice distribution based on relative occurrence (2002–2010, fish > 20.5 cm total length). Number of cells and proportion of cells meeting the classification criteria are shown for 10 binary variables and cells where the local spatial autocorrelation G_i* statistic value was significant (>1.645 and <-1.645 for hot spots and cold spots, respectively).

	Hot spot		Cold spot	
Variable	Count	Proportion	Count	Proportion
Geo_Plateau	322	0.86	82	0.33
Geo_Talus	6	0.02	14	0.06
Geo_Chenal	48	0.13	153	0.61
O2_12	24	0.06	22	0.09
O2_34	63	0.17	120	0.48
O2_56	124	0.33	26	0.10
O2_78	165	0.44	81	0.33
Sed1_S<300	237	0.63	188	0.76
Sed1_S >300	139	0.37	61	0.24
Sed2_R	89	0.24	73	0.29

Table 152. Environmental conditions prevailing in hot spots and cold spots of American plaice distribution based on catch in number (2002–2010, fish > 20.5 cm total length). Mean, median, and 5th, 25th, 75th, and 95th percentiles are shown for quantitative variables and cells where the local spatial autocorrelation G_i* statistic value was significant (>1.645 and <-1.645 for hot spots and cold spots, respectively).

Variable	Hot spot						Cold spot					
	Mean	5%	25%	Median	75%	95%	Mean	5%	25%	Median	75%	95%
MHVar_3x3	2.02	1.00	1.00	2.00	3.00	4.00	1.18	1.00	1.00	1.00	1.00	2.00
Sup_Protege	0.01	0.00	0.00	0.00	0.00	0.00	0.000	0.00	0.00	0.00	0.00	0.00
Sup_SemiExp	0.28	0.00	0.00	0.00	0.00	0.00	0.009	0.00	0.00	0.00	0.00	0.00
Cote_Dist	41960	7597	23534	37959	58223	88985	47799	14867	40563	50714	58959	71047
Bathy_Mean	-76.4	-141.6	-80.1	-67.4	-59.7	-44.0	-356.6	-487.0	-417.1	-382.4	-368.3	-20.2
Bathy_STD	7.4	1.6	2.6	4.2	7.6	27.6	9.7	2.9	5.7	8.3	13.0	21.3
Bathy_Max	-92.3	-197.0	-96.8	-76.3	-65.4	-49.6	-375.7	-504.5	-431.9	-409.1	-388.8	-27.0
Bathy_Min	-59.9	-102.1	-65.3	-58.0	-50.7	-27.7	-333.1	-478.0	-391.3	-362.6	-311.9	-14.5
Pente_Mean	0.21	0.06	0.09	0.13	0.21	0.67	0.22	0.068	0.15	0.19	0.27	0.46
Pente_STD	0.14	0.035	0.051	0.079	0.142	0.387	0.105	0.035	0.050	0.090	0.146	0.228
Pente_Min	0.01	0.000	0.000	0.003	0.010	0.042	0.03	0.000	0.005	0.014	0.025	0.148
Pente_Max	0.78	0.18	0.28	0.42	0.73	2.48	0.57	0.18	0.31	0.51	0.70	1.17
Geo2_Bosse	0.020	0.000	0.000	0.000	0.005	0.153	0.002	0.000	0.000	0.000	0.000	0.017
Geo2_Creux	0.021	0.000	0.000	0.000	0.009	0.128	0.005	0.000	0.000	0.000	0.002	0.029
Relief_var	2.26	1.00	1.00	1.00	3.00	6.00	1.91	1.00	1.00	1.50	2.00	4.70
SalMoyMoy	31.95	31.25	31.38	31.99	32.13	33.42	34.16	29.46	34.77	34.80	34.80	34.81
SalMinMoy	31.40	29.65	30.73	31.53	31.64	33.12	33.98	28.67	34.65	34.65	34.71	34.75
SalMaxMoy	32.41	31.56	32.16	32.31	32.71	33.63	34.37	30.04	34.83	34.94	35.04	35.04
SalMoyMin	31.59	30.22	31.29	31.54	31.99	32.77	34.13	29.38	34.64	34.80	34.80	34.80
SalMinMin	31.02	29.29	30.70	31.20	31.53	32.51	33.94	28.58	34.52	34.65	34.65	34.75
SalMaxMin	31.99	31.29	31.56	31.73	32.47	32.98	34.36	30.33	34.83	34.87	35.04	35.04
SalMoyMax	32.24	31.29	31.38	32.03	32.66	34.04	34.18	29.78	34.77	34.80	34.80	34.83
SalMinMax	31.72	30.40	30.73	31.53	32.35	33.82	34.01	29.11	34.65	34.65	34.71	34.75
SalMaxMax	32.76	32.16	32.31	32.47	33.02	34.22	34.42	30.65	34.83	34.94	35.04	35.04
TempMoyMoy	0.98	0.18	0.30	0.53	1.12	4.40	4.95	4.69	4.84	4.91	4.92	5.64
TempMinMoy	-0.33	-1.66	-1.15	-0.51	-0.22	1.98	3.75	-1.54	4.31	4.31	4.46	4.64
TempMaxMoy	2.70	1.11	1.34	2.30	2.77	5.59	6.17	5.10	5.32	5.32	5.42	13.94
TempMoyMin	1.15	0.18	0.36	0.56	1.32	4.56	5.08	4.69	4.84	4.91	4.92	6.11
TempMinMin	-0.85	-1.65	-1.57	-0.92	-0.51	0.41	3.78	-1.33	4.31	4.31	4.46	4.79
TempMaxMin	3.53	1.29	2.00	2.64	3.59	10.54	6.44	5.10	5.32	5.35	5.54	15.10
TempMoyMax	1.16	0.18	0.53	0.59	1.32	4.40	4.88	4.61	4.73	4.91	4.91	5.20
TempMinMax	0.11	-1.66	-0.51	-0.28	-0.15	3.97	3.77	-1.15	4.31	4.31	4.42	4.60
TempMaxMax	2.59	1.08	1.34	2.30	2.87	5.59	5.98	5.10	5.32	5.32	5.42	10.54

Table 153. Environmental conditions prevailing in hot spots and cold spots of American plaice distribution based on catch in number (2002–2010, fish > 20.5 cm total length). Number of cells and proportion of cells meeting the classification criteria are shown for 10 binary variables and cells where the local spatial autocorrelation G_i* statistic value was significant (>1.645 and <-1.645 for hot spots and cold spots, respectively).

	Hot spot		Cold spot	
Variable	Count	Proportion	Count	Proportion
Geo_Plateau	220	0.96	4	0.12
Geo_Talus	5	0.02	0	0.00
Geo_Chenal	5	0.02	30	0.88
O2_12	2	0.01	1	0.03
O2_34	12	0.05	23	0.68
O2_56	81	0.35	6	0.18
O2_78	135	0.59	4	0.12
Sed1_S<300	158	0.69	32	0.94
Sed1_S >300	72	0.31	2	0.06
Sed2_R	58	0.25	8	0.24

<u>Multiple regression analyses</u>

The following Tables (154–162) summarize the results of regression analyses for plaice.

Latitude and longitude effects

Table 154. Tests of the effects of latitude and longitude on the relative occurrence and local spatial autocorrelation G_i* statistic based on relative occurrence of American plaice for different time periods and two size categories. % variance, percentage of variance explained by latitude and longitude; Df, number of degrees of freedom; Effect, indicates significant parameter (Latitude, significant latitude effect; Combined, both latitude and longitude are significant); Transformation, type of transformation used on the dependent variables when required. Variables are described in Materials and Methods.

Variable	Parameter	% variance	F statistic	Df	P-value	Effect	Transformation
P_RO_7110	RO	2.7	3.59	2; 1896	0.028	Latitude	No
	Gi*	1.84	18.82	2; 1896	<0.0001	Combined	No
P_RO_8410	RO	1.9	2.68	2; 1870	0.0348	Latitude	No
	Gi*	1.62	16.38	2; 1870	<0.0001	Combined	No
P_RO_8410S	RO	3.41	33.2	2; 1821	<0.0001	Combined	No
	Gi*	8.71	87.92	2; 1821	<0.0001	Combined	No
P_RO_8410L	RO	1.06	1.97	2; 1821	0.044	Latitude	No
	Gi*	1.08	10.96	2; 1821	<0.0001	Latitude	No
P_RO_8492	RO	1.7	13.81	2; 1470	<0.0001	Latitude	No
	Gi*	5.84	46.65	2;1470	<0.0001	Combined	No
P_RO_8492S	RO	6.44	44.09	2; 1251	<0.0001	Combined	No
	Gi*	12.79	92.9	2; 1251	<0.0001	Combined	No
P_RO_8492L	RO	2.5	17.09	2;1251	<0.0001	Latitude	No
	Gi*	6.69	45.95	2; 1251	<0.0001	Latitude	No
P_RO_9301	RO	1.6	12.7	2;1462	<0.0001	Combined	No
	Gi*	6.4	50.88	2; 1462	<0.0001	Combined	No
P_RO_9301S	RO	7.9	62.98	2;1439	<0.0001	Combined	No
	Gi*	18.51	164.6	2; 1439	<0.0001	Combined	No
P_RO_9301L	RO	1.3	10.73	2; 1439	<0.0001	Latitude	No
	Gi*	5.2	40.29	2; 1439	<0.0001	Combined	No
P_RO_0210	RO	7.6	6.47	2;1418	<0.0016	Latitude	No
	Gi*	1	7.99	2; 1418	<0.0001	Latitude	No
P_RO_0210S	RO	0.6	5.21	2; 1417	<0.005	Combined	No
	Gi*	2.8	21.41	2;1417	<0.0001	Combined	No
P_RO_0210L	RO	1.3	9.64	2; 1417	<0.0001	Latitude	No
	Gi*	1.6	12.81	2; 1417	<0.0001	Latitude	No
P_RO_S8493	RO	1.09	8.43	2; 1347	<0.0001	Latitude	No
	Gi*	3.6	26.09	2;1347	<0.0001	Latitude	No
P_RO_W8493	RO	0.22	1.52	2; 464	> 0.05	No	Fourth root
	Gi*	0.36	1.84	2;464	> 0.05	No	Square root

Table 155. Tests of the effects of latitude and longitude on catch in number and local spatial autocorrelation G_i* statistic based on catch in number of American plaice for different time periods and two size categories. % variance, percentage of variance explained by latitude and longitude; Df, number of degrees of freedom; Effect, indicates significant parameter (Latitude, significant latitude effect; Combined, both latitude and longitude are significant); Transformation, type of transformation used on the dependent variables when required. Variables are described in Materials and Methods.

Variable	Parameter	% variance	F statistic	Df	P-value	Effect	Transformation
P_CN_8410	CN	6.05	59.75	2; 1821	<0.0001	Latitude	Square root
	Gi*	13.96	29.09	2; 1821	<0.0001	Combined	No
P_CN_8410S	CN	3.00	29.09	2; 1821	<0.0001	Combined	Square root
	Gi*	6.99	69.57	2; 1821	<0.0001	Combined	No
P_CN_8410L	CN	5.40	52.70	2; 1821	<0.0001	Latitude	Square root
	Gi*	12.48	131.00	2; 1821	<0.0001	Combined	No
P_CN_8492	CN	10.45	74.15	2; 1251	<0.0001	Combined	Square root
	Gi*	14.62	108.20	2;1251	<0.0001	Combined	No
P_CN_8492S	CN	4.96	33.68	2; 1251	<0.0001	Latitude	Square root
	Gi*	6.96	47.88	2; 1251	<0.0001	Combined	No
P_CN_8492L	CN	9.44	66.31	2;1251	<0.0001	Combined	Square root
	Gi*	13.49	98.70	2; 1251	<0.0001	Combined	No
P_CN_9301	CN	6.71	52.80	2;1439	<0.0001	Combined	Square root
	Gi*	10.04	81.04	2; 1439	<0.0001	Combined	No
P_CN_9301S	CN	5.44	42.48	2;1439	<0.0001	Combined	Square root
	Gi*	7.31	57.83	2; 1439	<0.0001	Combined	No
P_CN_9301L	CN	6.47	50.80	2; 1439	<0.0001	Combined	Square root
	Gi*	11.30	92.79	2; 1439	<0.0001	Combined	No
P_CN_0210	CN	2.54	19.47	2;1417	<0.0001	Combined	Square root
	Gi*	8.88	70.12	2; 1417	<0.0001	Combined	No
P_CN_0210S	CN	3.04	23.21	2; 1417	<0.0001	Combined	Square root
	Gi*	8.06	63.21	2;1417	<0.0001	Combined	No
P_CN_0210L	CN	2.02	15.66	2; 1417	<0.0001	Combined	Square root
	Gi*	7.57	59.13	2; 1417	<0.0001	Combined	No

Table 156. Tests of the effects of latitude and longitude on catch in weight and local spatial autocorrelation G_i* statistic based on catch in weight of American plaice for different time periods and two size categories. % variance, percentage of variance explained by latitude and longitude; Df, number of degrees of freedom; Effect, indicates significant parameter (Latitude, significant latitude effect; Combined, both latitude and longitude are significant); Transformation, type of transformation used on the dependent variables when required. Variables are described in Materials and Methods.

Variable	Parameter	% variance	F statistic	Df	P-value	Effect	Transformation
P_CW_8410	CW	7.35	73.34	2; 1821	<0.0001	Latitude	Square root
	Gi*	17.19	190.20	2; 1821	<0.0001	Latitude	No
P_CW_8492	CW	11.76	84.48	2; 1251	<0.0001	Combined	Square root
	Gi*	17.17	130.90	2;1251	<0.0001	Combined	No
P_CW_9301	CW	7.62	60.40	2;1439	<0.0001	Combined	Square root
	Gi*	15.35	131.50	2; 1439	<0.0001	Combined	No
P_CW_0210	CW	1.50	11.81	2;1417	<0.0001	Combined	Square root
	Gi*	6.56	50.82	2; 1417	<0.0001	Combined	No

Relative occurrences

Table 157. Results of multiple forward linear regressions between relative occurrence of American plaice and potential explanatory variables obtained from the megahabitat database (adapted from Dutil et al. 2011). The analyses were conducted on subsets of the data (e.g., 7110 refers to the period 1971–2010; suffix S and L to fish smaller and larger than 20.5 cm, respectively; prefix S and W to summer and winter, respectively). Only the significant explanatory variables are listed. *: p<0.10; **: p<0.05; ***: p<0.001; +: positive effect; -: negative effect; 1–4 and columnwise: contributions to the model explained variance are ranked from 1 to 4; <<: Model p < 0.001.

Variable	7110	8410	8410S	8410L	8492	8492S	8492L	9301	9301S	9301L	0210	0210S	0210L	S8493	W8493
MHVar_3x3	***		*	**										***	
Sup_Protege	***	***	***	***											
Sup_SemiExp	**		***	***	**	**						*		**	
Cote_Dist	***	***	***	***			**			***		**	***	**	
Bathy_Max	(3+)***		(4+)***	(3+)***	(2+)***	***						(3+)***		(3+)***	
Bathy_Min								(2+)***							
Pente_Mean								***							
Pente_Min							**							*	
Geo2_Bosse													(3-)***		
Geo2_Creux						*				**					
Relief_var			***	***		***						***			
SalMoyMin												***	***		
SalMaxMin	***	***					(3-)***								
SalMoyMax									(4-)***						
SalMinMax											***				
TempMoyMoy	(1-)***	(1-)***	(1-)***	(1-)***		(1-)***			(1-)***	(3-)***		(1-)***			
TempMinMoy					*			***							
TempMaxMoy								(3-)***			***		(2-)***		
TempMoyMin			***	(2-)***	(1-)***	***	(2-)***	(1-)***	(2-)***	(1-)*		(2-)***		(2-)***	
TempMinMin	***	***							***			***			(3+)*
TempMaxMin	(4-)***										***		**		
TempMoyMax												***			
TempMinMax			***	(4+)***	(4+)***	***								***	

TempMaxMax											(2+)***				
MHVar_3x3 ^{2}														**	
Sup_Protege^2								**	*	***					
Cote_Dist ^{2}	**	***	***	***			***	***		***			**	***	
Bathy_Mean ^{2}							(1-)***				(1-)***		(1-)***	(1-)**	
Bathy_STD ^{2}	**		***	***		(3-)***	***		***						
Bathy_Max ^{2}									(3-)***	(2-)**					
Bathy_Min ^{2}										***					
Pente_Mean ^{2}		(2-)***								***					
Pente_STD ^{2}							**							***	
Pente_Max ^{2}					*					*					
Geo2_Bosse ^{2}	***	***			*	***									
Geo2_Creux ^{2}			***	***		***		***	***	***					
Relief_var ^{2}	***	***								***					
SalMoyMoy ^{2}						***									
SalMaxMoy ^{2}											**	*			
SalMoyMin ^{2}			***				*								
SalMinMin ^{2}			***	***				*	***	**					
SalMaxMin ^{2}					***	***					*			***	(2+)***
SalMoyMax ^{2}						***				**				***	
SalMinMax ^{2}					***		***						***		
SalMaxMax ^{2}											***	(4-)***	***		
TempMoyMoy ^{2}							*			(4-)***					
TempMinMoy ^{2}															(1-)***
TempMaxMoy ^{2}					(3-)***										
TempMoyMin ^{2}								*							
TempMinMin ^{2}		(4-)***	(2-)**			(2-)**			**	***	***				
TempMaxMin ^{2}								***	*						
TempMoyMax ^{2}											***				
TempMinMax ^{2}			***			**				**			**		
TempMaxMax ^{2}	(2-)***	(3-)***	***	***			(4-)***	(4-)***	***		(3-)***	***	**	(4-)***	
Sed1_S	**	**	(3-)***	***		(4-)***		***	***	**	*	***	*		
Sed2_R	***	***	**	***	*	***				**	(4-)**		(4-)***	**	

O2_12										*			***		
O2_56			*	*	***		*							**	
Geo_Plateau	***														
Geo_Talus									***						
R^2 Adjusted	0.395	0.419	0.594	0.582	0.293	0.541	0.446	0.373	0.485	0.489	0.398	0.418	0.458	0.473	0.103
p-value	<<	<<	<<	<<	<<	<<	<<	<<	<<	<<	<<	<<	<<	<<	<<

Clustering of high relative occurrences

Table 158. Results of multiple forward linear regressions between G_i* (clusters of high relative occurrence for American plaice) and potential explanatory variables obtained from the megahabitat database (adapted from Dutil et al. 2011). The analyses were conducted on subsets of the data (e.g., 7110 refers to the period 1971–2010; suffix S and L to fish smaller and larger than 20.5 cm, respectively; prefix S and W to summer and winter, respectively). Only the significant explanatory variables are listed. *: p<0.10; **: p<0.05; ***: p<0.001; +: positive effect; -: negative effect; 1–4 and columnwise: contributions to the model explained variance are ranked from 1 to 4; <<: Model p < 0.001.

Variable	7110	8410	8410S	8410L	8492	8492S	8492L	9301	9301S	9301L	0210	0210S	0210L	S8493	W8493
MHVar_3x3	***	**	***	***			**	***		***	**	***		***	
Sup_SemiExp	*	***		***						***	**	**	**		
Cote_Dist		***	***	***	***	***	**	***	***	***	***	(4+)***	(4+)***	***	
Bathy_Max	(2+)***	(2+)***	(2+)***	(4+)***	(1+)***	***	(2+)***	(4+)***	(2+)***	(3+)***	***	***		***	
Pente_STD	***	***		***			***	***		***					
Pente_Min								*			(4-)***	(3-)***		(3-)***	
Pente_Max					***										
Geo2_Bosse											**				
Geo2_Creux		**	***						***					***	***
Relief_var						***	*								
SalMoyMin					***										
SalMinMin			***	*			***		***				**		
SalMaxMin	*	**													
SalMinMax													(3-)***		
TempMoyMoy	(1-)***	(1-)*	(1-)***	(2-)***		(1-)**		(1-)***		(1-)***	(2-)***	(2-)***		(2-)*	
TempMinMoy	(3+)***									(4+)***					
TempMoyMin									(1-)***	(2-)***			***		
TempMinMin			***		***		***								
TempMaxMin		(3-)***	(4-)***	***		***	(4-)***							***	
TempMoyMax										***					
TempMinMax		***	(3+)***		(3+)***			***	(3+)***					***	
TempMaxMax								***	(4-)***						
MHVar_3x3 ^{2}			***	***										***	***
Cote_Dist ^{2}	***	***	***	***	***	***	***	***	***	***	***	***	***	***	
Bathy_Mean ^{2}				(1-)***		(2-)***	(1-)***					(1-)***			

Bathy_STD ^{2}						(3-)***			***						
Bathy_Max ^{2}													***		
Bathy_Min ^{2}											(1-)***		(1-)***	(1-)***	
Pente_Mean ^{2}						**					***				
Pente_STD ^{2}														***	
Pente_Min ^{2}															**
Geo2_Creux ^{2}						***									
Relief_var ^{2}					***										
SalMinMoy ^{2}	*														(4+)*
SalMoyMin ^{2}						***				***	*			***	
SalMoyMax ^{2}					(2-)***	**	(3-)***								
SalMinMax ^{2}			***											***	***
SalMaxMax ^{2}		(4-)***		***							***	***	(2-)***		
TempMinMoy ^{2}															(3-)***
TempMaxMoy ^{2}													***		
TempMoyMin ^{2}	***												***		
TempMinMin ^{2}								(2-)***							
TempMaxMin ^{2}			***	**	***		***		**	**				**	
TempMoyMax ^{2}									***	***					
TempMinMax ^{2}	***	**	**	*					***	***					***
TempMaxMax ^{2}	(4-)***	***	***	(3-)***	(4-)***	***	***	(3-)***			(3-)***			(4-)***	
Sed1_S	***	***	***	***	***	***		***	***		***	***		***	
Sed2_R	***	***	***	***	***	(4-)***	***	**	**	***	**	*	***	***	
O2_12	*	***		***				***	***	***	***		***	***	***
O2_56		***	***	***	***	***	***	***				***		***	(2-)***
Geo_Plateau								**	**	**					(1-)***
R^2 Adjusted	0.692	0.712	0.782	0.782	0.604	0.712	0.720	0.656	0.733	0.737	0.637	0.660	0.681	0.758	0.357
P value	<<	<<	<<	<<	<<	<<	<<	<<	<<	<<	<<	<<	<<	<<	<<

Catch in number

Table 159. Results of multiple forward linear regressions between catch in number of American plaice and potential explanatory variables obtained from the megahabitat database (adapted from Dutil et al. 2011). The analyses were conducted on subsets of the data (e.g., 7110 refers to the period 1971–2010; suffix S and L to fish smaller and larger than 20.5 cm, respectively; prefix S and W to summer and winter, respectively). Only the significant explanatory variables are listed. *: p<0.10; **: p<0.05; ***: p<0.001; +: positive effect; -: negative effect; 1–4 and columnwise: contributions to the model explained variance are ranked from 1 to 4; <<: Model p < 0.001.

Variable	8410	8410S	8410L	8492	8492S	8492L	9301	9301S	9301L	0210	0210S	0210L
MHVar_3x3			***									***
Sup_Protege												
Sup_SemiExp	***		****	***	*	***	***		***			***
Cote_Dist												
Bathy_Mean	(2+)**											
Bathy_STD												
Bathy_Max		(3+)***		(2+)***	(3+)***			(2+)***		(4+)**		
Bathy_Min												
Pente_Mean							***					**
Pente_STD												
Pente_Min												
Pente_Max												
Geo2_Bosse												
Geo2_Creux							**					
Relief_var									***			
SalMoyMoy	***											
SalMinMoy							*		***			
SalMaxMoy						(3-)***						
SalMoyMin												
SalMinMin		(2-)***										*
SalMaxMin												
SalMoyMax			***									
SalMinMax										***		**
SalMaxMax												
TempMoyMoy			(1-)***		(1-)***		(1-)**	*	(2-)**	(1-)***	(1-)***	
TempMinMoy				***								
TempMaxMoy	(1-)***			(1-)***								

TempMoyMin				***		***	***	(1-)***	(1-)***		**	(1-)***
TempMinMin												
TempMaxMin		(1-)***	***		***							
TempMoyMax												*
TempMinMax					***	**		***		***		
TempMaxMax						(1-)***						
MHVar_3x3 ^{2}				**		**						
Sup_Protege^2				**	***							
Sup_SemiExp ^{2}							***		***			*
Cote_Dist ^{2}			**									
Bathy_Mean ^{2}			(2-)***						(4-)***			
Bathy_STD ^{2}				***	***	*						
Bathy_Max ^{2}						(2-)***					(2-)***	
Bathy_Min ^{2}				**			(4-)***					(2-)***
Pente_Mean ^{2}									***			
Pente_STD ^{2}		*										
Pente_Min ^{2}												
Pente_Max ^{2}												
Geo2_Bosse ^{2}												
Geo2_Creux ^{2}									**			
Relief_var ^{2}		*	**		*				**	***		**
SalMoyMoy ^{2}			***								***	
SalMinMoy ^{2}												
SalMaxMoy ^{2}												
SalMoyMin ^{2}				***	***	***	*					
SalMinMin ^{2}												
SalMaxMin ^{2}												
SalMoyMax ^{2}			***	***								
SalMinMax ^{2}					(4-)***							
SalMaxMax ^{2}	***	***					***	***	***	***	*	(4-)***
TempMoyMoy ^{2}			*									
TempMinMoy ^{2}	***		***				(2-)***	(4-)***	***	(3-)***	(4-)**	(3-)***
TempMaxMoy ^{2}												

TempMoyMin ^{2}	***		***									
TempMinMin ^{2}		*			***							
TempMaxMin ^{2}												
TempMoyMax ^{2}												
TempMinMax ^{2}	*			**	***	*		**			***	
TempMaxMax ^{2}											*	
Sed1_S	(3-)***	(4-)***	(3-)***	(3-)***	(2-)***	(4-)***	(3-)***	(3-)***	(3-)***	(2-)***	(3-)***	***
Sed2_R	(4-)***	***	(4-)***	(4-)***	***	***	***	**	***	*		**
O2_12				***	***	***						
O2_34				***	***	***	*	***	*			
O2_56		***		*								
O2_78	NA	NA	NA	NA	NA	NA	NA	NA	NA	NA	NA	NA
Geo_Talus				**	*		***		*			
Geo_Chenal	NA	NA	NA	NA	NA	NA	NA	NA	NA	NA	NA	NA
R^2 Adjusted	0.495	0.390	0.493	0.506	0.378	0.439	0.413	0.290	0.431	0.409	0.330	0.432
P value	<<	<<	<<	<<	<<	<<	<<	<<	<<	<<	<<	<<

Clustering of high catch in number

Table 160. Results of multiple forward linear regressions between G_i* (clusters of high catch in number for American plaice) and potential explanatory variables obtained from the megahabitat database (adapted from Dutil et al. 2011). The analyses were conducted on subsets of the data (e.g., 7110 refers to the period 1971–2010; suffix S and L to fish smaller and larger than 20.5 cm, respectively; prefix S and W to summer and winter, respectively). Only the significant explanatory variables are listed. *: p<0.10; **: p<0.05; ***: p<0.001; +: positive effect; -: negative effect; 1–4 and columnwise, contributions to the model explained variance are ranked from 1 to 4; <<: Model p < 0.001.

Variable	8410	8410S	8410L	8492	8492S	8492L	9301	9301S	9301L	0210	0210S	0210L
MHVar_3x3	***	***	***	*		***	***	***	***	***	**	(3-)***
Sup_SemiExp	***		***							***		***
Cote_Dist		***			***		***	***	***		**	
Bathy_STD								*				
Bathy_Max	(4+)***	(4+)***	(4+)***		(4+)***					(2+)***	(3+)***	
Bathy_Min												
Pente_Mean							***	(4-)***	***			
Pente_STD											***	
Pente_Max							*		**			
Geo2_Bosse											**	
Geo2_Creux	***	***								***	(2+)***	
SalMoyMin						(2-)***						
SalMaxMin		*									*	
SalMinMax	*											***
SalMaxMax												
TempMoyMoy		(1-)***			(1-)***				(1-)***		(1-)***	
TempMinMoy			*			**						
TempMaxMoy						(2-)***						
TempMoyMin							*			(1-)***		(1-)***
TempMinMin		***				***					**	
TempMaxMin	***	***		***	***	***		***			***	
TempMinMax					*							
TempMaxMax	(1-)***		(1-)***	(1-)***			(1-)***		(4-)***		***	
MHVar_3x3 ^{2}	***		***	***		***						
Sup_SemiExp ^{2}	**		**							**		***
Cote_Dist ^{2}		***			***		***	***	**		***	

Bathy_Mean ^{2}	(2-)***		(2-)***	(4-)***			(3-)***		***			
Bathy_STD ^{2}				***	***	***						
Bathy_Max ^{2}									(3+)**			(2-)***
Bathy_Min ^{2}						(4-)***						
Pente_Max ^{2}											**	*
Relief_var ^{2}			***									
SalMoyMoy ^{2}		***									***	
SalMinMoy ^{2}		**							**			
SalMaxMoy ^{2}					***							**
SalMinMin ^{2}				***	***	(3+)***						
SalMaxMin ^{2}				***		***			*			
SalMoyMax ^{2}				*-	***	***						
SalMaxMax ^{2}	***	***	***	(3+)*			***	(2-)***	***	(3-)***	(4-)***	***
TempMoyMoy ^{2}												
TempMinMoy ^{2}		***	***				(2-)***	***	***			
TempMaxMoy ^{2}												
TempMoyMin ^{2}				**		*						
TempMinMin ^{2}	***	(3-)***	**		*		**	(1-)***	**		***	**
TempMaxMin ^{2}												
TempMoyMax ^{2}				***		(1+)***					***	
TempMinMax ^{2}		***			**							
TempMaxMax ^{2}											***	
Sed1_S	***	***	***	***	(3-)***	***	***	***	***	(4-)***	***	***
Sed2_R	(3-)***	(2-)***	(3-)***	(2-)***	(2-)***	***	(4-)***	*	(2-)***	**		***
O2_12	*	**	**	***		***		***				
O2_34	***	***	***	***		***	*	(3-)***		*		(4-)**
O2_56				**		***		**				
Geo_Plateau									***			
Geo_Talus					**	*	**					
R^2 Adjusted	0.499	0.417	0.470	0.475	0.355	0.458	0.296	0.197	0.339	0.442	0.672	0.413
P value	<<	<<	<<	<<	<<	<<	<<	<<	<<	<<	<<	<<

Catch in weight

Table 161. Results of multiple forward linear regressions between catch in weight of American plaice and potential explanatory variables obtained from the megahabitat database (adapted from Dutil et al. 2011). The analyses were conducted on subsets of the data (e.g., 7110 refers to the period 1971–2010; suffix S and L to fish smaller and larger than 20.5 cm, respectively; prefix S and W to summer and winter, respectively). Only the significant explanatory variables are listed. *: p<0.10; **: p<0.05; ***: p<0.001; +: positive effect; -: negative effect; 1–4 and columnwise: contributions to the model explained variance are ranked from 1 to 4; <<: Model p < 0.001.

Variable	8410	8492	9301	0210
MHVar_3x3	***			*
Sup_SemiExp	***	***		
Bathy_Max	***	(3+)***	***	
SalMinMin			***	
SalMinMax				(4-)***
TempMoyMoy	(1-)***	(1-)**	(1-)***	
TempMoyMin				(1-)***
TempMinMin			***	
TempMaxMin	***	***	(2-)***	
TempMinMax				***
MHVar_3x3 ^{2}		**		
Sup_SemiExp ^{2}	*			
Cote_Dist ^{2}	***			
Bathy_Mean ^{2}	(2-)**			
Bathy_Max ^{2}				(2-)***
Pente_Max ^{2}			*	
Relief_var ^{2}	**			**
SalMoyMin ^{2}			***	
SalMaxMin ^{2}		***		
SalMoyMax ^{2}	***	(4-)***		
SalMaxMax ^{2}			***	***
TempMoyMoy ^{2}	***			
TempMinMoy ^{2}	*		(4-)***	
TempMoyMin ^{2}	***			
Sed1_S	(3-)***	(2-)***	***	***
Sed2_R	(4-)***	***	(3-)***	(3-)***
O2_12		***	**	
O2_34		**		
R^2 Adjusted	0.501	0.456	0.427	0.407
P value	<<	<<	<<	<<

Clustering of high catch in weight

Table 162. Results of multiple forward linear regressions between G_i* (clusters of high catch in weight for American plaice) and potential explanatory variables obtained from the megahabitat database (adapted from Dutil et al. 2011). The analyses were conducted on subsets of the data (e.g. 7110 refers to the period 1971–2010; suffix S and L to fish smaller and larger than 20.5 cm, respectively; prefix S and W to summer and winter, respectively). Only the significant explanatory variables are listed. *: p<0.10; **: p<0.05; ***: p<0.001; +: positive effect; -: negative effect; 1–4 and columnwise: contributions to the model explained variance are ranked from 1 to 4; <<: Model p < 0.001.

Variable	8410	8492	9301	0210
MHVar_3x3	***	**	***	***
Sup_Protege				
Sup_SemiExp	***			***
Cote_Dist			***	
Bathy_Mean				
Bathy_STD				
Bathy_Max	(4+)***		(4+)***	(4+)***
Bathy_Min				
Pente_Mean				
Pente_STD				
Pente_Min				
Pente_Max				***
Geo2_Bosse				
Geo2_Creux				
Relief_var				
SalMoyMoy				
SalMinMoy				
SalMaxMoy				***
SalMoyMin				
SalMinMin				
SalMaxMin				
SalMoyMax		(2-)***		
SalMinMax				
SalMaxMax				
TempMoyMoy			(1-)***	
TempMinMoy		***		
TempMaxMoy		(1-)***		
TempMoyMin		***		
TempMinMin				
TempMaxMin				
TempMoyMax				(1-)***
TempMinMax	(1+)***			(3+)***
TempMaxMax	***			
MHVar_3x3 ^{2}	***	***	**	
Sup_Protege^2				
Sup_SemiExp ^{2}	*			***
Cote_Dist ^{2}				
Bathy_Mean ^{2}		***		

Bathy_STD ^{2}		***		
Bathy_Max ^{2}				
Bathy_Min ^{2}	(2-)***			
Pente_Mean ^{2}				
Pente_STD ^{2}				
Pente_Min ^{2}				
Pente_Max ^{2}				
Geo2_Bosse ^{2}				
Geo2_Creux ^{2}				
Relief_var ^{2}	**			
SalMoyMoy ^{2}				
SalMinMoy ^{2}			***	
SalMaxMoy ^{2}				
SalMoyMin ^{2}				
SalMinMin ^{2}		***		
SalMaxMin ^{2}		***		
SalMoyMax ^{2}				
SalMinMax ^{2}				
SalMaxMax ^{2}	***		(3-)***	
TempMoyMoy ^{2}				
TempMinMoy ^{2}			***	
TempMaxMoy ^{2}				
TempMoyMin ^{2}				
TempMinMin ^{2}	***		***	(2-)***
TempMaxMin ^{2}			***	
TempMoyMax ^{2}		(4+)***		
TempMinMax ^{2}				
TempMaxMax ^{2}				
Sed1_S	***	***	***	***
Sed2_R	(3-)***	(3-)***	(2-)***	***
Geo_Plateau			***	
Geo_Talus		**		
Geo_Chenal				
O2_12	***	***		
O2_34	***	***		***
O2_56		***		
O2_78				
R^2 Adjusted	0.519	0.502	0.381	0.400
P value	<<	<<	<<	<<

Redundancy analysis

Mean catch in number per cell (square-root transformed) and cell local spatial autocorrelation Gi* statistic (Z-score, square-root transformed) were calculated based on sets with plaice present (see Methods in section 3) and the analysis was restricted to cells sampled in both periods (Tables 163–166). Triplots of the redundancy analyses are presented in Figures 166 and 167.

Catch in number

For the four periods and size categories considered (1984–1992 and 2002–2010, fish smaller and fish larger than 20.5 cm), there were significant effects of latitude and longitude on the catch in number. The relationship between the four response variables and the 17 significant explanatory variables selected by the stepwise regression was significant ($p<0.001$). Four canonical axes were significant ($p<0.01$) and together explained 54% (53% adjusted) of the variance in the catch in number of American plaice, with the first axis accounting for 92% of that value. The first principal component explained 20% of the unconstrained variance.

Table 163. Linear regression model statistics for the effects of latitude and longitude on the catch in number of American plaice for two periods (1984–1992 and 2002–2010) and for two size categories (fish smaller and fish larger than 20.5 cm).

Period and Size	F-statistic[1]	p-value	p-value for latitude	p-value for longitude	Adjusted R^2
1984–1992 < 20.5 cm	25.54	< 0.001	< 0.001	0.12	0.05
1984–1992 > 20.5 cm	23.24	< 0.001	< 0.001	0.31	0.04
2002–2010 < 20.5 cm	24.41	< 0.001	< 0.001	< 0.05	0.05
2002–2010 > 20.5 cm	3.34	<0.05	<0.01	0.88	0.01

[1] 2 and 962 degrees of freedom

Table 164. Redundancy analysis statistics for the effects of 17 environmental variables on the catch in number of American plaice for two periods (1984–1992 and 2002–2010) and for two size categories (fish smaller and fish larger than 20.5 cm).

	Degrees of freedom	Variance	F	N. perm	Pr (>F)	
Model	22	15.47	48.36	999	<0.001	
Residual	942	13.69				
RDA1	1	14.63	1025.80	999	<0.001	
RDA2	1	0.61	42.57	999	<0.001	
RDA3	1	0.16	11.18	999	<0.001	
RDA4	1	0.07	4.73	999	<0.010	
Residual	960	13.69				
Eigenvalue and contribution						
	RDA1	RDA2	RDA3	RDA4	PC1	PC2
Eigenvalue	14.632	0.607	0.159	0.067	7.717	14.632
Proportion explained	0.502	0.021	0.005	0.002	0.265	0.502
Cumulative proportion	0.502	0.523	0.528	0.530	0.795	0.502
Period and Size scores						
1984–1992 < 20.5 cm	-4.443	-0.901	0.558	0.274	3.650	-1.278
1984–1992 > 20.5 cm	-5.989	-0.593	-0.632	-0.120	4.492	-1.842
2002–2010 < 20.5 cm	-3.330	0.437	0.451	-0.479	2.295	2.741
2002–2010 > 20.5 cm	-4.175	1.462	-0.047	0.263	2.368	2.805

<u>Hot spots based on relative occurrence</u>

For the four periods and size categories considered (1984–1992 and 2002–2010, fish smaller and fish larger than 20.5 cm), there were significant effects of latitude and longitude on G_i*. The relationship between the four response variables and the 17 significant explanatory variables selected by the stepwise regression was significant (p<0.001). The three canonical axes were significant (p<0.001) and together explained 52% (51% adjusted) of the variance in the local spatial autocorrelation Gi* statistic for American plaice, with the first axis accounting for 91% of that value. The first principal component explained 30% of the unconstrained variance.

Table 165. Linear regression model statistics for the effects of latitude and longitude on the local spatial autocorrelation Gi* statistic (Z-score) as determined from the catch in number of American plaice in two periods (1984–1992 and 2002–2010) and for two size categories (fish smaller and fish larger than 20.5 cm).

Period and Size	F-statistic[1]	p-value	p-value for latitude	p-value for longitude	Adjusted R^2
1984–1992 < 20.5 cm	50.14	< 0.001	< 0.001	< 0.001	0.09
1984–1992 > 20.5 cm	97.89	< 0.001	< 0.001	< 0.001	0.17
2002–2010 < 20.5 cm	72.28	< 0.001	< 0.001	< 0.001	0.13
2002–2010 > 20.5 cm	33.69	< 0.001	< 0.001	<.05	0.06

[1] 2 and 962 degrees of freedom

Table 166. Redundancy analysis statistics for the effects of 17 environmental variables on the local spatial autocorrelation Gi* statistic (Z-score) as determined from the catch in number of American plaice in two periods (1984–1992 and 2002–2010) and for two size categories (fish smaller and fish larger than 20.5 cm).

	Degrees of freedom	Variance	F	N. perm	Pr (>F)	
Model	21	0.0882	48.99	999	0.001	
Residual	943	0.0809				
RDA1	1	0.0800	949.56	999	0.001	
RDA2	1	0.0059	69.83	999	0.001	
RDA3	1	0.0016	19.64	999	0.001	
Residual	960	0.0809				
Eigenvalue and contribution						
	RDA1	RDA2	RDA3	PC1	PC2	PC3
Eigenvalue	0.0800	0.0059	0.0017	0.0514	0.0189	0.0070
Proportion explained	0.473	0.035	0.010	0.304	0.112	0.042
Cumulative proportion	0.473	0.508	0.518	0.825	0.937	0.979
Period and Size scores						
1984–1992 < 20.5 cm	-0.838	-0.381	0.035	0.731	-0.615	
1984–1992 > 20.5 cm	-1.095	-0.396	-0.074	0.842	-0.754	
2002–2010 < 20.5 cm	-1.387	0.198	0.268	1.123	0.596	
2002–2010 > 20.5 cm	-1.489	0.321	-0.215	1.172	0.355	

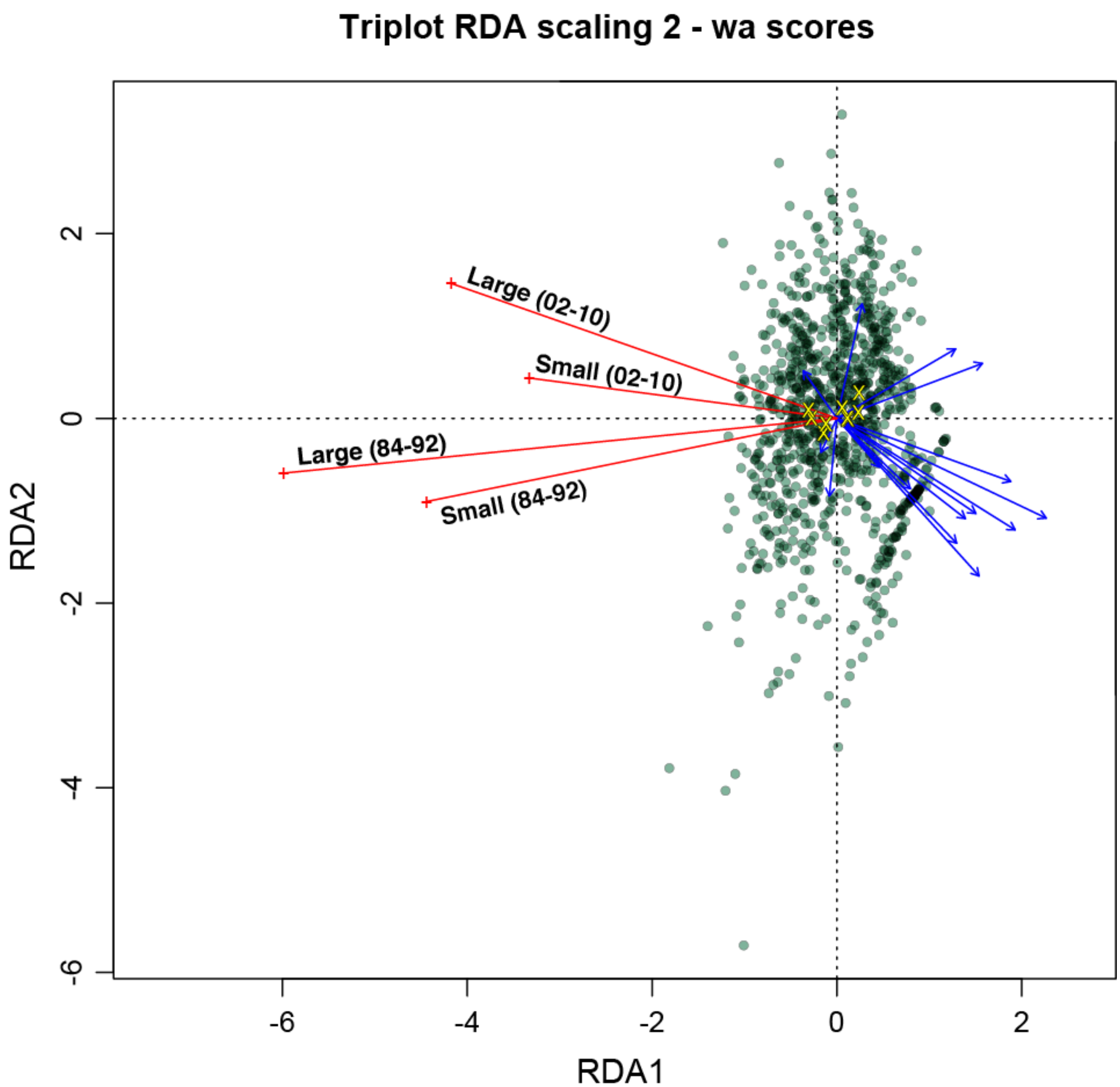

Figure 166. Results of a RDA analysis on the catch in number of American plaice in two periods (1984–1992 and 2002–2010) and for two size categories (fish smaller and fish larger than 20.5 cm). The triplot shows periods and size categories (red arrows; scores not to scale), environmental variables (blue arrows: quantitative; yellow marks: categorical), and cells. The first two RDA axes are shown.

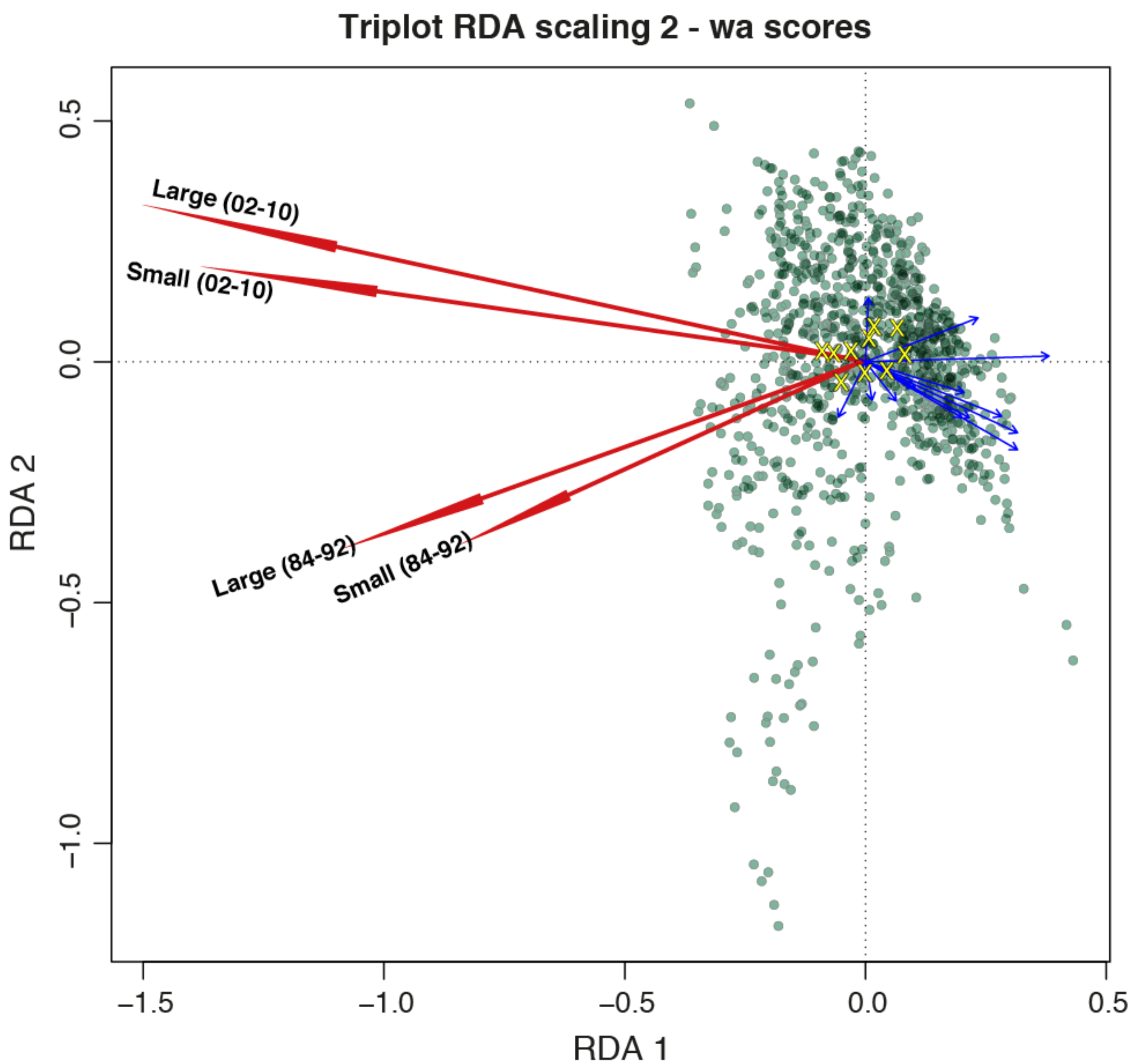

Figure 167. Results of a RDA analysis on the local spatial autocorrelation statistic G_i* for catch in number of American plaice in two periods (1984–1992 and 2002–2010) and for two size categories (fish smaller and fish larger than 20.5 cm). The triplot shows periods and size categories (red arrows; scores not to scale), environmental variables (blue arrows: quantitative; yellow marks: categorical), and cells. The first two RDA axes are shown.

Multivariate regression tree

The regression tree partitioned cells into ten different groups using environmental and fish assemblage (catch composition) data. The methods for tree partitioning analysis are presented in section 9 along with further details on the grouping results and the decision criteria. The results specific to plaice are summarized here.

Species composition

While the regression tree was formed on the basis of abundance data for 70 fish species, the distribution of the catch for individual species can be examined *a posteriori*, as highlighted in Figure 168. Based on catch abundance, American plaice occurred predominantly in group 1 of the regression tree. It was in fact the most abundant species in that group of cells. Other abundant species, and thus species with which plaice is likely to interact with frequently, included Atlantic cod, Atlantic herring, moustache sculpin, and daubed shanny. Four species were representative of the group based on distribution, fidelity, and abundance criteria, including American plaice with an indicator value (IndVal) of 0.158.

Using the relative occurrence data (1971–2010), the tree also revealed the placement of cells as hot spots and cold spots for plaice (coloured boxes and arrows in Figure 169). The hot spot cells ended out in the same group of cells (group 1) as the bulk of the catch, but apart from the cold spots which ended out in group 4.

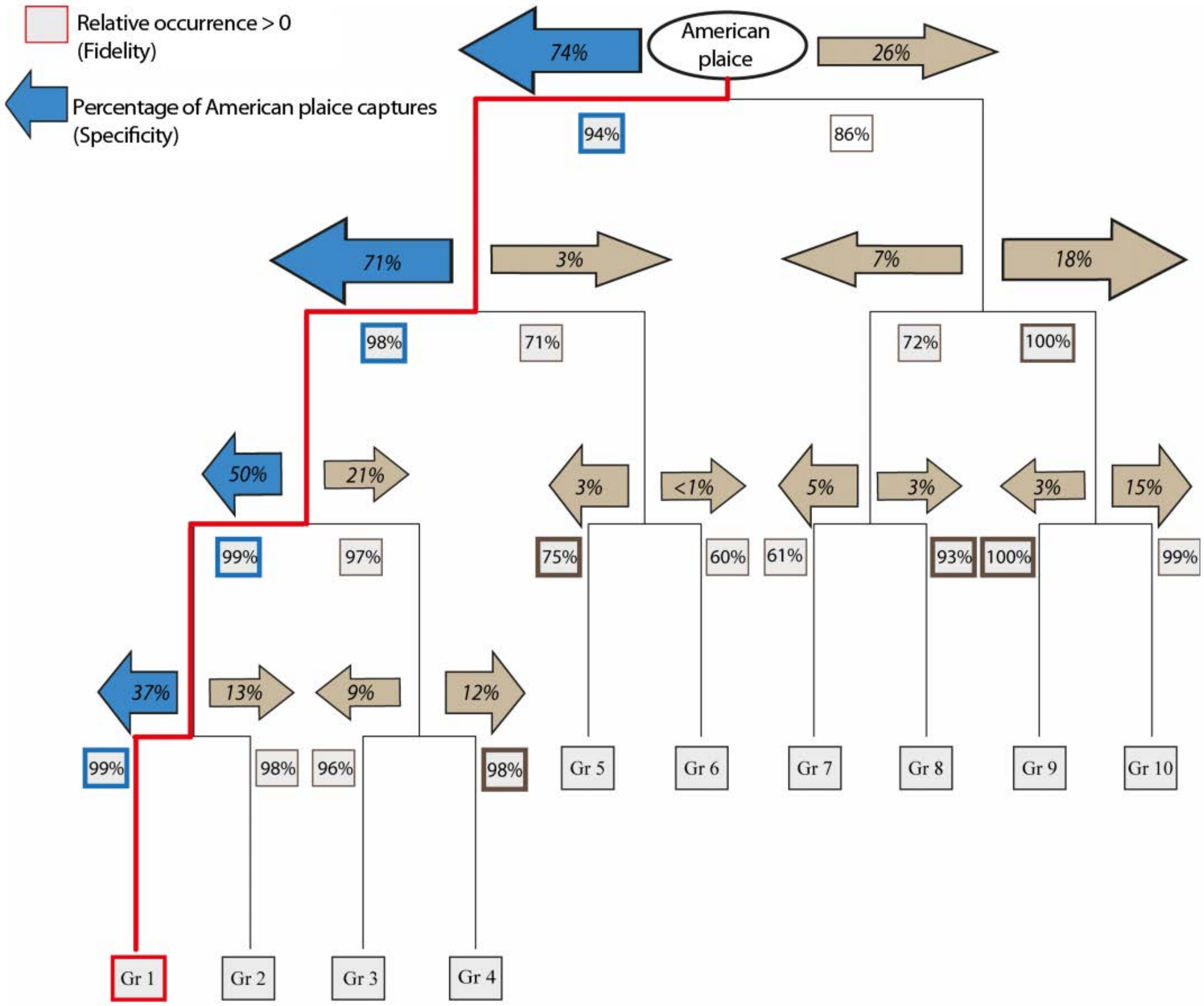

Figure 168. Recursive partitioning of American plaice catch in number data (blue arrows; period 2004–2010 in the fish assemblage database) highlighting the pathway of large plaice catches to group 1.

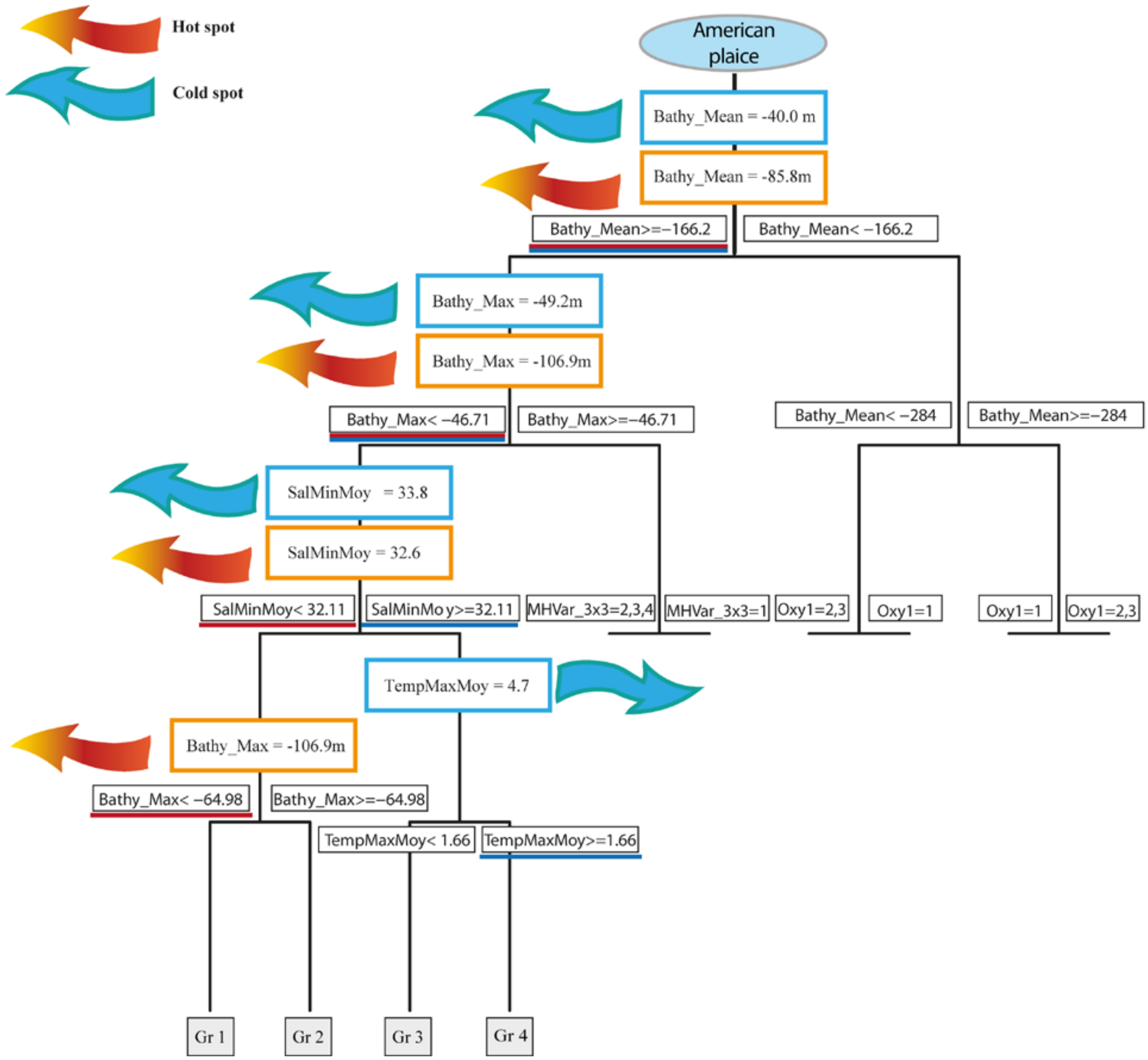

Figure 169. Recursive partitioning of American plaice based on mean environmental conditions of cells characterized as cold spots (blue arrows) and hot spots (red arrows) of relative occurrence (1971–2010). The mean levels of hot and cold spots at each split are highlighted in orange and blue, respectively.

9. MULTIVARIATE TREE ANALYSIS OF FISH SPECIES ASSEMBLAGES

Individual species form assemblages as a result of several processes. Species may share a common habitat because that habitat offers suitable living conditions or because one species depends on the other as a source of food for example. Furthermore, species may avoid a nearby habitat because of a higher risk of predation. The purpose of the multivariate tree analysis is to form groups of cells taking into consideration both catch data and habitat descriptors. Environmental criteria are selected that maximize differences in catch composition across groups of cells while minimizing differences between cells within each group. Thus, species assemblages are identified which are characteristic of a set of environmental conditions, pointing to potential interspecific relationships. For a further discussion of assemblages identified for the estuary and northern Gulf of St. Lawrence region, refer to Chouinard and Dutil (2011).

Materials and Methods

Habitat characterization

As described earlier (section 3, Methods), the habitat characteristics were obtained from Dutil et al. (2011). To summarize, the study area (St. Lawrence estuary, northern and southern Gulf) was divided into a grid of 100 km² cells. A hierarchical classification of the seabed at the scale of the megahabitat was proposed on the basis of physiographic and oceanographic features (Appendix 3). Each cell was assigned to one of 13 different megahabitats. Catch and effort data were matched with habitat categories and corresponding characteristics based on their set position in the grid.

Environmental variables

A list of the 38 environmental variables that were retained for the analysis is presented in Appendix 4. These were derived from the full list of variables shown in Table 56 (section 3) that were generated for use in the linear regression analysis.

Trawl survey data used

Fish assemblages and habitat associations were described on the basis of catches made during the bottom trawl surveys conducted annually in the lower estuary and Gulf of St. Lawrence (EGSL). The area coverage of these surveys is extensive (Figure 170), but pelagic and nearshore habitats as well as rough bottoms are not sampled. Sampling follows a stratified random design. Depth strata are predetermined and the number of sets per depth stratum is adjusted according to the planimetric area (*area* herein) of the stratum. Research survey data for the Gulf region and the Québec region were combined. When examining catch data, issues of catchability and identification need to be considered. Catchability issues may occur as a result of different gears and vessels being used over the years. The present study focussed on the period 2004–2010. During that period, the two regions concerned (Québec and Gulf) operated using the same vessel (CCGS *Teleost*) but not the same gear (Western IIa in the Gulf region and Campelen in the Québec region). While the surveys targeted pre-recruit and fully recruited groundfish of commercial importance, catches of other species were also recorded and species identification is considered to have been accurate. Documented issues with species identification precluded using data from earlier periods (Dutil et al. 2006). These issues may have occurred for several reasons, including not enough resources being available onboard for identifying rare and unfamiliar non-commercial fish species. The 2004–2010 surveys were conducted in August in the Québec region and in September in the Gulf region. Surveys conducted by the Gulf region take place in the southern Gulf whereas surveys conducted by the Québec region take place in the lower estuary and northern Gulf. However, in the present report, *northern Gulf* and *southern Gulf* refer to the location of an observation relative to the 200 m isobath south of the Laurentian Channel (Figure 170).

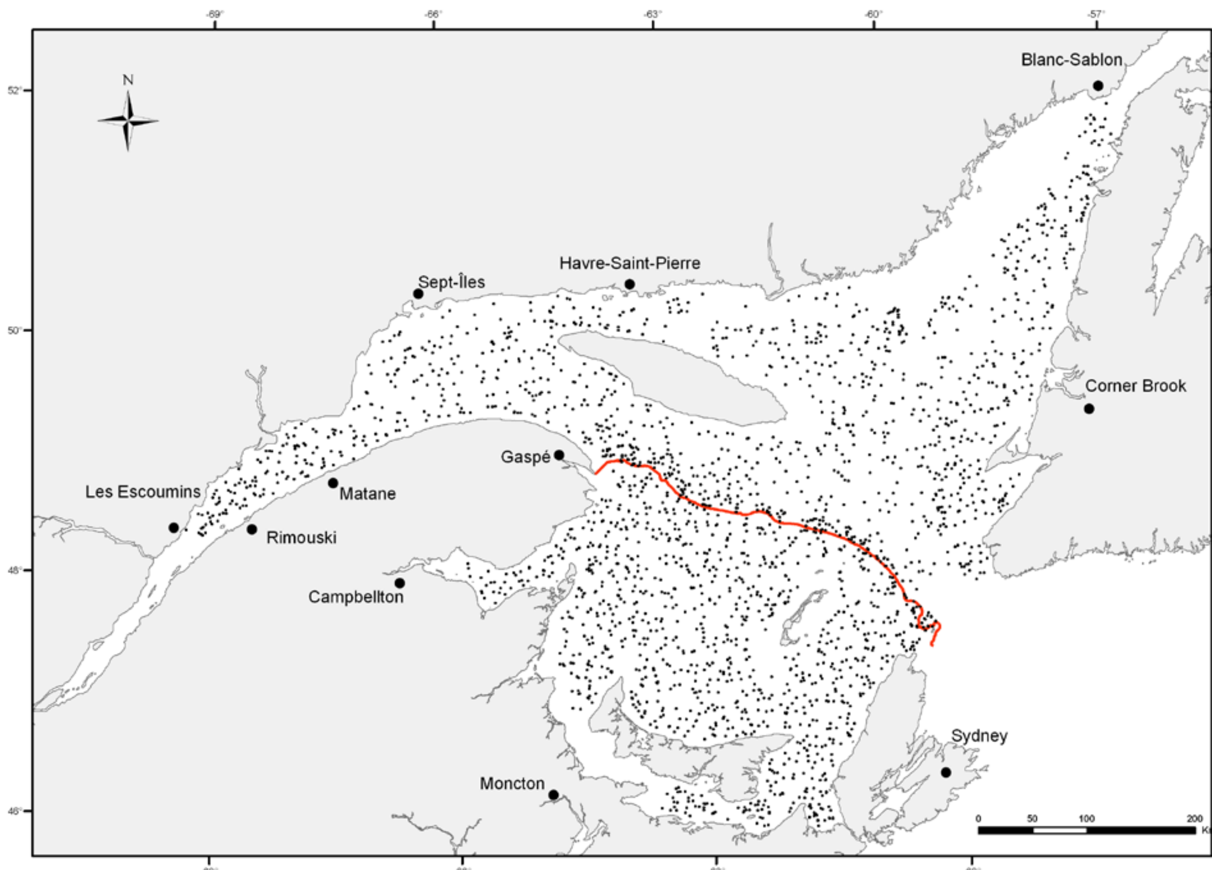

Figure 170. Map of the study area showing the locations of the 2004–2010 trawl sets (black dots) and an arbitrary dividing line (in red) between the northern and southern Gulf of St. Lawrence. The dividing line corresponds to the 200 m isobath south of the Laurentian Channel.

<u>Catch data by set</u>

For each set and each species, catches were recorded as number of fish and total weight (kg) of fish. Values were expressed per unit tow distance (1 nautical mile). A presence/absence matrix was prepared based on number and weight observations. A species was considered present in a set when catch in number (or weight) was > 0. Excluded from analysis were sets done outside of the study area, those that failed for any reason (e.g., damaged trawl), and those corresponding to cells with no matching megahabitat category as a result of lacking environmental data. Thus, data for presence/absence, catch in number, and weight were available for 2303 sets, with 1142 sets from the Gulf region surveys and 1161 sets from the Québec region surveys. Fish were present in all sets. A minimum of two species was caught in each set, and the maximum number of species caught in a set was 25.

Seventy species were included in the analysis of fish assemblages (Appendix 5). We included only species that were reported in at least one set and six years out of the seven years available. Because species of the genus *Sebastes* (*S. fasciatus* and *S. mentella*) and *Ammodytes* (*A. americanus* and *A. dubius*) can not be identified quickly using easily viewed criteria, their catches were reported at the genus level. Species caught in fewer years were also caught in low numbers and at few stations. Preliminary analyses have shown them to be of low impact in shaping assemblages, and thus they were not included in the analyses (41 species; Appendix 6). Capelin (*Mallotus villosus*) and silversides (*Menidia menidia*) were also excluded due to their pelagic distribution and, in the case of capelin, issues with the net liner that results in large catches being carried over subsequent trawl sets. Several specimens, mainly belonging to the genera *Liparis* and *Lycodes* and to the family Myctophidae, could not be identified to species and were left out. A rare morph of *Eumicrotremus* observed in the Belle Isle Strait area (species undetermined) was also not considered in the analyses.

The set data were compiled in a Microsoft Access database. The set information (2303 sets) appears in one table, and separate tables were prepared for presence/absence, catch in number, and catch in weight data (70 species, 2303 sets). The list of variables describing trawl sets and associated catches of fish in the DFO annual groundfish surveys conducted in the St. Lawrence estuary and Gulf during the period from 2004 to 2010 is shown in Appendix 7.

Catch data by cell

Species and set data were aggregated by cell using ESRI ArcGIS software. Out of 2432 cells for which a megahabitat category was available, 1237 cells were sampled during the period from 2004 to 2010, i.e., were trawled once or more. Fewer than two sets were done on average in each cell (maximum: eight sets). For presence/absence analyses, a species was considered present in a cell if reported in at least one set done in that cell. Occurrence was defined as the number of sets in a cell in which a species was reported, and relative occurrence was calculated as occurrence divided by effort (number of sets done in a cell). Mean catch in number and weight by cell was calculated on log-transformed values (including zeros; $\log_e$+1).

Statistics

Statistical analyses were performed using the R software package (version 2.14.0). A multivariate regression tree (MRT) was performed using the R function *mvpart*. Indicator values (IndVal) were calculated using the technique developed by Dufrêne and Lengendre (1997) and the R function *IndVal*. This index was calculated for each node and each terminal group formed by the MRT.

The concordance between species within groups and between indicator species of the same group were calculated using the Kendall method (Legendre 2005). Kendall concordance and Spearman correlation were calculated using the function implemented in the *vegan* package. The abundance of different species in each group was then calculated as well as the richness of each group formed by MRT analysis. A contingency table was produced in order to assess the overlap between the groups formed by MRT and megahabitats described in Dutil et al. (2011).

Background information on regression trees

Multivariate regression tree (MRT)

The multivariate regression tree method was chosen to achieve the earlier-stated goals regarding species assemblages. This method can form groups of cells taking into account the impact of the environment on the distribution of all species considered (70 species). It allows simultaneously the construction of a model and the selection of explanatory variables of interest (Legendre and Legendre 1998). This analysis generates a binary tree describing the environmental variables that best serve to distinguish the differences in species occurrences (Larsen and Speckman 2004). To do this, we calculate the impact that each successive division of a group of cells has on the sum of squared deviations from the mean group response matrix (matrix of species). The score (based on environmental variables) that minimizes this value represents the best division to retain. Tree partitioning is a nonparametric method that applies well to data that are not normally distributed (Legendre and Legendre 1998). In addition, this method can adequately model environmental data characterized by 1) non-linear relationships between the response variables (species richness) and the explanatory variables (environmental characteristics), 2) unimodal distribution response variables, and 3) unbalanced groups of different sizes (Brind'Amour 2005).

Primary divisions groups

The selection of the size of the final regression tree is based on various criteria, including the relative error produced by the model as well as the relative error of cross validation. This selection determines the number of groups of cells that are formed. It selects the tree that minimizes these two types of errors while producing a number of groups that remain consistent with the objectives of the study and the scale of environmental mechanisms observed.

Description of groups

From the groups of cells formed by this technique, we try to define species assemblages associated with each of these groups and the importance of environmental variables that explain the formation of these associations and their variability. Thus, assemblages formed are separated by hypervolumes similar to the environmental niche theory of Hutchinson, but applied to an assemblage of species rather than to a single species (Ouellette 2008).

Primary environmental variables determined by MRT

Thereafter, for each node and each terminal group, the variables that best explain each division are considered. These variables are called primary variables and they allow the partition (split at a given node) while maximizing the intragroup homogeneity of response variables (species).

Discriminating species determined by MRT

Once the groups are formed, the total species composition of cells constituting each group was analyzed to characterize them. For each of these divisions, the discriminant species have also been identified, being those that contribute most to the coefficient of determination or the least relative error (Legendre and Legendre 1998). Discriminating species provide an important contribution to the explained variance of the tree to a given node (Ouellette et al. 2005). This is particularly the case for species for which abundance differs significantly between groups in the same division. These species respond strongly to environmental variables identified for separating groups to a node. They are therefore the species best explained (smallest sum of squared errors) by this node, which itself is characterized by a primary environmental variable (Ouellette et al. 2005).

IndVal

Indicator species for each of the partitions have been defined for each node using the statistical method of finding indicator species (IndVal) developed by Dufrêne and Legendre (1997). This method characterizes the fidelity and specificity of species in each group to determine the group that best characterizes it. When a species shows a maximum indicator value for a group, it is associated with it and is considered an indicator species of this group.

Captures and species richness

<u>Captures</u>

To the north of the Gulf of St. Lawrence, 1142 stations were sampled between 2004 and 2010 compared to 1161 for the same period in the southern Gulf. These stations were collected in 1237 cells covering the study area. The total catch and the total average number per tow in the cells sampled (Figure 171) of each taxon and the frequency of their occurrence and capture are presented in Appendix 5.

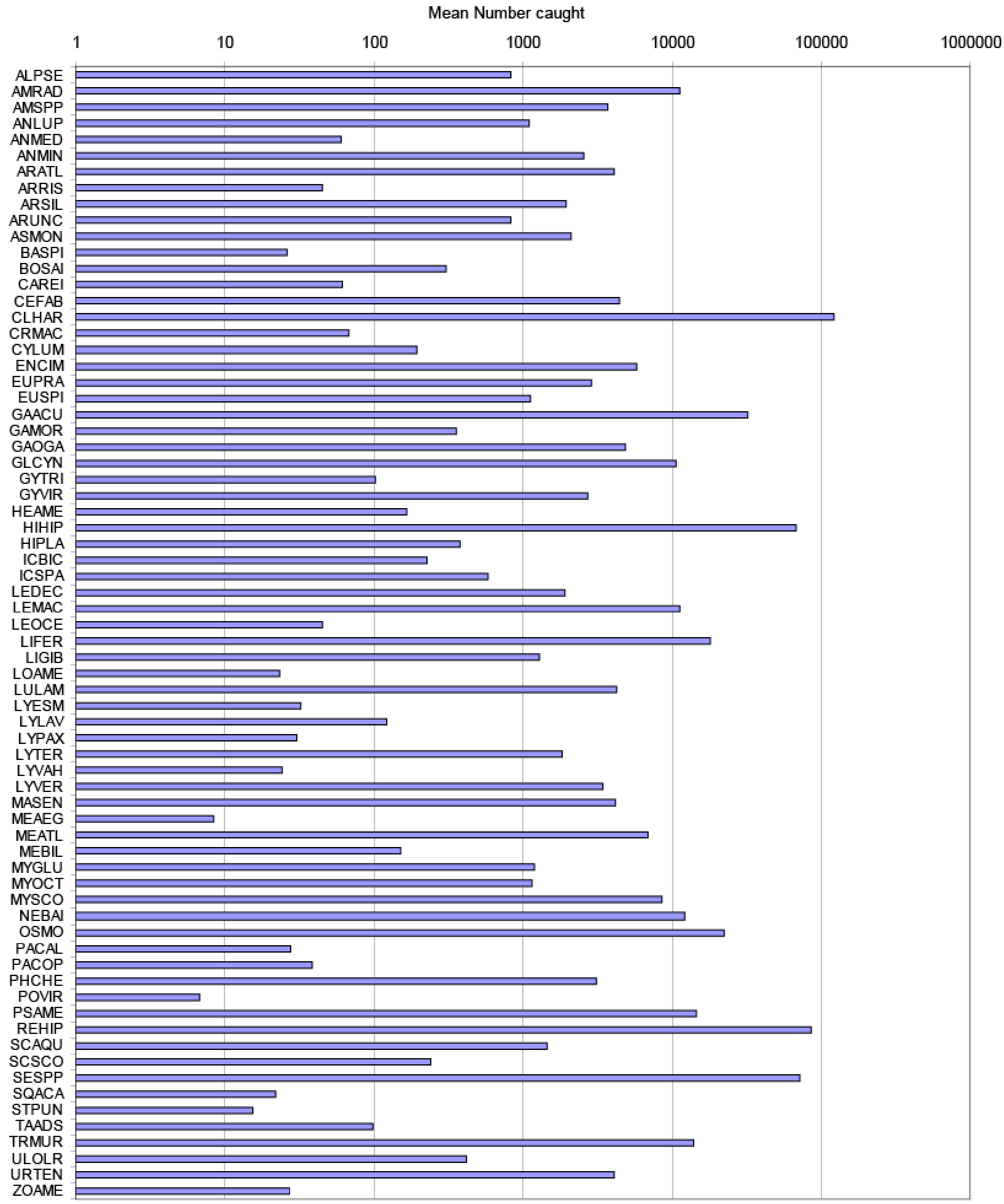

Figure 171. Standardized abundance (logarithmic scale) of species caught during the annual groundfish surveys (2004–2010). For each case, the horizontal bar represents the sum of the mean abundance per tow for each cell sampled during this period (n = 1237). Species are listed by their codes; see Appendix 5 for species names.

Species richness by station

Table 167 and Figures 172 and 173 show the distribution of species richness by sampling station for each region in the study area. The northern region had more diversity in catches than those from the southern Gulf.

Table 167. Minimum and maximum species richness observed in each region of the Gulf (northern = NR, southern = SR) and the total number for the study area.

Species richness	NR	SR	Total
Minimum	2	2	2
Maximum	25	22	25

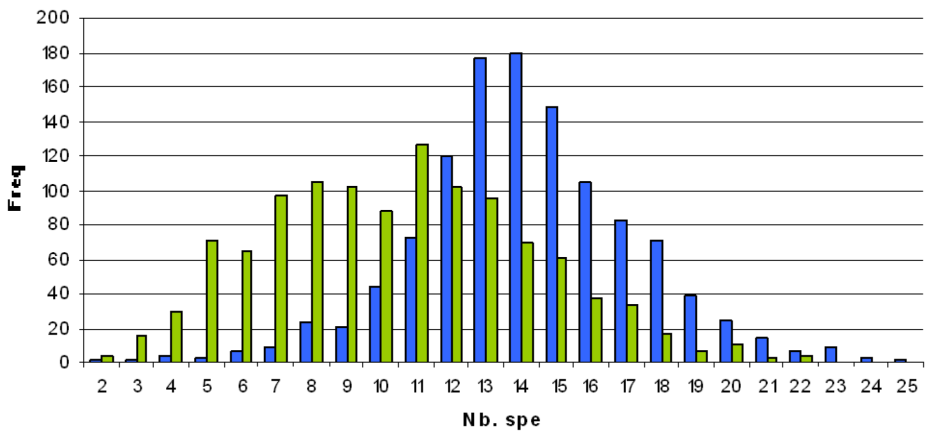

Figure 172. Species richness observed for the northern (green) and southern (blue) regions of the Gulf.

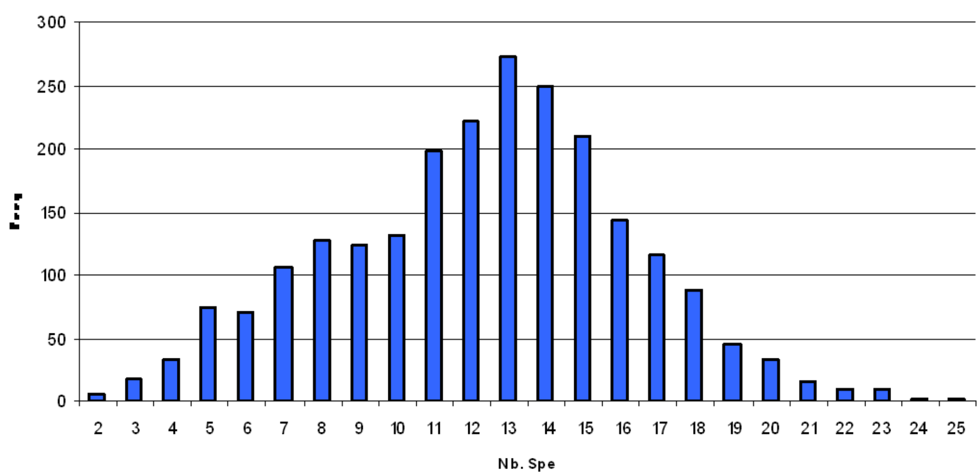

Figure 173. Species richness observed for both regions combined.

Species richness by cell

At the level of cells, captures most frequently revealed 13 or 14 species (Figure 174). Species were also not uniformly distributed in the study area (Figure 174).

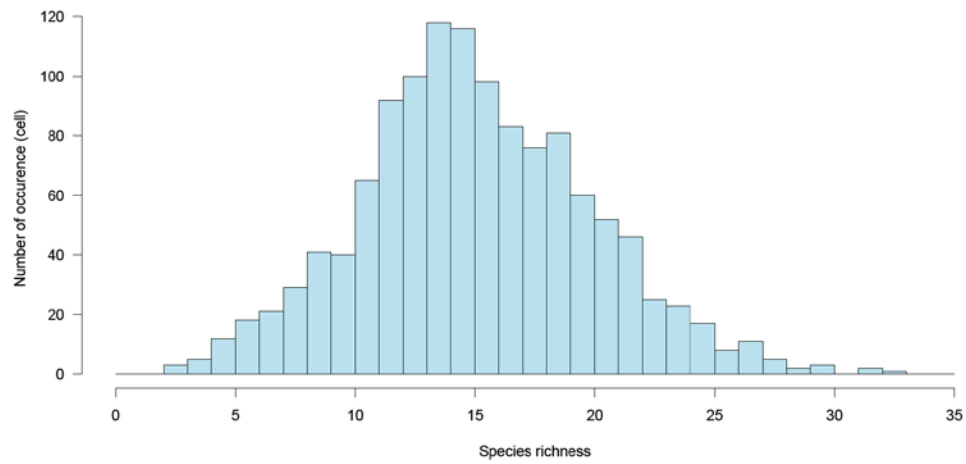

Figure 174. Species richness observed by cell.

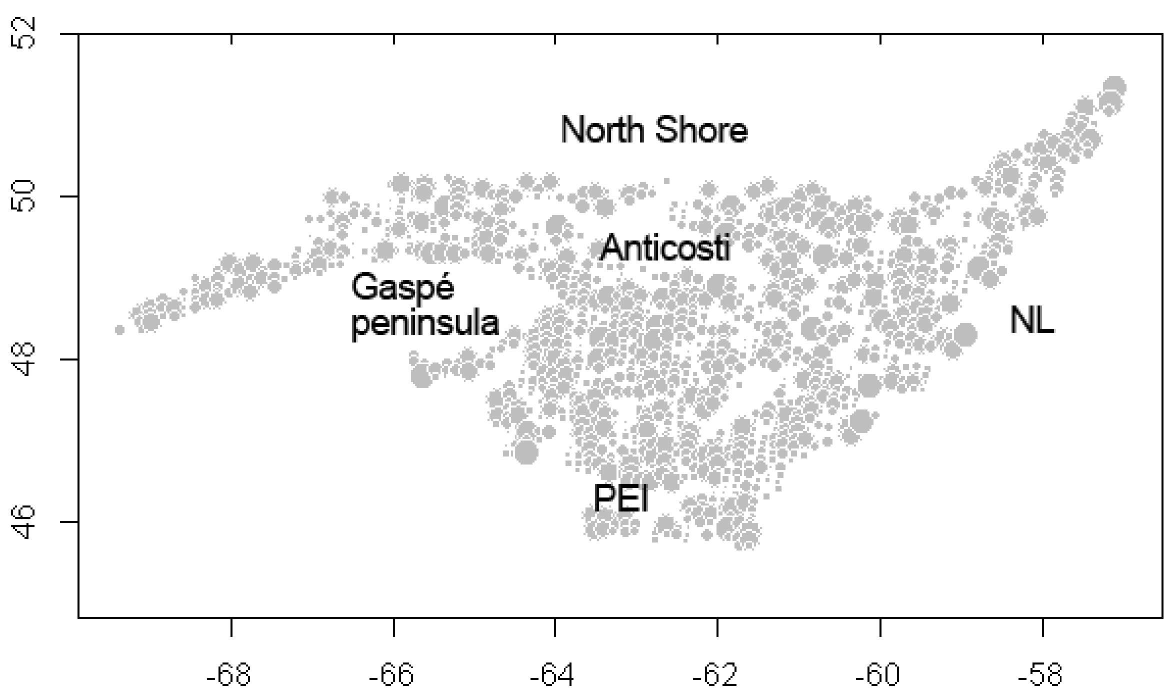

Figure 175. Map of the distribution of species richness.

Multivariate regression tree

Selection of groups

Figure 176 shows the R^2 (apparent and apparent from cross validation) and relative error as a function of the number of splits (partitions) considered, reaching a plateau between 8 and 10 groups using nine splits. Table 168 gives the values associated with successive splits of cells into nodes and groups.

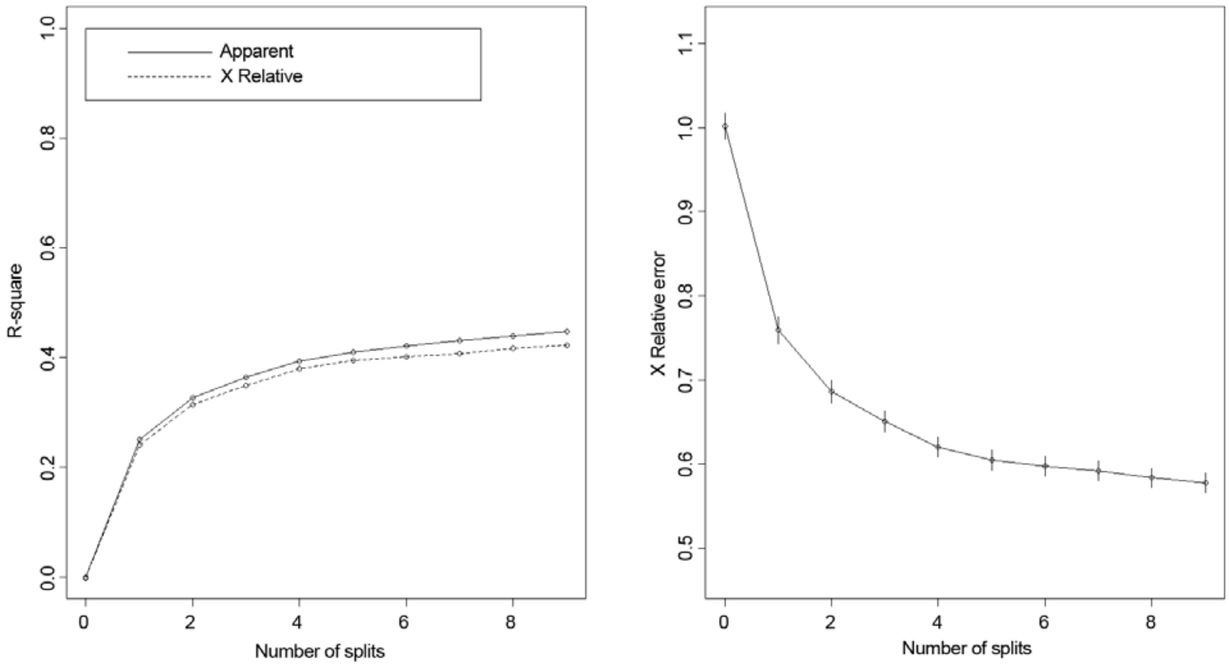

Figure 176. Plot of approximate R^2 (left) and relative error (right) for different splits.

Table 168. Successive splits into groupings (Node level = variance explained by the node).

Node level	No. of splits	Relative error
0.250	0	1
0.076	1	0.750
0.038	2	0.674
0.029	3	0.636
0.017	4	0.606
0.010	5	0.589
0.010	6	0.579
0.009	7	0.569
0.008	8	0.561
0.006	9	0.553

The results from the tree analysis have their groups summarized in terms of environmental variables, discriminating species, and species composition in the following sections.

Environment and nodes

Based on fish abundance in the estuary and Gulf of St. Lawrence, a tree was produced with 10 groups of cells that constitute the basic unit for describing assemblages and their associated habitat (Figure 177). This tree is composed of nine nodes that explain 55% of the total variation in the species composition of the St. Lawrence community. Environmental variables selected for the preparation of this tree are presented in Table 169. In order of importance, they are as follows: *mean bathymetry* separated the data into two limbs, the first with groups 1 to 6 for 750 observations and the other with groups 7 to 10 for 487 observations; *maximum bathymetry* separated groups 1 to 4 (625 observations) from groups 5 and 6 (125 observations), *minimum salinity* observed at mean depth separated groups 1 and 2 (397 observations) from groups 3 and 4 (228 observations); *mean bathymetry* separated groups 7 and 8 (236 observations) from groups 9 and 10 (251 observations); *megahabitat variability* in neighbouring cells separated groups 5 (95 observations) and 6 (30 observations); *oxygen* separated groups 7 (150 observations) and 8 (86 observations) at node 6; *maximum temperature* observed at mean depth split groups 3 (120 observations) and 4 (108 observations); *maximum bathymetry* split groups 1 (267 observations) and 2 (130 observations), *oxygen* also split groups 9 (78 observations) and 10 (173 observations) at node 7. Other primary environmental variables could also split the data similarly at different nodes. These variables are presented in Table 169, corresponding to the description of each node in the following section.

Table 169. Environmental factors involved in tree construction presented in descending order of importance (R^2) for splitting groups of cells at a node.

Node	Environmental factor	Environ. factor codename	R^2
1	Mean bathymetry	Bathy_Mean	25.020
2	Maximum bathymetry	Bathy_Max	7.613
4	Min. salinity observed at mean depth	SalMinMoy	3.814
3	Mean bathymetry	Bathy_Mean	2.947
5	Megahabitat variability	MHVar_3x3	1.680
6	Oxygen	Oxy	1.036
9	Max. temperature observed at mean depth	TempMaxMoy	0.951
8	Maximum bathymetry	Bathy_Max	0.878
7	Oxygen	Oxy	0.762

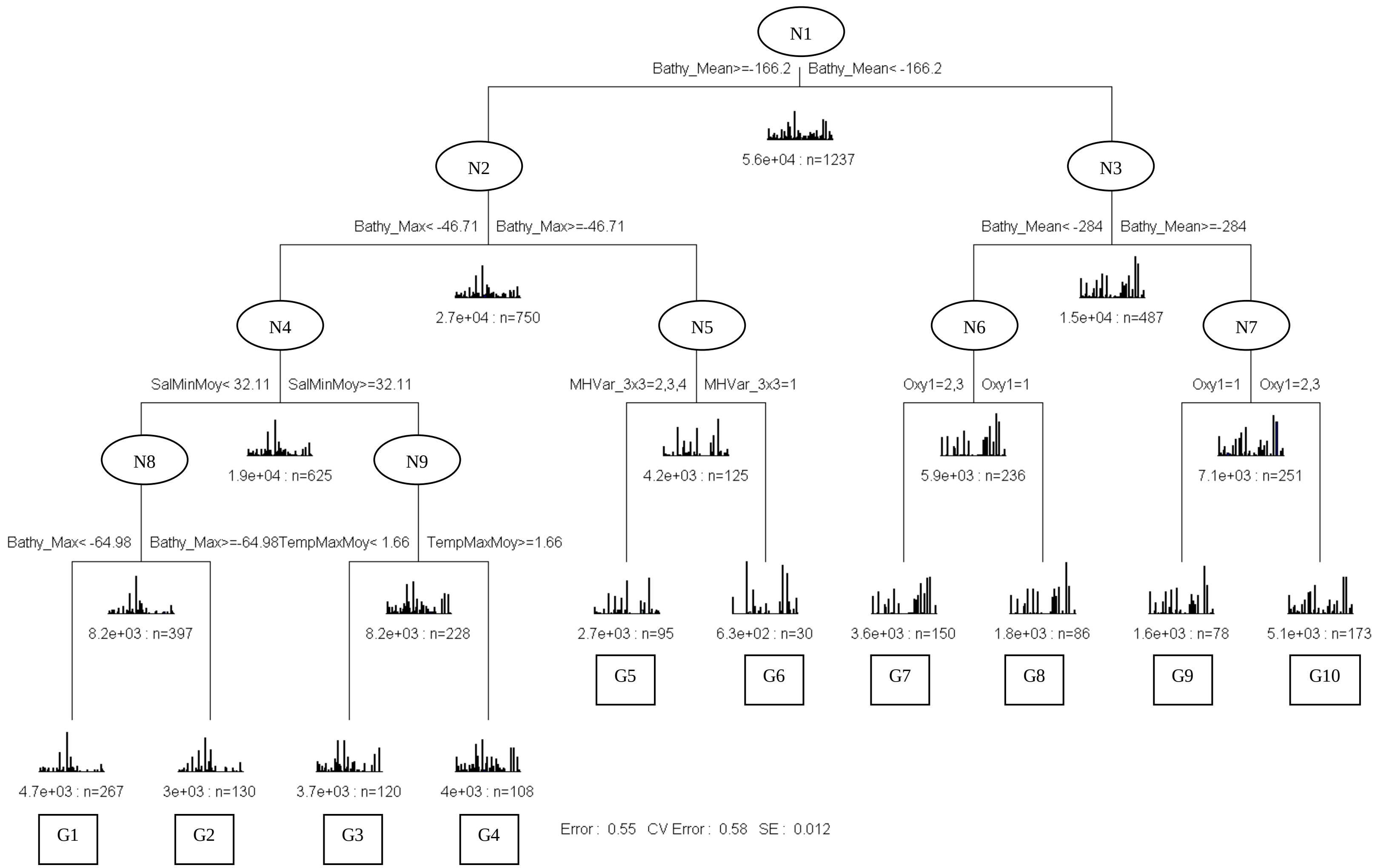

Figure 177. Regression tree constructed with estuary and Gulf of St. Lawrence capture data (2004–2010) as explained by the environmental variables at each splitting node (ovals). Terminal groups 1–10 (squares) are shown with their number of observations.

Species and nodes

The species considered as indicators for the splits at each node are summarized in Appendix 8. According to the partition of variance, discriminant species have been defined at each node. They are presented here along with the primary environmental variables (Tables 170–178).

At node 1 (N1: Figure 177), the discriminant species are *Reinhardtius hippoglossoides* (REHIP) and *Sebastes* spp. (SESPP). The average abundance of these two groups is greater in the right partition of the tree following the increase of the depth (≥166 m), with explanatory values of 26% and 15%, respectively (Table 170).

Table 170. Summary of node 1: primary environmental factors and discriminant species.

--- Node 1 ---		
Complexity (R^2) 25.01981		
Bathy_Mean≥-166.2 Bathy_Mean< -166.2		
Primary splits		
Bathy_Mean < -166.179 to the right		
Bathy_Max < -213.6135 to the right		
SalMinMoy < 33.38 to the left		
SalMoyMoy < 33.77692 to the left		
TempMinMoy < 2.745 to the left		
Discriminant species		
	REHIP	SESPP
% of expl. deviance	26.22	14.83
Mean on the left	0.56	0.72
Mean on the right	**4.07**	**3.36**
Summary		
Sum of probabilities	2.837	
Sum of indicator values	19.37	
Sum of significant indicator values	19.07	
Number of significant indicators	63	
Significant indicator distribution		
1	2	
35	28	

The species discriminating at the split for node 2 (N2: Figure 177) are *Clupea harengus* (CLHAR), *Limanda ferruginea* (LIFER), *Pseudopleuronectes americanus* (PSAME), and *Hippoglossoides platessoides* (HIPLA). The first three have abundances greater in the right partition following a reduction of the maximum depth (<46.7 m) versus PSAME. These species have explanatory values of 11%, 12%, 10%, and 31%, respectively (Table 171).

Table 171. Summary of node 2: primary environmental factors and discriminant species.

--- Node 2 ---				
Complexity (R^2) 7.613464				
Bathy_Max< -46.71 Bathy_Max≥-46.71				
Primary splits				
Bathy_Max < -46.70785 to the left				
SalMoyMax < 31.33111 to the left				
Bathy_Mean < -42.069 to the left				
TempMaxMoy < 6.09 to the left				
SalMoyMoy < 30.69636 to the right				
Discriminant species				
	CLHAR	HIPLA	LIFER	PSAME
% of expl. deviance	11.35	11.71	10.28	31.43
Mean on the left	0.66	**3.55**	0.69	0.09
Mean on the right	**2.81**	1.37	**2.73**	**3.66**
Summary				
Sum of probabilities	13.099			
Sum of indicator values	18.21			
Sum of significant indicator values	17.42			
Number of significant indicators	49			
Significant indicator distribution				
1	2			
30	19			

Node 4 (N4: Figure 177) is defined by the same discriminant species as node 1 (*Reinhardtius hippoglossoides* and *Sebastes* spp.), though now with higher values in salinity or temperature, and the species explaining 12% and 24%, respectively (Table 172).

Table 172. Summary of node 4: primary environmental factors and discriminant species.

--- Node 4 ---		
Complexity (R^2) 3.814203		
SalMinMoy< 32.11 SalMinMoy≥32.11		
Primary splits		
SalMinMoy < 32.115 to the left		
SalMinMax < 32.39 to the left		
TempMinMax < 0.135 to the left		
SalMoyMax < 32.775 to the left		
SalMoyMoy < 32.16117 to the left		
Discriminant species		
	REHIP	SESPP
% of expl. deviance	11.82	24.10
Mean on the left	0.19	0.17
Mean on the right	**1.50**	**2.05**
Summary		
Sum of probabilities	15.50	
Sum of indicator values	13.89	
Sum of significant indicator values	12.61	
Number of significant indicators	44.00	
Significant indicator distribution		
1	2	
11	33	

Node 8 (N8: Figure 177) resulted in the terminal groups 1 and 2. It is characterized by two discriminant species, *Clupea harengus* and *Limanda ferruginea*. Both species have a greater abundance in the right branch following an increase of the maximum bathymetry (≥65 m). These had an explanatory value of 21% and 53%, respectively (Table 173).

Table 173. Summary of node 8: primary environmental factors and discriminant species.

--- Node 8 ---		
Complexity (R^2) 0.8778993		
Bathy_Max< -64.98 Bathy_Max≥-64.98		
Primary splits		
Bathy_Max < -64.97825 to the left		
Bathy_Mean < -59.1069 to the left		
Bathy_Min < -48.38355 to the left		
SalMoyMoy < 31.31194 to the right		
TempMinMoy < -0.785 to the right		
Discriminant species		
	CLHAR	LIFER
% of expl. deviance	20.62	53.34
Mean on the left	0.38	0.50
Mean on the right	1.46	2.22
Summary		
Sum of probabilities	27.04	
Sum of indicator values	9.81	
Sum of significant indicator values	6.22	
Number of significant indicators	23.00	
Significant indicator distribution		
1	2	
12	11	

Node 9 (N9: Figure 177) led to the terminal groups 3 and 4. It is characterized by two discriminant species, *Lycodes vahlii* (LYVAH) and *Reinhardtius hippoglossoides*, both of which present the most significant abundances to the right branch following a decrease in maximum temperature for an average depth (<1.66°C). The variance explained by these species for this split is 12% and 34% (Table 174).

Table 174. Summary of node 9: primary environmental factors and discriminant species.

--- Node 9 ---		
Complexity (R^2) 0.9506249		
TempMaxMoy< 1.66 TempMaxMoy≥1.66		
Primary splits		
TempMaxMoy < 1.66 to the left		
Bathy_Max < -166.5275 to the right		
SalMaxMoy < 33.17 to the left		
TempMoyMoy < 1.13375 to the left		
SalMinMoy < 32.59 to the left		
Discriminant species		
	LYVAH	REHIP
% of expl. deviance	12.37	33.89
Mean on the left	0.27	0.66
Mean on the right	1.34	2.44
Summary		
Sum of probabilities	22.473	
Sum of indicator values	13.49	
Sum of significant indicator values	10.17	
Number of significant indicators	31	
Significant indicator distribution		
1	2	
12	19	

Node 5 (N5: Figure 177) is characterized by the discriminant species *Clupea harengus*, *Limanda ferruginea*, and *Osmerus mordax* (OSMOR). CLHAR and OSMOR had more marked abundances in the right partition of the tree while LIFER was more important in the left partition following an increase in the complexity of surrounding habitats. The variances explained by these species for this split are 25%, 13%, and 35%, respectively (Table 175).

Table 175. Summary of node 5: primary environmental factors and discriminant species.

--- Node 5 ---			
Complexity (R^2) 1.679732			
MHVar_3x3=2,3,4 MHVar_3x3=1			
Primary splits			
MHVar_3x3 splits as RLLL			
TempMaxMoy < 13.47 to the left			
SalMaxMoy < 30.17 to the right			
TempMaxMax < 10.415 to the left			
SalMinMax < 29.265 to the right			
Discriminant species			
	CLHAR	LIFER	OSMOR
% of expl. deviance	25.22	12.72	35.15
Mean on the left	2.04	**3.28**	1.08
Mean on the right	**5.25**	1.00	**4.88**
Summary			
Sum of probabilities	14.77		
Sum of indicator values	13.98		
Sum of significant indicator values	10.84		
Number of significant indicators	43		
Significant indicator distribution			
0	1	2	
20	10	13	

Node 3 (N3: Figure 177) is characterized by the discriminant species *Gadus morhua* (GAMOR), *Hippoglossoides platessoides* (HIPLA), *Melanostigma atlanticum* (MEATL), *Nezumia bairdii* (NEBAI), and *Phycis chesteri* (PHCHE). The average abundance of GAMOR and HIPLA is greater in the right split following a decrease of the average depth (< 284 m), with explanatory values of 19% and 13%, while MEATL, NEBAI, and PHCHE are associated with the left branch of the tree involving deeper stations (≥ 284 m) and with explanatory values of 12%, 15%, and 12%, respectively (Table 176).

Table 176. Summary of node 3: primary environmental factors and discriminant species.

--- Node 3 ---					
Complexity (R^2) 2.946754					
Bathy_Mean< -284 Bathy_Mean≥-284					
Primary splits					
Bathy_Mean < -284.0235 to the left					
SalMoyMoy < 34.54771 to the left					
SalMaxMin < 34.595 to the left					
SalMoyMin < 34.54771 to the left					
SalMaxMoy < 34.625 to the right					
Discriminant species					
	GAMOR	HIPLA	MEATL	NEBAI	PHCHE
% of expl. deviance	18.84	12.81	11.69	15.36	11.71
Mean on the left	0.10	1.47	**1.79**	**2.90**	**1.41**
Mean on the right	**1.69**	**2.78**	0.54	1.47	0.15
Summary					
Sum of probabilities	17.989				
Sum of indicator values	13.27				
Sum of significant indicator values	10.16				
Number of significant indicators	42				
Significant indicator distribution					
1	2				
15	27				

Node 6 (N6: Figure 177) led to the terminal groups 7 and 8. It is characterized by the discriminant species *Hippoglossoides platessoides*, *Melanostigma atlanticum*, *Phycis chesteri*, and *Reinhardtius hippoglossoides*. The first two species and REHIP have abundances greater in the right split of the tree, with oxygen concentrations corresponding to classes 2 and 3, while PHCHE abundances are more pronounced in the left branch, associated with class 1 oxygen. The variance explained by these species for this split are 13%, 11%, 28%, and 22%, respectively (Table 177).

Table 177. Summary of node 6: primary environmental factors and discriminant species.

--- Node 6 ---				
Complexity(R^2) 1.035744 Oxy1=2,3 Oxy1=1				
Primary splits				
Oxy1 splits as RLL-				
SalMaxMoy < 34.67 to the right				
Bathy_Max < -431.6515 to the right				
SalMoyMax < 34.71833 to the left				
SalMinMax < 34.635 to the left				
Discriminant species				
	HIPLA	MEATL	PHCHE	REHIP
% of expl. deviance	12.87	10.51	27.52	22.30
Mean on the left	1.04	1.41	**2.03**	3.59
Mean on the right	**2.21**	**2.46**	0.33	**5.13**
Summary				
Sum of probabilities	24.23			
Sum of indicator values	9.97			
Sum of significant indicator values	6.44			
Number of significant indicators	26			
Significant indicator distribution				
0	1	2		
9	9	8		

Node 7 (N7: Figure 177) led to the terminal groups 9 and 10. It is characterized by three discriminant species: *Gadus morhua*, *Melanostigma atlanticum*, and *Reinhardtius hippo-glossoides*. GAMOR has abundances greater in the right branch, following oxygen concentrations corresponding to classes 2 and 3, while the other two species are more predominant on the left side and associated with class 1 oxygen. The variances explained by these species for this split are 27%, 16%, and 15%, respectively (Table 178).

Table 178. Summary of node 7: primary environmental factors and discriminant species.

--- Node 7 ---			
Complexity (R^2) 0.762024			
Oxy1=1 Oxy1=2,3			
Primary splits			
Oxy1 splits as LRR-			
Bathy_Max < -269.9735 to the left			
SalMoyMax < 34.54771 to the right			
SalMaxMoy < 34.34 to the right			
Bathy_Mean < -235.287 to the left			
Discriminant species			
	GAMOR	MEATL	REHIP
% of expl. deviance	27.25	16.08	15.13
Mean on the left	0.68	1.31	4.75
Mean on the right	2.15	0.19	3.66
Summary			
Sum of probabilities	22.07		
Sum of indicator values	11.40		
Sum of significant indicator values	8.47		
Number of significant indicators	32		
Significant indicator distribution			
0	1	2	
7	13	12	

Group descriptions

The following figures and tables summarize species in terms of richness, proportional abundance, and value as indicators in assembling groups 1 through 10.

Group 1

This group consists of 267 cells, representing 22% of the area surveyed (2004-2010) and 9% of average total catch. It consists of a total of 56 species and has a maximum species richness of 28 species per cell (Figure 178).

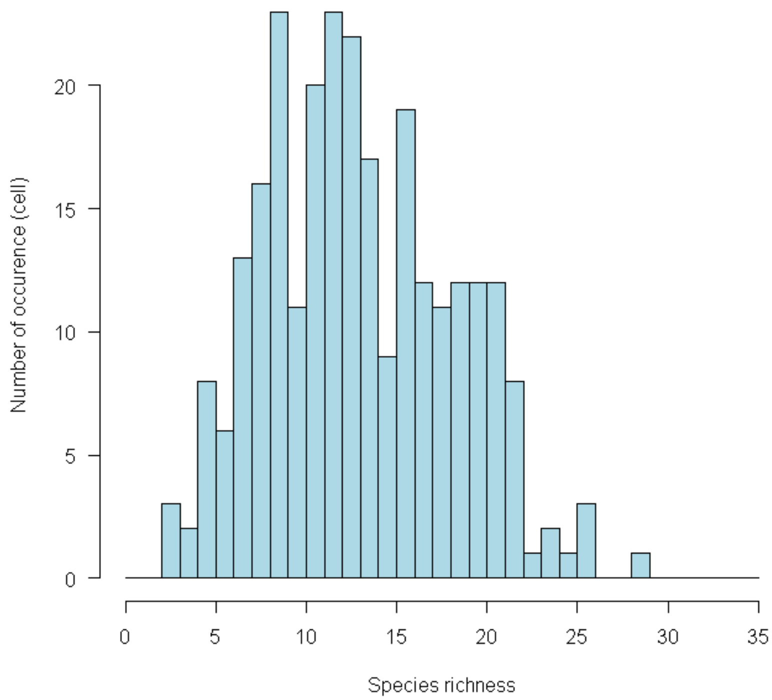

Figure 178. Species richness for cells belonging to group 1.

The most abundant species associated with this group is HIPLA followed by GAMOR, LEMAC, and CLHAR (Figure 179). Four species of this group had significant, albeit low, indicator values ($p < 0.05$) (Table 179). The distributions of these species are presented in Figure 180.

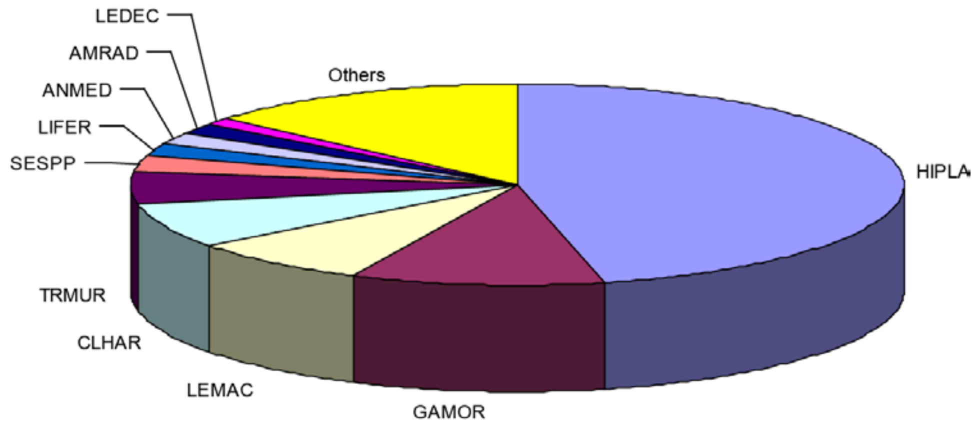

Figure 179. The most abundant species associated with group 1.

Table 179. Indicator species with their p-value and IndVal.

Species	Scientific name	IndVal	p-value
ANMED	*Anisarchus medius*	0.114	0.001
HIPLA	*Hippoglossoides platessoides*	0.158	0.001
ICSPA	*Icelus spatula*	0.170	0.001
ULOLR	*Ulcina olrikii*	0.202	0.001

The species of this group have a Kendall intra-group concordance of 45% (Appendix 9). The correlation between the indicator species is greater than 44% (Table 180). These species are found at an average depth of less than 166 m, a maximum depth of greater than 65 m, and salinity less than 32.

Table 180. Spearman rank correlation and Kendall concordance coefficients for group 1 indicator species.

	ANMED	HIPLA	ICSPA	ULOLR
Spearman correlation	0.255	0.271	0.330	0.350
Kendall concordance	0.441	0.453	0.498	0.512
p	0.001	0.001	0.001	0.001

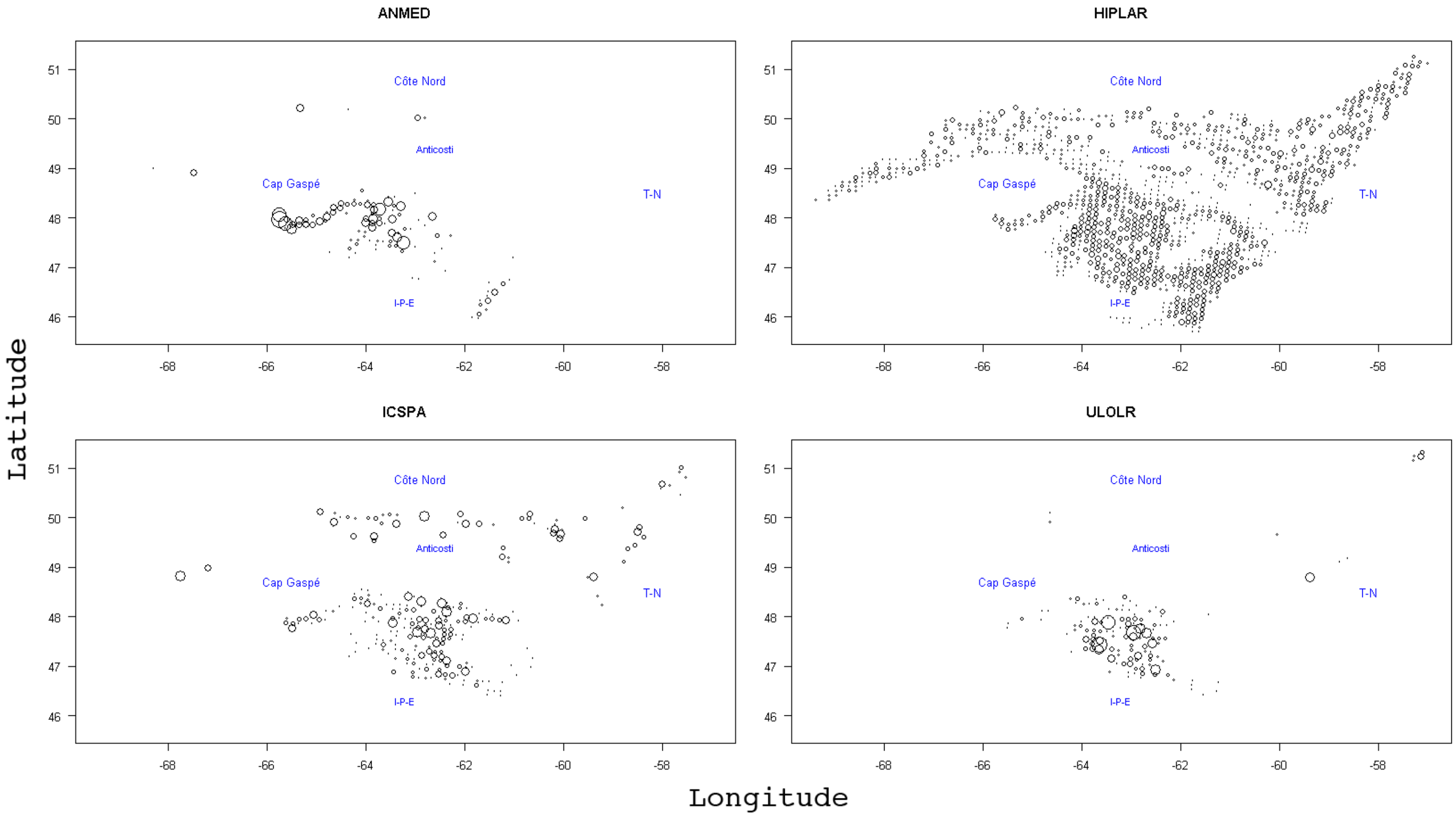

Figure 180. Distribution of group 1 indicator species (codes correspond to names in Table 178).

Group 2

This group consists of 130 cells, which represents 11% of the area surveyed (2004-2010) and 11% of average total catch. It is composed of 51 species in total and has a maximum richness of 27 species per cell (Figure 181).

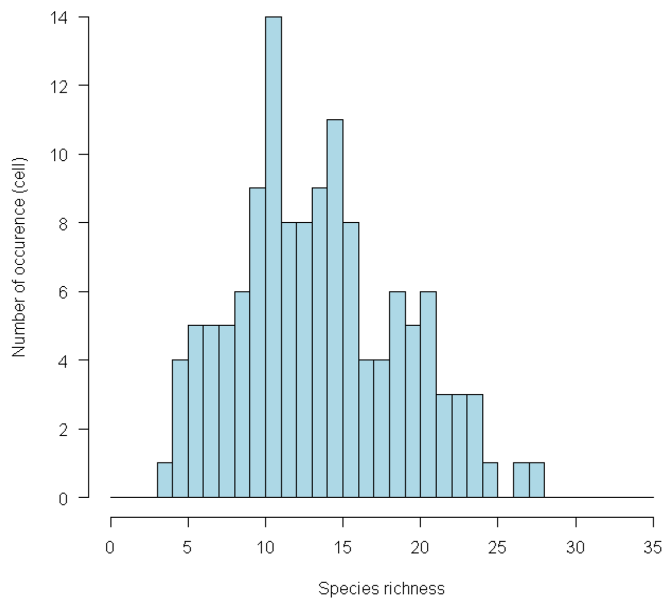

Figure 181. Species richness for cells belonging to group 2.

The most abundant species associated with group 2 are CLHAR, HIPLAS, LIFER, and GAMOR (Figure 182). Two species of this groups are notable for their significant ($p<0.05$), albeit low, indicator values (Table 181). Their distributions are presented in Figure 183.

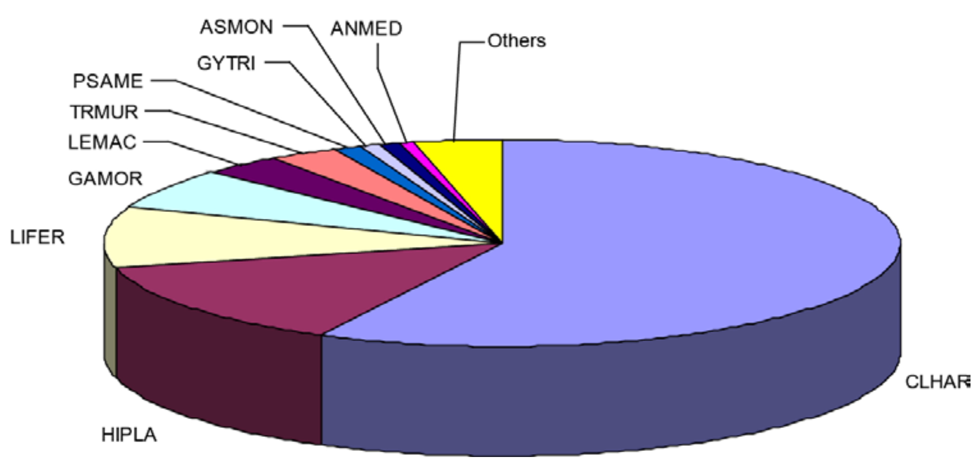

Figure 182. The most abundant species associated with group 2.

Table 181. Group 2 indicator species with their p-value and IndVal.

Species	Scientific name	IndVal	p-value
GYTRI	*Gymnocanthus tricuspis*	0.094	0.009
LIGIB	*Liparis gibbus*	0.111	0.001

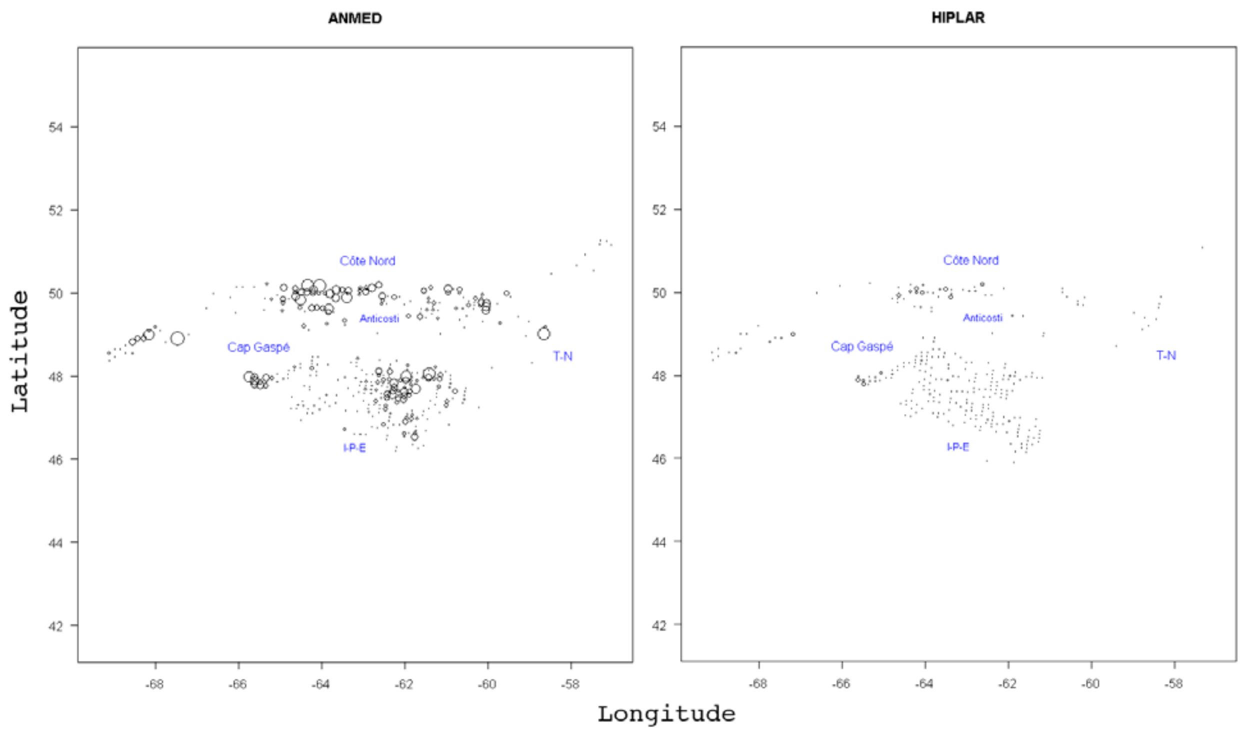

Figure 183. Distribution of group 2 indicator species.

The species of this group had a Kendall intra-group concordance of 70% (Appendix 9) and a concordance of 41% between indicator species (Table 182).

Table 182. Spearman rank correlation and Kendall concordance coefficients for group 2 indicator species.

	GYTRI	LIGIB
Spearman correlation	0.409	0.409
Kendall concordance	0.705	0.705
p	0.001	0.001

The species of this group are found in an environment with an average depth less than 166 m, a maximum depth greater than 47 m but less than 65 m, and a salinity of less than 32.

Group 3

This group consists of 120 cells, which represents 10% of the area surveyed (2004-2010) and 7% of average total catch. It is composed of 56 species in total and has a maximum richness of 29 species per cell (Figure 184).

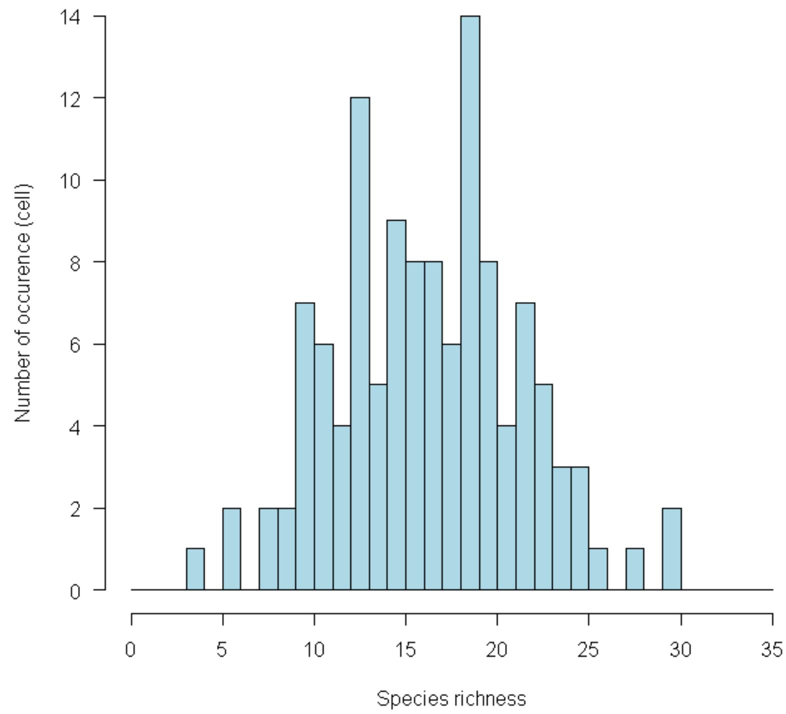

Figure 184. Species richness for cells belonging to group 3.

The most abundant species associated with this group are GAMOR, HIPLAS, SESPP, TRMUR, LEMAC, and REHIP (Figure 185).

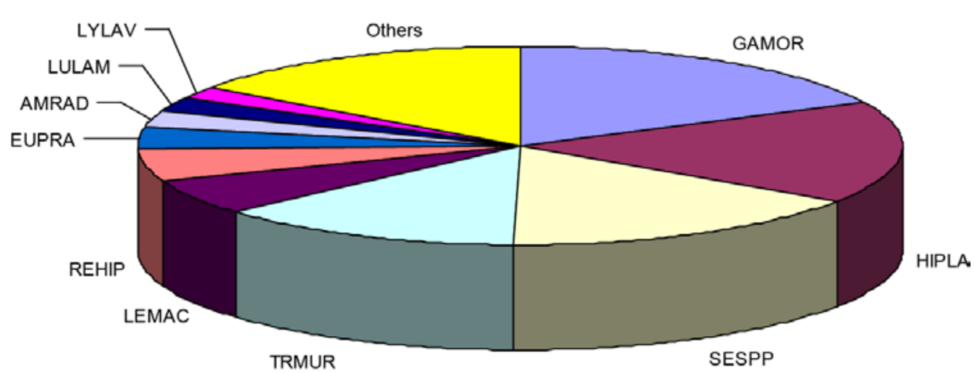

Figure 185. The most abundant species associated with group 3.

Eleven species present significant ($p<0.05$), albeit low, indicator values (Table 183).

Table 183. Indicator species of group 3 with p-value and IndVal.

Species	Scientific name	IndVal	p-value
GYVIR	*Gymnelus viridis*	0.058	0.006
ANMIN	*Anarhichas minor*	0.073	0.003
ARUNC	*Artediellus uncinatus*	0.101	0.001
ICBIC	*Icelus bicornis*	0.198	0.001
GAMOR	*Gadus morhua*	0.199	0.001
MYSCO	*Myoxocephalus scorpius*	0.204	0.001
ANLUP	*Anarhichas lupus*	0.209	0.001
LYLAV	*Lycodes lavalaei*	0.239	0.001
EUSPI	*Eumicrotremus spinosus*	0.312	0.001
TRMUR	*Triglops murrayi*	0.319	0.001
EUPRA	*Eumesogrammus praecisus*	0.328	0.001

The species of this group had a Kendall intra-group concordance of 37% (Appendix 8) and a concordance between indicator species varying from 23% to 46% (Table 184).

Table 184. Spearman rank correlation and Kendall concordance coefficients for group 3 indicator species.

	ANLUP	ANMIN	ARUNC	EUPRA	EUSPI	GAMOR
Spearman correlation	0.260	0.148	0.264	0.400	0.384	0.300
Kendall concordance	0.327	0.225	0.331	0.454	0.440	0.364
p	0.001	0.001	0.001	0.001	0.001	0.001

	GYVIR	ICBIC	LYLAV	MYSCO	TRMUR
Spearman correlation	0.216	0.254	0.351	0.265	0.404
Kendall concordance	0.287	0.322	0.410	0.332	0.458
p	0.001	0.001	0.001	0.001	0.001

The species of this group are found in an environment with average depth less than 166 m, maximum depth greater than 47 m, salinity less than 32, and temperature less than 1.7°C.

Group 4

This group consists of 108 cells, which represents 9% of the area surveyed (2004-2010) and 8% of average total catch. It is composed of 58 species in total and has a maximum richness of 32 species per cell (Figure 186).

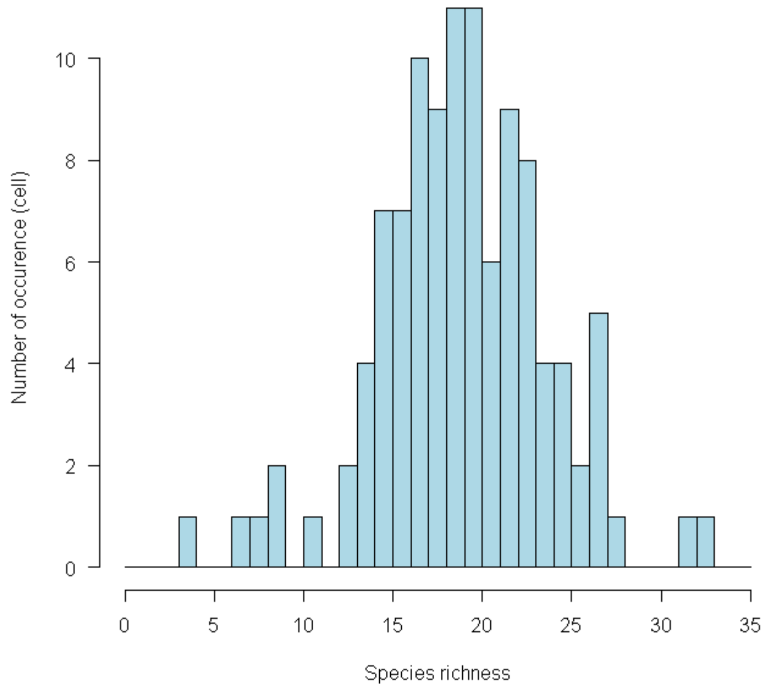

Figure 186. Species richness for cells belonging to group 4.

The most abundant species associated with group 4 are REHIP, HIPLA, SESPP, GAMOR, and TRMUR (Figure 187).

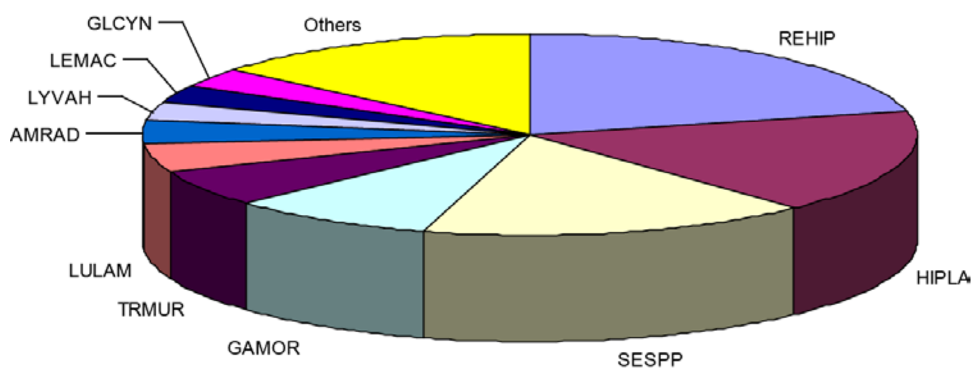

Figure 187. The most abundant species associated with group 4.

Ten species had significant (p<0.05), albeit low, indicator values (Table 185).

Table 185. Group 4 indicator species with p-value and IndVal.

Species	Scientific name	IndVal	p-value
MEAEG	*Melanogrammus aeglefinus*	0.019	0.048
CAREI	*Careproctus reinhardti*	0.043	0.014
BOSAI	*Boreogadus saida*	0.091	0.001
CYLUM	*Cryptacanthodes maculatus*	0.121	0.001
ARATL	*Artediellus atlanticus*	0.133	0.001
ASMON	*Aspidophoroides monopterygius*	0.158	0.001
LEMAC	*Leptoclinus maculatus*	0.181	0.001
LEDEC	*Leptagonus decagonus*	0.192	0.001
LYVAH	*Lycodes vahlii*	0.261	0.001
LULAM	*Lumpenus lampretaeformis*	0.301	0.001

The species of this group had a Kendall intra-group concordance of 28% (Appendix 9). The concordance between indicator species varied between 16% and 35% (Table 186).

Table 186. Spearman rank correlation and Kendall concordance coefficients for group 4 indicator species.

	ARATL	ASMON	BOSAI	CAREI	CYLUM
Spearman correlation	0.173	0.198	0.167	0.106	0.135
Kendall concordance	0.256	0.278	0.251	0.196	0.222
p	0.001	0.001	0.001	0.001	0.001

	LEDEC	LEMAC	LULAM	LYVAH	MEAEG
Spearman correlation	0.229	0.256	0.274	0.209	0.070
Kendall concordance	0.306	0.331	0.346	0.288	0.163
p	0.001	0.001	0.001	0.001	0.001

The species of this group were found in an environment with average depth less than 166 m, maximum depth greater than 47 m, salinity less than 32, and temperature greater than 1.7°C.

Group 5

This group consists of 95 cells, which represents 8% of the area surveyed (2004-2010) and 17% of the mean total catch. It is composed of 47 species in total and has a maximum richness of 29 species per cell (Figure 188).

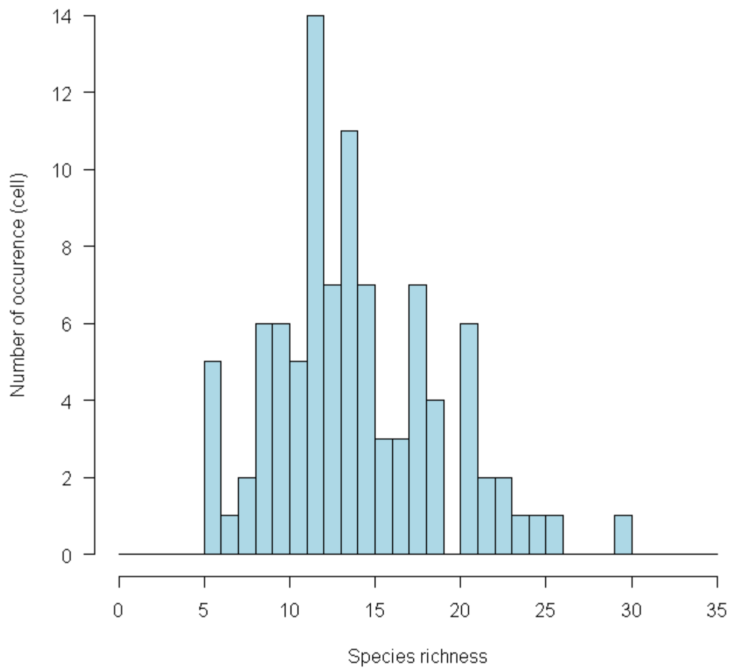

Figure 188. Species richness for cells belonging to group 5.

The most abundant species associated with group 5 is CLHAR_N, followed by LIFER, PSAME, OSMOR, and AMSPP (Figure 189).

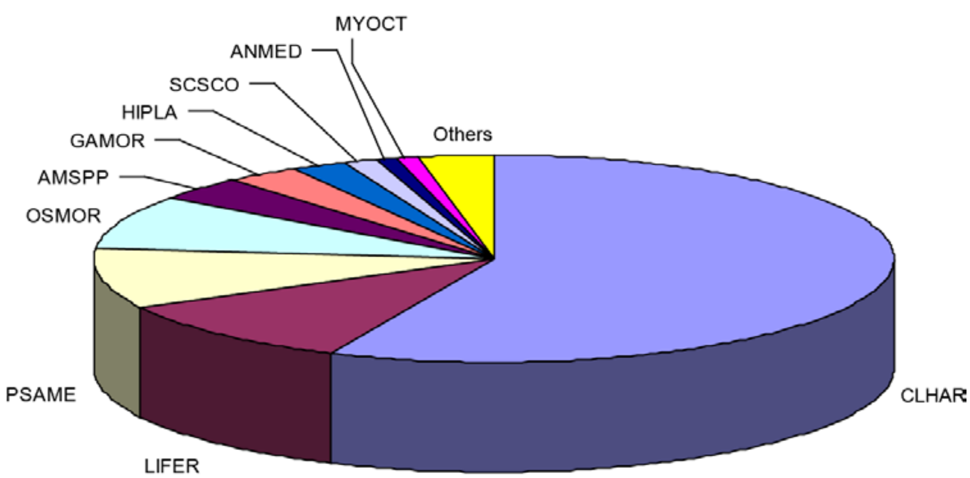

Figure 189. The most abundant species associated with group 5.

Six species had significant ($p<0.05$), albeit low, indicator values (Table 187).

Table 187. Group 5 indicator species with p-value and IndVal.

Species	Scientific name	IndVal	p
AMSPP	*Ammodytes*	0.107	0.002
LEOCE	*Leucoraja ocellata*	0.115	0.001
SCSCO	*Scomber scombrus*	0.176	0.001
HEAME	*Hemitripterus americanus*	0.307	0.001
MYOCT	*Myoxocephalus octodecemspinosus*	0.357	0.001
LIFER	*Limanda ferruginea*	0.440	0.001

The species of this group had a Kendall intra-group concordance of 39% (Appendix 9) and a concordance between indicator species varying from 27% to 47% (Table 188).

Table 188. Spearman rank correlation and Kendall concordance coefficients for group 5 indicator species.

	AMSPP	HEAME	LEOCE	LIFER	MYOCT	SCSCO
Spearman correlation	0.129	0.294	0.220	0.334	0.361	0.202
Kendall concordance	0.274	0.412	0.350	0.445	0.467	0.335
p	0.001	0.001	0.001	0.001	0.001	0.001

The species of this group are found at a depth averaging less than 166 m, a maximum depth of less than 47 m, and a heterogenous habitat with more than one type of different habitat nearby.

Group 6

This group consists of 30 cells, which represents 2% of the area surveyed (2004-2010) and 8% of average total catch. It is composed of 31 species in total and has a maximum richness of 24 species per cell (Figure 190).

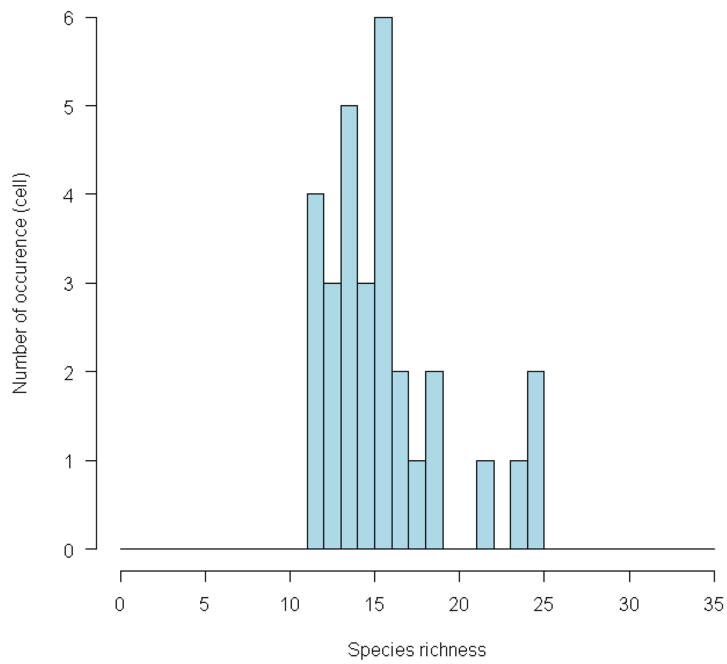

Figure 190. Species richness for cells belonging to group 6.

The most abundant species associated with this group are CLHAR, OSMOR, PSAME, and GAACU (Figure 191).

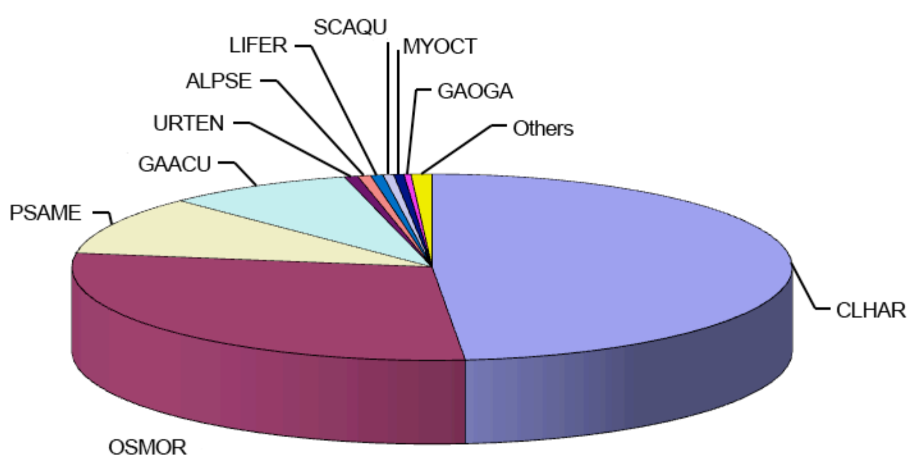

Figure 191. The most abundant species associated with group 6.

Twelve species had significant indicator values ($p<0.05$). Of these, five species had an IndVal significantly higher than 0.5 (Table 189).

Table 189. Group 6 indicator species with p-value and IndVal.

Species	Scientific name	IndVal	p-value
SQACA	*Squalus acanthias*	0.063	0.002
CRMAC	*Cryptacanthodes maculatus*	0.112	0.001
ZOAME	*Zoarces americanus*	0.189	0.001
URTEN	*Urophycis tenuis*	0.297	0.001
GAOGA	*Gadus ogac*	0.317	0.001
CLHAR	*Clupea harengus*	0.374	0.001
TAADS	*Tautogolabrus adspersus*	0.450	0.001
PSAME	*Pseudopleuronectes americanus*	0.505	0.001
GAACU	*Gasterosteus aculeatus*	0.596	0.001
SCAQU	*Scophthalmus aquosus*	0.657	0.001
ALPSE	*Alosa pseudoharengus*	0.668	0.001
OSMOR	*Osmerus mordax*	0.774	0.001

The species of this group had a Kendall intragroup concordance of 26% (Appendix 9). The concordance between indicator species varied between 16 and 44%, depending on the species (Table 190).

Table 190. Spearman rank correlation and Kendall concordance coefficients for group 6 indicator species.

	ALPSE	CLHAR	CRMAC	GAACU	GAOGA	OSMOR
Spearman correlation	0.393	0.208	0.113	0.241	0.124	0.364
Kendall concordance	0.443	0.274	0.187	0.305	0.197	0.417
p	0.001	0.001	0.001	0.001	0.001	0.001

	PSAME	SCAQU	SQACA	TAADS	URTEN	ZOAME
	0.340	0.320	0.081	0.330	0.140	0.259
Spearman correlation	0.395	0.377	0.157	0.386	0.211	0.321
Kendall concordance	0.001	0.001	0.001	0.001	0.001	0.001
p						

The species of this group are found at depths averaging less than 166 m, with a maximum depth of less than 47 m, and a heterogenous habitat with more than one type of different habitat nearby.

Group 7

This group consists of 150 cells, which represents 12% of the area surveyed (2004-2010) and 11% of average total catch. It is composed of 53 species in total and has a maximum richness of 23 species per cell (Figure 192).

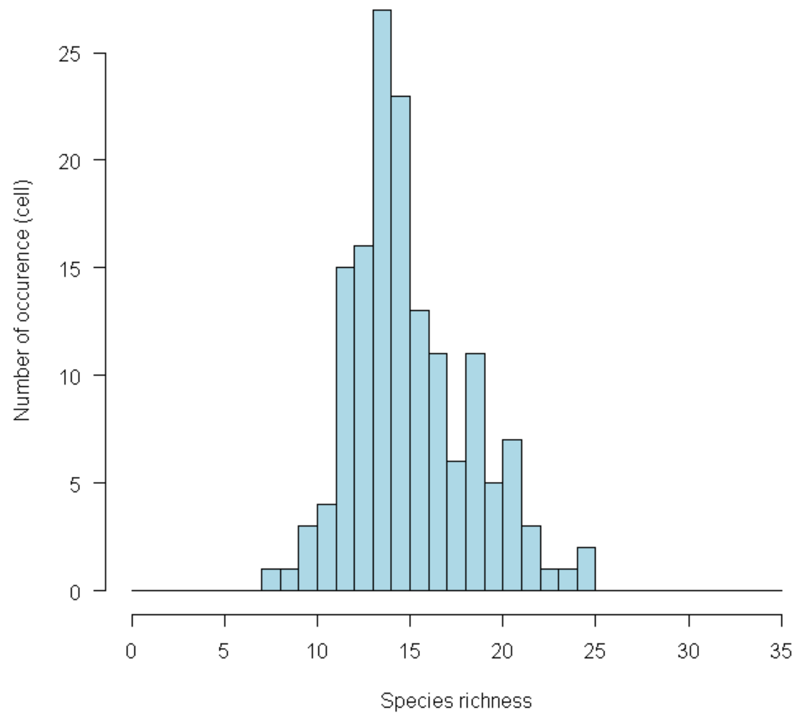

Figure 192. Species richness for cells belonging to group 7.

The most abundant species associated with Group 7 are SESPP, REHIP, and NEBAI (Figure 193).

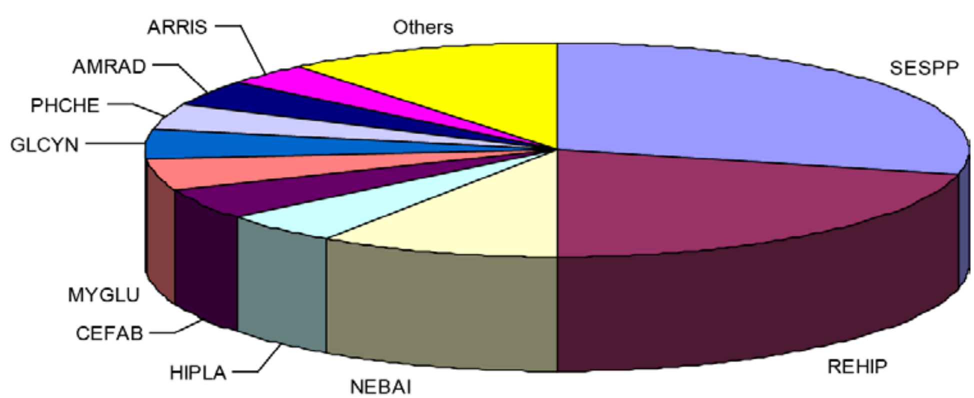

Figure 193. The most abundant species associated with group 7.

Fourteen species had significant indicator values ($p<0.05$). Of these, only one species had a significant IndVal greater than 0.5 (Table 191).

Table 191. Group 7 indicator species with p-value and IndVal.

Species	Scientific name	IndVal	p-value
BASPI	*Bathyraja spinicauda*	0.031	0.031
LOAME	*Lophius americanus*	0.054	0.003
LYPAX	*Lycenchelys paxillus*	0.064	0.001
LYTER	*Lycodes terraenovae*	0.067	0.001
LYESM	*Lycodes esmarkii*	0.084	0.001
PACOP	*Paraliparis copei*	0.133	0.001
GLCYN	*Glyptocephalus cynoglossus*	0.198	0.001
PACAL	*Paraliparis calidus*	0.203	0.001
SESPP	*Sebastes*	0.208	0.001
MYGLU	*Myxine glutinosa*	0.229	0.001
CEFAB	*Centroscyllium fabricii*	0.235	0.001
NEBAI	*Nezumia bairdii*	0.326	0.001
ARRIS	*Arctozenus risso*	0.362	0.001
PHCHE	*Phycis chesteri*	0.668	0.001

The species of this group had a Kendall intragroup concordance of 37% (Appendix 9) and a concordance between indicator species varying between 19% and 45% (Table 192).

Table 192. Spearman rank correlation and Kendall concordance coefficients for group 7 indicator species.

	ARRIS	BASPI	CEFAB	GLCYN	LOAME	LYESM	LYPAX
Spearman correlation	0.388	0.150	0.315	0.326	0.134	0.159	0.129
Kendall concordance	0.432	0.211	0.364	0.374	0.196	0.219	0.192
p	0.001	0.001	0.001	0.001	0.001	0.001	0.001

	LYTER	MYGLU	NEBAI	PACAL	PACOP	PHCHE	SESPP
Spearman correlation	0.155	0.337	0.407	0.216	0.178	0.370	0.317
Kendall concordance	0.215	0.384	0.449	0.272	0.236	0.415	0.366
p	0.001	0.001	0.001	0.001	0.001	0.001	0.001

Group 7 species were found at depth averaging more than 284 m, with an oxygen threshold corresponding to oxygen classes 2 and 3.

Group 8

This group consists of 86 cells, which represents 7% of the area surveyed (2004-2010) and 8% of average total catch. It is composed of 42 species in total and has a maximum richness of 20 species per cell (Figure 194).

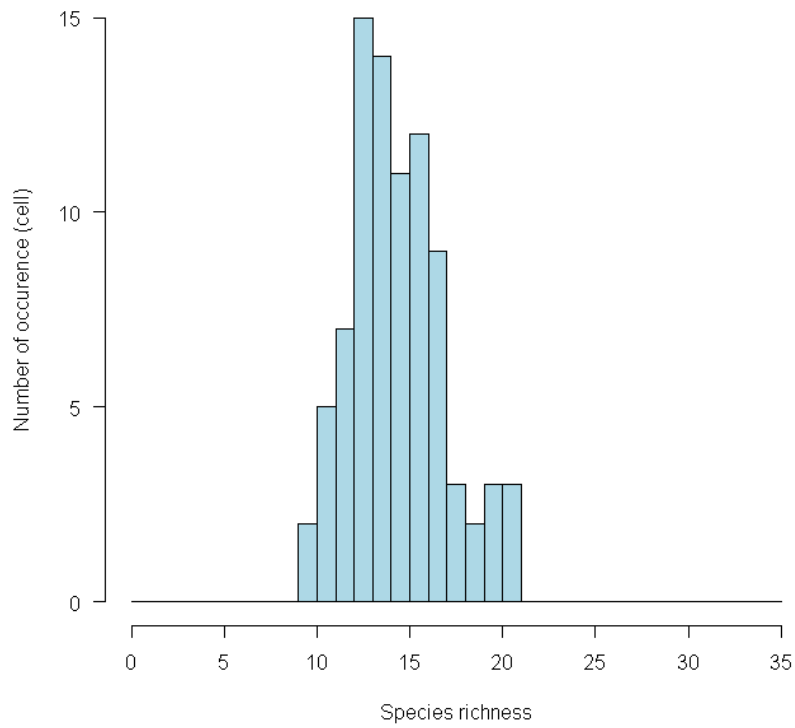

Figure 194. Species richness for cells belonging to group 8.

The most abundant species associated with this group are REHIP, SESPP, MYGLU, MEATL, and NEBAI (Figure 195).

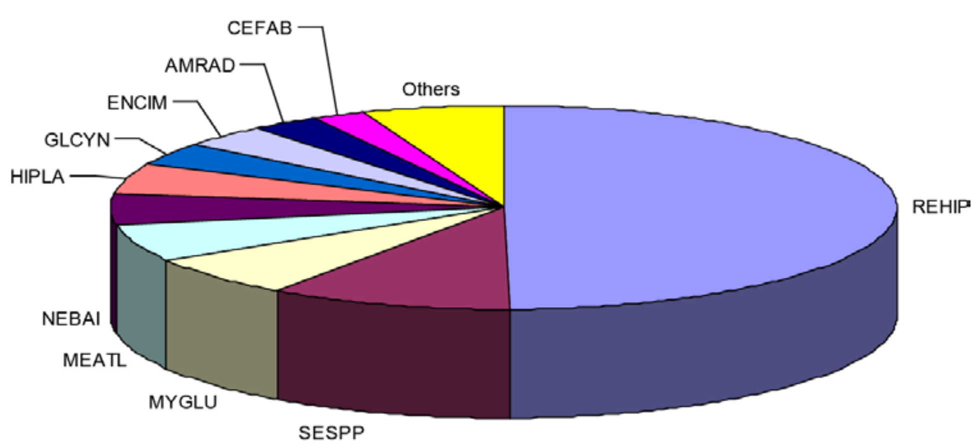

Figure 195. The most abundant species associated with group 8.

Three species had significant ($p<0.05$), albeit low, indicator values (Table 193).

Table 193. Group 8 indicator species with p-value and IndVal.

Species	Scientific name	IndVal	p-value
REHIP	*Reinhardtius hippoglossoides*	0.249	0.001
ENCIM	*Enchelyopus cimbrius*	0.267	0.001
MEATL	*Melanostigma atlanticum*	0.366	0.001

The species of this group had a Kendall intragroup concordance of 74% (Appendix 9). The concordance between indicator species varied from 69% to 77% (Table 194).

Table 194. Spearman rank correlation and Kendall concordance coefficients for group 8 indicator species.

	ENCIM	MEATL	REHIP
Spearman correlation	0.655	0.533	0.646
Kendall concordance	0.770	0.689	0.764
p	0.001	0.001	0.001

The species of this group were found at a depth averaging more than 284 m and with an oxygen threshold corresponding to oxygen class 1.

Group 9

This group consists of 78 cells, which represents 6% of the area surveyed (2004-2010) and 6% of average total catch. It is composed of 49 species in total and has a maximum richness of 31 species per cell (Figure 196).

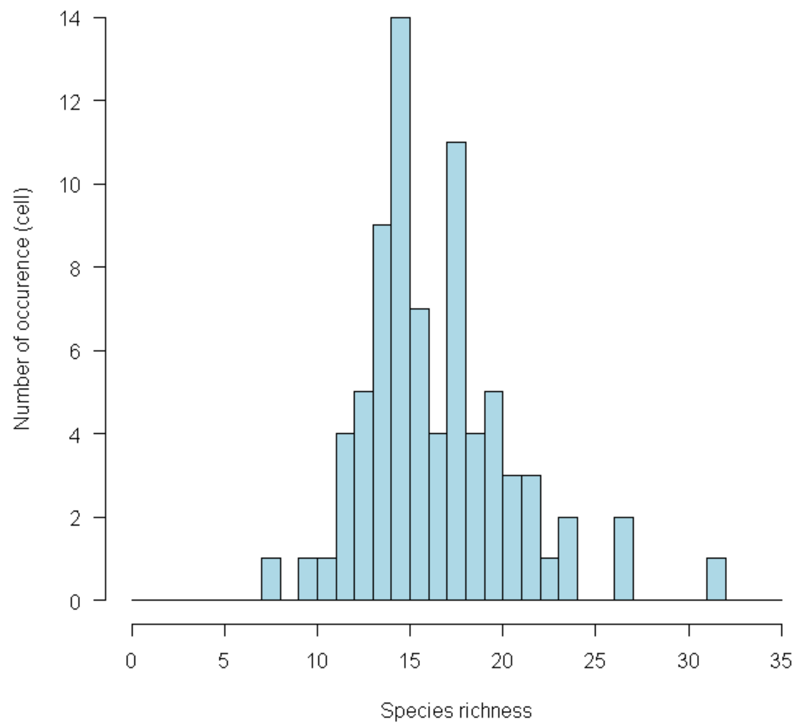

Figure 196. Species richness for cells belonging to group 9.

The most abundant species associated with group 9 are REHIP, SESPP, and HIPLA (Figure 197).

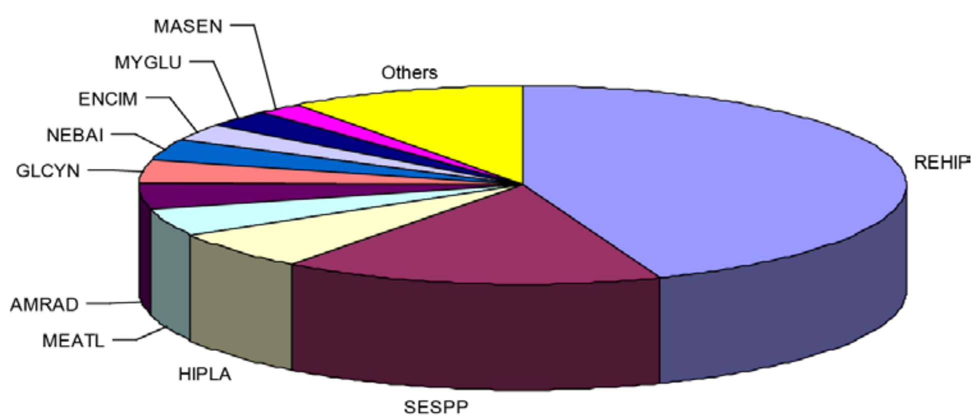

Figure 197. The most abundant species associated with group 9.

Three species had significant (p<0.05), albeit low, indicator values (Table 195).

Table 195. Group 9 indicator species with p-value and IndVal.

Species	Scientific name	IndVal	p
LYVER	*Lycenchelys verrillii*	0.114	0.001
AMRAD	*Amblyraja radiata*	0.199	0.001
MASEN	*Melanogrammus aeglefinus*	0.250	0.001

The species of this group had a Kendall intragroup concordance of 60% (Appendix 9). The concordance between indicator species varied from 49% to 65% (Table 196).

Table 196. Spearman rank correlation and Kendall concordance coefficients for group 9 indicator species

	AMRAD	LYVER	MASEN
Spearman correlation	0.442	0.234	0.471
Kendall concordance	0.628	0.489	0.647
p	0.001	0.001	0.001

The species of this group are found in an environment of average depth less than 284 m and an oxygen threshold corresponding to oxygen class 1.

Group 10

This group consists of 173 cells, which represents 14% of the area surveyed (2004-2010) and 15% of average total catch. It is composed of 59 species in total and has a maximum richness of 28 species per cell (Figure 198).

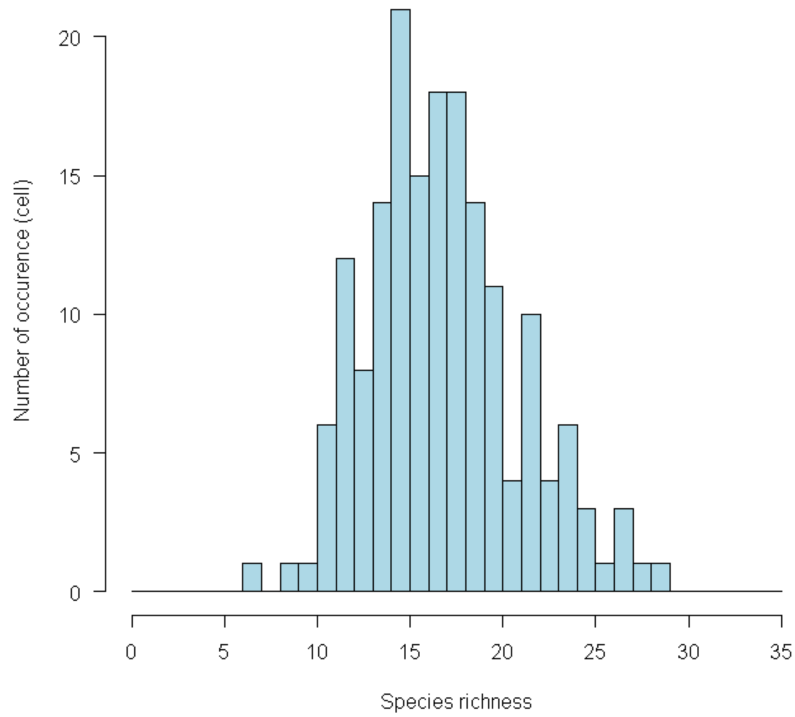

Figure 198. Species richness for cells belonging to group 10.

The most abundant species associated with this group are SESPP, REHIP, HIPLA, and GAMOR (Figure 199).

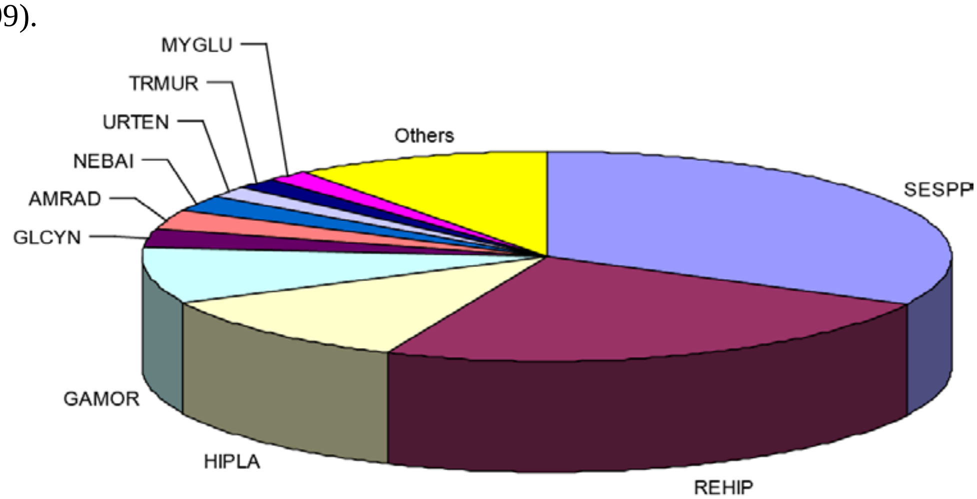

Figure 199. The most abundant species associated with group 10.

Three species had significant ($p<0.05$), albeit low, indicator values (Table 197).

Table 197. Group 10 indicator species with p-value and IndVal.

Species	Scientific name	IndVal	p
ARSIL	*Argentina silus*	0.065	0.001
HIHIP	*Hippoglossus hippoglossus*	0.137	0.001
MEBIL	*Merluccius bilinearis*	0.168	0.001

The species of this group had a Kendall intragroup concordance of 42% (Appendix 9). The concordance between indicator species varied by species from 40% to 48% (Table 198).

Table 198. Spearman rank correlation and Kendall concordance coefficients for group 10 indicator species.

	ARSIL	HIHIP	MEBIL
Spearman correlation	0.097	0.131	0.224
Kendall concordance	0.398	0.421	0.483
p	0.001	0.001	0.001

The species of this group were found at depths averaging less than 284 m with an oxygen threshold corresponding to oxygen classes 2 and 3.

Agreement between the two classification systems of habitat

The groupings of cells produced using a regression tree on the basis of both biological and environmental data at times corresponded to the megahabitats as determined using a cluster analysis of the physiographic and oceanographic data. The maximum number of cells in a tree group corresponding to a megahabitat is highlighted in green (Table 199). Groups 7–10 had the most cells in megahabitat 1, while groups 1 and 2 were mostly represented by megahabitat 10. The remaining groups shared most cells with 1 megahabitat, i.e., group 3 with megahabitat 11, group 4 with megahabitat 3, group 5 with megahabitat 8, and group 6 with megahabitat 5.

Viewed from the cluster classification, megahabitat 1 had its cells spread across tree groups 7–10. Megahabitats 3 and 10 had most cells in tree groups 4, and 1 and 2, respectively.

The number of cells contributing to a group is shown as proportional histograms in Figure 200 as tree groups coloured by megahabitat groups versus megahabitat groups by tree groups.

Table 199. Cross-table of the number of cells belonging to either tree groups (MRT) 1 to 10 or megahabitat clusters 1 to 13. Total no. corresponds to the the number of groups belonging to a class in the other classification system.

	Group as per MRT											
Megahabitat	1	2	3	4	5	6	7	8	9	10	Total	Total no.
1							139	85	47	93	364	4
2							2			5	7	2
3	5		6	48					3	29	91	5
4				11			9	1	20	41	82	5
5		3			45	30					78	3
7	10	1	4	9					1	1	26	6
8	13	51		2	50						116	4
9	39	7	27								73	3
10	179	68	20								267	3
11	14		50	19							83	3
12	4		4	7							15	3
13	3		9	12					7	4	35	5
Total	267	130	120	108	95	30	150	86	78	173	1237	
Total no.	8	5	7	7	2	1	3	2	5	6		

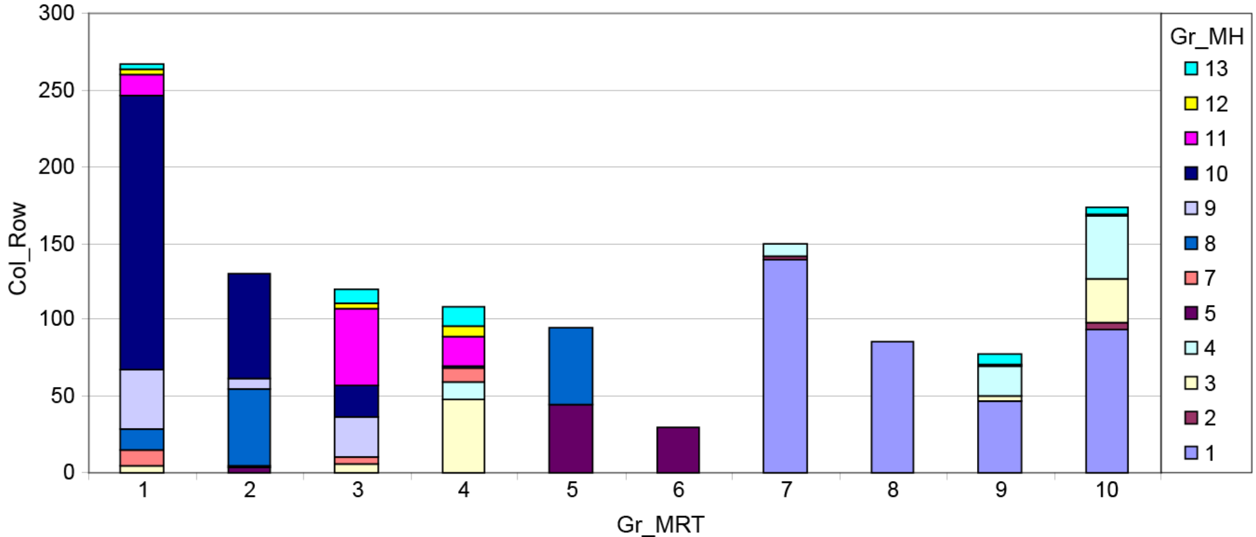

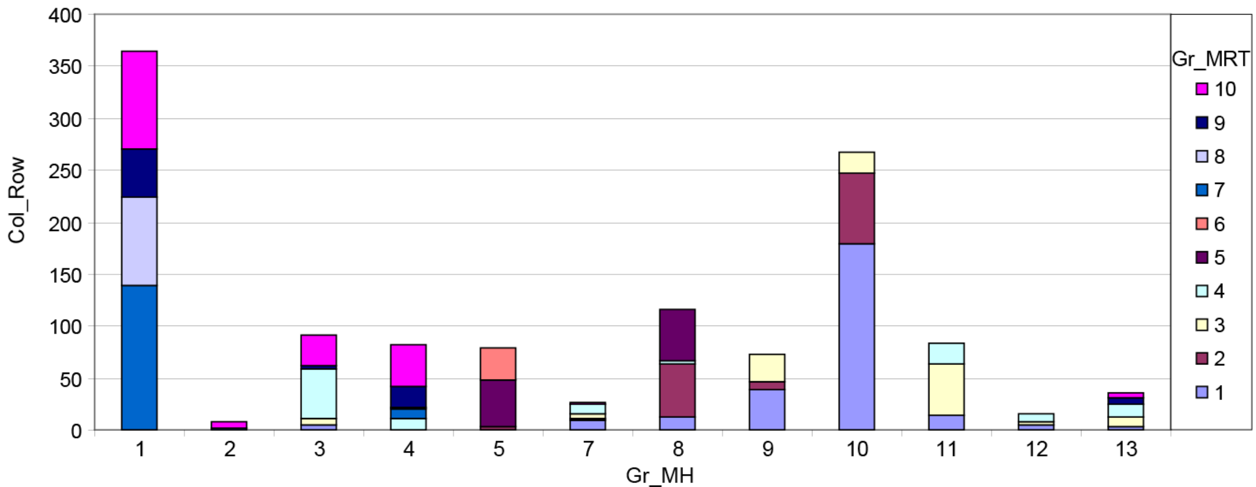

Figure 200. Histogram distribution of cells (Col_Row) by groupings. Above: regression tree groups (Gr_MRT), with columns coloured proportionally by megahabitats (Gr_MH). Below: megahabitat clusters coloured by tree groups.

CONCLUSION

Managing our marine resources in an efficient manner is a major task that may at times appear to be overwhelming considering the spatial scale and diversity of issues to be addressed. Whether the goal is to locate the habitat of species at risk or areas of greater ecological value, mapping a network of marine protected areas, or implementing a multi-species risk-based approach, two key aspects will have a major incidence on the degree of success of our decision making: a vast amount of basic scientific infomation and a great capacity to deliver an advice on the basis of that information.

This report proposes an integrative approach by which physiographic and oceanographic data on one hand and catch data obtained from routine research surveys of fish abundance on the other hand can be matched to provide a substantial amount of information on species as well as on habitats. The manuscript goes into a wealth of details about the methodology, and lists a large number of outputs in the form of tables and figures. However, these should only be regarded as examples of the potential products that can be obtained. Key to this approach was the use of spatial tools and the delivery of standardized datasets that can be improved and used again to address new species/issues in a timely fashion.

From the managers' perspective, the proposed methodology has several advantages, it builds on the existing data, as opposed to requiring more data from the field, it uses a common spatial reference system (the 100 km^2 grid) which could also be used to feed additional information on human risk factors, and it can pinpoint the location and planimetric area of important habitats from a monospecific or multispecific (biodiversity) standpoint. For planning purposes, it also has a great potential. The spatial extent of conservation measures and activities can be determined. The efficiency of monitoring activities and sampling protocols can be improved.

The method also has its disadvantages. The current habitat classification is a static one; changes in the habitats over time are not taken into consideration. Furthermore, the spatial scale used here may be inappropriate for describing key aspects of the ecology of many species. More field observations and more specifically better field observations, such as high resolution bathymetry and photography, will be required over large areas before a better resolution can be achieved. This will be useful only if meaningful observations on living organisms are made at a similar resolution.

ACKNOWLEDGMENTS

Many people were involved in the production of this report. The authors would like to thank the following individuals in particular: Hugues Benoît, Roderick Morin, Toby Surette (Gulf); and Denis Bernier, Hugo Bourdages, Johanne Gauthier, Sylvain Hurtubise, Richard Larocque (Québec). We would also like thank Joe Crocker (Ottawa) and Nicole Bouchard (Québec) for their support, and to Laure Devine and Ross Alexander for reviewing the text.

REFERENCES

Benoît, H.P. and D.P. Swain, 2003a. Accounting for length and depth-dependent diel variation in catchability of fish and invertebrates in an annual bottom-trawl survey. ICES J. Mar. Sci. 60: 1298–1317.

Benoît, H.P. and D.P. Swain, 2003b. Standardizing the southern Gulf of St. Lawrence bottom-trawl survey time series: adjusting for changes in research vessel, gear and survey protocol. Can. Tech. Rep. Fish. Aquat. Sci. 2505: iv + 95 pp.

Bourdages, H., L. Savard, D. Archambault, and S. Valois. 2007. Results from the August 2004 and 2005 comparative fishing experiments in the northern Gulf of St. Lawrence between the CCGS *Alfred Needler* and the CCGS *Teleost*. Can. Tech. Rep. Fish. Aquat. Sci. 2750: ix + 57 pp.

Brind'Amour, A. 2005. Arbre de régression multivariable: application à une communauté de poissons littoraux d'un lac du Bouclier canadien. Comptes rendus des 12èmes rencontres de la Société Francophone de Classification tenues à Montréal du 30 mai au 1er juin 2005. V. Makarenkov, G. Cucumel, F.-J. Lapointe, éditeurs. Université du Québec à Montréal.

Chouinard, P.-M. and J.-D. Dutil. 2011. The structure of demersal fish assemblages in a cold, highly stratified environment. ICES J. Mar. Sci. 68: 1896–1908.

Dufrêne, M. and P. Legendre. 1997. Species assemblages and indicator species: the need for a flexible asymmetrical approach. Ecological Monographs 67: 345–366.

Dutil, J.-D., S. Proulx, P. S. Galbraith, J. Chassé, N. Lambert, and C. Laurian. 2012. Coastal and epipelagic habitats of the estuary and Gulf of St. Lawrence. Can. Tech. Rep. Fish. Aquat. Sci. 3009: ix + 87 pp.

Dutil, J.-D., S. Proulx, P.-M. Chouinard, and D. Borcard. 2011. A hierarchical classification of the seabed based on physiographic and oceanographic features in the St. Lawrence. Can. Tech. Rep. Fish. Aquat. Sci. 2916: vii + 72 pp.

Dutil, J.-D., R. Miller, C. Nozères, B. Bernier, D. Bernier, and D. Gascon. 2006. Révision des identifications de poissons faites lors des relevés scientifiques annuels de l'abondance des poissons de fond et de la crevette nordique dans l'estuaire et le nord du golfe du Saint-Laurent. Rapp. manus. can. sci. halieut. aquat. 2760: x + 87 p.

Getis, A., and Ord, J. K. 2010. The analysis of spatial association by use of distance statistics. In: L. Anselin and S. J. Rey (eds), Perspectives on Spatial Data Analysis, pp. 127-145. Springer, Berlin Heidelberg.

Hernández, H. M. and M. Navarro. 2007. A new method to estimate areas of occupancy using herbarium data. Biodiv. Conserv. 16: 2457–2470.

Larsen, D. R. and P. L. Speckman. 2004. Multivariate regression trees for analysis of Abundance data. Biometrics 60: 54–549.

Legendre, P. 2005. Species associations: the Kendall coefficient of concordance revisited. J. Agr. Biol. Envir. St. 10: 226–245.

Legendre, P. and L. Legendre. 1998. Numerical ecology, 2nd English edition: Developments in environmental modeling 20. Amsterdam, Elsevier Science BV, 832 pp.

McGarigal, K., S.A. Cushman, M.C. Neel, and E. Ene. 2002. FRAGSTATS: Spatial pattern analysis program for categorical maps. Computer software program produced by the authors at the University of Massachusetts, Amherst. Available at the following web site: http://highlighted.umass.edu/landeco/research/fragstats/fragstats.html

Ouellette, M.-H., J.-L. DesGranges, P. Legendre and D. Borcard. 2005. L'arbre de régression multivariables: classification d'assemblage d'oiseaux fondée sur les caractéristiques de leur habitat. Société Francophone de Classification, Montréal.

Ouellette, M.-H. 2008. Arbres de régression multivariable ou « multivariate regression trees ». Supplément au chapitre 3. Université de Montréal. 9 pp.

APPENDICES

Appendix 1. Summary statistics for descriptors used in cluster analysis of seafloor habitats

For a full description of the data set, refer to Dutil et al. 2011.

Depth categories

Class	Bathy_Min	Bathy_Mean	Bathy_Max	Bathy_STD
Bathy_1	-10.73	-23.22	-37.92	6.45
Bathy_2	-43.84	-65.08	-90.08	10.27
Bathy_3	-81.94	-144.38	-205.56	29.47
Bathy_4	-389.83	-416.20	-435.05	10.31
Bathy_5	-236.49	-281.64	-312.51	18.00

Salinity categories

Class	Sal Min Min	Sal Moy Min	Sal Max Min	Sal Min Moy	Sal Moy Moy	Sal Max Moy	Sal Min Max	Sal Moy Max	Sal Max Max
S_1	28.1	29.2	30.6	28.5	29.5	30.6	29.2	30.0	31.0
S_2	34.3	34.5	34.6	34.5	34.6	34.7	34.5	34.6	34.7
S_3	32.6	32.9	33.1	33.6	33.8	34.1	34.1	34.3	34.5
S_4	30.1	30.9	31.6	30.4	31.2	31.8	30.8	31.4	32.0
S_5	31.9	32.3	32.6	32.5	32.8	33.0	33.2	33.4	33.7
S_6	31.0	31.6	32.1	31.7	32.1	32.4	32.1	32.4	32.7
S_7	27.5	29.3	30.9	31.8	32.3	32.7	33.3	33.6	33.8

Temperature categories

Class	T Min Min	T Moy Min	T Max Min	T Min Moy	T Moy Moy	T Max Moy	T Min Max	T Moy Max	T Max Max
T_1	-1.29	7.10	15.97	-1.33	5.78	13.02	-1.26	4.42	10.06
T_2	4.33	4.79	5.28	4.47	4.93	5.41	4.49	4.95	5.44
T_3	0.38	1.23	2.10	2.60	3.24	3.85	4.11	4.60	5.09
T_4	-0.83	0.55	2.11	-0.32	0.66	1.87	0.17	1.05	2.14
T_5	-1.22	2.53	6.81	-0.81	0.67	2.26	-0.15	0.87	1.96
T-6	-1.11	4.18	10.81	-0.75	1.97	4.93	0.28	1.88	3.61

Slope categories

Class	Slope_Mean	Slope_STD	Slope_Min	Slope_Max
P-1	0.22	0.12	0.02	0.63
P-2	0.10	0.05	0.01	0.28
P-3	0.38	0.21	0.05	1.13
P-4	0.60	0.35	0.05	1.84
P-5	0.87	0.52	0.09	2.69
P-6	1.13	0.79	0.09	4.28

Landscape

Geomorph_1		
Code	Title	Description
1	Shelf	mean depth < 200 m and mean slope < 0.8°
2	Slope	mean slope > 0.8°
3	Channel	mean depth > 200 m and mean slope < 0.8°

Geomorph_2	
Code	Description
1	Uniform terrain
2	Seafloor with humps
3	Seafloor with pits

Geomorph_3	
Code	Description
0	Non coastal
1	Coastal

Dissolved oxygen

Class	Saturation (%)
1	<25
2	25–35
3	35–45
4	45–55
5	55–65
6	65–75
7	75–85
8	>85

Surface sediments

Class	Description
110	Pelite and calcipelite
120	Sandy pelite
130	Pelite with coarse sand or gravel
210	Fine to coarse sand
310	Coarse sand to gravel
410	Gravel
512	Rock with pelite
530	Rock with coarse sand
540	Rock with gravel

Appendix 2. Megahabitat flowcharts

Results from a cluster analysis are summarized as three flowcharts characterizing the deep (I) and shallow (II and III) water habitats. Labels are those attributed to the habitats as presented in the first chapter (section 1). The letters correspond to the 13 megahabitat groups (see Dutil et al. 2011). The spatial area (in km^2) and general location names of groups are shown in the white boxes.

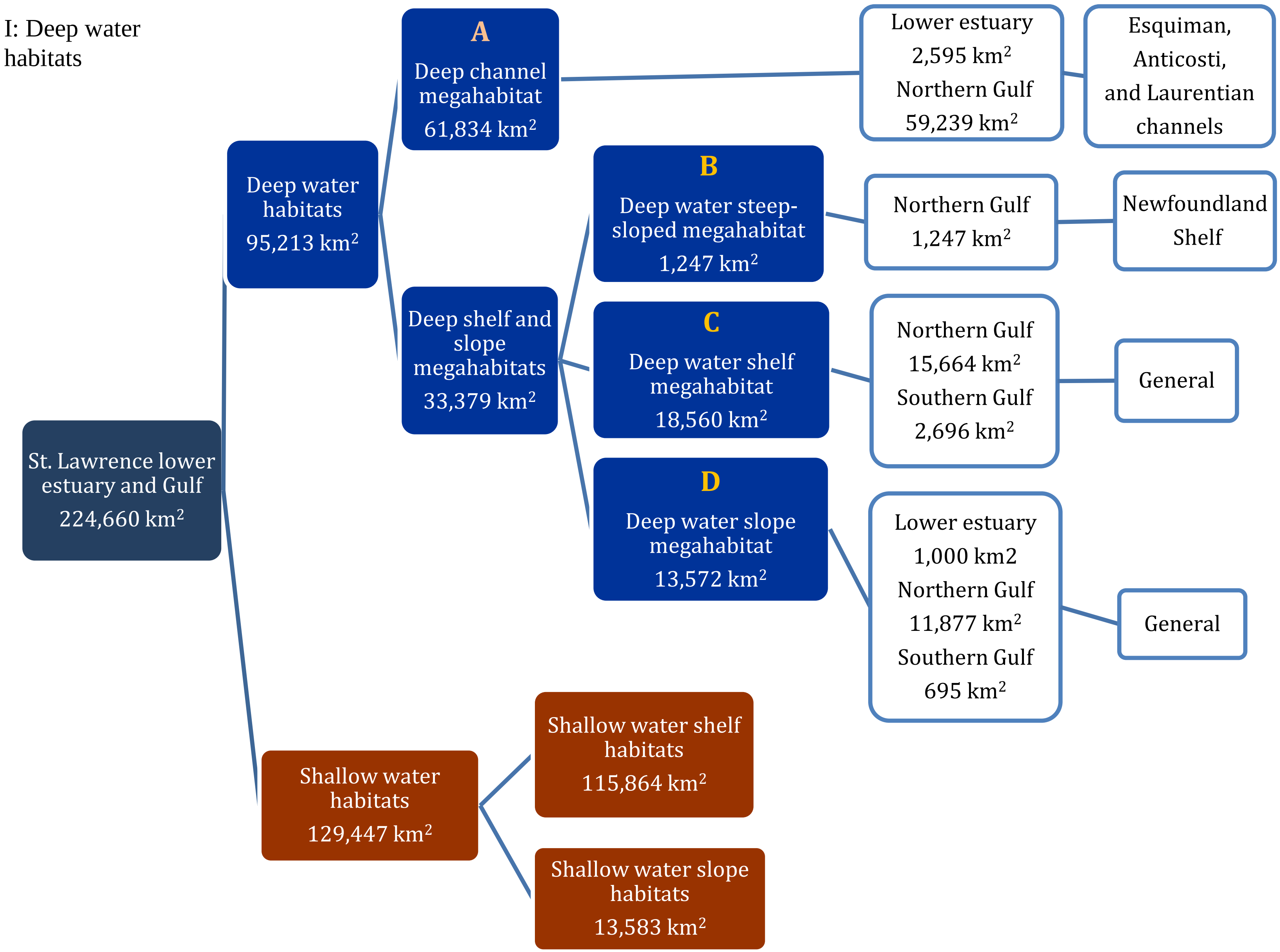
I: Deep water habitats
St. Lawrence lower estuary and Gulf
224,660 km²
Deep water habitats
95,213 km²
A
Deep channel megahabitat
61,834 km²
Lower estuary
2,595 km²
Northern Gulf
59,239 km²
Esquiman, Anticosti, and Laurentian channels
Deep shelf and slope megahabitats
33,379 km²
B
Deep water steep-sloped megahabitat
1,247 km²
Northern Gulf
1,247 km²
Newfoundland Shelf
C
Deep water shelf megahabitat
18,560 km²
Northern Gulf
15,664 km²
Southern Gulf
2,696 km²
General
D
Deep water slope megahabitat
13,572 km²
Lower estuary
1,000 km2
Northern Gulf
11,877 km²
Southern Gulf
695 km²
General
Shallow water habitats
129,447 km²
Shallow water shelf habitats
115,864 km²
Shallow water slope habitats
13,583 km²

II: Shallow water habitats

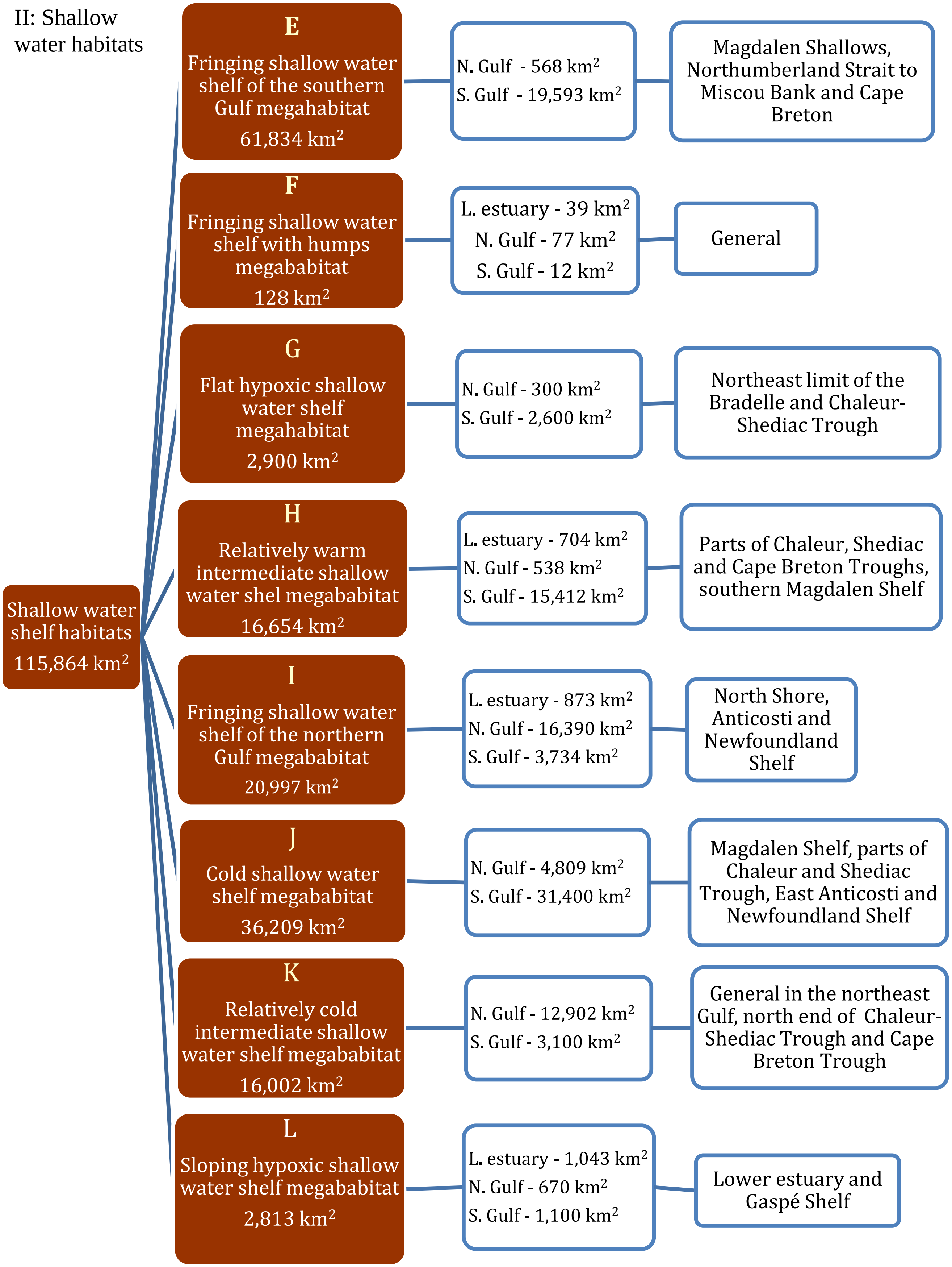

III: Shallow water habitats

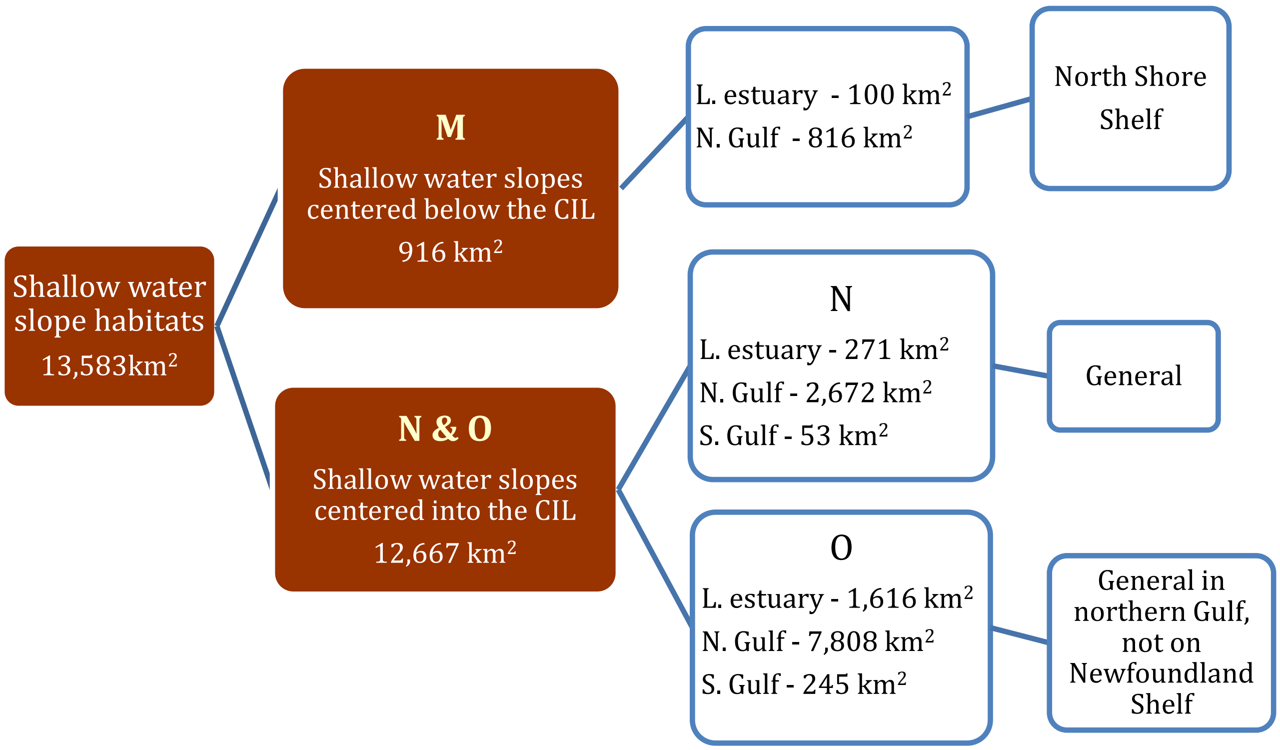

Appendix 3. Description of variables from geospatial analysis

Col_Row: Cell (10 km × 10 km) designation using column number (1 to 115) and row number (1 to 85) from left to right and from top to bottom (9775 cell matrix).

Cell address (100 km^2)

GiZScore: Getis and Ord local Gi* statistic indicating clusters of relative occurrences.

*Gi**

SPOT: Class variable indicating the close proximity of high (hot spots) and low (cold spots) relative occurrence values, respectively. Hot spots have values >1.65 (SPOT=2), cold spots values < -1.65 (SPOT=1); SPOT=0 for -1.65> GIZScore >1.65 (GIZScore not significant).

Cold spot / Hot spot

Area_KD90: Cell surface area within the 90% volume density contour (KDE) based on relative occurrences.

Surface area, 90% contour for KDE

Area_KD50: Cell surface area within the 50% volume density contour (KDE) based on relative occurrences.

Surface area, 50% contour for KDE

Area_AOO: Degree of overlap (cell surface area) of cell with the area of occupancy, as determined by the Hernández and Navarro (2007) method.

Surface area, area of occupancy

KD: Class variable based on values for Area_KD90 and Area_KD50. KD=50 when Area_KD50 represents >50% of the cell surface area; KD=90 when Area_KD90 represents >50% of the cell surface area; KD=100 otherwise.

KDE category

AOO: Binary variable based on the value of Area_AOO. AOO=1 when Area_AOO > 50% of the cell surface area; AOO=0 otherwise.

Class, area of occupancy

Megahabitat: Hierarchical classification of cells into 13 megahabitats as per Dutil et al (2011).

Megahabitat

Appendix 4. Environmental variables retained for multivariate regression tree analysis

As adapted from the full list of environmental variables (presented in Table 56, section 3) that were used in the linear regression analysis.

Variable	Abbreviation
Megahabitat variability	MHVar_3x3
Number of ridges (maximum of 9) represented in cell	Relief_var
Cell with sheltered marine area	Sup_Protege
Cell with semi-exposed marine area	Sup_SemiExp
Cell with exposed marine area	Sup_Expose
Distance between the centroid of the cell and the nearest coast	Cote_Dist
Average depth	Bathy_Mean
Maximum depth	Bathy_Max
Minimum depth	Bathy_Min
Average slope	Pente_Mean
Standard deviation of the mean slope	Pente_STD
Minimum slope	Pente_Min
Maximum slope	Pente_Max
Proportion of the surface of the cell classified as uniform by its roughness	Geo2_Uniforme
Proportion of the area of the cell classified as humps by its roughness	Geo2_Bosse
Proportion of the area of the cell classified as pits by its roughness	Geo2_Creux
Mean bottom annual mean salinity	SalMoyMoy
Mean bottom monthly minimum salinity	SalMinMoy
Mean bottom monthly maximum salinity	SalMaxMoy
Minimum bottom annual mean salinity	SalMoyMin
Minimum bottom monthly minimum salinity	SalMinMin
Minimum bottom monthly maximum salinity	SalMaxMin
Maximum bottom annual mean salinity	SalMoyMax
Maximum bottom monthly minimum salinity	SalMinMax
Maximum bottom monthly maximum salinity	SalMaxMax
Mean bottom annual mean temperature	TempMoyMoy
Mean bottom monthly minimum temperature	TempMinMoy
Mean bottom monthly maximum temperature	TempMaxMoy
Minimum bottom annual mean temperature	TempMoyMin
Minimum bottom monthly minimum temperature	TempMinMin
Minimum bottom monthly maximum temperature	TempMaxMin
Maximum bottom annual mean temperature	TempMoyMax
Maximum bottom monthly minimum temperature	TempMinMax
Maximum bottom monthly maximum temperature	TempMaxMax
Oxygen saturation classes (1: 0–35%, 2: 35–55%, 3: 55–75%, 4: 75–100%)	Oxy1
Geomorphology (in terms of the slope and depth: shelf, slope, and channel)	Geo1
Sediments (a category from clay to gravel)	Sed1
Rocky outcrops	Sed2

Appendix 5. Taxa caught during the bottom trawl surveys

Taxa caught during the bottom trawl surveys conducted annually in the lower estuary and Gulf of St. Lawrence (2004–2010) and considered in the analysis of assemblages and habitat associations. TSN code: taxonomic serial number; Species code: codes used in the geospatial database; Standardized catch: sum of average catch in number by set over all cells sampled; Number of sets: number of sets with the species present; Number of years: number of years when the species was observed.

Scientific name	French common name	English common name	TSN code	Species code	Total catch in number	Standardized catch	Number of sets	Number of years
Alosa pseudoharengus	Gaspareau	Alewife	161706	ALPSE	3747	815	167	7
Amblyraja radiata	Raie épineuse	Thorny skate	564149	AMRAD	21420	11334	1246	7
Ammodytes	Lançon (genre *Ammodytes*)	Sand lance (Genus *Ammodytes*)	171671	AMSPP	14456	3688	126	7
Anarhichas lupus	Loup atlantique	Striped wolffish	171341	ANLUP	1710	1103	312	7
Anisarchus medius	Lompénie naine	Stout eelblenny	171620	ANMED	11142	61	190	7
Anarhichas minor	Loup tacheté	Spotted wolffish	171342	ANMIN	107	2569	76	7
Artediellus atlanticus	Hameçon atlantique	Atlantic hookear sculpin	167208	ARATL	4128	4095	639	7
Arctozenus risso	Lussion blanc	White barracudina	644687	ARRIS	7128	45	698	7
Argentina silus	Grande argentine	Atlantic argentine	162064	ARSIL	81	1940	21	6
Artediellus uncinatus	Hameçon neigeux	Snowflake hookear sculpin	167207	ARUNC	1991	817	308	7
Aspidophoroides monopterygius	Alligator atlantique	Alligatorfish	167439	ASMON	5420	2109	829	7
Bathyraja spinicauda	Raie à queue épineuse	Spinytail skate	160932	BASPI	55	26	21	7
Boreogadus saida	Saïda franc	Arctic cod	164706	BOSAI	730	305	174	7
Careproctus reinhardti	Petite limace de mer	Sea tadpole	167522	CAREI	201	61	13	7
Centroscyllium fabricii	Aiguillat noir	Black dogfish	160703	CEFAB	6254	4379	147	7
Clupea harengus	Hareng atlantique	Atlantic herring	161722	CLHAR	412197	121893	1229	7
Cryptacanthodes maculatus	Terrassier tacheté	Wrymouth	171609	CRMAC	158	67	95	7
Cyclopterus lumpus	Grosse poule de mer	Lumpfish	167612	CYLUM	398	194	242	7
Enchelyopus cimbrius	Motelle à quatre barbillons	Fourbeard rockling	164748	ENCIM	10356	5763	897	7
Eumesogrammus praecisus	Quatre-lignes atlantique	Fourline snakeblenny	171601	EUPRA	5829	2882	482	7
Eumicrotremus spinosus	Petite poule de mer atlantique	Atlantic spiny lumpsucker	167545	EUSPI	2574	1121	440	7
Gasterosteus aculeatus	Épinoche à trois épines	Threespine stickleback	166365	GAACU	18463	32423	190	7

Scientific name	French common name	English common name	TSN code	Species code	Total catch in number	Standardized catch	Number of sets	Number of years
Gadus morhua	Morue franche	Atlantic cod	164712	GAMOR	80314	352	1679	7
Gadus ogac	Ogac	Greenland cod	164717	GAOGA	1404	4898	290	7
Glyptocephalus cynoglossus	Plie grise	Witch flounder	172873	GLCYN	22246	10565	1171	7
Gymnocanthus tricuspis	Tricorne arctique	Arctic staghorn sculpin	167275	GYTRI	7962	103	556	7
Gymnelus viridis	Unernak caméléon	Fish doctor	631028	GYVIR	512	2685	152	7
Hemitripterus americanus	Hémitriptère atlantique	Sea raven	167289	HEAME	594	167	215	7
Hippoglossus hippoglossus	Flétan atlantique	Atlantic halibut	172933	HIHIP	910	67154	414	7
Hippoglossoides platessoides	Plie canadienne	American plaice	172877	HIPLA	191066	376	2189	7
Icelus bicornis	Icèle à deux cornes	Twohorn sculpin	167188	ICBIC	448	228	84	6
Icelus spatula	Icèle spatulée	Spatulate sculpin	167192	ICSPA	1620	577	375	7
Leptagonus decagonus	Agone atlantique	Atlantic poacher	167478	LEDEC	5799	1899	507	7
Leptoclinus maculatus	Lompénie tachetée	Daubed shanny	171603	LEMAC	36656	11246	1049	7
Leucoraja ocellata	Raie tachetée	Winter skate	564145	LEOCE	153	45	55	7
Limanda ferruginea	Limande à queue jaune	Yellowtail flounder	172909	LIFER	58937	17899	621	7
Liparis gibbus	Limace marbrée	Variegated snailfish	167561	LIGIB	3435	1291	438	7
Lophius americanus	Baudroie d'Amérique	Monkfish	164499	LOAME	60	23	51	7
Lumpenus lampretaeformis	Lompénie-serpent	Snakeblenny	631023	LULAM	7380	4203	457	7
Lycodes esmarkii	Lycode d'Esmark	Esmark's eelpout	630982	LYESM	42	32	30	6
Lycodes lavalaei	Lycode de Laval	Newfoundland eelpout	165276	LYLAV	4665	121	622	7
Lycenchelys paxillus	Snakeblenny	Common wolf eel	165248	LYPAX	40	30	24	6
Lycodes terraenovae	Lycode atlantique	Atlantic eelpout	630981	LYTER	34	1826	28	7
Lycodes vahlii	Lycode à carreaux	Checker eelpout	165284	LYVAH	6573	24	484	7
Lycenchelys verrillii	Lycode à tête longue	Wolf eelpout	631024	LYVER	225	3440	88	7
Malacoraja senta	Raie à queue de velours	Smooth skate	564151	MASEN	7234	4123	876	7
Melanogrammus aeglefinus	Aiglefin	Haddock	164744	MEAEG	72	8	19	6
Melanostigma atlanticum	Mollasse atlantique	Atlantic soft pout	165296	MEATL	12868	6917	421	7
Merluccius bilinearis	Merlu argenté	Silver hake	164791	MEBIL	307	152	145	7
Myxine glutinosa	Myxine du nord	Atlantic hagfish	159772	MYGLU	14693	1192	526	7
Myoxocephalus octodecemspinosus	Chaboisseau à dix-huit épines	Longhorn sculpin	167320	MYOCT	4296	1143	366	7
Myoxocephalus scorpius	Chaboisseau à épines courtes	Shorthorn sculpin	167318	MYSCO	2309	8498	539	7
Nezumia bairdii	Grenadier du Grand Banc	Marlin-spike	165395	NEBAI	22025	12228	740	7
Osmerus mordax	Éperlan arc-en-ciel	Rainbow smelt	162041	OSMOR	88011	22343	187	7

Scientific name	French common name	English common name	TSN code	Species code	Total catch in number	Standardized catch	Number of sets	Number of years
Paraliparis calidus	Limace ardente	Lowfin snailfish	167604	PACAL	57	28	38	7
Paraliparis copei	Limace à museau noir	Blacksnout seasnail	167605	PACOP	59	39	22	7
Phycis chesteri	Merluche à longues nageoires	Longfin hake	164734	PHCHE	5489	3104	332	7
Pollachius virens	Goberge	Pollock	164727	POVIR	31	7	10	6
Pseudopleuronectes americanus	Plie rouge	Winter flounder	172905	PSAME	64023	14587	357	7
Reinhardtius hippoglossoides	Flétan du Groenland	Greenland halibut	172930	REHIP	156592	84925	1193	7
Scophthalmus aquosus	Turbot de sable	Windowpane	172746	SCAQU	917	1441	68	7
Scomber scombrus	Maquereau bleu	Atlantic mackerel	172414	SCSCO	5455	243	192	7
Sebastes	Sébaste (genre *Sebastes*)	Redfish (genus *Sebastes*)	166705	SESPP	134134	71997	1258	7
Squalus acanthias	Aiguillat commun	Spiny dogfish	160617	SQACA	131	22	22	7
Stichaeus punctatus	Stichée arctique	Arctic shanny	171596	STPUN	58	15	18	7
Tautogolabrus adspersus	Tanche-tautogue	Cunner	170481	TAADS	464	98	81	7
Triglops murrayi	Faux-trigle armé	Moustache sculpin	167375	TRMUR	135540	13949	1393	7
Ulcina olrikii	Alligator arctique	Arctic alligatorfish	643658	ULOLR	1214	412	213	7
Urophycis tenuis	Merluche blanche	White hake	164732	URTEN	12945	4091	695	7
Zoarces americanus	Loquette d'Amérique	Ocean pout	630979	ZOAME	119	27	61	7

Appendix 6. Taxa caught occasionally and not considered for analysis

Taxa caught occasionally during the bottom trawl surveys conducted annually in the lower estuary and Gulf of St. Lawrence (2004–2010) and not considered in the analysis of assemblages and habitat associations. TSN code: taxonomic serial number; Species code: codes used in the geospatial database; Number of sets: number of sets with the species present; Number of years: number of years when the species was observed.

Scientific name	French common name	English common name	TSN code	Species code	Number caught	Number of sets	Number of years
Alosa sapidissima	Alose savoureuse	American shad	161702	ALSAP	125	20	5
Anarhichas denticulatus	Loup à tête large	Northern wolffish	550561	ANDEN	10	3	2
Anguilla rostrata	Anguille d'Amérique	American eel	161127	ANROS	1	1	1
Argyropelecus gigas	Grande hache d’argent	Greater silver Hatchetfish	162218	ARGIG	1	1	1
Benthosema glaciale	Lanterne glaciaire	Glacier lanternfish	162680	BEGLA	3	2	1
Chauliodus sloani	Chauliode très lumineux	Sloane's viperfish	162281	CHSLO	7	6	4
Cottunculus microps	Cotte polaire	Polar sculpin	167408	COMIC	12	9	4
Cryptopsaras couesii	Pêcheur à trèfle	Triplewart seadevil	623188	CRCOU	3	2	2
Cyclothone microdon	Cyclothone à petites dents	Veiled anglemouth	162170	CYMIC	9	7	5
Dipturus laevis	Grande raie	Barndoor skate	564139	DILAE	1	1	1
Gaidropsarus argentatus	Mustèle argentée	Silver rockling	164768	GAARG	16	16	5
Gaidropsarus ensis	Mustèle arctique à trois barbillons	Threebeard rockling	164769	GAENS	1	2	1
Gasterosteus wheatlandi	Épinoche tachetée	Blackspotted stickleback	166385	GAWHE	22	2	1
Lamna nasus	Maraîche	Porbeagle	159911	LANAS	1	1	1
Lampadena speculigera	Lampe à nez denté	Mirror lanternfish	162708	LASPE	2	2	1
Leucoraja erinacea	Raie hérisson	Little skate	564130	LEERI	2	2	2
Liparis coheni	Limace de Cohen	Gulf snailfish	167580	LICOH	1	1	1
Liparis fabricii	Limace gélatineuse	Gelatinous snailfish	550548	LIFAB	42	19	5
Lumpenus fabricii	Lompénie élancée	Slender eelblenny	631020	LUFAB	31	12	5
Lycodes pallidus	Lycode pâle	Pale eelpout	165277	LYPAL	3	2	2
Lycodes polaris	Lycode polaire	Canadian eelpout	165266	LYPOL	30	8	2
Micromesistius poutassou	Poutassou	Blue whiting	164774	MIPOU	1	1	1
Microgadus tomcod	Poulamon atlantique	Atlantic tomcod	164720	MITOM	5	3	3
Myoxocephalus aenaeus	Chaboisseau bronzé	Grubby	167321	MYAEN	18	9	4
Neoscopelus macrolepidotus	Lanterne à grandes écailles	Glowingfish	162774	NEMAC	9	2	1
Nemichthys scolopaceus	Avocette ruban	Slender snipe eel	161624	NESCO	2	2	1
Notoscopelus elongatus	Lanterne	Lanternfish	162659	NOELO	1	1	1
Petromyzon marinus	Lamproie marine	Sea lamprey	159722	PEMAR	2	2	2
Peprilus triacanthus	Stromatée à fossettes	Butterfish	172567	PETRI	145	18	4

Scientific name	French common name	English common name	TSN code	Species code	Number caught	Number of sets	Number of years
Pholis gunnellus	Sigouine de roche	Rock gunnel	171645	PHGUN	9	8	3
Polyipnus clarus	Hache du talus continental	Star-eye hatchetfish	622357	POCLA	7	7	4
Rajella fyllae	Raie ronde	Round skate	564135	RAFYL	5	5	3
Salmo salar	Saumon atlantique	Atlantic salmon	161996	SASAL	5	5	4
Scomberesox saurus	Balaou	Atlantic saury	165612	SCSAU	52	13	3
Serrivomer beanii	Serrivomer trapu	Stout sawpalate	635762	SEBEA	4	4	2
Sebastes norvegicus	Sébaste orangé	Golden redfish	166781	SENOR	237	3	3
Stomias boa	Dragon boa	Boa dragonfish	162292	STBOA	3	3	2
Synaphobranchus kaupii	Anguille égorgée	Northern cutthroat eel	635794	SYKAU	4	4	3
Triglops nybelini	Faux-trigle à grands yeux	Bigeye sculpin	167376	TRNYB	11	7	3
Triglops pingelii	Faux-trigle bardé	Ribbed sculpin	644643	TRPIN	11	5	2
Ulvaria subbifurcata	Ulvaire deux-lignes	Radiated shanny	171616	ULSUB	49	10	3

Appendix 7. List of trawl survey variables

List of variables describing bottom trawl sets and associated fish catches in the DFO annual groundfish surveys conducted in the St. Lawrence estuary and Gulf during the period from 2004 to 2010.

Variable	Legend	Description
SET_ID	Trawl set ID	Trawl set identification. The code contains the information required to trace set data in the corporate databases. The first two digits designate the DFO region (variable REGION). For the DFO Québec region surveys, the code indicates the source project, survey number, vessel code, and set number. For the DFO Gulf region surveys, the code indicates the cruise number, vessel code, and set number.
REGION	DFO region	DFO region responsible for the data and the surveys. NR: Québec Region; SR: Gulf Region.
SET_LAT	Latitude of set	Position of the trawl set in decimal degrees, WGS84 (World Geodetic System, 1984 revision).
SET_LON	Longitude of set	Position of the trawl set in decimal degrees, WGS84 (World Geodetic System, 1984 revision).
DATE	Date	Trawl set date as DD-MMM-YYYY.
YEAR	Year	Year of the survey.
MONTH	Month	Month when the trawl set took place.
DAY	Day	Day when the trawl set took place.
TIME	Hour	Time of day (24-hour clock) when the trawl set took place.
NAFO	NAFO division	NAFO division where the trawl set occurred.
NAFO_SUB	NAFO subdivision	NAFO subdivision where the trawl set occurred.
*_N	Catch in number (*)	Catch in number expressed per unit tow distance (one nautical mile). The star stands for the scientific name five-digit code for the species. For instance, GAMOR_N refers to catches of Atlantic cod. Species codes are shown in Appendix 5.
*_W	Catch in weight (*)	Catch in weight expressed per unit tow distance (one nautical mile). The star stands for the scientific name five-digit code for the species. For instance, HIPLA_W refers to catches of American plaice. Species codes are shown in Appendix 5.
*_P	Presence/absence (*)	Presence/absence of species. The star stands for the scientific name five-digit code for the species. For instance, ANLUP refers to presence/absence data for striped wolffish. Species codes are shown in Appendix 5.
*_O	Occurrence (*)	Number of sets with species present. The star stands for the scientific name five-digit code for the species. For instance, ANLUP refers to presence/absence data for striped wolffish. Species codes are shown in Appendix 5.
*_R	Relative occurrence (*)	Relative occurrence of species (occurrence/number of sets). The star stands for the scientific name five-digit code for the species. For instance, ANLUP refers to presence/absence data for striped wolffish. Species codes are shown in Appendix 5.
COL_ROW	Cell ID	Location of set in a grid. Cell designation uses column number from left to right (1 to 115) and row number from top to bottom (1 to 85). Each cell represents 100 km^2 (10 km × 10 km).
MEGAHABITA	Megahabitat	Class of megahabitat to which the cell belongs; classes described in Dutil et al. 2011.

Appendix 8. Summary of indicator species associated with terminal groups of cells

Final partition	
Summary	
Sum of probabilities	0.53
Sum of indicator values	15.79
Sum of significant indicator values	15.77
Number of significant indicators	68

Group	no. indicator sp.
1	4
2	2
3	11
4	10
5	6
6	12
7	14
8	3
9	3
10	3

Species	Scientific name	cluster	IndVal	probability
ANMED	*Anisarchus medius*	1	0.114	0.001
HIPLA	*Hippoglossoides platessoides*	1	0.158	0.001
ICSPA	*Icelus spatula*	1	0.170	0.001
ULOLR	*Ulcina olrikii*	1	0.202	0.001
GYTRI	*Gymnocanthus tricuspis*	2	0.094	0.009
LIGIB	*Liparis gibbus*	2	0.111	0.001
GYVIR	*Gymnelus viridis*	3	0.058	0.006
ANMIN	*Anarhichas minor*	3	0.073	0.003
ARUNC	*Artediellus uncinatus*	3	0.101	0.001
ICBIC	*Icelus bicornis*	3	0.198	0.001
GAMOR	*Gadus morhua*	3	0.199	0.001
MYSCO	*Myoxocephalus scorpius*	3	0.204	0.001
ANLUP	*Anarhichas lupus*	3	0.209	0.001
LYLAV	*Lycodes lavalaei*	3	0.239	0.001
EUSPI	*Eumicrotremus spinosus*	3	0.312	0.001
TRMUR	*Triglops murrayi*	3	0.319	0.001
EUPRA	*Eumesogrammus praecisus*	3	0.328	0.001
MEAEG	*Melanogrammus aeglefinus*	4	0.019	0.048
CAREI	*Careproctus reinhardti*	4	0.043	0.014
BOSAI	*Boreogadus saida*	4	0.091	0.001
CYLUM	*Cryptacanthodes maculatus*	4	0.121	0.001
ARATL	*Artediellus atlanticus*	4	0.133	0.001
ASMON	*Aspidophoroides monopterygius*	4	0.158	0.001

Species	Scientific name	cluster	IndVal	probability
LEMAC	*Leptoclinus maculatus*	4	0.181	0.001
LEDEC	*Leptagonus decagonus*	4	0.192	0.001
LYVAH	*Lycodes vahlii*	4	0.261	0.001
LULAM	*Lumpenus lampretaeformis*	4	0.301	0.001
AMSPP	*Ammodytes*	5	0.107	0.002
LEOCE	*Leucoraja ocellata*	5	0.115	0.001
SCSCO	*Scomber scombrus*	5	0.176	0.001
HEAME	*Hemitripterus americanus*	5	0.307	0.001
MYOCT	*Myoxocephalus octodecemspinosus*	5	0.357	0.001
LIFER	*Limanda ferruginea*	5	0.440	0.001
SQACA	*Squalus acanthias*	6	0.063	0.002
CRMAC	*Cryptacanthodes maculatus*	6	0.112	0.001
ZOAME	*Zoarces americanus*	6	0.189	0.001
URTEN	*Urophycis tenuis*	6	0.297	0.001
GAOGA	*Gadus ogac*	6	0.317	0.001
CLHAR	*Clupea harengus*	6	0.374	0.001
TAADS	*Tautogolabrus adspersus*	6	0.450	0.001
PSAME	*Pseudopleuronectes americanus*	6	0.505	0.001
GAACU	*Gasterosteus aculeatus*	6	0.596	0.001
SCAQU	*Scophthalmus aquosus*	6	0.657	0.001
ALPSE	*Alosa pseudoharengus*	6	0.668	0.001
OSMOR	*Osmerus mordax*	6	0.774	0.001
BASPI	*Bathyraja spinicauda*	7	0.031	0.031
LOAME	*Lophius americanus*	7	0.054	0.003
LYPAX	*Lycenchelys paxillus*	7	0.064	0.001
LYTER	*Lycodes terraenovae*	7	0.067	0.001
LYESM	*Lycodes esmarkii*	7	0.084	0.001
PACOP	*Paraliparis copei*	7	0.133	0.001
GLCYN	*Glyptocephalus cynoglossus*	7	0.198	0.001
PACAL	*Paraliparis calidus*	7	0.203	0.001
SESPP	*Sebastes*	7	0.208	0.001
MYGLU	*Myxine glutinosa*	7	0.229	0.001
CEFAB	*Centroscyllium fabricii*	7	0.235	0.001
NEBAI	*Nezumia bairdii*	7	0.326	0.001
ARRIS	*Arctozenus risso*	7	0.362	0.001
PHCHE	*Phycis chesteri*	7	0.668	0.001
REHIP	*Reinhardtius hippoglossoides*	8	0.249	0.001
ENCIM	*Enchelyopus cimbrius*	8	0.267	0.001
MEATL	*Melanostigma atlanticum*	8	0.366	0.001
LYVER	*Lycenchelys verrillii*	9	0.114	0.001
AMRAD	*Amblyraja radiata*	9	0.199	0.001
MASEN	*Melanogrammus aeglefinus*	9	0.250	0.001
ARSIL	*Argentina silus*	10	0.065	0.001
HIHIP	*Hippoglossus hippoglossus*	10	0.137	0.001
MEBIL	*Merluccius bilinearis*	10	0.168	0.001

Appendix 9. Intragroup concordance (Kendall's coefficient)

Group	W	F	Prob. F	Corrected prob. F	Chi²	Prob. perm	Corrected prob. perm
1	0.448	2.439	<0.001	<0.001	2216.848	0.001	0.011
2	0.704	2.375	<0.001	<0.001	1739.450	0.001	0.011
3	0.366	5.777	<0.001	<0.001	4978.519	0.001	0.011
4	0.276	3.424	<0.001	<0.001	3406.695	0.001	0.011
5	0.387	3.156	<0.001	<0.001	2869.820	0.001	0.011
6	0.258	3.819	<0.001	<0.001	3822.647	0.001	0.011
7	0.336	6.581	<0.001	<0.001	5815.438	0.001	0.011
8	0.742	5.738	<0.001	<0.001	2749.651	0.001	0.011
9	0.601	3.018	<0.001	<0.001	2230.263	0.001	0.011
10	0.424	1.472	<0.001	<0.001	1571.747	0.001	0.011